Peptidomimetic Foldamers of β-Secondary Structural Elements

Jonathan E. Ross

A dissertation presented in partial fulfilment of the requirements for the award of the degree of

Doctor of Philosophy

Of

University of Oxford

Chemistry Research Laboratory
12 Mansfield Road
Oxford
OX1 3TA

Pembroke College
St Aldate's
Oxford
OX1 1DW

April 2016

Declaration of Authorship

This thesis describes work carried out in the Chemistry Research Laboratory between October 2012 and April 2016. The thesis is a result of my own work unless stated otherwise in the text or included in the list below:

Chapter 2: Compounds **1-19** were synthesised by E. A. German (MChem 2014, Part II Student, Hamilton Group, University of Oxford). X-ray crystal structures were solved by Dr P. C. Knipe (post-doctoral research assistant, Hamilton Group, University of Oxford). Portions of this chapter were previously published:

> German, E. A., Ross, J. E., Knipe, P. C., Don, M. F., Thompson, S., Hamilton, A. D., 'β-Strand mimetic foldamers rigidified through dipolar repulsion', *Angew. Chem. Int. Ed.*, **2015**, 54, 2469-2652.

Chapter 3: X-ray crystal structures were solved by Dr P. C. Knipe. Portions of this chapter were previously published:

> Ross, J. E., Knipe, P. C., Thompson, S., Hamilton, A. D., 'Hybrid Diphenylalkyne-Dipeptide Oligomers Induce Multistrand β-Sheet Formation', *Chem. Eur. J.*, **2015**, 21, 14699-14702.

Chapter 5: Compounds **130-154** were synthesised by O. Neale (MChem 2015, Part II Student, Hamilton Group, University of Oxford).

Acknowledgements

I returned to Oxford after a brief stint in the ‘real world’ and it is a testament to those below, and many others, that I have not once regretted my decision. The research experience has met all of its expected clichés, from the fist-clenching to the fist-pumping, but the memories of the latter shall live on that bit longer. The DTC, with its support from the EPSRC, was a truly fantastic place to commence a research career and their continuing support and input has been greatly valued.

Mention that your boss is the Vice-Chancellor and the most frequent response is surely you don’t ever see him? Nothing could be further from the truth. I feel that research, in the best possible way, is Professor Hamilton’s professional hobby, and the resulting enthusiasm and ideas that he brought in his every spare moment have been of great benefit.

To the post docs; Sam - from the tolerance of my distractions in Wallingford in the opening months, to the vital assistance in the last few weeks - thank you; Pete - your eye for detail, appreciation of Alan Partridge and tolerance of endless questions on the 1st year biochemistry syllabus has been exemplary - good luck in Belfast; Hayden - I never thought I’d learn so much about drafts, uplifts and thermals, nor proteins, assays and HPLC - who knows which set will prove more useful!; Matteo - my fellow director and cheestrepeneur, climb the greasy pole faster and I’ll see you in Unilever House soon!

To my fellow DPhils; the soon to be Dr. Dr. Lucarelli - thank you for the introduction to the world of competitive eating on the 4th July and the sailing in Boston; Madu - for the Sri Lankan cooking and the Jack Cox fine cuts for four, I hope my figures go some way towards matching yours; Tom - from the opening days of dominoes and videos at the DTC to the long nights in the NMR hall just gone, we’ve faced it together with aplomb - thank you.

To the more fleeting (and invariably more mature) members of the lab - Hannah, Mel, Tohru, and Natalie - thank you for the wise words and the attempts to improve the lab's productivity!

To my Part II's, Lizzie and Olivia, I couldn't have asked for a better duo. Be it alongside boundless enthusiasm for 'Team β-strand' (your parting message to the fumehood still stands) or the Park End cheese-floor, your willingness to grapple with the frustrations of synthesis, the finer aspects of protein folding, or simply a Thursday morning hangover, never failed to impress.

To PCBC, from the near misses of undergraduate to the fantastic success of 2012 onwards, it's been a tiring, stressful, but most of all, enthralling and rewarding experience.

To the 'Real Bullingdon Club', in all its iterations - I don't yet know what to do with the plaque, the two square metre canvas and the empty bottle of Bollinger - but it's been a fine place to rest my head at the end of each day.

Finally the largest thank you of all to my parents; it has been over five years since that fateful dinner when I announced I wanted to do a DPhil and despite the initial trepidation, the support since has been immense. I promise I'll give the law at least six months….

Abstract

Foldamers have the potential to be the synthetic equivalent of Nature's macromolecules; man-made oligomers that use a range of non-covalent interactions to fold into well-defined structures.

Chapter 1 introduces the challenges laid down by Gellman to chemists in creating foldamers; i) to design new polymers that reliably display interesting folding properties; ii) to be able to include novel and unnatural functional groups; and iii) render them simple to synthesise. Each of the foldamers made in this thesis will be evaluated against these challenges.

Chapter 2 develops a mimic of the linear β-strand, based on alternating pyridyl/urea units, with the conformation enforced by dipolar repulsion. Conformational bias is demonstrated in the solution phase by computational and NMR studies, and in the solid phase by X-ray crystallography. The concept is extended to the inclusion of hydrophilic residues and conformation is maintained in a polar protic solvent.

Chapter 3 describes the design and synthesis of a three- and four-stranded β-sheet mimic templated by the diphenylacetylene motif. The folding is enforced by a hydrogen bonding network demonstrated *via* extensive solution phase studies and X-ray crystallography.

Chapter 4 explores the scope of this new architecture. The meander is successfully elongated to seven strands, and the structure shown to be amenable to the inclusion of D-amino acids and hydrophilic residues. The foldamer is therefore shown to meet all of Gellman's criteria.

Chapter 5 uses the diphenylacetylene motif to study the factors involved in the formation of β-sheets, specifically the effect of side-chain identity on hydrogen bond strength. The difference in strengths is shown to be minimal, suggesting that β-sheet propensity is due to the energy changes in forming the extended conformation rather than forces between strands.

Abbreviations

Å	Angstrom
Aβ	Amyloid β
Ar	Aryl
ATR	Attenuated total reflectance
Bak BH3	Bcl-2 homologous antagonist killer Bcl-2 homology domain 3
Bcl-x_L	B-cell lymphoma 2
Boc	*tert*-Butyloxycarbonyl
Bpy	2,2'-Bipyridine
Bu	Butyl
cal	Calorie
CCDC	Cambridge Crystallographic Data Centre
CD	Circular dichroism
COSY	Homonuclear correlation spectroscopy
Da	Dalton
DCC	*N,N'*-dicyclohexylcarbodiimide
DFT	Density functional theory
DIPEA	*N,N*-diisopropylethylamine
DMAP	4-Dimethylaminopyridine
DME	1,2-Dimethoxyethane
DMSO	Dimethylsulfoxide
DNA	Deoxyribonucleic acid
EDC	1-Ethyl-3-(3-dimethylaminopropyl)carbodiimide
ESI	Electrospray ionisation
Et	Ethyl
F_c	Fragment crystallisable
Fmoc	Fluorenylmethyloxycarbonyl
GB1	Immunoglobin-binding domain from protein G
GPCR	G-protein coupled receptor
HBTU	(2-(1*H*-Benzotriazol-1-yl)-1,1,3,4-tetramethyluornium hexafluorophosphate
HDM2	Human double minute 2 homolog

HIF	Hypoxia Inducible Factor
HIV	Human immunodeficiency virus
HMBC	Heteronuclear multiple-bond correlation spectroscopy
HOBt	Hydroxybenzotriazole
HPLC	High-performance liquid chromatography
HSQC	Heteronuclear single-bond correlation spectroscopy
IC_{50}	Half-maximal inhibitory concentration
IgG	Immunoglobin G
Il-4	Interleukin-4
IR	Infra-red
IRS	Insulin Receptor Substrate
K	Kelvin
KHMDS	Potassium bis(trimethylsilyl)amide
k	Kilo
L	Litre
LDA	Lithium diisopropylamide
m	Metre
m	Milli (as prefix)
M	Molar
Mad	Mitotic arrest deficient
MDM2	Mouse double minute 2 homolog
MMFF	Merck Molecular Force Field
MOE	Molecular Operating Environment
mol	Mole
n	nano
NMR	Nuclear magnetic resonance
NOE	Nuclear Overhauser effect
NOESY	Nuclear Overhauser effect spectroscopy
p53	Tumor protein p53
P_C	Random coil propensity
PDB	Protein Data Bank
PDZ	Post synaptic density protein; Drosophilia disc large tumor suppressor; Zonula occludens-1 protein
PG	Protecting group

PKA	Protein Kinase A
ppb	Parts per billion
PPI	Protein-protein interaction
ppm	Parts per million
P_α	Helix propensity
P_β	Sheet propensity
Q	Quaternary
Raf	Serine/threonine-protein kinase A-Raf
RAP1A	Rap GTP-binding protein 1A
Ras	Rat sarcoma
RMSD	Root mean squared deviation
RNA	Ribonucleic acid
ROESY	Rotating-frame nuclear Overhauser effect spectroscopy
SAR	Structure-Activity Relationship
SEM	2-(Trimethylsilyl)ethoxymethyl
S_N	Substitution nucleophilic
TBAF	Tetra-*n*-butylammonium fluoride
tert	Tertiary
TFA	Trifluoroacetic acid
TFE	1,1,1-Trifluoroethanol
THF	Tetrahydrofuran
TLC	Thin layer chromatography
TMS	Trimethylsilyl
UV	Ultraviolet
Δ	Change in
μ	Micro

One and three letter amino acid codes are used throughout.

All reactions proceed at room temperature unless otherwise indicated.

Table of Contents

Chapter 1 - Foldamers

1.1 The Allure of Foldamers

In the macromolecules, DNA, RNA and proteins, Nature has created exquisite machines whose precise function is defined by their structure. Be they the enzymes that mediate reactions, the gate-keepers of the cell, or the molecules responsible for transport and information storage, these polymers, determined by their primary sequence and surroundings are guided by intra- and inter-molecular forces into folded states. It is the chemist's challenge to design new polymers and incorporate novel structural elements to probe, disrupt and perhaps even improve upon the molecules of Nature.

In his 'Manifesto', Gellman designated this new field as that of 'foldamers'.[1] He defined a foldamer as any polymer that has 'a strong tendency to adopt a specific conformation'. His ultimate aim for the field is for chemists to be able to control secondary and tertiary structure, and therefore design and synthesise 'unnatural polymeric agents … capable of performing useful functions'. To that end, he challenged the chemical community to address three major strands of research in the development of new foldamers:

i) the design of new polymeric backbones that could reliably display interesting folding properties,

ii) the ability to include novel, and in particular unnatural functional groups and,

iii) the ease of synthesis.

In the intervening seventeen years, each of these targets, and in particular the first, has been addressed. Chemists have been able to use hydrogen bonding, π-stacking,[2] van der Waals forces,[3] electrostatic interactions[4] and the hydrophobic effect[5] as controlling elements of novel foldamers. They have incorporated azides and alkynes for 'click' chemistry,[6] alongside

new motifs to reinforce conformational preference. Many of these new polymers are amenable to existing automated synthetic methods, enabling the rapid creation of foldamer libraries. These foldamers go beyond merely the academic study of remarkable conformational preferences; they have been used to target a huge range of diseases, [7–10] in the design of gels and vesicles for application in drug delivery,[11] and in the development of molecular machines.[12]

1.2 Hydrogen Bonding

1.2.1 Homologated-Amino Acids

Much of the earliest foldamer work focused on the modified amino acid family; polymers consisting solely of β- and γ-amino acids as well as those containing mixed monomer units (Figure 1.1). Gellman and Seebach have been the pioneers of this field, building an appreciation of the rules that govern the conformational preferences of these homologated peptides. For much of this class, the driving factor in folding is hydrogen bonding.

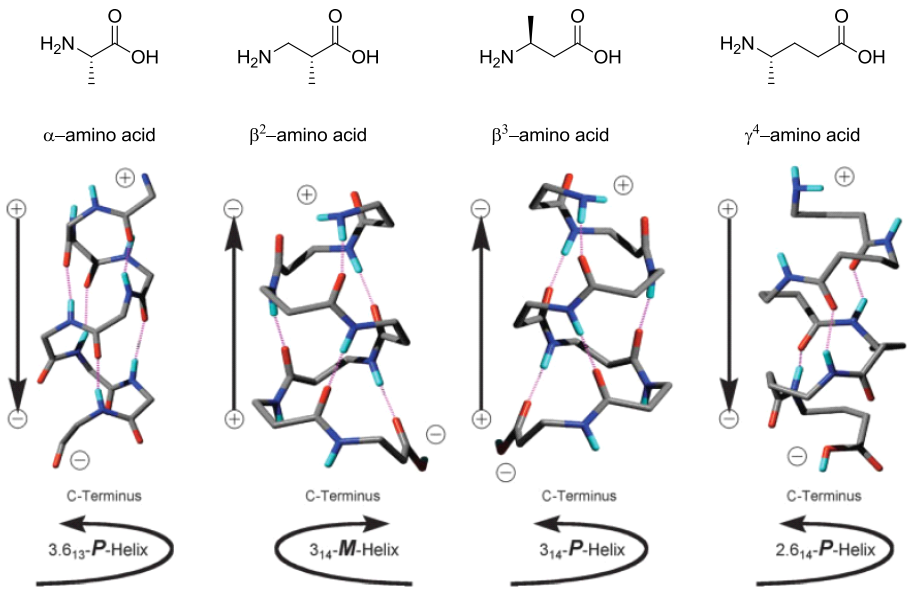

Figure 1.1 α-, β-, and γ-amino acids. Figure by Seebach *et al.*[13] and reproduced with permission from 'John Wiley and Sons'.

It is well established that short oligomers of the proteogenic α-amino acids can form stable helices in solution with as few as four monomer units and Seebach has demonstrated that helical stability increases for both β- and γ-amino acids when compared to α-amino acids. Furthermore, in progressing from three (α) to four (β) to five (γ) chain atoms the handedness of the helix switches with each homologation step.[13]

1.2.1.1 β-Peptides

β-Peptides are the most thoroughly studied and the use of different side-chains has enabled the identifaction of five different helix types, each defined by the size of the hydrogen-bonded rings formed. These are the 8-, 10-, 12-, 12/10, and 14-helix. The 14-helix is the most extensively researched and forms a regular, three residue repeating arrangement with the hydrogen bond between the N-H of the i^{th} residue, and the C=O of the *i + 2* residue. Due to steric clashes only small (H, F) groups are permitted in the axial position and this allows control of helical preference (Figure 1.2).[14]

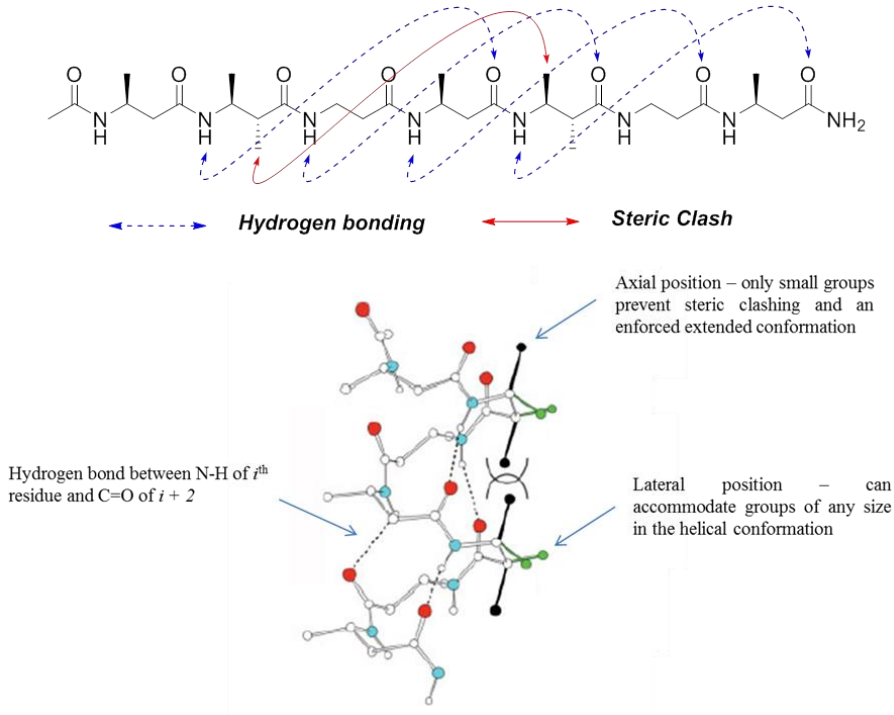

Figure 1.2 Model of the 14-helix showing the axial and lateral clashes. Figure adapted from Seebach *et al.*[13] and reproduced with permission from 'John Wiley and Sons'.

By inserting an alkyl group into this position the chain is forced into an extended conformation,[15] and the use of a turn inducer such as a geminally disubstituted $\beta^{2,2}$-amino acid allows for the construction of parallel or anti-parallel sheet like structures.[16] By understanding and utilising this rule the chemist can now have greater control over conformation than through the use of α-amino acids; as shall be highlighted in later chapters the design of peptides that adopt the β-sheet conformation is a non-trivial exercise. Additionally these sheets are distinct from those of α-amino acids as the amide and carbonyl groups all point in the same direction as opposed to alternating (Figure 1.3).

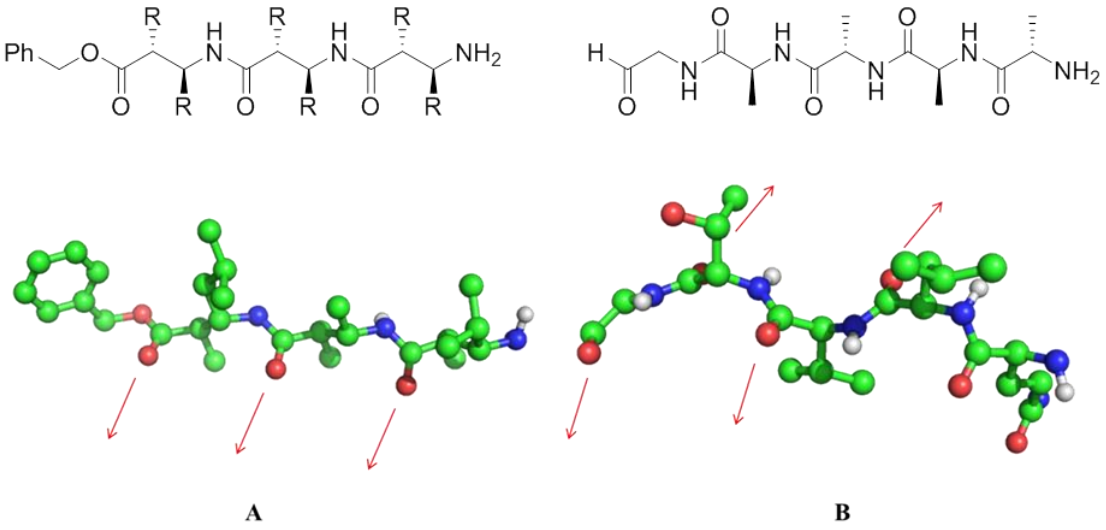

Figure 1.3 Crystal structure of an extended β-peptide (A; CCDC: 113798) and natural β-strand composed of α-peptides (B; PDB: 4GD4). Hydrogen atoms omitted for clarity.

By contrast, the 12/10-helix demonstrates the flexibility of novel foldamers. Working from the observation that β^2 and β^3 amino acids are both accommodated in the 14-helix, it was anticipated that a polymer of alternating β^3 and β^2 residues would fold into the three residue turn 14-helix. Instead, a 2.7 residue turn 12/10-helix was observed with a macrodipole and a novel pattern of side-chains across the helix.[17-18] This novel side-chain display opens options beyond the capabilities of using solely α-amino acids.

The 8-, and 10-helices are of particular interest and a demonstration of the power of synthetic foldamers as they both represent a novel helix type not seen in natural amino acids. The 8-helix is a folded staircase with each step being composed of the eight membered hydrogen-bonded ring (Figure 1.4).[19]

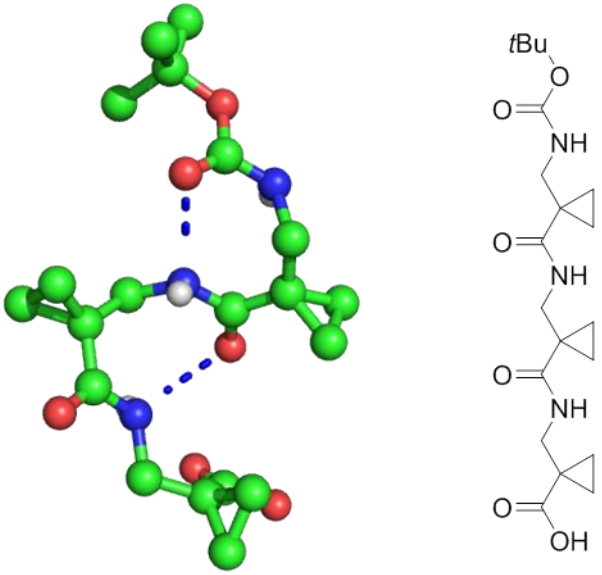

Figure 1.4 8-helix adopting the conformation of a folded staircase (CCDC: 129239).

The above examples show that homologated peptides fulfil the first of Gellman's foldamer criteria; they reliably display interesting folding properties with a range of designed helical and extended conformations.

1.2.1.2 γ-Peptides

The Smith group has explored the conformation of γ-peptides when the chain has been constrained by a carbo- or heterocyclic ring. Solid state studies showed that the inclusion of a cyclopropane ring resulted in a parallel sheet structure stabilized by inter-strand hydrogen bonds (Figure 1.5).[20]

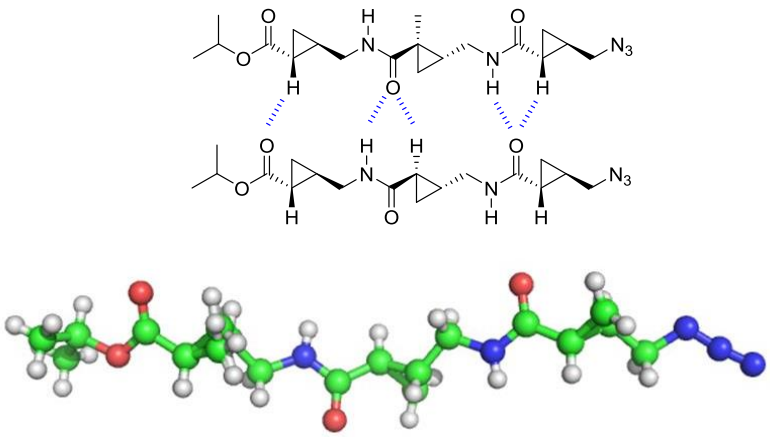

Figure 1.5 Parallel sheet structure of a γ-peptide reinforced by a cyclopropane ring (CCDC: 617972).

By contrast the synthesis of the five-membered ring analogue was found to promote intra- as opposed to intermolecular hydrogen bonding, with the resultant conformation described as a bend-ribbon (Figure 1.6).[21]

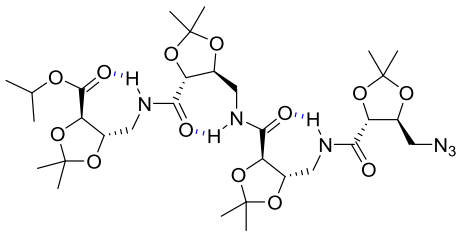

Figure 1.6 Bend-ribbon conformation of a γ-peptide templated by 7-membered hydrogen-bonded rings.

1.2.1.3 Biological Application of β-peptides

By understanding and applying these folding rules Gellman created helical, cationic and amphiphilic oligomers of β-peptides that mimic amphipathic peptides and thus show antimicrobial activity *via* a membrane disruption mechanism (Figure 1.7).[22] These compounds display a key advantage over the parent antibiotic comprised of α-amino acids, in that they underwent extremely slow proteolytic degradation as the homologated amino acids are not recognised by the protease enzymes. This demonstrates his second criteria in action; incorporating unnatural groups, here a methylene unit, provides the foldamer with an advantage in its application.

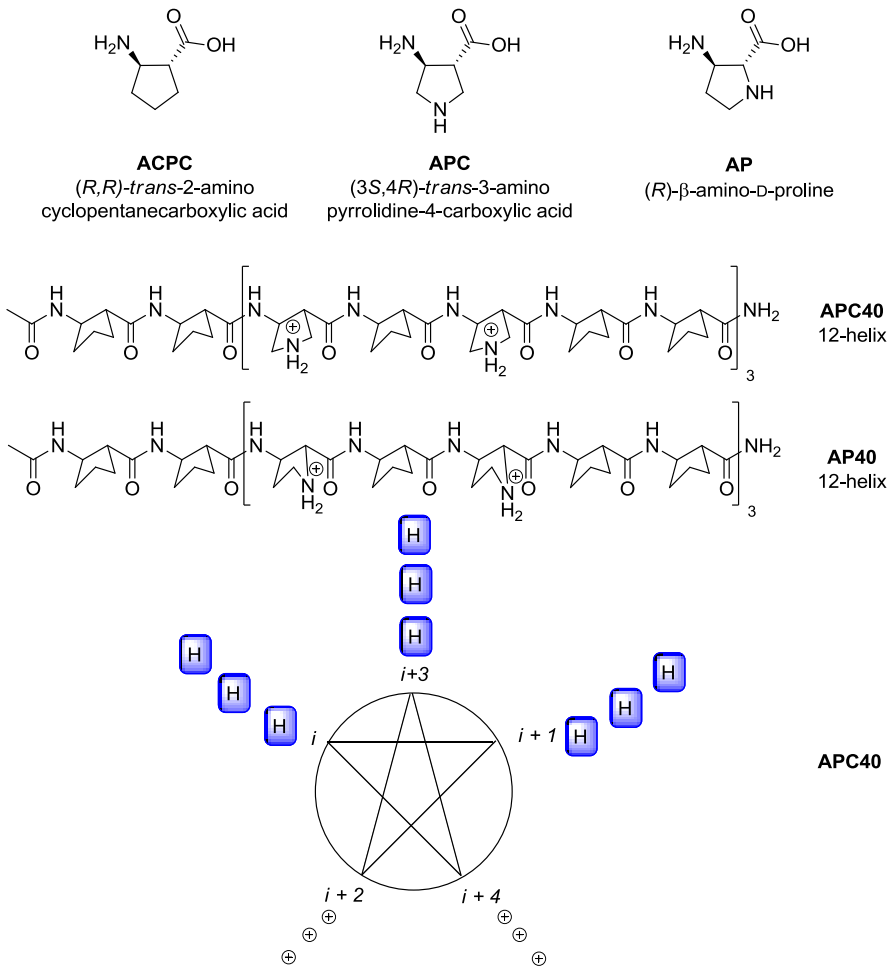

Figure 1.7 i) The monomer units, ACPC, APC and AP used in the construction of antibiotic oligomers; ii) Structures of APC40 and AP40, two of the oligomers synthesised; iii) View down the helix of APC40, showing the projection of cationic residues ("+") and hydrophobic residues (ACPC ring, "H"). Cationic residues are protonated at physiological pH.

Turning to the third criteria, ease of synthesis, the use of β-amino acids is unfortunately limited by their availability; extension of the *C*-terminus *via* the Arndt-Eistert homologation to give β^3 peptides is trivial,[23] but extension of the *N*-terminus for β^2 peptides remains synthetically challenging.

1.2.2 Aromatic Amide Foldamers

Beyond homologated amino acids hydrogen bonding remains one of the most popular methods of imparting conformational preference.[24] The field of aromatic amide foldamers combines the rigidity and planarity of the aromatic rings and the strength of hydrogen bonds

to create polymers with a highly biased conformational preference that is often simple to design and predict.

Early examples include the anthranilamide oligomers of Hamilton and co-workers[25] and the work of DeGrado incorporating an N-H-S hydrogen bond (Figure 1.8).[26]

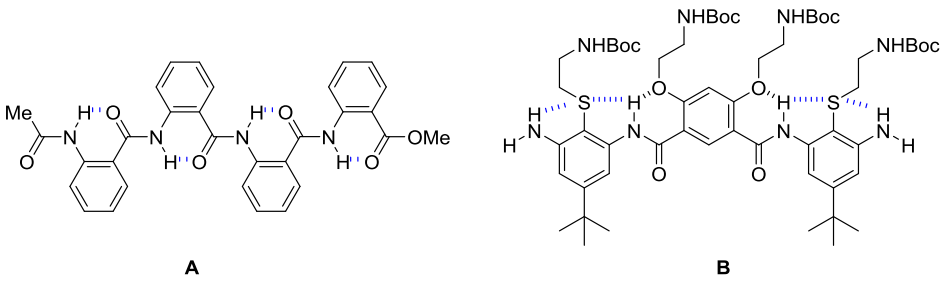

Figure 1.8 **A**: Anthranaliamide of Hamilton *et al.*; **B**: Sulfur hydrogen bonding motif of DeGrado *et al*.

The work grew more directed as researchers aimed to use these strategies in the design of scaffolds for α-helix mimicry. Hamilton and co-workers created the first oligopyridylamides[27] before Ahn and Wilson produced similar designs based around a five-membered hydrogen-bonded ring.[28, 29] Although researched independently they differed only in their *R* and terminal groups (Figure 1.9).

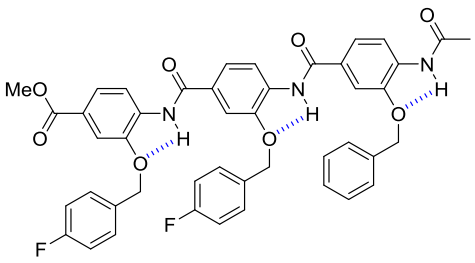

Figure 1.9 Benzamides of Ahn and Wilson.

Hamilton and Kulikov have extended this work by showing such scaffolds to be amenable to the incorporation of a large array of side-chains suitable for SAR studies.[30]

However extension to higher order oligomers proved difficult due to problems of solubility and therefore a new scaffold had to be developed. The benzoylurea oligomer, with a facile

and iterative synthesis, uses six-membered hydrogen bonded rings to impart conformational preorganisation whilst maintaining excellent solubility through the urea moiety. This allowed for the creation of a helix mimetic extended out to 3.7 nm, of similar length to a seven-turn, thirty residue, natural α-helix (Figure 1.10).[31]

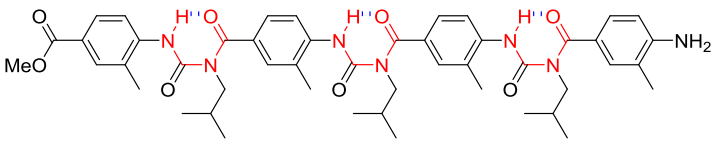

Figure 1.10 Extended benzoyl urea mimic developed by Hamilton *et al*. Intramolecularly hydrogen bonded urea ring that enforces the conformation and adds solubility highlighted in red.

The work of Gong *et al*. shows how the aromatic amide motif can be incorporated into aliphatic chains, and more specifically a peptide strand to induce an extended conformation.[32] The six-membered hydrogen bonded ring allows for the correct display of hydrogen bond donors and acceptors to create hetero- and homodimers (Figure 1.11).[33]

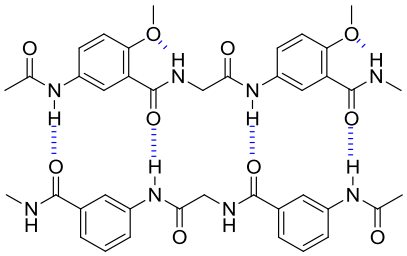

Figure 1.11 Incorporation of an aromatic amide motif into a peptide chain to induce extended conformation.

The work detailed above describes just some of the vast range of structural types developed in the field. This class meets all three of Gellman's criteria; their folding properties are often simple to predict and thus amenable to precise design, the aromatic rings are amenable to extensive functionalisation, and there is a huge library of reagents to facilitate the formation of the amide bonds.

Such is the range of structures formed that they have been successfully applied to a range of different problems; macrocyclisation,[34] molecular recognition,[35,36] chemical biology,[26,37] and catalysis.[38]

1.2.2.1 Biological Application

Aromatic amide foldamers have also been extensively applied to biological problems. DeGrado used his sulfur hydrogen bonding motif to create an amphiphilic molecule, with a cationic and hydrophobic face, to mimic the magainin peptides in the same fashion as Gellman.[39] Hamilton used the α-helix mimetics, both pyridyl and benzoylureas, to target the Bak BH3/Bcl-x_L protein-protein interaction.[27,31] These scaffolds have proven amenable to a high level of diversification with Boger creating a 400 unit library for screening against the HDM2/p53 complex.[40] Huc has designed a quinolone based monomer[41] that adopts a remarkably stable helix conformation and binds G-quadruplex DNA (Figure 1.12).[42]

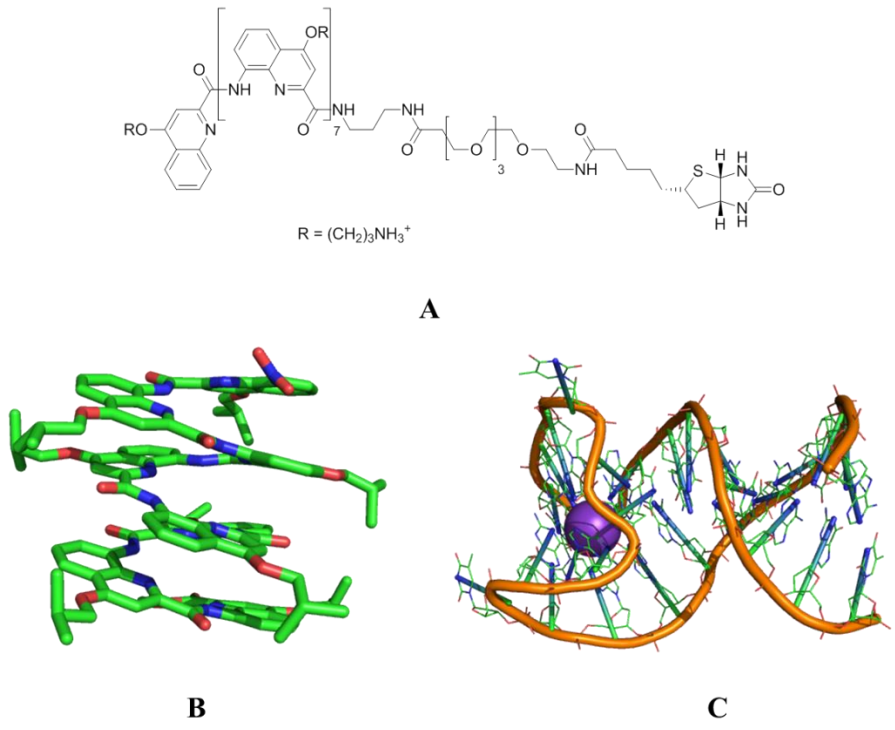

Figure 1.12 **A**: Biotin adducted foldamer targeting G-quadruplex DNA; **B**: Crystal structure of foldamer showing helical conformation (CCDC: 208068); **C**: NMR solution structure of G-quadruplex DNA (PDB: 5CMX).

1.2.2.2 Macrocyclisation and Molecular Recognition

Macrocylic oligomers can be used in molecular recognition as the pre-organisation reduces the entropic penalty that would otherwise be paid for the rigidity that binding imposes. However that entropic penalty has to be paid at some point, most often in the initial synthesis. The use of foldamers allows this to be overcome through the pre-organisation of reactive termini in close proximity.

For example Gong *et al*. prepared a cyclic hexamer from simple aniline and acid chloride precursors (Figure 1.13).[43] Despite having to simultaneously form six amide bonds this one-pot reaction proceeded in high yield (69 – 82%) with the pre-organisation clearly playing a key role in promoting the final cyclisation step.

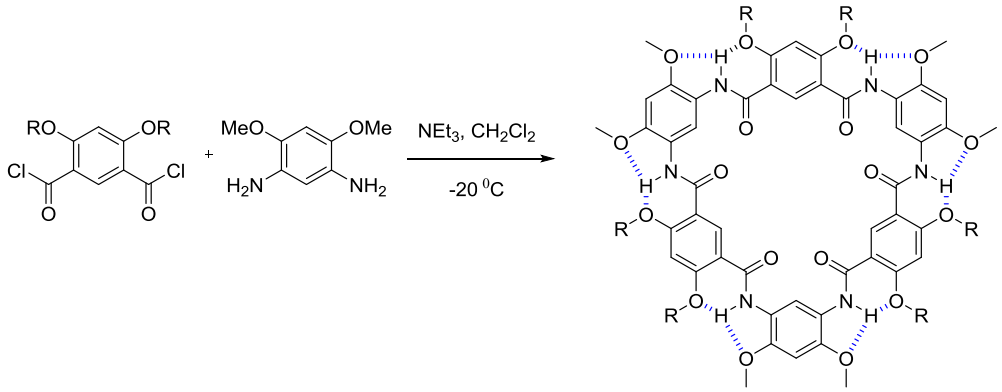

Figure 1.13 Macrocyclisation of two simple monomer units into a cyclic hexamer.

This work has been expanded more recently to create vast polycyclic structures such as the rotaxane and platinum heterocycles of Li *et al*.[44,45]

Aromatic amide foldamers have been used as a host for a huge variety of molecules, including sugars,[46] dioctylammonium,[47] water and formic acid,[48] cations, and anions.[49,50] Some of the most visually arresting work in this space is the use of aromatic amide foldamers as a template for molecular tweezers. Li *et al*. designed bisporphyrin molecules that have complexed a number of different fullerenes (Figure 1.14).[51] The incorporation of fullerenes

containing chiral adducts allowed for the creation of supramolecular chirality, whilst swapping the *tert*-butylphenyl groups for pyridines afforded water solubility.[52]

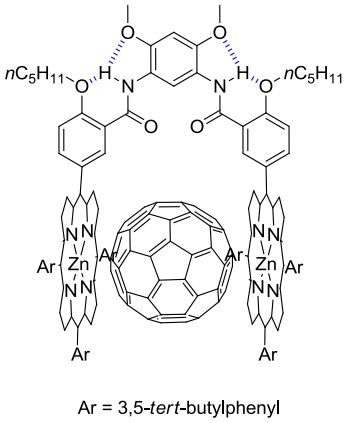

Figure 1.14 Zinc porphyrin tweezers templated by an aromatic amide tip.

1.2.2.3 Catalysis

The Smith group sought to use the hydrogen bonding imparted by an aromatic amide foldamer to improve the efficiency of enantioselective catalysts.[38] It was reasoned that pre-organisation as a result of the non-covalent interactions within the catalyst structure would minimise the entropic cost of transition-state binding and consequently afford greater stabilization of that transition state. The principle was successfully applied to a model Mannich reaction with improved yields and enantioselectivities over a control unable to hydrogen bond (Figure 1.15).

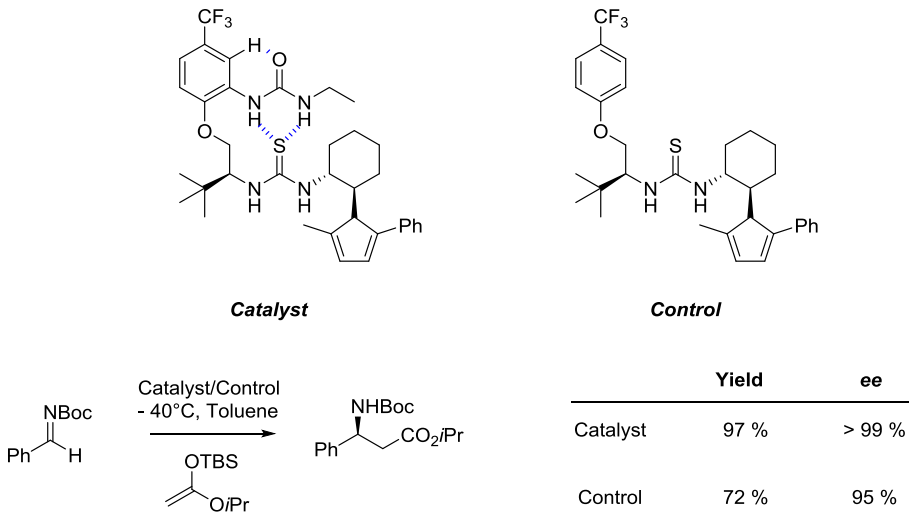

Figure 1.15 Positive cooperativity enhancing catalyst efficiency and enantioselectivity in the Mukaiyama-Mannich reaction.

This shows how synthetic foldamers can copy the function of nature's macromolecules, as the principles that govern the excellent catalytic properties of enzymes are applied to a synthetic foldamer.

1.3 Anion Controlled Foldamers

Extensive research has also been performed on removing the hydrogen bond acceptor to create foldamers whose conformation can be controlled *via* the presence of an anion.[4] These rely on hydrogen bond donors to coordinate the anion and have been used with oligoindoles, pyrroles, and triazoles (Figure 1.16).

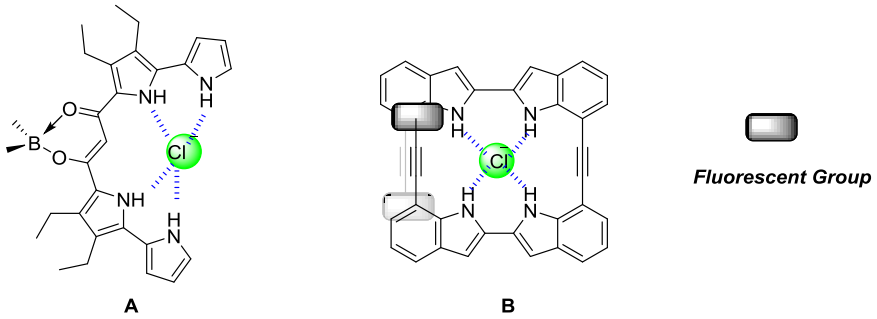

Figure 1.16 **A**: Pyrrole-based oligomer displaying curved conformation in the presence of a chloride anion.[53] **B**: Oligo-indole adopting a helical conformation in the presence of an anion.[54] The alkyne is covalently bonded to a fluorescent group that allows for detection of helical folding *via* fluorescent quenching.

The oligo-indole example highlights another potential application of foldamers; their use as molecular switches. The molecule only folds in the presence of the chloride ion, at which point the two termini are brought into close proximity and fluorescent quenching occurs. The molecule can thus act as a chloride ion sensor.

1.4 Hydrophobic Forces

All of the above examples rely on hydrogen bonding but unfortunately many structures successfully templated by hydrogen bonds structures in non-polar solvents lose conformational preference in the aqueous environment due to solvent competition. The loss of such control would fail the first of Gellman's criteria. However in water the strength of a solvophobic effect is likely to increase.[55] Therefore could this effect be successfully utilised in the design of foldamers?

Initially the hydrophobic effect, although clearly playing a role in protein folding,[56] was thought to be too non-specific and lacking in directionality to be used as a design principle in foldamers.

However Wolynes *et al*. sought to challenge this assertion and design a helix whose formation was driven purely by solvophobic interactions.[5] The researchers computationally tested a series of *meta*-phenylacetylene oligomers, revealing that upon increasing $n > 7$, the ordered helical state displayed a lower free energy than any open state (Figure 1.17).

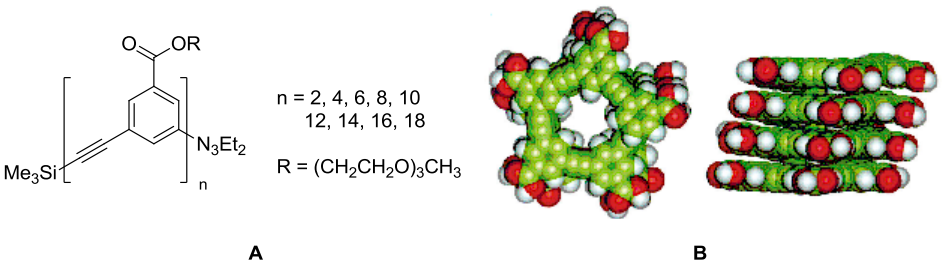

Figure 1.17 A: Phenylacetylene oligomer B: Computational prediction of helix formation for $n > 7$. Reprinted by permission from The American Association for the Advancement of Science, Copyright 1997.

Armed with this knowledge they synthesised a suite of oligomers of varying chain length and examined their conformation *via* the hypochromic effect, UV and NMR spectroscopy. Across all three experiments they observed a solvent dependent indication of helix formation when $n > 8$. In chloroform no helicity was observed, whereas in acetonitrile and mixed acetonitrile/water the transformation did occur, indicative of solvophobically driven folding to create a hydrophobic core.

A recent application of this work from the Flood research group has seen hydrophobic collapse used to bind chloride in aqueous acetonitrile solutions, a difficult task to achieve with water present.[57] The hydrophobic core creates a low dielectric constant microenvironment that strengthens the hydrogen bonds within it, making the crucial difference that allows for extraction of ions from an aqueous solvent. The researchers were able to obtain a beautiful crystal structure of the helical oligomer complexing the chloride anion (Figure 1.18).

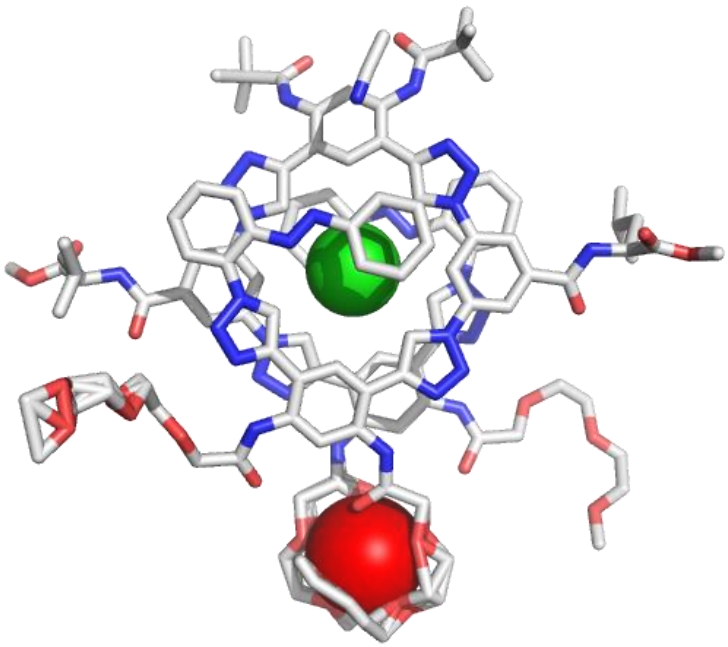

Figure 1.18 Crystal structure showing the binding of chloride (green) and sodium (red) within a helical foldamer. There is some disorder around chain termini and the sodium ion. Hydrogen atoms have been omitted for clarity.

1.5 π-π Interactions

Chemists have used a force much less common in nature to control foldamer conformation, that of π-π interactions. In 2000, Lehn and co-workers used these interactions to stabilise the formation of double helices of 2'-pyridyl-2-pyridinecarboxamide oligomers (Figure 1.19).[58]

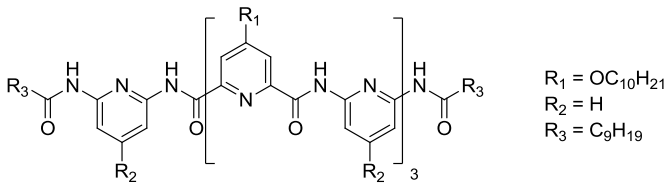

Figure 1.19 2'Pyridyl-2-pyridinecarboxamide oligomer.

Prior to this work formation of double helices from synthetic foldamers was little known, with a few examples utilising base-pair hydrogen bonding, as found in duplex DNA, and through coordination to metal ions in a similar manner to that found in the anion controlled foldamers above. The strands themselves are forced into a helical conformation through intramolecular hydrogen bonding, before the π-π driven inter-strand recognition creates the double helix (Figure 1.20).

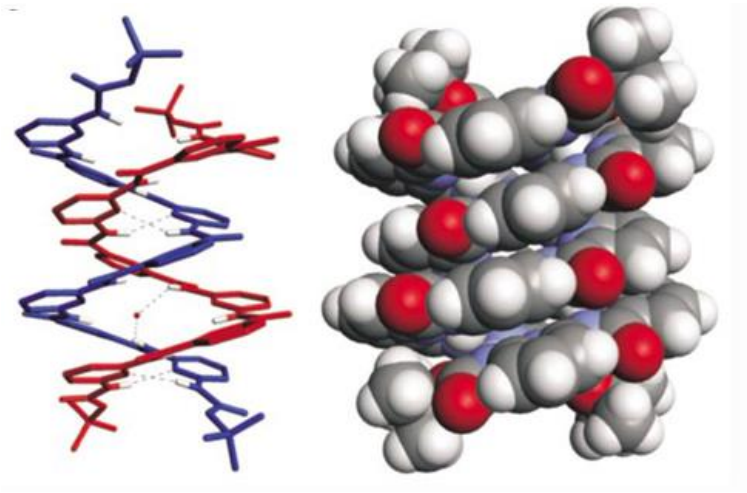

Figure 1.20 Crystal structure of Lehn's π-stacked double helix. Reprinted by permission from Macmillan Publishers Ltd: Nature, **407**, 720-723, Copyright 2000.

More recently Huc *et al.* have demonstrated the use of π-π stacking in the design of multi-stranded sheets (Figure 1.21).[2] Their rationale was to use forces strong enough to ensure conformational preference, but weak enough to prevent aggregation, the bane of many small, synthetic sheets.

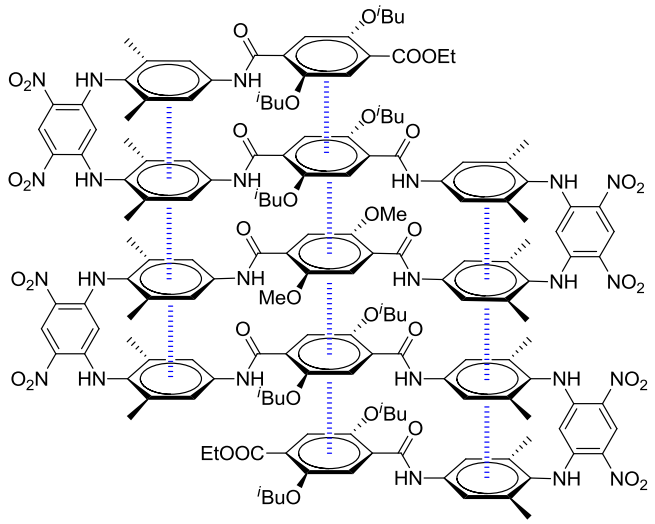

Figure 1.21 An aromatic amide foldamer conformationally organised by π-π interactions.

These compounds were shown to adopt a sheet conformation by both solution state NMR studies in chloroform, and the procurement of beautiful crystal structures (Figure 1.22).

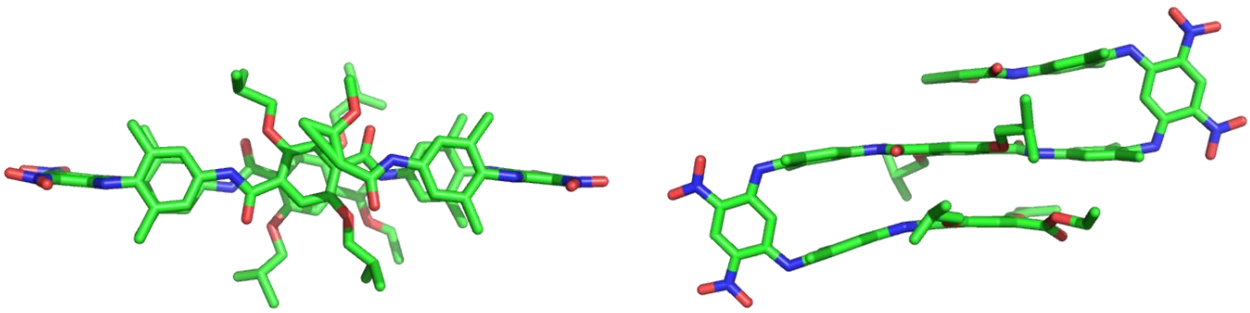

Figure 1.22 Left: Top elevantion of nonamer of Huc's architecture. Right: Side elevation (CCDC: 1425515).

These molecules represent a new and elegant design class, and one which the researchers feel can be extended to 'a variety of patterns' to give 'rise to novel layered aromatic architectures of controlled size and shape.'

1.6 Foldamers and Peptidomimetics

A number of the structures above have been used in biological applications. A key extension of foldamers is into the field of peptidomimetics: using artificial molecules and scaffolds to create mimics of proteins and peptides. This rapidly developing area is particularly important in targeting protein-protein interactions (PPIs).[59]

Thus far most drugs on the market target enzymes and membrane proteins such as G-protein coupled receptors (GPCRs).[60] However, PPIs have been implicated in a vast number of pathologies, including HIV,[61] cancer[62] and amyloid based diseases such as type II diabetes,[9] Parkinson's[63] and Alzheimer's.[64] To be able to design effective inhibitors of these interactions would therefore open up a new range of possibilities in the development of therapies for these indications.

However this challenge is extremely difficult. Whereas enzymes have a small, well-defined, binding pocket, often containing a number of hydrophilic residues, and bind their substrates tightly, PPIs are weak, and quite often transient, interactions across huge surface areas.[65] These areas are often overwhelmingly hydrophobic, making the binding less specific than the interactions seen in enzymes (Figure 1.23).

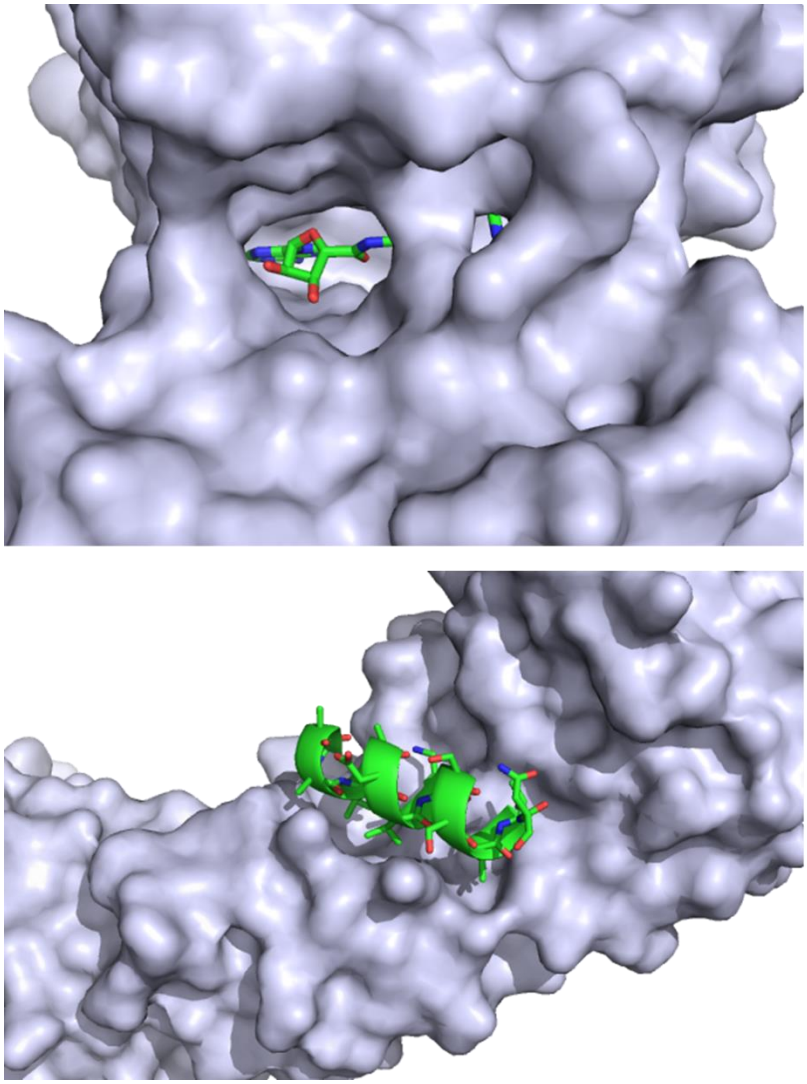

Figure 1.23 **A**: Crystal structure of haspin kinase GSG2 in complex with bi-substrate inhibitor ARC-3372 (PDB: 5HTC). **B**: Crystal structure of β-catenin in complex with T-cell factor showing some hotspots within the large surface area of a protein-protein interaction (PDB: 2GL7).[67]

However despite the seemingly herculean task of targeting such interactions with small, drug-like molecules, there are some glimmers of hope. For some PPIs, such as the HIF-1α/p300[68] and barnase/barnstar[69] interactions, single point mutations can dramatically weaken binding. Similarly, mutagenesis studies have shown that the majority of the binding energy within a PPI is localised to only a few residues, termed 'hotspots'.[70] If enough structural information about the interaction, either solution phase or X-ray crystal structure, can be gathered, then this can facilitate the start of an inhibitor development program.

The structural information shows that these hot spots are often present on well-defined secondary structural elements; α-helices, β-strands and β-sheets.[71,72] All these secondary structures have a defined hydrogen bonding pattern that creates a predictable structure and projects the amino acid side-chains in a consistent spatial arrangement.

Truncated peptides of a parent protein within the PPI can be used in initial binding studies but are unsuitable as drugs. Short sequences often show little preference for the desired binding conformation,[73] and peptides are prone to proteosomal degradation and display poor cell penetration (unless specifically designed cell-penetrating peptides).[74]

This application therefore provides the ideal opportunity for foldamers to be used as peptidomimetics. As shown above, chemists can exert fine control over conformation and utilise non-peptidic scaffolds to overcome metabolic liability and poor pharmacokinetic properties. The creation of a rigid scaffold reduces the entropic penalty paid by the molecule upon binding. Furthermore, with access to the full toolkit of organic chemistry, rather than just the twenty naturally occurring α-amino acids, huge increases in potency, solubility and stability can be achieved.

The strategy is to create surface mimics that prevent the association of two proteins at the interface. Once the hotspots on a secondary structural element have been identified the peptidomimetic aims to mimic those residues responsible for the interaction and thus displace the endogenous binder. This would prevent the downstream effects of the PPI, for example uncontrolled cell growth. The most common secondary structural element found at these interfaces is the α-helix,[72] and a large number of scaffolds, some of which have been explored above (Figures 1.8, 1.9, 1.10) have been specifically developed to mimic this helix. These scaffolds are then used to project side-chains in the same fashion as the existing α-helix. Such scaffolds could aim to inhibit the helix-helix PPI highlighted in red in Figure 1.25.

This strategy has been successfully used by a number of researchers, for example by Hamilton in targeting PPIs such as the p53/HDM2 interaction.[71] Indeed, Navitoclax, a helix PPI inhibitor that was designed as an antagonist of the Bcl family of anti-apoptotic proteins, has reached Phase I clinical trials as a treatment for small-cell lung cancers (Figure 1.24).[76]

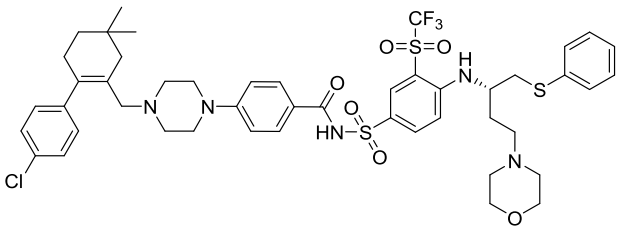

Figure 1.24 Navitoclax, a PPI inhibitor that has reached Phase I clinical trials.

However this thesis will focus on the design of foldamers that fulfil Gellman's criteria and mimic β-structure to target the interactions such as the one highlighted in blue (Figure 1.25). Compared to the number of α-helix scaffolds there remains a paucity of β-strand and sheet mimics,[77] whilst the continuing identification of therapeutically important strand and sheet mediated PPIs creates greater need.

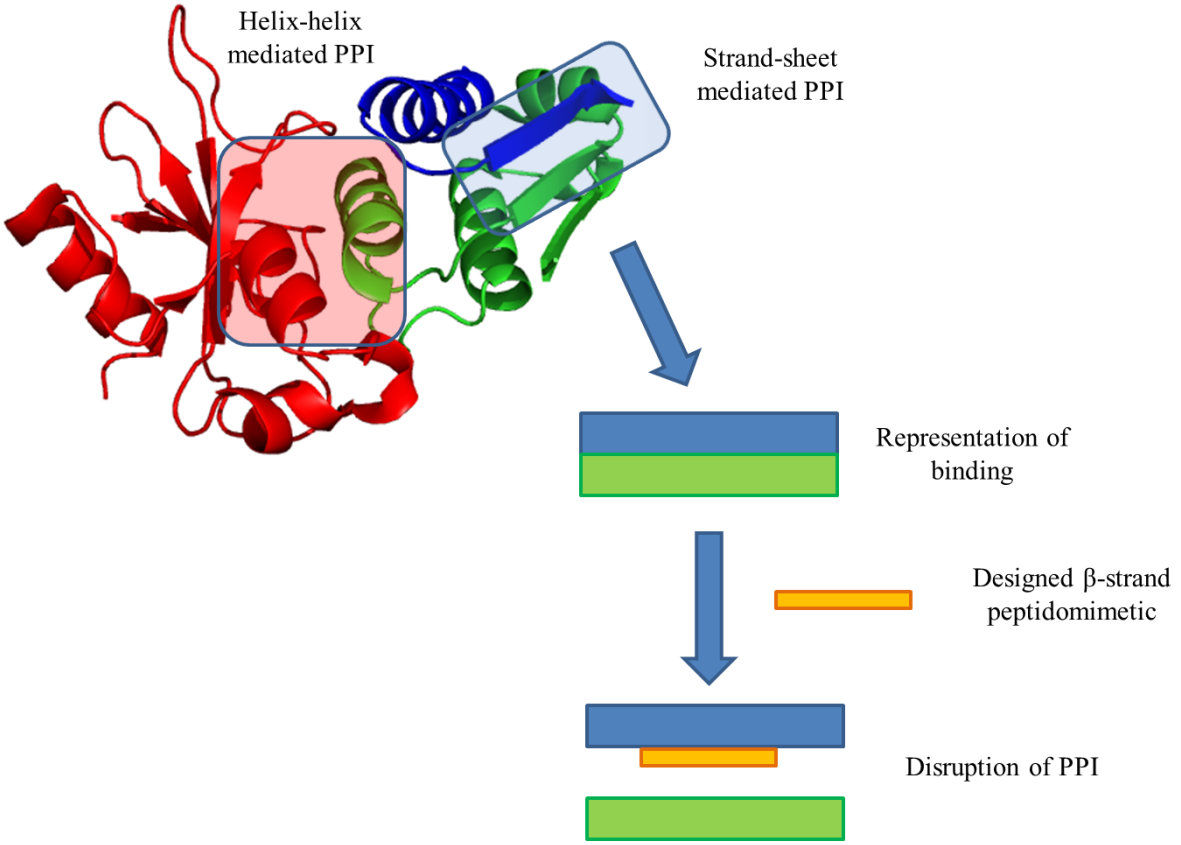

Figure 1.25 Demonstration of the strategy for PPI inhibition and the use of a strand peptidomimetics to effect this strategy (PDB 2ZA4).

1.7 Conclusions

The above examples present an overview of the strategies and applications of foldamers since Gellman first laid down the challenge in 1998. Although much progress has been made, with a huge number of different strategies and templates developed, much remains to be done. This is particularly true for extended conformations and sheet architecture, which are plagued by problems of weak conformational preferences and aggregation.

Therefore this thesis describes efforts to design, synthesise and evaluate new foldamers that mimic the β-strand (Chapter 2) and β-sheet (Chapters 3 & 4) secondary structural elements. Each of these new foldamers will be assessed against Gellman's criteria. Finally in Chapter 5 the foldamers shall be put to a new purpose, assessing the forces involved in protein folding.

1.2 References

1. Gellman, S. H. Foldamers: A Manifesto. *Acc. Chem. Res.* **31,** 173–180 (1998).
2. Sebaoun, L., Maurizot, V., Granier, T., Kauffmann, B. & Huc, I. Aromatic Oligoamide β-Sheet Foldamers. *J. Am. Chem. Soc.* **136,** 2168–2174 (2014).
3. Butterfoss, G. L., Drew, K., Renfrew, P. D., Kirshenbaum, K. & Bonneau, R. Conformational preferences of peptide–peptoid hybrid oligomers. *Pept. Sci.* **102,** 369–378 (2014).
4. Juwarker, H. & Jeong, K.-S. Anion-controlled foldamers. *Chem. Soc. Rev.* **39,** 3664–3674 (2010).
5. Nelson, J. C., Saven, J. G., Moore, J. S. & Wolynes, P. G. Solvophobically Driven Folding of Nonbiological Oligomers. *Science* **277,** 1793–1796 (1997).
6. Holub, J. M. & Kirshenbaum, K. Tricks with clicks: modification of peptidomimetic oligomers via copper-catalyzed azide-alkyne [3 + 2] cycloaddition. *Chem. Soc. Rev.* **39,** 1325–1337 (2010).
7. Fülöp, L. *et al.* A Foldamer-Dendrimer Conjugate Neutralizes Synaptotoxic β-Amyloid Oligomers. *PLoS ONE* **7,** e39485 (2012).
8. Yap, J. L. *et al.* Relaxation of the rigid backbone of an oligoamide-foldamer-based α-helix mimetic: identification of potent Bcl-xL inhibitors. *Org. Biomol. Chem.* **10,** 2928–2933 (2012).
9. Kumar, S. & Miranker, A. D. A foldamer approach to targeting membrane bound helical states of islet amyloid polypeptide. *Chem. Commun.* **49,** 4749–4751 (2013).
10. Lee, E. F. *et al.* High-Resolution Structural Characterization of a Helical α/β-Peptide Foldamer Bound to the Anti-Apoptotic Protein Bcl-xL. *Angew. Chem. Int. Ed.* **48,** 4318–4322 (2009).
11. You, L.-Y., Wang, G.-T., Jiang, X.-K. & Li, Z.-T. Hydrogen bonded aromatic hydrazide foldamers for the self-assembly of vesicles and gels. *Tetrahedron* **65,** 9494–9504 (2009).
12. Prabhakaran, P., Priya, G. & Sanjayan, G. J. Foldamers: They're Not Just for Biomedical Applications Anymore. *Angew. Chem. Int. Ed.* **51,** 4006–4008 (2012).
13. Seebach, D., Hook, D. F. & Glättli, A. Helices and other secondary structures of β- and γ-peptides. *Pept. Sci.* **84,** 23–37 (2006).
14. Aurora, R. & Rosee, G. D. Helix capping. *Protein Sci.* **7,** 21–38 (1998).

15. Seebach, D., Abele, S., Gademann, K. & Jaun, B. Pleated Sheets and Turns of β-Peptides with Proteinogenic Side Chains. *Angew. Chem. Int. Ed.* **38,** 1595–1597 (1999).

16. Seebach, D. *et al.* Preparation and Structure of β-Peptides Consisting of Geminally Disubstituted β2,2- and β3,3-Amino Acids: A Turn Motif for β-Peptides. *Helv. Chim. Acta* **81,** 2218–2243 (1998).

17. Rueping, M., Schreiber, J. V., Lelais, G., Jaun, B. & Seebach, D. Mixed β2/β3-Hexapeptides and β2/β3-Nonapeptides Folding to (P)-Helices with Alternating Twelve- and Ten-Membered Hydrogen-Bonded Rings. *Helv. Chim. Acta* **85,** 2577–2593 (2002).

18. Hanessian, S., Luo, X., Schaum, R. & Michnick, S. Design of Secondary Structures in Unnatural Peptides: Stable Helical γ-Tetra-, Hexa-, and Octapeptides and Consequences of α-Substitution. *J. Am. Chem. Soc.* **120,** 8569–8570 (1998).

19. Abele, S., Seiler, P. & Seebach, D. Synthesis, Crystal Structures, and Modelling of β-Oligopeptides Consisting of 1-(Aminomethyl)cyclopropanecarboxylic Acid: Ribbon-Type Arrangement of Eight-Membered H-Bonded Rings. *Helv. Chim. Acta* **82,** 1559–1571 (1999).

20. Qureshi, M. K. N. & Smith, M. D. Parallel sheet structure in cyclopropane γ-peptides stabilized by C–H···O hydrogen bonds. *Chem. Commun.* 5006–5008 (2006).

21. Kothari, A., Qureshi, M. K. N., Beck, E. M. & Smith, M. D. Bend-ribbon forming γ-peptides. *Chem. Commun.* 2814–2816 (2007).

22. Porter, E. A., Weisblum, B. & Gellman, S. H. Mimicry of Host-Defense Peptides by Unnatural Oligomers: Antimicrobial β-Peptides. *J. Am. Chem. Soc.* **124,** 7324–7330 (2002).

23. Podlech, J. & Seebach, D. The Arndt–Eistert Reaction in Peptide Chemistry: A Facile Access to Homopeptides. *Angew. Chem. Int. Ed. Engl.* **34,** 471–472 (1995).

24. Zhang, D.-W., Zhao, X., Hou, J.-L. & Li, Z.-T. Aromatic Amide Foldamers: Structures, Properties, and Functions. *Chem. Rev.* **112,** 5271–5316 (2012).

25. Hamuro, Y., Geib, S. J. & Hamilton, A. D. Oligoanthranilamides. Non-Peptide Subunits That Show Formation of Specific Secondary Structure. *J. Am. Chem. Soc.* **118,** 7529–7541 (1996).

26. Tew, G. N., Scott, R. W., Klein, M. L. & DeGrado, W. F. De Novo Design of Antimicrobial Polymers, Foldamers, and Small Molecules: From Discovery to Practical Applications. *Acc. Chem. Res.* **43,** 30–39 (2010).

27. Ernst, J. T., Becerril, J., Park, H. S., Yin, H. & Hamilton, A. D. Design and Application of an α-Helix-Mimetic Scaffold Based on an Oligoamide-Foldamer Strategy: Antagonism of the Bak BH3/Bcl-xL Complex. *Angew. Chem. Int. Ed.* **42,** 535–539 (2003).

28. Ahn, J.-M. & Han, S.-Y. Facile synthesis of benzamides to mimic an α-helix. *Tetrahedron Lett.* **48,** 3543–3547 (2007).

29. Plante, J. *et al.* Synthesis of functionalised aromatic oligamide rods. *Org. Biomol. Chem.* **6,** 138–146 (2007).

30. Kulikov, O. V. & Hamilton, A. D. Synthesis of the novel trimeric benzamides—potential inhibitors of protein–protein interactions. *RSC Adv.* **2,** 2454–2461 (2012).

31. Rodriguez, J. M. & Hamilton, A. D. Benzoylurea oligomers: Synthetic foldamers that mimic extended alpha helices. *Angew. Chem.-Int. Ed.* **46,** 8614–8617 (2007).

32. Gong, B. *et al.* A New Approach for the Design of Supramolecular Recognition Units: Hydrogen-Bonded Molecular Duplexes. *J. Am. Chem. Soc.* **121,** 5607–5608 (1999).

33. Zeng, H. *et al.* An extremely stable, self-complementary hydrogen-bonded duplex. *Chem. Commun.* 1556–1557 (2003).

34. Gong, B. Hollow Crescents, Helices, and Macrocycles from Enforced Folding and Folding-Assisted Macrocyclization. *Acc. Chem. Res.* **41,** 1376–1386 (2008).

35. Hou, J.-L. *et al.* Hydrogen Bonded Oligohydrazide Foldamers and Their Recognition for Saccharides. *J. Am. Chem. Soc.* **126,** 12386–12394 (2004).

36. Li, C. *et al.* F···H-N Hydrogen Bonding Driven Foldamers: Efficient Receptors for Dialkylammonium Ions. *Angew. Chem. Int. Ed.* **44,** 5725–5729 (2005).

37. Li, Z.-T., Hou, J.-L. & Li, C. Peptide Mimics by Linear Arylamides: A Structural and Functional Diversity Test. *Acc. Chem. Res.* **41,** 1343–1353 (2008).

38. Jones, C. R., Dan Pantoş, G., Morrison, A. J. & Smith, M. D. Plagiarizing Proteins: Enhancing Efficiency in Asymmetric Hydrogen-Bonding Catalysis through Positive Cooperativity. *Angew. Chem. Int. Ed.* **48,** 7391–7394 (2009).

39. Tew, G. N. *et al.* De novo design of biomimetic antimicrobial polymers. *Proc. Natl. Acad. Sci.* **99,** 5110–5114 (2002).

40. Shaginian, A. *et al.* Design, Synthesis, and Evaluation of an alpha-Helix Mimetic Library Targeting Protein - Protein Interactions. *J. Am. Chem. Soc.* **131,** 5564–5572 (2009).

41. Jiang, H., Léger, J.-M. & Huc, I. Aromatic δ-Peptides. *J. Am. Chem. Soc.* **125,** 3448–3449 (2003).

42. Delaurière, L. *et al.* Deciphering Aromatic Oligoamide Foldamer–DNA Interactions. *Angew. Chem. Int. Ed.* **51,** 473–477 (2012).

43. Yuan, L. *et al.* Highly Efficient, One-Step Macrocyclizations Assisted by the Folding and Preorganization of Precursor Oligomers. *J. Am. Chem. Soc.* **126,** 11120–11121 (2004).

44. Wu, Z.-Q., Jiang, X.-K. & Li, Z.-T. Hydrogen bonding-mediated self-assembly of square and triangular metallocyclophanes. *Tetrahedron Lett.* **46,** 8067–8070 (2005).

45. Xu, X.-N. *et al.* Hydrogen-Bonding-Mediated Dynamic Covalent Synthesis of Macrocycles and Capsules: New Receptors for Aliphatic Ammonium Ions and the Formation of Pseudo[3]rotaxanes. *Chem. Eur. J.* **15,** 5763–5774 (2009).

46. Yi, H.-P. *et al.* Hydrogen bonding-mediated oligobenzamide foldamer receptors that efficiently bind a triol and saccharides in chloroform. *New J. Chem.* **29,** 1213–1218 (2005).

47. Yi, H.-P., Li, C., Hou, J.-L., Jiang, X.-K. & Li, Z.-T. Hydrogen-bonding-induced oligoanthranilamide foldamers. Synthesis, characterization, and complexation for aliphatic ammonium ions. *Tetrahedron* **61,** 7974–7980 (2005).

48. Huc, I., Maurizot, V., Gornitzka, H. & Léger, J.-M. Hydroxy-substituted oligopyridine dicarboxamide helical foldamers. *Chem. Commun.* 578–579 (2002).

49. Kim, Y. H., Calabrese, J. & McEwen, C. CaCl3- or Ca2Cl4 Complexing Cyclic Aromatic Amide. Template Effect on Cyclization. *J. Am. Chem. Soc.* **118,** 1545–1546 (1996).

50. Choi, K. & Hamilton, A. D. Rigid Macrocyclic Triamides as Anion Receptors: Anion-Dependent Binding Stoichiometries and 1H Chemical Shift Changes. *J. Am. Chem. Soc.* **125,** 10241–10249 (2003).

51. Wu, Z.-Q. *et al.* Hydrogen-Bonding-Driven Preorganized Zinc Porphyrin Receptors for Efficient Complexation of C60, C70, and C60 Derivatives. *J. Am. Chem. Soc.* **127,** 17460–17468 (2005).

52. Liu, H., Wu, J., Xu, Y.-X., Jiang, X.-K. & Li, Z.-T. Complexation of hydrogen bonding-driven preorganized di- and hexacationic bisporphyrin receptors for C60 in aqueous and DMSO media. *Tetrahedron Lett.* **48,** 7327–7331 (2007).

53. Maeda, H. & Haketa, Y. Selective iodinated dipyrrolyldiketone BF2 complexes as potential building units for oligomeric systems. *Org. Biomol. Chem.* **6,** 3091–3095 (2008).

54. Kim, U.-I., Suk, J., Naidu, V. R. & Jeong, K.-S. Folding and Anion-Binding Properties of Fluorescent Oligoindole Foldamers. *Chem. Eur. J.* **14,** 11406–11414 (2008).

55. Lehn, J.-M. Perspectives in Supramolecular Chemistry—From Molecular Recognition towards Molecular Information Processing and Self-Organization. *Angew. Chem. Int. Ed. Engl.* **29,** 1304–1319 (1990).

56. Kauzmann, W. in *Advances in Protein Chemistry* (ed. C.B. Anfinsen, M. L. A., Kenneth Bailey and John T. Edsall) **14,** 1–63 (Academic Press, 1959).

57. Hua, Y., Liu, Y., Chen, C.-H. & Flood, A. H. Hydrophobic Collapse of Foldamer Capsules Drives Picomolar-Level Chloride Binding in Aqueous Acetonitrile Solutions. *J. Am. Chem. Soc.* **135,** 14401–14412 (2013).

58. Berl, V., Huc, I., Khoury, R. G., Krische, M. J. & Lehn, J.-M. Interconversion of single and double helices formed from synthetic molecular strands. *Nature* **407,** 720–723 (2000).

59. Morelli, X., Bourgeas, R. & Roche, P. Chemical and structural lessons from recent successes in protein-protein interaction inhibition (2P2I). *Curr. Opin. Chem. Biol.* **15,** 475–481 (2011).

60. Overington, J. P., Al-Lazikani, B. & Hopkins, A. L. How many drug targets are there? *Nat. Rev. Drug Discov.* **5,** 993–996 (2006).

61. Chan, D. C., Chutkowski, C. T. & Kim, P. S. Evidence that a prominent cavity in the coiled coil of HIV type 1 gp41 is an attractive drug target. *Proc. Natl. Acad. Sci.* **95,** 15613–15617 (1998).

62. Ivanov, A. A., Khuri, F. R. & Fu, H. Targeting protein–protein interactions as an anticancer strategy. *Trends Pharmacol. Sci.* **34,** 393–400 (2013).

63. Haass, C. & Selkoe, D. J. Soluble protein oligomers in neurodegeneration: lessons from the Alzheimer's amyloid β-peptide. *Nat. Rev. Mol. Cell Biol.* **8,** 101–112 (2007).

64. Hamley, I. W. The Amyloid Beta Peptide: A Chemist's Perspective. Role in Alzheimer's and Fibrillization. *Chem. Rev.* **112,** 5147–5192 (2012).

65. Ozbabacan, S. E. A., Engin, H. B., Gursoy, A. & Keskin, O. Transient protein–protein interactions. *Protein Eng. Des. Sel.* **24,** 635–648 (2011).

66. Wells, J. A. & McClendon, C. L. Reaching for high-hanging fruit in drug discovery at protein–protein interfaces. *Nature* **450,** 1001–1009 (2007).

67. Sampietro, J. *et al.* Crystal Structure of a β-Catenin/BCL9/Tcf4 Complex. *Mol. Cell* **24,** 293–300 (2006).

68. Appelhoff, R. J. *et al.* Differential function of the prolyl hydroxylases PHD1, PHD2, and PHD3 in the regulation of hypoxia-inducible factor. *J. Biol. Chem.* **279,** 38458–38465 (2004).

69. Urakubo, Y., Ikura, T. & Ito, N. Crystal structural analysis of protein–protein interactions drastically destabilized by a single mutation. *Protein Sci. Publ. Protein Soc.* **17,** 1055–1065 (2008).

70. Cunningham, B. C. & Wells, J. A. High-resolution epitope mapping of hGH-receptor interactions by alanine-scanning mutagenesis. *Science* **244,** 1081–1085 (1989).

71. Ross, N. T., Katt, W. P. & Hamilton, A. D. Synthetic mimetics of protein secondary structure domains. *Philos. Trans. R. Soc. Lond. Math. Phys. Eng. Sci.* **368,** 989–1008 (2010).

72. Bullock, B. N., Jochim, A. L. & Arora, P. S. Assessing Helical Protein Interfaces for Inhibitor Design. *J. Am. Chem. Soc.* **133,** 14220–14223 (2011).

73. Hatakeyama, Y., Sawada, T., Kawano, M. & Fujita, M. Conformational Preferences of Short Peptide Fragments. *Angew. Chem. Int. Ed.* **48,** 8695–8698 (2009).

74. Bechara, C. & Sagan, S. Cell-penetrating peptides: 20 years later, where do we stand? *FEBS Lett.* **587,** 1693–1702 (2013).

75. Yin, H. *et al.* Terphenyl-based helical mimetics that disrupt the p53/HDM2 interaction. *Angew. Chem.-Int. Ed.* **44,** 2704–2707 (2005).

76. Gandhi, L. *et al.* Phase I Study of Navitoclax (ABT-263), a Novel Bcl-2 Family Inhibitor, in Patients With Small-Cell Lung Cancer and Other Solid Tumors. *J. Clin. Oncol.* **29,** 909–916 (2011).

77. Loughlin, W. A., Tyndall, J. D. A., Glenn, M. P., Hill, T. A. & Fairlie, D. P. Update 1 of: Beta-Strand Mimetics. *Chem. Rev.* **110,** PR32–PR69 (2010).

Chapter 2 - β-Strand Mimetics

2.1 β-Strands and their Role in Biology

The β-strand is often described as the simplest of the secondary structural elements. It is the fully extended, linear conformation of a peptide strand, with coplanar amide bonds and side-chains alternating above and below the backbone. β-Strands are most commonly found as the constituent part of a β-sheet and in fact isolated strands within the PDB are rare. It was therefore previously considered, when observed, to be a random part of secondary structure. However, recent studies have shown that the isolated β-strand is a key recognition element for a broad range of biological interactions. These include proteases,[1] major histocompability complexes,[2] and transferases.[3] Interestingly it is also thought that the β-strand plays a key role in recognition between proteins and DNA by binding into the major groove (Figure 2.1).[4]

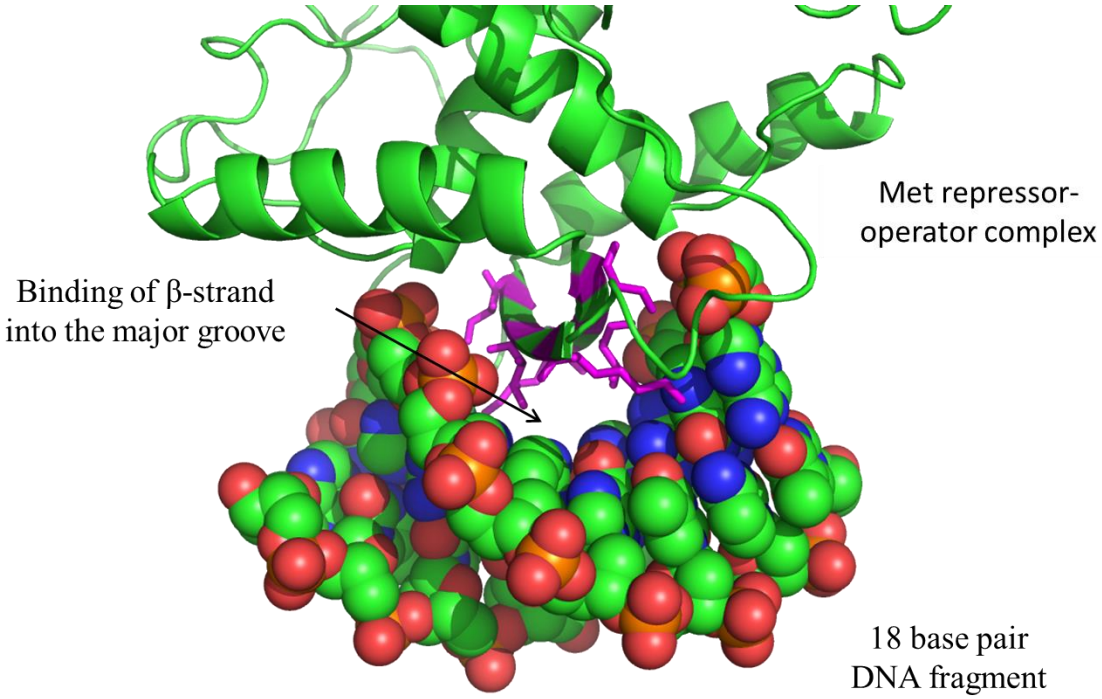

Figure 2.1 Crystal structure of the *met* repressor-operator complex revealing DNA recognition by β-strands (PDB: 1CMA). Side chains responsible for binding shown in magenta.

With such a wide range of biological targets in a number of important therapeutic areas the need for strand mimics is now well recognised.[5]

2.2 Considerations in Mimetic Design

In creating a strand mimic it is highly important to consider the structural elements that make it distinct from the other types of secondary structure. The extended β-strand, such as found in complex with a protease, displays an *i* to *i + 4* distance of 14.5 Å, in contrast to the 13.2 Å observed in a β-sheet.[6] Most important are the number of different recognition surfaces available. The β-strand has maximum exposure of two side-chain faces, and complete availability of main chain carbonyl and amide groups for hydrogen bonding (Figure 2.2).

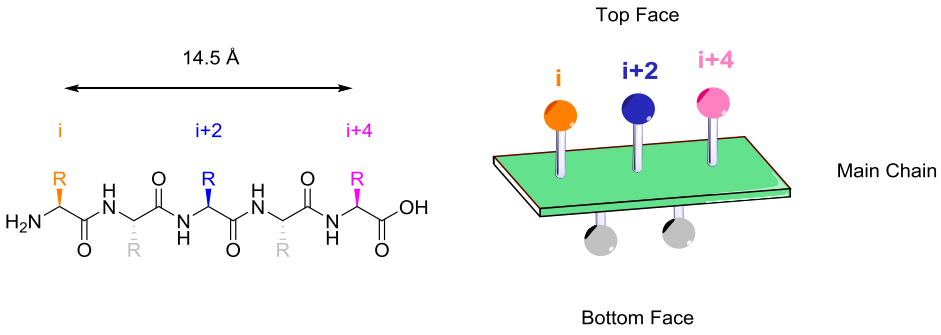

Figure 2.2 Schematic representation of a β-strand displaying the inter-residue distance and recognition domains.

Within the sheet, some of these potential main-chain bonding interactions are removed. Within an α-helix the *i* to *i+4* inter-residue distance is considerably smaller at 6.3 Å and all main-chain hydrogen bonds are already satisfied within the helix motif. The crystal structure of the RAP1A – Raf complex, a key protein-protein interaction within the Ras pathway, heavily implicated in numerous cancers, provides the perfect example of different domains in which a successful β-strand mimic must interact (Figure 2.3).[7]

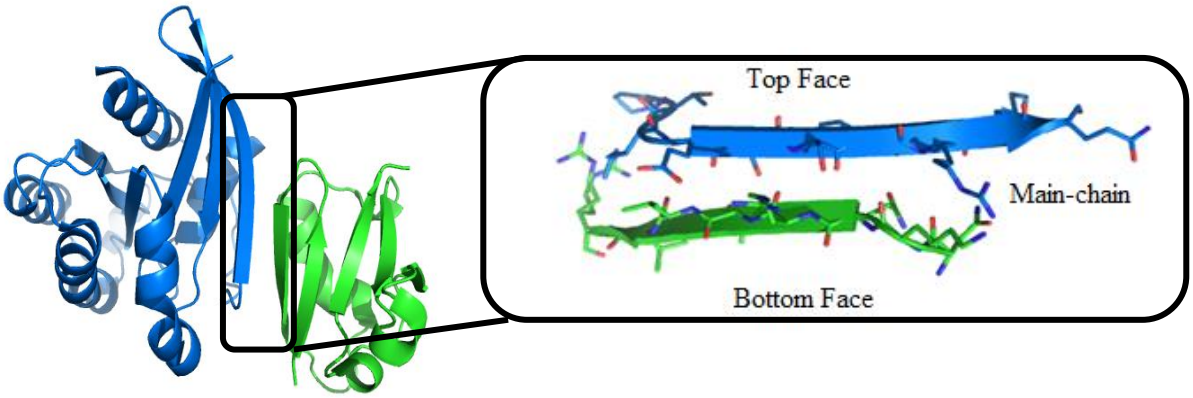

Figure 2.3 Crystal structure of the RAP1A-Raf complex (PDB: 1C1Y). RAP1A (blue) is highly homologous with Ras. Zoomed section shows three domains involved in the interaction; the main chain and the side-chains both above and below the peptide backbone.

2.3 Macrocyclisation of Peptides

Nature has been able to impart conformational constraints on peptides and proteins through macrocyclisation, for example in the formation of disulfide bonds, and chemists are able to do the same. This cyclisation can be achieved through either side-chain to side-chain, or side-chain to main-chain constraints (Figure 2.4).

This side-chain to main-chain approach has been particularly successful in targeting HIV-1 protease, in both *in vitro* and cellular assays. This is best evidenced by the work of Fairlie *et al*. in their synthesis and biological testing of macrocyclic peptides.[8] The macrocyclisation stabilizes the strand conformation required for binding, and delivers extremely potent IC_{50} values in a cellular assay, alongside low toxicity, and crucially, excellent stability towards acidic conditions, degradative proteases, gastric juices and human immune cells. Furthermore crystal structures of these compounds showed both how tightly the peptidomimetic sits in the binding pocket and the goodness of fit with the parent peptide (Figure 2.5).

Side-chain to side-chain linking has been extensively used in peptide stapling, whereby the incorporation of quaternary amino acids bearing terminal olefin side-chains amenable to a metathesis reaction increases the proportion of helical conformation.[9]

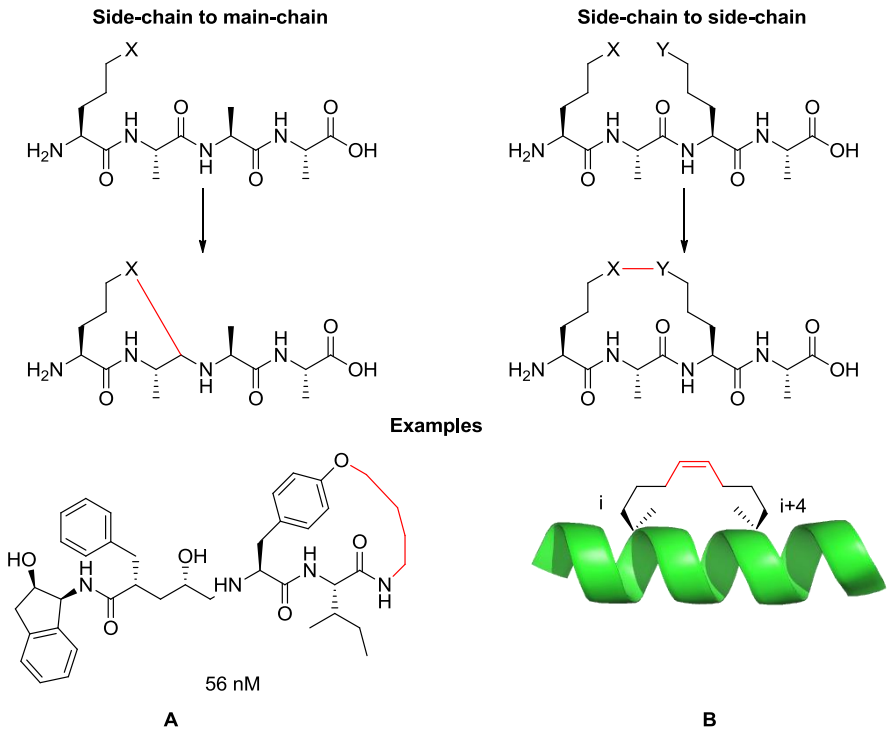

Figure 2.4 Top: Schematic showing the principle of side-chain to main-chain and side-chain to side-chain linking strategies. Examples: **A**: Macrocylic peptides as strand inducers used in the inhibition of HIV-1 protease by Fairlie *et al*.[8] **B**: Helix-stapling technique *via* olefin metathesis, the chemistry pioneered by Grubbs[9] and the biological application by Verdine.[10]

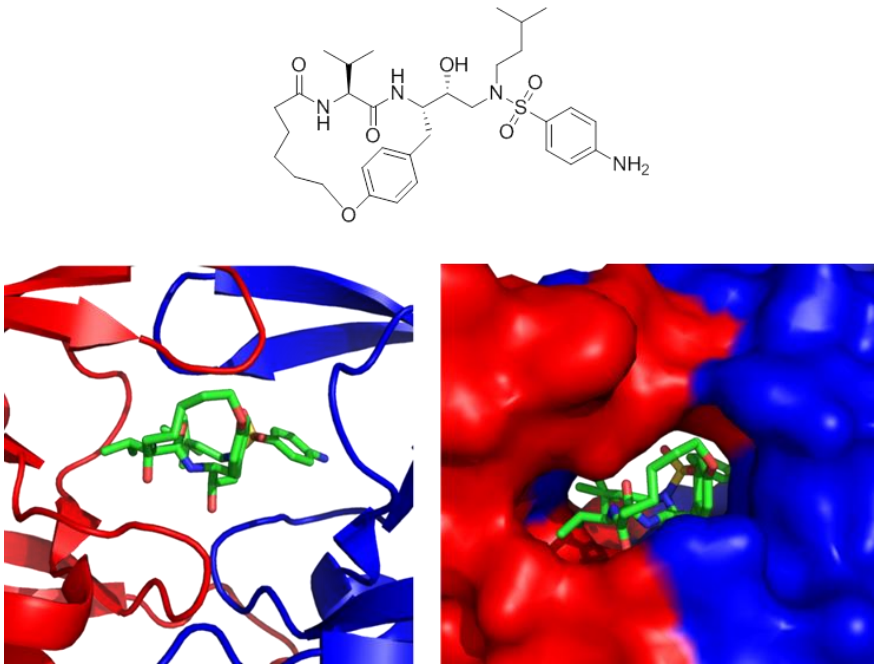

Figure 2.5 Top: Structure of macrocyclic peptide inhibitor Left: Ribbon representation of macrocyclic peptide within the HIV-1 protease binding pocket showing the C_2 symmetric nature of the pocket. Right: Surface representation showing the nature of the tight binding pocket and the ability of the extended peptide to fill the pocket (PDB: 1D4L).

2.4 Use of Rigidifying Rings

In a similar manner to the tactics adopted in aromatic amide foldamers (Chapter 1, Section 1.2.2), the use of rings, both aliphatic and aromatic, can add a rigid template that enforces the required extended confirmation. An excellent example of this comes from the development of inhibitors of Ras farnesylation, a pathway strongly implicated in a huge variety of cancers.[11] Gierasch *et al*. developed a series of tetrapeptides that showed inhibition of the farnesyl transferase in purified protein assays, but were inactive, presumably due to degradation, upon moving to cell-based assays.[12] Fortunately replacement of aliphatic residues with rigidifying aromatic rings created potent inhibitors that were even able to limit tumor growth in mice (Figure 2.6).[3,13]

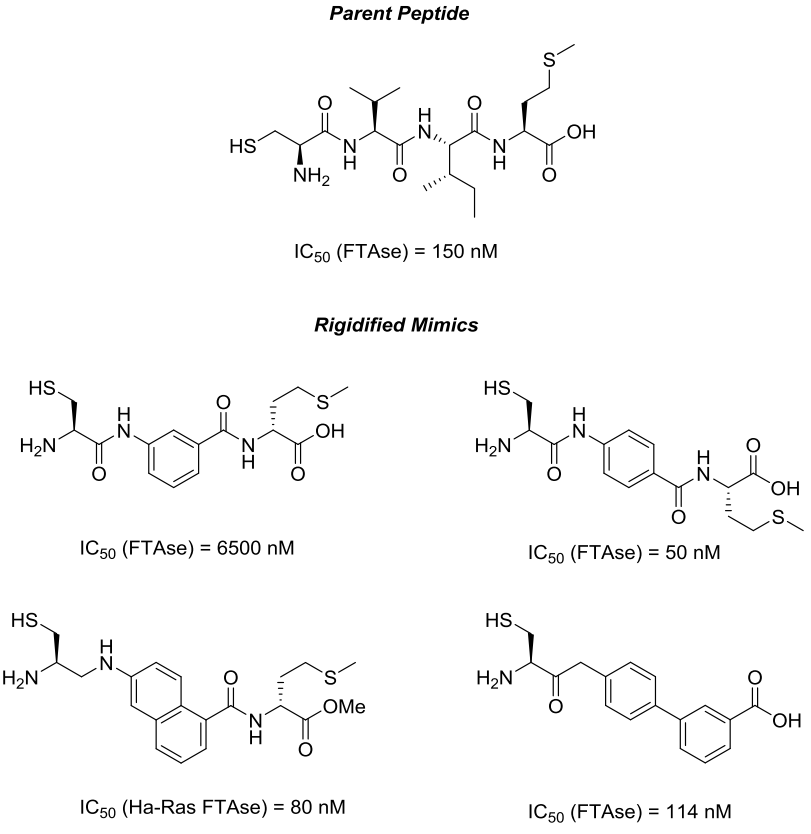

Figure 2.6 Tetrapeptide mimics against farnesyl transferase containing an aromatic rigidifying scaffold.

Nowick has used a similar strategy in the development of his strand mimics. The aromatic linker provides sufficient rigidity so as to allow for exact copying of the hydrogen bonding

capabilities of the main chain peptide (Figure 2.7). This results in the formation in solution of antiparallel β-sheet conformations.[14] In turn Kiso *et al*. were able to show that this scaffold could successfully inhibit HIV-1 protease with an IC_{50} of 30 μM.[15] The ability of Nowick's design to template β-sheets will be explored in greater depth in Chapter 3.

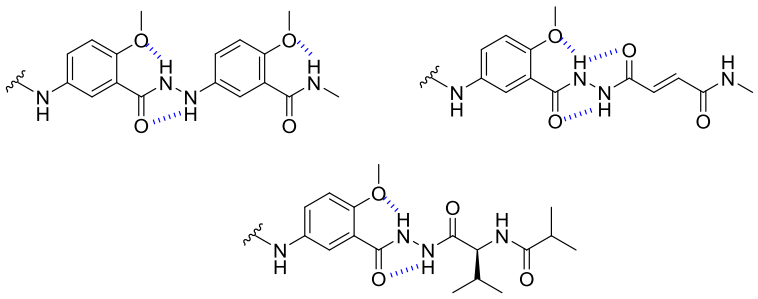

Figure 2.7 Nowick's β-strand scaffolds.

2.5 Heterocyclic Scaffolds

Researchers have also enjoyed considerable success progressing beyond purely carbocylic compounds and utilising heteroatoms to afford greater synthetic feasability. Hammond *et al*. incorporated oxopiperazine as an amino acid substitute (Figure 2.8).[16]

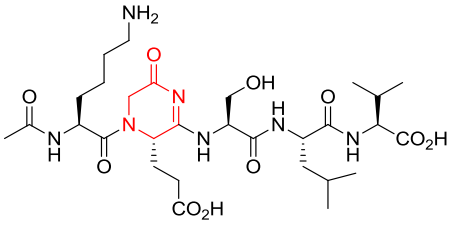

Figure 2.8 Pentapeptide of Hammond incorporating an oxopiperazine amino acid (highlighted in red) as a rigidifying scaffold.

This afforded a facile synthesis with a pentapeptide mimic that showed greater affinity for the inhibition of a PDZ domain than the parent peptide, demonstrating the potential positive effects of providing a rigid scaffold.

However despite the above successes, all the examples remain peptidic in underlying nature. As such, although they are amenable to design and reliably sit in the extended conformation,

the retention of a peptidic backbone leaves them liable to disadvantages such as poor cell penetration.

Hirschmann *et al*. were the first to develop a truly non-peptidic scaffold with their synthesis of a bispyrrolinone mimic as an inhibitor of HIV-1 protease (Figure 2.9).[17,18]

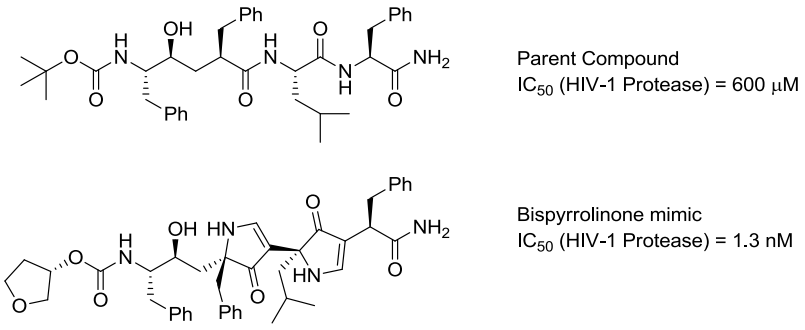

Figure 2.9 Parent peptidic compound developed by Merck[19] and the designed bispyrrolinone mimic of Hirschmann *et al*.[18]

The beauty of this compound was that it maintained the ability to interact in all three domains with successful display of side-chains above and below the plane of the main chain, and the retention of hydrogen bond donors and acceptors despite the removal of the peptide bonds. However, this class fails the third limb of Gellman's test, as the synthesis was non trivial and struggles to incorporate many non-aliphatic amino acids.

2.6 Previous Work in the Hamilton Group

More recently, the Hamilton group has turned its attention to the development of entirely non-peptidic β-strand mimetics. Within this field the focus has been on the design of scaffolds that are able to copy the spatial and angular projection of the amino acid side-chains. Although this approach neglects the domain of the main-chain hydrogen bonding pattern, recent work by Remaut *et al*. have shown that, upon examination of the PDB, there are a considerable number of β-strand interactions that occur solely *via* their side-chains.[20]

The first generation mimic was the alkyne linked 2,2-disubstituted indolin-3-one (Figure 2.10 **A**).[21] The alkyne enforced the correct inter-residue distance whilst the intramolecular hydrogen bond controlled the conformation. This was proved *via* solution state NMR studies and X-ray crystal structures (Figure 2.10 **B**) that showed the inter-residue *i* to *i + 4* distance to be 13.2 Å. However, with the synthesis starting from a tetra-substituted phenyl ring, it was subject to poor yields and a large number of steps.

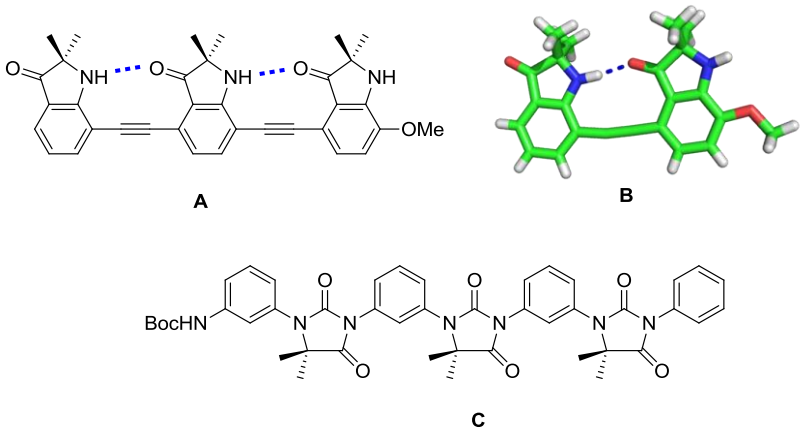

Figure 2.10 **A**: Alkyne-linked 2,2-disubstituted indolin-3-one **B**: Crystal structure showing rigidity of scaffold and projection of side-chains (CCDC: 739198) **C**: 1,3-pehnyl linked hydantoin.

Many of these synthetic problems were eliminated through the design of the 1,3-phenyl linked hydantoin scaffold (Figure 2.10 **C**).[22] Although no crystal structure could be obtained, computational modelling and solution phase studies, including NOESY NMR, was consistent with partial population of desired conformation.

However both these scaffolds included the *gem*-dimethyl group to prevent epimerisation. This necessitates the inclusion in the synthesis of α-α, disubstituted amino acids, creating far greater expense in their synthesis. Additionally the synthesis of high enantio-enriched quaternary centres remains challenging. This problem was overcome in the next generation, through the replacement of the proximal carbonyl with a methylene unit to create the aryl-linked imidazolidin-2-one oligomer (Figure 2.11).[23]

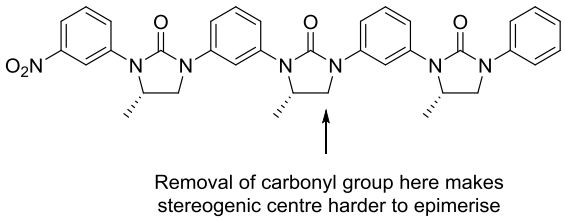

Figure 2.11 Aryl-linked imidazolidin-2-one oligomer.

Computational studies showed that an energy minimised conformation could be overlaid on a natural β-strand with a good fit, and the synthesis proved facile and scalable with chirality introduced through reducing the amino acid to the corresponding alcohol. Crucially racemisation was no longer a problem with enantio- and diastereopurity maintained through the synthesis. However solution phase conformational studies on the final molecule showed it was conformationally flexible. With no constraints on the N_{urea}-C_{aryl} bond it could undergo free rotation and adopt a number of different conformations (Figure 2.12). NOESY NMR showed all these confirmations to be populated to a considerable extent at room temperature.

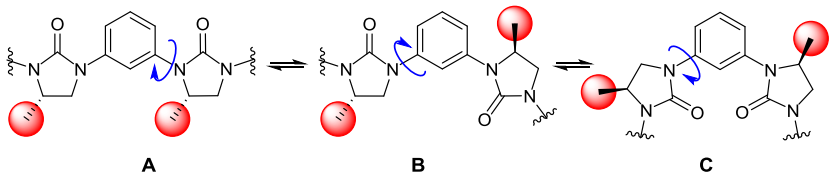

Figure 2.12 Conformational flexibility of the aryl-linked imidazolidin-2-one oligomer.

2.7 Novel Scaffold Design

The earliest mimics showed excellent control of conformation but at the expense of ease of synthesis with the need for α,α-di-substituted amino acids, a small starting pool that also limited inclusion of novel and interesting chemical moieties. By contrast the aryl-imidazolidinone scaffold provided a much simpler synthesis but at the cost of conformational control.

A new scaffold was therefore sought, in which the side-chain spatial distribution of the previous aryl-linked imidazolidin-2-one scaffold was maintained, but with a greater

conformational bias imparted through non-covalent interactions. In order to pass all three elements of Gellman's test the synthesis must remain simple and amenable to alternative side-chains.

Malone *et al*. had shown that the use of dipolar repulsion between a carbonyl group and a pyridine could successfully bias conformation (Figure 2.13).[24]

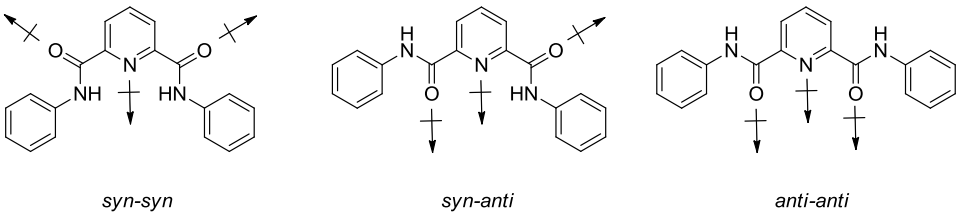

Figure 2.13 Conformations of aromatic amides. Inclusion of pyridine strengthens conformational preference for *syn-syn* due to dipolar repulsion.

By adopting the same strategy it was hoped that the replacement of the phenyl group with a pyridyl ring would bias the desired conformation (Figure 2.14).

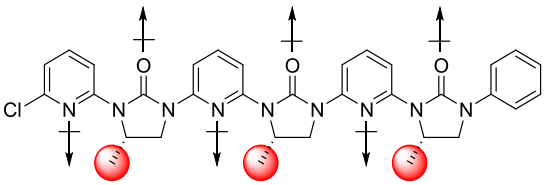

Figure 2.14 Dipolar repulsion imparting conformational bias.

To assess the likely conformational behaviour of this scaffold it was subjected to molecular mechanics computation.[25] A conformational search showed the conformation in Figure 2.15 to be the lowest in energy by 6 kcal.mol^{-1}.[26] At room temperature (298 K) this corresponds to > 99 % of the population sitting in the desired conformation. This compared extremely favourably with the previous scaffold where eighteen conformations lay within 0.7 kcal.mol^{-1} of the computed energy minima.

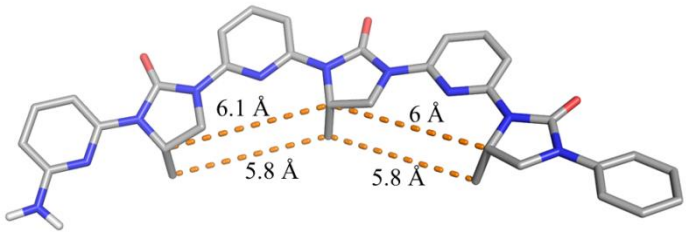

Figure 2.15 Lowest energy conformation from a molecular mechanics computation of the proposed scaffold.

A second calculation provided further evidence of the preferred conformation. By holding all the other bonds fixed, rotating the N_{urea}-C_{aryl} bond in degree increments and calculating the relative energy of each conformation the Boltzmann distribution for model aryl and pyridyl systems could be calculated (Figure 2.16).

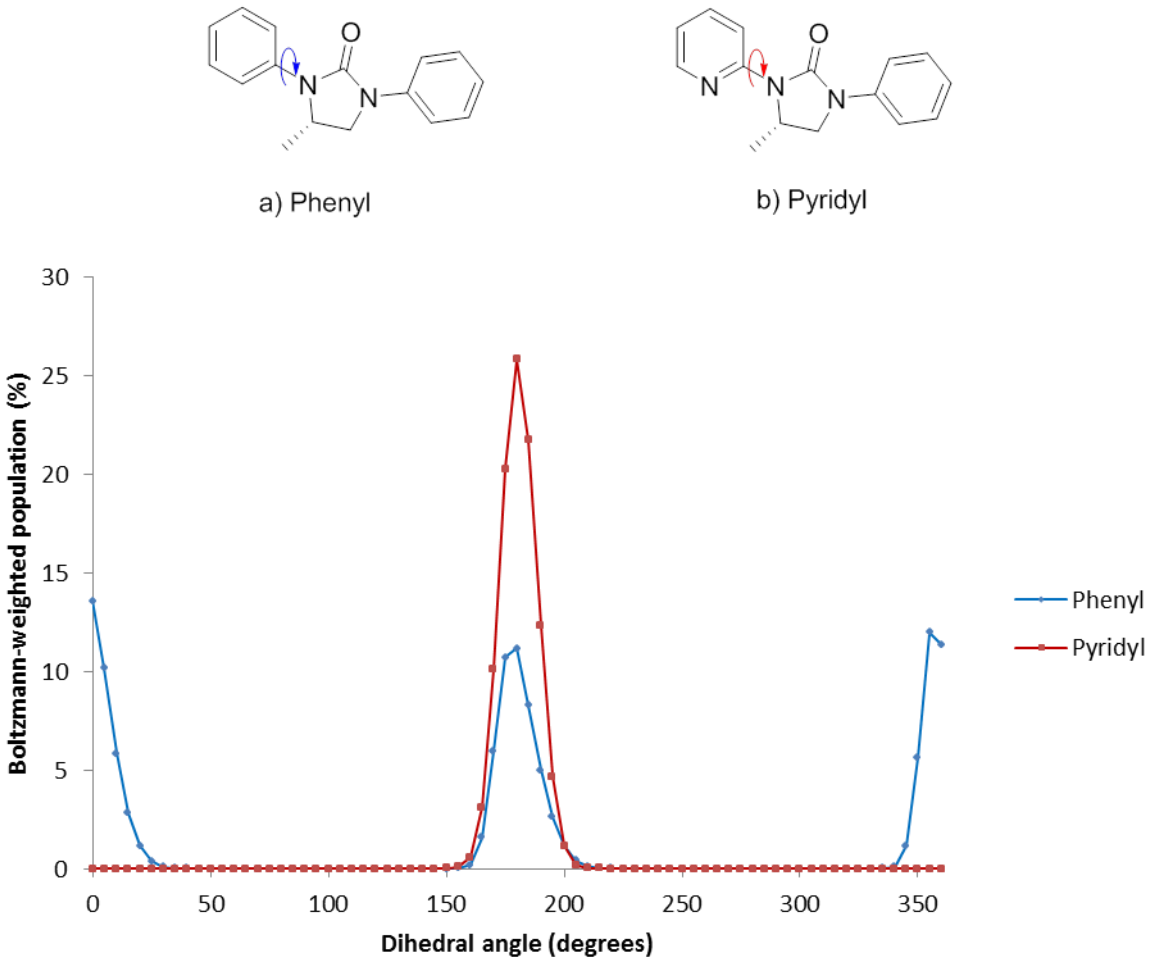

Figure 2.16 Computational calculation of the Boltzmann weighted population at 298 K due to rotation about the N_{urea}-C_{aryl} bond.

In both models there is effectively zero population away from completely planar systems, due to the loss of conjugation on moving away from planarity. However, crucially, whereas the aryl system displays roughly equal population density in each planar regime, the pyridyl system exclusively populates the desired conformation.

2.8 Synthesis

The computational studies gave good confidence in the proposed scaffold extensively populating the desired conformation. Therefore the synthesis of a model compound dimer and trimer, using a methyl group as a side-chain for proof-of-principle, was embarked upon. The initial synthetic plan was to use a similar route to that devised by Hamilton *et al*. in their synthesis of the aryl-linked system.[22]

Alcohol **1** was formed in 82 % yield by the S_NAr reaction of L-alaninol with 2,6-dichloropyridine at high temperature and pressure. The literature suggested that such forcing conditions were required due to the reluctance of the pyridine ring to undergo S_NAr.[27] The free alcohol could subsequently be protected as a silyl ether **2** in near quantitative yield (Scheme 2.1).[28]

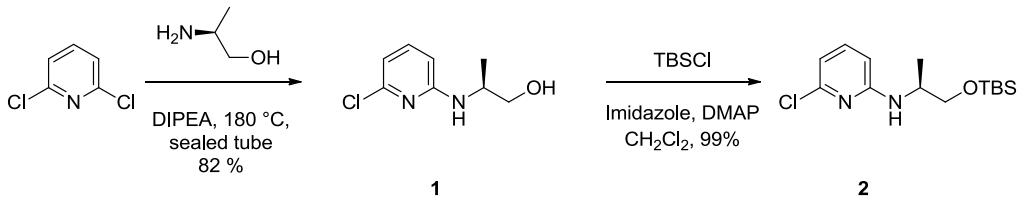

Scheme 2.1 S_NAr and subsequent alcohol protection.

The first stage in the construction of the five membered urea ring was to use the secondary aniline **2** as a nucleophile in an addition reaction with phenyl isocyanate. Extensive optimisation was required due to the reduced nucleophilicity of this amine (Table 2.1).

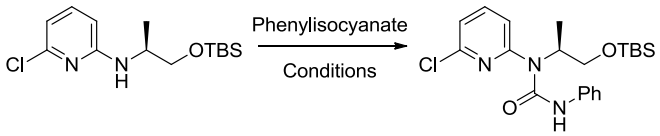

2 **3**

Entry	Scale (mmol)	Solvent	Conditions	Time (h)	Temperature (°C)	Yield (%)
1	0.33	CH_2Cl_2	DMAP (cat.)	5	40	14
2	0.33	CH_2Cl_2	DMAP (cat.)	18	40	38
3	0.33	CH_2Cl_2	DMAP (cat.)	72	40	72
4	0.33	THF	KHMDS (1.3 eq.)	1 + 2	-78 to 20	9
5	0.33	THF	KHMDS (1.3 eq.)	1 + 2	-78 to 20	37
6	0.33	THF	LDA (1.3 eq.)	1 + 2	-78 to 20	-
7	0.33	THF	*n*-BuLi (1.3 eq.)	1 + 2	-78 to 20	68
8	1.00	THF	*n*-BuLi (1.3 eq.)	1 + 2	-78 to 20	68
9	2.00	THF	*n*-BuLi (1.3 eq.)	1 + 2	-78 to 20	56
10	4.00	THF	*n*-BuLi (1.05 eq.)[a]	1 + 2	-78 to 20	58

a) Fewer equivalents of *n*-BuLi used on scale up due to increased confidence in still delivering a slight excess of *n*-BuLi and allowing for complete deprotonation.

Table 2.1 Optimisation of condensation of secondary aniline with phenylisocyanate.

The first three entries detail attempts to perform this reaction with an amine using DMAP as a nucleophilic catalyst. Even with elevated temperatures and after prolonged reaction times the reaction could not be forced towards the urea product, confirming the suspicion around the poor reactivity of the amine. It was therefore decided to attempt to first deprotonate the amine, and subsequently add the phenylisocyanate to the resulting anion. With *n*-BuLi as base this proceeded in a moderate yield and proved amenable to scale up.

The silyl group was removed from alcohol **3** using TBAF in THF, buffered with acetic acid. This reaction was never observed to go to completion, and under prolonged reaction times underwent degradation to an intractable mixture. The literature suggested the reaction could proceed to completion through the use of HF and pyridine, but with an already acceptable yield of 78 % it was considered prudent to avoid these potentially dangerous reagents.[29] An intramolecular Mitsunobu afforded cyclic urea **5** in 79 % yield (Scheme 2.2).

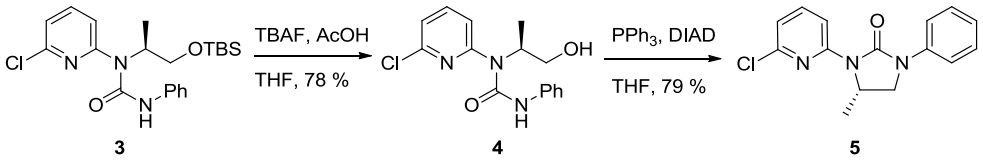

Scheme 2.2 Alcohol deprotection and subsequent ring closure.

To complete the synthesis of the monomer unit, the chlorine substituent had to be converted into an aniline. The amine was successfully introduced as a protected species through the Buchwald-Hartwig coupling of benzylamine in a high yield.[30] Subsequent deprotection by hydrogenation, catalysed by palladium hydroxide on carbon, proceeded well but required extended reaction times of 48 hours and 100 % catalyst loadings, possibly due to catalyst poisoning by pyridine (Scheme 2.3).[31] By way of evidence a similar reaction in the synthesis of the phenyl-linked oligomer required only 0.5 % catalyst loading.[23]

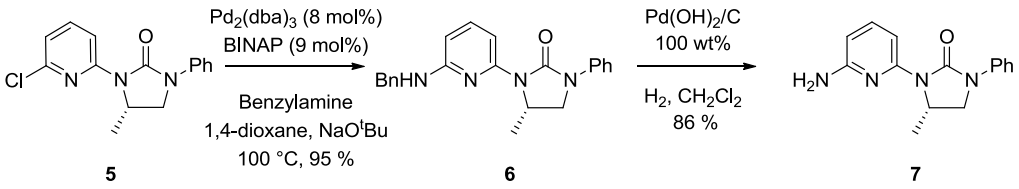

Scheme 2.3 Buchwald-Hartwig coupling with benzylamine and subsequent benzyl deprotection.

At this stage in the previous synthesis the construction of the dimer had proceeded *via* the conversion of aniline **7** into an isocyanate, subsequent coupling with secondary aniline **2** and a second intramolecular Mitsunobu reaction to close the ring (Scheme 2.4).

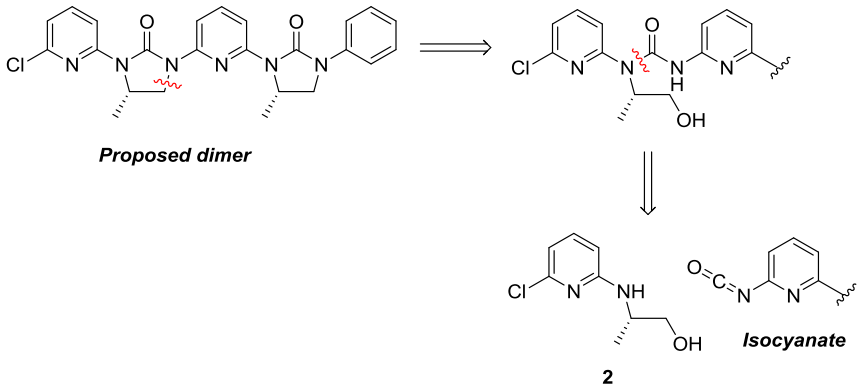

Scheme 2.4 Adaptation of a previously utilised strategy that proved unsuccessful with pyridyl rings.

Unfortunately all attempts to synthesise the proposed isocyanate with triphosgene proved unsuccessful. Reports in the literature indicated similar difficulties in performing this reaction on a substrate of this nature but provided no reasons for the observed lack of reactivity.[32] This necessitated alternative strategies to complete the synthesis. The first was to attempt an intermolecular Mitsunobu reaction and complete the synthesis *via* a ring closing urea formation (Scheme 2.5).

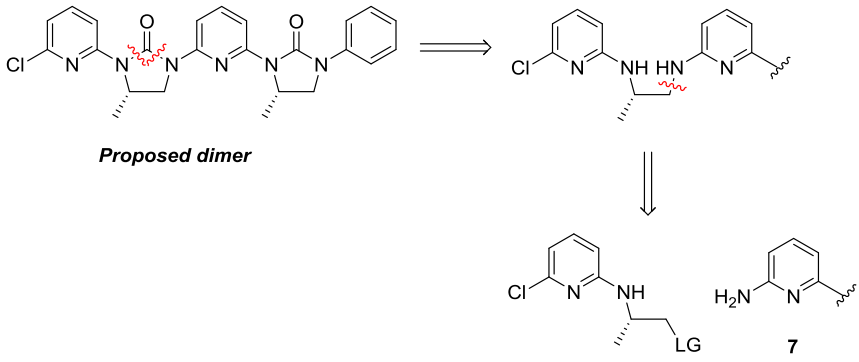

Scheme 2.5 Retrosynthesis of route proceeding *via* an intermolecular Mitsunobu reaction and urea formation to effect the subsequent ring closure.

For this first reaction to be successful secondary aniline **2** had to be protected in order to prevent both cross-reaction and aziridation products. Unfortunately Boc protection of the nitrogen was unsuccessful, as exclusive protection of the alcohol occurred in excellent yield (Scheme 2.6).

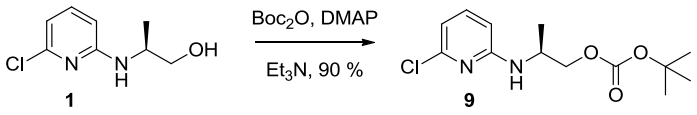

Scheme 2.6 Boc-protection of the primary alcohol instead of the desired secondary aniline.

This necessitated the development of an alternative second route (Scheme 2.7).

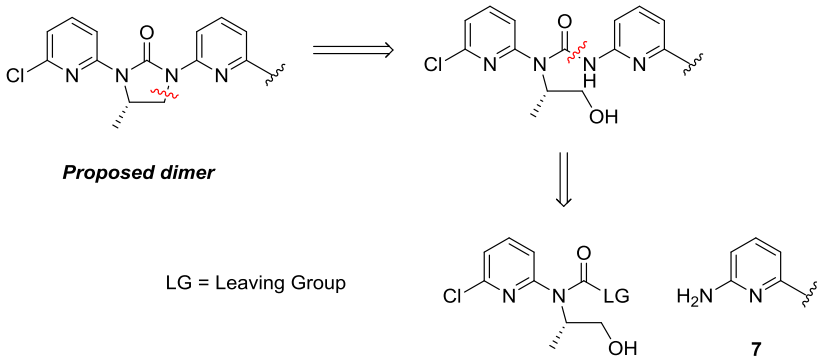

Scheme 2.7 Retrosynthesis of route proceeding *via* a condensation reaction before a Mitsunobu reaction to effect the subsequent ring closure.

The proposed leaving group was a phenolate, to be introduced with phenyl chloroformate. Initial attempts to create the carbamate using DIPEA as a base were unsuccessful, but reverting to the complete deprotonation *via* *n*-BuLi as for the synthesis of **3**, resulted in a successful reaction with a pleasing yield of 84 %. A test reaction with 2-chloro-6-amino pyridine provided hope that this strategy would be successful (Scheme 2.8). Efforts were made to improve the disappointing yield but these were unsuccessful.

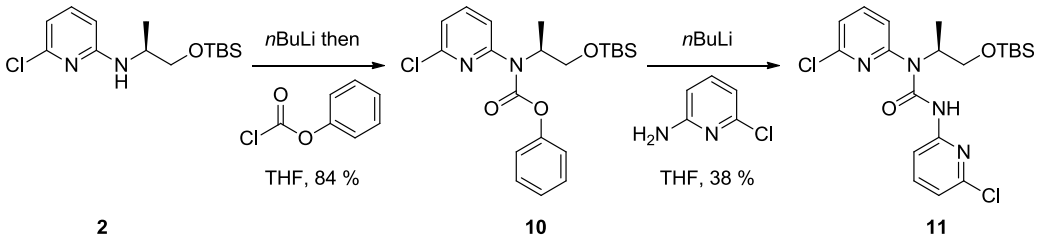

Scheme 2.8 Test reaction for the coupling of a primary analine with the phenyl carbamate.

With the strategy validated, and coupling conditions in hand, the synthesis of dimer **14** could be completed *via* alcohol deprotection and Mitsunobu reactions (Scheme 2.9).

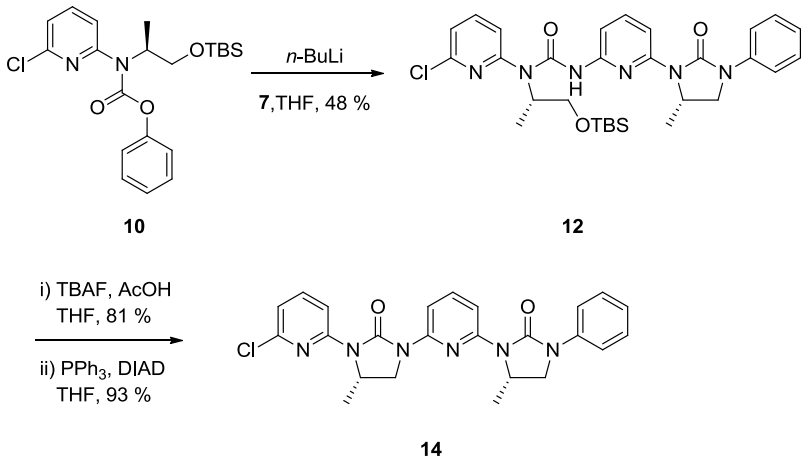

Scheme 2.9 Synthesis of dimer **14** as a mimic of the *i* and *i+2* residues of a canonical β-strand.

With a successful strategy in hand, the synthesis of trimer **19** was straightforward, although yields were generally more modest than those observed in constructing the monomer and dimer. In particular the aniline coupling with the carbamate to synthesise **17** was temperamental with a maximum yield of 17 %. However there was sufficient material to allow for completion of the synthesis (Scheme 2.10).

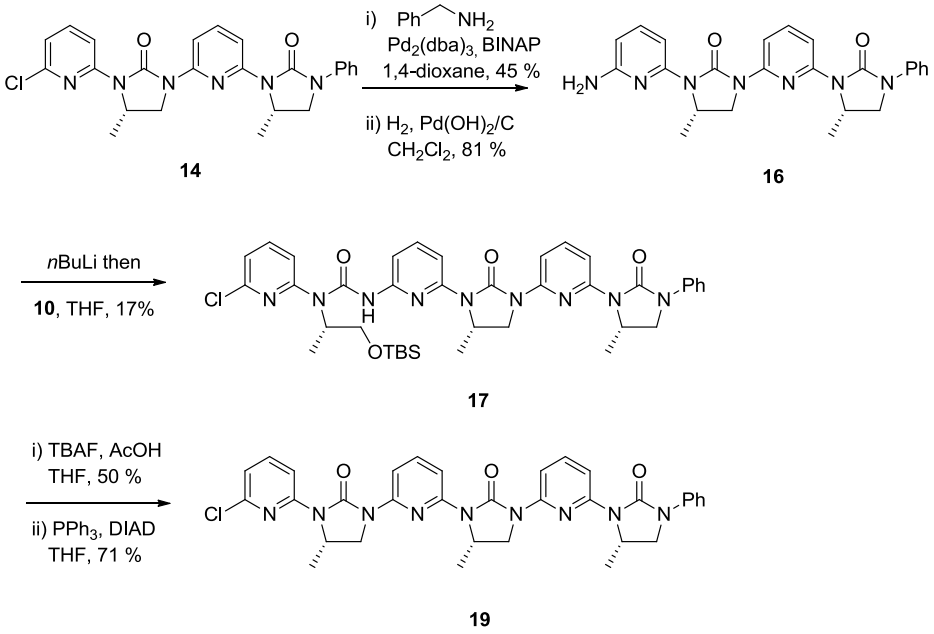

Scheme 2.10 Synthesis of trimer **19** as a mimic of the *i*, *i+2*, and *i+4* residues of a canonical β-strand

2.9 Conformational Analysis

2.9.1 Solution Phase Studies

The solution phase conformation of this new strand mimic could be studied through NOE NMR experiments. In dimer **14** the comparison of the signals between *H*3 and *H*5, and between *H*12 and *H*14 should give an indication of the population of each conformation. Similarly in the trimer **19** the pairings of *H*3 and *H*5, *H*12 and *H*14, *H*21 and *H*23 should give similar information. This is because the signal due to the pairing onto the aryl ring should be strong given free rotation about the N-C(Ar) bond, whereas if the dipolar repulsion achieves the desired effect the other pairings should have a much reduced or zero signal intensity (Figure 2.17). The reason for this is that NOE intensity scales off with distance as $1/r^6$, resulting in 5 Å being around the limit of detection.

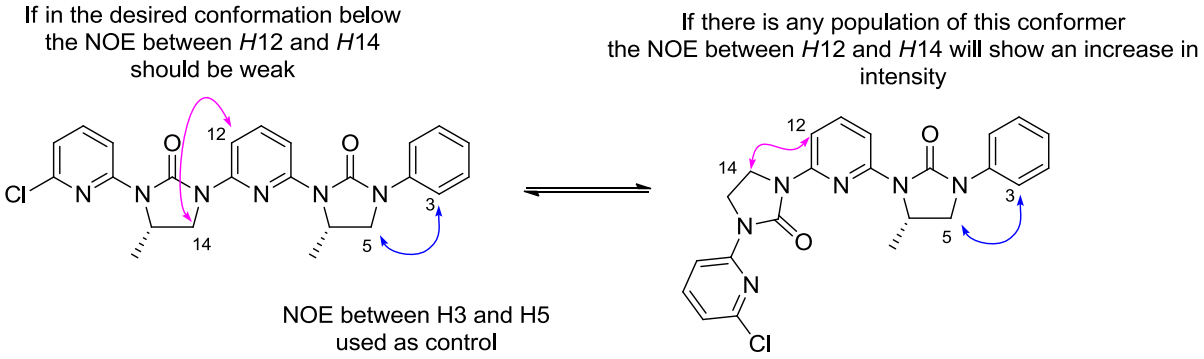

Figure 2.17 Rationale for NOE experiments to study solution phase conformation.

Therefore NOESY (dimer **14**) and ROESY (trimer **19**) spectra were initially taken in deuterated chloroform at room temperature (298 K).

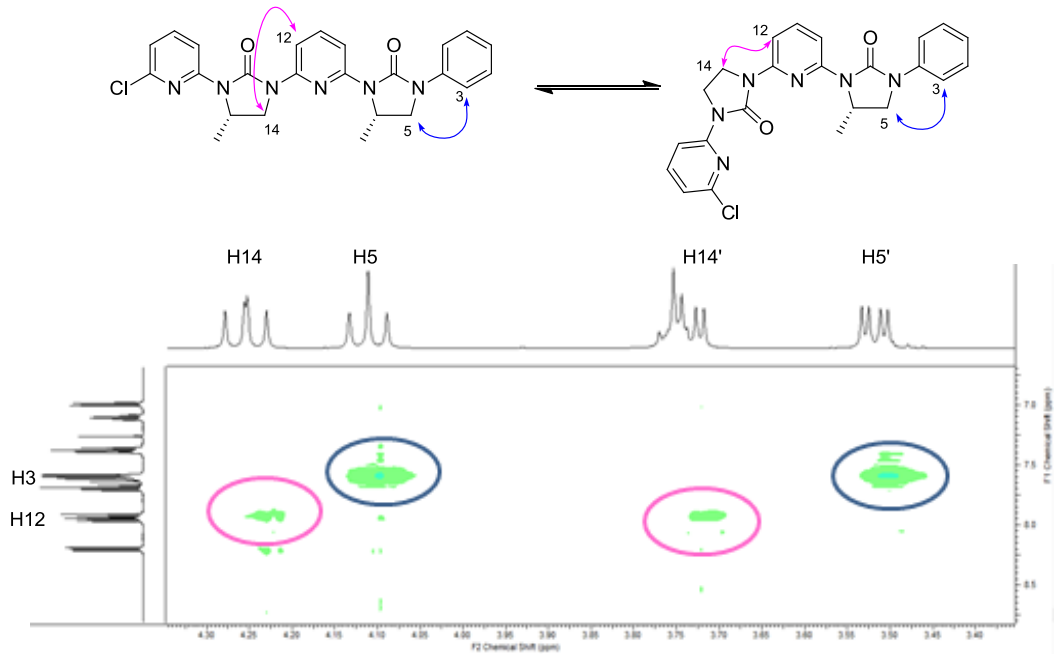

Figure 2.18 NOESY spectrum of dimer **14** in $CDCl_3$. The colour of each circle corresponds to the NOE interaction shown in the molecules above.

As expected a much stronger signal is observed for the *H*3-*H*5 (blue) interaction than the *H*12-*H*14 (purple) one. There are two peaks for each interaction as *H*5 and *H*14 have diastereotopic protons. These three-dimensional peaks can be integrated to give a ratio of 40:1. Given that *H*3 has two protons, this suggests a 20:1 relative intensity between the through-space interactions. Unfortunately given the scaling of NOESY interactions with distance (intensity decreases as $1/r^6$) it is invalid to make firm quantitative conclusions based on this data.

There are two possible explanations for the presence of a weak *H*12 - *H*14 signal. Measurement of *H*12 to *H*14 on the crystal structure (see Section 2.9.2) reveals a distance of 4.5 Å, on the outer-detection limit of nOe interactions and therefore able to contribute a small signal. Alternatively, as posited in Figure 2.17 above the dipolar repulsion may not confer a complete conformational bias and a major and minor conformation are both populated to an extent that can be detected by a time averaged experiment such as NMR.

The ROESY experiment on trimer **19** revealed the same overall picture (Figure 2.19).

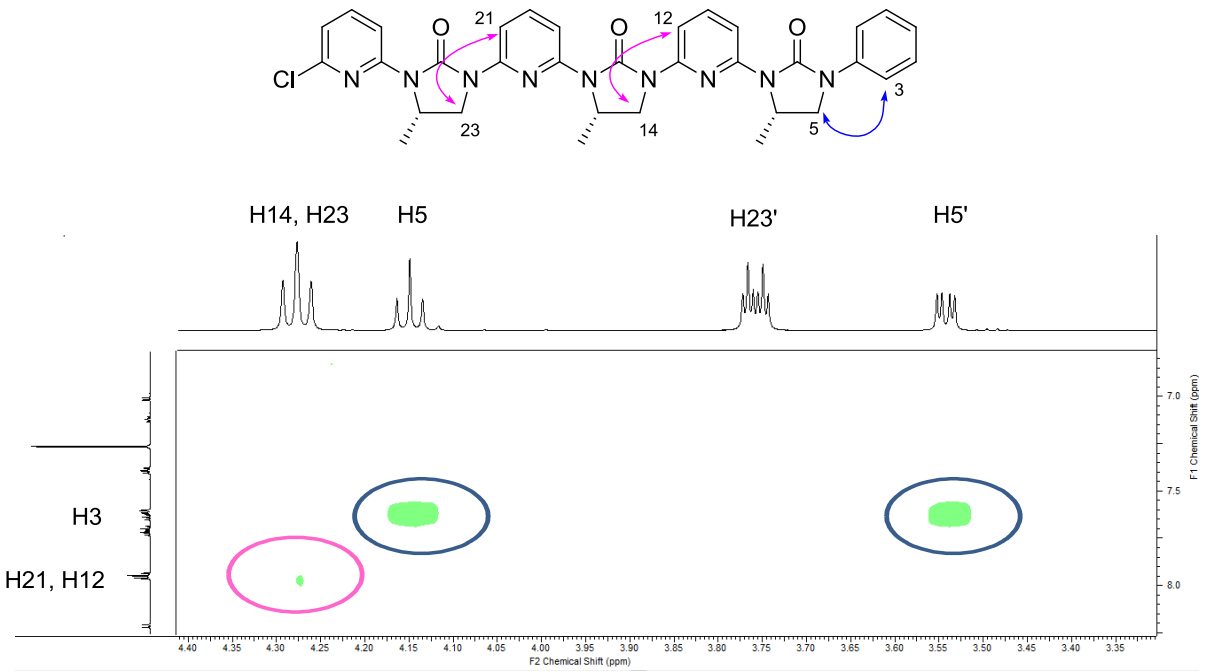

Figure 2.19 ROESY spectrum of trimer **19** in $CDCl_3$. The colour of each circle corresponds to the NOE interaction shown in the molecules above.

The correlation between *H*3 and *H*5 (blue) is much stronger than between *H*12 and *H*14, and, *H*21 and *H*23. With no correlation observed between *H*23' and *H*21, nor *H*14' and *H*21, the evidence suggests a stronger bias towards the preferred conformation in the trimer than the dimer.

In order to probe the relative populations of these compounds two further through-space experiments were conducted. First a high temperature (348 K) NOESY experiment was conducted on dimer **14**. This showed no change to the spectrum recorded at 298 K, providing some, but not conclusive evidence of the less intense peaks from the interaction between *H*12 and *H*14 being due to the distance between the protons, rather than population of the minor conformation. This is because the signal would be expected to increase at higher temperature were it due to the presence of a minor conformer. This is because for any equilibrium a change in the temperature alters the Boltzmann distribution such that the higher energy state grows in population.

A second experiment was to examine the trimer **19** in a more challenging solvent system, where the bias imparted by the dipolar repulsion might be expected to have a lesser effect. This is because in a solvent with a higher dipole a molecule with a large macrodipole can be stabilised. Therefore ROESY spectra of timer **19** were recorded in DMSO-d_6 at room temperature and 350 K. Pleasingly in both cases the only peaks observed were those due to the interaction between *H*3 and *H*5 (Figure 2.20).

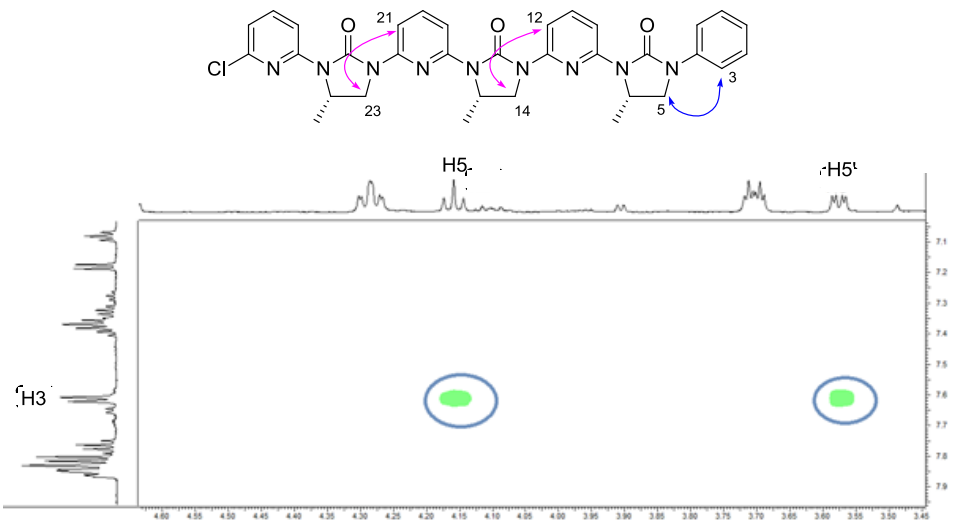

Figure 2.20 ROESY spectrum of trimer **19** in DMSO-d_6. The colour of each circle corresponds to the NOE interaction shown in the molecules above.

2.9.2 Solid Phase Studies

The single crystal X-ray structures of both dimer **14** and trimer **19** were obtained, **14** *via* vapour diffusion of petroleum ether into diethyl ether, and **19** *via* vapour diffusion of petroleum ether into ethyl acetate. Both structures support the initial hypothesis of dipolar repulsion enabling conformational bias, further supporting the solution state analysis.

For dimer **14** two different structures were present in the asymmetric unit, with the methyl groups representing the amino acid side-chain projected on the same face of the molecule. The measured distance between the α-carbon atoms in both structures is 5.8 Å, comparable to the 6.6 Å found within a canonical β-strand. The distance between the β-carbons varied

between 5.2 and 6.0 Å, indicating a degree of conformational flexibility. Within the scope of the conformational bias imparted, this degree of flexibility is not disheartening, as it would allow the mimetic to bind to a protein in an 'induced fit' model and thus adapt to a given target (Figure 2.21).[33]

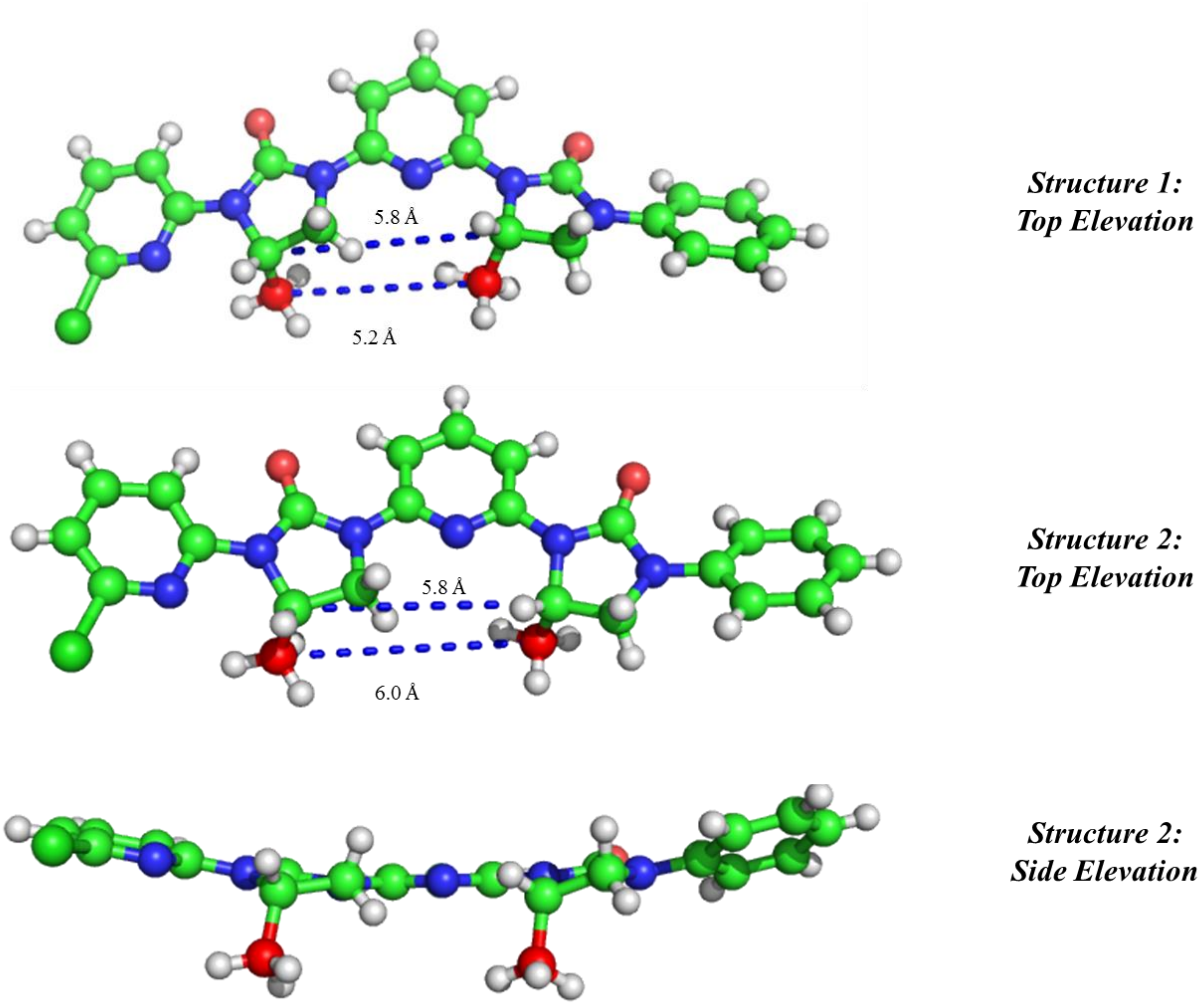

Figure 2.21 Single crystal X-ray structure of dimer **14** mimicking two alanine residues in the *i* and *i+2* positions (CCDC: 1030068).

With a view towards using these strand mimetics as inhibitors of PPIs the crystal structure of **14** was overlaid on the structure of the Raf protein (previously noted at Figure 2.3). The methyl groups were matched to corresponding atoms of an arginine and asparagine side-chains projecting from the same face of the Raf β-strand. With a four-point calculated RMSD, based on an overlay of the α and β positions, of 0.67 Å, there is strong evidence that

the new scaffold is able to display side-chains at the same distance and angular projection as a natural, and indeed therapeutically relevant, protein (Figure 2.22).

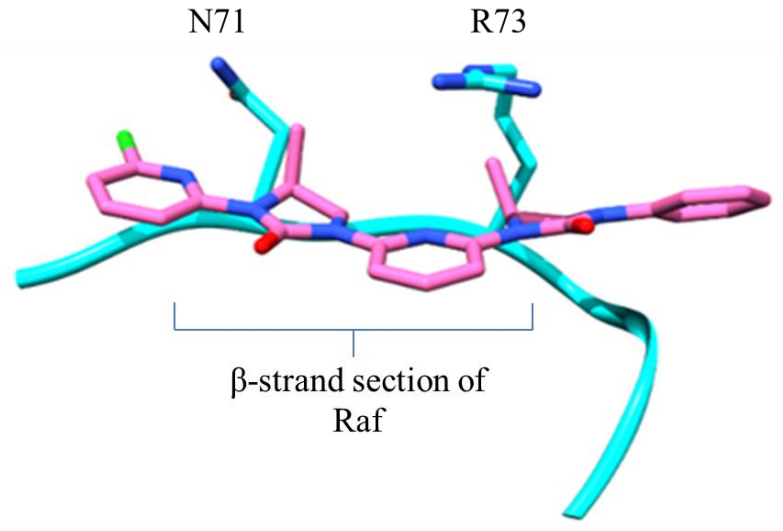

Figure 2.22 Overlay of the single crystal X-ray structure of dimer 14 (pink) and Raf protein (cyan). Mimic side-chains aligned with the α and β positions of N71 and R73 (PDB: 1RRB).[34]

The data from the crystal structure of trimer **19** was of a lower resolution but still provided sufficient information to extract distances and angular projections. Again the molecule adopted the desired conformation with all the methyl groups were projected from the same face. The interatomic distances showed good correlation with those observed in a natural β-strand. However, upon extension to the trimer, an extensive curvature to the molecule in the plane of the scaffold backbone was revealed (Figure 2.23).

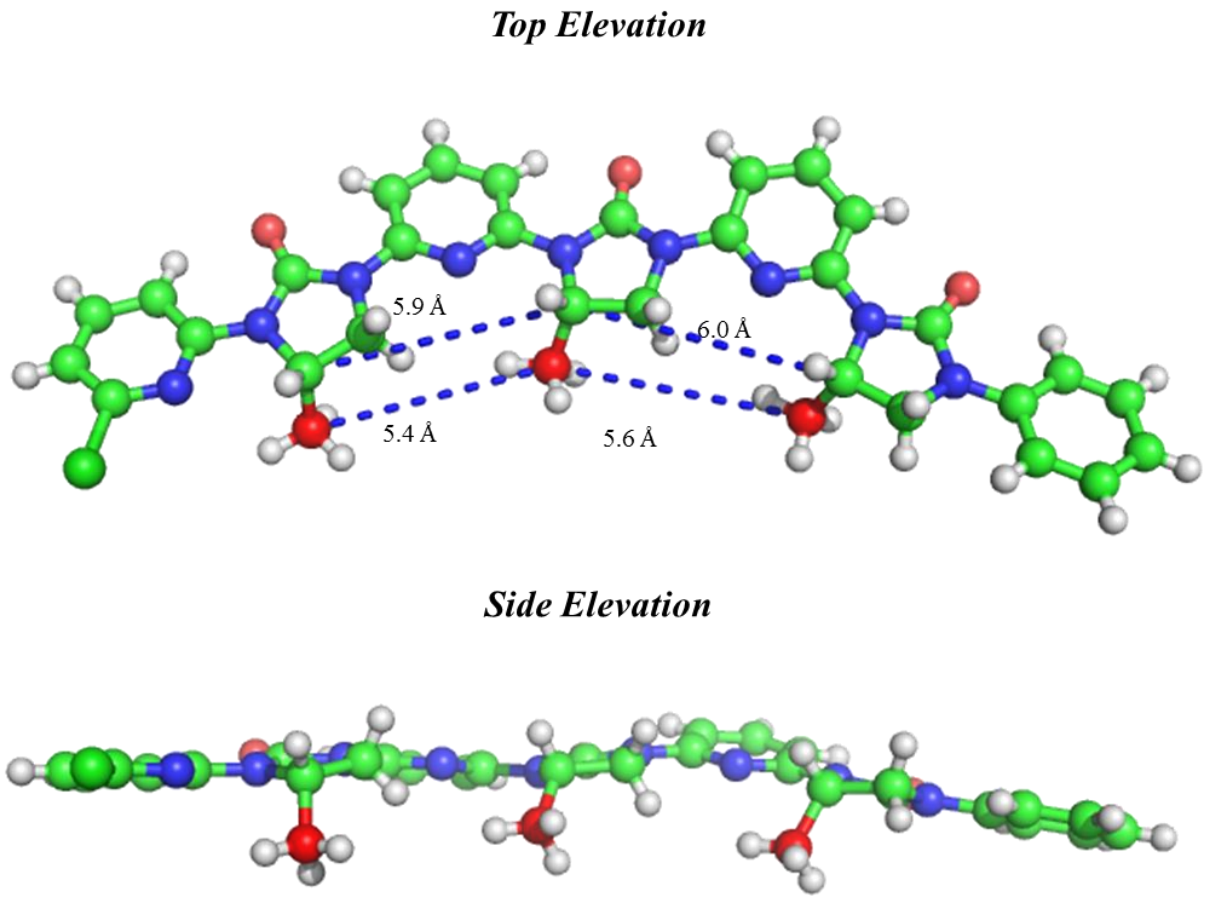

Figure 2.23 Single crystal X-ray structure of trimer **19** mimicking three alanine residues in the *i*, *i+2*, and *i+4* positions (CCDC 1030069).

2.10 Conclusions

These novel foldamers can now be assessed against Gellman's criteria; in the incorporation of the pyridyl moiety there is a new polymeric backbone that shows conformational bias due to dipolar repulsion. This has been provided by robust evidence from computational, solution and solid phase studies. Additionally for dimer **14** the side-chain display compares favourably with the geometries of natural and therapeutically relevant β-strands.

The synthesis requires no enantioselective steps, nor particularly expensive or toxic reagents or catalysts and uses only simple purification procedures. However it is iterative with each ring constructed on the growing chain and the later steps in particular prone to low yields. In

the incorporation of different side-chains, or unnatural functional groups these yields may decrease further.

The next part of this chapter will seek to extend this system with hydrophilic side-chains and incorporate them through a new and modular synthesis.

2.11 Incorporation of Hydrophilic Residues

The above work provides a proof of principle, demonstrating the ability of this scaffold to control conformation in the desired manner. However, to show suitability for biological applications it is essential to incorporate hydrophilic residues. This would allow for water solubility and to test the conformational bias in aqueous media.

2.11.1 Synthesis

An alternative strategy has been developed towards a modular synthesis (Scheme 2.11).

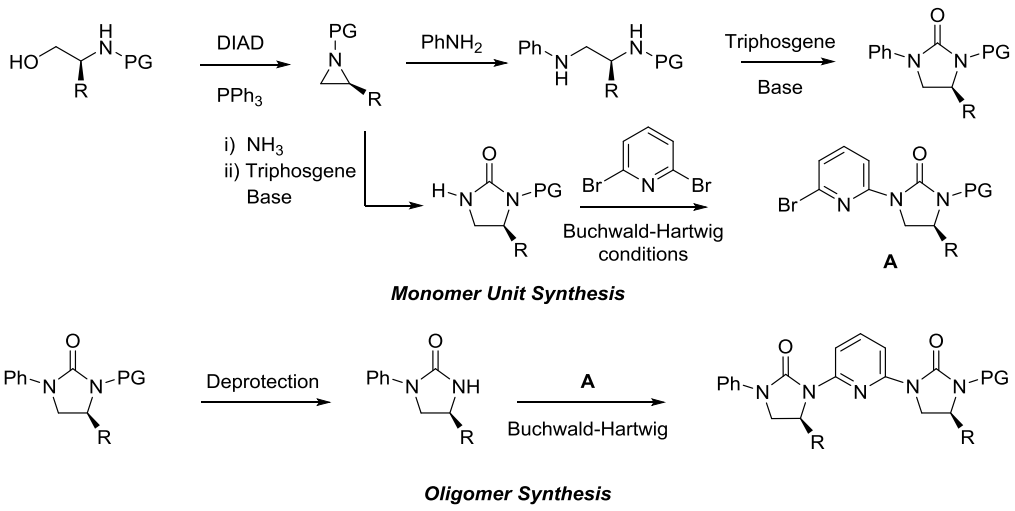

Scheme 2.11 Modular synthetic strategy amenable to incorporation of hydrophilic side-chains.

This modular synthesis has been successfully applied using a phenylalaninol as the starting material to enable the rapid construction of pentamers and hexamers with a benzyl group as the side-chain.

2.11.1.1 Amino Acid Reduction

The amino alcohol of lysine is not commercially available and therefore various conditions were explored to effect the reduction of the free acid (Table 2.2).

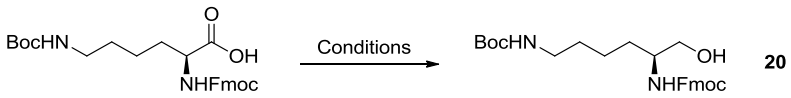

Entry	Reducing Agent	Solvent	Time (h)	Yield (%)	Comments
1	$NaBH_4$, I_2	THF	2	20	Fmoc deprotection
2	$NaBH_4$, I_2	THF	16	33	Fmoc deprotection
3	$NaBH_4$, I_2	THF	120	19	Fmoc deprotection
4	$NaBH_4$, H_2SO_4	THF/Et_2O	16	-	No reaction
5	$NaBH_4$, I_2, AcOH	THF	72	-	No reaction
6	$LiAlH_4$	THF	1	-	Intractable gel
7	$LiAlH_4$	Et_2O	1	-	Poor solubility
8	Ethyl chloroformate, NMM then $NaBH_4$, H_2O	DME	0.1	92	-

Table 2.2 Optimisation of acid reduction in the presence of the Fmoc group.

Direct reduction of the acid with sodium borohydride and iodine to proceed *via* the borane, or with lithium aluminium hydride, was unsuccessful with poor yields and extensive Fmoc deprotection. Fortunately, using ethyl chloroformate to create the mixed anhydride and subsequent reduction with sodium borohydride was extremely successful and amenable to scale up.

2.11.1.2 Protecting Group Selection

At this point the remainder of the synthesis necessitated a protecting group swap from Fmoc due to incompatibility in later steps, to tosyl or nosyl. The synthetic route for each protecting group was investigated simultaneously to ascertain the optimal synthetic strategy. Standard Fmoc removal conditions use piperidine in dichloromethane in a 1:3 ratio,[35] but removal of

piperidine *in vacuo* proved difficult, as in the subsequent nosyl or tosyl protection residual piperidine was frequently protected instead of the target compound. 1 M Dimethylamine in ethanol also facilitated deprotection, and was easier to remove under vacuum, therefore allowing for both tosyl and nosyl protection of the free amine (Scheme 2.12). The subsequent Mitsunobu reaction to form aziridines **23** and **24** proved temperamental in tetrahydrofuran, predominantly showing no reaction and recovery of starting material, but highly reliable in acetonitrile with good yields.

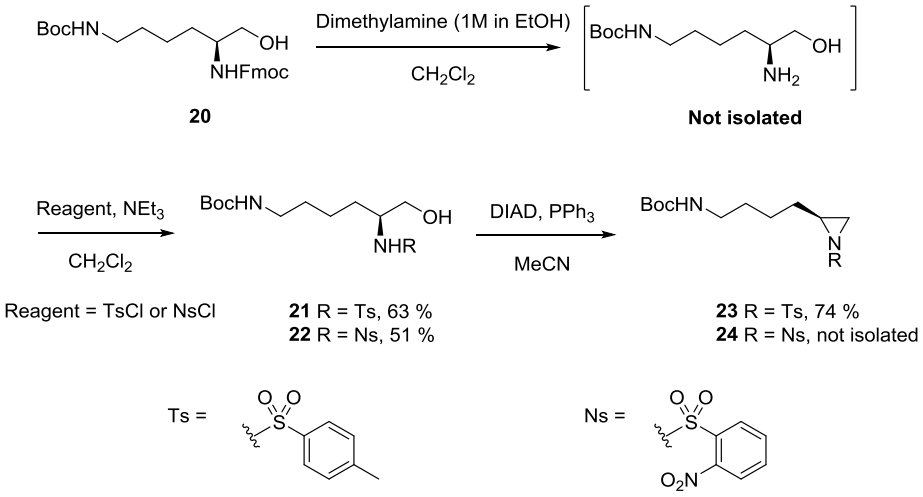

Scheme 2.12 Synthesis of tosyl- and nosyl- protected aziridines representing common intermediate for further synthesis.

There was a fear that aziridines **23** and **24** would be liable to polymerisation.[36,37] Tosyl protected compound **23** was air and room temperature stable for at least one week, but the corresponding nosyl derivative **24** was prone to forming an insoluble solid, presumed to be the polymer. Polymerisation was therefore avoided by incomplete removal of solvent following flash column chromatography. The aziridine was the common intermediate for the synthesis of both the terminal and repeating units and therefore at this point the synthesis diverged (Scheme 2.13).

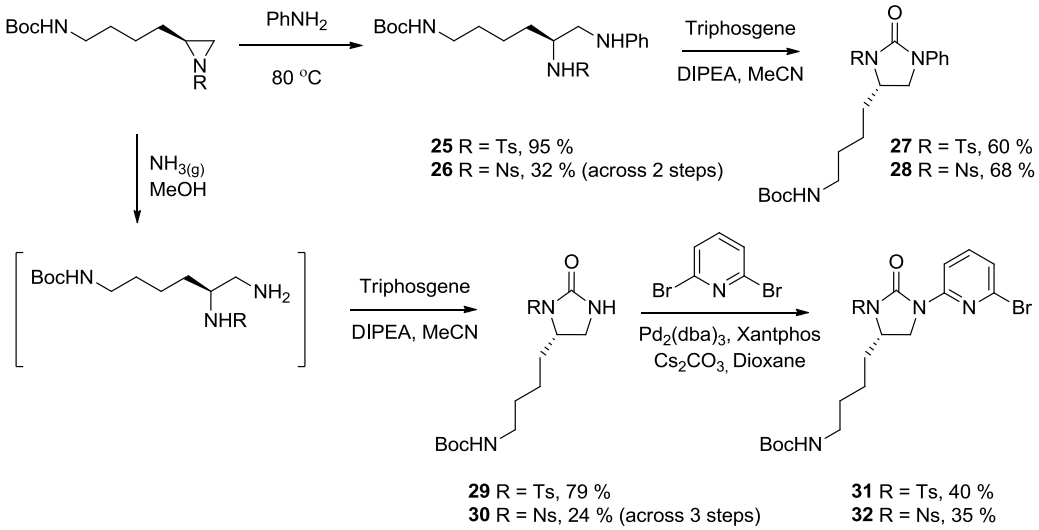

Scheme 2.13 Elaboration of common aziridine building blocks into terminal (**27**, **28**) and monomer units (**31**, **32**).

The aziridine was successfully and regioselectively opened using either aniline or ammonia to afford the corresponding diamines (**25** and **26** for opening with aniline, corresponding compounds opened with ammonia were not isolated). From these the five-membered urea ring was closed using triphosgene. The repeating monomer unit (**31**, 40 % or **32**, 35 %) was then completed through the Buchwald-Hartwig coupling of the urea to 2,6-dibromopyridine. Although no double addition product was isolated this reaction was found to be low yielding for both protecting groups.

2.11.1.3 Combining the Modules

Iterative deprotection and Buchwald-Hartwig coupling were then used to construct the dimer. Tosylated amine **27** was deprotected by treatment with magnesium metal in methanol and sonication, whilst the nosyl group on urea **28** was removed by thiophenol in an S_NAr reaction. The tosyl deprotection was found to be low yielding, and although dimer **34** was successfully purified, insufficient material could be isolated post deprotection to successfully synthesise the trimer (Scheme 2.14).

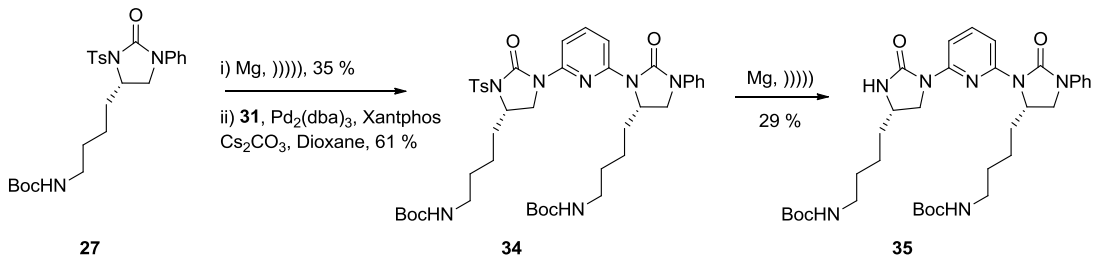

Scheme 2.14 Synthesis of tosyl protected dimer **35**.

This was because the reaction formed an insoluble gel around the magnesium that sequestered much of the product. Previous work in the group had shown that this gel could be broken up with prolonged stirring in the presence of hydrochloric acid,[37] but with the Boc protecting groups in place this was not a viable strategy. Fortunately nosyl deprotection of both the monomer and dimer proceeded in acceptable yields allowing for synthesis of the trimer. The Boc-groups were successfully removed in TFA and the final deprotected molecule **38** purified by reverse-phase HPLC displaying excellent solubility in water of greater than 10 mg / mL (Scheme 2.15).

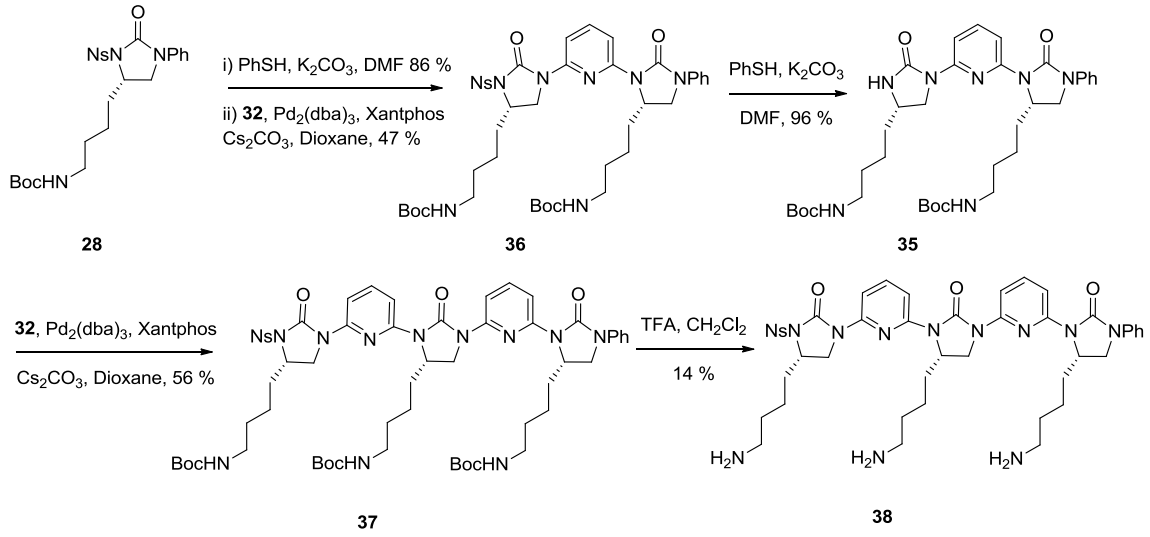

Scheme 2.15 Synthesis of nosyl protected trimer **38.**

2.12 Conformational Analysis

Initial characterisation of trimer **38** was carried out in deuterated methanol for ease of recovery of material. Pleasingly, the through-space interactions revealed from a ROESY

spectrum were as seen for the all alanine trimer **19**, with the expected peak between *H*45 and *H*47 and an absence of any others (Figure 2.24).

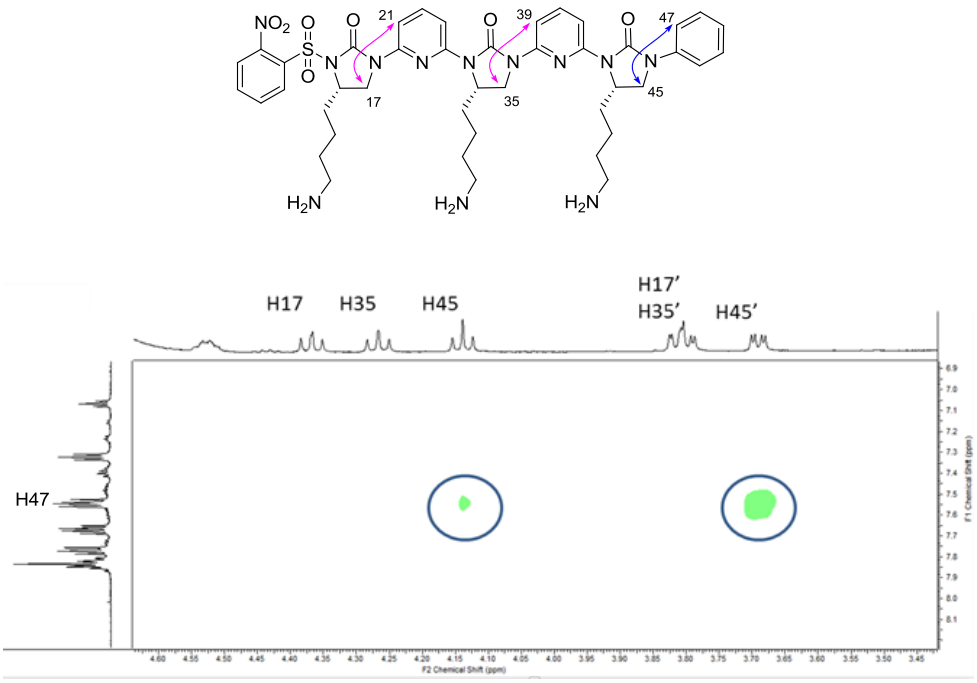

Figure 2.24 ROESY spectrum of trimer **38** in MeOD. The colour of each circle corresponds to the NOE interaction shown in the molecules above.

Pleasingly this indicates the preservation of a strong conformational bias for this hydrophilic molecule in a polar protic solvent. Unfortunately attempts to repeat the experiment in H_2O or an H_2O/D_2O mix could not reveal anything as the peaks are coincident with the water peak and are therefore also affected by solvent suppression.

2.13 Conclusions and Future Work

2.13.1 Meeting Gellman's Criteria

Through the second half of this chapter the case for this scaffold has been strengthened yet further. It has proved amenable to a modular synthesis that allows for the incorporation of hydrophilic side-chains. The use of a nosyl group as the protecting group strategy for nitrogen, which is removed with thiophenol at room temperature, an extremely mild procedure, should allow for the incorporation of a broad range of natural and unnatural

chemical side-chain mimics, either unprotected if stable to the synthesis conditions, or themselves protected with orthogonal protecting groups which could be either acid or base labile. With the hydrophilic compound retaining its conformational bias, all three challenges laid down by Gellman have therefore been met.

2.13.2 Future Work

2.13.2.1 Overcoming Curvature

Although dimer **14** displayed good overlap with a canonical β-strand, the curvature noted in trimer **19** would perhaps prevent extended mimics of four or five residues from adopting the required conformation. It was proposed that this curvature was due to the alternating 5,6 ring system, with the five-membered ring introducing the curvature. Therefore it was reasoned that substituting the five-membered urea for a six-membered homologue would force the adoption of a more linear conformation. Work in the group has shown this to be the case (Figure 2.25).[36]

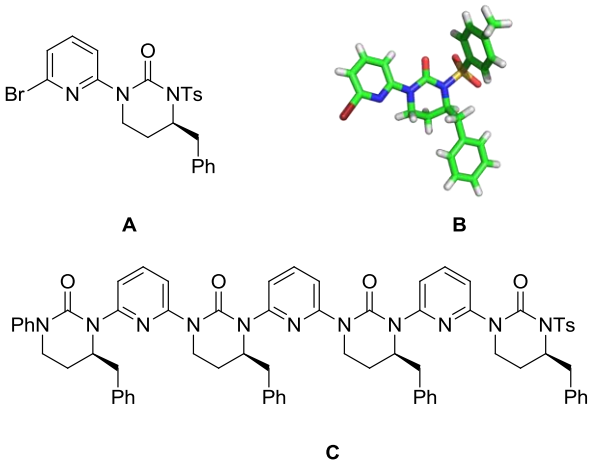

Figure 2.25 A: Monomer unit with a 6-membered urea ring B: Crystal structure of monomer unit showing the dipolar conformational lock to still be effective (CCDC: 1056842). C: Tetramer, with the desired conformation shown by computational and solution state studies.

2.13.2.2 Utilising Curvature

Alternatively the curvature can be used to create an adaptable monomer capable of switching from sheet to helical conformation in the presence of an external stimulus.

This has been achieved by the group using acid, which promotes the change from a linear, dipolar repulsion enforced conformation to a helical, hydrogen-bonded, one (Figure 2.26).[37]

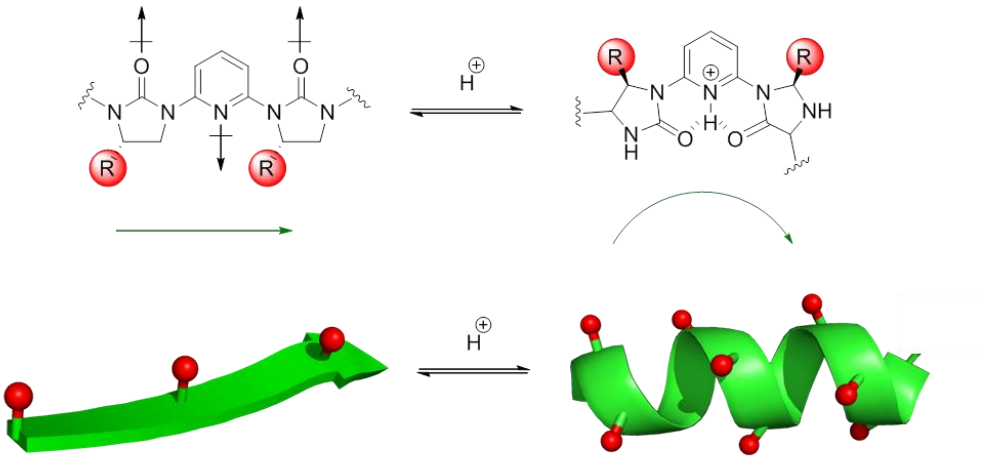

Figure 2.26 The acid-mediated conformational switching of the pyridiyl-linked oligomer from strand to helix.

2.13.2.3 Biological Applications

With the dimer displaying good side-chain overlap, further work by the group demonstrating how linearity could be maintained, and a modular synthesis amenable to the inclusion of a broad range of amino acid residues, this novel scaffold presents the ideal opportunity to mimic natural β-strands and disrupt PPIs. Figure 2.27 showcases the range of diseases that could be targeted with strands varying in length from two to five residues.

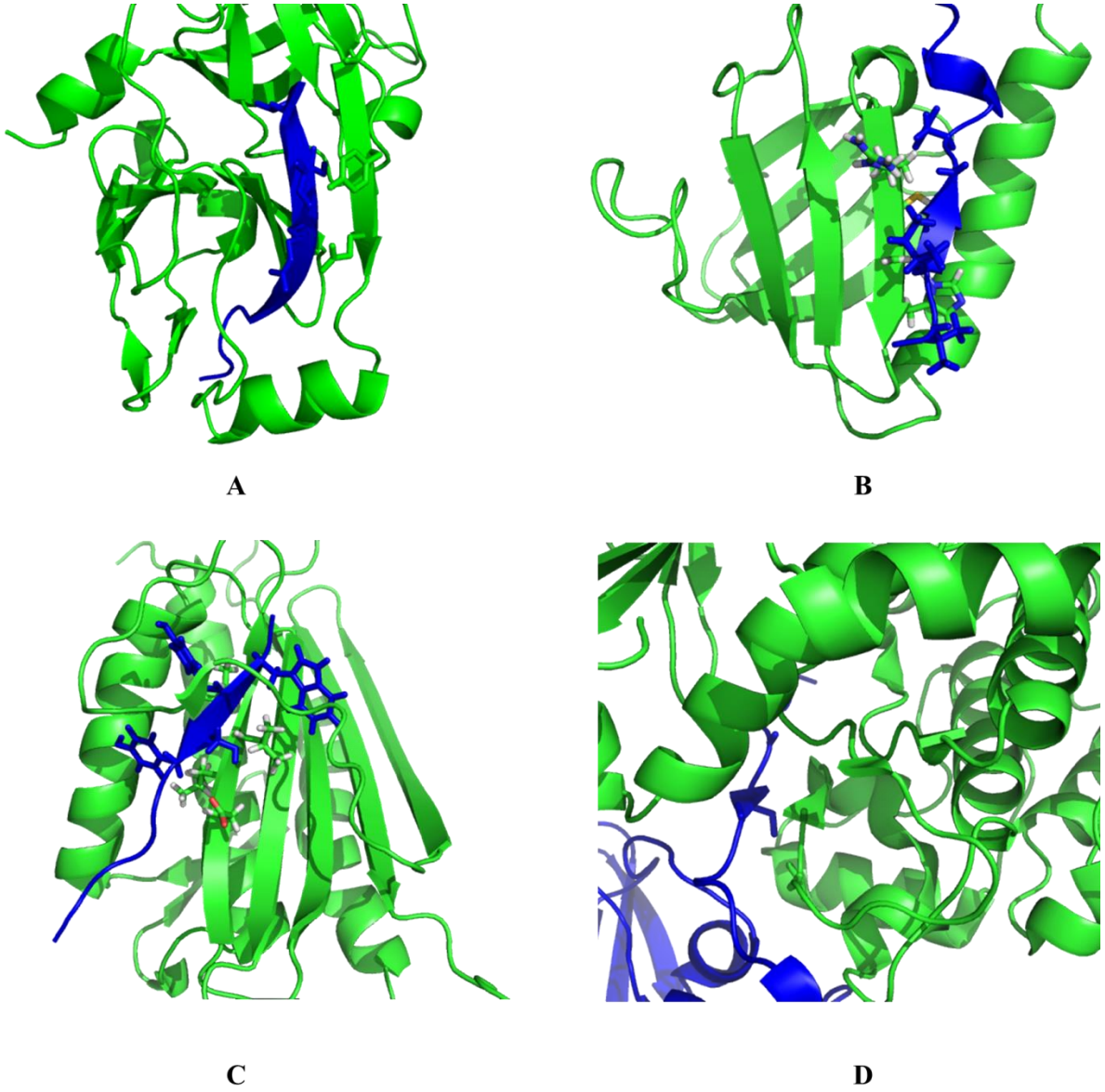

Figure 2.27 **A**: Crystal structure of NS3 protease and NS4a peptide (PDB: 1NS3). Inhibition of this complex by a protease inhibitor and interferon is known to inhibit viral RNA replication.[38] **B**: NMR solution structure of IL-4 receptor phosphopeptide recognition by the IRS-1 PTB domain (PDB: 1IRS). IRS1 is a critical element in insulin-signalling pathways and implicated in type 2 diabetes.[39] **C**: Crystal structure of the Mad2 Spindle Checkpoint Protein bound to Mad1 (PDB: 1KLQ). Correct regulation of this protein prevents chromosome mis-segregation during mitosis and meiosis, implicated in many cancers.[40] **D**: Crystal structure of the catalytic and regulatory subunits of PKA (PDB: 3FHI). PKA is implicated in the regulation of transcription in eukaryotic cells.[41]

Initially the scaffold will be validated against the strand interactions with well-established assays and known to been amenable to peptidomimetics such as the HIV-1 protease dimerization targeted successfully by Fairlie[8] and Smith.[18]

2.14 Experimental

2.14.1 General Information

2.14.1.1 Solvents and Reagents

All non-aqueous reactions were carried out under an atmosphere of argon or nitrogen in oven or flame-dried glassware unless otherwise stated. Anhydrous tetrahydrofuran and dichloromethane (from commercial sources) were obtained filtration through activated alumina (powder ~150 mesh, pore size 58 Å, basic, Sigma-Aldrich) columns, or were dried on an MB-SPS-800 dry solvent system. Other solvents and reagents were used directly as received from commercial suppliers without further purification. PE refers to distilled light petroleum of fraction (30 ˚C – 40 ˚C). Inorganic solutions refer to saturated aqueous solutions, unless otherwise indicated. Brine refers to a saturated aqueous solution of sodium chloride. The notation 'mL.mmol^{-1}' is the number of mL of solvent used in the specified work up procedure per mmol of starting material.

2.14.1.2 Chromatography

Flash column chromatography was carried out using Merck Geduran Si 60 silica gel (40 – 63µm). Thin-layer chromatography was carried out using Merck Kieselgel 60 F254 (230 – 400 mesh) fluorescent treated silica, visualised under UV light (254 nm) and by staining with aqueous potassium permanganate solution or ninhydrin in ethanol. High performance liquid chromatography was performed using a Waters 1525 pump, 2707 autosampler, and 2849 detector. Phenomonex Luna columns (250 mm long, 5 µm beads, C18 reverse-phase medium) were used for HPLC separations. Analytical HPLC was run using 1 mL min^{-1} flow through a 4.6 mm diameter column. Sample injections for analytical runs consisted of 40 µL of a 1 mg.mL^{-1} sample solution. Semi-preparative HPLC was run using 10 mL.min^{-1} flow through a 21.1 mm diameter column. Sample injections for semi-preparative runs consisted

of 500 µL of solution containing no more than 50 mg of sample. HPLC solvents were degassed by sonication for 30 min and contained 0.1 % v/v TFA.

2.14.1.3 Spectroscopy

^{1}H and ^{13}C NMR spectra were recorded using a Bruker 600, 500, or 400 MHz spectrometer running Topspin™ software and are quoted in ppm for measurement against a residual solvent peak as an internal standard. The ^{1}H NMR spectra are reported as follows: δ / ppm (multiplicity, coupling constant, number of protons, assignment). Multiplicity is abbreviated as follows: s = singlet, br = broad, d = doublet, dd = doublet of doublets, t = triplet, dt = doublet of triplets, q = quartet, qn = quintet, m = multiplet). Coupling constants are given in Hertz. Compound names are those generated by ChemBioDraw™ (CambridgeSoft) following IUPAC nomenclature. However, the NMR assignment numbering used is arbitrary and does not follow any particular convention. The numbering of compounds is illustrated on the spectra themselves; *vide infra*. The ^{13}C NMR spectra are reported in δ / ppm. Two-dimensional (COSY, HSQC, HMBC) NMR spectroscopy was used to assist the assignment of the signals in the ^{1}H and ^{13}C NMR spectra. IR spectra were recorded on a Bruker Tensor 27 FT-IR spectrometer from a thin film deposited onto a diamond ATR module. Only selected maximum absorbances (ν_{max}) of the most intense peaks are reported (cm^{-1}). Peaks in the region of 2350 cm^{-1} are attributed to the C-D stretch in $CDCl_3$. High-resolution mass spectra were recorded on a Bruker MicroTof mass spectrometer (ESI) by the internal service at the Department of Organic Chemistry, University of Oxford. Meting points were recorded using a Leica Galen III hot-stage microscope apparatus and are reported uncorrected in degrees Celsius (˚C). Optical rotations were recorded using a Perkin Elmer 341 polarimeter and are reported in degrees using concentrations in $g.100\ mL^{-1}$.

2.14.2 General Experimental Procedures

General procedure (2a): S_NAr Reaction

Amine (1.0 eq.) and *N*,*N*-diisopropylethylamine (2.3 eq.) were added to 2,6-dichloropyridine (4.0 eq.) in a sealed tube. The reaction mixture was heated to 180 °C for 18 h. After cooling to room temperature the reaction was diluted with dichloromethane (10 mL.mmol^{-1}), partitioned with ammonium chloride (10 mL.mmol^{-1}) and extracted with dichloromethane (3 x 10 mL.mmol^{-1}). The combined organic layers were dried over magnesium sulfate, filtered and the reaction concentrated *in vacuo*.

General procedure (2b): Silyl protection of alcohol

TBSCl (2.0 eq.) was added to a stirring solution of alcohol (1.0 eq.), imidazole (3.0 eq.) and DMAP (trace) in DMF (0.6 M). The reaction was stirred at room temperature for 12 h and subsequently diluted with dichloromethane (10 mL.mmol^{-1}). The solution was partitioned with ammonium chloride (10 mL.mmol^{-1}) and extracted with dichloromethane (3 x 10 mL.mmol^{-1}). The combined organic layers were dried over magnesium sulfate, filtered and the reaction concentrated *in vacuo*.

General procedure (2c): Amide bond formation

To a stirring solution of amine (1.00 eq.) in THF (0.7 M) at -78 °C was added *n*BuLi (1.05 eq.). After 1 h the carbonyl electrophile (1.30 eq.) was added and the reaction brought to room temperature and stirred for a further 2 h. Acetic acid (1.10 eq.) was added and the reaction diluted with dichloromethane (0.08 M). The mixture was partitioned with water and extracted with dichloromethane (3 x 10 mL.mmol^{-1}). The combined organic layers were dried over magnesium sulfate, filtered and the reaction concentrated *in vacuo*.

General procedure (2d): Removal of silyl protecting group

Acetic acid (3.0 eq.) was added dropwise to a stirred solution of protected alcohol (1.0 eq.) in tetrahydrofuran (0.1 M). Tetra-*n*-butyl ammonium fluoride (1 M in tetrahydrofuran, 1.2 eq.) was added dropwise and the reaction stirred at room temperature for 5 h. The reaction was diluted with dichloromethane (0.08 M) and the resulting solution partitioned with ammonium chloride (10 $mL.mmol^{-1}$) and extracted with dichloromethane (3 x 10 $mL.mmol^{-1}$). The combined organic layers were dried over magnesium sulfate, filtered and the reaction concentrated *in vacuo*.

General procedure (2e): Mitsunobu reaction

Triphenylphosphine (1.5 eq.) and DIAD (1.5 eq.) were added to a stirring solution of alcohol (1.0 eq.) in tetrahydrofuran (0.1 M). The reaction was stirred at room temperature for 30 min and concentrated *in vacuo*.

General procedure (2f): Buchwald-Hartwig Coupling

Sodium *tert*-butoxide (3 eq.) and amine (3 eq.) were added to the aryl halide (1 eq.) in 1,4-dioxane (0.15 M). The solution was degassed with argon for 20 min before the addition of $Pd_2(dba)_3$ (8 mol %) and BINAP (9 mol %). The solution was stirred at 100 °C for 5 h, the reaction filtered through Celite® and concentrated *in vacuo*.

General procedure (2g): Reduction of benzylamines

The benzylamine (1 eq.) was dissolved in dichloromethane (0.06 M) and a drop of acetic acid added. $Pd(OH)_2/C$ (100 wt %) was added and the mixture degassed with argon for 20 min. A positive pressure of H_2 gas was applied *via* balloon and the reaction left to stir at room

temperature for 2 h. The reaction mixture was passed through Celite®, washed with dichloromethane (20 mL. $mmol^{-1}$) and concentrated *in vacuo*.

General procedure (2h): Boc protection

According to a literature procedure,[41] triethylamine (1 eq.), DMAP (1 eq.) and *tert*-butyldicarbonate (2 eq.) were added to a stirring solution of amine (1 eq.) in tetrahydrofuran (0.1 M), and the reaction stirred at room temperature for 2 h. The reaction was diluted with dichloromethane (0.08 M) and the solution partitioned with ammonium chloride (10 $mL.mmol^{-1}$) and extracted with dichloromethane (3 x 10 $mL.mmol^{-1}$). The combined organic layers were dried over magnesium sulfate, filtered and the reaction concentrated *in vacuo*.

General procedure (2i): Acid reduction

According to a literature procedure,[42] ethyl chloroformate (1.10 eq.) was added to a stirring solution of acid (1.00 eq.) and *N*-methylmorpholine (1.05 eq.) in glyme (0.1 M) at -15 °C. The reaction mixture was stirred for 5 min and the resultant slurry filtered and washed with diethyl ether (20 $mL.mmol^{-1}$). The filtrate was cooled to -15 °C and $NaBH_4$ (3.00 eq.) in water (1 M) was added dropwise. The reaction flask was left open to allow for evolution of gas and upon cessation of effervescence ten times the initial volume of water was added. The reaction was warmed to room temperature and stirred for 1 h, at which point the reaction was further diluted with water (20 $mL.mmol^{-1}$) and extracted with dichloromethane (3 x 10 $mL.mmol^{-1}$). The combined organic layers were dried and concentrated *in vacuo*.

General procedure (2j): Fmoc deprotection

To a stirring solution of Fmoc protected amine (1 eq.) in dichloromethane (0.1 M) was added a solution of dimethylamine in ethanol (1 M, final ratio *v:v*, 1:1). The reaction was stirred for 1 h at room temperature and concentrated *in vacuo*.

General procedure (2k): Tosylation

To a stirring solution of amine (1 eq.) in dichloromethane (0.1 M) was added triethylamine (3 eq.) and tosyl chloride (2 eq.). The reaction was stirred at room temperature for 1 h and subsequently diluted with dichloromethane (0.05 M). The solution was partitioned with ammonium chloride (10 $mL.mmol^{-1}$) and extracted with dichloromethane (3 x 10 $mL.mmol^{-1}$). The combined organic layers were dried over magnesium sulfate, filtered and the reaction concentrated *in vacuo*.

General procedure (2l): Nosylation

To a stirring solution of amine (1 eq.) in dichloromethane (0.10 M) was added triethylamine (2 eq.) and nosyl chloride (2 eq.). The reaction was stirred at room temperature for 16 h and subsequently diluted with dichloromethane (0.05 M). The solution was partitioned with ammonium chloride (10 $mL.mmol^{-1}$) and extracted with dichloromethane (3 x 10 $mL.mmol^{-1}$). The combined organic layers were dried over magnesium sulfate, filtered and the reaction concentrated *in vacuo*.

General procedure (2m): Aziridine ring opening with aniline

Aziridine (1 eq.) was dissolved in aniline (1 M) and the reaction stirred at 80 °C for 2 h and concentrated *in vacuo*.

General procedure (2n): Aziridine ring opening with ammonia

Aziridine (1 eq.) was dissolved in methanol (0.1 M) in a sealed tube. At 0 °C, ammonia gas was bubbled through the solution for 20 min, before the tube was sealed, heated to 80 °C and stirred for 2 h. The reaction mixture was transferred to a round-bottomed flask and the reaction concentrated *in vacuo*.

General procedure (2o): Urea formation

To a stirring solution of diamine (1.0 eq.) and *N*,*N*-diisopropylethylamine (1.1 eq.) in acetonitrile (0.25 M) was added triphosgene (0.4 eq, 0.25 M in acetonitrile) by syringe pump over the course of 1 h. The reaction was stirred for a further 30 min, diluted with water (0.05 M) and extracted with dichloromethane (3 x 10 mmol.ml^{-1}). The combined organic layers were dried over magnesium sulfate, filtered and the reaction concentrated *in vacuo*.

General procedure (2p): Tosyl deprotection

Magnesium powder (2 eq.) was added to tosyl protected amine (1 eq.) in methanol. The solution was sonicated for 1 h, diluted with water (10 mL.mmol^{-1}) and extracted with dichloromethane (3 x 10 mmol.ml^{-1}). The combined organic layers were dried over magnesium sulfate, filtered and the reaction concentrated *in vacuo*.

General procedure (2q): Buchwald-Hartwig coupling

To a stirring solution of amine (1.0 eq.) in 1,4-dioxane was added caesium carbonate (2.0 eq.), $Pd(dba)_2$ (5 mol %) and Xantphos (15 mol %). The mixture was degassed with argon for 15 min before the addition of aryl bromide (1.2 eq.). The reaction was heated to 80 °C and stirred for 2 h. Upon completion the mixture was diluted with water (10 mL.mmol^{-1}) and extracted with dichloromethane (3 x 10 mmol.ml^{-1}). The combined organic layers were dried over magnesium sulfate, filtered and the reaction concentrated *in vacuo*.

General procedure (2r): Nosyl deprotection

To a stirring solution of *N*-nosylurea (1.0 eq.) in DMF (0.1 M) was added potassium carbonate (3.0 eq.) and the suspension degassed with argon for 10 min. Thiophenol (1.5 eq.) was added with the immediate development of a rich yellow colour. The reaction was stirred

at room temperature for 1 h and subsequently diluted with diethyl ether (150 mL.mmol^{-1}), washed with saturated sodium bicarbonate solution (3 x 20 mL.mmol^{-1}), and the combined aqueous layers extracted with diethyl ether (3 x 20 mL.mmol^{-1}). The combined organic layers were dried over magnesium sulfate, filtered and the reaction concentrated *in vacuo*.

General procedure (2s): Boc deprotection

To a stirring solution of Boc-protected amine (1 eq.) in dichloromethane (0.1 M) was added TFA (1:1 volume ratio with dichloromethane). The reaction was stirred at room temperature for 30 min before the solvent was removed *in vacuo*. The residual TFA was removed *via* co-evaporation three times with toluene.

2.14.3 Characterisation Data

(S)-2-((6-Chloropyridin-2-yl)amino)propan-1-ol 1

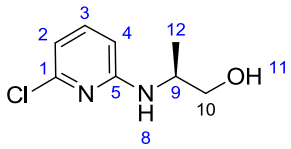

According to *general procedure (2a)*: L-Alaninol (1.00 g, 13.3 mmol) and 2,6-dichloropyridine (7.88 g, 53.3 mmol) gave the *title compound* **1** (2.04 g, 82 %) as a white solid after purification by flash column chromatography (PE:Et_2O, 4:6); $[\alpha]_D^{23.5}$ -19.6 (*c* 0.55, $CHCl_3$); δ_H (400 MHz, $CDCl_3$) 7.34 (t, *J* 7.8, 1H, H3), 6.58 (d, *J* 7.6, 1H, H2), 6.32 (d, *J* 8.1, 1H, H4), 4.62 (d, *J* 5.9, 1H, H8), 3.94 - 4.03 (m, 1H, H9), 3.71 - 3.79 (m, 1H, H10), 3.55 - 3.63 (m, 1 H, H10'), 2.99 (t, *J* 5.0, 1H, H11), 1.24 (d, *J* 6.8, 3H, H12); δ_C (101 MHz, $CDCl_3$) 158.4 (C5) 149.4 (C1), 139.7 (C3), 112.1 (C2), 105.7 (C4), 67.6 (C10), 49.7 (C9), 17.6 (C12); HRMS calculated for $C_8H_{12}{}^{35}ClN_2O$ $[M+H]^+$: 187.0633, found 187.0632; IR (CH_2Cl_2) 3307, 2967, 2361, 1603, 1568.

(S)-N-(1-((tert-Butyldimethylsilyl)oxy)propan-2-yl)-6-chloropyridin-2-amine 2

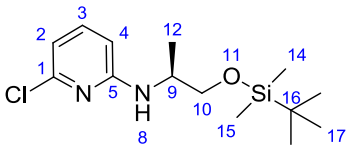

According to *general procedure (2b)*: Alcohol **1** (1.00 g, 5.37 mmol) gave the *title compound* **2** (1.60 g, 99 %) as a yellow oil after purification by flash column chromatography (PE:Et_2O, 4:6); $[\alpha]_D^{23.5}$ -8.0 (*c* 1.3, $CHCl_3$); δ_H (400 MHz, $CDCl_3$) 7.30 - 7.35 (m, 1H, H3), 6.54 (d, *J* 7.3, 1H, H2), 6.27 (d, *J* 8.3, 1H, H4), 4.73 - 4.82 (m, 1H, H8), 3.82 - 3.92 (m, 1H, H9), 3.63 (m, 2 H, H10, H10'), 1.22 (d, *J* 6.6, 3H, H12), 0.89 (s, 9H, H17), 0.06 (s, 3H, H14), 0.05 (s, 3H, H15); δ_C (101 MHz, $CDCl_3$) 158.2 (C5), 149.6 (C1), 139.5 (C3), 111.5 (C2), 104.8 (C4), 66.3 (C10), 48.5 (C9), 25.9 (C17), 18.3 (C16), 17.4 (C12), -5.4 (C14, C15);

HRMS calculated for $C_{14}H_{26}{}^{35}ClN_2OSi$ $[M+H]^+$: 301.1497, found 301.1499; IR(CH_2Cl_2) 2929, 2857, 1793.

(S)-1-(1-((tert-Butyldimethylsilyl)oxy)propan-2-yl)-1-(6-chloropyridin-2-yl)-3-phenylurea 3

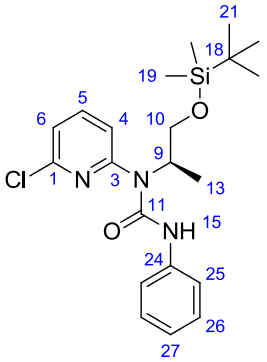

According to *general procedure (2c)*: Amine **2** (300 mg, 1.01 mmol) and phenylisocyanate gave the *title compound* **3** (294 mg, 68 %) as a yellow oil after purification by flash column chromatography (PE:Et_2O, 19:1); $[\alpha]_D^{23.5}$ +34.8 (*c* 0.75, $CHCl_3$); δ_H (400 MHz, $CDCl_3$) 9.95 (s, 1H, H15), 7.56 - 7.62 (m, 1H, Ar-H), 7.34 - 7.44 (m, 3H, Ar-H), 7.19 - 7.29 (m, 2H, Ar-H), 6.95 - 7.05 (m, 2H, Ar-H), 4.33 - 4.44 (m, 1H, H9), 4.21 (dd, *J* 10.4, 7.2, 1H, H10), 3.87 (dd, *J* 10.3, 4.6, 1H, H10'), 1.39 (d, *J* 7.1, 3H, H13), 0.82 (s, 9H, H21), 0.03 (s, 3H, H19), 0.00 (s, 3H, 19'); δ_C (101 MHz, $CDCl_3$) 155.9 (C11), 153.3, 147.8, 140.4, 138.7, 128.8, 123.1, 119.9, 119.0, 116.3 (9 x Ar-C), 66.2 (C10), 57.9 (C9), 25.9 (C21), 18.3 (C18), 15.9 (C13), -5.3 (C19), -5.4 (C19'); HRMS calculated for $C_{21}H_{30}{}^{35}ClN_3NaO_2Si$ $[M+Na]^+$: 442.1688, found 442.1706; IR (CH_2Cl_2) 3456 (weak), 2970, 1738, 1716.

(S)-1-(6-Chloropyridin-2-yl)-1-(1-hydroxypropan-2-yl)-3-phenylurea 4

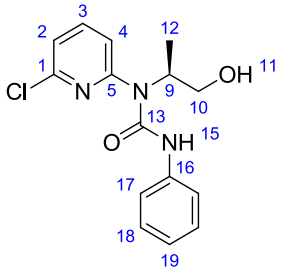

According to *general procedure (2d)*: Urea **3** (497 mg , 1.19 mmol) gave the *title compound* **4** (281 mg, 78 %) as a white solid after purification by flash column chromatography

(PE:Et_2O, 3:7); $[\alpha]_D^{23.5}$ +64.4 (*c* 0.85, $CHCl_3$); δ_H (400 MHz, $CDCl_3$) 9.26 (s, 1H, H15), 7.59 (t, *J* 7.9, 1H, H3), 7.28 - 7.34 (m, 2H, H17), 7.16 - 7.22 (m, 2H, H18), 7.12 (d, *J* 7.8, 1H, H2), 7.04 (d, *J* 8, 1H, H4), 6.93 - 6.99 (m, 1H, H19), 4.64 - 4.93 (m, 1H, H11), 4.40 - 4.49 (m, 1H, H9), 3.77 - 3.86 (m, 2H, H10, H10'), 1.23 (d, *J* 6.7, 3H, H12); δ_C (101 MHz, $CDCl_3$) 154.7 (C13), 154.0 (C1 or C5), 148.6 (C1 or C5), 140.9 (C3), 138.2 (C16), 128.8 (C18), 123.5 (C19), 120.4 (C4), 120.0 (C17), 117.3 (C2), 65.6 (C10), 57.0 (C9), 15.0 (C12); HRMS calculated for $C_{15}H_{16}{}^{35}ClN_3NaO_2$ $[M+Na]^+$: 328.0823, found 328.0828; IR (CH_2Cl_2) 3456, 3016, 1739.

(S)-3-(6-Chloropyridin-2-yl)-4-methyl-1-phenylimidazolidin-2-one 5

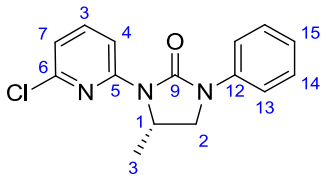

According to *general procedure (2e)*: Alcohol **4** (143 mg, 0.469 mmol) gave the *title compound* **5** (106 mg, 79 %) as a white solid after purification by flash column chromatography (PE:Et_2O, 7:3); $[\alpha]_D^{23.5}$ -10.0 (*c* 0.1, $CHCl_3$); δ_H (400 MHz, $CDCl_3$) 8.13 (d, *J* 8.3, 1H, H4), 7.48 - 7.57 (m, 3H, H3, H13), 7.31 (t, *J* 7.9, 2H, H14), 7.01 - 7.09 (m, 1H, H15), 6.89 (d, *J* 7.8, 1H, H7), 4.75 - 4.86 (m, 1H, H1), 4.04 (t, *J* 8.8, 1H, H2), 3.44 (dd, *J* 9.0, 3.1, 1H, H2'), 1.43 (d, *J* 6.1, 3H, H3); δ_C (101 MHz, $CDCl_3$) 153.9 (C5), 151.6 (C9), 148.7 (C6), 139.9 (C13), 139.6 (C12), 129.0 (C14), 123.6 (C15), 118.5 (C3), 117.8 (C7), 112.1 (C4), 49.8 (C2), 47.6 (C1), 20.0 (C3); HRMS calculated for $C_{15}H_{14}{}^{35}ClN_3NaO$ $[M+Na]^+$: 310.0718, found 310.0721; IR (CH_2Cl_2) 3456 (weak), 2970, 1738, 1716.

(S)-3-(6-(Benzylamino)pyridin-2-yl)-4-methyl-1-phenylimidazolidin-2-one 6

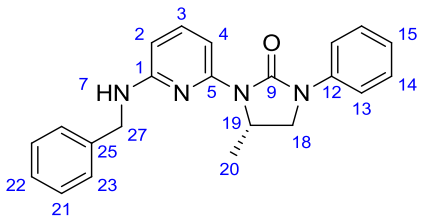

According to *general procedure (2f)*: Urea **5** (106 mg, 0.37 mmol) and benzylamine (40 µL, 0.37 mmol) gave the *title compound* **6** (126 mg, 95 %) as a yellow solid after purification by flash column chromatography (PE:Et_2O, 7:3); $[\alpha]_D^{23.5}$ +164.0 (*c* 0.25, $CHCl_3$); δ_H (400 MHz, $CDCl_3$) 7.49 - 7.54 (m, 2H, Ar-H), 7.45 (d, *J* 7.8, 1H, H4), 7.34 (t, *J* 7.9, 1H, H3), 7.23 - 7.32 (m, 6H, Ar-H), 7.20 (dd, *J* 6.0, 2.6, 1H, Ar-H), 7.01 (t, *J* 7.3, 1H, Ar-H), 6.03 (d, *J* 7.8, 1H, H2), 4.70 (m, 1H, H19), 4.66 (1H, H7), 4.45 (d, *J* 4.4, 2H, H27, H27'), 3.96 (t, *J* 8.8 1H, H18), 3.36 (dd, *J* 8.7, 3.5, 1H, H18'), 1.31 (d, *J* 6.1, 3H, H20); δ_C (101 MHz, $CDCl_3$) 157.0, 154.3, 150.3, 140.1, 139.8, 139.0, 128.8, 128.5, 127.2, 127.1, 123.0, 118.2, 102.8, 100.9 (13 x Ar-C), 49.7 (C18), 47.3 (C19), 46.1 (C27), 20.2 (C20); HRMS calculated for $C_{22}H_{23}N_4O$ $[M+H]^+$: 359.1866, found 359.1867; IR (CH_2Cl_2) 3377 (weak), 3060 (weak), 3029 (weak), 2975 (weak), 2361, 2341, 1705.

(S)-3-(6-Aminopyridin-2-yl)-4-methyl-1-phenylimidazolidin-2-one 7

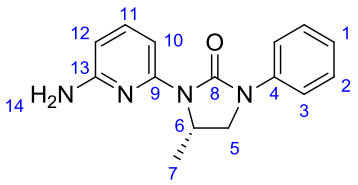

According to *general procedure (2g)*: Protected aniline **6** (295 mg, 0.82 mmol) gave the *title compound* **7** (189 mg, 86 %) as a yellow solid after purification by flash column chromatography (PE:Et_2O, 4:6); $[\alpha]_D^{23.5}$ -30.9 (*c* 0.94, $CHCl_3$); δ_H (400 MHz, $CDCl_3$) 7.52 (m, 3H, H3, H10), 7.36 (dd, *J* 7.9 1H, H11), 7.26 - 7.33 (m, 2H, H2), 7.02 (t, *J* 1.0, 1H, H1), 6.11 (d, *J* 7.8, 1H, H12), 4.72 - 4.84 (m, 1H, H6), 4.00 (t, *J* 8.7, 1H, H5), 3.64 - 4.56 (m, 2H, H14), 3.37 - 3.43 (m, 1H, H5'), 1.40 (d, *J* 6.1, 3H, H7); δ_C (101 MHz, $CDCl_3$) 156.8 (C13),

154.3 (C9), 150.4 (C8), 140.1 (C4), 139.4 (C11), 128.9 (C2), 123.1 (C1), 118.3 (C3), 104.1 (C10), 102.2 (C12), 49.7 (C5), 47.3 (C6), 20.2 (C7); HRMS calculated for $C_{15}H_{17}N_4O$ $[M+H]^+$: 269.1397, found 269.1402; IR (CH_2Cl_2) 3355, 2930, 1704, 1614.

(S)-tert-butyl (2-((6-chloropyridin-2-yl)amino)propyl) carbonate 9

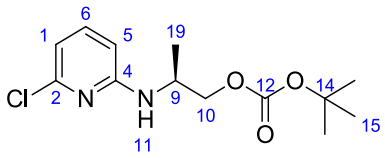

According to *general procedure (2h)*: Alcohol **1** (100 mg, 0.54 mmol) and di-*tert*-butyldicarbonate (234 mg, 1.08 mmol) gave the *title compound* **9** (138 mg, 90 %) as a yellow oil after purification by flash column chromatography (PE:Et_2O, 6:4); $[\alpha]_D^{23.5}$ -13.3 (*c* 0.15 , $CHCl_3$); δ_H (400 MHz, $CDCl_3$) 7.34 (t, *J* 7.8, 1H, H6), 6.57 (d, *J* 7.3, 1H, H1), 6.30 (d, *J* 8.1, 1H, H5), 4.63 - 4.75 (m, 1H, H11), 4.17 (d, *J* 7.6, 2H, H9, H10), 4.06 (d, *J* 5.9, 1 H, H10'), 1.49 (s, 9H, H15), 1.24 - 1.30 (m, 3H, H19); δ_C (101 MHz, $CDCl_3$) 157.7 (C12), 153.6 (C4), 149.6 (C2), 139.6 (C6), 112.1 (C1), 105.1 (C5), 82.4 (C14), 69.4 (C10), 46.1 (C9), 27.7 (C15), 17.6 (C19); HRMS calculated for $C_{13}H_{20}N_2O_3$ $[M+H]^+$: 287.1157, found 287.1154; IR ($CHCl_3$) 3396, 2980, 2360, 1742, 1598.

Phenyl (S)-(1-((tert-butyldimethylsilyl)oxy)propan-2-yl)(6-chloropyridin-2-yl)carbamate 10

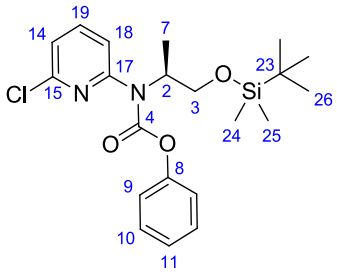

According to *general procedure (2c)*: Secondary amine **2** (500 mg, 1.67 mmol) and phenylchloroformate (315 µl, 2.51 mmol) gave the *title compound* **10** (589 mg, 84 %) as a yellow oil after purification by flash column chromatography (PE:Et_2O, 9:1); $[\alpha]_D^{23.5}$ +42.8 (*c* 0.65, $CHCl_3$); δ_H (400 MHz, $CDCl_3$) 7.60 (dd, *J* 7.8, 1H, H19), 7.26 - 7.35 (m, 3H, H18,

H10), 7.11 - 7.18 (m, 2H, H11, H14), 7.03 - 7.08 (m, 2H, H9), 4.47 - 4.47 (m, 1H, H2), 3.90 (dd, *J* 10.3, 7.8, 1H, H3), 3.73 (dd, *J* 10.4, 6.2, 1H, H3'), 1.30 (d, *J* 6.8, 3H, H7), 0.81 - 0.84 (s, 9H, H26), 0.00 (s, 6H, H24, H25); δ_C (101 MHz, $CDCl_3$) 153.5 (C4), 153.3 (C15), 150.9 (C17), 149.3 (C8), 139.7 (C19), 129.3 (C10), 125.6 (C11), 122.2 (C14), 121.8 (C18), 121.6 (C9), 64.8 (C3), 56.9 (C2), 25.9 (C26), 18.2 (C23), 15.5 (C7), -5.3 (C25), -5.4 (C24); HRMS calculated for $C_{21}H_{30}{}^{35}ClN_2O_3Si$ $[M+H]^+$: 421.1709, found 421.1698; IR (CH_2Cl_2) 2930, 2857, 2360, 1729, 1581.

(S)-1-(1-((tert-Butyldimethylsilyl)oxy)propan-2-yl)-1,3-bis(6-chloropyridin-2-yl)urea 11

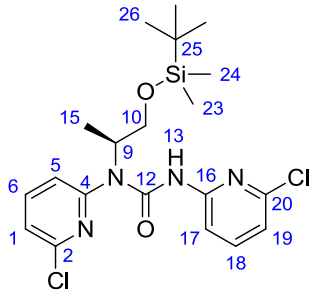

According to *general procedure (2c)*: Protected alcohol **10** (59 mg, 0.14 mmol) and 2-amino-6-chloro-pyridine (21 mg, 0.17 mmol) gave the *title compound* **11** (24 mg, 38 %) as a yellow oil after purification by flash column chromatography (PE:Et_2O, 7:3); $[\alpha]_D^{23.5}$ +24.2 (*c* 0.65, $CHCl_3$); δ_H (400 MHz, $CDCl_3$) 8.87 (s, 1H, H13), 7.97 - 8.00 (m, 1H, Ar-H), 7.70 (t, *J* 7.9, 1H, Ar-H), 7.59 (t, *J* 7.9, 1H, Ar-H), 7.40 - 7.44 (m, 1H, Ar-H), 7.21 (dd, *J* 7.8, 0.5, 1H, Ar-H), 6.95 (dd, *J* 7.6, 0.5, 1H, Ar-H), 4.55 - 4.66 (m, 1H, H9), 4.09 (dd, J 10.3, 7.3, 1H, H10), 3.84 (dd, *J* 10.4, 4.5, 1H, H10'), 1.31 (d, *J* 7.1, 3H, H15), 0.88 - 0.92 (m, 9H, H26), 0.11 (s, 3H, H23), 0.09 (s, 3H, H24); δ_C (101 MHz, $CDCl_3$) 154.0 (C12), 153.1, 152.4, 149.6, 148.8, 140.4, 121.6, 119.9, 118.3, 111.4 (10 x Ar-C), 66.1 (C10), 56.6 (C9), 25.9 (C26), 18.4 (C25), 15.6 (C15), -5.4 (C23, C24); HRMS calculated for $C_{20}H_{28}{}^{35}Cl_2N_4NaO_2Si$ $[M+Na]^+$: 477.1251, found 477.1246; IR ($CHCl_3$) 3664, 3540, 3248, 2977, 2955, 2857, 1687.

1-((S)-1-((tert-Butyldimethylsilyl)oxy)propan-2-yl)-1-(6-chloropyridin-2-yl)-3-(6-((S)-5-methyl-2-oxo-3-phenylimidazolidin-1-yl)pyridin-2-yl)urea 12

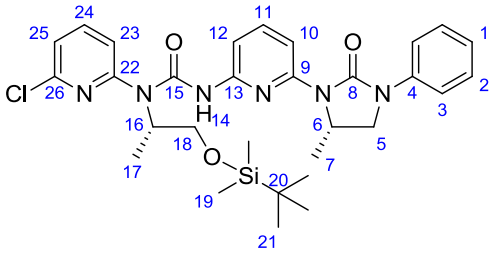

According to *general procedure (2c)*: Electrophile **10** (1.96 g, 4.68 mmol) and primary amine **7** (1.05 g, 3.90 mmol) gave the *title compound* **12** (1.10 g, 48 %) as a yellow oil after purification by flash column chromatography (PE:Et_2O, 6:4); $[\alpha]_D^{23.5}$ +14.7 (*c* 0.6, $CHCl_3$); δ_H (400 MHz, $CDCl_3$) 10.12 (s, 1H, H14), 7.82 - 7.88 (m, 1H, H11), 7.64 (t, *J* 7.9, 1H, H24), 7.59 (m, 2H, H12 H10), 7.54 (dd, *J* 8.8, 1.0, 2H, H3), 7.40 (d, *J* 7.8, 1H, H23), 7.33 (m, 7.5, 2H, H2), 7.08 - 7.12 (m, 1H, H25), 7.05 (s, 1H, H1), 4.75 - 4.85 (m, 1H, H6), 4.29 - 4.40 (m, 1H, H16), 4.16 - 4.25 (m, 1H, H18), 4.01 - 4.09 (m, 1H, H5), 3.87 (dd, *J* 10.3, 4.9, 1H, H18'), 3.43 (dd, *J* 8.8, 3.4, 1H, H5'), 1.45 (d, *J* 6.1, 3H, H7), 1.38 (d, *J* 7, 3H, H17), 0.80 - 0.85 (s, 9H, H21), 0.03 (s, 3H, H19), 0.00 (s, 3H, H19'); δ_C (101 MHz, $CDCl_3$) 155.7 (C26), 154.2 (C8 or C15), 152.6 (C8 or C15), 150.2 (C9 or C13), 150.1 (C9 or C13), 148.1 (C22), 140.6 (C24), 139.9 (C4), 139.6 (C10), 128.8 (C2), 123.2 (C1), 119.9 (C25), 118.3 (C3), 117.1 (C23), 108.6 (C11), 107.1 (C12), 65.8 (C18), 58.4 (C16), 49.8 (C5), 47.4 (C6), 25.9 (C21), 20.2 (C7), 18.2 (C20), 15.8 (C17), -5.4 (C19), -5.4 (C19'); HRMS calculated for $C_{30}H_{40}O_3N_6{}^{35}ClSi$ $[M+H]^+$: 595.2614, found 595.2597; IR (CH_2Cl_2) 2954, 2930, 2857, 1738, 1715, 1689.

1-(6-Chloropyridin-2-yl)-1-((S)-1-hydroxypropan-2-yl)-3-(6-((S)-5-methyl-2-oxo-3-phenylimidazolidin-1-yl)pyridin-2-yl)urea 13

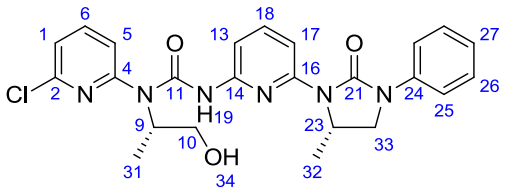

According to *general procedure (2d)*: Protected alcohol **12** (190 mg, 0.32 mmol) gave the *title compound* **13** (124 mg, 81 %) as a yellow oil after purification by flash column chromatography (PE:Et_2O, 1:9); $[\alpha]_D^{23.5}$ +6.5 (*c* 0.65, $CHCl_3$); δ_H (400 MHz, $CDCl_3$) 9.35 (br. s., 1H, H19), 7.81 - 7.89 (m, 1H, H17), 7.70 (t, *J* 7.9, 1H, H6), 7.56 - 7.61 (m, 2H, H18 H13), 7.51 (m, 2H, H25), 7.27 - 7.34 (m, 2H, H26), 7.15 - 7.20 (m, 2H, H1, H5), 7.01 - 7.06 (m, 1H, H27), 4.71 (m, 1H, H23), 4.43 - 4.53 (m, 1H, H9), 4.02 (t, *J* 8.8, 1H, H33), 3.88 (m, 2H, H10, H10'), 3.45 - 3.76 (br. s, 1H, H34), 3.37 - 3.42 (m, 1H, H33'), 1.39 (d, *J* 6.1, 3H, H32), 1.31 (d, *J* 6.8, 3H, H31); δ_C (101 MHz, $CDCl_3$) 154.6 (C21), 154.1 (C4), 153.2 (C11), 150.1 (C16), 149.7 (C14), 149.1 (C2), 141.1 (C6), 139.8 (C24), 139.7 (C18), 128.9 (C26), 123.2 (C27), 121.1 (C1 or C5), 118.3 (C25), 117.7 (C1 or C5), 108.9 (C17), 106.9 (C13), 65.7 (C10), 57.5 (C9), 49.7 (C33), 47.4 (C23), 20.1 (C32), 15.1 (C31); HRMS calculated for $C_{24}H_{25}{}^{35}ClN_6NaO_3$ $[M+Na]^+$: 503.1569, found 503.1573; IR (CH_2Cl_2) 3418 (broad), 2972, 2881, 1707, 1687.

(S)-3-(6-Chloropyridin-2-yl)-4-methyl-1-(6-((S)-5-methyl-2-oxo-3-phenylimidazolidin-1-yl)pyridin-2-yl)imidazolidin-2-one 14

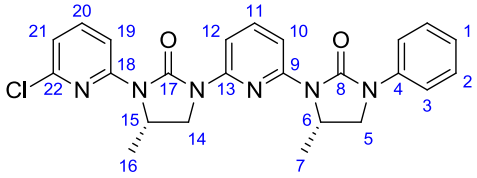

According to *general procedure (2e)*: Amine **13** (100 g, 0.21 mmol) gave the *title compound* **14** (73 mg, 75 %) as a yellow solid after purification by flash column chromatography

(PE:Et_2O, 8:2); $[\alpha]_D^{23.5}$ +5.7 (*c* 0.65, $CHCl_3$); δ_H (400 MHz, $CDCl_3$) 8.21 (d, *J* 8.3, 1H, H19), 7.89 (d, *J* 8.2, 1H, H10) 7.85 (d, *J* 7.9, 1H, H12), 7.67 - 7.74 (m, 1H, H11), 7.58 - 7.66 (m, 3H, H3 H20), 7.35 - 7.42 (m, 2H, H2), 7.11 (t, *J* 7.3, 1H, H1), 7.00 (d, *J* 7.6, 1H, H21), 4.80 - 4.91 (m, 2H, H6, H15), 4.25 (dd, *J* 10.4, 9.2, 1 H, H14), 4.11 (t, *J* 8.8, 1H, H5), 3.70 - 3.75 (m, 1 H, H14'), 3.49 - 3.55 (m, 1H, H5'), 1.55 (d, *J* 6.1, 3H, H7), 1.52 (d, *J* 6.1, 3H, H16); δ_C (101 MHz, $CDCl_3$) 154.1 (C8), 153.6 (C17), 151.4 (C21), 149.9 (C9 or C13), 149.8 (C9 or C13), 148.7 (C18), 139.9 (C20), 139.8 (C4), 139.3 (C11), 128.9 (C2), 123.3 (C1), 118.3 (C3), 118.1 (C22), 112.4 (C19), 108.2 (C10), 107.1 (C12), 49.7 (C5), 48.3 (C14), 47.5 (C6 or C15), 47.5 (C6 or C15), 20.3 (C7 or C16), 20.2 (C7 or C16); HRMS calculated for $C_{24}H_{24}{}^{35}ClN_6O_2$ $[M+H]^+$: 463.1644, found 463.1635; IR ($CHCl_3$) 2975, 2361, 1716; mp: 166 – 168 °C (diethyl ether).

(S)-3-(6-(Benzylamino)pyridin-2-yl)-4-methyl-1-(6-((S)-5-methyl-2-oxo-3-phenylimidazolidin-1-yl)pyridin-2-yl)imidazolidin-2-one 15

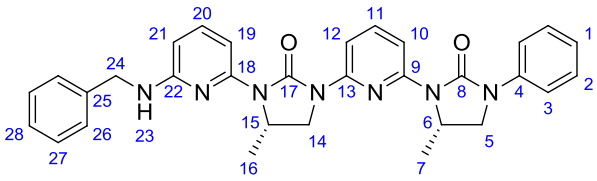

According to *general procedure (2f)*: 2-chloropyridine derivative **14** (50 mg, 0.108 mmol) and benzylamine (12 µl, 0.108 mmol) gave the *title compound* **15** (26 mg, 45 %) as a yellow oil after purification by flash column chromatography (PE:Et_2O, 7:3); $[\alpha]_D^{23.5}$ -46.1 (*c* 0.95, $CHCl_3$); δ_H (400 MHz, $CDCl_3$) 7.88 (d, *J* 8.2, 1H, H12), 7.83 (d, *J* 8.0, 1H, H10), 7.59 (t, *J* 8.1, 1H, H11), 7.52 (dd, *J* 8.7, 0.9, 2H, H3), 7.44 (d, *J* 7.9, 1H, H19), 7.34 - 7.40 (m, 1H, H20), 7.30 - 7.33 (m, 2H, H2), 7.25 - 7.29 (m, 4H, H26, H27), 7.19 - 7.22 (m, 1H, H28), 7.03 (t, *J* 7.4, 1H, H1), 6.06 (d, *J* 7.9, 1H, H21), 4.73 - 4.81 (m, 1H, H6), 4.68 (m, 2H, H15, H23), 4.46 (s, 2 H, H24), 4.10 (t, *J* 9.6, 1 H, H14), 4.03 (t, *J* 8.7, 1H, H5), 3.58 (dd, *J* 10.2, 3.8, 1H, H14'), 3.39 - 3.47 (m, 1H, H5'), 1.46 (d, *J* 6.1, 3H, H7), 1.31 (d, *J* 6.1, 3H, H16);

δ_C (101 MHz, $CDCl_3$) 156.0 (C22), 153.2 (C8 or C17), 152.9 (C8 or C17), 149.3 (Ar-C), 149.1 (Ar-C), 148.7 (Ar-C), 138.9 (Ar-C), 138.7 (Ar-C), 138.2 (C11), 138.0 (C20), 127.9 (Ar-C), 127.6 (Ar-C), 126.2 (Ar-C), 126.1 (Ar-C), 122.2 (C1), 117.3 (C3), 106.8 (C10), 106.1 (C12), 102.1 (C19), 100.3 (C21), 48.7 (C5), 47.3 (C14), 46.5 (C6), 46.3 (C15), 45.1 (C24), 19.5 (C7 or C16), 19.3 (C7 or C16); HRMS calculated for $C_{31}H_{32}N_7O_2$ $[M+H]^+$: 534.2612, found 534.2611; IR ($CHCl_3$) 3457, 3016, 2970, 2947, 2132, 1739.

(S)-3-(6-Aminopyridin-2-yl)-4-methyl-1-(6-((S)-5-methyl-2-oxo-3-phenylimidazolidin-1-yl)pyridin-2-yl)imidazolidin-2-one 16

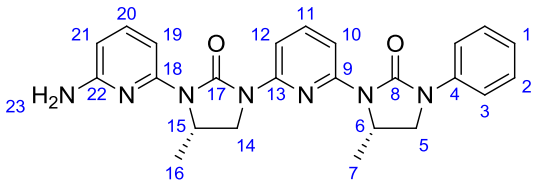

According to *general procedure (2g)*: Protected amine **15** (9 mg, 0.017 mmol) gave the *title compound* **16** (6 mg, 81 %) as a white solid after purification by flash column chromatography (PE:Et_2O, 2:8); $[\alpha]_D^{23.5}$ -11.1 (*c* 0.36, $CHCl_3$); δ_H (500 MHz, $CDCl_3$) 7.88 - 8.01 (m, 2H, H10, H12), 7.67 (t, *J* 8.2, 1H, H11), 7.54 - 7.62 (m, 3 H, H3, H19), 7.42 - 7.49 (m, 1H, H20), 7.34 - 7.41 (m, 2H, H2), 7.06 - 7.13 (m, 1H, H1), 6.16 - 6.23 (m, 1H, H21), 4.74 - 4.89 (m, 2H, H6, H15), 4.31 (br. s., 2H, H23), 4.19 (dd, *J* 10.3, 9.0, 1H, H14), 4.08 (t, *J* 8.8, 1H, H5), 3.67 (dd, *J* 10.3, 3.9, 1H, H14'), 3.49 (dd, *J* 8.8, 3.4, 1H, H5'), 1.54 (d, *J* 6.1, 3H, H7), 1.43 - 1.49 (m, 3H, H16); δ_C (126 MHz, $CDCl_3$) 156.8 (C22), 154.1 (C8), 153.9 (C17), 150.3 (C18), 150.1 (C13), 149.7 (C9), 139.8 (C4), 139.3 (C11 or C20), 139.2 (C11 or C20), 128.8 (C2), 123.2 (C1), 118.3 (C3), 107.7 (C10 or C12), 107.1 (C10 or C12), 104.3 (C19), 102.4 (C21), 49.7 (C5), 48.3 (C14), 47.4 (C6), 47.2 (C15), 20.4 (C7 or C16), 20.3 (C7 or C16); HRMS calculated for $C_{24}H_{26}N_7O_2$ $[M+H]^+$: 444.2143, found 444.2136; IR ($CHCl_3$) 3482, 3366, 3062, 2976, 2896, 1707, 1580.

1-((S)-1-((tert-Butyldimethylsilyl)oxy)propan-2-yl)-1-(6-chloropyridin-2-yl)-3-(6-((S)-5-methyl-3-(6-((S)-5-methyl-2-oxo-3-phenylimidazolidin-1-yl)pyridin-2-yl)-2-oxoimidazolidin-1-yl)pyridin-2-yl)urea 17

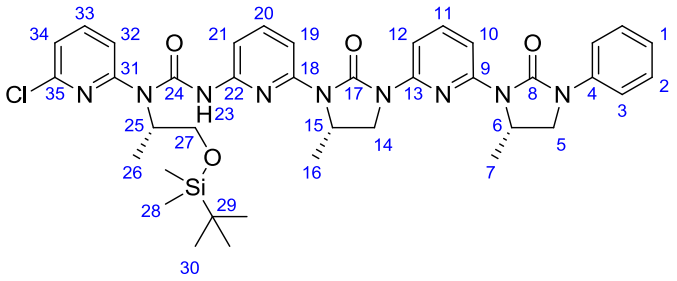

According to *general procedure (2c)*: Activated carbonyl **10** (72 mg, 0.17 mmol) and primary amine **16** (58 mg, 0.13 mmol) gave the *title compound* **17** (17 mg, 17 %) as a yellow oil after purification by flash column chromatography (PE:Et_2O, 7:3); $[\alpha]_D^{23.5}$ -33.5 (*c* 0.95, $CHCl_3$); δ_H (500 MHz, $CDCl_3$) 10.23 (s, 1H, H23), 7.88 - 7.98 (m, 3H, Ar-H), 7.65 - 7.73 (m, 4H, Ar-H), 7.61 (dd, *J* 8.8 1.0, 2H, H3), 7.47 (d, *J* 8.1, 1H, Ar-H), 7.39 (dd, *J* 8.6 7.3, 2H, H2), 7.16 (d, *J* 7.8, 1H, Ar-H), 7.11 (t, *J* 8, 1H, H1), 4.79 - 4.91 (m, 2H, H6, H15), 4.35 - 4.44 (m, 1H, H25), 4.20 - 4.30 (m, 2H, H14, H27), 4.09 - 4.15 (m, 1H, H5), 3.90 - 3.95 (m, 1H, H27'), 3.69 - 3.75 (m, 1H, H14'), 3.52 (dd, *J* 8.8, 3.4, 1H, H5'), 1.56 (d, *J* 6.1, 3H, H16), 1.51 (d, *J* 6.1, 3H, H7), 1.43 - 1.46 (m, 3H, H26), 0.89 (s, 9H, H30), 0.09 (s, 3H, H28), 0.06 (s, 3H, H28'); δ_C (126 MHz, $CDCl_3$) 155.8 (C31), 154.2 (C8), 153.9 (C17), 152.6 (C24), 150.3 (C=O), 150.3 (C=O), 149.9 (C=O), 149.8 (Ar-C), 148.1 (Ar-C), 140.6 (Ar-C), 139.9 (C4), 139.7 (Ar-C), 139.3 (C20), 128.9 (C2), 123.3 (C1), 119.9 (Ar-C), 118.4 (C3), 117.1 (Ar-C), 108.9 (Ar-C), 108.0 (Ar-C), 107.5 (Ar-C), 107.2 (C21), 65.9 (C27), 58.5 (C25), 49.8 (C5), 48.4 (C14), 47.5 (C15/C6), 47.4 (C15/C6), 25.9 (C30), 20.5 (C7), 20.4 (C16), 18.3 (C29), 15.9 (C26), -5.3 (C28), -5.4 (C28'); HRMS calculated for $C_{39}H_{49}N_9O_4{}^{35}ClSi$ $[M+H]^+$: 770.3360, found 770.3342; IR ($CHCl_3$) 2929, 2856, 2361, 1718.

1-(6-Chloropyridin-2-yl)-1-((S)-1-hydroxypropan-2-yl)-3-(6-((S)-5-methyl-3-(6-((S)-5-methyl-2-oxo-3-phenylimidazolidin-1-yl)pyridin-2-yl)-2-oxoimidazolidin-1-yl)pyridin-2-yl)urea 18

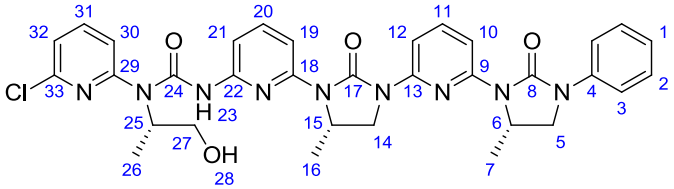

According to *general procedure (2d)*: Protected alcohol **17** (28 mg, 0.036 mmol) gave the *title compound* **18** (12 mg, 50 %) as a white solid after purification by flash column chromatography (PE:Et_2O, 2:8); $[\alpha]_D^{23.5}$ -50.0 (*c* 0.04 , $CHCl_3$); δ_H (500 MHz, $CDCl_3$) 9.51 (s, 1H, H23), 7.89 - 7.98 (m, 3H, Ar-H), 7.78 (t, *J* 7.8, 1H, H31), 7.66 - 7.72 (m, 3 H, Ar-H), 7.61 (d, *J* 7.8, 2H, H3), 7.39 (t, *J* 8.1, 2H, H2), 7.23 - 7.30 (m, 2H, H30, H32), 7.12 (t, *J* 7.5, 1H, H1), 4.82 - 4.91 (m, 1H, H6), 4.73 - 4.82 (m, 1H, H15), 4.51 - 4.58 (m, 1H, H25), 4.23 (t, *J* 9.7, 1H, H14), 4.13 (t, *J* 8.9, 1H, H5), 3.97 (d, *J* 5.4, 2H, H27, H27'), 3.71 (dd, *J* 10.5, 3.7, 1H, H14'), 3.53 (dd, *J* 8.9, 3.3, 1H, H5'), 3.48 - 3.64 (br s, 1H, H28), 1.56 (d, *J* 6.4, 3H, H7), 1.48 (d, *J* 6.1, 3H, H16), 1.39 (d, *J* 7.1, 3H, H26); δ_C (126 MHz, $CDCl_3$) 154.7 (Q), 154.1 (Q), 153.8 (Q), 153.3 (Q), 150.2 (Q), 149.9 (Q), 149.8 (Q), 149.8 (Q), 149.1 (Q), 141.2 (C31), 139.8 (Ar-C), 139.3 (Ar-C), 135.8 (C4), 128.9 (C2), 123.3 (C1), 121.1 (C32/C30), 118.4 (C3), 117.6 (C32/C30), 109.2 (Ar-C), 108.0 (Ar-C), 107.3 (Ar-C), 107.2 (Ar-C), 65.8 (C27), 57.6 (C25), 49.7 (C5), 48.4 (C14), 47.5 (C6 or C15), 47.3 (C6 or C15), 20.4 (C7 or C16), 20.4 (C7 or C16), 15.1 (C26);. HRMS calculated for $C_{33}H_{34}N_9O_4{}^{35}Cl$ $[(M+H)]^+$: 656.2495, found 656.2490; IR ($CHCl_3$) 2924, 2361, 1716, 1583.

(S)-3-(6-Chloropyridin-2-yl)-4-methyl-1-(6-((S)-5-methyl-3-(6-((S)-5-methyl-2-oxo-3-phenylimidazolidin-1-yl)pyridin-2-yl)-2-oxoimidazolidin-1-yl)pyridin-2-yl)imidazolidin-2-one 19

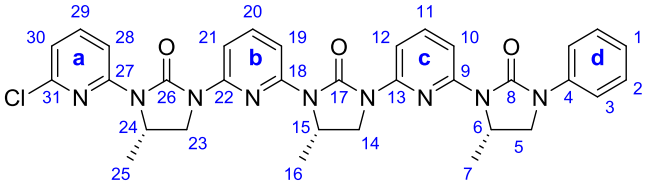

According to *general procedure (2e)*: Alcohol **18** (12 mg, 0.018 mmol) gave the *title compound* **19** (8 mg, 71 %) as a yellow solid after purification by flash column chromatography (PE:Ethyl Acetate, 8:2); $[\alpha]_D^{23.5}$ -12.5 (*c* 0.08, $CHCl_3$); δ_H (500 MHz, $CDCl_3$) 8.22 (d, *J* 8.3, 1H, H28), 7.92 - 7.99 (m, 4H, Ar-H ring **b**/**c**), 7.72 (m, 2H, Ar-H ring **b**/**c**), 7.66 - 7.69 (m, 1H, H29), 7.60 - 7.65 (m, 2H, H3), 7.40 (m, 2H, H2), 7.09 - 7.16 (m, 1H, H1), 7.02 (d, *J* 7.6, 1H, H30), 4.81 - 4.93 (m, 3H, H6, H15, H24), 4.27 (s, 2H, H14, H23), 4.15 (s, 1H, H5), 3.72 - 3.79 (m, 2H, H14', H23'), 3.51 - 3.58 (m, 1H, H5'), 1.51 - 1.60 (m, 9H, H7, H16, H25); δ_C (126 MHz, $CDCl_3$) 154.1 (C17 or C26), 153.8 (C17 or C26), 153.6 (C8), 151.4 (C27 or C31), 150.1 (Ar ring **b**/**c**), 150.0 (Ar ring **b**/**c**), 149.8 (Ar ring **b**/**c**), 149.7 (Ar ring **b**/**c**), 148.8 (C27 or C31), 140.0 (C29), 139.9 (C4), 139.4 (C11 or C20), 139.3 (C11 or C20), 128.9 (C2), 123.3 (C1), 118.4 (C3), 118.1 (Ar ring **a**), 112.4 (Ar ring **a**), 108.6 (Ar ring **b**/**c**), 108.2 (Ar ring **b**/**c**), 107.5 (Ar ring **b**/**c**), 107.2 (Ar ring **b**/**c**), 49.8 (C5), 48.4 (C14 or C23), 48.3 (C14 or C23), 47.5 (C6 or C15 or C24), 47.5 (C6 or C15 or C24), 47.4 (C6 or C15 or C24), 20.6 (C7 or C16 or C25), 20.4 (C7 or C16 or C25), 20.2 (C7 or C16 or C25); HRMS calculated for $C_{33}H_{32}N_9O_3{}^{35}Cl$ $[M+H]^+$: 638.2389, found 638.2383; IR (CH_2Cl_2) 2924, 2853, 1717, 1583; mp: 179 – 183 °C (diethyl ether).

(S)-(9H-Fluoren-9-yl)methyl tert-butyl (6-hydroxyhexane-1,5-diyl)dicarbamate 20

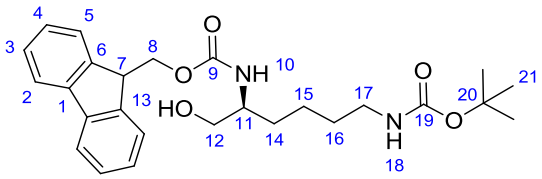

According to *general procedure (2i)*: Fmoc-Lys(Boc)-OH (5.0 g, 10.7 mmol) gave the *title compound* **20** (4.0 g, 82 %) as a white solid after purification by flash column chromatography (Et_2O); $[\alpha]_D^{25.0}$ -30.1 (*c* 0.1, $CHCl_3$); δ_H (400 MHz, $CDCl_3$) 7.76 (d, *J* 7.6, 2 H, H5), 7.60 (d, *J* 7.6, 2H, H2), 7.37 - 7.43 (m, 2 H, H4), 7.28 - 7.34 (m, 2 H, H3), 5.25 (d, *J* 7.6, 1 H, H10), 4.65 - 4.73 (m, 1 H, H18), 4.40 (d, *J* 6.6, 2 H, H8, H8'), 4.15 - 4.25 (m, 1 H, H7), 3.49 - 3.74 (m, 3 H, H11, H12, H12'), 2.99 - 3.23 (m, 2 H, H17, H17'), 1.57 - 1.68 (m, 1 H, H14), 1.41 - 1.52 (m, 12 H, H14', H16, H16', H21), 1.30 - 1.40 (m, 2 H, H15, H15'); δ_C (101 MHz, $CDCl_3$) 156.7 (C=O), 156.4 (C=O), 143.8 (C6), 141.2 (C1), 127.6 (C4), 127.0 (C3), 125.0 (C2), 119.9 (C5), 79.2 (C20), 66.5 (C8), 64.6 (C12), 52.9 (C11), 47.2 (C7), 39.6 (C17), 30.4 (C14), 29.8 (C16), 28.3 (C21), 22.6 (C15); HRMS calculated for $C_{26}H_{43}N_2O_5Na$ $[M+Na]^+$: 477.2360, found 477.2357; IR (CH_2Cl_2) 3330, 2936, 2864, 2361, 2340, 1759, 1689, 1524.

(S)-tert-Butyl (6-hydroxy-5-(4-methylphenylsulfonamido)hexyl)carbamate 21

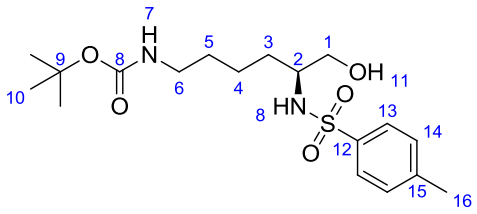

According to *general procedure (2j)*: Fmoc-protected amine **20** (2.00 g, 4.4 mmol) gave Residue **A**. According to *general procedure (2k)*: Residue **A** and tosyl chloride (1.67 g, 8.8 mmol) gave *title compound* **21** (1.07 g, 63 %) as a colourless oil after purification by flash column chromatography (Et_2O); $[\alpha]_D^{25.0}$ +9.0 (*c* 1.00, $CHCl_3$); δ_H (500 MHz, DMSO-d_6) 7.68

(d, *J* 7.0, 2 H, H13), 7.35 - 7.39 (m, 3 H, H8, H14), 6.64 - 6.70 (m, 1 H, H7), 4.60 (t, *J* 6.0, 1 H, H11), 3.20 - 3.29 (m, 1 H, H1), 3.05 - 3.13 (m, 1 H, H1'), 2.92 - 3.01 (m, 1 H, H2), 2.71 – 2.75 (m, 2 H, H6, H6'), 2.38 (s, 3 H, H16), 1.42 - 1.50 (m, 1 H, H3), 1.38 (s, 9 H, H10), 1.16 (m, 4 H, H3', H4, H5, H5'), 0.84 - 0.99 (m, 1 H, H4'); δ_C (126 MHz, DMSO-d_6) 156.0 (C8), 142.7 (C12), 139.6 (C15), 129.9 (C14), 126.9 (C13), 77.8 (C9), 63.9 (C1), 55.4 (C2), 39.9 (C6), 31.1 (C3), 29.7 (C5), 28.7 (C10), 22.6 (C4), 21.4 (C16); HRMS calculated for $C_{18}H_{30}N_2O_5NaS$ $[M+Na]^+$: 409.1768, found 409.1768; IR (CH_2Cl_2) 3528, 3366, 3282, 2930, 2865, 1681, 1598, 1526.

(S)-tert-Butyl (6-hydroxy-5-(4-nitrophenylsulfonamido)hexyl)carbamate 22

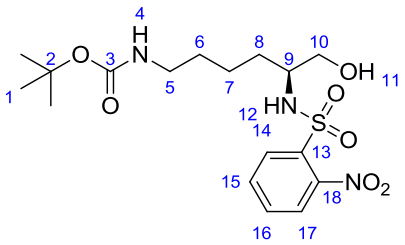

According to *general procedure (2j)*: Fmoc-protected amine **20** (1.60 g, 3.50 mmol) gave Residue **A** as a white solid. According to *general procedure (2l)*: Residue **A** and nosyl chloride (750 mg, 3.39 mmol) gave the *title compound* **22** (750 mg, 51 %) as a white foam after purification by flash column chromatography (PE:Et_2O, 1:4); $[\alpha]_D^{25.0}$ +2.10 (*c* 1.00, $CHCl_3$); δ_H (400 MHz, $CDCl_3$) 8.08 - 8.13 (m, 1 H, Ar-H), 7.80 - 7.84 (m, 1 H, Ar-H), 7.70 - 7.74 (m, 2 H, Ar-H), 4.72 (t, *J* 5.9, 1 H, H4), 4.28 (br. s., 2 H, H11, H12), 3.47 - 3.52 (m, 2 H, H10, H10'), 3.40 - 3.46 (m, 1 H, H9), 2.89 - 3.01 (m, 2 H, H5, H5'), 1.47 - 1.58 (m, 2 H, H8, H8'), 1.39 (s, 9 H, H1), 1.31 - 1.36 (m, 2 H, H6, H6'), 1.13 - 1.29 (m, 2 H, H7, H7'); δ_C (101 MHz, $CDCl_3$) 156.1 (C3), 147.5, 134.5, 133.4, 132.8, 130.4, 125.1, 79.0 (C2), 63.9 (C10), 56.4 (C9), 39.7 (C5), 30.9 (C6), 29.4 (C8), 28.2 (C1), 22.3 (C7); HRMS calculated for $C_{17}H_{26}N_3O_7S$ $[M-H]^-$: 416.1497, found 416.1497; IR (CH_2Cl_2) 3352 (broad), 2938, 2868, 2253, 1686, 1540.

(S)-tert-Butyl (4-(1-tosylaziridin-2-yl)butyl)carbamate 23

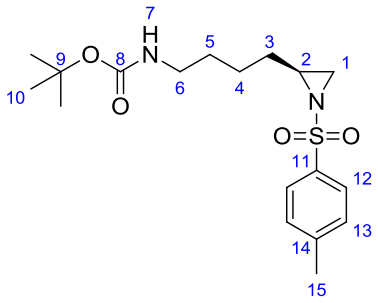

According to *general procedure (2e)*: Alcohol **21** (1.07 g, 2.77 mmol) gave the *title compound* **23** (750 mg, 74 %) as a colourless oil after purification by flash column chromatography (Et_2O); $[\alpha]_D^{25.0}$ +80.3 (*c* 0.10, $CHCl_3$); δ_H (400 MHz, $CDCl_3$) 7.74 (d, *J* 7.2, 2 H, H12), 7.27 (d, *J* 8.6, 2 H, H13), 4.48 - 4.60 (m, 1 H, H7), 2.89 - 2.98 (m, 2 H, H6, H6'), 2.61 – 2.65 (m, 1 H, H2), 2.54 (d, *J* 6.8, 1 H, H1), 2.37 (s, 3 H, H15), 1.98 (d, *J* 4.4, 1 H, H1'), 1.50 - 1.58 (m, 1 H, H3), 1.30 - 1.41 (m, 11 H, H5, H5', H10), 1.18 - 1.28 (m, 3 H, H3', H4, H4'); δ_C (101 MHz, $CDCl_3$) 155.8 (C8), 144.4 (C11), 134.9 (C14), 129.5 (C13), 127.9 (C12), 78.9 (C9), 40.1 (C2), 39.9 (C6), 33.7 (C1), 30.7 (C3), 29.2 (C5), 28.3 (C10), 23.8 (C4), 21.5 (C15); HRMS calculated for $C_{18}H_{28}N_2O_4NaS$ $[M+Na]^+$: 391.1662, found 391.1668; IR (CH_2Cl_2) 3391 (broad), 2977, 2932, 2865, 1697, 1455.

(S)-tert-Butyl (5-(4-methylphenylsulfonamido)-6-(phenylamino)hexyl)carbamate 25

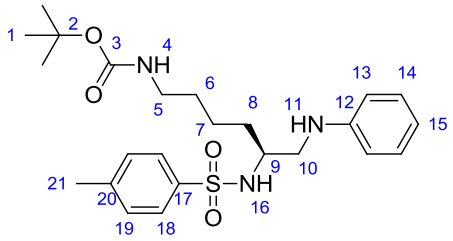

According to *general procedure (2m)*: Aziridine **23** (100 mg, 0.27 mmol) and aniline (1 mL) gave the *title compound* **25** (118 mg, 95 %) as a white solid after purification by flash column chromatography (Diethyl ether); $[\alpha]_D^{25.0}$ -23.3 (*c* 0.9, $CHCl_3$); δ_H (400 MHz, $CDCl_3$) 7.67 (d, *J* 8.1, 2 H, H18), 7.17 (d, *J* 8.1, 2 H, H14), 7.03 (dd, *J* 8.2, 7.0, 2 H, H19), 6.57 - 6.63 (m,

1 H, H15), 6.36 (d, *J* 7.8, 2 H, H13), 5.23 (br. s., 1 H, H11), 4.47 (br. s, 1 H, H4), 3.23 - 3.34 (m, 1 H, H9), 2.96 - 3.05 (m, 2 H, H10, H10'), 2.88 - 2.94 (m, 2 H, H5, H5'), 2.33 (s, 3 H, H21), 1.35 - 1.37 (m, 11 H, H1, H8, H8'), 1.21 - 1.26 (m, 2 H, H6, H6'), 1.17 - 1.19 (m, 1 H, H7), 0.97 - 1.08 (m, 1 H, H7'); δ_C (101 MHz, $CDCl_3$) 156.1 (C3), 147.6 (C12), 143.4 (C17), 137.6 (C20), 129.6 (C14), 129.1 (C19), 127.1 (C18), 117.4 (C15), 112.8 (C13), 79.1 (C2), 53.1 (C9), 47.8 (C10), 39.8 (C5), 32.6 (C8), 29.6 (C6), 28.4 (C1), 22.2 (C7), 21.4 (C21); HRMS calculated for $C_{24}H_{36}N_3O_4S$ $[M+H]^+$: 462.2421 found 462.2420; IR (CH_2Cl_2) 3398 (broad), 2976, 2932, 2864, 1688, 1603, 1510.

(S)-tert-Butyl (5-(4-nitrophenylsulfonamido)-6-(phenylamino)hexyl)carbamate 26

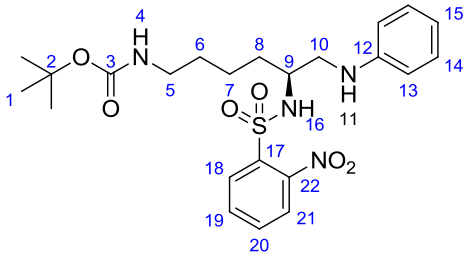

According to *general procedure (2e)*: Amino-alcohol **22** (183 mg, 0.44 mmol) gave residue **A** which was purified by flash column chromatography (PE:Et_2O, 1:4) and the reaction concentrated *in vacuo* to a total volume of 2 mL. According to *general procedure (2m)*: 2 mL solvent containing Residue **A** gave the *title compound* **26** (70 mg, 32 % across 2 steps) as a white foam after purification by flash column chromatography (Et_2O); $[\alpha]_D^{25.0}$ +38.5 (*c* 1.00, $CHCl_3$); δ_H (400 MHz, $CDCl_3$) 7.93 (dd, *J* 7.5, 1.6, 1 H, Ar-H), 7.65 - 7.69 (m, 1 H, Ar-H), 7.45 - 7.55 (m, 2 H, Ar-H), 6.97 (dd, *J* 8.3, 7.6 Hz, 2 H, H14), 6.54 - 6.59 (m, 1 H, Ar-H), 6.27 (d, *J* 7.8, 2 H, H13), 5.56 (d, *J* 7.6, 1 H, H16), 4.48 (br. s., 1 H, H4), 3.55 (td, *J* 7.6, 5.1, 2 H, H9, H11), 3.12 (dd, *J* 15.0, 5.0, 1 H, H10), 3.02 (dd, *J* 15.0, 5.0, 1 H, H10'), 2.90 - 2.98 (s, 2 H, H5), 1.44 - 1.54 (m, 2 H, H6, H6'), 1.33 - 1.40 (m, 13 H, H1, H7, H7', H8, H8'); δ_C (101 MHz, $CDCl_3$) 156.0 (C3), 147.4, 147.1, 134.3, 133.3, 132.7, 130.5, 129.1, 125.1, 117.5, 112.5 (10 x Ar-C), 79.1 (C2), 54.3 (C9), 47.8 (C10), 39.9 (C5), 32.9 (C8), 29.6 (C6),

28.4 (C1), 22.4 (C7); HRMS calculated for $C_{23}H_{33}N_4O_6S$ $[M+H]^+$: 493.2115, found 493.2112; IR (CH_2Cl_2) 3344 (broad), 2955, 2912, 2875, 2211, 1670, 1550.

(S)-tert-Butyl 6-azido-2-(2-iodobenzamido)hexanoate 27

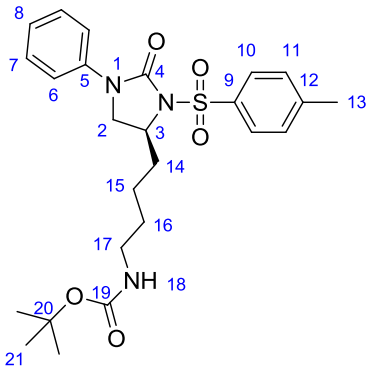

According to *general procedure (2o)*: Diamine **25** (110 mg, 0.24 mmol) and triphosgene (30 mg, 0.10 mmol) gave the *title compound* **27** (70 mg, 60 %) as a colourless residue after purification by flash column chromatography (PE:Et_2O, 1:2); $[\alpha]_D^{25.0}$ -30.1 (*c* 0.50, $CHCl_3$); δ_H (400 MHz, $CDCl_3$) 7.91 (d, *J* 8.0, 2 H, H10),7.33 - 7.39 (m, 2 H, H11), 7.21 - 7.28 (m, 4 H, H6, H7), 6.99 - 7.05 (m, 1 H, H8), 4.45 - 4.55 (m, 1 H, H18), 4.32 - 4.40 (m, 1 H, H3), 3.93 (t, *J* 9.2, 1 H, H2), 3.44 (dd, *J* 9.0, 3.0, 1 H, H2'), 2.98 - 3.06 (m, 2 H, H17, H17'), 2.34 (s, 3 H, H13), 1.92 - 2.02 (m, 1 H, H14), 1.75 - 1.86 (m, 1 H, H14'), 1.39 - 1.52 (m, 2 H, H16, H16'), 1.35 (s, 9 H, H21), 1.23 - 1.31 (m, 2 H, H15, H15'); δ_C (101 MHz, $CDCl_3$) 156.0 (C19), 151.5 (C4), 144.8, 138.3, 136.1, 129.5, 128.9, 128.2, 124.2, 118.6, 79.1 (C20), 53.3 (C3), 48.0 (C2), 40.0 (C17), 34.5 (C14), 29.8 (C16), 28.3 (C21), 21.6 (C13), 20.9 (C15); HRMS calculated for $C_{25}H_{33}N_3O_5NaS$ $[M+Na]^+$ 510.2033, found 510.2032; IR (CH_2Cl_2) 3396 (broad), 3064, 2975, 2930, 2866, 2115, 1725, 1598, 1503, 1458.

(S)-tert-Butyl (4-(3-((4-nitrophenyl)sulfonyl)-2-oxo-1-phenylimidazolidin-4-yl)butyl)carbamate 28

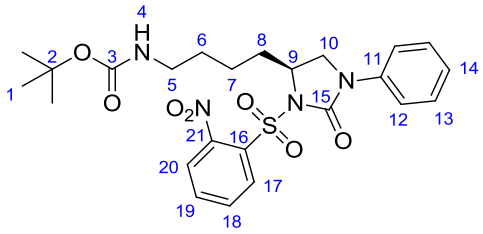

According to *general procedure (2o)*: Diamine **26** (50 mg, 0.10 mol) gave the *title compound* **28** (35 mg, 68 %) as a white solid after purification by flash column chromatography (PE:Et_2O, 1:1); $[\alpha]_D^{25.0}$ +154 (*c* 1.00, $CHCl_3$); δ_H (400 MHz, $CDCl_3$) 8.36 - 8.43 (m, 1 H, Ar-H), 7.64 - 7.69 (m, 3 H, Ar-H), 7.32 - 7.37 (m, 2 H, Ar-H), 7.22 - 7.28 (m, 2 H, Ar-H), 7.01 - 7.07 (m, 1 H, Ar-H), 4.42 - 4.57 (m, 2 H, H4, H9), 4.21 (t, *J* 8.9, 1 H, H10'), 3.49 (dd, *J* 9.2, 1.6, 1 H, H10), 3.03 - 3.12 (m, 2 H, H5, H5'), 1.84 - 1.98 (m, 2 H, H8, H8'), 1.41 - 1.53 (m, 4 H, H6, H6', H7, H7'), 1.35 (s, 9 H, H1); δ_C (101 MHz, $CDCl_3$) 156.1 (C3), 151.0 (C15), 147.9, 138.2, 134.9, 134.7, 132.0, 131.9, 129.1, 124.6, 124.3, 118.8 (10 x Ar-C), 79.2 (C2), 54.4 (C9), 48.6 (C10), 40.1 (C5), 35.6 (C8), 29.9 (C6), 28.4 (C1), 21.5 (C7); HRMS calculated for $C_{24}H_{30}N_4O_7SNa$ $[(M+H)]^+$ 541.1727 found 541.1723; IR (CH_2Cl_2) 2980, 2933, 2865, 1734, 1705.

(S)-tert-Butyl (4-(2-oxo-3-tosylimidazolidin-4-yl)butyl)carbamate 29

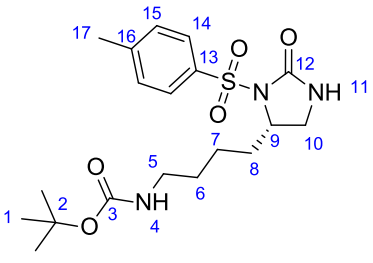

According to *general procedure (2n)*: Aziridine **23** (250 mg, 0.67 mmol) gave Residue **A**. According to *general procedure (2o)*: Residue **A** and triphosgene (80 mg, 0.27 mmol) gave the *title compound* **29** (220 mg, 79 % over two steps) as a white solid after purification by

flash column chromatography (Et_2O); $[\alpha]_D^{25.0}$ -23.0 (*c* 1.00, $CHCl_3$); δ_H (400 MHz, $CDCl_3$) 7.82 (d, *J* 8.3, 2 H, H14), 7.23 (d, *J* 8.1, 2 H, H15), 6.31 (s, 1 H, H11), 4.55 - 4.67 (m, 1 H, H4), 4.20 - 4.30 (m, 1 H, H9), 3.44 (t, *J* 9.2, 1 H, H10), 3.05 (dd, *J* 9.2, 3.5, 1 H, H10'), 2.96 - 3.03 (m, 2 H, H5, H5'), 2.35 (s, 3 H, H17), 1.78 - 1.89 (m, 1 H, H8), 1.67 - 1.78 (m, 1 H, H8'), 1.35 - 1.44 (m, 11 H, H1, H6, H6'), 1.19 - 1.27 (m, 2 H, H7, H7'); δ_C (101 MHz, $CDCl_3$) 156.1 (C=O), 155.9 (C=O), 144.4 (C13), 136.2 (C16), 129.4 (C15), 127.7 (C14), 79.0 (C2), 56.9 (C9), 42.9 (C10), 40.0 (C5), 34.3 (C8), 29.6 (C6), 28.3 (C1), 21.5 (C17), 20.9 (C7); HRMS calculated for $C_{19}H_{29}N_3O_5NaS$ $[M+Na]^+$: 434.1720, found 434.1720; IR (CH_2Cl_2) 3342 (broad), 2691, 2914, 2890, 2854, 1744, 1712.

(S)-tert-Butyl (4-(3-((4-nitrophenyl)sulfonyl)-2-oxoimidazolidin-4-yl)butyl)carbamate 30

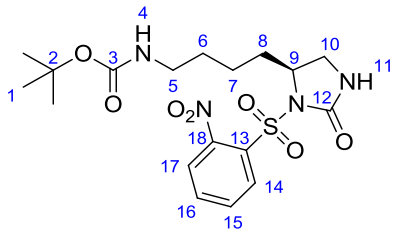

According to *general procedure (2e)*: Amino-alcohol **22** (548 mg, 1.31 mmol) gave Residue **A** which was purified by flash column chromatography (PE:Et_2O, 1:4) and reaction concentrated *in vacuo* to a total volume of 4 mL. According to *general procedure (2n)*: 4 mL of solvent containing residue **A** gave residue **B**. According to *general procedure (2o)*: Residue **B** gave the *title compound* **30** (140 mg, 24 % across 3 steps) as a yellow foam after purification by flash column chromatography (CH_2Cl_2:MeOH, 19:1); $[\alpha]_D^{25.0}$ +9.00 (*c* 1.00, $CHCl_3$); δ_H (400 MHz, $CDCl_3$) 8.24 - 8.35 (m, 1 H, Ar-H), 7.62 - 7.70 (m, 3 H, Ar-H), 5.98 (s, 1 H, H4), 4.68 (br. s., 1 H, H11), 4.35 - 4.45 (m, 1 H, H9), 3.66 (t, *J* 8.9, 1 H, H10), 3.13 (d, *J* 9.0, 1 H, H10'), 3.06 (d, *J* 6.1, 2 H, H5, H5'), 1.78 - 1.85 (m, 2 H, H8, H8'), 1.42 - 1.51 (m, 2 H, H6, H6'), 1.37 (s, 9 H, H1), 1.31 - 1.34 (m, 2 H, H7, H7'); δ_C (101 MHz, $CDCl_3$) 169.3 (C12), 155.0 (C3), 147.7, 134.5, 134.3, 131.9, 131.7, 124.0 (6 x Ar-C), 79.0 (C2), 57.8

(C9), 43.4 (C10), 40.1 (C5), 35.3 (C8), 29.6 (C6), 28.3 (C1), 21.3 (C7); HRMS calculated for $C_{18}H_{26}N_4O_7SNa$ $[M+H]^+$: 465.1414, found 465.1411; IR (CH_2Cl_2) 3337, 3096, 2978, 2934, 2865, 1711, 1685.

(S)-tert-Butyl (4-(1-(6-bromopyridin-2-yl)-2-oxo-3-tosylimidazolidin-4-yl)butyl)carbamate 31

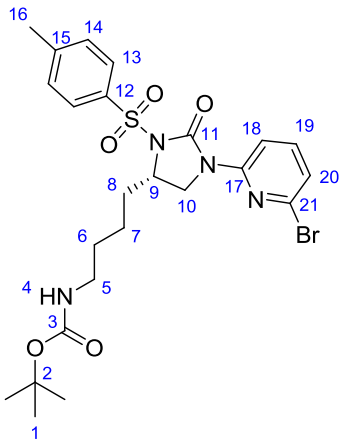

According to *general procedure (2q)*: Amine **29** (200 mg, 0.49 mmol) and 2,6-dibromopyridine (136 mg, 0.58 mmol) gave the *title compound* **31** (110 mg, 40 %) as a colourless oil after purification by flash column chromatography (PE:Et_2O, 1:1); $[\alpha]_D^{25.0}$ +24.5 (*c* 1.00, $CHCl_3$); δ_H (400 MHz, $CDCl_3$) 8.01 (dd, *J* 8.3, 0.7, 1 H, H20), 7.90 (d, *J* 8.5, 2 H, H13), 7.39 (t, *J* 8.1, 1 H, H19), 7.27 (d, *J* 8.1, 2 H, H14), 7.08 (dd, *J* 7.6, 0.5, 1 H, H18), 4.48 - 4.58 (m, 1 H, H4), 4.36 (br. s., 1 H, H9), 4.01 (dd, *J* 11.0, 9.3, 1 H, H10), 3.76 (dd, *J* 10.9, 3.3, 1 H, H10'), 2.98 – 3.06 (m, 2 H, H5, H5'), 2.35 (s, 3 H, H16), 1.90 - 2.02 (m, 1 H, H8), 1.69 - 1.83 (m, 1 H, H8'), 1.41 - 1.52 (m, 2 H, H6, H6'), 1.36 (s, 9 H, H1), 1.24 - 1.31 (m, 2 H, H7, H7'); δ_C (101 MHz, $CDCl_3$) 156.0 (C3 or C11), 156.0 (C3 or C11), 151.3 (Ar-C), 150.9 (Ar-C), 145.1 (Ar-C), 139.8 (C19), 135.9 (Ar-C), 129.7 (C14), 128.3 (C13), 123.0 (C18), 112.0 (C20), 79.2 (C2), 53.6 (C9), 46.8 (C10), 40.1 (C5), 34.5 (C8), 29.8 (C6), 28.4 (C1), 21.7 (C16), 21.0 (C7); HRMS calculated for $C_{24}H_{31}N_4O_5NaBrS$ $[M+Na]^+$:

591.1070, found 591.1070; IR (CH_2Cl_2) 3566 (broad), 2960, 2914, 2890, 2853, 1736, 1713, 1442.

(S)-tert-Butyl (4-(1-(6-bromopyridin-2-yl)-3-((2-nitrophenyl)sulfonyl)-2-oxoimidazolidin-4-yl)butyl)carbamate 32

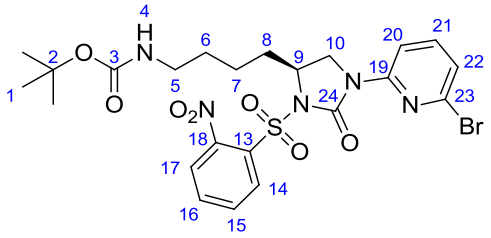

According to *general procedure (2q)*: Amide **30** (130 mg, 0.29 mmol) and 2,6-dibromopyridine (81 mg, 0.35 mmol) gave the *title compound* **32** (60 mg, 35 %) as a pale yellow foam after purification by flash column chromatography (PE:Et_2O, 1:1); $[\alpha]_D^{25.0}$ +254 (*c* 1.00, $CHCl_3$); δ_H (400 MHz, $CDCl_3$) 8.37 - 8.41 (m, 1 H, Nosyl-H), 7.91 (d, *J* 8.1, 1 H, H22), 7.66 - 7.73 (m, 3 H, Nosyl-H), 7.39 (t, *J* 8.1, 1 H, H21), 7.10 (d, *J* 7.6, 1 H, H20), 4.42 - 4.55 (m, 2 H, H4, H9), 4.22 (dd, *J* 10.9, 8.9, 1 H, H10), 3.87 (dd, *J* 10.9, 2.1, 1 H, H10'), 3.03 - 3.13 (m, 2 H, H5, H5'), 1.83 - 1.94 (m, 2 H, H8, H8'), 1.46 - 1.54 (m, 2 H, H6, H6'), 1.36 (s, 9 H, H1), 1.17 - 1.33 (m, 2 H, H7, H7'); δ_C (101 MHz, $CDCl_3$) 156.0 (C3), 150.8 (C24), 150.7 (C19), 148.0 (C18), 139.8 (C21), 139.4 (C23), 135.0 (Nosyl-C), 134.8 (Nosyl-C), 132.0 (Nosyl-C), 131.6 (C13), 124.4 (Nosyl-C), 123.2 (C20), 112.0 (C22), 79.2 (C2), 54.7 (C9), 47.4 (C10), 40.1 (C5), 35.6 (C8), 29.8 (C6), 28.4 (C1), 21.4 (C7); HRMS calculated for $C_{23}H_{29}N_5O_7SBr$ $[M+H]^+$: 598.0966, found 598.0969; IR (CH_2Cl_2) 3296 (broad), 2980, 1733, 1716, 1698, 1684, 1652.

(S)-tert-Butyl (4-(2-oxo-1-phenylimidazolidin-4-yl)butyl)carbamate 33

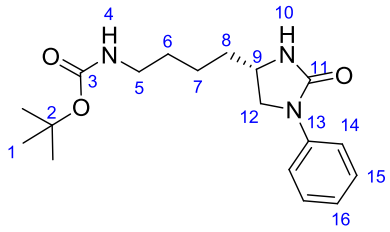

According to *general procedure (2p)*: Tosyl protected amine **27** (60 mg, 0.12 mmol) gave the *title compound* **33** (14 mg, 35 %) as a colourless oil after purification by flash column chromatography (Et_2O); $[\alpha]_D^{25.0}$ +5.00 (*c* 1.00, $CHCl_3$); δ_H (400 MHz, $CDCl_3$) 7.46 (dd, *J* 9.0, 1.0, 2 H, H14), 7.24 - 7.29 (m, 2 H, H15), 6.95 - 7.00 (m, 1 H, H16), 5.07 (br. s., 1 H, H10), 4.51 (br. s., 1 H, H4), 3.93 (t, *J* 8.8, 1 H, H12), 3.68 - 3.75 (m, 1 H, H9), 3.46 (dd, *J* 8.8, 6.3, 1 H, H12'), 3.02 - 3.11 (m, 2 H, H5, H5'), 1.55 - 1.59 (m, 2 H, H8, H8'), 1.44 - 1.50 (m, 2 H, H6, H6'), 1.37 (s, 9 H, H1), 1.29 - 1.35 (m, 2 H, H7, H7'); δ_C (101 MHz, $CDCl_3$) 158.8 (C=O), 156.0 (C=O), 140.0 (C13), 128.8 (C15), 122.6 (C16), 117.7 (C14), 79.2 (C2), 50.9 (C12), 49.0 (C9), 40.2 (C5), 35.6 (C6), 30.3 (C8), 28.4 (C1), 22.4 (C7); HRMS calculated for $C_{18}H_{28}N_3O_3$ $[M+H]^+$: 334.2125, found 334.2119; IR (CH_2Cl_2) 2980, 2948, 2322, 1698, 1558, 1541.

Tosyl-protected Dimer 34

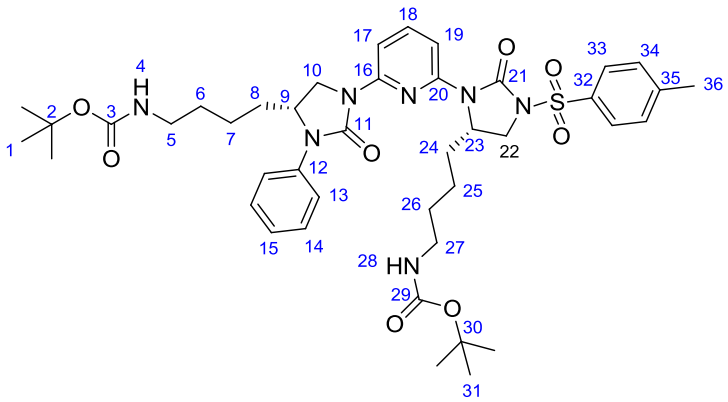

According to *general procedure (2q)*: Amide **33** (14 mg, 0.04 mmol) and bromide **31** (29 mg, 0.05 mmol) gave the *title compound* **34** (21 mg, 61 %) as a colourless oil after purification by flash column chromatography (PE:Et_2O, 1:4); $[\alpha]_D^{25.0}$ +25.4 (*c* 1.00, $CHCl_3$);

δ_H (500 MHz, $CDCl_3$) 7.92 (d, *J* 8.4, 2 H, H13), 7.88 (d, *J* 8.0, 1 H, H17 or H19), 7.67 (d, *J* 7.9, 1 H, H17 or H19), 7.55 (t, *J* 8.0, 1 H, H18), 7.48 - 7.52 (m, 2 H, H33 or H34), 7.25 - 7.33 (m, 4 H, H14, H33 or H34), 7.01 - 7.07 (m, 1 H, H15), 4.91 - 5.00 (m, 1 H, H4 or H28), 4.76 - 4.84 (m, 1 H, H4 or H28), 4.53 - 4.61 (m, 1 H, H9 or H23), 4.32 - 4.39 (m, 1 H, H9 or H23), 4.03 (t, *J* 9.0, 1 H, H10 or H22), 3.98 (t, *J* 9.0, 1 H, H10 or H22), 3.64 - 3.72 (m, 1 H, H10' or H22'), 3.53 (dd, *J* 9.0, 3.0, 1 H, H10' or H22'), 2.96 - 3.06 (m, 4 H, H5, H5', H27, H27'), 2.36 (s, 3 H, H36), 1.97 - 2.04 (m, 1 H, H6 or H26), 1.89 - 1.96 (m, 1 H, H6 or H26), 1.77 - 1.85 (m, 1 H, H6' or H26'), 1.60 - 1.69 (m, 1 H, H6' or H26'), 1.38 - 1.54 (m, 4 H, H8, H8', H24, H24'), 1.36 (s, 9 H, H1 or H31), 1.34 (s, 9 H, H1 or H31), 1.24 - 1.30 (m, 4 H, H7, H7' H25, H25'); δ_C (126 MHz, $CDCl_3$) 156.1 (2C, C3, C29), 154.1 (C11 or C21), 151.3 (C11 or C21), 149.8 (Ar-C), 148.8 (Ar-C), 144.9 (Ar-C), 139.6 (C18), 139.5 (Ar-C), 136.0 (Ar-C), 129.6 (C14 or C33 or C34), 128.9 (C14 or C33 or C34), 128.3 (C13), 123.5 (C15), 118.4 (C33 or C34), 108.9 (C17 or C19), 107.4 (C17 or C19), 79.1 (2C, C2, C30), 53.4 (C9 or C23), 51.3 (C9 or C23), 47.5 (C10 or C22), 46.6 (C10 or C22), 40.4 (2C, C5, C27), 34.8 (C6 or C26), 32.8 (C6 or C26), 30.3 (C8 or C24), 30.0 (C8 or C24), 28.4 (2C, C1, C31), 22.2 (C7 or C25), 21.7 (C36), 21.4 (C7 or C25); HRMS calculated for $C_{42}H_{58}N_7O_8S$ $[M+H]^+$: 820.4062, found 820.4058; IR (CH_2Cl_2) 3015, 3001, 2998, 2963, 1657, 1545.

Deprotected Dimer 35

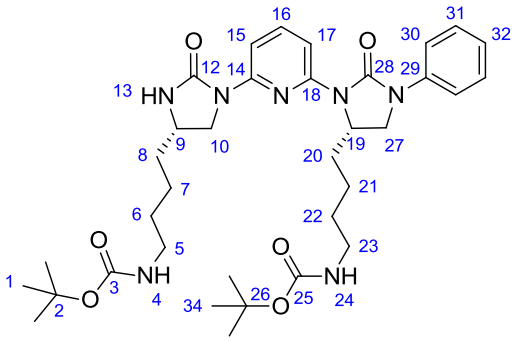

According to *general procedure (2r)*: *N*-nosyl urea **36** (21 mg, 0.025 mmol) gave the *title compound* **35** (16 mg, 96 %) as a pale yellow residue after purification by flash column

chromatography (CH_2Cl_2:MeOH, 9:1); $[\alpha]_D^{23.5}$ +20.7 (*c* 0.10, $CHCl_3$); δ_H (600 MHz, $CDCl_3$) 7.79 (dd, *J* 8.1, 3.9, 1 H, Ar-H), 7.65 - 7.73 (m, 1 H, Ar-H), 7.49 - 7.56 (m, 3 H, Ar-H), 7.30 (t, *J* 7.9, 2 H, Ar-H), 7.00 - 7.06 (m, 1 H, Ar-H), 5.04 (br. s., 1 H, H4 or H24), 4.70 - 4.80 (m, 1 H, H4 or H24), 4.56 - 4.68 (m, 1 H, H19), 4.21 - 4.28 (m, 1 H, H13), 4.16 (t, *J* 9.5, 1 H, H10), 3.99 (t, *J* 8.9, 1 H, H27), 3.66 - 3.75 (m, 1 H, H9), 3.55 - 3.60 (m, 1 H, H10'), 3.53 (dd, *J* 8.9, 3.2, 1 H, H27'), 2.99 - 3.09 (m, 4 H, H5, H5', H23, H23'), 1.84 - 2.02 (m, 2 H, H8, H20), 1.42 - 1.71 (m, 10 H, H6, H6', H7, H7', H8', H20', H21, H21', H22, H22), 1.33 - 1.38 (m, 18 H, H1, H34); (151 MHz, $CDCl_3$) 158.0 (C12 or C28), 156.1 (C12 or C28), 156.1 (C3 or C25), 154.3 (C3 or C25), 150.3, 149.6, 139.8, 139.2, 134.8, 131.7, 128.9, 123.3, 118.3 (9 x Ar-C), 79.1 (2C, C2, C26), 51.2 (C19), 49.6 (C9), 48.8 (C10), 47.5 (C27), 40.4 (C5 or C23), 40.2 (C5 or C23), 35.8 (C8 or C20), 32.8 (C8 or C20), 30.3 (C6 or C22), 29.9 (C6 or C22), 28.4 (C1 or C34), 28.4 (C1 or C34), 22.5 (C7 or C1), 22.0 (C7 or C21); HRMS calculated for $C_{35}H_{52}N_7O_6$ $[M+H]^+$: 666.3974, found 666.3968; IR (CH_3Cl) 3344 (broad), 2923, 2853, 1710, 1522, 1399, 1366.

Nosyl-protected Dimer 36

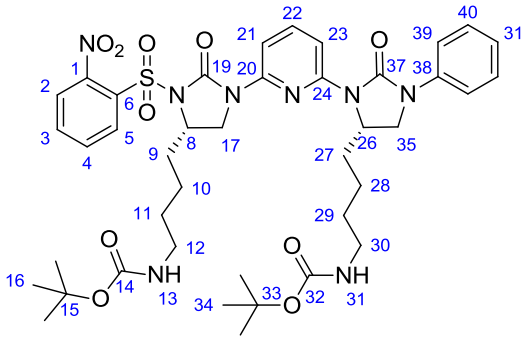

According to *general procedure (2q)*: Amide **33** (20 mg, 0.06 mmol) and bromide **32** (30 mg, 0.05 mmol) gave the *title compound* **36** (20 mg, 47 %) as a yellow residue after purification by flash column chromatography (CH_2Cl_2:MeOH, 9:1); $[\alpha]_D^{23.5}$ -164.0 (*c* 0.10, $CHCl_3$); δ_H (500 MHz, $CDCl_3$) 8.39 - 8.43 (m, 1 H), 7.91 (dd, *J* 6.0, 2.0, 1 H, Ar-H), 7.66 - 7.71 (m, 3 H, Ar-H), 7.53 - 7.56 (m, 2 H, Ar-H), 7.50 (d, *J* 7.9, 2 H, Ar-H), 7.30 (t, *J* 7.9, 2 H, Ar-H),

7.04 (t, *J* 7.4, 1 H, Ar-H), 4.95 - 5.10 (m, 1 H, H13 or H31), 4.72 - 4.83 (m, 1 H, H13 or H31), 4.57 - 4.65 (m, 1 H, H8 or H26), 4.43 - 4.50 (m, 1 H, H8 or H26), 4.25 (t, *J* 9.5, 1 H, H17 or H35), 3.98 (t, *J* 9.0, 1 H, H17 or H35), 3.76 (d, *J* 9.0, 1 H, H17' or H35'), 3.54 (dd, *J* 9.0, 2.9, 1 H, H17' or H35'), 3.01 - 3.10 (m, 4 H, H12, H12', H30, H30'), 1.88 - 2.00 (m, 3 H, 3 of H9, H9', H27, H27'), 1.65 - 1.72 (m, 1 H, 1 of H9, H9', H27, H27'), 1.39 - 1.56 (m, 8 H, H10, H10', H11, H11', H28, H28', H29, H29'), 1.34 - 1.37 (m, 18 H, H16, H34); δ_C (126 MHz, $CDCl_3$) 156.2, 156.1, 154.1, 150.8 (4 x C=O), 150.0, 148.6, 147.9, 139.6, 139.5, 134.9, 134.8, 132.0, 131.7, 128.9, 124.4, 123.5, 118.4, 109.1, 107.2 (15 x Ar-C), 79.1 (C15 or C33), 79.1 (C15 or C33), 54.5 (C8 or C26), 51.3 (C8 or C26), 47.5 (C17 or C35), 47.2 (C17 or C35), 40.4 (2C, C12, C30), 35.8 (C9 or C27), 32.9 (C9 or C27), 30.5 (C11 or C29), 30.3 (C11 or C29), 28.4 (2C, C16, C34), 22.2 (C10 or C28), 21.8 (C10 or C28); HRMS calculated for $C_{41}H_{54}N_8O_{10}SNa$ $[M+Na]^+$: 873.3576 found 873.3554; IR (CH_2Cl_2) 3367 (broad), 2928, 2858, 1709, 1584, 1485.

Boc-Protected Trimer 37

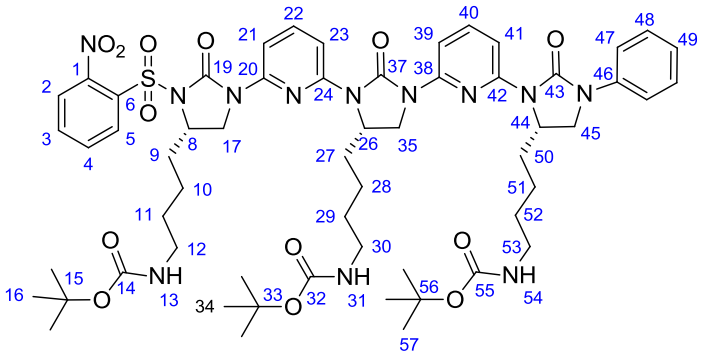

According to *general procedure (2q)*: Amide **36** (20 mg, 0.03 mmol) and bromide **32** (50 mg, 0.05 mmol) gave the *title compound* **37** (20 mg, 56 %) as a yellow residue after purification by flash column chromatography (CH_2Cl_2:MeOH, 9:1); $[\alpha]_D^{25.0}$ +14.0 (*c* 0.5, $CHCl_3$); δ_H (500 MHz, $CDCl_3$) 8.42 (s, 1 H, Ar-H), 7.90 - 7.92 (m, 1 H, Ar-H), 7.88 (d, *J* 8.0, 1 H, Ar-H), 7.84 (d, *J* 7.9, 1 H, Ar-H), 7.70 (d, *J* 1.3, 1 H, Ar-H), 7.69 (br. s., 1 H, Ar-H), 7.67 - 7.68 (m, 1 H, Ar-H), 7.61 (s, 1 H, Ar-H), 7.57 - 7.59 (m, 2 H, Ar-H), 7.53 (d, *J* 7.7, 2 H, Ar-H),

7.32 (d, J 1.1, 2 H, Ar-H), 7.03 - 7.05 (m, 1 H, Ar-H), 5.51 (br. s, 1 H, NH), 5.13 (br. s, 1 H, NH), 4.79 (br. s, 1 H, NH), 4.64 - 4.67 (m, 1 H, H8 or H26 or H44), 4.57 - 4.61 (m, 1 H, H8 or H26 or H44), 4.45 - 4.48 (m, 1 H, H8 or H26 or H44), 4.23 - 4.26 (m, 1 H, H17 or H35 or H45), 4.06 - 4.11 (m, 1 H, H17 or H35 or H45), 4.01 (t, *J* 9.0, 1 H, H17 or H35 or H45), 3.77 (br. d, *J* 9.0, 2 H, 2 of H17', H35', H45'), 3.56 (dd, *J* 9.0, 3.0, 1 H, H17' or H35' or H45'), 3.04 - 3.08 (m, 6 H, H12, H12', H30, H30', H53, H53'), 1.81 - 2.07 (m, 8 H, 8 of H9, H9', H11, H11', H27, H27', H29, H29', H50, H50', H52, H52'), 1.60 - 1.72 (m, 4 H, 4 of H9, H9', H11, H11', H27, H27', H29, H29', H50, H50', H52, H52'), 1.41 - 1.44 (m, 3 H, H10, H28, H51), 1.36 (d, *J* 2.0, 18 H, 2 of H16 or H34 or H57), 1.34 (s, 9 H, H16 or H34 or H57), 1.17 - 1.21 (m, 3 H, H10', H28', H51'); δ_C (126 MHz, $CDCl_3$) 156.4, 156.2, 156.2, 154.2, 153.7, 150.7 (6 x C=O), 149.9, 149.8, 149.7, 148.7, 147.9, 147.6, 139.7, 139.4, 134.9, 134.9, 134.8, 132.1, 131.7, 128.9, 125.5, 124.4, 123.4, 118.4, 109.3, 108.1, 107.5, 107.1 (22 x Ar-C), 79.2 (2C, 2 of C15, C33, C56), 79.0 (C15 or C33 or C56), 54.5 (C6 or C26 or C44), 51.4 (C6 or C26 or C44), 51.2 (C6 or C26 or C44), 47.5 (C17 or C35 or C45), 47.3 (C17 or C35 or C45), 47.1 (C17 or C35 or C45), 40.7 (C12 or C30 or C53), 40.5 (C12 or C30 or C53), 40.4 (C12 or C30 or C53), 35.8 (C9 or C27 or C50), 33.3 (C9 or C27 or C50), 33.0 (C9 or C27 or C50), 30.7 (C11 or C29 or C52), 30.5 (C11 or C29 or C52), 29.9 (C11 or C29 or C52), 28.5 (C16 or C34 or C57), 28.4 (C16 or C34 or C57), 28.4 (C16 or C34 or C57), 22.7 (C10 or C28 or C51), 22.5 (C10 or C28 or C51), 21.8 (C10 or C28 or C51); IR (CH_2Cl_2) 3350 (broad), 2945, 2956, 2844, 1723, 1699, 1535; HRMS calculated for $C_{58}H_{78}N_{12}O_{13}NaS$ $[M+Na]^+$: 1205.5424, found 1205.5432;

Deprotected Trimer 38

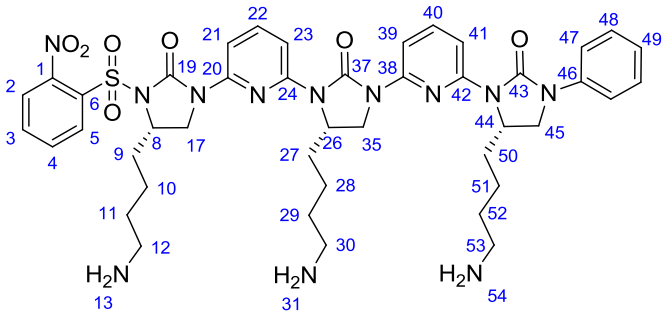

According to *general procedure (2s)*: Boc-protected amine **37** (20 mg, 0.016 mmol) gave the *title compound* **38** (2 mg, 14 %) as a colourless oil after purification by reverse phase HPLC (MeCN:H_2O); $[\alpha]_D^{25.0}$ +11.5 (*c* 0.10, H_2O); δ_H (600 MHz, CD_3OD) 8.35 (d, *J* 7.4, 1 H, H2), 7.80 - 7.87 (m, 4 H, Ar-H), 7.78 (d, *J* 8.4, 1H, Ar-H), 7.77 (d, *J* 7.9, 1 H, Ar-H), 7.68 (td, *J* 8.2, 6.3, 2 H, Ar-H), 7.56 (d, *J* 7.9, 2 H, H47), 7.54 (d, *J* 8.2, 1 H, Ar-H), 7.33 (t, *J* 8.4, 2 H, H48), 7.08 (t, *J* 7.4, 1 H, H49), 4.82 - 4.88 (m, 2 H, H44, 1 of H8 or H28), 4.50 - 4.55 (m, 1 H, H8 or H28), 4.37 (dd, *J* 10.8, 9.2, 1 H, H17 or H35), 4.27 (t, *J* 10.3, 1 H, H17 or H35), 4.14 (t, *J* 9.2, 1 H, H45), 3.80 (td, *J* 8.9, 3.1, 2 H, H17', H35'), 3.69 (dd, *J* 8.9, 3.1, 1 H, H45'), 2.91 - 2.95 (m, 2 H, 2 of H12, H12', H30, H30', H53, H53'), 2.81 - 2.88 (m, 4 H, 4 of H12, H12', H30, H30', H53, H53'), 1.87 - 2.00 (m, 6 H, H9, H9', H27, H27', H50, H50'), 1.70 - 1.77 (m, 2 H, 2 of H11, H11', H29, H29', H52, H52'), 1.63 - 1.69 (m, 2 H, H11, H11', H29, H29', H52, H52'), 1.53 - 1.61 (m, 4 H, 4 of H10, H10', H11, H11', H28, H28', H29, H29', H51, H51', H52, H52'), 1.40 - 1.47 (m, 4 H, 4 of H10, H10', H28, H28', H51, H51'); δ_C (126 MHz, CD_3OD) 154.8 (C=O), 154.2 (C=O), 150.9 (C=O), 150.2 (C20 or C24 or C38 or C42), 150.0 (C20 or C24 or C38 or C42), 149.9 (C20 or C24 or C38 or C42), 149.1 (C20 or C24 or C38 or C42), 148.0 (C1), 139.6 (Ar-C), 139.4 (Ar-C), 139.0 (Ar-C), 135.6 (Ar-C), 134.2 (C2), 131.8 (Ar-C), 130.8 (C6), 128.6 (C48), 124.5 (Ar-C), 123.4 (C49), 118.8 (C47), 109.4 (Ar-C), 108.2 (Ar-C), 107.7 (Ar-C), 107.4 (Ar-C), 54.2 (C8 or C28), 51.2 (C8 or C28), 50.8 (C44), 46.0 (C17 or C35), 39.2 (2C, 2 of C12, C30, C53), 39.1 (C12 or C30 or C53),

35.2 (C9 or C27 or C50), 32.4 (C9 or C27 or C50), 32.2 (C9 or C27 or C50), 27.4 (2C, 2 of C11, C29, C52), 26.8 (C11 or C29 or C52), 20.9 (C10 or C28 or C51), 20.5 (C10 or C28 or C51), 20.4 (C10 or C28 or C51); C45 and C17/35 are obscured by the solvent peak but were identified by HSQC as being at 47.0 and 47.4 respectively; LRMS calculated for $C_{43}H_{55}N_{12}O_7S$ $[M+H]^+$: 883.4 found 883.4; IR (CH_2Cl_2) 3420 (broad), 2928, 2465 (broad), 1582, 1484, 1450.

2.14.4 X-Ray Crystallography

Low temperature[44] single crystal X-ray diffraction studies were carried out on **14** using MoK_α radiation on a Nonius Kappa CCD diffractometer equipped with an area detector and graphite monochromator, within the University of Oxford Chemistry Department. Data for **19** were collected using Beamline I19(EH1) at Diamond Light Source.[45] Raw frame data were reduced using CrysAlisPRO [CrysAlisPRO, Oxford Diffraction /Agilent Technologies UK Ltd, Yarnton, England.] (for **19**) and DENZO/SCALEPACK[46] and the structures were solved using SIR92[47] (for **7**) or SuperFlip.[48] Full-matrix least-squares refinement of the structures were carried out using CRYSTALS.[49,50] Compound **19** was found to be twinned by rotation about the *a* axis.[51] Full refinement details are given in the supplementary material (CIF). Crystallographic data (excluding structure factors) have been deposited with the Cambridge Crystallographic Data Centre (CCDC 1030066-9) and copies of these data can be obtained free of charge *via* www. ccdc.cam.ac.uk/data_request/cif.

Single-crystal X-ray diffraction data for two-residue mimic 14 (CCDC 1030068)

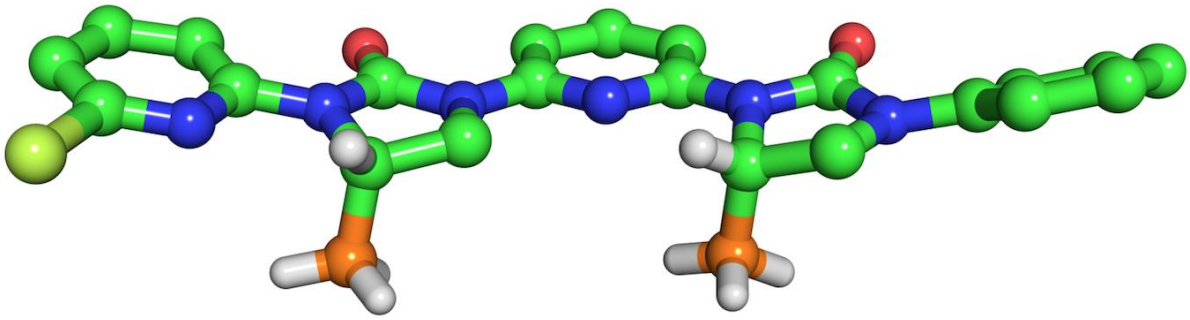

Crystal Data

a = 11.99400(10) Å α = 90°
b = 18.01090(10) Å β = 90°
c = 20.5992(2) Å γ = 90°

Volume	4449.90(6) Å^3	*Crystal Class*	orthorhombic
Space group	P 2_1 2_1 2_1	*Z* =	8
Formula	C_{24} H_{23} Cl_1 N_6 O_2	M_r	462.94
Cell determined from	19908 reflections	*Cell θ range* =	5 - 27°
Temperature	150K		
Shape	needle		
Colour	clear_pale_colourless	*Size*	0.18 × 0.24 × 0.42 mm
D_x	1.38 Mg m^{-3}	*F000*	1936.000

μ	0.207 mm^{-1}		
Absorption correction	multi-scan		
T_{min}	0.88	T_{max}	0.96

Data Collection

Diffractometer	multi-scan
Scan type	ω scans
Reflections measured	105496
Independent reflections	10151
Rint	0.0573
θ_{max}	27.5198
h =	-15 → 15
k =	-23 → 23
l =	-26 → 26

Refinement

$\Delta\rho_{min}$ =	-0.23 e $Å^{-3}$
$\Delta\rho_{max}$ =	0.31 e $Å^{-3}$
Reflections used	10151
Cutoff: I >	-3.00σ(I)
Parameters refined	596
S =	0.99
R-factor	0.044
weighted R-factor	0.069
Δ/σ_{max}	0.0007
Flack parameter	-0.07(4)
Refinement on	F^2
w =	$w' \times [1 - (\Delta F_{obs} / 6 \times \Delta F_{est})^2]^2$
w′ =	$[P_0T_0'(x) + P_1T_1'(x) + ...P_{n-1}T_{n-1}'(x)]^{-1}$, where P_i are the coefficients of a Chebychev series in $t_i(x)$, and $x = F_{calc}^2/F_{calc}^2{}_{max}$.

Single-crystal X-ray diffraction data for three-residue mimic 19 (CCDC 1030069)

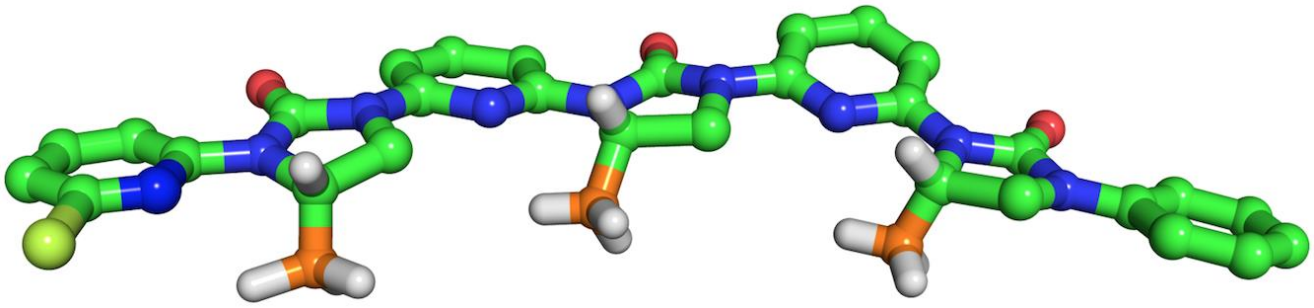

Crystal Data

a = 7.3961(2) Å α = 90°
b = 26.2836(8) Å β = 95.017(2)°
c = 15.8744(4) Å γ = 90°

Volume	3074.10(15) Å^3	*Crystal Class*	monoclinic
Space group	P 2_1	*Z* =	4
Formula	C_{33} H_{32} Cl_1 N_9 O_3	M_r	638.13
Cell determined from	16129 reflections	*Cell θ range* =	2 - 26°
Temperature	120K		
Shape	needles		
Colour	clear_pale_colourless	*Size*	0.01 × 0.02 × 0.05 mm
D_x	1.38 Mg m^{-3}	*F000*	1336.000
μ	0.176 mm^{-1}		
Absorption correction	multi-scan		
T_{min}	0.76	T_{max}	1.00

Data Collection

Diffractometer	multi-scan
Scan type	ω scans
Reflections measured	27824
Independent reflections	11323
Rint	0.0490
θ_{max}	26.1930
h =	-9 → 9
k =	-28 → 32
l =	-19 → 19

Refinement

$\Delta\rho_{min}$ =	-1.17 e Å^{-3}
$\Delta\rho_{max}$ =	0.95 e Å^{-3}
Reflections used	11278
Cutoff: I >	-3.00σ(I)
Parameters refined	830
S =	0.95
R-factor	0.089
weighted R-factor	0.217
Δ/σ_{max}	0.0011
Refinement on	F^2
w =	$w' \times [1 - (\Delta F_{obs} / 6 \times \Delta F_{est})^2]^2$
w′ =	$[P_0T_0'(x) + P_1T_1'(x) + ...P_{n-1}T_{n-1}'(x)]^{-1}$, where P_i are the coefficients of a Chebychev series in $t_i(x)$, and $x = F_{calc}^2/F_{calc}^2{}_{max}$.

2.15 References

1. Fairlie, D. P. *et al.* Conformational Selection of Inhibitors and Substrates by Proteolytic Enzymes: Implications for Drug Design and Polypeptide Processing. *J. Med. Chem.* **43,** 1271–1281 (2000).

2. Brown, J. H. *et al.* Three-dimensional structure of the human class II histocompatibility antigen HLA-DR1. *Nature* **364,** 33–39 (1993).

3. Qian, Y. *et al.* Design and structural requirements of potent peptidomimetic inhibitors of p21ras farnesyltransferase. *J. Biol. Chem.* **269,** 12410–12413 (1994).

4. Somers, W. S. & Phillips, S. E. V. Crystal structure of the met represser–operator complex at 2.8 Å resolution reveals DNA recognition by β-strands. *Nature* **359,** 387–393 (1992).

5. Leung, D., Abbenante, G. & Fairlie, D. P. Protease Inhibitors: Current Status and Future Prospects. *J. Med. Chem.* **43,** 305–341 (2000).

6. Loughlin, W. A., Tyndall, J. D. A., Glenn, M. P. & Fairlie, D. P. β-Strand Mimetics. *Chem. Rev.* **104,** 6085–6118 (2004).

7. Nassar, N. *et al.* The 2.2 Å crystal structure of the Ras-binding domain of the serine/threonine kinase c-Raf1 in complex with RaplA and a GTP analogue. *Nature* **375,** 554–560 (1995).

8. Tyndall, J. D. A. *et al.* Synthesis, Stability, Antiviral Activity, and Protease-Bound Structures of Substrate-Mimicking Constrained Macrocyclic Inhibitors of HIV-1 Protease. *J. Med. Chem.* **43,** 3495–3504 (2000).

9. Blackwell, H. E., Grubbs, R. H. Highly Efficient Synthesis of Covalently Cross-Linked Peptide Helices by Ring-Closing Metathesis. *Angew. Chem. Int. Ed.* **37,** 3281-3284 (1998).

10. Schafmeister, C. E., Po, J., Verdine, G. L. An All-Hydrocarbon Cross-Linking System for Enhancing the Helicity and Metabolic Stability of Peptides. *J. Am. Chem. Soc.* **122,** 5891-5892 (2000).

11. Casey, P. J., Solski, P. A., Der, C. J. & Buss, J. E. p21ras is modified by a farnesyl isoprenoid. *Proc. Natl. Acad. Sci.* **86,** 8323–8327 (1989).

12. Goldstein, J. L., Brown, M. S., Stradley, S. J., Reiss, Y. & Gierasch, L. M. Nonfarnesylated tetrapeptide inhibitors of protein farnesyltransferase. *J. Biol. Chem.* **266,** 15575–15578 (1991).

13. Santagada, V. *et al.* Synthesis, Pharmacological Evaluation, and Molecular Modeling Studies of Novel Peptidic CAAX Analogues as Farnesyl-Protein-Transferase Inhibitors. *J. Med. Chem.* **49,** 1882–1890 (2006).

14. Tsai, J. H., Waldman, A. S. & Nowick, J. S. Two New β-strand Mimics. *Bioorg. Med. Chem.* **7,** 29–38 (1999).

15. Song, M., Rajesh, S., Hayashi, Y. & Kiso, Y. Design and synthesis of new inhibitors of HIV-1 protease dimerization with conformationally constrained templates. *Bioorg. Med. Chem. Lett.* **11,** 2465–2468 (2001).

16. Hammond, M. C., Harris, B. Z., Lim, W. A. & Bartlett, P. A. β Strand Peptidomimetics as Potent PDZ Domain Ligands. *Chem. Biol.* **13,** 1247–1251 (2006).

17. Smith, A. B. *et al.* De Novo Design, Synthesis, and X-ray Crystal Structures of Pyrrolinone-Based .beta.-Strand Peptidomimetics. *J. Am. Chem. Soc.* **116,** 9947–9962 (1994).

18. Smith, A. B. *et al.* Pyrrolinone-Based HIV Protease Inhibitors. Design, Synthesis, and Antiviral Activity: Evidence for Improved Transport. *J. Am. Chem. Soc.* **117,** 11113–11123 (1995).

19. Lyle, T. A. *et al.* Benzocycloalkyl amines as novel C-termini for HIV protease inhibitors. *J. Med. Chem.* **34,** 1228–1230 (1991).

20. Remaut, H. & Waksman, G. Protein–protein interaction through β-strand addition. *Trends Biochem. Sci.* **31,** 436–444 (2006).

21. Wyrembak, P. N. & Hamilton, A. D. Alkyne-Linked 2,2-Disubstituted-indolin-3-one Oligomers as Extended β-Strand Mimetics. *J. Am. Chem. Soc.* **131,** 4566–4567 (2009).

22. Jamieson, A. G., Russell, D. & Hamilton, A. D. A 1,3-phenyl-linked hydantoin oligomer scaffold as a β-strand mimetic. *Chem. Commun.* **48,** 3709–3711 (2012).

23. Sutherell, C. L., Thompson, S., Scott, R. T. W. & Hamilton, A. D. Aryl-linked imidazolidin-2-ones as non-peptidic beta-strand mimetics. *Chem. Commun.* **48,** (2012).

24. Malone, J. F., Murray, C. M., Dolan, G. M., Docherty, R. & Lavery, A. J. Intermolecular Interactions in the Crystal Chemistry of N,N‘-Diphenylisophthalamide, Pyridine-2,6-dicarboxylic Acid Bisphenylamide, and Related Compounds. *Chem. Mater.* **9,** 2983–2989 (1997).

25. *Molecular Operating Environment (MOE)*, 2013.08; Chemical Computing Group Inc., 1010 Sherbrooke St. West, Suite 910, Montreal, QC, Canada, H3A 2R7, **2016**..

26. *MMFF94x Force Field with 10,000 rejections, and RMS gradient of 0.005, an RMSD limit of 0.25 and an MM Iteration Limit of 500. Computed with water as an implicit solvent.*

27. Verheij, M. H. P. *et al.* Design, Synthesis, and Structure–Activity Relationships of Highly Potent 5-HT3 Receptor Ligands. *J. Med. Chem.* **55,** 8603–8614 (2012).

28. Bajpai, R. & Curran, D. P. Synthesis and Spectroscopic Analysis of a Stereoisomer Library of the Phytophthora Mating Hormone α1 and Derived Bis-Mosher Esters. *J. Am. Chem. Soc.* **133,** 20435–20443 (2011).

29. Shepard, M. S. & Carreira, E. M. Asymmetric Photocycloadditions with an Optically Active Allenylsilane: Trimethylsilyl as a Removable Stereocontrolling Group for the Enantioselective Synthesis of exo-Methylenecyclobutanes. *J. Am. Chem. Soc.* **119,** 2597–2605 (1997).

30. Muci, A. R. & Buchwald, S. L. in *Cross-Coupling Reactions* (ed. Miyaura, P. N.) 131–209 (Springer Berlin Heidelberg, 2002).

31. McDonald, C. G. & Shannon, J. S. Selective poisoning of palladium-catalysed hydrogen-exchange reactions. *Tetrahedron Lett.* **4,** 1349–1351 (1963).

32. Kung, P.-P. *et al.* Structure activity relationships of quinoline-containing c-Met inhibitors. *Eur. J. Med. Chem.* **43,** 1321–1329 (2008).

33. Weikl, T. R. & von Deuster, C. Selected-fit versus induced-fit protein binding: kinetic differences and mutational analysis. *Proteins* **75,** 104–110 (2009).

34. Terada, T. *et al.* Nuclear magnetic resonance and molecular dynamics studies on the interactions of the ras-binding domain of raf-1 with wild-type and mutant ras proteins 1. *J. Mol. Biol.* **286,** 219–232 (1999).

35. Vuljanic, T., Bergquist, K.-E., Clausen, H., Roy, S. & Kihlberg, J. Piperidine is preferred to morpholine for Fmoc cleavage in solid phase glycopeptide synthesis as exemplified by preparation of glycopeptides related to HIV gp120 and mucins. *Tetrahedron* **52,** 7983–8000 (1996).

36. Yamashita, T., Knipe, P. C., Busschaert, N., Thompson, S. & Hamilton, A. D. A Modular Synthesis of Conformationally Preorganised Extended β-Strand Peptidomimetics. *Chem. Eur. J.* **21,** 14699–14702 (2015).

37. Knipe, P. C., Thompson, S. & Hamilton, A. D. Manuscript Accepted. doi: 10.1039/c6cc01496h.

38. Lin, K., Kwong, A. D. & Lin, C. Combination of a Hepatitis C Virus NS3-NS4A Protease Inhibitor and Alpha Interferon Synergistically Inhibits Viral RNA Replication and Facilitates Viral RNA Clearance in Replicon Cells. *Antimicrob. Agents Chemother*. **48,** 4784–4792 (2004).

39. Kovacs, P. *et al.* The role of insulin receptor substrate-1 gene (IRS1) in type 2 diabetes in Pima Indians. *Diabetes* **52,** 3005–3009 (2003).

34. Malmanche, N., Maia, A. & Sunkel, C. E. The spindle assembly checkpoint: Preventing chromosome mis-segregation during mitosis and meiosis. *FEBS Lett.* **580,** 2888–2895 (2006).

41. Srivastava, R. K. *et al.* The RIIβ regulatory subunit of protein kinase A binds to cAMP response element: An alternative cAMP signaling pathway. *Proc. Natl. Acad. Sci. U. S. A.* **95,** 6687–6692 (1998).

42. Flynn, D. L., Zelle, R. E. & Grieco, P. A. A mild two-step method for the hydrolysis of lactams and secondary amides. *J. Org. Chem.* **48,** 2424–2426 (1983).

43. Aaseng, J. E. & Gautun, O. R. Synthesis of substituted (S)-2-aminotetralins via ring-opening of aziridines prepared from l-aspartic acid β-tert-butyl ester. *Tetrahedron* **66,** 8982–8991 (2010).

44. Cosier, J., & Glazer, A. M. A nitrogen-gas-stream cryostat for general X-ray diffraction studies. *J. Appl. Cryst.***19,** 105-107 (1986).

45. Nowell, H., Barnett, S. A., Christensen, K. E., Teat, S. J., Allan, D. R. I19, the small-molecule single-crystal diffraction beamline at Diamond Light Source. *J. Synchotron Rad*. **19,** 435-431 (2012).

46. Otwinowski, Z. & Minor, W. in *Methods in Enzymology* (ed. Carter, C. W. & Sweet, R. M.) (Academic Press, 1997).

47. Altomare, A., Cascarano, G., Giacovazzo, C., Guagliardi, A., Burla, M. C., Polidori, G., Camalli, M. *SIRPOW*.92 - a program for automatic solution of crystal structures by direct methods optimized for powder data. *J. Appl. Cryst.* **27,** 435-436 (1994).

48. Palatinus, L. & Chapuis, G. *SUPERFLIP* - a computer program for the solution of crystal structures by charge flipping in arbitary dimensions. *J. Appl. Cryst*. **40,** 786-790 (2007).

49. Betteridge, P. W., Carruthers, J. R., Cooper, R. I., Prout, K., Watkin, D. J., *CRYSTALS* version 12: software for guided crystal analysis. *J. Appl. Cryst.* **36,** 1487 (2003).

50. Cooper, R. I., Thompson, A. L., Watkin, D. J. *CRYSTALS* enhancements: dealing with hydrogen atoms in refinement. *J. Appl. Cryst.* **43,** 1100-1107 (2010).

51. Cooper, R. I., Gould, R. O., Parsons, S., Watkin, D. J. The derivation of non-merohedral twin laws during refinement by analysis of poorly fitting intensity data and the refinement of non-merohedrally twinned crystal structures in the program *CRYSTALS*. *J. Appl. Cryst.* **35,** 168-174 (2002).

Chapter 3 - β-Sheet Mimetics

3.1 β-Sheets in Nature

The edge-to-edge hydrogen bonding between two or more β-strands (Chapter 2) creates a β-sheet. This hydrogen bonding places the Cα's of adjacent strands 4.7 – 4.8 Å apart with a residue length of 3.3 – 3.5 Å.[1] This residue length is slightly shorter than the corresponding distance in an ideal β-strand highlighting the ability of the main chain to move away from the fully extended conformation to accommodate sheet formation. The inter-strand hydrogen bonds that stabilise the sheet structure are between 1.9 and 2.3 Å in length. The strands can arrange themselves in parallel or anti-parallel alignments (Figure 3.1).

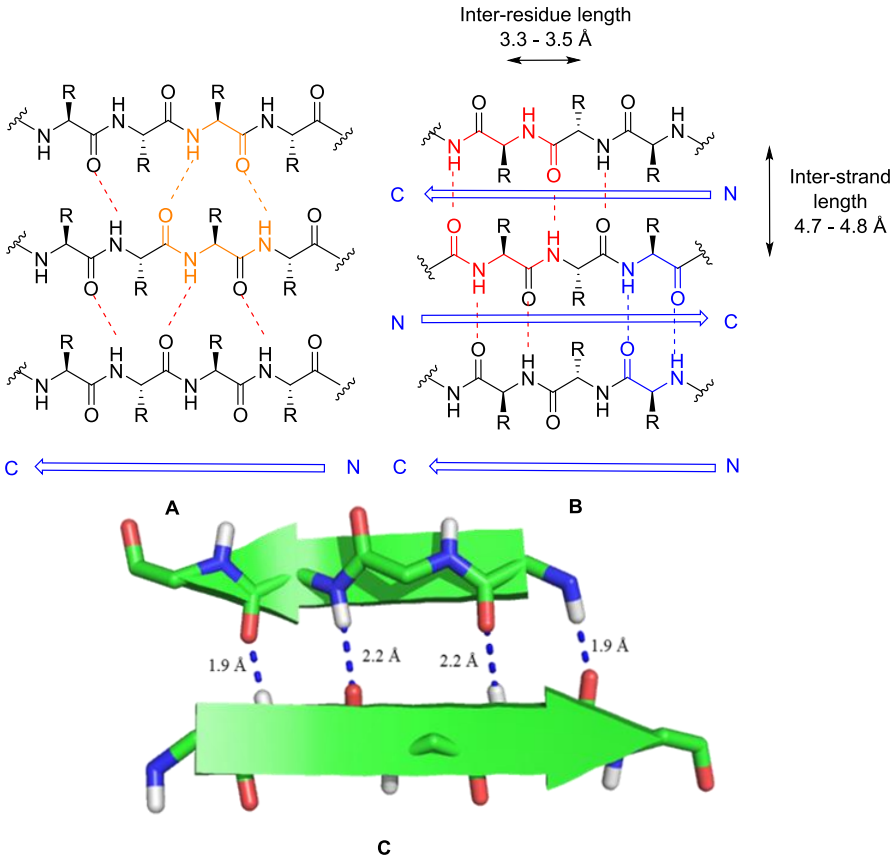

Figure 3.1 **A**: Parallel β-sheet, 12-membered hydrogen-bonded ring shown in orange. **B**: Anti-parallel β-sheet, 14-membered hydrogen bonded ring shown in red, 10-membered hydrogen bonded ring shown in blue. **C**: Crystal structure of anti-parallel β-sheet showing hydrogen bond lengths (PDB: 1IL8).

Parallel sheets contain only twelve-membered hydrogen-bonded rings whereas anti-parallel sheets alternate between ten and fourteen-membered rings. It is generally thought that the anti-parallel arrangement is more stable due to better amide and carbonyl alignment for hydrogen bond formation.[2] Mixed sheets of parallel and anti-parallel strands are also found.[3] Sheets can be formed from a contiguous sequence connected by a β-turn or hairpin units, or from stretches of peptide far apart in sequence or from two entirely different peptides.

The β-sheet is a structural motif frequently used in Nature, and as such is found in key structural proteins such as spider silk fibroin.[4] They are also constituent parts of complex architectures and super-secondary structures such as the β-barrel, a key motif in many membrane proteins[5] and molecular transporters,[6] and the β-propeller (Figure 3.2).

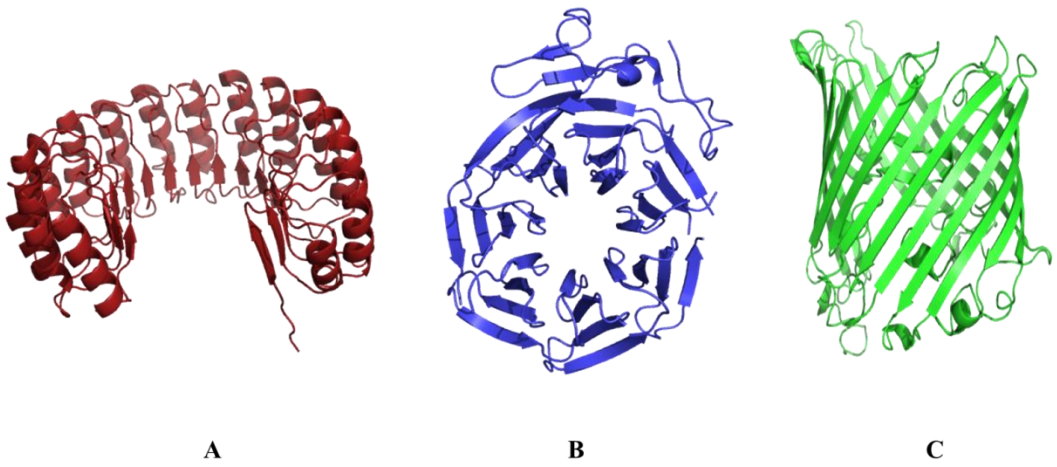

Figure 3.2 **A**: Crystal structure of the placental ribonuclease inhibitor showing a ring of parallel β-sheets (PDB:1A4Y).[7] **B**: Crystal structure of the C-terminal domain of Tup1, a compressor transcriptor in yeast showing the β-propeller motif (PDB: 1ERJ).[8] **C**: Crystal structure of the sucrose-specific porin ScrY from Salmonella typhimurium showing the β-barrel motif (PDB: 1A0S).[9]

β-Sheets play roles beyond that of a rigid wall however, with their interactions involved in processes ranging from electron transfer[10] and protein dimerization[11] to recognition by proteolytic enzymes.[12] They are also heavily implicated in a number of pathologies, and in particular amyloid based diseases.

3.2 The Trouble with β-Sheets

The structure of β-strands may be simple, but forcing two or more of them together to form a β-sheet is a non-trivial exercise. In contrast to α-helices, a relatively stable secondary structure which is readily accommodated by small peptides,[13–15] β-sheets are somewhat reluctant to form stable monomers in solution. This is due to low stability, tendency to aggregate, and the poor solubility of peptides likely to form sheets given their high hydrophobic residue content.[16] β-Sheet propensity and the stability of β-sheets will be discussed fully in Chapter 5.

There has been success in the design of peptides that can form a β-sheet in an aqueous environment, but these are rarely fully folded in solution and are therefore difficult to study.[17–19] This has prompted the design and study of artificial β-sheets to better understand sheet formation, and for application in materials engineering[20] and the biomedical field.[21]

3.3 Artificial β-Sheets

The development of artificial β-sheets has been advanced through the implementation of three different strategies; the incorporation of unnatural turn inducing elements to force two peptide strands into proximity, the use of rigidifying linkers to force a strand into the extended conformation and assert the correct hydrogen bonding pattern, and the modification of the peptide chain to prevent aggregation. Much of the early work focused on creating sheets in organic solvents such as chloroform or dichloromethane, whilst more recent efforts have found solutions for folding in the more demanding aqueous environment.

3.3.1 Early Turn Inducers

In 1986, Feigel was the first to use a rigid aromatic template to align two peptide strands and create an artificial β-sheet.[22] By combining an artificial linker with a tripeptide the researchers were able to create a macrocycle that adopted the correct hydrogen bonding

pattern for an antiparallel β-sheet (Figure 3.3). The conformation was probed *via* ^{1}H NMR NOE studies and variable temperature NMR in DMSO-d_6.

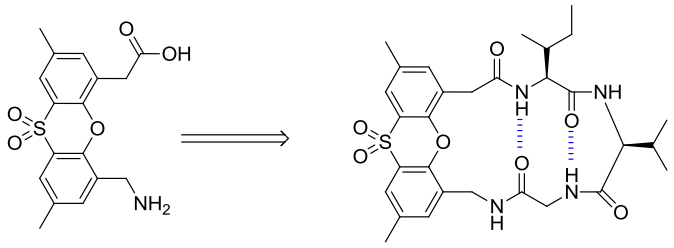

Figure 3.3 Unnatural rigid amino acid used to template a peptide macrocycle into a β-sheet formation with two intermolecular hydrogen bonds.

Subsequent work was able to incorporate two templating groups to form the macrocycle (Figure 3.4).[23,24] Interestingly both molecules are prone to inversions of the marcocyclic ring at room temperature, creating broad NMR signals and therefore the NOE experiments had to be conducted at -61°C for the signals to be resolved.

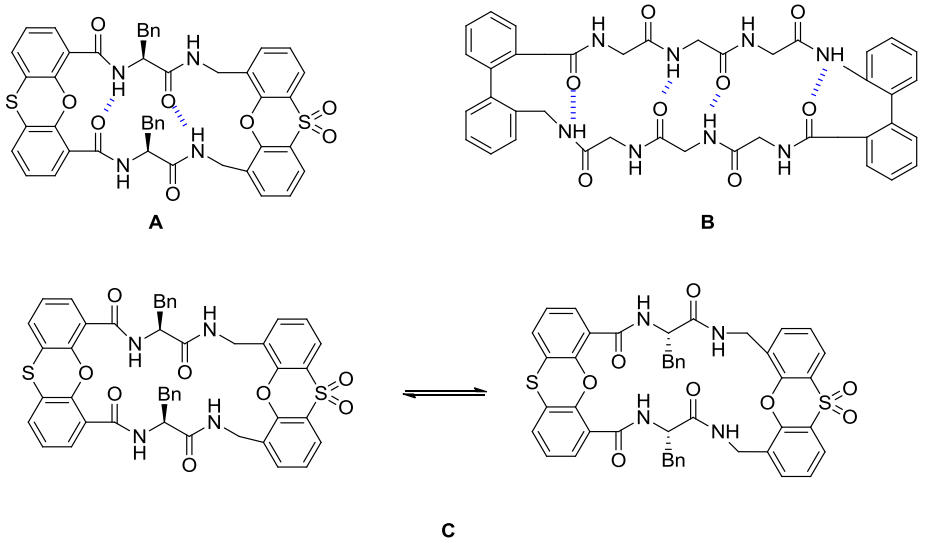

Figure 3.4 Feigel's use of two templating units to form parallel (**A**) and anti-parallel (**B**) artificial β-sheets. **C**: Inversion of macrocyclic ring at room temperature leading to broad NMR signals.

Numerous other templates were developed for studies within organic solvents, including the *trans*-alkene of Gellman,[25] Kemp's diphenylacetylene,[26] and the $Ru(bpy)_3^{2+}$ complex of Ogawa (Figure 3.5).[27]

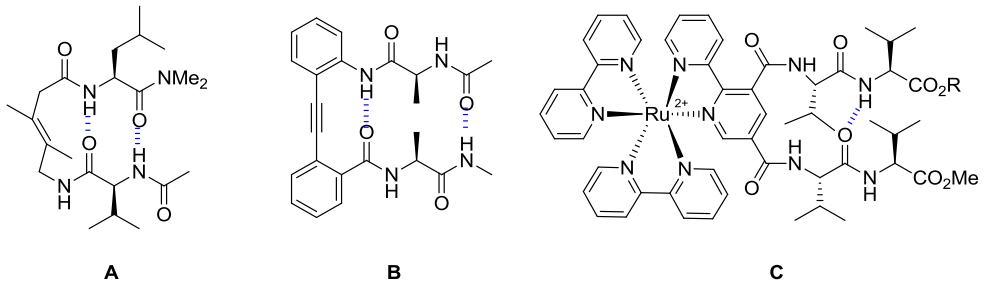

Figure 3.5 **A**: *trans*-Alkene turn inducer. **B**: Diphenylacetylene turn inducer. **C**: $Ru(bpy)_3^{2+}$ turn inducer.

3.3.1.1 Turn Inducers as Biological Tools

The two-stranded β-sheet, or β-hairpin is an extremely common motif in the mediation of molecular recognition between proteins. These early turn inducers therefore presented the ideal opportunity for the design of 'protein epitope mimics', through the insertion of a template into an otherwise natural peptide sequence (Figure 3.6). Robinson has been a pioneer in this field and has used a variety of templates to mimic antibody loops,[28–30] antimicrobial and antiviral peptides,[31–33] and to target proteases,[34] p53/MDM2,[35] and protein/RNA interactions.[36] In some of these interactions the hairpin epitope is used to mimic other secondary structures, such as α-helices.[37]

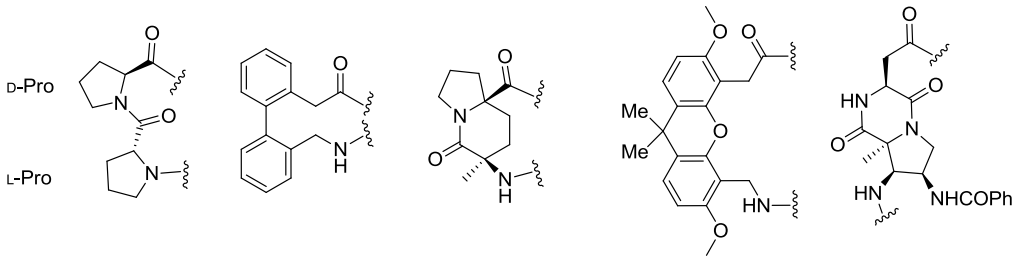

Figure 3.6 Turn inducers used by Robinson to synthesise hairpin motifs for use against a variety of biological targets.

This strategy has proved successful as these templating units are extremely easy to incorporate into vast libraries of macrocyclic peptides through late stage incorporation after a conventional solid phase peptide synthesis.

However, little has been done to study the exact nature of folding within this class of molecules to prove a β-sheet conformation, or to extend them to incorporate more than two peptide strands.

3.3.2 The Use of Turn Inducers and Rigidfying Units

Kemp first generated a three-stranded sheet mimic *via* the incorporation of an epindolidione β-strand mimetic connected by two Pro-D-Ala turns and urea linking groups (Figure 3.7).[38–40] The epindolidione motif, as an elongated aromatic system adds rigidity to one of the strands and pre-organises some of the hydrogen bonding. The researchers showed extensive solution and solid phase data to confirm sheet conformation and the scaffold demonstrated the same β-sheet propensities for different amino acids as observed in natural proteins.

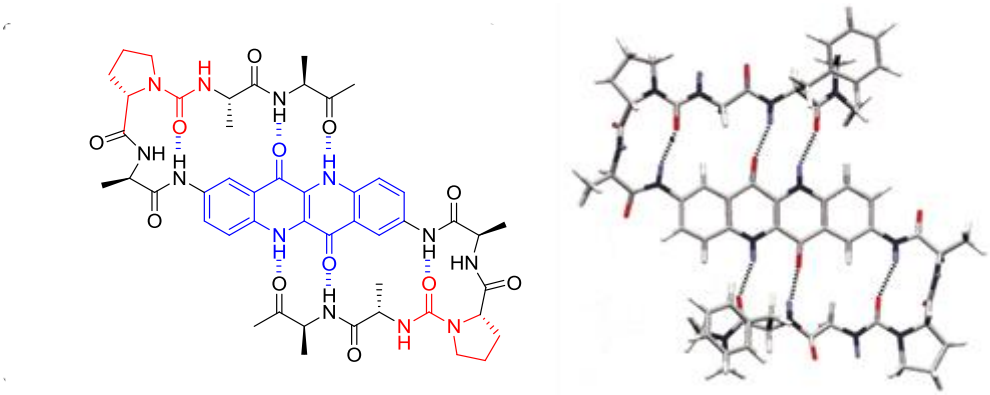

Figure 3.7 Templation of a three-stranded β-sheet by an epindolidione strand mimic (blue) and turn inducers (red). Figure of crystal structure adapted from 'Artificial β-Sheets'[21] with permission from the Royal Society of Chemistry.

Nowick used the *Hao* motif, composed of a **H**ydrazine, 5-**A**mino-2-methoxybenzoic acid and an **O**xalic acid, in his construction of three-stranded sheets templated by an oligourea scaffold (Figure 3.8).[41] He envisioned the ability to create large sheets using this strategy and was able to show that two stranded versions of this structure could dimerize in solution.[42] However these templated sheets teetered on the edge of equilibrium with an unfolded state, an indication that the sheet conformation is not rigidly enforced.

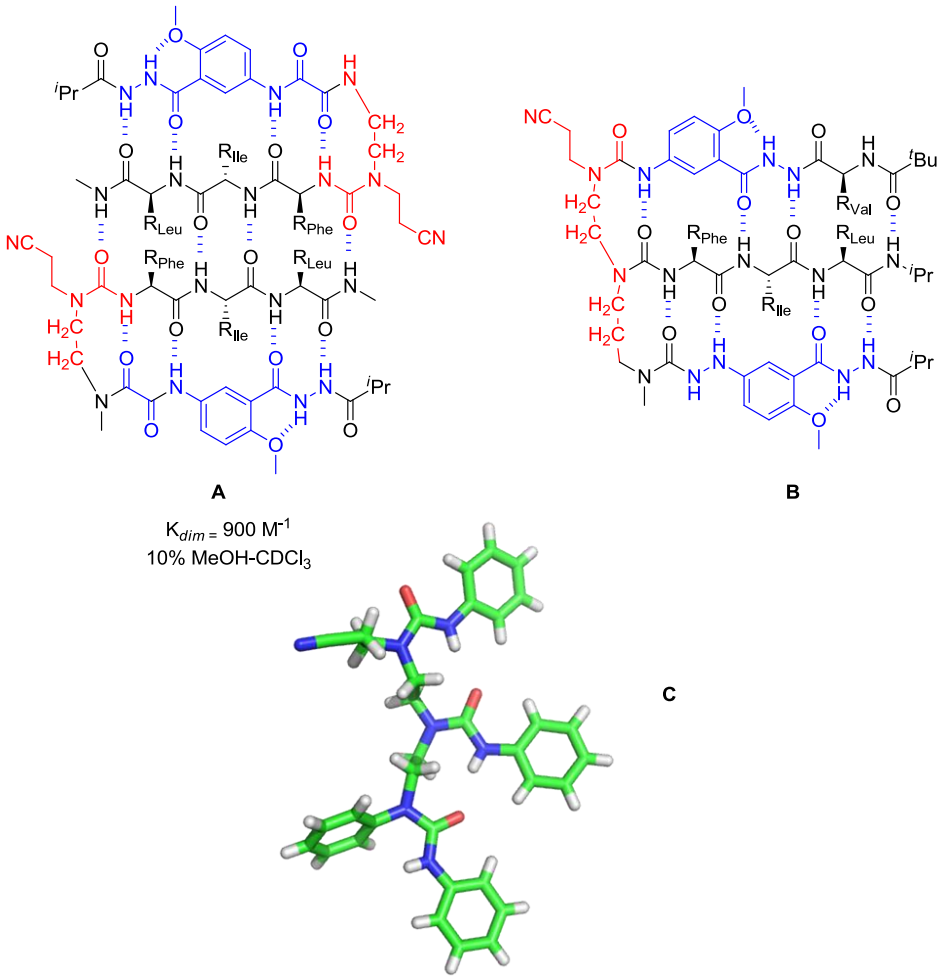

Figure 3.8 **A**: Two-stranded artificial sheet dimerizing in solution. **B**: Three-stranded sheet templated by an oligourea scaffold. Rigidfying strand mimetic shown in blue, oligourea turn linker shown in red. **C**: Crystal structure of the tri-urea scaffold projecting phenyl groups in place of peptide strands (CCDC: ZOTGAQ).

3.3.3 Use of a Central Template

An alternative strategy is to insert the linking template in the middle of the two-strands and thus have control over bi-directional sheet formation. Gellman looked to adopt such an approach through the formation of inter-strand disulfide bonds between cysteine side-chains.[43] Such bonds linking two together strands are rare in Nature, primarily due to the reduction of the disulfide bond under physiological conditions, but when formed do stabilize parallel β-sheets. However, this can only occur in one direction as the accommodation of the covalent disulfide bond forces the strand out of the extended conformation (Figure 3.9).

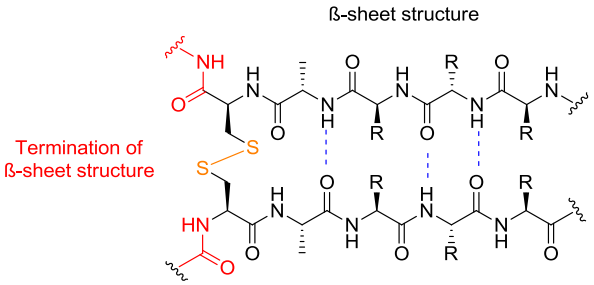

Figure 3.9 Representation of the termination of β-sheet structure by a disulfide bond.

Hamilton *et al*. were able to adapt the diphenylacetylene motif developed by Kemp to template the sheet in two directions.[44] Crystal structures and H/D exchange provided proof of principle for all alanine residues (Figure 3.10), whilst incorporation of hydrophilic residues showed that conformation was maintained in mixed DMSO/aqueous environments.

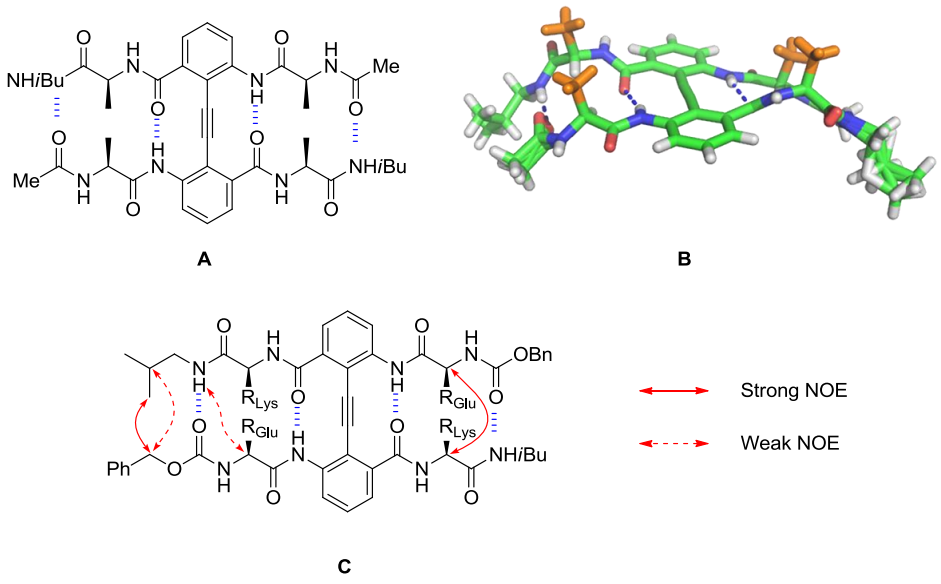

Figure 3.10 **A**: Bidirectional sheet formation templated by the diphenylacetylene motif. **B**: Crystal structure of **A** with display of side-chain highlighted in orange (CCDC: 915931). **C**: Incorporation of hydrophilic side-chains and observed NOE's in a mixed DMSO/aqueous environment.

3.3.4 Extension into aqueous solvents

Early work by Nowick showed the challenge of moving into more competitive solvents. He examined the folding of a urea-templated sheet in chloroform, methanol, 50 % aqueous methanol and DMSO. The interstrand NOEs detected in chloroform were reduced in number

and intensity in methanol and aqueous methanol, and all but disappeared in DMSO. They were replaced by short range interactions around the urea group that were inconsistent with the adoption of a sheet conformation (Figure 3.11).[45]

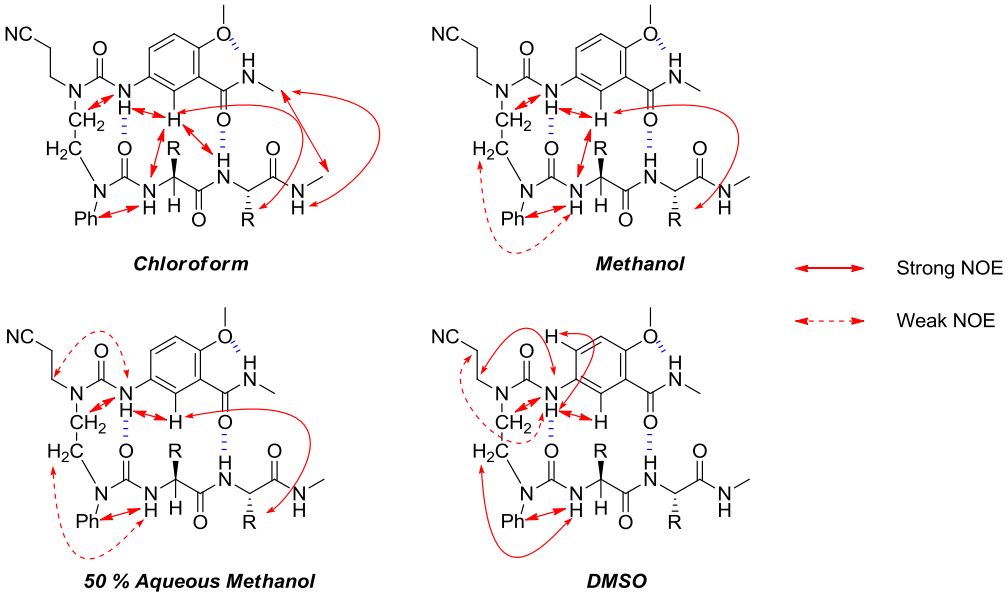

Figure 3.11 NOEs observed on a urea-templated sheet mimic in a variety of solvents.

3.3.4.1 Use of the Hydrophobic Effect

In attempting to design sheets that can successfully maintain conformation in a competitive solvent, Kelly adopted a similar approach to Feigel, Kemp and others by using an aromatic turn inducer to bring the strands closer together. However, rather than using two templates or macrocyclisation as a tool to enforce sheet formation across the whole molecule, he used the hydrophobic effect to keep the strands together. The group synthesised a series of different peptides on the same dibenzofuran template to probe the effect of creating a hydrophobic cluster. The sheet characteristics were probed by FT-IR, variable temperature NMR and X-ray crystallography and their result confirmed that incorporation of a hydrophilic residue such as lysine (**C**) or a smaller residue such as alanine (**B**) disrupts sheet formation (Figure 3.12).[46]

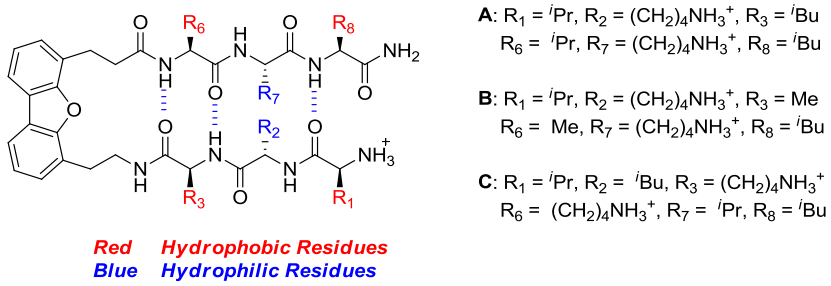

Figure 3.12 Exploration of the effect of hydrophobic clusters on sheet formation in aqueous solution when templated by a dibenzofuran linker.

3.3.4.2 Avoiding Aggregation

Further developing this work, Kelly developed a series of turn templates that were found to aggregate extensively. However, modification of the peptide chain to include *N*-methyl groups prevented the main chain from forming intermolecular hydrogen bonds, inhibiting aggregation (Figure 3.13).[47,48]

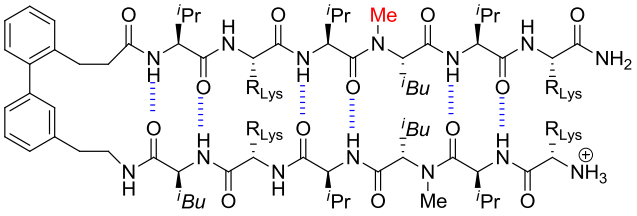

Figure 3.13 *N*-methylation (highlighted in red) prevents aggregation of a β-sheet stabilized by an aromatic linker and a hydrophobic cluster.

Lengyel and Horne have used a similar backbone modification strategy to design an artificial β-sheet.[49] Using β-amino acids and building on the well-established α→β substitution rules for helix mimicry,[50,51] they developed a strategy for the stabilisation of a sheet conformation in water. Although the work presented was for a model peptide, there is a fantastic opportunity to extend the work to substitution in a complete protein and thus build towards the design and modification of tertiary structure.

Gellman has used *cis*-1,2-cyclohexanedicarboxylic acid as a parallel sheet promoter. Using protonated basic residues such as lysine to avoid aggregation, the compounds showed excellent sheet behaviour in water, as deduced by NOE experiments (Figure 3.14).[52]

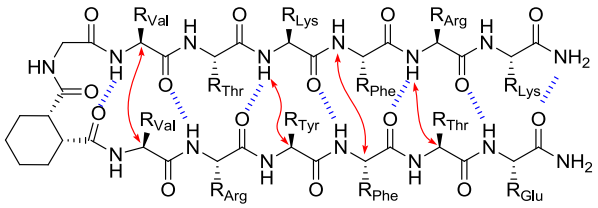

Figure 3.14 Di-acid turn linker promoting parallel sheet formation in aqueous solvent. Selected NOE's shown.

Furthermore Gellman showed that the di-acid linkers are not the 'dominant drivers of parallel β-sheet formation' but instead merely the enablers by bringing the strands close together. It is therefore the inter-strand interactions, and predominantly the main chain hydrogen bonding that contributes to sheet stability. Whether this conclusion can be extrapolated to all turn linkers is unclear.

Similarly Nowick has included a mix of residues to both promote sheet formation and avoid aggregation to create a series of sheets that have been used to extensively study sheet interactions.[1]

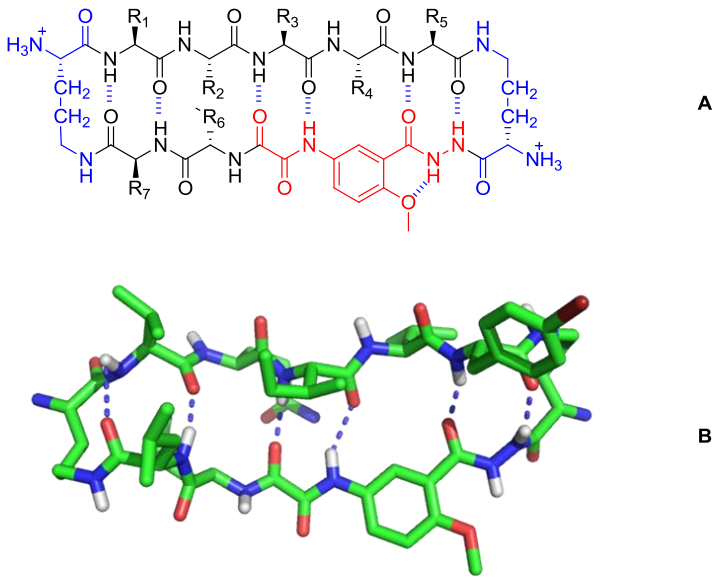

Figure 3.15 **A**: Macrocylic β-sheet developed by Nowick for probing sheet interactions. The sheet incorporates two unnatural amino acids, 'Hao' in red, and '$^{\delta}$Orn' in blue. **B**: Crystal structure of one of the macrocyclic sheets (PDB: 3Q9G).

The synthesis of such macrocycles is relatively straightforward with the incorporation of two unnatural amino acids, *Hao*[42] and *$^{\delta}$Orn*,[45,46] that promote and rigidify sheet conformation, but are amenable to solid phase synthesis. Experiments revealed in exquisite detail, and with beautiful crystal structures, the ability of these artificial sheets to form dimers and tetramers, both edge-to-edge and face-to-face (Figure 3.16).[53]

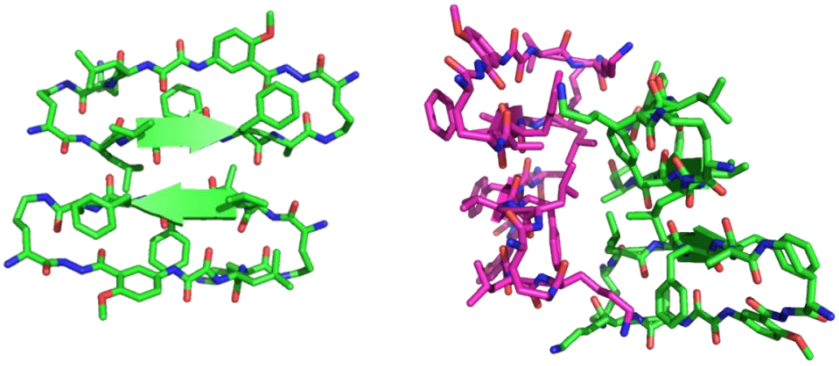

Figure 3.16 Edge-to-edge dimer (left), and face-to-face tetramer (right) of macrocyclic β-sheets (PDB: 3Q9H).

These motifs have also been used to inhibit amyloid aggregation (for a complete exploration see Section 3.5.2).

3.4 Multi-Stranded β-Sheets

The turn inducers described above form only a small part of peptidic and non-peptidic scaffolds capable of forming two-stranded β-sheet. As shown by many of the authors, in particular Robinson in targeting a huge range of indications from bacterial and viral infections to cancer,[37,54,55] these minimal peptidomimetics can be extremely useful. However with many interactions being mediated *via* larger surfaces and more sophisticated macromolecules requiring more complex building blocks, there is a need for sheet architectures with greater numbers of strands.

Through an iterative design process, Serrano *et al*. synthesised the twenty-amino acid, three-stranded sheet Betanova (Figure 3.17).[56]

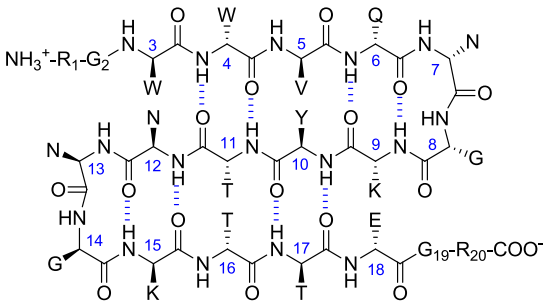

Figure 3.17 Betanova, a designed three-stranded β-sheet peptide. Amino acid side-chains are indicated by single letter codes.

To produce a stable, non-aggregating molecule that displayed considerable β-sheet character in water the researchers started from a known β-hairpin design using the Asn-Gly turn inducer and further considered sheet propensities, preferences for inter-strand residue pairs, and overall hydrophobic surface area. The conformation was probed and proved by long range inter-strand NoE's, analysis of $^{3}J_{NH\alpha}$ coupling constants and chemical shift profiles. The authors also noted that a key feature of folded structures such as sheets is a cooperative folding/unfolding transition and so assessed this under both thermal and chemical denaturation by circular dichroism and fluorescence spectroscopy. The authors hoped that by

rationally designing a small β-sheet peptide the avenues would be open for greater study and understanding of folding and aggregation.

Concurrently Schenk and Gellman also designed a three-stranded β-sheet and used this scaffold to assess the cooperativity of sheet folding.[57] They used the ^{D}Pro-Xxx turn inducer as through replacement of ^{D}Pro with ^{L}Pro the hairpin was no longer present, and hence a suitable control was available. The sequence was designed to have a +2 charge to prevent aggregation, and a library of peptides was synthesised containing two (^{D}Pro^{D}Pro), one (^{D}Pro^{L}Pro or ^{L}Pro^{D}Pro) or zero (^{L}Pro^{L}Pro) of the hairpin inducers. Global conformation was probed with circular dichroism, with the double hairpin molecule displaying well defined maxima and minima indicative of β-sheet structure, the zero showing random coil structure and the single hairpin displaying a spectrum between the two. Having established conformational control the influence of cooperativity was examined through NOESY and ^{1}H chemical shift analysis. Long-range cross-strand interactions appeared to indicate that the disruption of one hairpin reduced the number and intensity of signals in the second, suggesting positive cooperativity perpendicular to strand direction. This was further confirmed by the chemical shift analysis (Figure 3.18).

This assessment of cooperativity was supported by the work of Sharman and Searle in a thorough evaluation of an Asn-Gly hairpin linked three-stranded β-sheet.[58] They concluded that ‘the larger number of hydrogen bonding interactions within the sheet gives rise to [a] greater degree of cooperativity’.

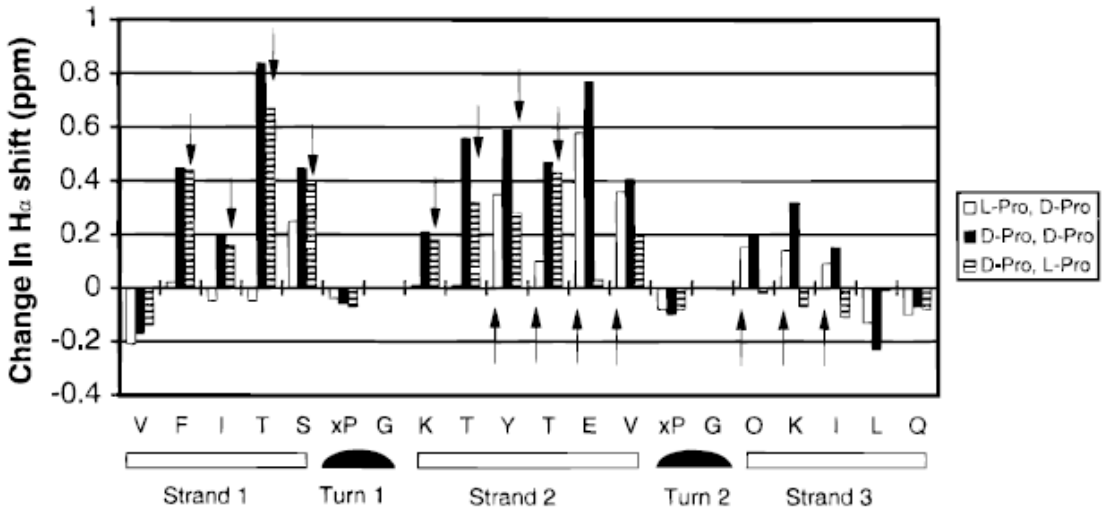

Figure 3.18 ^{1}H chemical shift analysis of three-stranded sheet (^{D}Pro^{D}Pro) and controls (^{D}Pro^{L}Pro or ^{L}Pro^{D}Pro). The graph shows $\Delta\delta = \delta_{observed} - \delta_{random\ coil}$ for each residue. A larger value of $\Delta\delta$ indicates greater β-sheet character. Reprinted with permission from Journal of the American Chemical Society. Copyright 1998 American Chemical Society.

In the construction of these multi-stranded sheets aggregation remained a persistent problem. Many researchers used polycationic molecules to both aid solubility and prevent aggregation, but Doig showed that the strategy of *N*-methylation remained a viable option (Figure 3.19).[59]

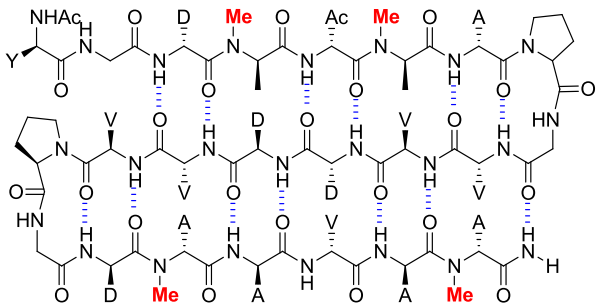

Figure 3.19 23-mer Peptide containing four *N*-methyl alanine residues forming a non-aggregating three-stranded β-sheet.

The 23-mer contained four *N*-methyl alanine residues and its conformation was studied using circular dichroism. Somewhat unusually it was found that the β-sheet conformation was most populated upon heating to 333 K, but no explanation was offered in the paper. This could be as a result of the fine balancing of the equilibrium as entropic and enthalpic contributions of both the peptide and the associated waters contribute to the total free energy.

Finally, Balaram has used the ^{D}Pro-Xxx hairpin to extend out to four and five-stranded sheets.[60,61] Although the five-stranded sheet was found to only fold in methanol and not in aqueous environments, it included a metal ion binding motif that paved the way for possible assembly of more complex architectures such as β-sandwiches and β-barrels.

3.5 Biologically Active Designed Sheets

3.5.1 Anginex

These principles have been successfully applied to the design and synthesis of the anti-parallel β-sheet forming 33-mer peptide anginex.[62] Angiogenesis, the formation of new blood vessels, is a crucial biological activity for functions such as embryogenesis and wound-healing but is also hijacked in cancer to help develop blood supply to tumours. The inhibition of angiogenesis was therefore seen to be an extremely viable therapeutic strategy,[63] with a number of endogenous inhibitors including platelet factor 4,[64] angiostatin,[65] and bactericidal permeability increasing protein (BPI)[66] discovered. The active portion of these proteins were all found to display predominantly cationic and hydrophobic side-chains, and were structurally similar, with these residues projected from an anti-parallel β-sheet.

This prompted Mayo *et al*. to attempt to design an artificial peptide, incorporating elements of these anti-angiogenic proteins and β-sheet design principles.[62] From a library of thirty peptides, anginex was found to be an extremely potent *in vitro* and *in vivo* inhibitor (Figure 3.20).

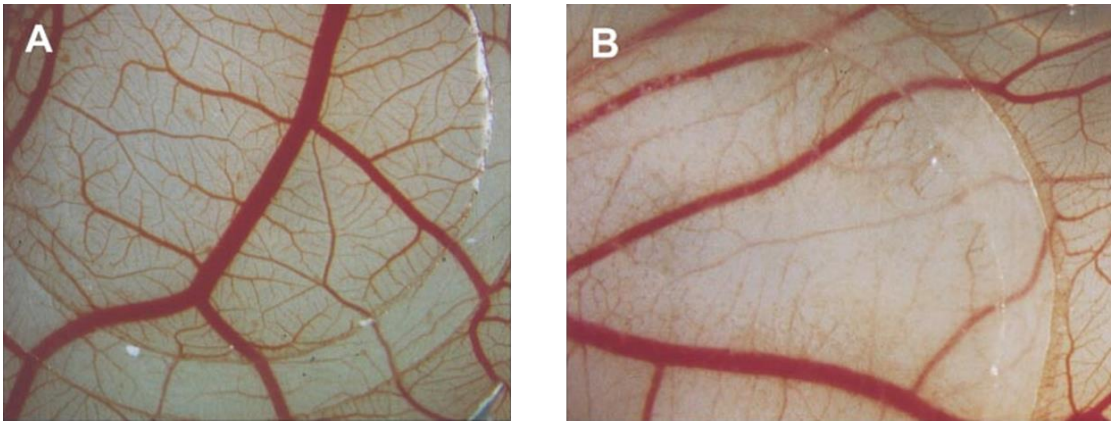

Figure 3.20 Blood vessel development in chick embryo chorio-allantonic membrane. **A**: Control **B**: Following four daily applications of 64 µL of anginex solution there is considerably less vasculature. Reprinted with permission from Biochemical Journal. Copyright 2001, Portland Press Limited.

Subsequent work has shown the necessity of β-sheet formation for biological activity,[67] and anti-tumor activity.[68] Finally the Martinek group has shown the ability to modify the anginex peptide to include β-amino acids and maintain sheet conformation and biological effect (Figure 3.21).[69]

Figure 3.21 **A**: Representative structure of anginex with the β-sheet forming region highlighted in brown. **B**: β^3-amino acid substitutions made by Martinek *et al*. that maintained sheet structure and biological activity.

3.5.2 Protein Aggregation and Amyloidysis

As Haas and Selkoe so eloquently phrase it in their review on soluble protein oligomers, ‘degenerative diseases of the human brain have long been viewed as among the most

enigmatic and intractable problems in biomedicine.'[70] Amyloid deposits, a hallmark of such disorders, have long been used to confirm clinical diagnoses post-death clinical conformation, but with little understanding of how and why they form (Figure 3.22).

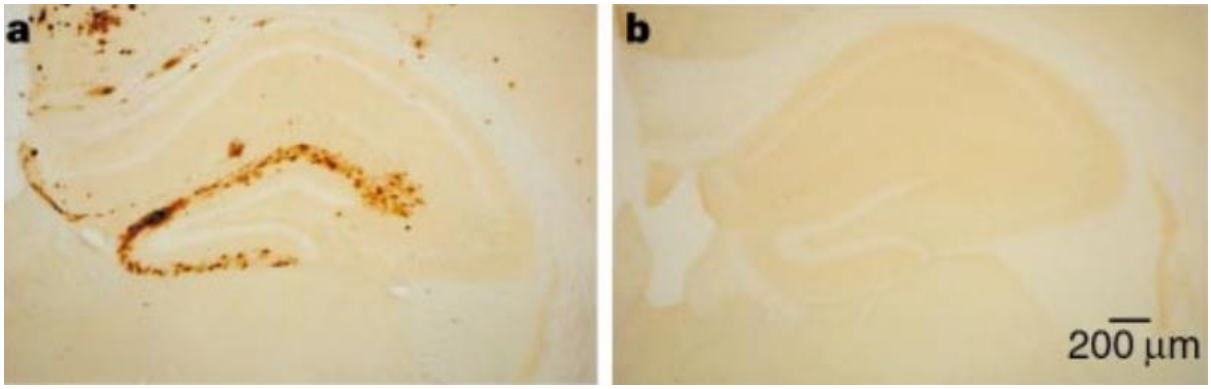

Figure 3.22 Hippocampal Aβ deposition **a**. Extensive deposition in the outer molecular layer of the hippocampal dentate gyrus. **b.** Immunized mouse shows no such deposition.[71] Reprinted by permission from Macmillan Publishers Ltd: Nature, **400**, 173-177, Copyright 1999.

However with X-ray diffraction revealing these fibrils to be made up of a highly ordered, pleated, β-sheet structure, the possibility of sheet mimics to both build our understanding of such structures and investigate ways to disrupt their formation opened up.

3.5.2.1 β-Sheet Peptidomimetics as Probes

The structures of the micro- or even macro-scopic fibrils found in amyloid deposits are now well established but research has indicated that, although highly symptomatic of amyloid diseases, these visible deposits probably play little role in progressing the pathology. Instead, it is the small, still soluble oligomers that most likely play the bioactive and toxic role.[72] However their unstable and heterogenous nature have made these oligomers extremely difficult to study.

A number of techniques have been developed to better study these molecules, such as the $^{13}C_{methyl}$-DEST NMR experiment developed by Clore,[73] and the use of surfaces with different peptide binding properties to elucidate aggregation kinetics by Lund.[74] However Lund's

method reveals little around the structural factors affecting the kinetics and the NMR technique is limited to methyl bearing side-chains. Fortunately the chemistry developed to form sheet foldamers can be of great assistance in structural elucidation.

Nowick was able to combine his *Hao* and *Orn* linked system shown above (Figure 3.16) to provide conformational stability to key sections of misfolded proteins and thus enable structural studies. For example, through the use of a double *Hao* system he was was able to template $A\beta_{15\text{-}23}$, a series of key residues in the important central region of Aβ (Figure 3.23).[75]

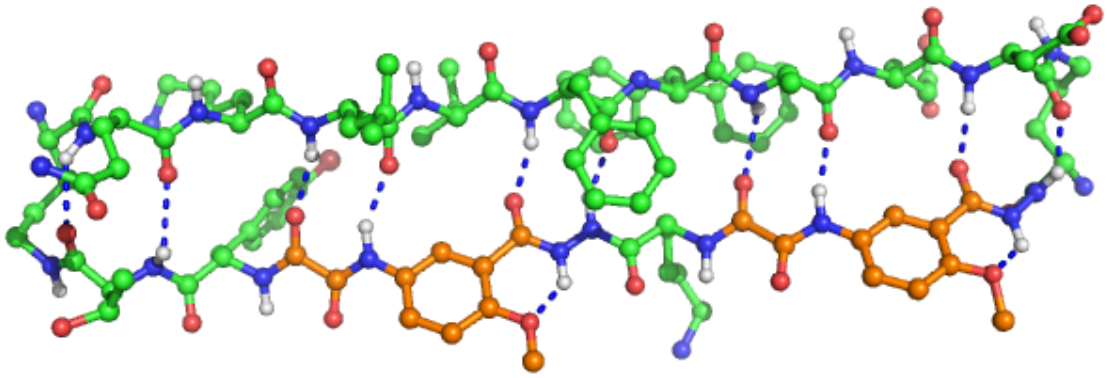

Figure 3.23 X-Ray crystal structure of $A\beta_{15\text{-}23}$ (top strand) templated by a *Hao* strand inducer (bottom strand) and *Orn* turn inducer units (PDB: 4IVH).

This macrocycle was amenable to crystallisation and formed oligomers of cruciform tetramers and triangular dodecamers. The triangular dodecamer revealed a hydrophobic cavity that could provide some insight into how these oligomers insert into, and form a pore within, the cell membrane. This pore formation is a current hypothesis for the toxicity of such oligomers.[76]

More recently Nowick's group have sought to 'naturalise' the peptide as much as possible by removing the peptidomimetic elements whilst maintaining the amenability to study. This is exemplified by two papers, the first on Aβ and the second on α-synuclein.

With Aβ the researchers were able to remove the *Hao* template and simply enforce a hairpin structure *via* macrocyclisation with *Orn* and a cross-strand disulfide linker.[77] The incorporation of a single *N*-methyl group was able to prevent uncontrolled aggregation. Pleasingly these less intrusive modifications again allowed for the crystallisation of hairpins oligomerised into trimers, dodecamers and annular pores. These results supported a previously outlined model that β-hairpins were the key conformational determinant of non-fibrillar oligomers (Figure 3.24).

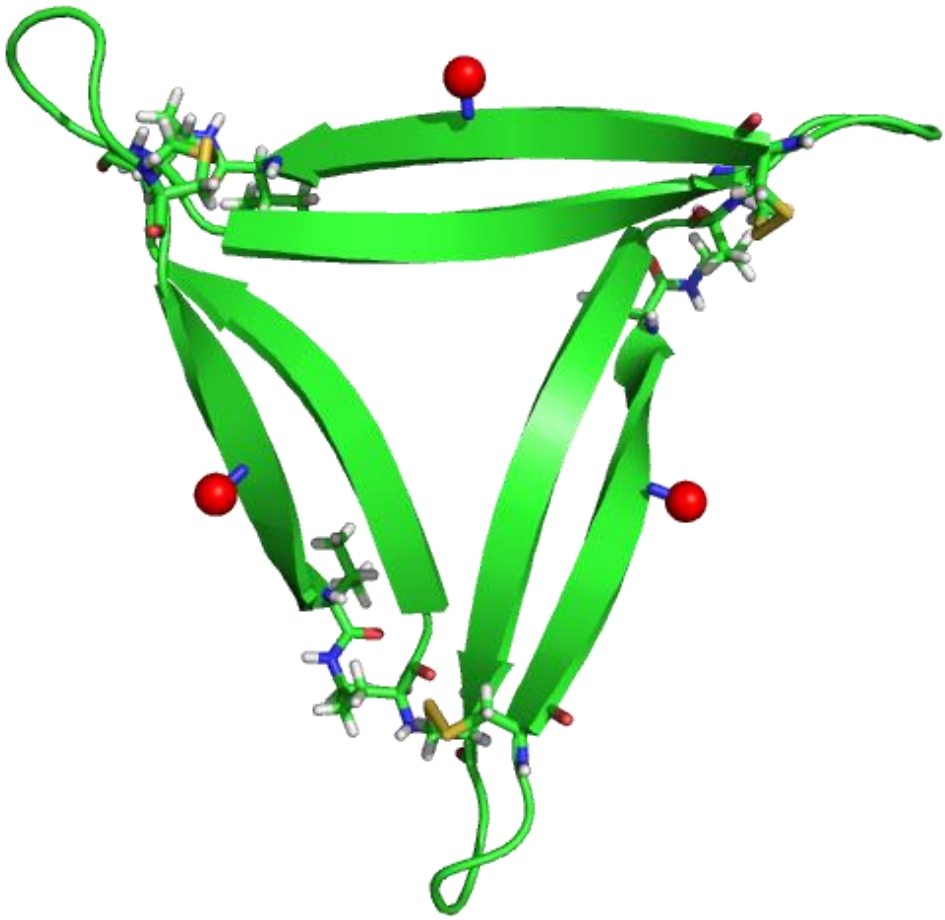

Figure 3.24 X-Ray crystal structure of the trimer formed from Aβ hairpins (PDB: 5HOY). Hairpin shown in cartoon form, Orn linkers and disulfide bridges shown as sticks. *N*-methyl groups shown as red spheres.

Similar modifications were made to a section of the α-synuclein peptide, with two Orn linkers, *N*-methylation and a single site mutation of a glycine to an alanine to enhance folding.[78] Again these allowed for crystallisation into triangular trimers and a basket shaped

nonamer. These oligomers displayed similar properties to those of full length peptide, validating the model that they provided.

That such a similar technique worked for a different system bodes well for this becoming a general approach towards a better understanding of 'difficult-to-crystallise' peptides. Indeed the approach has also been applied to the study of IAPP oligomers.[79] This elegantly shows how building an understanding of folding through the design of foldamers can be applied to tackle previously intractable problems.

3.5.2.2 Peptidomimetics as Therapeutics

Furthemore, our appreciation of how to design foldamers, can also be applied to the prevention of such aggregation. Using the same techniques as highlighted above, one of Nowick's *Hao* templated macrocycles was shown to slow the onset and subsequent growth of Aβ oligomers, with a resultant decrease in neuronal cell death.[80] A similar strategy was used to target the aggregation of tau-protein-derived peptide AcPHF6.[81] Through mutational studies the researchers were able to show that an extremely hydrophobic recognition surface with valine, isoleucine and leucine residues, was essential to inhibitory activity, and conclude that a molecule that presents two well-defined surfaces would be useful in future studies of amyloid inhibition. Such a challenge is ideally suited to the field of β-sheet peptidomimetic foldamers.

3.6 Template Assembled Synthetic Proteins

Sheet architectures have been used in the design and synthesis of mini-proteins containing mixed protein architectures. In the template assembled synthetic proteins (TASPs) pioneered by Mutter *et al.*,[82] the sheet structure acts as a template for a variety of additional protein structures, including α-helices,[83–85] β-barrels or both.[82] This work allows the chemist to construct a *de novo* protein, overcoming the problems of folding design and elongated

peptide synthesis, and allowing for the incorporation of unnatural residues and peptidomimetics (Figure 3.25).

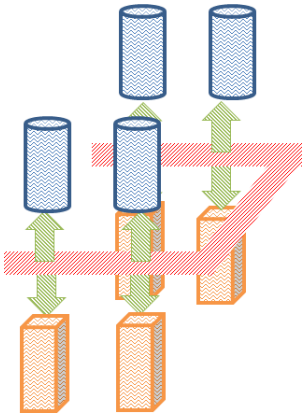

Figure 3.25 Demonstration of the TASP concept. The red turn element represents the template, with the green arrows the connecting linkers. The elongated cubs and barrels are the additional elements that can be selectively incorporated to create a multi-domain structure incorporating different elements of secondary structure.

The sheet elements are constructed from synthetic turn elements such as substituted naphthalenes, with rigid templation enforced by strategies such as peptide or disulphide macrocyclisation.[86] The peptide chains always contain orthogonally *N*-protected lysine residues (often Boc and Fmoc) to allow for selective modification with the secondary structural elements (Figure 3.26).

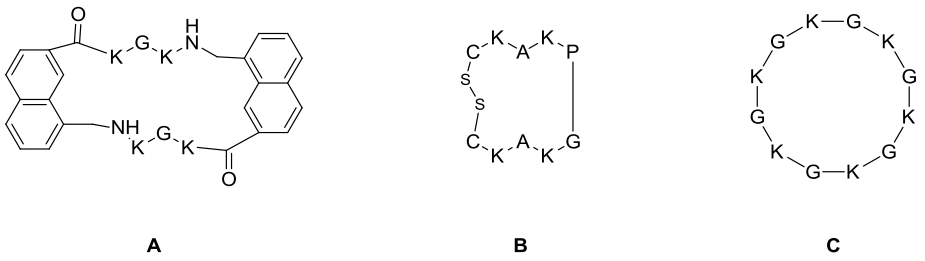

Figure 3.26 Strategies for the synthesis of suitable TASP templates. **A**: Macrocyclisation with rigid turn linker **B**: Macrocyclisation through the formation of a disulphide bond **C**: Peptide macrocyclisation.

These synthetic proteins are functional as well as structural, with a TASP able to act as an antigen for the raising of highly specific antibodies.[86] By appending the α-helix bundle from the MHC protein the researchers were able to raise mouse antibodies that recognised the native protein of origin, showing the potential for therapeutic antibody development.

3.7 Design of a Novel β-Sheet Architecture

Many β-sheets are formed as β-meanders, where the anti-parallel strands are connected by β-turns and the complete sequence is contiguous. These structures are common within proteins and are one of Nature's ways of creating extended surfaces. Despite the progress highlighted above there remains a need for a β-meander template that adopts a stable conformation across the full range of solvents. It must be adaptable in length and number of strands, thereby allowing for the creation of a surface of variable size. The synthesis should be rapid, scalable and able to incorporate natural and unnatural side-chain residues.

The diphenylacetylene motif developed by Kemp in 1995 has many of these virtues; it displays an excellent ability to template two-stranded sheet formation;[26] is easily synthesised using well-established chemistry and recent work by Spivey has shown it is amenable to inclusion in solid phase synthesis and capable of displaying hairpin loops with biological activity.[87,88] As such the 'Kemp turn' offers the ideal motif for the development of an artificial meander (Figure 3.27).

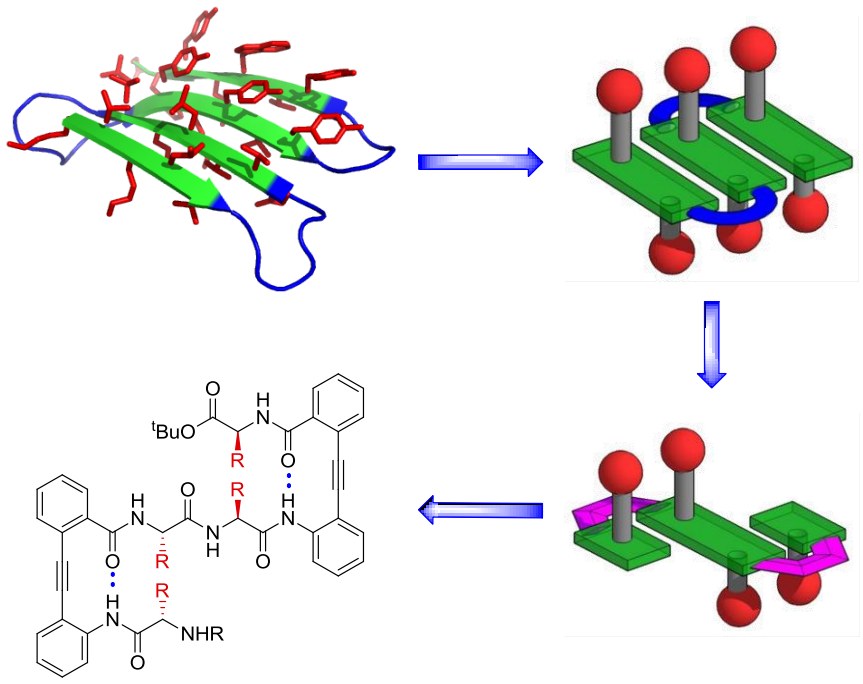

Figure 3.27 β-Meander mimicry: schematic design for the incorporation of the 'Kemp turn' motif into an artificial β-sheet (PDB: 3AUM).[89]

The β-turns connecting the β-meander together can be considered as superfluous to the recognition domains of the sheet, and can instead be replaced by an artificial linker, in this case the diphenyl acetylene. These linkers could in theory be used indefinitely to create a multi-stranded sheet.

For an initial test of this concept a conformational search on the proposed three-stranded meander was carried out in MOE using MMFF94X as the force field and water as an implicit solvent (Figure 3.28).[90]

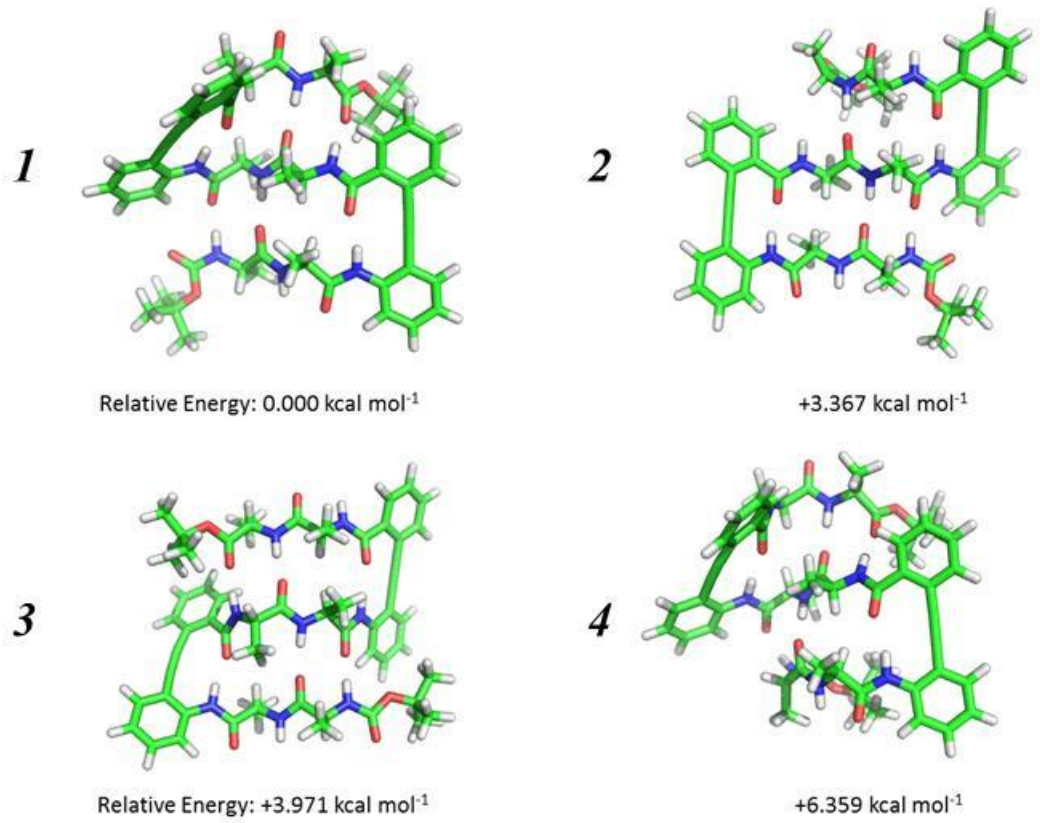

Figure 3.28 Conformational search of three-stranded, two residues per strand, all alanine meander with *tert*-butyl ester and N-Boc protecting groups. Calculations performed in MOE[90] and the outcomes visualised in Pymol.[91]

The search found four conformations that sat within local minima, and all of them showed the desired hydrogen bonding network and side-chain display. The differences appear to arise from two different effects; the diphenylacetylene linkers moving out of each other's plane, as observed in conformations **1** and **4**, or the fraying of the protected termini away from the plane of the molecule, as evidenced in all conformations except **3**. The same search was conducted on the four-stranded meander, but none of the results displayed the desired planar conformation with an extended hydrogen bonding network. However it was reasoned that with a molecule approaching this size (~ 1500 Da) the program would struggle to sample sufficient conformations to necessarily find the global minimum.

With these encouraging computational results in hand, it was decided to embark on the synthesis of the three and four-stranded molecules as a proof-of-concept. Alanine residues

were incorporated as these are known to promote β-sheet formation and their simple structure would aid in synthesis, characterisation and analysis.

It was envisaged that the meander could be formed *via* the coupling of monomer unit **A**. This necessitated the construction of **A** with orthogonal protecting groups (Figure 3.29).

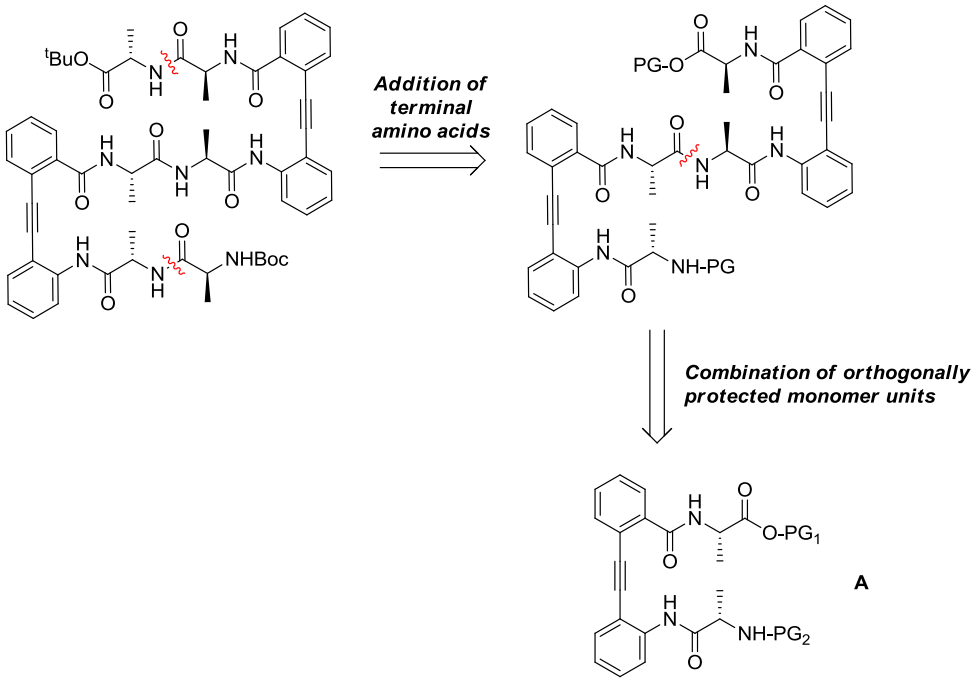

Figure 3.29 Retrosynthetic strategy for the synthesis of the 'meander'.

3.8 Synthesis of the 'Meander'

3.8.1 Synthesis of a Modular Building Block

Modular building block **48** was synthesised on a multi-gram scale from readily available starting materials. 2-Iodoaniline **41** was subjected to Sonogashira coupling with TMS-acetylene, and subsequently deprotected with potassium carbonate in methanol to yield **43** in 87 % yield over two steps. Meanwhile benzoyl chloride **44** was coupled with the *tert*-butyl ester of L-alanine, with DMAP as a nucleophilic catalyst to yield iodide **45** in good yield. Iodide **45** and terminal alkyne **43** were then united with a second Sonogashira reaction to form aniline **46** in a good yield (Scheme 3.1). Increased reaction times and heating to 50 °C

were required to force this Sonogashira reaction to completion, presumably due to the increased steric hindrance.

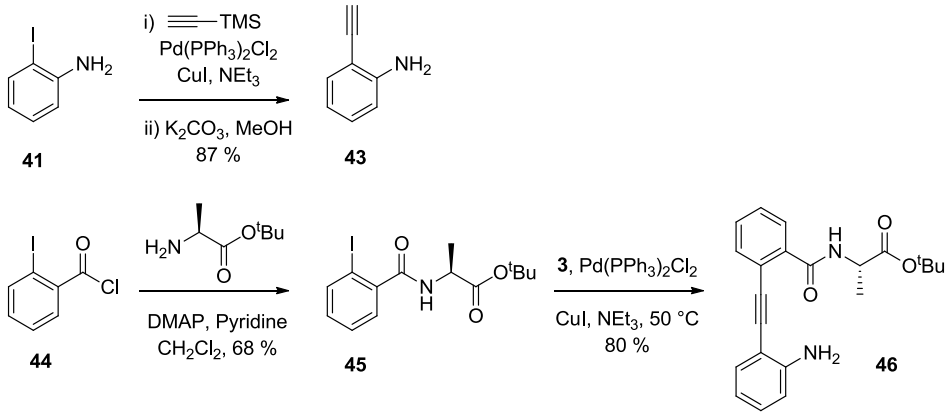

Scheme 3.1 Initial steps in the synthesis of modular building block **48**.

The final step to form the modular building block required the coupling of the resultant aniline **46** with Fmoc-Ala-OH. Initial attempts at the amide bond formation were unsuccessful and thus optimisation was carried out with 2-iodoaniline **41** and Boc-Ala-OH.

3.8.2 Optimisation of Aniline Coupling

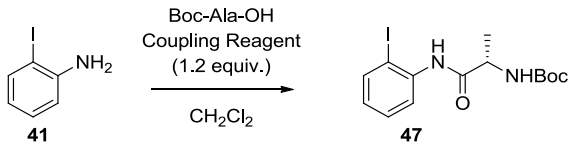

Entry	Coupling Reagent	Scale (mmol)	Solvent	Time (h)	Activation temperature (°C)	Yield (%)
1	DCC/HBTU	0.46	THF	16	20	0
2	Mukaiyama	0.46	THF	16	20	0
3	DCC/HBTU	0.46	CH_2Cl_2	16	20	42
4	DCC	0.46	CH_2Cl_2	16	20	74
5	HBTU	0.46	CH_2Cl_2	16	20	0

6	EDC / HOBt	0.46	CH_2Cl_2	16	20	0
7	DCC	0.46	CH_2Cl_2	48	20	67
8	DCC	0.46	CH_2Cl_2	16	0	93
9	DCC	0.46	CH_2Cl_2	6	0	98
10	DCC	0.46	CH_2Cl_2	16	0	95
11	DCC	2.30	CH_2Cl_2	16	0	54
12	DCC	2.30	CH_2Cl_2	6	0	70

Table 3.1 Optimisation of aniline and amino acid coupling.

Previous work in the group had shown that anilines could form amide bonds with DCC and HBTU as activating reagents in THF.[44] Although good solubility of the reagents was observed in THF, the reaction did not proceed under DCC/HBTU or Mukaiyama conditions.[92] Change of solvent to dichloromethane resulted in a successful reaction and a 42 % isolated yield. Further exploration of coupling conditions showed that DCC alone afforded the best yield. For longer peptide systems there were concerns over racemisation when DCC is used in isolation, due to oxazalone formation and the resultant increased acidity of the α-proton. However in this system, and indeed the targeted modular building block, **48**, oxazalone formation is not possible. As evidence of this, all molecules were, as part of their synthesis, subsequently elaborated to those with more than one stereocentre, and diastereomers were not observed.

Performing the activation of the acid with DCC at 0 °C and shortening the reaction time to six hours resulted in an excellent 98 % yield. Upon scale up to 2.30 mmol of 2-iodoaniline this was found to reduce to a moderate 70%. These optimised conditions were applied to the coupling of aniline **46** and Fmoc-Ala-OH to yield orthogonally protected building block **48** in 70 % yield (Scheme 3.2).

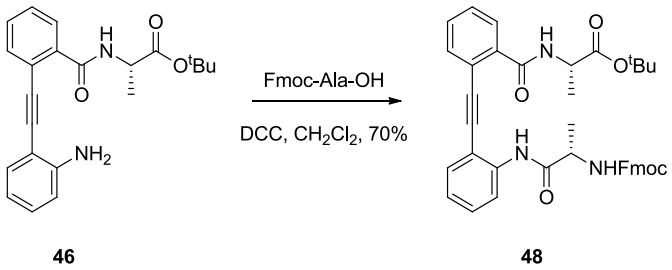

46 48

Scheme 3.2 Completion of orthogonally protected modular building block **48** for β-meander formation.

3.8.3 Demonstrating Orthogonality of Protecting Groups

Before embarking on amide coupling it was necessary to test the orthogonality of the Fmoc and *tert*-butyl ester protecting groups. Building block **48** was subjected to TFA and upon completion, as judged by TLC, the presence of the free acid but protected amine was confirmed by mass spectrometry. The TFA was removed *in vacuo* with any residual acid removed by subsequent co-evaporation with toluene. Similarly, exposure to piperidine was found by mass spectrometry to reveal only the amine and leave the *tert*-butyl ester intact (Scheme 3.3).

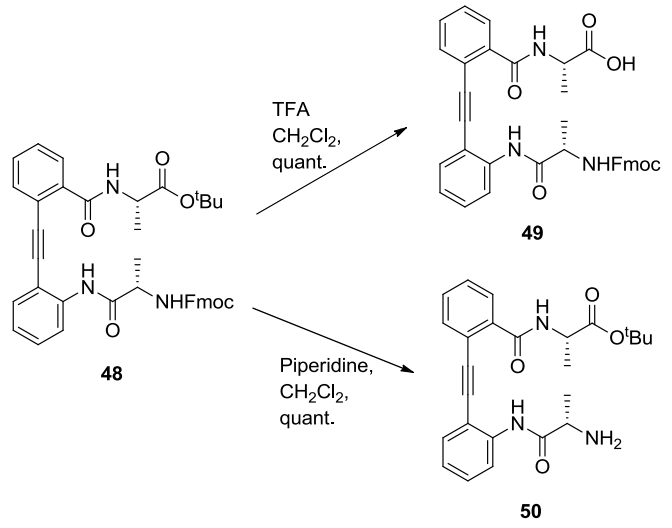

48 49 50

Scheme 3.3 Orthogonal deprotection of modular building block for β-meander formation.

3.8.4 Test Coupling of Alkyl Amines

Optimisation of the coupling of alkyl amines was carried out on a model system before embarking on the final meander formation. Test compound **52** was synthesised through the

optimised DCC coupling of aniline **43** and Boc-Ala-OH and subsequent deprotection with TFA (Scheme 3.4).

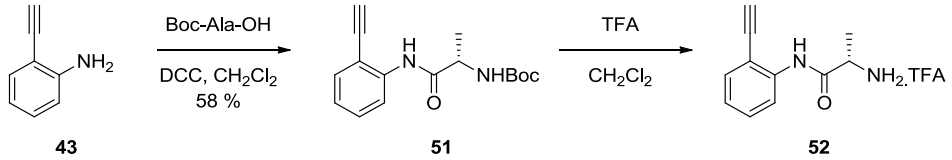

Scheme 3.7 Synthesis of test compound for alkyl amine and carboxylic acid coupling

The TFA salt was used without further purification and coupled with a further Boc-Ala-OH to create the two amino acid chain **53**.

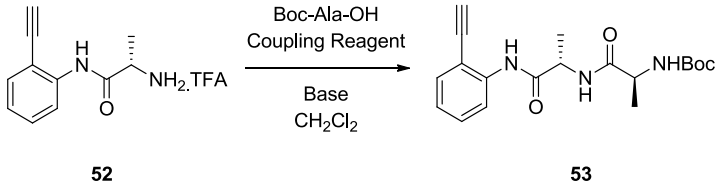

Entry	Coupling Reagents (equiv.)	Base (equiv.)	Yield (%)
1	EDC, HOBt (2)	DIPEA (3)	58
2	EDC (2)	DIPEA (3)	40
3	DCC (2)	DIPEA (3)	38
4	HBTU (2)	DIPEA (3)	78
5	HBTU (1)	DIPEA (3)	58
6	HBTU (2)	DIPEA (1)	26
7	HBTU (2)	DIPEA (5)	39

Table 3.2 Optimisation of alkyl amine and acid coupling.

These results indicated that two equivalents of the uronium reagent, HBTU, and three equivalents of Hünig's base resulted in a good yield of 78 %. Adjusting the equivalents of coupling reagent or base resulted in reduced yield.

3.8.5 Initial Formation of Three Stranded Meander

With alkyl amine coupling conditions now in hand attempts were made to couple two of the building blocks to form compound **54**. Initially, neither the free amine, nor the free acid, were subjected to further purification after deprotection and the resultant yield was a disappointing 5 %, presumably due to residual piperidine reacting with acid **50**, although this side-product could not be isolated. Fortunately it was possible to purify the free amine *via* column chromatography and the yield increased to 49 % (Scheme 3.5).

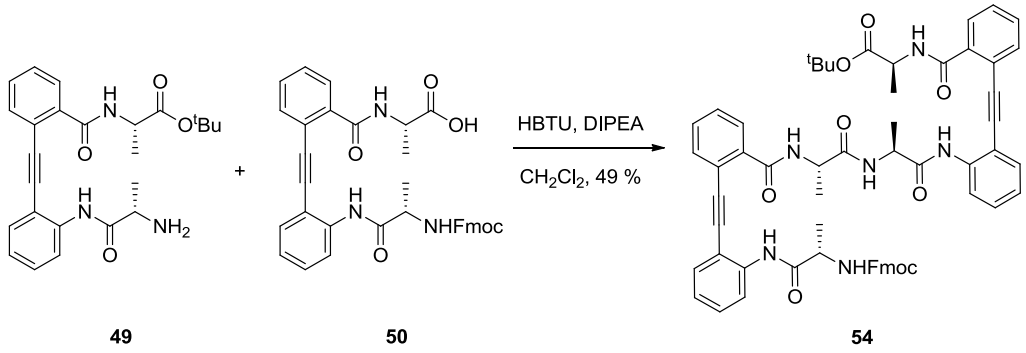

Scheme 3.5 Initial formation of three-stranded meander.

3.8.6 Completion of Meander and Extension to Four Strands

It was now possible to sequentially add one further alanine at each terminus. The *tert*-butyl ester was removed to reveal the terminal acid, and the extension performed with *tert*-butyl ester L-alanine. It was then discovered that the tetra-methyl urea side product from the use of HBTU co-eluted with the product and the coupling reagents were therefore changed to EDC and HOBt with minimal reduction in yield. Finally Fmoc deprotection followed by amide bond formation with Boc-Ala-OH revealed the complete three-stranded meander **56**.

Similarly the four-stranded meander could be synthesised by *tert*-butyl ester deprotection of the initial meander **54** and EDC/HOBt mediated amide bond formation with the free amine of modular building block **48**. The single amino acid extensions were performed to give final molecule **59** (Scheme 3.6).

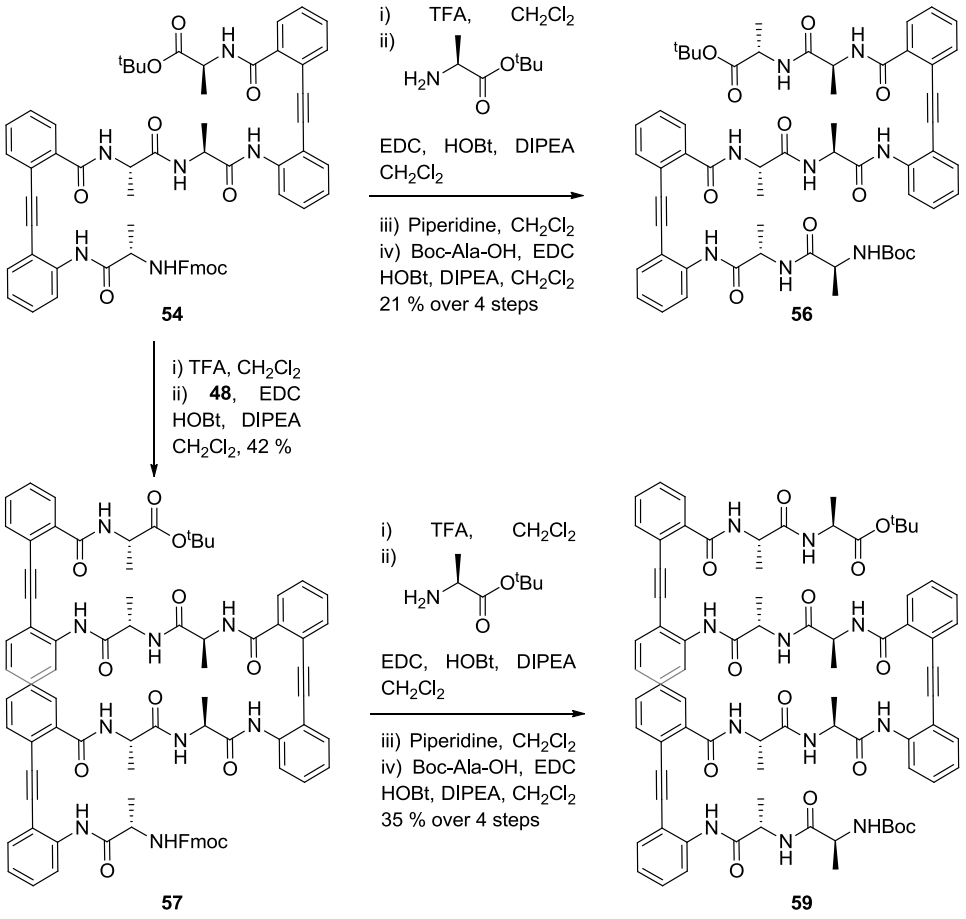

Scheme 3.6 Elongation to complete the three- and four-stranded meanders.

3.8.7 Synthesis of Control Compounds

For solution state analysis it was necessary to synthesise a series of control compounds that would mimic each of the strands in isolation. These are outlined below (Figure 3.30):-

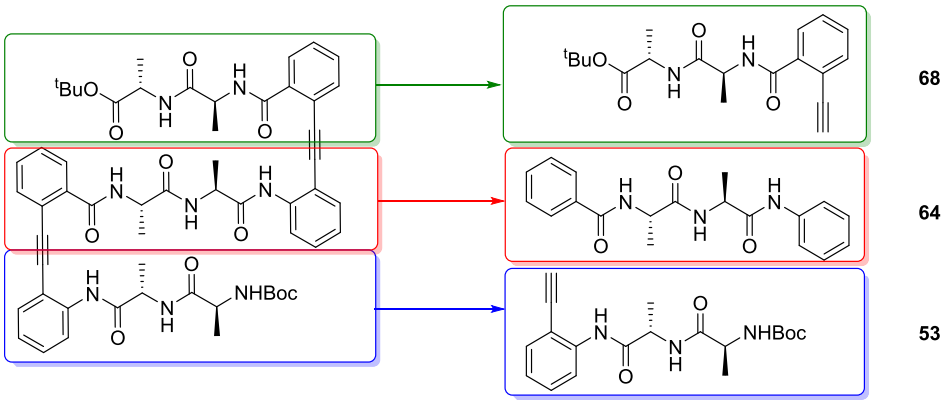

Figure 3.30 Schematic showing the rationale behind the selection of the control molecules.

Control molecules **53** and **64** were synthesised in a similar manner to the meanders as outlined below (Scheme 3.7).

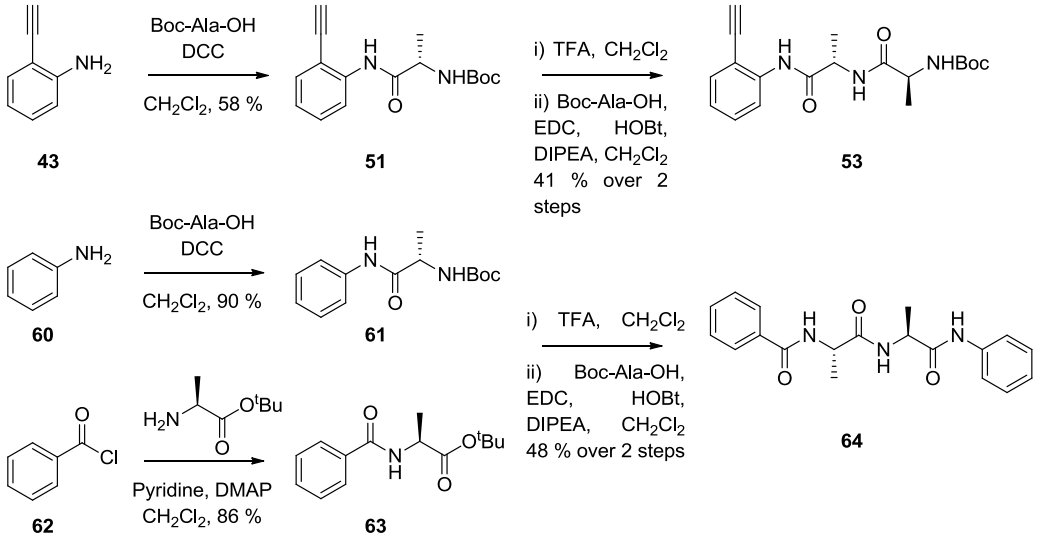

Scheme 3.7 Synthesis of single strand control compounds (**53** - blue - bottom strand, **64** - red - middle strand).

The synthesis of silyl-protected acetylene **66**, the precursor to the blue control compound proceeded well (Scheme 3.8).

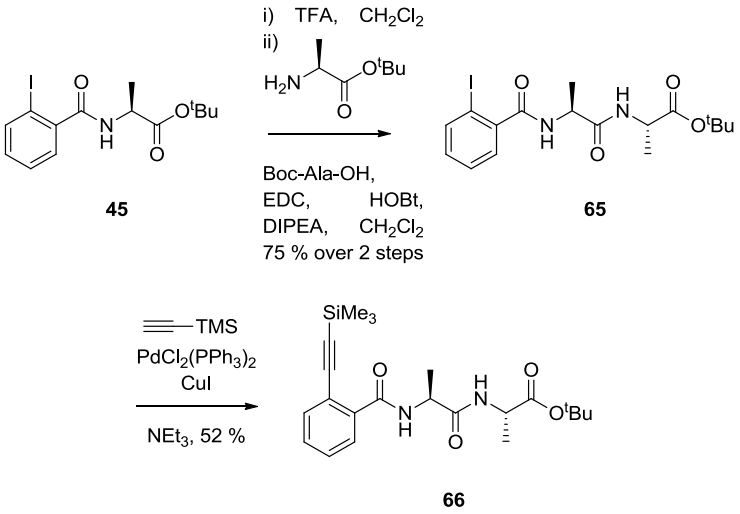

Scheme 3.8 Early steps towards tge synthesis of the final, top single strand (green – **68**) control compound.

However, upon deprotection of the trimethysilyl group with potassium carbonate in methanol, the desired terminal alkyne was not produced. Instead cyclic molecule **67** was

formed in 32 % yield (Scheme 3.9). ^{1}H and ^{13}C connectivity, and a NOESY spectrum showing the proximity of *H*a and *H*b were used to aid in assignment.

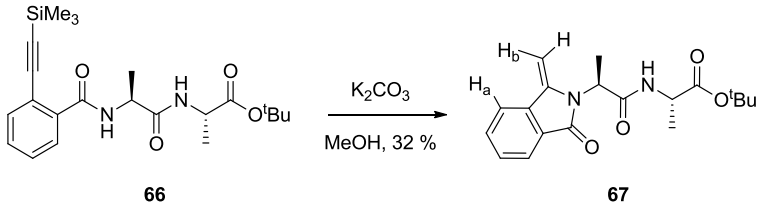

Scheme 3.9 Unwanted cyclisation upon silyl deprotection.

The literature included extensive precedent for this base mediated 5-exo-dig cyclisation.[93,94] This literature showed that a base was necessary to effect this cyclisation, and therefore when the reaction was performed with TBAF, buffered with a small amount of acetic acid, the control strand **68** was successfully isolated in 93 % yield (Scheme 3.10).

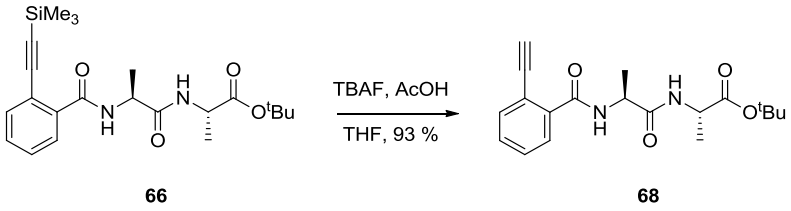

Scheme 3.10 Alternative reaction conditions furnish the desired control compound (**68** - green - top strand).

Finally a series of two-stranded molecules were synthesised for further comparison studies, the first being the extended Kemp turn **70** (Scheme 3.11).

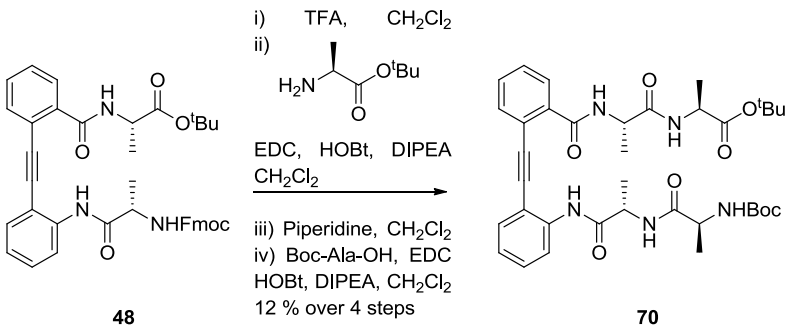

Scheme 3.11 Synthesis of two-stranded turn mimic **70** as a control.

The second was a molecule containing the diphenyacetylene motif but unable to form the proposed hydrogen bonding network as the amide and carbonyl groups would not align (Scheme 3.12).

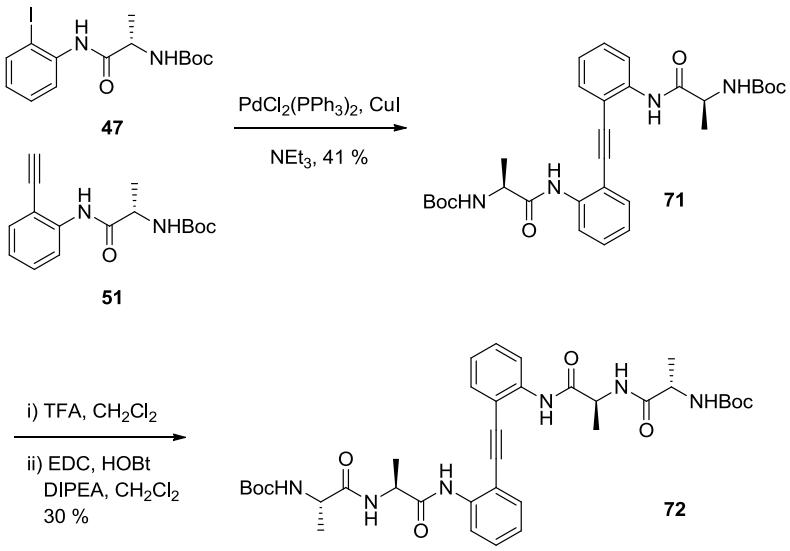

Scheme 3.12 Synthesis of four-residue control, unable to create a hydrogen-bonding network.

3.9 Analysis of Three- and Four-Stranded Meanders

3.9.1 Full Characterisation of Meanders 56 and 59

The characterisation of these molecules was non-trivial, requiring a number of 1D and 2D NMR techniques. The process is exemplified below with the assignment of four-stranded meander **59**.

The amide N-Hs within the Kemp turn motif were easily identifiable as singlets downfield of 9 ppm. Similarly the carbonyl carbons within the motif were distinct from the other carbonyl groups, owing to their proximity to the aromatic system, and fell between 165 - 167 ppm. The remaining amide N-Hs were identified by the lack of signal within HSQC and their ^{1}H-^{1}H coupling in the COSY spectrum to the neighbouring α-proton. Using the HSQC and COSY spectrums the α- and β-proton and carbons could be identified and grouped together. These groups are shown as cyan circles in Figure 3.31.

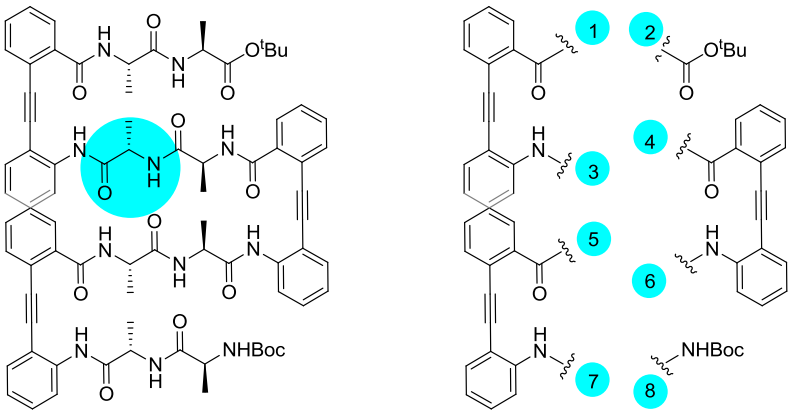

Figure 3.31 Method for complete structural assignment of mimic **59**.

It was hoped that the HMBC spectrum would enable the identification of the carbonyl group through the multiple bond correlation with the β-hydrogens of the proximal methyl group, and therefore enable complete connectivity for each strand to be established. However, given the proximity of the carbonyl resonances, the resolution was not sufficiently high to allow for unambiguous assignment (Figure 3.32).

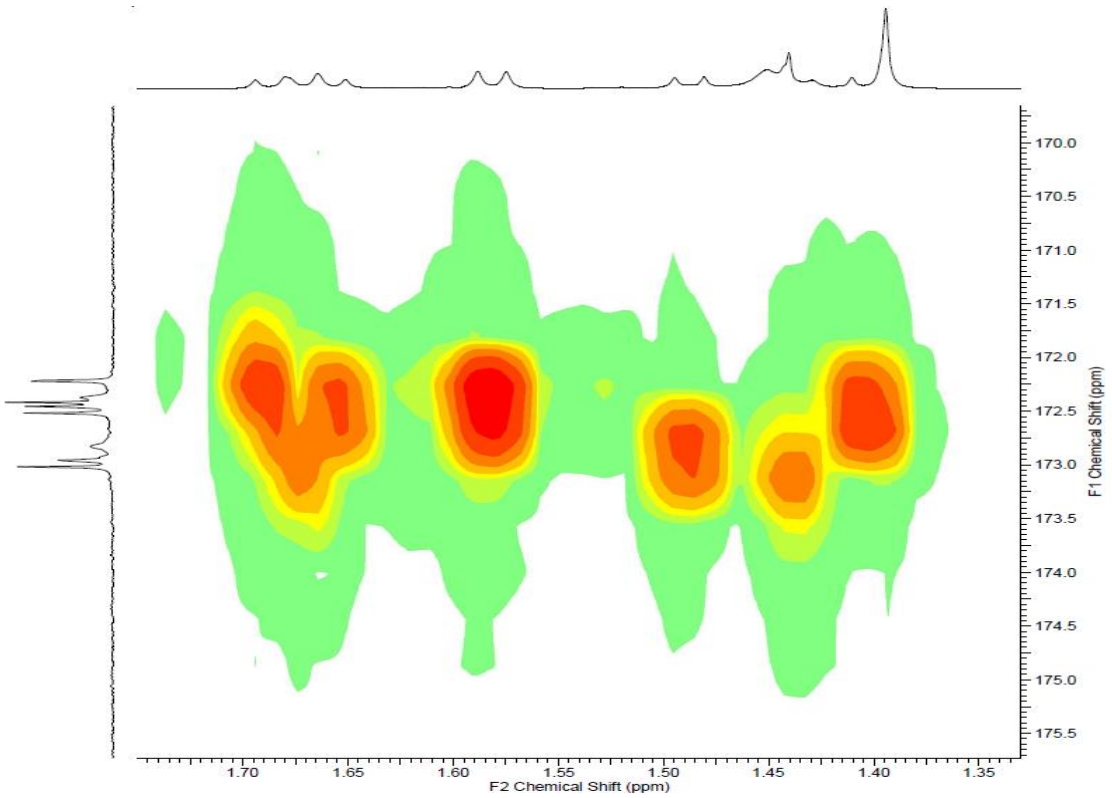

Figure 3.32 Selected region of HMBC spectrum of mimic **59** showing the low resolution.

Fortunately, band selective HMBC yields a higher resolution spectrum and enabled assignment (Figure 3.33).[95] The initial resolution problem is caused by the large (~ 200 ppm) ^{13}C shift range that must be indirectly sampled in order to obtain the final 2D spectrum. To keep experiment times within acceptable limits this range is normally scanned with a low resolution. Therefore the region of interest can be excited selectively for a more efficient use of time; however peak overlap then occurs due to the appearance of homonuclear proton *J*-couplings in the indirect ^{13}C dimension. This is then overcome by the suppression of the homonuclear coupling modulations to produce a high resolution spectrum.

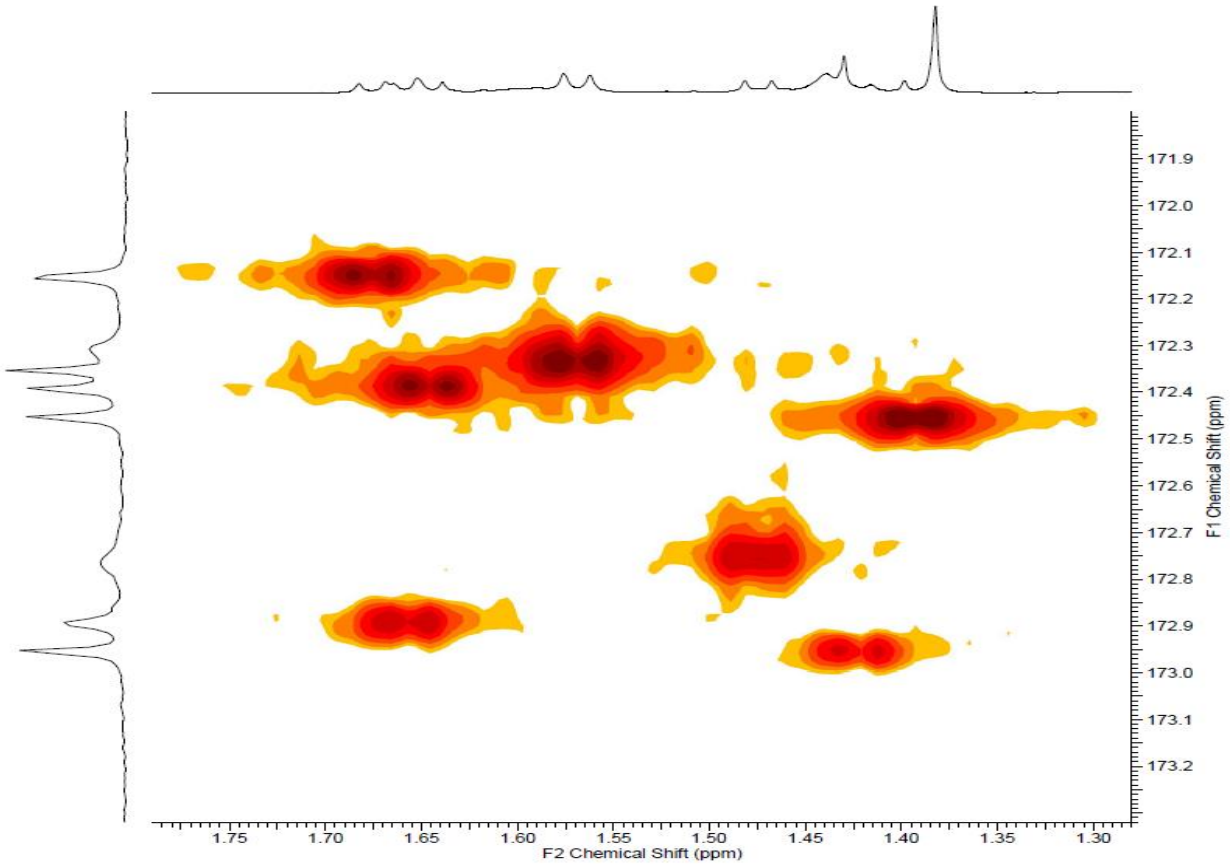

Figure 3.33 Selected region of a band selective HMBC of mimic **59** showing much higher resolution.

With the connectivity of each strand identified the ordering of the strands could now be investigated. The two outer strands were identified *via* the presence of the ester and carbamate groups as opposed to amide bonds. With the outer strands known, final

characterisation of the three stranded meander **56** became trivial, whilst the four stranded **59** required ROESY analysis to show the location of each strand relative to each other (Figure 3.34).

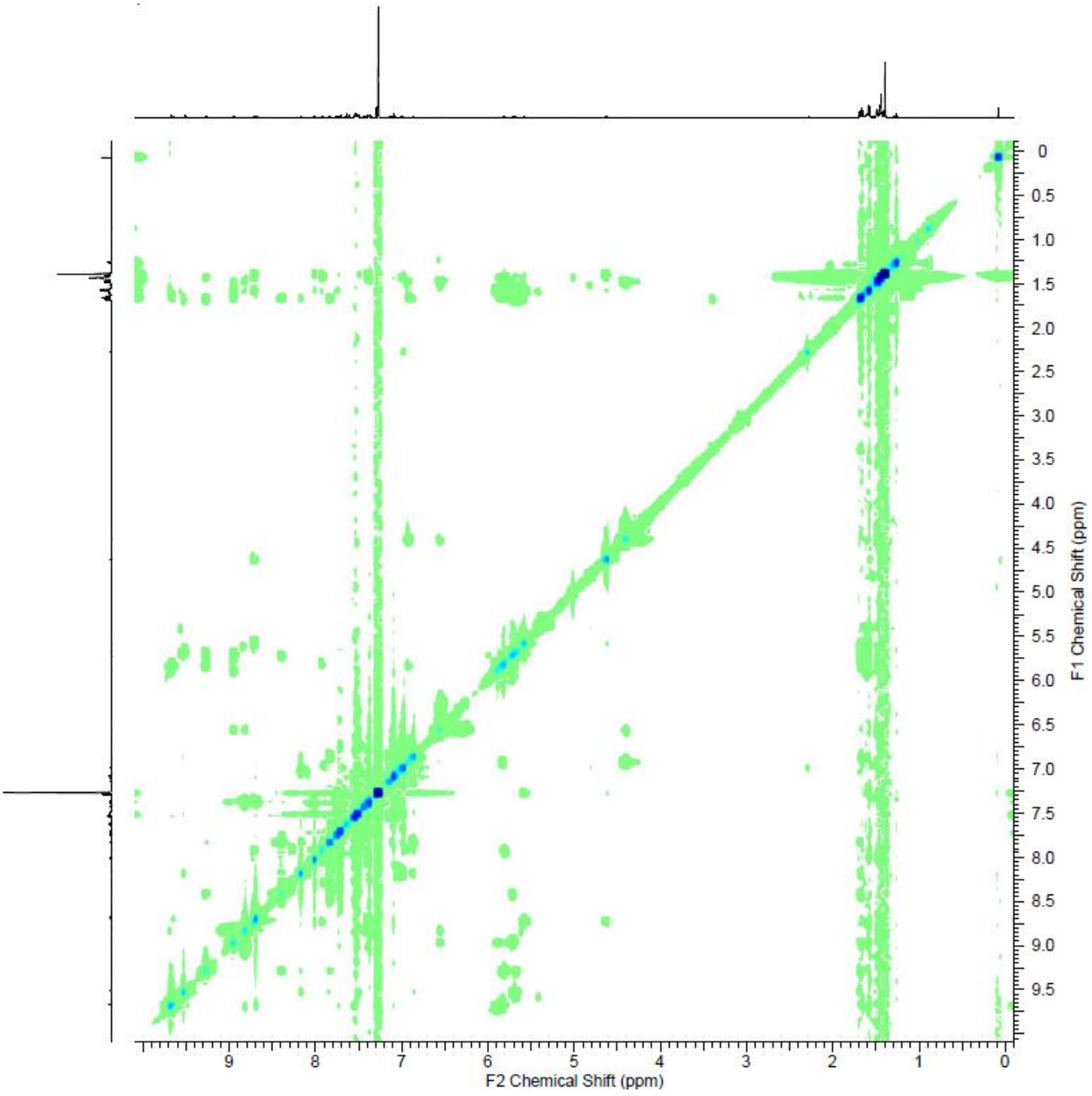

Figure 3.34 ROESY spectrum of four-stranded meander **59**.

3.9.2 Aggreation Assay

The meanders of interest and controls were assessed for aggregation in chloroform. A recent paper by Beaulieu *et al*. gives a simple NMR assay for determining aggregation.[96] Having

taken ^{1}H NMR spectra across two orders of magnitude of concentration, resonances showing change in chemical shift or shape are indicative of aggregation. Three spectra of each meander **56** and **59**, at concentrations of 10 mM (green), 1.0 mM (red) and 100 µM (blue), were obtained, overlaid and visually compared (Figure 3.35).

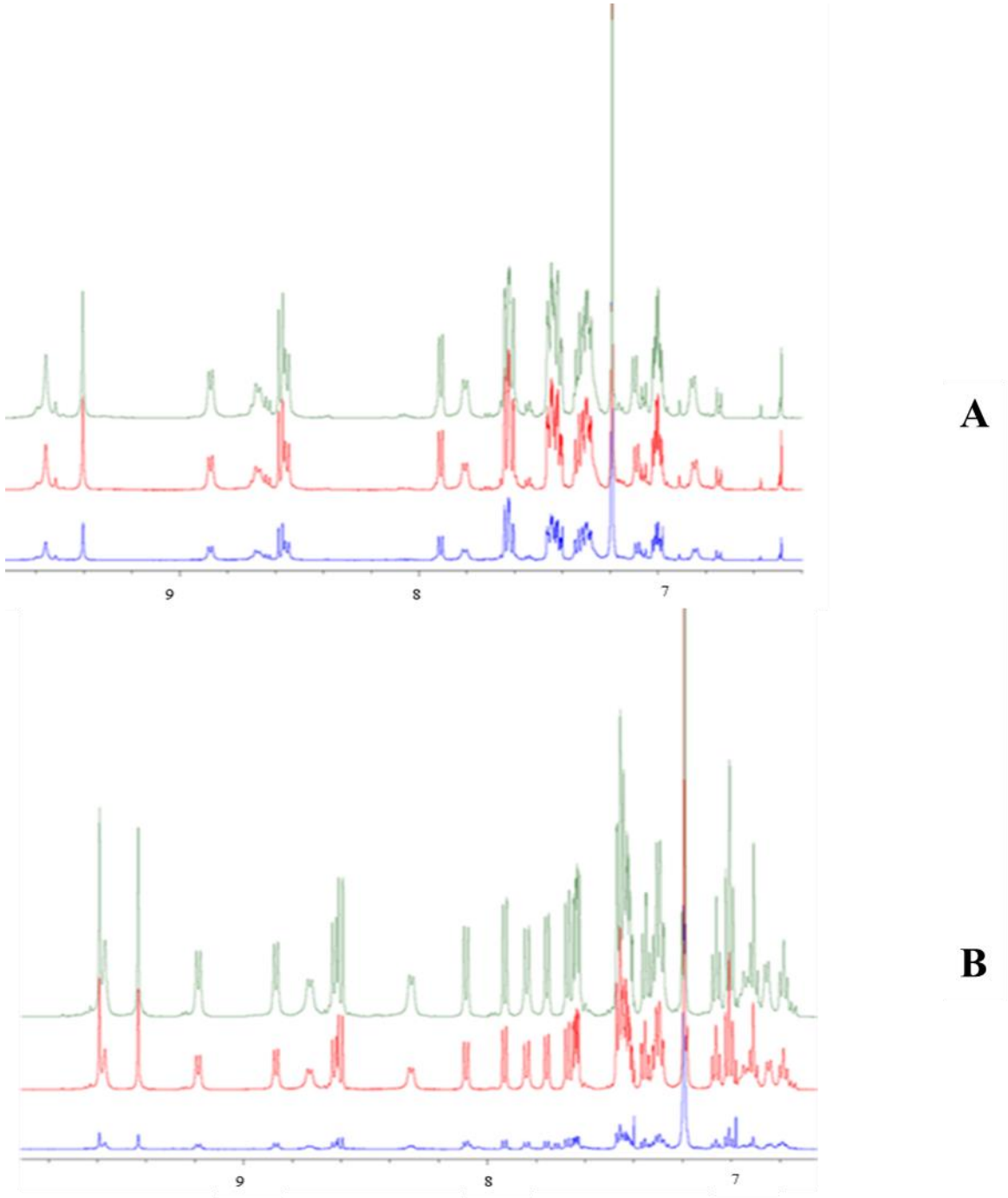

Figure 3.35 ^{1}H NMR overlay from an aggregation assay for three-stranded meander **56** (**A**) and four-stranded meander **59** (**B**) showing no change in chemical shift or peak shape as a result of changing concentration. Green, 10 mM; Red 1 mM; Blue 100 µM

Both meanders display no aggregation, with all resonances showing the same chemical shift and shape across the full range of concentrations. This, combined with the excellent peak dispersion in the ^{1}H spectra, provides good evidence of minimal aggregation of these sheet mimics.

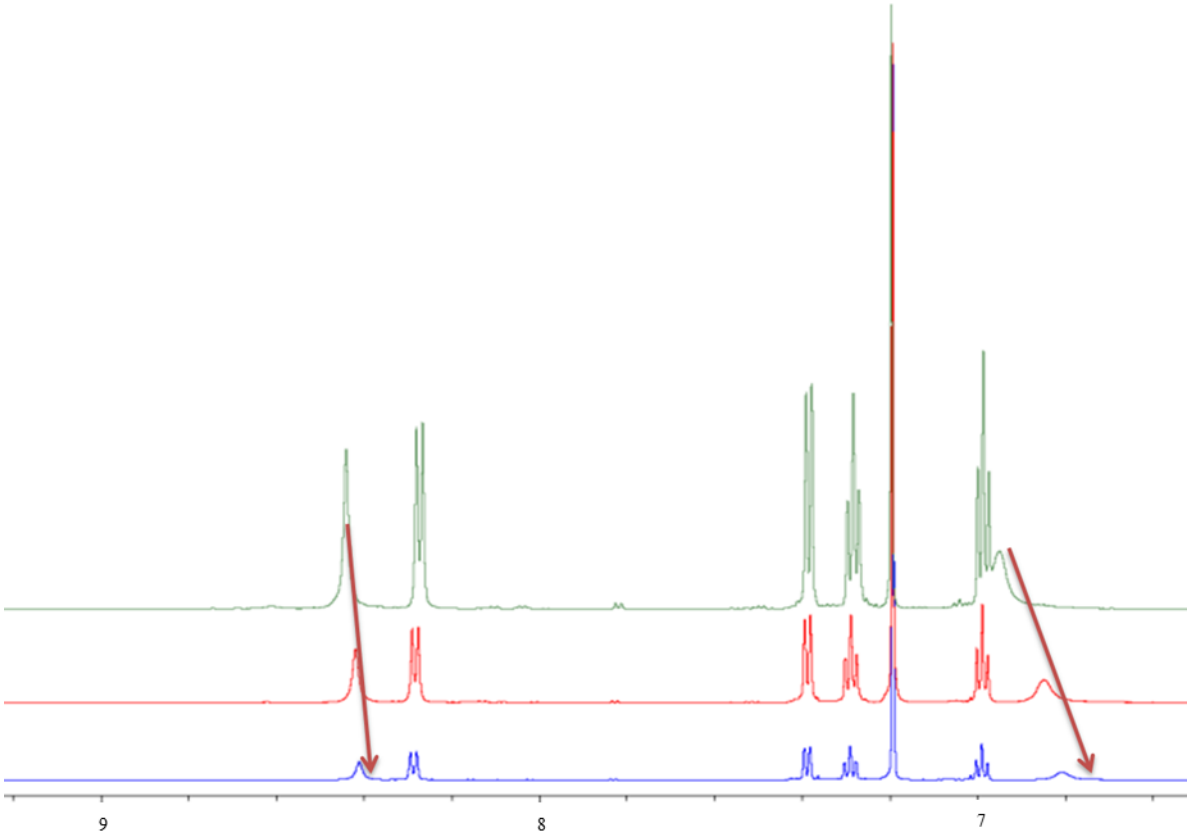

Figure 3.36 ^{1}H NMR spectral overlay from an aggregation assay for control molecule **53**. Amide peaks with changing chemical shift highlighted, indicative of aggregation. Green, 10 mM; Red 1 mM; Blue 100 µM

However, for all the control molecules small changes in chemical shift and clear changes in peak shape were observed, indicating a degree of aggregation (Figure 3.36). Given the propensity of small hydrophobic peptide fragments to aggregate it is perhaps unsurprising that this behaviour is observed. This means that it is imperative to carefully consider the potential impact of concentration and possible aggregation on future experiments.

3.9.3 ROESY Analysis

Both meanders with molecular weights between 1000 and 1500 Da are in the cross-over region of tumbling speed for NOESY spectra and were therefore only suitable for ROESY analysis. The ROESY spectrum of **56** at a concentration of 10 mM in $CDCl_3$ shows cross-strand correlations between the Cα hydrogens, Cβ hydrogens and amide N-Hs (Figure 3.37).

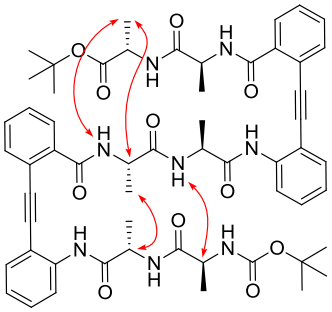

56

Figure 3.37 Cross-strand correlations indicated by a ROESY experiment on meander **56** indicating the population of the desired conformation in solution.

Some of these are only weak interactions as would be expected for interactions between opposite faces. They could come about as the molecule twists out of the plane. Unfortunately the data shows too high an incidence of resonances in the desired region to observe cross-strand Cβ-Cβ hydrogen interactions. However, a much stronger interaction is observed between the *tert*-butyl ester and a group of three aromatic hydrogens. Complete assignment of the aromatic hydrogens was not possible due to spectral coincidence, and there are therefore two possible conformations in which this interaction can occur (Figure 3.38).

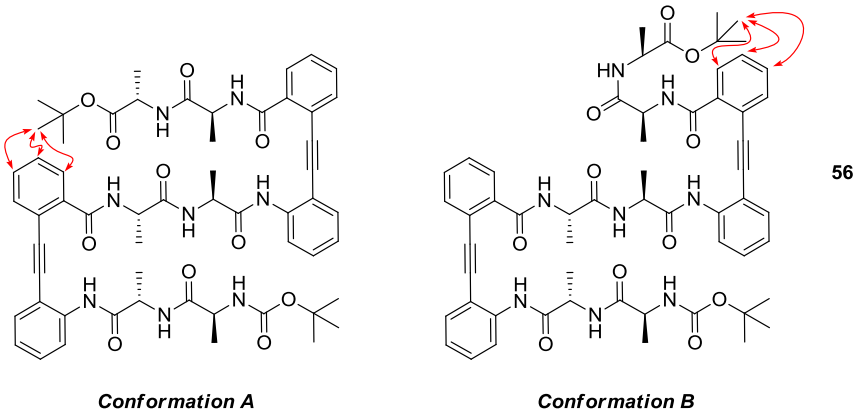

Figure 3.38 Two possible conformations arising from observed ROESY correlations between *tert*-butyl and aromatic protons.

Analysis of the spectrum for other correlations that provide further evidence for either of these conformations was unsuccessful. However given the wealth of data from other solution phase experiments, the correlations arising from conformation ***A*** would appear to be more likely.

Interestingly the corresponding interaction between the *tert*-butyl of the Boc protecting group and any aromatic hydrogens is not observed. Assuming that conformation ***A*** is preferred, it is hypothesised that the additional methylene unit equivalent within the carbamate, as compared to the ester, results in a steric clash between the *tert*-butyl group and the aromatic hydrogens, forcing the group away and preventing the hydrogen bonding network from completely forming. This hypothesis is reinforced by both the computational studies (Section 3.7) and the X-ray crystal structure (Section 3.9.10) that show the carbamate group being forced away from the aromatic linker system.

A ROESY spectrum of **59** at a concentration of 10 mM in $CDCl_3$ shows very similar correlations (Figure 3.39). The cross-strand interactions are again present, as are the *tert*-butyl – aromatic interactions. However the αH to NH cross-strand interactions slightly confuse the picture. This could be a result of spin diffusion. Alternatively the low barrier to

rotation around the central acetylene axis (~ 1 kcal.mol^{-1}) can result in extensive puckering that allow for such interactions.

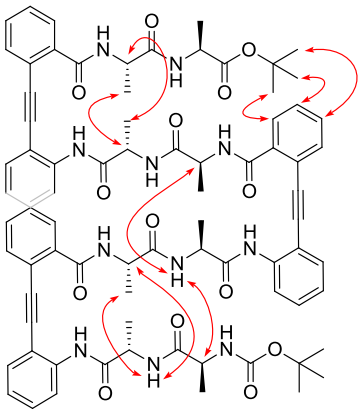

59

Figure 3.39 Cross-strand correlations indicated by a ROESY experiment on mimic **59**.

3.9.4 NMR Shift Analysis

It is well established that within a peptide strand the shift of the α-proton will move downfield as the strand is extended and becomes more β-sheet like.[97,98] Gellman has used these shift changes as evidence of the population of the folded state.[99]

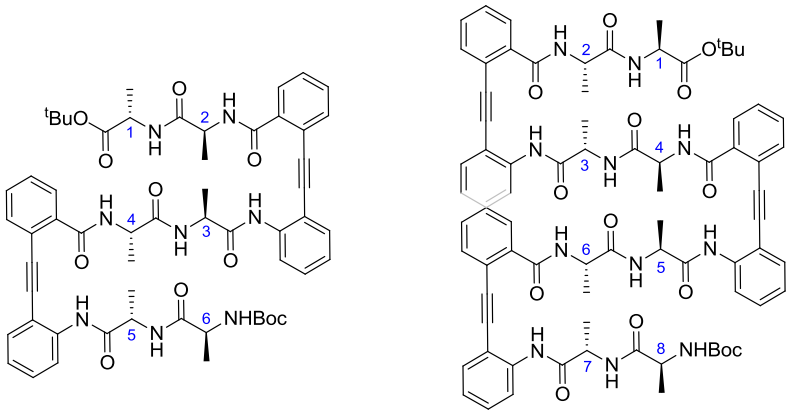

56 **59**

Figure 3.40 Numerical assignment of residues in meanders **56** and **59**.

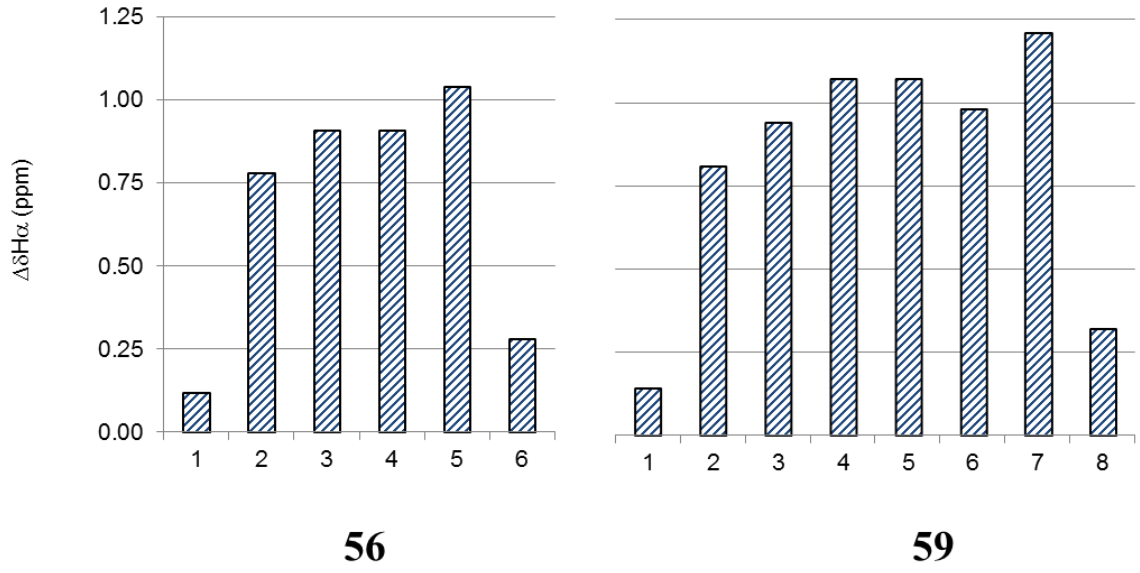

Figure 3.41 ^{1}H NMR chemical shift values of the α-hydrogens in meanders **56** and **59** relative to the corresponding positions in single-stranded controls **53**, **64**, and **68**.

By comparing the chemical shift values of the α-proton within the completed meanders **56** and **59** to the relevant control (Figure 3.41) it is possible to analyse the extent to which β-sheet character is imposed by the meander motif. The non-terminal amino acids show downfield shifts of 0.78 – 1.21 ppm relative to the controls. The corresponding range for terminal amino acids is 0.12 – 0.32 ppm, indicative of less pronounced β-sheet structure and fraying at the end of each strand. The average downfield shift for non-terminal residues in three-stranded **56** is 0.90 ppm and in four-stranded **59**, 1.00 ppm. This increase indicates the possibility of a cooperative effect, whereby the presence of each additional strand within the meander system reinforces the conformational preference.

This prompted further analysis of the chemical shifts of both the α- and amide N-H's to probe for a cooperative effect. The amide N-H's were included as it would be expected that as the strength of this hydrogen bond increases the signal moves further downfield due to more extensive deshielding when involved in a cooperatively enhanced hydrogen bond.[100]

As the number of strands is increased it is possible to track the shift of equivalent protons. The strands for each molecule are designated numerically according to Figure 3.42. The α- and N-H's are numbered from 1-3 (red for N-H, blue for α-proton) from left to right within each strand. For each strand it is then possible to track the change in chemical shift of the α- and amide protons. These changes are shown in Figures 3.43 - 3.45.

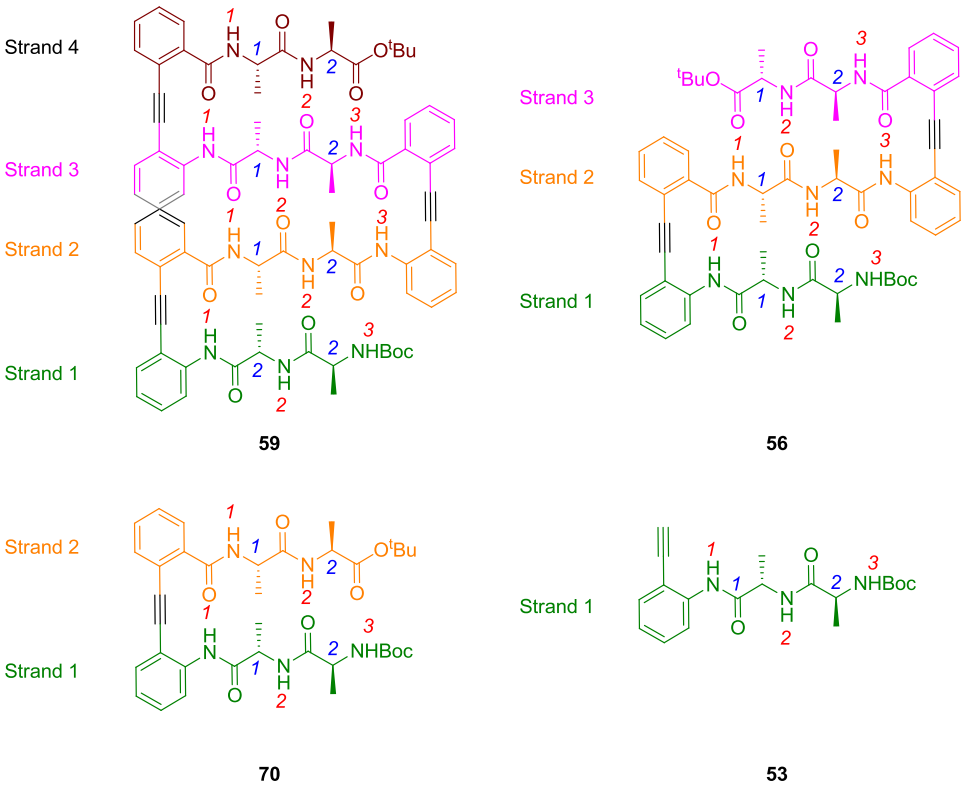

Figure 3.42 Residue labels for cooperativity analysis in ^{1}H NMR shifts,

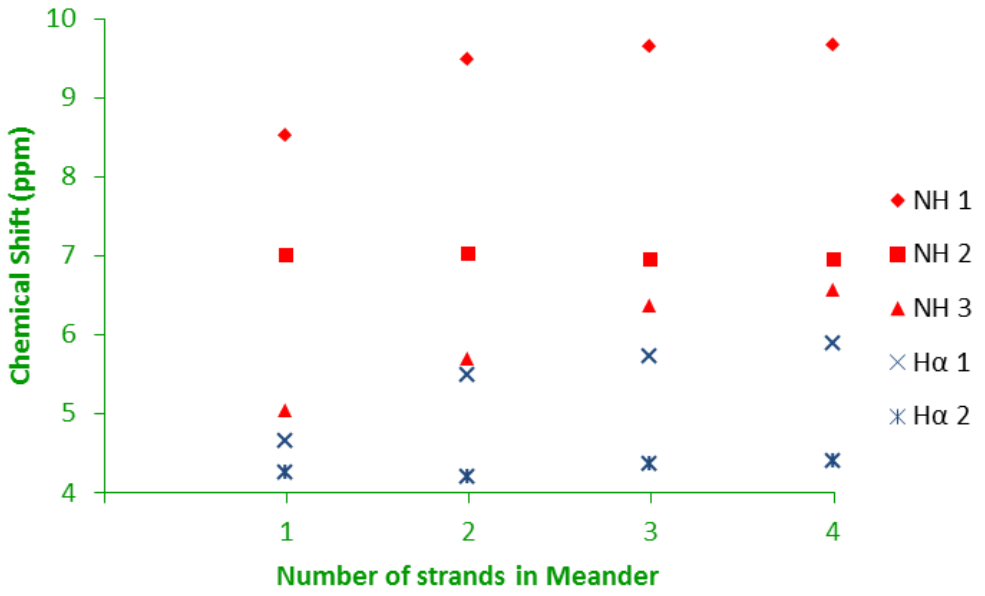

Figure 3.43 Change in chemical shift for α- and amide N-Hs in Strand 1. The increasing value is indicative of the formation of sheet structure and shows a positive cooperative effect whereby the addition of each strand reinforces the strength of the hydrogen bonds in the existing sheet.

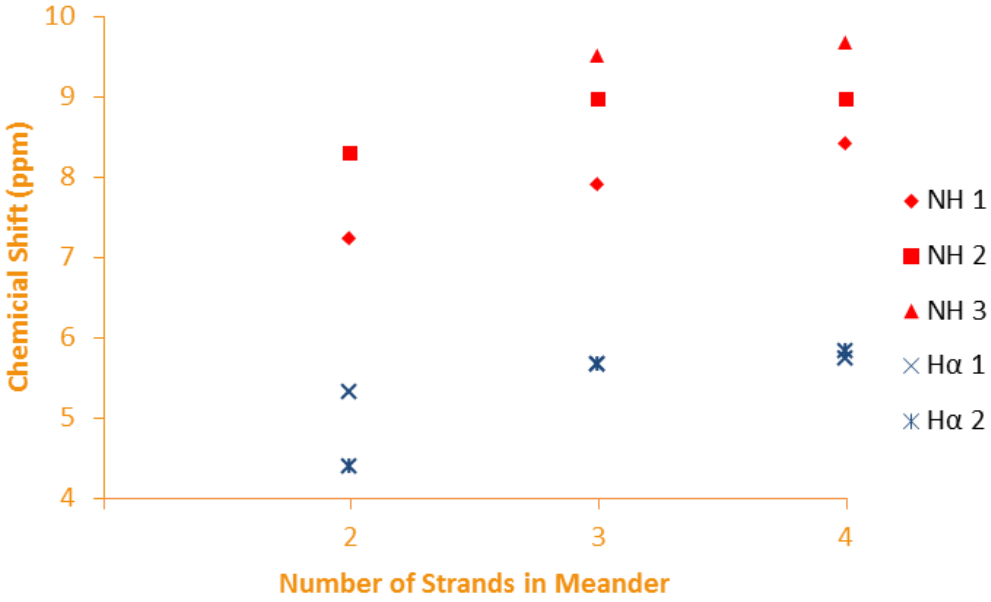

Figure 3.44 Change in chemical shift for α- and amide N-Hs in Strand 2. The increasing value is indicative of the formation of sheet structure and shows a positive cooperative effect whereby the addition of each strand reinforces the strength of the hydrogen bonds in the existing sheet.

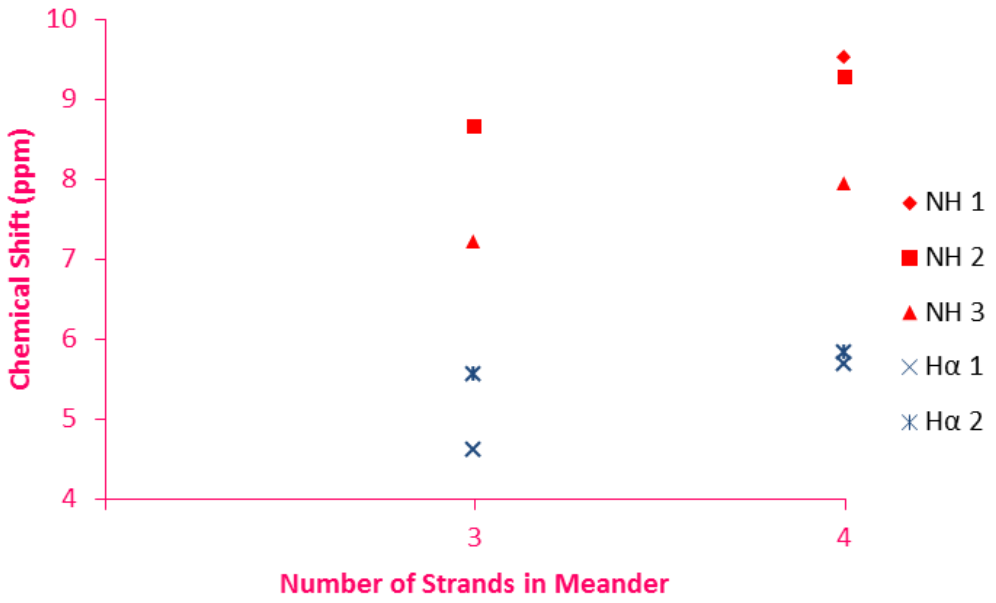

Figure 3.45 Change in chemical shift for α- and amide N-Hs in Strand 3. The increasing value is indicative of the formation of sheet structure and shows a positive cooperative effect whereby the addition of each strand reinforces the strength of the hydrogen bonds in the existing sheet.

The data shows that increasing the number of strands moves the shift of the α-protons downfield in all cases. This change is greatest for the non-terminal residues. For example in Strand 1, α-proton 1 shows a much larger downfield shift than the terminal α-proton *b*. The amide N-Hs that are involved in hydrogen bonds similarly show a downfield shift. Those not involved in a hydrogen bond, for example N-*H*-2 in Strand 1 show no change. Interestingly the amide N-Hs involved in the Kemp turn, after the formation of the first hydrogen bond show no further downfield shift with an increasing number of strands. By contrast, the amide N-Hs involved in hydrogen bonds in the middle of the strands do show a continuing downfield shift.

This continued downfield shift of α-protons as the number of strands increases therefore supports the hypothesis of a degree of cooperation in the formation of increasingly large structures. That this effect is also present for the amide N-Hs is further strong evidence. Both of these analyses indicate that the mimics show a strong preference for the formation of the extended β-sheet conformation.

3.9.5 Secondary Structure Propensity Score

A computational method developed by Forman-Kay *et al*.[101] provides the ability to score each residue on its β-sheet or α-helix character, and subsequently provide an overall indication of the character of the molecule as a whole. In 1994 Wishart and Sykes developed a method known as secondary chemical shifts as a simple measure of secondary structure. The ^{1}H NMR shift of the α-proton is observed and Δδ derived as follows;

$$\Delta\delta = \delta_{observed} - \delta_{coil}$$

where Δδ > 0 indicates α-helix and Δδ < 0 indicates β-strand.[102] However this simple method does not take into account the sensitivity of different amino acids for determining secondary structure.[103] Forman-Kay therefore developed a method that uses the chemical shifts of the $^{1}H^{N}$, $^{1}H^{\alpha}$, $^{13}C^{\alpha}$, $^{13}C^{\beta}$, $^{13}C^{C=O}$, the nature of the amino acid and weights all these contributions by their sensitivity to α and β structure to produce a final numerical score between -1 and 1. Within natural peptides a score of 1 is indicative of complete α-helix character and -1 complete β-sheet. The score of each residue in chloroform is shown in Figure 3.46, but the nature of the calculation means that no score is provided for the residue at the *C*-terminus. The numbering of the residues is as in Figure 3.40.

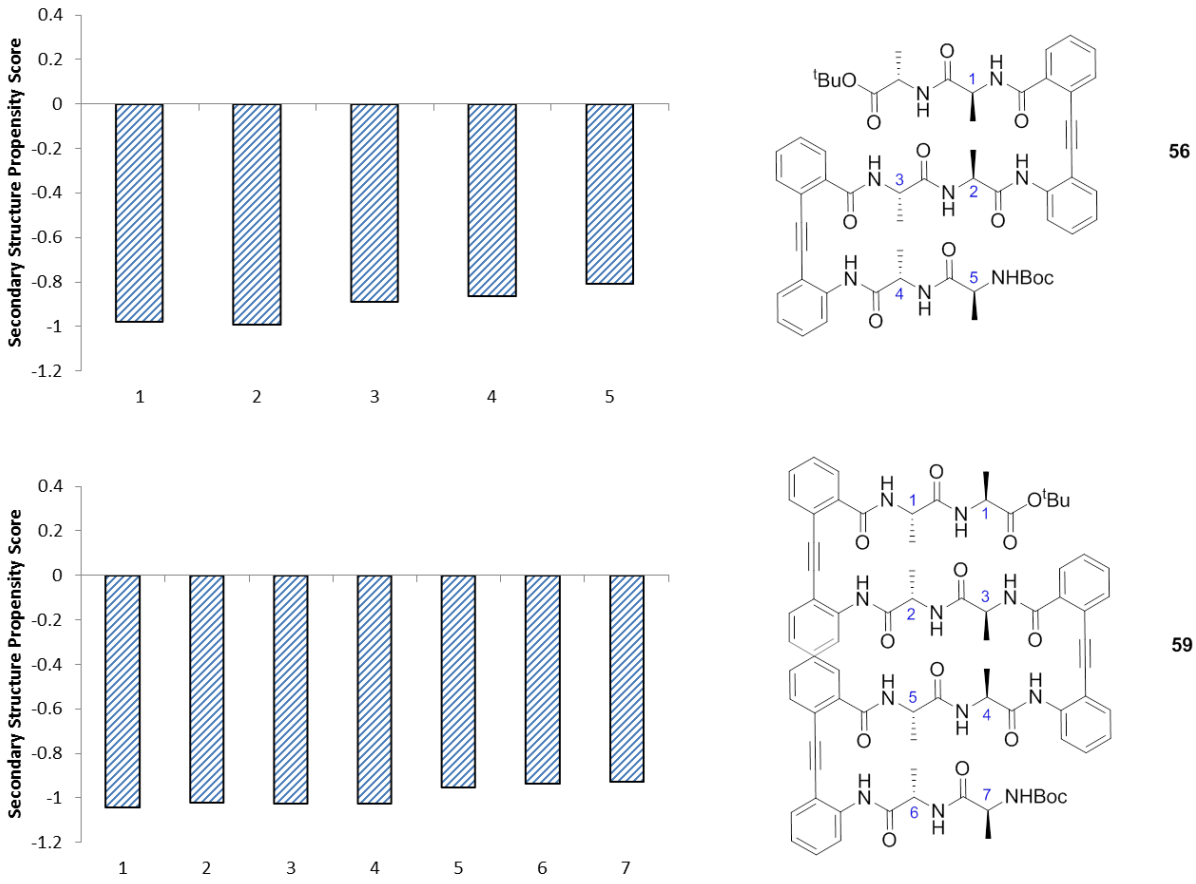

Figure 3.46 Secondary structure propensity scores in $CDCl_3$ for three-stranded meander **56** (Top) and four-stranded meander **59** (Bottom). Negative scores are indicative of β-sheet structure.

The individual residue scores clearly show that each residue provides NMR shift data that points strongly towards a β-sheet like environment. Some residues in the four-stranded mimic **59** have a score of marginally less than -1, perhaps indicating that the metric is incorrectly calibrated for the inclusion of non-natural elements such as the diphenylacetylene within the molecule, and for use in a non-aqueous solvent. However when these scores are considered relative to the control molecules (see below), a strong qualitative argument for β-sheet structure remains.

These individual residue scores can be combined to give an overall score for the molecule, expressed as a percentage of β-sheet or α-helix character. The mean β-sheet score was 94.0 % for three-stranded meander **56** and 99.8 % for four-stranded meander **59**, both with an α-helix

score of 0 %. Once again a degree of positive cooperativity was observed with the four-stranded meander having a greater β-sheet character than the three-stranded.

The experiment was repeated on control molecules **53**, **64**, and **68**, whilst **72** was specifically used to investigate the effect on the propensity scores of the artificial diphenylacetylene linker. In all cases the overall β-sheet character was between 0 and 32 % demonstrating that appreciable β-sheet character has been imparted by the designed meander motif.

The experiment was repeated in DMSO-d_6 as an alternative solvent (Figure 3.47).

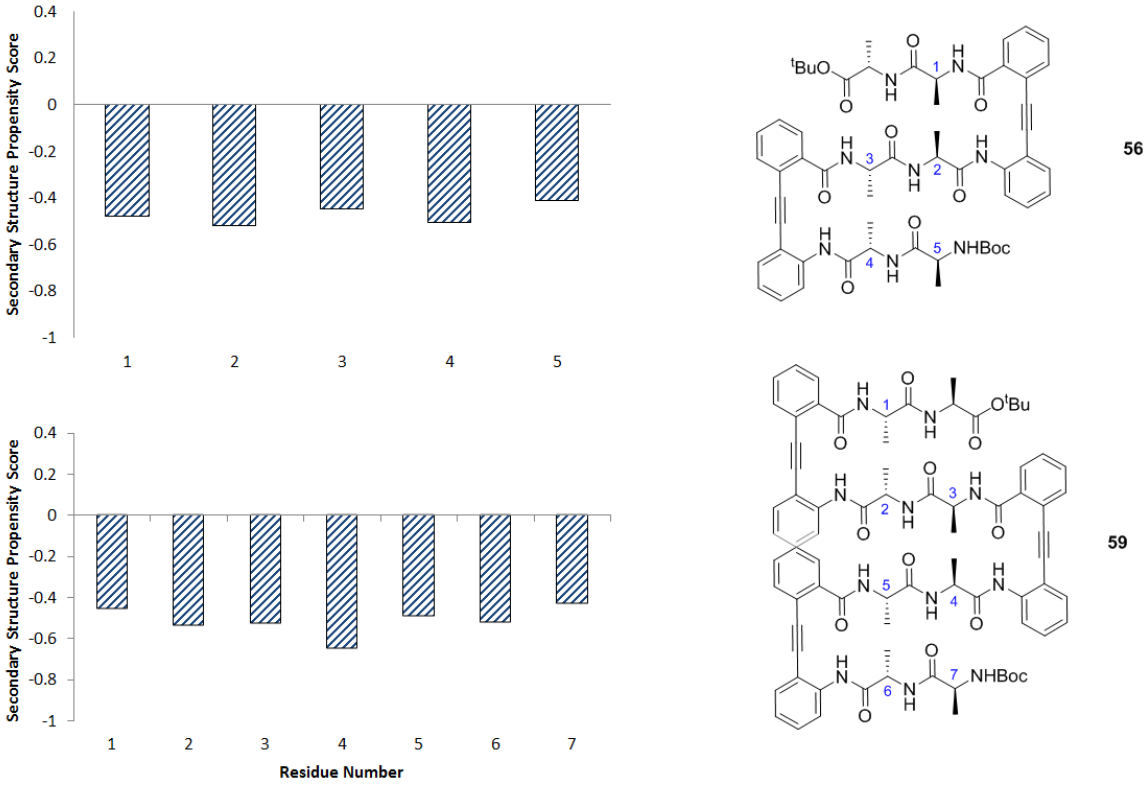

Figure 3.47 Secondary structure propensity scores in DMSO-d_6 for three-stranded meander **56** (Top) and four-stranded meander **59** (Bottom). Negative scores are indicative of β-sheet structure.

As a hydrogen bond acceptor, DMSO has the ability to significantly disrupt any hydrogen bonding networks. It is therefore unsurprising that the scores are reduced when compared to chloroform. The mean β-sheet scores for each molecule were 48.8 % and 51.6 %, again with no α-helix character. When compared to scores for sheet segments of natural proteins these

scores remain extremely favourable, and indicate that a strong conformational bias is still present. For example the SSP score for the sheet forming regions of anginex (see Section 3.5.1 above) fall between -0.2 and -0.4.[104]

3.9.6 Hydrogen-Deuterium Exchange

Further support for the proposed structure is provided by deuterium exchange experiments, whereby the hydrogen-bonded amide N-Hs would be expected to exchange less rapidly than those exposed to solvent. This technique is applicable to the study of hydrogen bonding in both complete proteins[105] and small molecules,[106] and as such is an ideal technique for the meanders in this study.

Adapting a literature procedure,[107] an initial ^{1}H NMR spectrum was recorded (10.48 mM in 480 µL $CDCl_3$). CD_3OD (20 µL, resulting in a final substrate concentration of 10.00 mM and a methanol concentration of 0.99 M) was added at time = 0 and a spectrum acquired five minutes later, marking time = 5 mins. Further spectra were acquired at two-minute intervals until t = 100 mins. A distinct non-exchanging signal was used as an internal integration reference. Integration ranges for exchanging protons are user-defined, and self-consistent within each experiment. The *y*-intercept is taken as the calculated value at $t = 0$, and this value was used to normalize the data to % hydrogen remaining. The values for all compounds were averaged from three runs. For all data presented any amide N-Hs not shown on the graph completely exchange before the first reading is taken at time = 5 min.

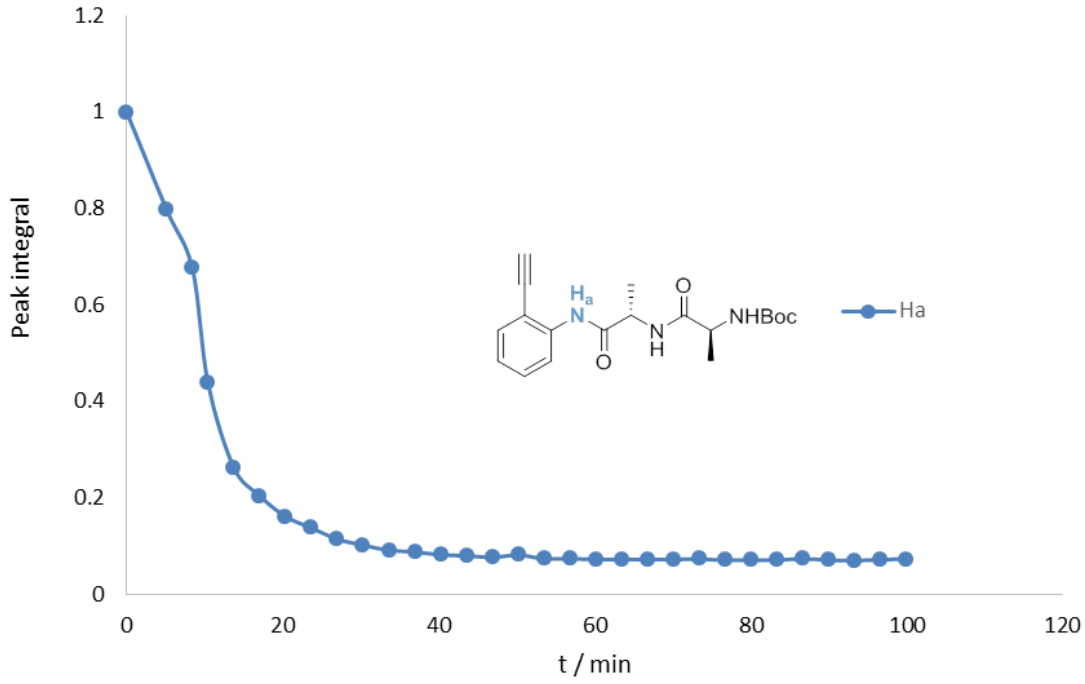

Figure 3.48 Hydrogen/deuterium exchange for control molecule **53**. Amide N-Hs that underwent complete exchange prior to the first ^{1}H spectrum acquisition at t = 5 min are omitted for clarity.

For control molecule **53** complete exchange was observed for amides *H*b and *H*c within five minutes (Figure 3.48). *H*a undergoes complete exchange within forty minutes with a half-life of nine minutes. All of these amide N-Hs are expected to be fully exposed to solvent and therefore undergo the observed fast exchange. The difference between the exchange rates presumably lies in the different kinetic acidities of the aromatic and peptidic amides. The aggregation of this control in chloroform must be acknowledged for this experiment and would probably confound any exact quantitative analysis. However in providing evidence for the fast exchange of all protons in a molecule completely exposed to solvent and allowing a qualitative comparison to the meanders of interest, the small extent of the aggregation should not affect the qualitative interpretation.

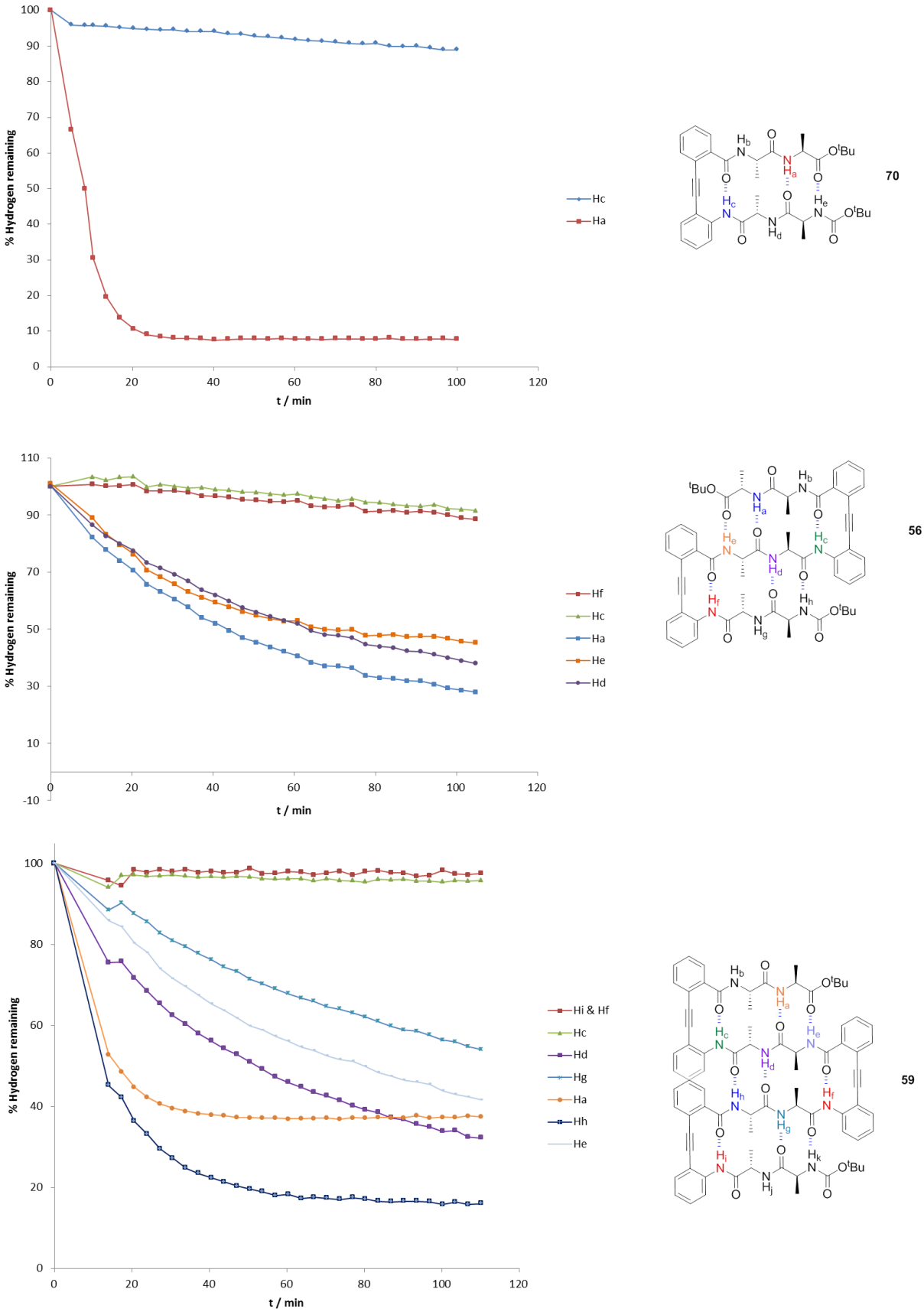

Figure 3.49 Hydrogen/deuterium exchange for double strand **70**, three-stranded **56**, and four-stranded **59**. Amide N-Hs that underwent complete exchange prior to the first ^{1}H spectrum acquisition at t = 5 min are omitted for clarity.

This complete exchange was observed for all the amide N-Hs on the 'outside' of the meanders (*H*b and *H*d for double-stranded **70**, *H*b and *H*g for three-stranded **56**; *H*b and *H*j for four-stranded **59**) providing evidence for their exposure to solvent.

For all molecules the amide N-Hs within the Kemp turn (*H*c for **70**; *H*c and *H*f for **56**; *H*c, *H*f and *H*i for **59**) display a very slow rate of exchange. This is expected from the nature of the linker that conformationally pre-organises these amide N-Hs into a hydrogen bond and the large downfield shift of these protons within the ^{1}H NMR spectrum. The protons in the middle of the strands show an intermediate rate of exchange. This could be due to weaker hydrogen bonds in the middle of the strands but the fact that the aromatic amide had a slower rate of exchange in the control molecule could be skewing the interpretation of these results, and therefore no firm conclusion regarding hydrogen bond strength can be reached.

Of interest is that for four-stranded meander **59**, and within the proposed bonding network, *H*h shows the fastest rate of exchange. This could be explained by the fact that the phenylacetylene linkers would clash if the molecule was sitting in a flat conformation and therefore the molecule must be slightly twisted out of plane, potentially weakening this hydrogen bond (Figure 3.50).

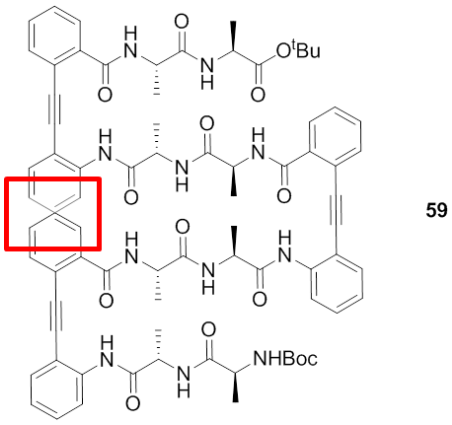

59

Figure 3.50 Four-stranded **59** with the potential clash between phenyl rings highlighted.

Finally *H*e, (double-stranded **70**), H_h (three-stranded **56**) and *H*k (four-stranded **59**) exchange completely within five minutes. As part of a carbamate group rather than an amide, the proton is less acidic, and therefore a weaker hydrogen bond donor.[108] This would be expected to result in slower exchange. Therefore the observed rapid exchange requires an explanation. No firm conclusions can be drawn from comparison to the control compound as that also undergoes complete exchange within five minutes. A putative explanation is provided by the NOE data, whereby the extra methylene unit equivalent within the carbamate compared to the *C*-terminal ester results in a steric clash between the *tert*-butyl group and the aromatic protons, forcing the group away and preventing the hydrogen bonding.

These H/D exchange results provide good evidence for the proposed hydrogen bonding network, whilst also painting a more nuanced picture of some aspects of the meanders.

3.9.7 Variable Temperature Studies

The use of variable temperature ^{1}H NMR studies to identify hydrogen bonding is a well-established technique.[109] When placed in DMSO, the hydrogen bonded amide N-Hs are protected from the solvent, whereas those that are not will be exposed to solvent. As the temperature is varied the non-hydrogen bonded protons will therefore experience a more rapidly changing environment as the temperature change has a greater effect on the behaviour of the DMSO. This will manifest itself in a greater change in chemical shift of the proton. It is widely held that a move of greater than 6 ppb.K^{-1} indicates no internal hydrogen bonding network, whereas less than 4 ppb.K^{-1} is evidence of one.[110,111] This deduction is based on the assumption of no major conformational changes as a result of increasing temperature.

To perform the experiment 500 µL of a 10 mM solution of each molecule was made up in DMSO-d_6. ^{1}H, and COSY spectra to aid in assignment, were recorded at 5 K intervals from 298 K to 343 K. The chemical shift of each amide N-H was recorded for each temperature

and then plotted to determine the rate of change of chemical shift against temperature in ppb K^{-1}.

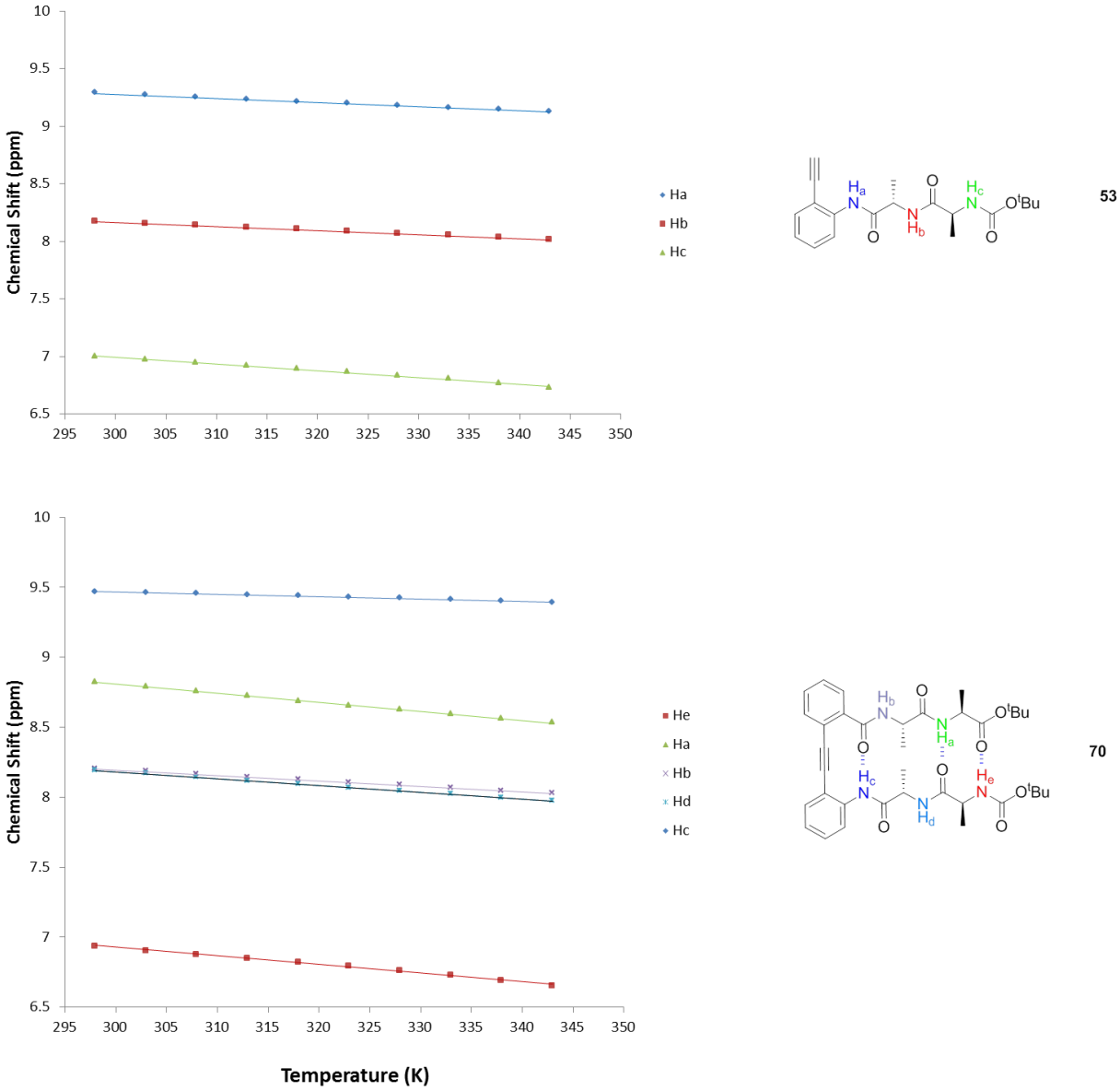

Figure 3.51 Amide N-H chemical shifts during variable temperature study on control molecule **53** and two-stranded turn mimic **70** in DMSO.

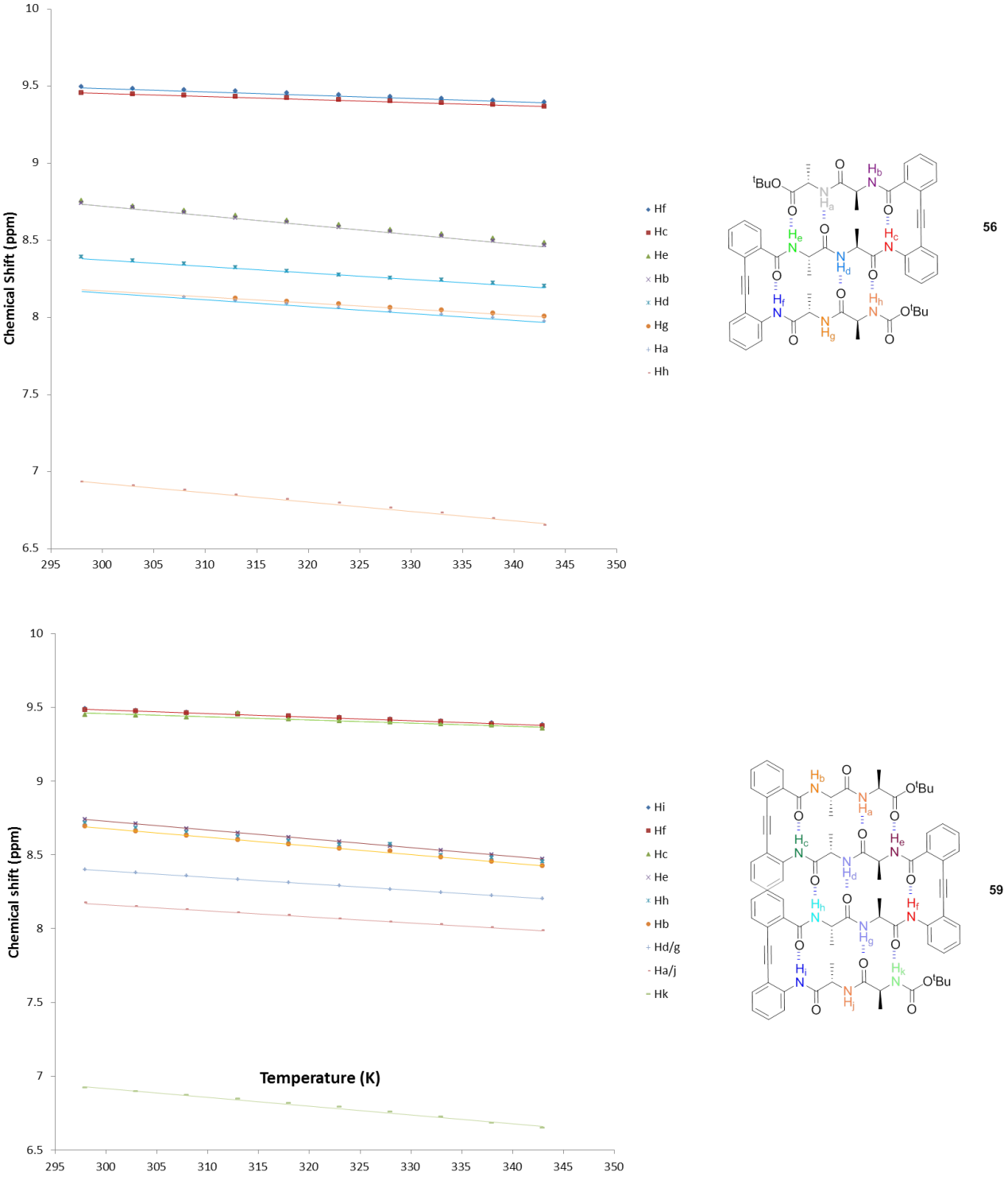

Figure 3.52 Amide N-H chemical shifts during variable temperature study on three-stranded **56** and four-stranded turn **59** in DMSO. For four-stranded meander **59** selected resonances were coincident throughout the experiment and so could not be distinguished from each other. Amide N-H *f* could not be distinguished from the aromatic peaks due to spectral coincidence and so was not recorded.

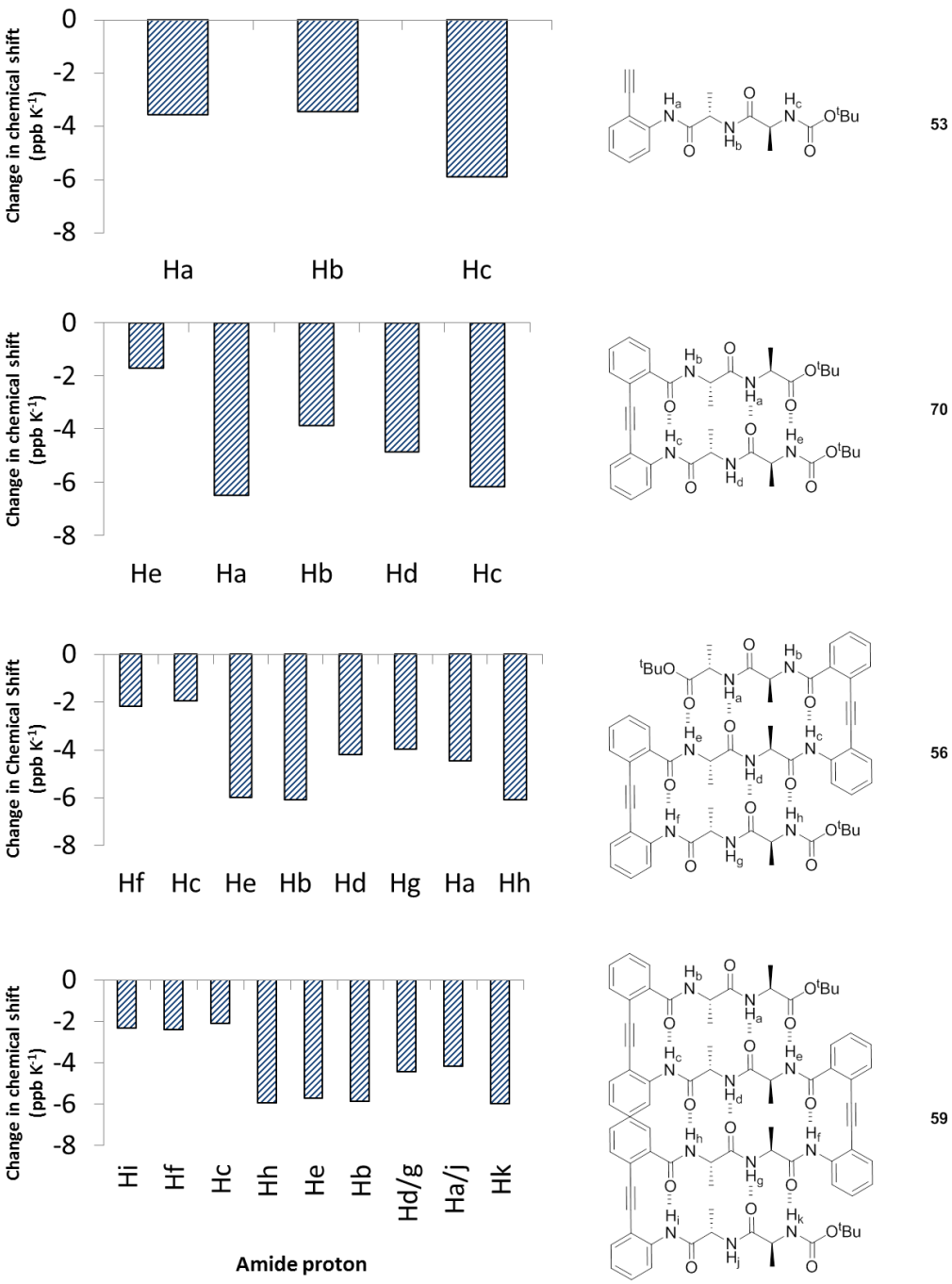

Figure 3.53 Gradient of chemical shift for each amide N-H in control molecule **53**, two-stranded turn **70**, three-stranded meander **56** and four-stranded meander **59**.

These results show that for molecules, **70**, **56**, and **59** the proton proximal to the aryl ring has a gradient of less than 2.5 ppb K^{-1}, providing further evidence of the hydrogen bond with the Kemp turn motif being strong. However beyond this none of the other amide N-Hs give values consistent with intramolecular hydrogen bonding. These results in isolation would therefore either imply that the molecules have not adopted the desired conformation in the

more competitive DMSO solvent or undergo large changes in conformation as a result of temperature changes. However given the linear nature of all the data, and the expectation of a step change for an unfolding event, this seems unlikely.

3.9.8 Chloroform-DMSO Titration

This titration experiment probes the response of amide N-Hs to changes in solvent composition, particularly in the progression from a non-hydrogen bonding solvent to a hydrogen bonding one. DMSO is capable of acting as a hydrogen bond acceptor and therefore a typical interaction with an amide N-H will result in a downfield shift as the nuclei become less shielded. As a result of this hydrogen bonding interaction, DMSO has the ability to disrupt hydrogen bonding networks. Where major disruption occurs the pattern and dispersion of the ^{1}H NMR spectrum should be significantly altered relative to that of chloroform. A minor disruption of the bonding network would manifest itself as a small downfield shift, as the strong intramolecular bonds are slightly weakened.

Adapting literature procedures,[112] a spectrum was taken of a sample at 10 mM in 500 µL of $CDCl_3$. DMSO was added in aliquots according to Table 3.3.

DMSO Added (µL)	Total DMSO (µL)	% DMSO
0	0	0
10	10	2
20	30	6
20	50	9
50	100	17
50	150	23
50	200	29

Table 3.3 Amount of DMSO added and corresponding % DMSO of total solution within each experiment.

Following each addition the sample was allowed to equilibrate for twenty minutes and the sample relocked and shimmed. To aid in assignment a COSY spectrum was taken at each titration point. Each spectrum was referenced to the residual $CHCl_3$ peak and the amide chemical shift values recorded and graphed.

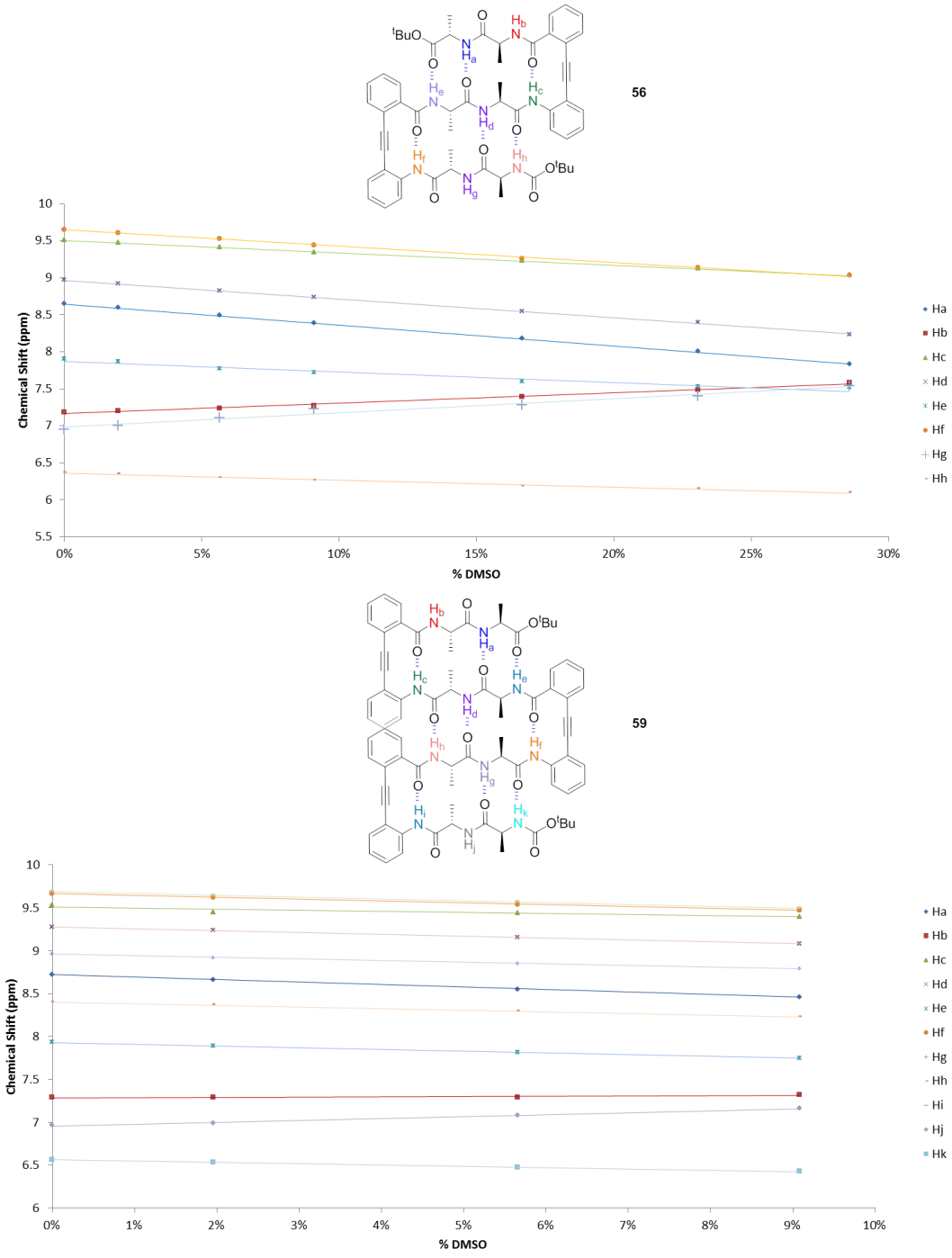

Figure 3.54 Plot of ^1H chemical shift (δ/ppm) against % DMSO added for three-stranded meander **56** and four-stranded meander **59**.

The gradients of each line can be calculated and shown in bar chart format for each amide proton (Figure 3.55).

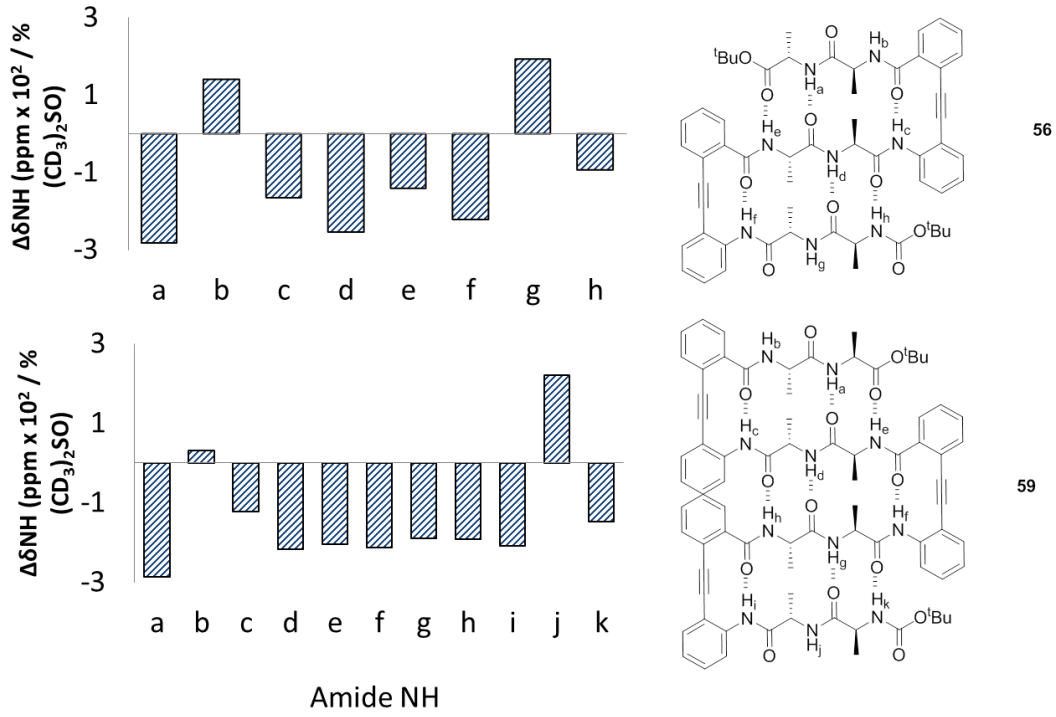

Figure 3.55 Gradient of change in chemical shift for each amide N-Hin meanders **56** and **59**. Positive values are indicative of a proton exposed to solvent whilst negative values are indicative of protons sitting with a pre-existing hydrogen bond.

Control molecule, **53**, and two-stranded **70**, produced the following data under the same experimental conditions (Figure 3.56).

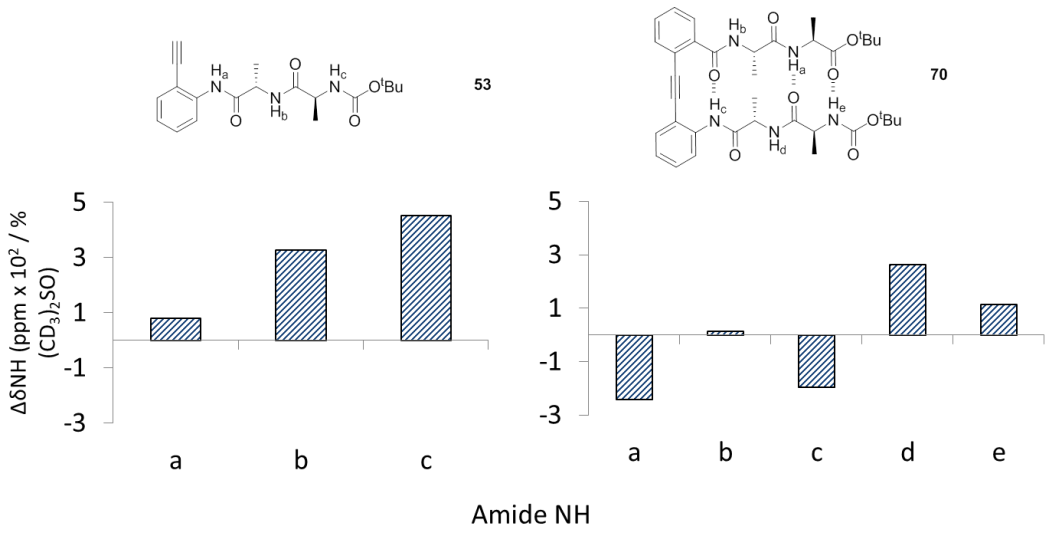

Figure 3.56 Gradient of change in chemical shift for each amide N-H in control **53** and turn mimic **70**.

As discussed in Section 3.9.4, an increase in hydrogen bonding results in a downfield shift. DMSO, unlike chloroform, is capable of forming intermolecular hydrogen bonds and so exposed amide N-H would be expected to move downfield.

In control molecule **53** (Figure 3.56) all of the amide N-H's are fully exposed to solvent, and as expected the addition of DMSO sees a downfield shift in the NMR spectrum. For all of the meander systems this pattern of exposed protons shifting upfield is observed (N-H *b* and *g* for **56**, N-H *b* and *j* for **59**, Figure 3.55). Where the amide N-Hs are already part of an intramolecular hydrogen bond this upfield shift would not be expected to occur. Instead a small downfield shift will occur as the more challenging solvent slightly disrupts the hydrogen bonding network. This pattern is observed for all the other amide N-Hs, providing further supporting evidence for the hydrogen bonding network proposed.

3.9.9 'A Value' Calculation

The use of deuterated chloroform and DMSO as NMR solvents can be extended to provide another measure of hydrogen bond strength. Abraham *et al*. have recently shown that the presence of an intramolecular hydrogen bond can be probed through the recording of the

chemical shift of a given O-H or N-H residue in both chloroform and DMSO.[113] The difference between the two chemical shifts can be directly related to the hydrogen bond acidity, ***A***, which can be used as a quantitative assessment of intramolecular hydrogen bonding.

$$\Delta\delta = \delta(DMSO) - \delta(CDCl_3)$$

$$\boldsymbol{A} = 0.0065 + 0.133\Delta\delta$$

A Value	Hydrogen Bond
A > 0.16	No
0.05 < ***A*** < 0.16	Maybe
0.05 > ***A***	Yes

Table 3.4 '***A*** value' calculation and interpretation.

Therefore NMR spectra of meanders **56** and **59**, turn mimic **70**, and control strand **53**, were obtained in DMSO-$_{d6}$ and the molecules fully characterised as described in Section 3.9.1. It should be noted that the dispersion of peaks observed in chloroform was repeated in DMSO. The chemical shift of each N-H residue was then inputted into the formula above and the ***A*** value computed. This value is overlaid on each molecule in Figure 3.57. Colours are used to indicate presence of a hydrogen bond; green for definitely present, orange for the uncertain region and red for definitely absent.

As would be expected the control molecule shows two red and one orange N-Hs, indicating a lack of hydrogen bonding. The amide N-H adjacent to the aryl ring, as observed in the deuterium exchange experiment behaves differently so the fact that it is observed in the indeterminate region is not unexpected. Progressing from one to four strands the same trends emerge; the formation of a clear hydrogen bonding network amongst the internal amide N-

Hs, whilst the N-Hs that would be expected to be exposed to solvent give no indication of intramolecular bonds being formed.

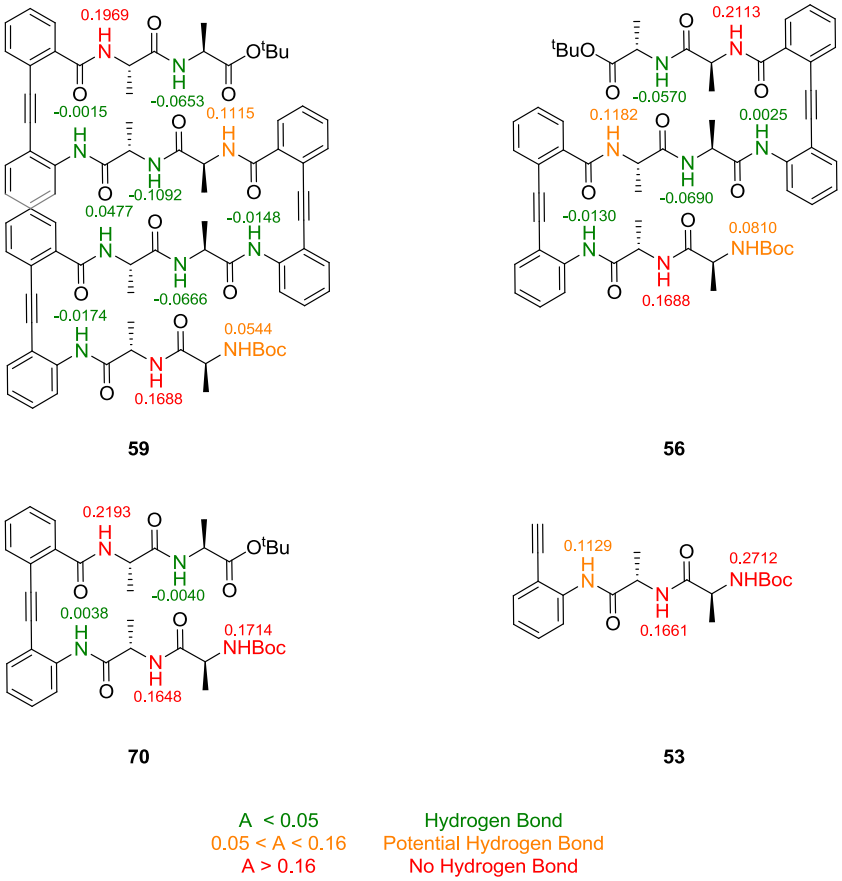

Figure 3.57 '***A*** values' and corresponding hydrogen bond strength interpretation overlaid onto the meanders and controls.

Again it is possible to observe the increased cooperative effect as the number of strands increases as the ***A*** value for the equivalent proton steadily descends, indicating a stronger hydrogen bond as the number of strands increases.

For the four-stranded meander **59** the data are consistent with some of the finer points to emerge from the deuterium exchange experiments. Recall that amide N-H ***h***, near where the two phenyl rings could clash showed the fastest rate of exchange indicating a weak hydrogen bond. Here the ***A*** value of 0.0477 is at the upper bound of hydrogen bonding. Considering all of the other ***A*** values within the network are below zero, this provides further evidence for the hypothesis of the two rings clashing and therefore either lengthening and weakening the

proximal hydrogen bond, or resulting in a number of different conformers, with the desired conformer only populated to a limited extent.

This data also provides evidence of the termini fraying but still displaying a cooperative effect with increasing strand number. For example considering the N-H within the carbamate group there is a clear trend towards increasing hydrogen bond strength (Table 3.5).

Number of Strands	***A*** Value
1	0.2712
2	0.1714
3	0.0810
4	0.0544

Table 3.5 ***A*** value of the carbamate group N-H as the number of strands increases.

3.9.10 Solid Phase Studies

Crystals of meander **56** were grown by vapour diffusion, data collected at the Diamond Synchrotron and the X-ray crystal structures solved. Four different conformers of **56** were present within the asymmetric unit.

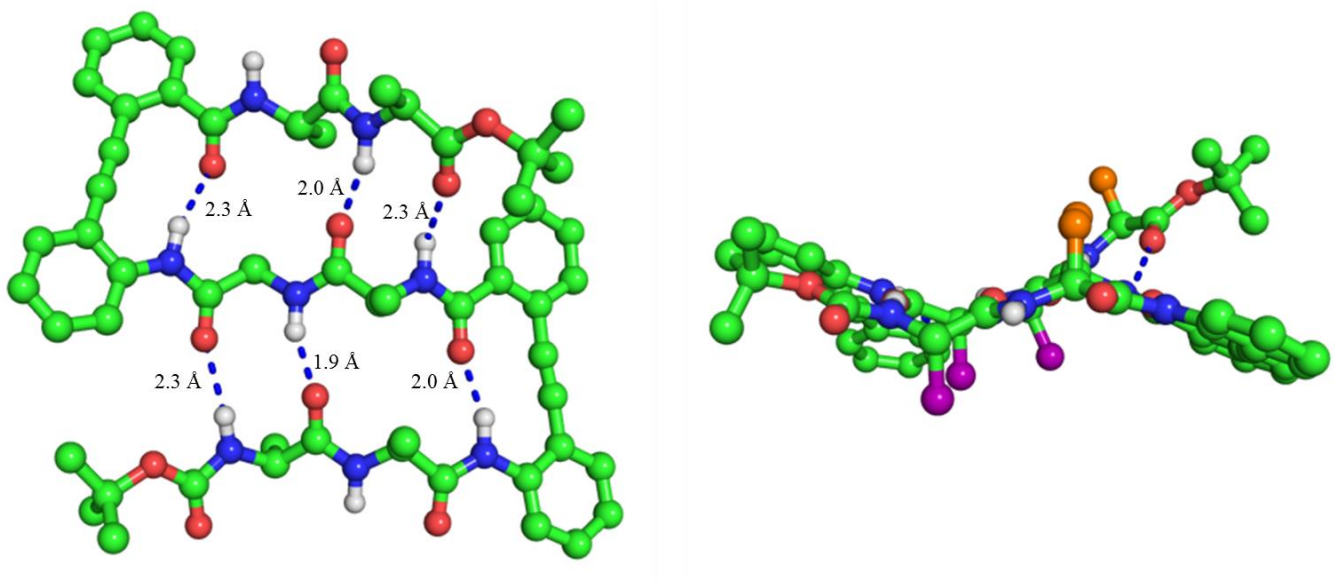

Figure 3.58 Single crystal X-ray structure of meander **56**. **Left**: Top elevation showing hydrogen bonding network with H-O distances indicated in Å. **Right**: Side view showing control over side-chain display and pleated appearance. Coloured spheres indicate side-chain display above (orange) and below (purple) the plane of the molecule (CCDC: 1049256).

The crystal structure agrees well with the overall picture provided by the solution phase NMR data, with three intramolecularly hydrogen-bonded strands and a network of six intramolecular hydrogen bonds. The hydrogen bond lengths range from 1.9 to 2.3 Å, in good agreement with those found in a natural β-sheet. Similarly the intra-strand α-C to α-C distances range from range from 4.0 to 5.5 Å, and the β-C to β-C distances of 3.8 to 5.5 Å, both comparable with the conventional β-sheet. This hydrogen bonding network provides the platform for the projection of side-chains above and below the plane. This unequivocally demonstrates the ability of the system to control side-chain display in the solid state. Indeed a structural overlay of the crystal structure with the β-sheet found in the OspA mutant membrane protein of Borreliella burgdorferi shows excellent overlap with a five vector RMSD of 0.992 Å (Figure 3.59).

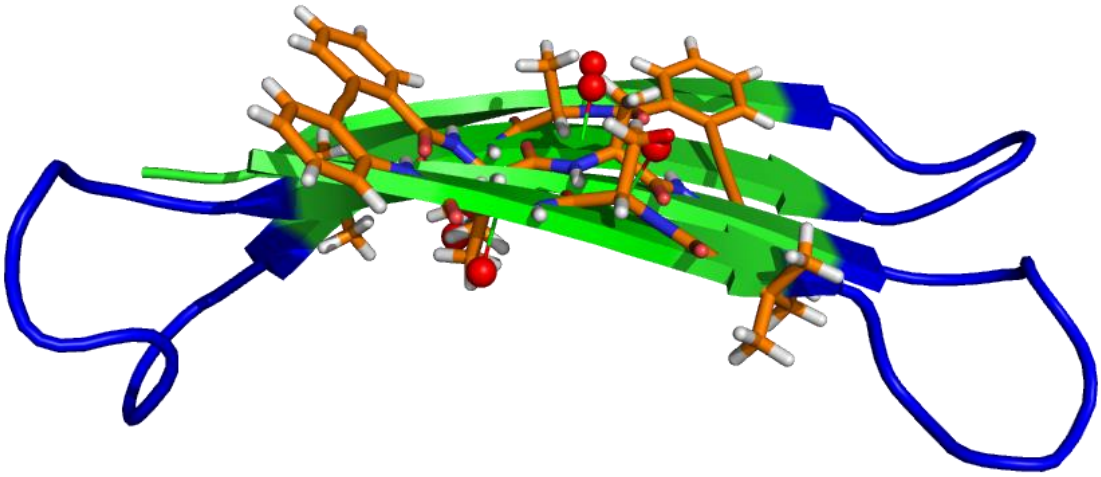

Figure 3.59 Five vector overlay of three-stranded meander **56** with selected β-sheet region of the OspA mutant membrane protein of Borreliella burgdorferi. **56** coloured in orange, β-carbons of the overlapping residues shown as red spheres. The rest of the side-chain was omitted for clarity (PDB: 3AUM).

Interestingly the X-ray crystal structure also provides insight into the behaviour of the termini, and some of this appears to be in disagreement with the solution phase studies. Both terminal amide bonds are measured as 2.3 Å, at the upper bound of the measured distances for the inter-strand hydrogen bonds. However, no firm links can be drawn to the solution phase data given that one of the bonds within the Kemp turn, proven to be one of the strongest, also measures 2.3 Å.

The proximity of the *tert*-butyl group to the adjacent aryl ring can also be measured. Recall that the ROESY and deuterium exchange experiments suggested that the *tert*-butyl ester, as opposed to the carbamate showed the greater proximity to the phenyl ring. However, as shown in Figure 3.60, the *tert*-butyl ester is clearly bent away from the ring at a 45° angle, whereas the carbamate group remains in the plane of the molecule. The distances are shown to be 4.0 and 3.6 Å respectively.

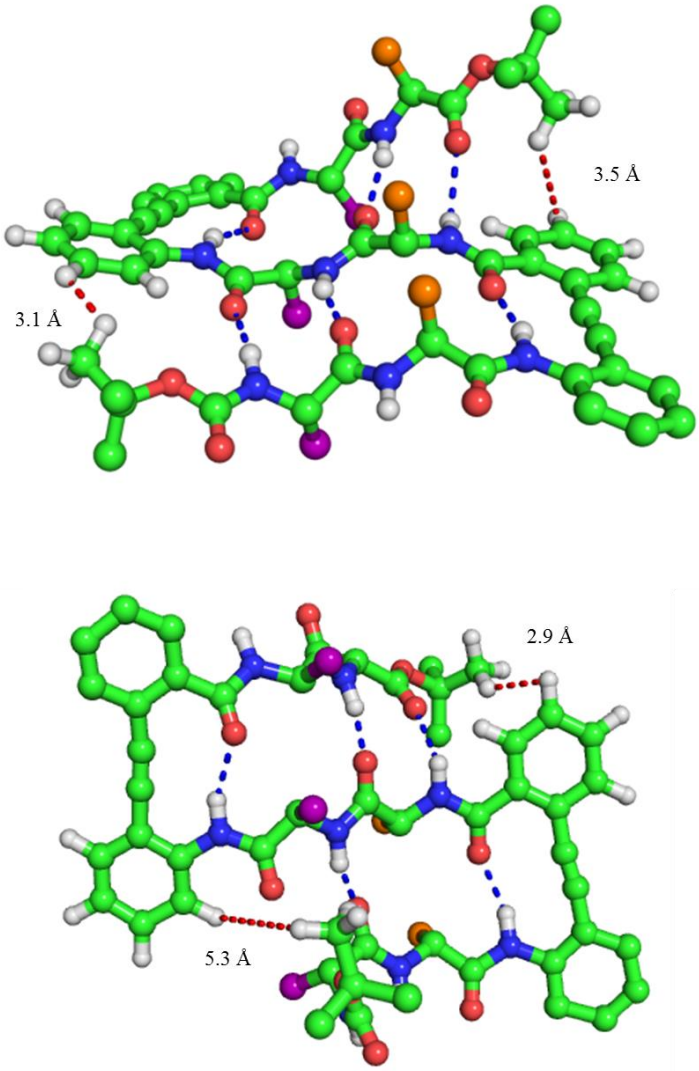

Figure 3.60 Perspective showing distance between aromatic rings and *tert*-butyl termini on two different crystal structures

This deviation from the solution phase data can however be rationalised: an NMR experiment represents the time average of the molecule in a dynamic state, whereas the crystal structure represents a single snapshot in the solid state. It is reasonable to envision the two terminal strands in a dynamic equilibrium, rapidly interchanging which one is in, and which is out of the plane. Similarly the terminal *tert*-butyl groups themselves can experience a great deal of flexibility, with the methylene equivalent in the carbamate group offering a large range of motion.

This possibility is borne out by the crystal structure of a second molecule within the same asymmetric unit. Here the carbamate group is bent well away from the aryl ring to a distance of 5.3 Å, right on the edge of detection as an NMR through space interaction whilst the ester is only 2.9 Å away.

This second single crystal X-ray structure has two molecules within the asymmetric unit, with inter-molecular hydrogen bonds of distance 3.0 Å creating an extended surface of six parallel strands. This intermolecular interaction shows the ability for these artificial molecules to behave much like many of their predecessors, most notably Nowick's *Hao* and $^{\delta}$*Orn* linked sheets,[1] and more importantly like a natural β-sheet (Figure 3.61).

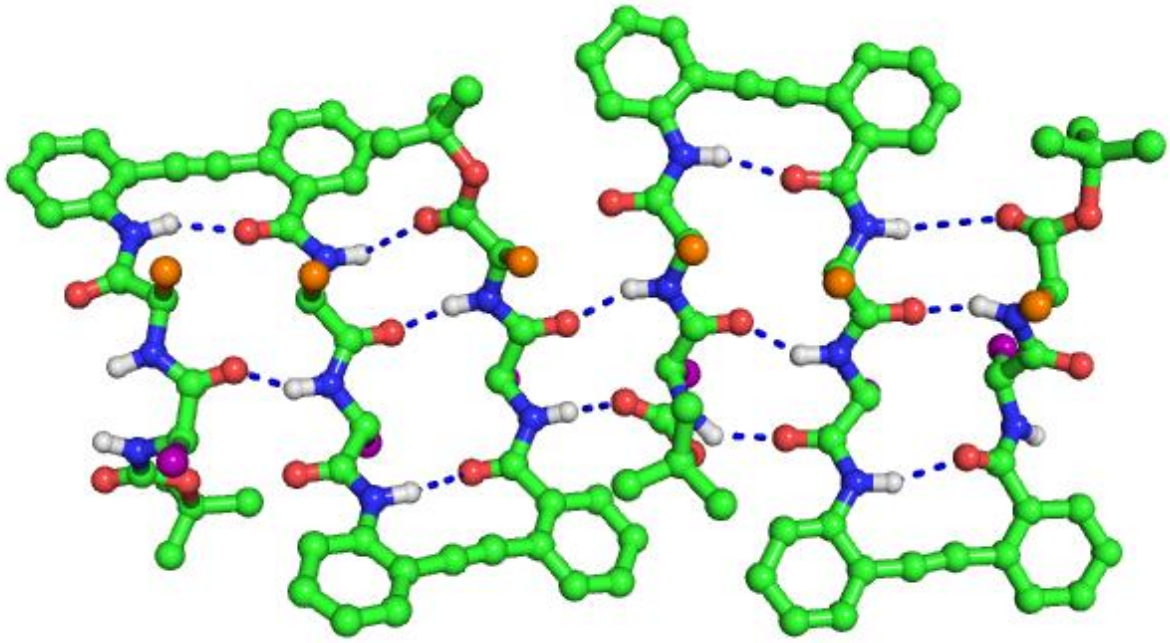

Figure 3.61 X-Ray crystal structure of the dimer formed by edge-to-edge non-covalent interactions. Inter-sheet hydrogen bonding indicated with N-O distances measured in Å.

3.9.10.1 Analysis of Dihedral Angles

With a crystal structure in hand it was possible to calculate the dihedral angle for each residue using Pymol[91] and place them on a Ramachandran plot (Figure 3.62). The dihedral angle was calculated for each of the four different conformations within the asymmetric unit.

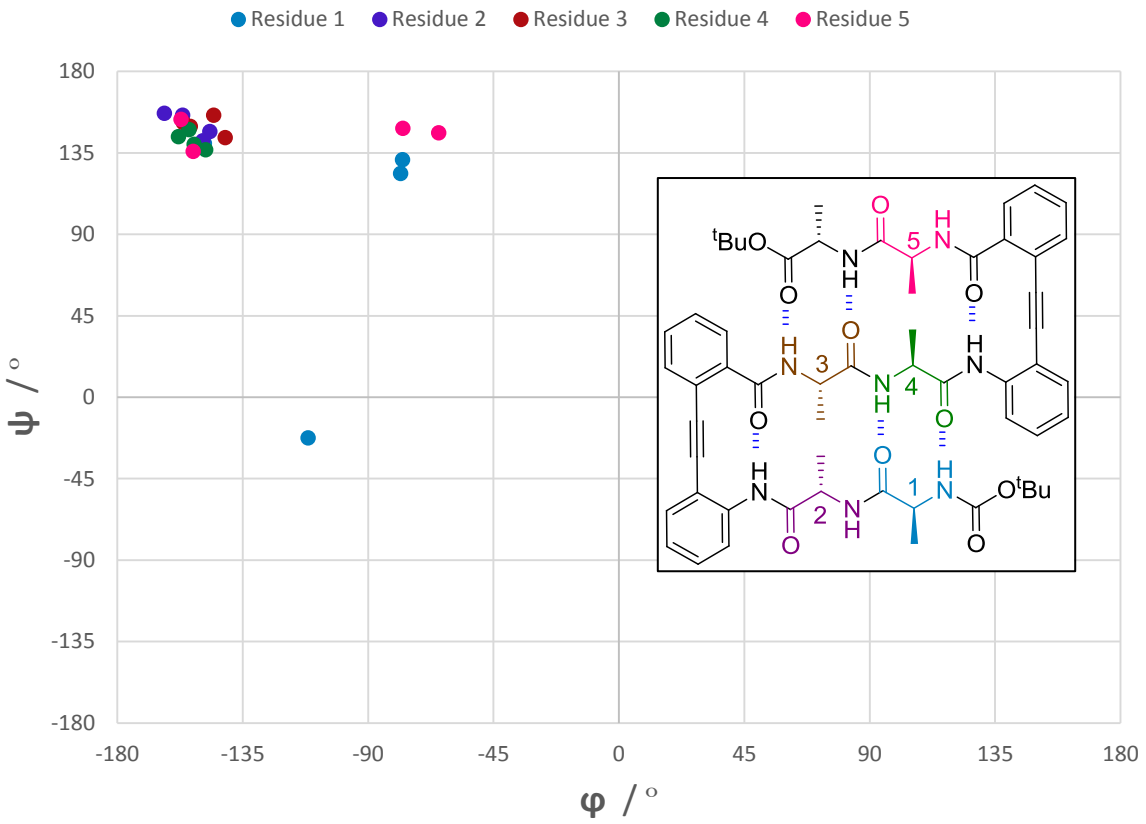

Figure 3.62 Analysis of dihedral angles generated from the crystal structure of 3-stranded meander **59** showing that the majority of the residues sit within the φ and ψ angles of a canonical β-sheet.

The calculated values compare extremely favourably with the canonical β-sheet dihedral angles of (φ,ψ) = (-135°, 135°). The average values across all residues were (φ,ψ) = (- 135 ± 32°, 136 ± 37°). As the plot shows, the large standard deviations are due to outliers on the terminal residues.

3.10 Conclusions

A three-, and four-stranded meander have been successfully formed *via* a simple, robust and scalable synthesis. These meanders have, through a variety of solution phase experiments and the collection of single crystal X-ray data, been shown to adopt the desired conformation in organic solvents and in the solid state. As such these molecules have met the first and third of Gellman's challenges; reliable and preditable folding behaviour with a trivial synthesis.

These molecules represent the first step in the creation of a fully adaptable surface. The architecture of the surface is now in place and the next chapter will explore the flexibility of this architecture in creating larger and differentially modified surfaces, thus fulfilling the second of Gellman's challenges.

3.11 Experimental

3.11.1 General Information

For ‘Solvents and Reagents’, ‘Chromatography’, and ‘Spectroscopy’, see Chapter 2, Section 2.14.1.

3.11.2 General Experimental Procedures

General procedure (3a): Sonogashira cross-coupling

According to a modified literature procedure,[114] a solution of iodide (1.0 eq.) was dissolved in triethylamine (0.1 M) and the solution degassed by bubbling argon through for 10 min. Copper(I) iodide (10 mol %) and $PdCl_2(PPh_3)_2$ (2.5 mol %) were added followed by dropwise addition of acetylene (2.0 eq.), or degassed solution thereof. The resulting mixture was heated to 50 ˚C for 16 h and then cooled to room temperature and poured into water (20 mL.mmol^{-1}). The aqueous layer was extracted with ethyl acetate (3 x 10 mL.mmol^{-1}), dried (magnesium sulfate) and the mixture concentrated *in vacuo*.

General procedure (3b): Trimethylsilyl deprotection

According to a modified literature procedure,[114] trimethyl silyl protected alkyne (1.0 eq.) was dissolved in methanol (0.1 M) and to the stirring solution was added potassium carbonate (1.05 eq.). After 1 h the reaction mixture was diluted with water (10 mL.mmol^{-1}) and extracted with dichloromethane. The organic layer was dried (magnesium sulfate) and the mixture concentrated *in vacuo*.

General procedure (3c): Aniline amide coupling

According to a modified literature procedure,[115] a solution of acid (1.0 eq.) was dissolved in dichloromethane (0.1 M) and to the stirring solution was added *N*,*N*-dicyclohexylcarbodiimide (1.3 eq.). The reaction mixture was cooled to 0 ˚C and stirred

for 10 min before the addition of aniline (1.0 eq.). The reaction was allowed to come to room temperature and stirred overnight before dilution with dichloromethane (10 mL.mmol^{-1}) and subsequently washed with sodium bicarbonate (3 x 10 mL.mmol^{-1}). The organic layer was dried (magnesium sulfate) and the mixture concentrated *in vacuo*.

General procedure (3d): Acid chloride amide coupling

According to a modified literature procedure,[116] acid chloride (1.0 eq.) was dissolved in dichloromethane (0.2 M). To the stirring solution was added 4-dimethylaminopyridine (0.1 mol %) and pyridine (1.5 eq.) dropwise. Amine (1.0 eq.) was dissolved in dichloromethane (0.1 M) and added dropwise. The reaction mixture was stirred at room temperature for 90 min. Upon completion the reaction was diluted with dichloromethane (20 mL.mmol^{-1}) and washed with 2 *N* hydrochloric acid (3 x 20 mL.mmol^{-1}), sodium hydrogen carbonate (3 x 20 mL.mmol^{-1}) and brine (3 x 20 mL.mmol^{-1}). The organic layer was dried (magnesium sulfate) and the mixture concentrated *in vacuo*.

General procedure (3e): Alkyl amine amide coupling

According to a modified literature procedure,[115] a solution of acid (1.0 eq.) was dissolved in dichloromethane (0.1 M) and to the stirring solution was added *N*,*N*,*N*',*N*'-tetramethyl-*O*-(1*H*-benzotraizol-1-yl)uranium hexafluorophosphate (2.0 eq.). The reaction mixture was stirred for 10 min before the addition of amine (1.0 eq.) and *N*,*N*-diisopropylethylamine (3.0 eq.). The reaction was stirred overnight before dilution with dichloromethane (10 mL.mmol^{-1}) and subsequently washed with sodium bicarbonate (3 x 10 mL.mmol^{-1}), ammonium chloride (3 x 10 mL.mmol^{-1}), and brine (3 x 10 mL.mmol^{-1}). The organic layer was dried (magnesium sulfate) and the mixture concentrated *in vacuo*.

General procedure (3f): Boc/O^{t}Bu deprotection

Boc protected amine/acid (1.0 eq.) was dissolved in dichloromethane (0.1 M) and to the stirring solution was added trifluoroacetic acid (1:1 dichloromethane:trifluoroacetic acid). The reaction was stirred at room temperature for 15 min (Boc)/ 3 h (O^{t}Bu) and the mixture concentrated *in vacuo*. The residual trifluoroacetic acid was removed by co-evaporation with toluene (3 x 15 mL.mmol^{-1}).

General procedure (3g): Fmoc deprotection

Fmoc protected amine (1.0 eq.) was dissolved in dichloromethane (0.1 M) and to the stirring solution was added piperidine (4:1, dichloromethane:piperidine). The reaction was stirred at room temperature for 15 min and the mixture concentrated *in vacuo*.

General procedure (3h): TBAF silyl deprotection

Silyl protected acetylene (1.0 eq.) was dissolved in THF (0.1 M) and to the stirring solution was added TBAF (1M in THF, 1.1 eq.). The reaction was stirred at room temperature for 30 min, quenched with aqueous $NaHCO_3$ (15 mL.mmol^{-1}), extracted with dichloromethane (3 x 15 mL.mmol^{-1}) and the mixture concentrated *in vacuo*.

3.11.3 Characterization Data

2-((Trimethylsilyl)ethynyl)aniline 42

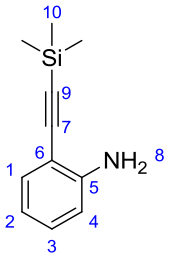

According to *general procedure (3a)*: 2-iodoaniline **41** (10.0 g, 45.6 mmol) and ethynyltrimethylsilane (12.7 mL, 90 mmol) gave the *title compound* **42** (7.89 g, 93 %) as a dark yellow oil after purification by flash column chromatography (PE:Et_2O, 9:1); δ_H (400 MHz, $CDCl_3$) 7.10 (d, *J* 7.6, 1 H, H1), 6.92 (td, *J* 7.7, 1.2, 1 H, H3), 6.43 – 6.51 (m, 2 H, H2, H4), 4.03 (br. s, 2 H, H8), 0.07 (s, 9 H, H10); δ_C (101 MHz, $CDCl_3$) 148.2 (C5), 132.2 (C1), 129.8 (C3), 117.7 (C2), 114.1 (C7), 107.7 (C4), 101.8 (C6), 99.7 (C9), 0.1 (C10); HRMS calculated for $C_{11}H_{15}NNaSi$ $[M+Na]^+$: 212.0866, found 212.0869; IR ($CHCl_3$) 3478, 3382, 2958, 2145, 1613.

2-Ethynylaniline 43

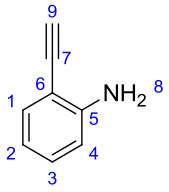

According to *general procedure (3b)*: Silylacetylene **42** (7.0 g, 40 mmol) gave the *title compound* **43** (4.2 g, 90 %) as a pale yellow oil; δ_H (400 MHz, $CDCl_3$) 7.20 (dd, *J* 8.0, 1.8, 1 H, H1), 7.00 (td, *J* 8.0, 1.5, 1 H, H3), 6.52 - 6.57 (m, 2 H, H2, H4), 4.09 (br, 2 H, H8), 3.25 (s, 1 H, H9); δ_C (101 MHz, $CDCl_3$) 148.4 (C5), 132.5 (C1), 130.0 (C3), 117.6 (C2), 114.2 (C4), 106.4 (C6), 82.4 (C7), 80.6 (C9); IR ($CHCl_3$) 3469, 3377, 3278, 2096 1613; HRMS: calculated for C_8H_7NNa $[M+Na]^+$:140.0471, found 140.0473.

(S)-tert-Butyl 2-(2-iodobenzamido)propanoate 45

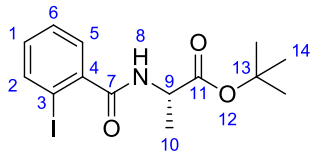

According to *general procedure (3d)*: 2-benzoyl chloride **44** (10.0 g, 37.6 mmol) and L-alanine *tert*-butyl ester hydrochloride (6.8 g, 37.6 mmol) gave the *title compound* **45** (12.2 g, 87 %) as a colourless oil after purification by flash column chromatography (PE:Et_2O, 3:2); $[\alpha]_D^{23.5}$ –1.10 (*c* 1.30, $CHCl_3$); δ_H (400 MHz, $CDCl_3$) 7.78 (dd, 1H, *J* 8.1, 0.7, H1), 7.33 (dd, 1H, *J* 7.6, 1.7, H2), 7.29 (td, 1H, *J* 7.3, 1.0, H5), 7.01 (td, 1H, *J* 7.8, 1.5, H6), 6.44 (br. s, 1H, H8), 4.57 (q, 1H, *J* 7.2, H9), 1.43 (d, 3H, *J* 7.1, H10), 1.41 (s, 9H, H14); δ_C (101 MHz, $CDCl_3$) 171.8 (C11), 168.3 (C7), 141.5 (C4), 139.8 (C2), 131.1 (C1), 128.2 (C6), 128.0 (C5), 92.3 (C3), 82.1 (C13), 49.1 (C9), 27.9 (C14), 18.4 (C10); IR ($CHCl_3$) 3293, 2978, 1729; HRMS calculated for $C_{14}H_{18}INNaO_3$ $[M+Na]^+$: 398.0224, found 398.0206.

(S)-tert-Butyl 2-(2-((2-aminophenyl)ethynyl)benzamido)propanoate 46

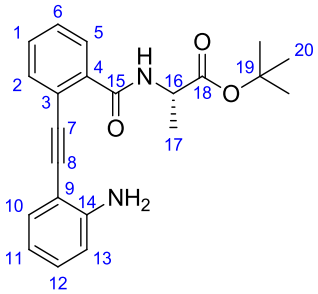

According to *general procedure (3a)*: Iodide **45** (9.15 g, 24.4 mmol) and alkyne **42** (2.8 g, 24.4 mmol) gave the *title compound* **46** (6.02 g, 70 %) as a pale yellow oil after purification by flash column chromatography (PE:Et_2O, 1:1); $[\alpha]_D^{23.5}$ +5.00 (*c* 0.20, $CHCl_3$); δ_H (400 MHz, $CDCl_3$) 7.70 (dd, 1H, *J* 7.8, 1.0, Ar-H), 7.51 (dd, 1H, *J* 7.6, 1.2, Ar-H), 7.34 (td, 1H, *J* 7.3, 1.5, Ar-H), 7.28 (m, 2H, Ar-H), 7.21 (d, 1H, *J* 6.9, N-H), 7.04 (dt, 1H, *J* 7.3, 1.5, Ar-H), 6.59 (m, 2H, Ar-H), 4.57 (m, 3H, NH_2 and H16), 1.39 (d, 3H, *J* 7.1, H17), 1.37

(s, 9H, H20); δ_C (101 MHz, $CDCl_3$) 172.0 (C18), 168.7 (C15), 149.1, 135.8, 133.1, 132.0, 130.4, 130.2, 128.4, 128.0, 121.2, 117.2, 114.2, 106.7 (12 x Ar-C), 92.4, 92.2 (C7, 8), 82.0 (C19), 49.4 (C16), 27.9 (C20), 18.5 (C17); IR (CH_2Cl_2) 3324, 2979, 1642; HRMS calculated for $C_{22}H_{24}N_2NaO_3$ $[M+Na]^+$ 387.1679, found 387.1666.

(S)-tert-Butyl (1-((2-iodophenyl)amino)-1-oxopropan-2-yl)carbamate 47

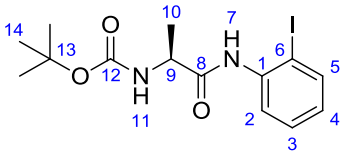

According to *general procedure (3c)*: N-Boc-Ala-OH (435 mg, 2.30 mmol) and 2-iodoaniline **41** (500 mg, 2.30 mmol) gave the *title compound* **47** (498 mg, 56 %) as a white solid after purification by flash column chromatography (PE:Et_2O, 7:3); $[\alpha]_D^{23.5}$ –22.9 (*c* 0.90, $CHCl_3$); δ_H (400 MHz, $CDCl_3$) 8.32 (br. s., 1 H, H11), 8.12 (d, *J* 7.6, 1 H, H2), 7.68 (dd, *J* 8.1, 1.2, H4), 7.23 (t, *J* 7.7, 1 H, H3), 6.75 (td, *J* 7.5, 1.2, 1 H, H5), 5.20 - 5.29 (br. s, 1 H, H7), 4.27 - 4.37 (m, 1 H, H9), 1.41 (d, *J* 7.3, 3 H, H10), 1.39 (s, 9 H, H14); δ_C (100 MHz, $CDCl_3$) 171.1 (C8), 155.4 (C12), 138.8 (C1), 137.9 (C2), 129.1 (C4), 126.0 (C3), 122.0 (C5), 90.0 (C6), 80.4 (C13), 51.1 (C9), 28.3 (C14), 18.1 (C10); IR ($CHCl_3$) 3307, 2932, 1682; HRMS calculated for $C_{14}H_{19}IN_2O_3$ $[M+Na]^+$: 413.0333, found 413.0327.

(S)-tert-Butyl 2-(2-((2-((S)-2-((((9H-fluoren-9-yl)methoxy)carbonyl)amino)propanamido)phenyl)ethynyl)benzamido)propanoate 48

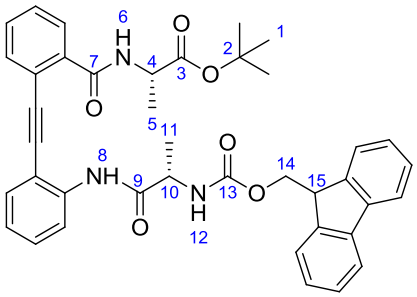

According to *general procedure (3c)*: Fmoc-Ala-OH (1.85 g, 6.1 mmol) and aniline **46** (1.1 g, 3.0 mmol) gave the *title compound* **48** (1.2 g, 59 %) as an off-white solid after purification by flash column chromatography (PE:Et_2O, 1:1); $[\alpha]_D^{23.5}$ -17.3 (*c* 0.80, $CHCl_3$); δ_H (400 MHz, $CDCl_3$) 9.32 (s, 1H, H8), 8.46 (d, 1H, *J* 8.3, Ar-H), 7.66 (d, 2H, *J* 7.3, Ar-H) 7.54 (m, 2H, Ar-H), 7.43 (m, 3H, Ar-H), 7.25 (m, 7H, Ar-H), 7.00 (t, 1H, *J* 7.6, Ar-H), 6.88 (d, 1H, *J* 6.6, H6), 6.49 (d, 1H, *J* 8.3, H12), 4.84 (q, 1H, *J* 7.4, α-H), 4.62 (q, 1H, *J* 6.9, α-H), 4.15 (dd, 1H, *J* 10.3, 8.1, H14), 4.03 (dd, 1H, *J* 10.3, 7.3, H14'), 3.93 (t, 1H, *J* 7.6, H15), 1.53 (d, 3H, *J* 7.1, Me-H), 1.42 (d, 3H, *J* 6.8, Me-H), 1.33 (s, 9H, H31); δ_C (101 MHz, $CDCl_3$) 172.3, 166.9, 155.7, 144.0 (4 x C=O), 143.8, 141.2, 140.1, 136.2, 133.5, 131.7, 130.7, 129.9, 128.5, 127.6, 127.4, 127.0, 125.2, 125.1, 123.4, 121.5, 119.8, 112.1 (18 x Ar-C), 94.0, 89.5 (2 x alkynyl-C), 82.5 (C2), 68.8 (C14), 51.4, 49.5 (2 x α-C), 47.0 (C15), 27.8 (C34), 19.6, 18.6 (2 x β-C); IR ($CHCl_3$) 3294, 2979, 1721, 1649; HRMS calculated for $C_{40}H_{39}N_3NaO_6$ $[M+Na]^+$: 680.2371, found 680.2711.

(S)-2-(2-((2-((S)-2-((((9H-Fluoren-9-yl)methoxy)carbonyl)amino)propanamido)phenyl)ethynyl)benzamido)propanoic acid 49

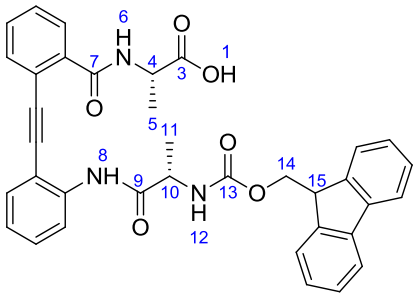

According to *general procedure (3f)*: *tert*-Butyl ester **48** (100 mg, 0.15 mmol) gave the *title compound* **49** (88 mg, 98 %) as a yellow residue; $[\alpha]_D^{25.0}$ +33.7 (*c* 1.00, $CHCl_3$); δ_H (400 MHz, $CDCl_3$) 11.76 (br. s, 1 H, H1), 9.30 (s, 1 H, H8), 8.41 (d, *J* 8.3, 2 H, Ar-H), 7.66 (d, *J* 7.3, 2 H, Ar-H), 7.58 (t, *J* 8.4, 2 H, Ar-H), 7.47 (d, *J* 6.4, 2 H, Ar-H), 7.42 (d, *J* 7.6, 1 H, Ar-H), 7.26 - 7.31 (m, 4 H, Ar-H), 7.18 - 7.23 (m, 3 H, Ar-H), 6.91 - 6.97 (m, 1 H, H6), 6.29 - 6.37 (m, 1 H, H12), 4.92 - 5.02 (m, 1 H, H10), 4.79 - 4.90 (m, 1 H, H4), 4.21 (d, *J* 7.3, 2 H, H14, H14'), 4.02 - 4.08 (m, 1 H, H15), 1.50 (d, *J* 6.8, 3 H, H11), 1.47 (d, *J* 7.1, 3 H, H5); δ_C (101 MHz, $CDCl_3$) 176.9 (C3), 172.1 (C9), 166.9 (C7), 156.4 (C13), 143.7, 143.5, 141.2, 139.9, 133.9, 132.1, 131.1, 129.9, 128.4, 127.7, 127.4, 127.2, 127.0, 125.2, 125.1, 123.6, 119.9, 112.4 (18 x Ar-C), 94.5, 89.9 (2 x alkynyl-C), 67.4 (C14), 51.1 (C10), 49.0 (C4), 46.9 (C15), 20.2 (C11), 18.3 (C5); IR ($CHCl_3$); 3293 (broad), 3065, 2942, 2856, 1708, 1649, 1579, 1527; HRMS calculated for $C_{36}H_{32}N_3O_6$ $[M+H]^+$: 602.2286, found 602.2285.

(S)-tert-Butyl 2-(2-((2-((S)-2-aminopropanamido)phenyl)ethynyl)benzamido)propanoate 50

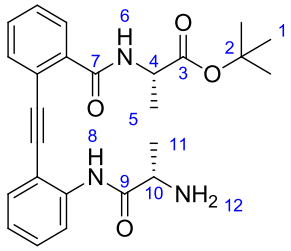

According to *general procedure (3g)*: Fmoc-protected amine **48** (1.00 g, 0.48 mmol) gave the free amine **50** (0.66 g, 95 %) as a yellow oil after purification by flash column chromotography (CH_2Cl_2:MeOH, 19:1); $[\alpha]_D^{23.5}$ +34.1 (*c* 0.75, $CHCl_3$); δ_H (400 MHz, $CDCl_3$) 10.15 (s, 1 H, H8), 8.43 (d, *J* 8.4, 1 H, H6), 7.75 (dd, *J* 7.5, 1.6, 1 H, Ar-H), 7.57 - 7.61 (m, 1 H, Ar-H), 7.39 - 7.45 (m, 2 H, Ar-H), 7.32 (td, *J* 7.2, 1.6, 2 H, Ar-H), 7.26 (td, *J* 7.8, 1.5, 1 H, Ar-H), 6.95 (td, *J* 7.5, 1.3, 1 H, Ar-H), 4.55 (qn, *J* 7.1, 1 H, H10), 3.67 (q, *J* 7.1, 1 H, H24), 1.73 (br, 2 H, H12), 1.36 (d, *J* 7.3, 3 H, H5), 1.32 - 1.35 (m, 12 H, H1, 11); δ_C (101 MHz, $CDCl_3$) 174.6, 171.8 (2 x C=O), 166.1 (C7), 139.6, 135.9, 133.2, 131.5, 130.4, 129.9, 128.8, 128.6, 122.9, 120.0, 119.0, 111.5 (12 x Ar-C), 93.5, 90.2 (2 x alkynyl-C), 82.0 (C2), 51.2 (C10), 49.3 (C4), 27.7 (C2), 21.4 (C11), 18.4 (C5); IR ($CHCl_3$) 3081, 2979, 1730, 1649; HRMS calculated for $C_{25}H_{30}N_3O_4$ $[M+H]^+$: 436.2231, found 436.2212.

(S)-tert-Butyl (1-((2-ethynylphenyl)amino)-1-oxopropan-2-yl)carbamate 51

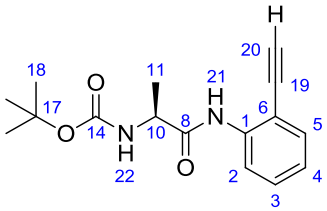

According to *general procedure (3c)*: Boc-Ala-OH (2.80 g, 14.9 mmol) and aniline **43** (1.45 g, 12.4 mmol) gave the terminal acetylene **51** (2.08 g, 58 %) as a pale yellow oil after purification by flash column chromatography (PE:Et_2O, 5:1); $[\alpha]_D^{23.5}$ -69.4 (*c* 0.70, $CHCl_3$) δ_H (400 MHz, $CDCl_3$) 8.79 (br, 1 H, H22), 8.39 (d, *J* 8.3, 1 H, H2), 7.41 (dd, *J* 7.7, 1.2, 1 H,

H4), 7.31 (t, *J* 8.3, 1 H, H3), 6.92 - 7.10 (m, 1 H, H5), 5.36 (br. s., 1 H, H21), 4.22 - 4.52 (m, 1 H, H10), 3.52 (s, 1 H, H20), 1.41 - 1.49 (m, 12 H, H11, H18); δ_C (101 MHz, $CDCl_3$) 171.0 (C8), 155.2 (C14), 139.2 (C1), 132.0 (C2), 130.0 (C4), 123.4 (C3), 119.1 (C5), 111.0 (C6), 84.6 (C19), 80.3 (C17), 78.8 (C20), 51.2 (C10), 28.2 (C18), 18.1 (C11); IR ($CHCl_3$) 3299, 2979, 1687. HRMS calculated for $C_{16}H_{20}N_2NaO_3$ $[M+Na]^+$: 311.1366, found 311.1362.

tert-Butyl ((S)-1-(((S)-1-((2-ethynylphenyl)amino)-1-oxopropan-2-yl)amino)-1-oxopropan-2-yl)carbamate 53

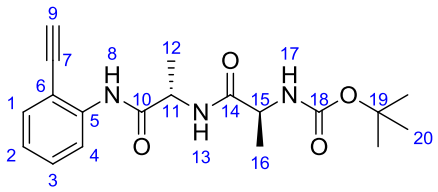

According to *general procedure (3f)*: Boc-protected amine (490 mg, 1.28 mmol) gave yellow solid **52**. According to *general procedure (3e)*: Amine **52** and Boc-Ala-OH (483 mg, 2.56 mmol) gave the terminal acetylene **53** (197 mg, 41 %) as an off-white solid after purification by flash column chromatography (PE:Et_2O, 1:1); $[\alpha]_D^{23.5}$ -143 (*c* 0.55, $CHCl_3$); δ_H (400 MHz, $CDCl_3$) 8.52 (br. s., 1 H, H8), 8.34 (d, *J* 8.3, 1 H, H4), 7.46 (dd, *J* 7.8, 1.5, 1 H, H1), 7.32 - 7.38 (m, 1 H, H3), 7.06 (td, *J* 7.6, 1.1, 1 H, H2), 7.00 (br. s, 1 H, H13), 5.04 (d, *J* 7.3, 1 H, H17), 4.61 - 4.71 (m, 1 H, H11), 4.25 (br. s., 1 H, H15), 3.56 (s, 1 H, H9), 1.49 (d, *J* 7.1, 3 H, H12), 1.45 (s, 9 H, H20), 1.39 (d, *J* 7.1, 3 H, H16); δ_C (101 MHz, $CDCl_3$) 172.7 (C10), 170.1 (C14), 155.7 (C18), 139.2 (C5), 132.2 (C1), 130.1 (C3), 123.7 (C2), 119.6 (C4), 111.4 (C6), 84.7 (C9), 80.5 (C7), 79.0 (C19), 49.9 (C15), 49.8 (C11), 28.3 (C20), 18.0 (C12), 17.9 (C16); IR ($CHCl_3$) 3407, 3283, 3263, 2980, 1693; δ_H (DMSO-d_6, 500 MHz) 9.32 (s, 1 H, H9), 8.20 (d, *J* 7.5, 1 H, H13), 7.92 (d, *J* 8.3, 1 H, H7), 7.52 (dd, *J* 7.7, 1.4, 1 H, H4), 7.43 (td, *J* 8.0, 1.0, 1 H, H6), 7.18 (td, *J* 7.5, 1.1, 1 H, H5), 7.03 (d, *J* 8.0, 1 H, H17), 4.57 (s, 1H, H1), 4.49 - 4.56 (m, 1 H, H11), 4.02 - 4.13 (m, 1 H, H15), 1.42 (s, 9 H, H20), 1.38 (d, *J* 7.1, 3 H,

H12), 1.25 (d, *J* 7.1, 3 H, H16); δ_C (DMSO-d_6, 126 MHz) 173.3 (C10), 171.6 (C14), 155.6 (C18), 139.6 (C8), 133.0 (C4), 130.0 (C6), 124.9 (C5), 122.6 (C7), 114.4 (C3), 87.5 (C1), 79.8 (C19), 78.6 (C2), 49.9 (C15), 49.4 (C11), 28.7 (C20), 18.6 (C16), 18.3 (C12); HRMS calculated for $C_{30}H_{38}N_4NaO_6$ $[M+Na]^+$:573.2684, found 573.2683.

(S)-tert-Butyl 2-(2-((2-((S)-2-((S)-2-(2-((2-((S)-2-((((9H-fluoren-9-yl)methoxy)carbonyl)amino)propanamido)phenyl)ethynyl)benzamido)propanamido)propanamido)phenyl)ethynyl)benzamido)propanoate 54

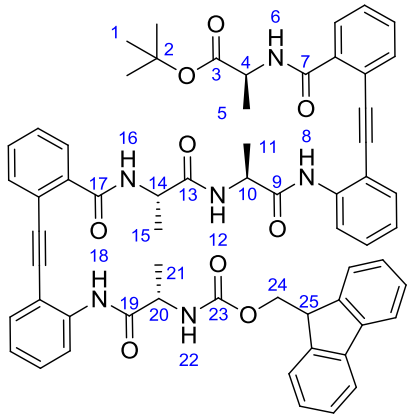

According to *general procedure (3f)*: tBu-ester protected acid **48** (500 mg, 0.76 mmol) gave residue **49**. According to *general procedure (3e)*: Acid **49** and amine **50** (330 mg, 0.76 mmol) gave the *title compound* **54** (227 mg, 31 %) as a white solid after purification by flash column chromatography (PE:Et_2O, 1:1); $[\alpha]_D^{23.5}$ -3.50 (*c* 1.25, $CHCl_3$); δ_H (500 MHz, $CDCl_3$) 9.60 (s, 1 H, H8 or H18), 9.40 (s, 1 H, H8 or H18), 8.65 (d, *J* 8.5, 1 H, Ar-H), 8.45 (d, *J* 8.5, 1 H, Ar-H), 7.91 (d, *J* 7.9, 1 H, N-H), 7.75 (d, *J* 7.6, 2 H, Ar-H), 7.62 - 7.70 (m, 6 H, Ar-H), 7.43 - 7.54 (m, 4 H, Ar-H), 7.34 - 7.41 (m, 6 H, Ar-H), 7.28 - 7.33 (m, 1 H, Ar-H), 7.22 - 7.27 (m, 2 H, Ar-H), 7.03 - 7.13 (m, 3 H, 1x N-H, 2 x Ar-H), 6.57 (s, 1 H, N-H), 6.11 (d, *J* 8.2, 1 H, N-H), 5.37 (t, *J* 7.2, 1 H, H20), 5.22 (t, *J* 7.0, 1 H, H10), 5.16 (t, *J* 7.1, 1 H, H14), 4.72 (t, *J* 7.1, 1 H, H4), 4.58 (dd, *J* 10.0, 7.0, 1 H, H24), 4.44 (dd, *J* 10.6, 7.4, 1 H, H24'), 4.24 (t, *J* 7.0, 1 H, H25), 1.59 (d, *J* 6.6, 3 H,H21), 1.51 (d, *J* 6.9, 3 H, H15), 1.40 - 1.45 (m, 6 H, H5,

H11), 1.39 (s, 9 H, H1); δ_C (126 MHz, $CDCl_3$) 172.4, 172.3, 172.3, 171.5, 166.7, 166.0 (6 x C=O), 155.9 (C23), 143.9, 143.8, 142.1, 141.3, 141.2, 140.6, 140.5, 136.2, 134.3, 134.0, 133.4, 132.1, 131.7, 131.0, 130.7, 129.9, 129.9, 128.5, 127.6, 127.5, 127.3, 127.0, 125.3, 123.3, 123.2, 122.5, 121.6, 119.9, 119.9, 119.5, 112.1 (30 x Ar-C), 95.1, 94.0, 89.9, 89.8 (4 x alkynyl-C), 82.3 (C2), 67.1 (C24), 50.9 (C20), 49.5 (C14), 49.4 (C10), 49.0 (C4), 47.1 (C24), 27.8 (C1), 20.9 (C21), 20.4 (C15), 19.0 (C11), 18.6 (C5); IR ($CHCl_3$) 3285, 2980, 2249, 1644; HRMS calculated for $C_{61}H_{58}N_6NaO_9$ $[M+Na]^+$: 1041.4157, found 1041.4146.

(S)-tert-Butyl 2-((S)-2-(2-((2-((S)-2-((S)-2-(2-((2-((S)-2-((((9H-fluoren-9-yl)methoxy)carbonyl)amino)propanamido)phenyl)ethynyl)benzamido)propanamido)propanamido)phenyl)ethynyl)benzamido)propanamido)propanoate 55

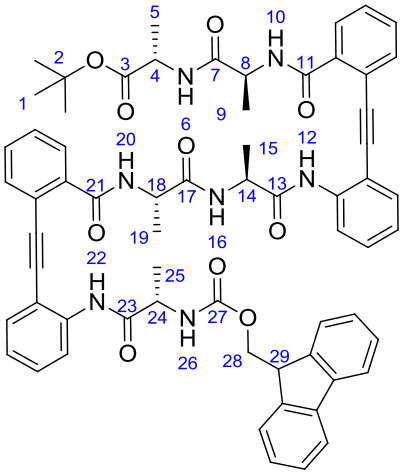

According to *general procedure (3f)*: *tert*-Butyl protected ester **54** (100 mg, 0.10 mmol) gave intermediate **A** as a yellow residue. According to *general procedure (3e)*: Residue **A** and L-alanine tert-butyl ester hydrochloride (30 mg, 0.20 mmol) gave the product **55** (62 mg, 57 %) as a pale yellow residue after purification by flash column chromatography (PE:Et_2O, 1:2); $[\alpha]_D^{23.5}$ +10.7 (*c* 0.90, $CHCl_3$); δ_H (500 MHz, $CDCl_3$) 9.65 (s, 1 H, H12 or H22), 9.37 (s, 1 H, H12 or H22), 8.63 - 8.69 (m, 2 H, Ar-H, H20), 8.60 (d, *J* 8.2, 1 H, Ar-H), 8.36 (d, *J* 8.2, 1 H, H6), 7.92 (d, *J* 8.5, 1 H, H16), 7.88 (d, *J* 7.4, 1 H, Ar-H), 7.73 - 7.77 (m, 3 H, Ar-H),

7.70 (s, 1 H, Ar-H), 7.68 (s, 1 H, Ar-H), 7.67 (dd, *J* 4.4, 3.3, 2 H, Ar-H), 7.50 - 7.54 (m, 3 H, Ar-H), 7.48 - 7.49 (m, *J* 1.3, 1 H, Ar-H), 7.37 - 7.41 (m, 3 H, Ar-H), 7.35 - 7.37 (m, 2 H, Ar-H), 7.19 - 7.24 (m, 3 H, Ar-H), 7.12 (d, *J* 7.7, 1 H, H10), 7.08 (td, *J* 7.6, 0.9, 1 H, Ar-H), 7.04 (td, *J* 7.5, 1.1, 1 H, Ar-H), 6.04 (d, *J* 8.4, 1 H, H26), 5.60 - 5.68 (m, *J* 6.9, 6.9, 2 H, H18, H24), 5.47 - 5.52 (m, 1 H, H14), 5.41 - 5.46 (m, *J* 1.3, 1 H, H8), 4.60 - 4.69 (m, *J* 7.6, 7.6, 2 H, H28, H28'), 4.52 - 4.59 (m, 1 H, H4), 4.30 - 4.35 (m, 1 H, H29), 1.62 (d, *J* 7.0, 3 H, H25), 1.52 (d, *J* 7.0, 3 H, H19), 1.47 (d, *J* 6.9, 3 H, H9), 1.42 (d, *J* 6.8, 3 H, H15), 1.37 (s, 9 H, H1), 1.25 (d, *J* 4.4, 3 H, H5); δ_C (126 MHz, $CDCl_3$) 172.7, 172.6, 172.6, 172.4, 172.0 (5 x C=O), 166.5 (C21, C11), 156.1 (C27), 144.1, 143.9, 141.3, 141.2, 140.9, 135.0, 134.6, 134.0, 133.8, 132.2, 131.9, 130.9, 130.8, 130.0, 129.9, 128.1, 128.1, 127.7, 127.5, 127.0, 125.4, 125.4, 123.2, 122.9, 122.7, 122.5, 119.8, 119.4, 119.3, 112.0, 111.6 (30 x Ar-C), 95.3, 94.8, 89.9, 89.9 (4 x alkynyl-C), 82.0 (C2), 67.3 (C28), 50.8 (C24), 49.7 (C18), 49.0 (C8), 48.8 (C14), 48.6 (C4), 47.2 (C29), 27.9 (C1), 21.2 (C25), 20.2 (C9, C19), 19.7 (C15), 19.2 (C5); IR ($CHCl_3$) 3288, 3065, 2978, 2933, 2873, 2250, 2216, 1695; HRMS calculated for $C_{64}H_{63}N_7NaO_{10}$ $[M+Na]^+$: 1112.4529, found 1061.4743.

(S)-tert-Butyl 2-((S)-2-(2-((2-((S)-2-((S)-2-(2-((2-((S)-2-((S)-2-((tert-butoxycarbonyl)amino)propanamido)propanamido)phenyl)ethynyl)benzamido)propanamido)propanamido)phenyl)ethynyl)benzamido)propanamido)propanoate 56

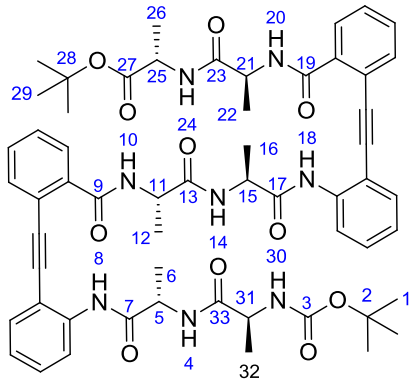

According to *general procedure (3g)*: Fmoc-protected amine **55** (700 mg, 0.65 mmol) gave amine **A** as a white solid. According to *general procedure (3e)*: Amine **A** and Boc-Ala-OH (215 mg, 1.14 mmol) gave the *title compound* **56** (273 mg, 40 %) as a white solid after purification by flash column chromatography (PE:Et_2O, 1:1); $[\alpha]_D^{23.5}$ +12.6 (*c* 1.25, $CHCl_3$); δ_H (500 MHz, $CDCl_3$) 9.64 (br, 1 H, H8), 9.48 (s, 1 H, H18), 8.95 (d, *J* 7.5, 1 H, H14), 8.75 (d, *J* 7.5, 1 H, Ar-H), 8.62 - 8.67 (m, 2 H, Ar-H, H24), 7.99 (d, *J* 7.7, 1 H, Ar-H), 7.89 (d, *J* 8.0, 1 H, H10), 7.66 - 7.73 (m, 3 H, Ar-H), 7.47 - 7.55 (m, 4 H, Ar-H), 7.33 - 7.43 (m, 4 H, Ar-H), 7.19 (d, *J* 7.7, 1 H, H20), 7.08 (tdd, *J* 7.5, 3.9, 0.9, 2 H, Ar-H), 6.95 (d, *J* 7.7, 1 H, H4), 6.37 (d, *J* 8.0, 1H, H30), 5.77 - 5.87 (m, 1 H, H5), 5.60 - 5.70 (m, *J* 7.1, 2 H, H11, 15), 5.50 - 5.57 (m, 1 H, H21), 4.57 - 4.64 (m, 1 H, H25), 4.30 - 4.43 (m, 1 H, H31), 1.61 (d, *J* 6.8, 3 H, H6), 1.58 (d, *J* 6.9, 3 H, H16), 1.52 (d, *J* 6.8, 3 H, H22), 1.50 (d, *J* 6.9, 3 H, H12), 1.47 (d, *J* 6.9, 3 H, H32), 1.42 (br, 9 H, H1), 1.38 - 1.40 (m, 12 H, H26, H29); δ_C (126 MHz, $CDCl_3$) 172.9 (C13), 172.8 (C3), 172.5 (C27), 172.5 (C23), 172.4 (C33), 172.1 (C17), 166.3 (C19), 165.9 (C9), 155.9 (C3), 142.1, 140.8, 140.8, 140.6, 134.6, 134.3, 134.0, 132.2, 132.1, 131.0, 130.9, 130.0, 128.2, 128.1, 127.7, 127.2, 123.3, 123.2, 122.9, 122.6, 119.5, 119.3, 112.0, 111.9 (24 x Ar-C), 95.6, 95.0, 90.0, 90.0 (4 x alkynyl-C), 81.9 (C28), 79.3 (C2), 50.3

(C15 and C31), 49.7 (C5), 48.9 (C11), 48.8 (C21), 48.6 (C25), 28.4 (C29), 27.9 (C1), 20.6 (C6 and C16), 20.5 (C22), 20.1 (C12), 19.4 (C32), 19.3 (C32); δ_H (DMSO-d_6, 500 MHz) 9.49 (s, 1 H, H8), 9.45 (s, 1 H, H18), 8.71 - 8.76 (m, 2 H, H10, H20), 8.38 (d, *J* 7.8, 1 H, H14), 8.27 (d, *J* 8.0, 1 H, Ar-H), 8.21 - 8.23 (m, 1 H, Ar-H), 8.14 - 8.20 (m, 2 H, H4, H24), 7.75 - 7.77 (m, 1 H, Ar-H), 7.71 - 7.74 (m, 2 H, Ar-H), 7.68 - 7.71 (m, 1 H, Ar-H), 7.55 - 7.61 (m, 2 H, Ar-H), 7.50 - 7.54 (m, 4 H, Ar-H), 7.38 - 7.43 (m, 1 H, Ar-H), 7.34 - 7.38 (m, 1 H, Ar-H), 7.08 - 7.15 (m, 2 H, Ar-H), 6.93 (d, *J* 8.0, 1 H, H30), 4.95 - 5.05 (m, 2 H, H5, H15), 4.69 - 4.79 (m, 1 H, H11), 4.51 - 4.59 (m, 1 H, H21), 4.00 - 4.10 (m, 1 H, H31), 3.93 - 3.98 (m, 1 H, H25), 1.35 - 1.39 (m, 12 H, H6, H29), 1.32 - 1.35 (m, 15 H, H1, H11, H15), 1.27 (d, *J* 7.0, 3 H, H15), 1.16 - 1.18 (m, 3 H, H32), 1.14 (d, *J* 7.3, 3 H, H26); δ_C (DMSO-d_6, 126 MHz) 173.3 (C27), 172.6 (C7), 172.6 (C33), 172.4 (C17), 172.4 (C13), 172.0 (C23), 167.5 (C19), 167.5 (C9), 155.5 (C3), 140.5, 140.3, 137.5, 137.4, 133.1, 132.9, 132.3, 131.0, 130.9, 130.2, 130.2, 129.1, 129.1, 128.8, 128.7, 124.1, 124.0, 121.0, 120.9, 120.8, 120.7, 114.4, 113.0, 112.8 (24 x Ar-C), 94.6, 94.6, 89.3, 89.3 (4 x alkynyl-C), 80.7 (C28), 78.5 (C2), 49.9 (C31), 49.3 (C5), 49.3 (C15), 49.2 (C11), 49.1 (C21), 48.8 (C25), 28.6 (C28), 28.0 (C2), 19.4 (C6), 19.1 (C16), 18.5 (C32), 18.4 (C12), 18.2 (C22), 17.0 (C26); IR ($CHCl_3$) 3284, 2978, 2913, 1695, 1640; HRMS calculated for $C_{57}H_{66}N_8NaO_{11}$ $[M+Na]^+$: 106.4710, found 1061.4743.

(S)-tert-Butyl 2-(2-((2-((S)-2-((S)-2-(2-((2-((S)-2-((S)-2-(2-((2-((S)-2-((((9H-fluoren-9-yl)methoxy)carbonyl)amino)propanamido)phenyl)ethynyl)benzamido)propanamido)propanamido)phenyl)ethynyl)benzamido)propanamido)propanamido)phenyl)ethynyl)benzamido)propanoate 57

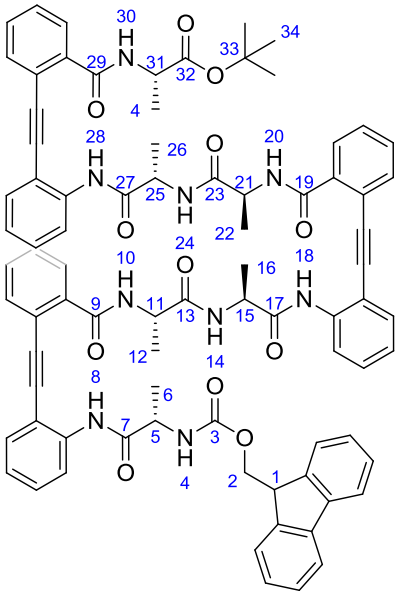

According to *general procedure (3f)*: *tert*-Butyl protected ester **54** (146 mg, 0.15 mmol) gave intermediate **A** as a yellow residue. According to *general procedure (3e)*: Residue **A** and amine **50** (67 mg, 0.15 mmol) gave the *title compound* **57** (85 mg, 44 %) as a pale yellow residue after purification by flash column chromatography (PE:Et_2O, 1:2); $[\alpha]_D^{23.5}$ +58.4 (*c* 0.70, $CHCl_3$); δ_H (500 MHz, $CDCl_3$) 9.69 (s, 1 H, N-H), 9.55 (s, 1 H, N-H), 9.45 (s, 1 H, N-H), 8.81 (d, *J* 8.0, 1 H, N-H), 8.69 (d, *J* 8.4, 1 H, Ar-H), 8.61 (d, *J* 8.4, 1 H, Ar-H), 8.34 (dd, *J* 11.3, 8.6, 2 H, N-H), 8.11 (d, *J* 8.4, 1 H, Ar-H), 7.80 (d, *J* 7.7, 1 H, Ar-H), 7.74 - 7.78 (m, *J* 7.3, 5.0, 3 H, Ar-H), 7.73 (d, *J* 7.6, 1 H, Ar-H), 7.68 - 7.71 (m, *J* 7.1, 7.1, 3 H, Ar-H), 7.66 (d, *J* 7.6, 1 H, Ar-H), 7.57 (dd, *J* 7.7, 0.8, 1 H, Ar-H), 7.49 - 7.54 (m, 5 H, Ar-H), 7.44 (td, *J* 7.6, 1.1, 1 H, Ar-H), 7.36 - 7.40 (m, 4 H, Ar-H), 7.21 - 7.27 (m, 4 H, 1 x N-H, 3 x Ar-H), 7.12 - 7.16 (m, 1 H, Ar-H), 7.03 - 7.11 (m, 3 H, Ar-H), 6.98 (d, *J* 6.9, 1 H, N-H), 6.91 - 6.95 (m, 1 H, Ar-H), 6.06 (d, *J* 8.4, 1 H, N-H), 5.64 - 5.74 (m, *J* 7.3 Hz, 2 H, Hα), 5.55 - 5.62 (m, 1 H, Hα), 5.46 - 5.52 (m, 1 H, Hα), 5.34 - 5.41 (m, 1 H, Hα), 4.77 - 4.84 (m, 1 H,

Hα), 4.65 - 4.75 (m, 2 H, H2, H2'), 4.33 - 4.38 (m, 1 H, H1), 1.66 (t, *J* 6.9, 6 H, Hβ), 1.59 (d, *J* 6.8, 3 H, Hβ), 1.52 (d, *J* 7.1, 3 H, Hβ), 1.49 (d, *J* 6.9, 3 H, Hβ), 1.44 (s, 9 H, H34), 1.42 (d, *J* 6.8, 3 H, Hβ); δ_C (126 MHz, $CDCl_3$) 172.8, 172.7, 172.4, 172.3, 172.2, 172.2 (6 x C=O), 166.9, 166.4, 166.2 (3 x C=O, adjacent to phenyl groups), 156.0 (C3), 144.1, 144.0, 141.3, 141.2, 141.0, 140.8, 140.3, 136.0, 134.8, 134.5, 133.9, 133.6, 133.4, 132.2, 131.9, 131.5, 130.9, 130.6, 129.9, 129.8, 129.6, 128.5, 128.3, 128.0, 127.9, 127.5, 127.5, 127.2, 127.0, 127.0, 125.5, 125.5, 125.4, 123.4, 123.2, 122.9, 122.6, 122.3, 121.9, 120.2, 119.9, 119.8, 119.4, 112.4, 112.1, 111.6 (48 x Ar-C), 95.5, 94.8, 94.4, 90.1, 89.6, 89.5 (6 x alknyl-C), 82.4 (C33), 67.2 (C2), 50.9, 49.7, 49.5, 49.4, 49.2, 49.0 (6 x αC), 47.2 (C1), 27.9 (C34), 21.2, 20.7, 20.5, 20.4, 19.9, 18.9 (6 x βC); IR ($CHCl_3$) 3285, 3065, 2979, 2932, 2872, 2248, 1692; HRMS calculated for $C_{82}H_{77}N_9NaO_{12}$ $[M+Na]^+$: 1402.5584, found 1402.5568.

Precursor to Four-Stranded Sheet Mimic 58

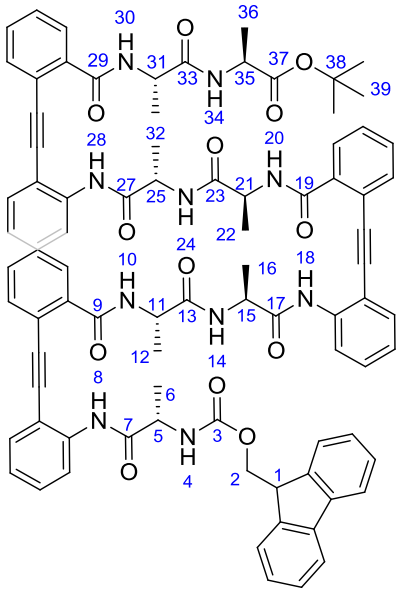

According to *general procedure (3f)*: *tert*-Butyl protected ester **57** (135 mg, 0.10 mmol) gave intermediate **A** as a yellow residue. According to *general procedure (3e)*: Residue **A** and L-alanine *tert*-butyl ester hydrochloride (30 mg, 0.20 mmol) gave the *title compound* **58**

(79 mg, 57 %) as a pale yellow residue after purification by flash column chromatography (Et_2O); δ_H (500 MHz, $CDCl_3$) 9.61 (s, 1 H, N-H), 9.45 (s, 1 H, N-H), 9.41 (s, 1 H, N-H), 9.12 (d, *J* 7.9, 1 H, N-H), 8.61 (d, *J* 8.4, 1 H, Ar-H), 8.24 (d, *J* 8.4, 1 H, Ar-H), 8.15 (d, *J* 8.4, 1 H, N-H), 7.87 (d, *J* 7.6, 1 H, N-H), 7.72 (d, *J* 8.7, 1 H, N-H), 7.70 (d, *J* 8.2, 1 H, N-H), 7.64 - 7.68 (m, 5 H, Ar-H), 7.62 (dd, *J* 3.2, 0.9, 1 H, Ar-H), 7.60 (dd, *J* 3.2, 0.9, 1 H, Ar-H), 7.38 - 7.45 (m, 6 H, Ar-H), 7.33 (td, *J* 7.6, 1.2, 1 H, Ar-H), 7.25 - 7.30 (m, 4 H, Ar-H), 7.19 (d, *J* 7.6, 1 H, N-H), 7.11 - 7.17 (m, 3 H, Ar-H), 7.07 (td, *J* 7.6, 0.9 Hz, 1 H, Ar-H), 6.91 - 7.04 (m, 4 H, Ar-H), 6.77 (td, *J* 7.0, 0.8, 1 H, Ar-H), 5.99 (d, *J* 8.2, 1 H, N-H), 5.76 (quin, *J* 7.2, 1 H, αH), 5.62 - 5.69 (m, 1 H, αH), 5.49 - 5.60 (m, 2 H, αH), 5.39 - 5.47 (m, 2 H, αH), 4.59 - 4.67 (m, 2 H, αH, H2a), 4.48 - 4.55 (m, 1 H, H2b), 4.23 - 4.29 (m, 1 H, H1), 1.61 (d, *J* 6.9, 3 H, Me-H), 1.57 (d, *J* 6.9, 3 H, Me-H), 1.55 (d, *J* 6.9, 3 H, Me-H), 1.46 (d, *J* 6.8, 3 H, Me-H), 1.38 (d, *J* 6.9, 3 H, Me-H), 1.29 - 1.33 (m, 12 H, H38, Me-H), 1.27 (d, *J* 6.8, 3 H, Me-H); δ_C (126 MHz, $CDCl_3$) 173.0, 172.8, 172.7, 172.4, 172.4, 172.3, 172.2 (7 x C=O), 166.9, 166.0, 166.0 (3 x C=O adjacent to aryl ring), 156.0 (C3), 144.1, 144.1, 141.3, 141.1, 140.9, 140.3, 134.5, 134.4, 134.3, 134.2, 134.1, 133.6, 132.1, 132.0, 131.9, 131.1, 130.8, 130.5, 130.0, 129.8, 129.7, 128.3, 128.3, 128.0, 127.8, 127.5, 127.2, 127.0, 125.4, 123.2, 123.1, 122.9, 122.8, 122.5, 122.3, 119.8, 119.5, 119.4, 119.2, 112.1, 112.0, 111.6 (42 x Ar-C), 95.6, 95.3, 95.3, 90.1, 89.9, 89.5 (6 x alkynyl-C), 82.0 (37), 67.2 (C2), 50.9, 50.2, 49.6, 49.2, 48.8, 48.7, 48.6, 47.3 (C1), 27.9 (C38), 25.6, 24.9, 21.2, 20.8, 20.5, 20.2, 20.0 (7 x β-C); IR ($CHCl_3$) 3278, 3058, 2972, 2936, 2242, 1695; HRMS calculated for $C_{85}H_{82}N_{10}NaO_{13}$ $[M+Na]^+$: 1473.5955, found 1473.5982.

Four-Stranded Sheet Mimic 59

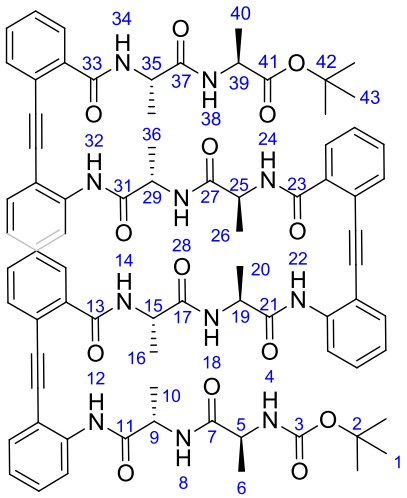

According to *general procedure (3g)*: Fmoc-protected amine **58** (80mg, 0.06 mmol) gave amine **A** as a white solid. According to *general procedure (3e)*: Amine **A** and Boc-Ala-OH (30 mg, 0.12 mmol) gave the *title compound* **59** (19 mg, 21 %) as a white solid after purification by flash column chromatography (Et_2O); $[\alpha]_D^{23.5}$ +9.91 (*c* 1.10, $CHCl_3$); δ_H (500 MHz, $CDCl_3$) 9.67 (s, 1 H, H12), 9.65 (br, 1 H, H22), 9.51 (s, 1 H, H32), 9.27 (d, *J* 7.5, 1 H, H28), 8.95 (d, *J* 7.9, 1 H, H8), 8.81 (d, *J* 7.5, 1 H, Ar-H), 8.71 (d, *J* 7.9, 1 H, H38), 8.68 (d, *J* 8.4, 1 H, Ar-H), 8.37 - 8.42 (m, 1 H, H14), 8.17 (d, *J* 8.4, 1 H, Ar-H), 8.01 (d, *J* 7.7, 1 H, Ar-H), 7.92 (d, *J* 8.7, 1 H, H24), 7.84 (d, *J* 7.7, 1 H, Ar-H), 7.75 (d, *J* 7.4, 1 H, Ar-H), 7.71 (ddd, *J* 7.5, 5.4, 0.9, 2 H, Ar-H), 7.62 (t, *J* 7.9, 1 H, Ar-H), 7.52 - 7.55 (m, 4 H, Ar-H), 7.47 - 7.51 (m, 2 H, Ar-H), 7.43 (td, *J* 7.6, 1.2, 1 H, Ar-H), 7.35 - 7.40 (m, 3 H, Ar-H), 7.28 (d, *J* 7.1, 1 H, H34), 7.14 (t, *J* 7.5, 1 H, Ar-H), 7.09 (t, *J* 7.5, 2 H, Ar-H), 7.01 - 7.04 (m, 1 H, Ar-H), 6.97 - 7.01 (m, 2 H, Ar-H), 6.93 - 6.96 (m, 1 H, H18), 6.87 (t, *J* 7.5, 1 H, Ar-H), 6.53 - 6.59 (m, 1 H, H4), 5.85 - 5.93 (m, 1 H, H9), 5.77 - 5.84 (m, 2 H, H19, 25), 5.70 - 5.75 (m, 1 H, H15), 5.65 - 5.70 (m, *J* 7.3, 1 H, H29), 5.54 - 5.61 (m, 1 H, H35), 4.59 - 4.66 (m, 1 H, H39), 4.35 - 4.46 (m, 1 H, H5), 1.64 - 1.70 (m, 9 H, H16, H20, H30), 1.58 (d, *J* 6.8, 6 H, H10, 36), 1.49 (d, *J* 7.0 Hz, 3 H, H6), 1.42 - 1.47 (m, 12 H, H26, H43), 1.37 - 1.42 (m, 12 H, H1, H40); δ_C (126 MHz, $CDCl_3$) 173.0 (C27), 173.0 (C21), 172.8 (C7), 172.5 (C41), 172.5

(C17), 172.4 (C11), 172.4 (C37), 172.2 (C31), 166.6 (C13), 166.1 (C33), 165.8 (C23), 155.9 (C3), 150.6, 141.0, 140.8, 140.7, 140.3, 134.3, 134.3, 134.2, 133.9, 132.1, 132.1, 131.1, 130.9, 130.5, 129.8, 128.4, 128.3, 128.1, 127.8, 127.7, 127.3, 123.2, 123.1, 122.8, 122.6, 122.3, 119.6, 119.3, 112.2, 111.9, (30 x Ar-C), 95.8, 95.6, 95.2, 90.2, 90.0, 89.6 (6 x alkynyl-C), 82.1 (C42), 79.3 (C2), 50.2 (C5), 50.2 (C29), 50.1 (C9), 49.9 (C19), 49.1 (C15), 48.9 (C35), 48.7 (C39), 48.6 (C25), 28.4 (C43), 27.9 (C1), 20.8 (C10, 36), 20.6 (C30), 20.6 (C16, 20), 20.2 (C26), 19.5 (C6), 19.4 (C40); δ_H (DMSO-d_6, 500 MHz) 9.47 - 9.51 (m, 2 H, H12, H22), 9.45 (s, 1 H, H32), 8.67 - 8.75 (m, 3 H, H14, H24, H34), 8.37 - 8.42 (m, 2 H, H18, H28), 8.19 - 8.24 (m, 3 H, Ar-H), 8.15 - 8.19 (m, 2 H, H8, 38), 7.75 - 7.77 (m, 1 H, Ar-H), 7.68 - 7.74 (m, 5 H, Ar-H), 7.48 - 7.57 (m, 9 H, Ar-H), 7.32 - 7.41 (m, 3 H, Ar-H), 7.07 - 7.15 (m, 3 H, Ar-H), 6.92 (d, *J* 8.0, 1 H, H4), 4.95 - 5.05 (m, 3 H, H9, H19, H29), 4.73 - 4.80 (m, 1 H, H15), 4.64 - 4.71 (m, 1 H, H25), 4.50 - 4.57 (m, 1 H, H35), 4.01 - 4.10 (m, 1 H, H5), 3.91 - 3.98 (m, 1 H, H39), 1.39 (d, *J* 7.0, 3 H, H10), 1.34 - 1.37 (m, 12 H, H30, H43), 1.33 (s, 9 H, H1), 1.30 (d, *J* 6.1, 3 H, H16), 1.24 - 1.29 (m, 9 H, H20, H26, H30), 1.17 (d, *J* 7.5, 3 H, H6), 1.12 (d, *J* 7.3, 3 H, H40); δ_C (DMSO-d_6, 126 MHz) 172.7 (C41), 172.6, 172.4, 172.4, 172.4, 172.4, 172.3, 172.0 (7 x C=O), 167.5 (C13), 167.5 (C23), 167.4 (C33), 155.5 (C3), 140.5, 140.4, 140.3, 137.5, 137.5, 137.4, 133.1, 133.0, 132.9, 132.3, 131.0, 130.9, 130.2, 130.2, 130.1, 129.1, 128.7, 125.4, 124.1, 124.1, 121.0, 120.9, 120.9, 120.8, 120.7, 113.0, 113.0, 112.8 (36 x Ar-C), 94.7, 94.6, 94.5, 89.4, 89.3, 89.3 (6 x alkynyl-C), 80.7 (C42), 78.5 (C2), 49.9 (2C, C5, C15), 49.4 (C25), 49.2 (3C, C9, C19, C29) 49.1 (C35), 48.8 (C39), 28.6 (C43), 28.0 (C1), 19.4 (C10), 19.2 (C20), 19.1 (C30), 18.5 (C6), 18.5 (C16), 18.3 (C26), 18.2 (C36), 17.0 (C40); IR ($CHCl_3$) 3280, 2977, 2931, 1695, 1633; HRMS calculated for $C_{78}H_{85}N_{11}NaO_{14}$ $[M+Na]^+$: 1422.6170, found 1422.6177.

(S)-tert-Butyl (1-oxo-1-(phenylamino)propan-2-yl)carbamate 61

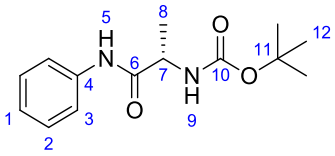

According to *general procedure (3c)*: Boc-Ala-OH (659 mg, 3.49 mmol) and aniline **60** (250 µL, 2.69 mmol) gave the *title compound* **61** (639 mg, 90 %) as a white solid after purification by flash column chromatography (PE:Et_2O, 4:1); $[\alpha]_D^{23.5}$ +34.5 (*c* 1.50, $CHCl_3$); δ_H (400 MHz, $CDCl_3$) 8.89 (br. S, 1 H, H5), 7.41 (d, *J* 7.8, 2 H, H3), 7.08 - 7.18 (m, 2 H, H2), 6.91 - 7.00 (m, 1 H, H1), 5.53 (d, *J* 7.6, 1 H, H9), 4.31 - 4.48 (m, 1 H, H7), 1.34 - 1.38 (m, 12 H, H8, H12); δ_c (101 MHz, $CDCl_3$) 171.5 (C6), 156.1 (C10), 137.9 (C4), 128.7 (C2), 124.0 (C1), 119.8 (C3), 80.3 (C11), 50.7 (C7), 28.2 (C12), 18.0 (C8); IR ($CHCl_3$) 3289, 3205, 3146, 3101, 2978, 2932, 2856, 2362, 1664; HRMS calculated for $C_{14}H_{20}O_3N_2Na$ $[M+Na]^+$: 287.1366, found 287.1363.

(S)-tert-Butyl 2-benzamidopropanoate 63

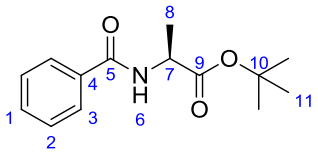

According to *general procedure (3d)*: Benzoyl chloride **62** (291 µL, 2.5 mmol) and alanine *tert*-butyl ester hydrochloride (500 mg, 2.75 mmol) gave the *title compound* **63** (535 mg, 86 %) as a colourless oil after purification by flash column chromatography (PE: Et_2O, 1:1); $[\alpha]_D^{23.5}$ –65.4 (*c* 1.66, $CHCl_3$); δ_H (400 MHz, $CDCl_3$) 7.68 - 7.73 (m, 2 H, H3), 7.32 - 7.38 (m, 1 H, H1), 7.24 - 7.30 (m, 2 H, H2), 7.05 (d, *J* 7.5, 1 H, H6), 4.52 - 4.63 (m, 1 H, H7), 1.38 (s, 9 H, H11), 1.37 (d, *J* 7.1, 3 H, H8); δ_c (101 MHz, $CDCl_3$) 172.4 (C9), 166.5 (C5), 133.9 (C4), 131.2 (C1), 128.2 (C2), 126.8 (C3), 81.7 (C10), 48.8 (C7), 27.7 (C11), 18.3 (C8); IR ($CHCl_3$)

3323, 3063, 2980, 2936, 2361, 1735; HRMS calculated for $C_{14}H_{19}O_3NNa$ $[M+Na]^+$: 272.1257, found 272.1257.

N-((S)-1-Oxo-1-(((S)-1-oxo-1-(phenylamino)propan-2-yl)amino)propan-2-yl)benzamide 64

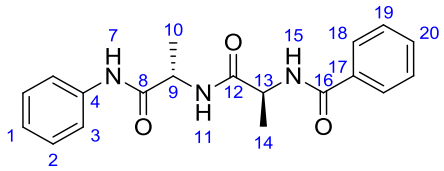

According to *general procedure (3f)*: *tert*-Butyl protected acid **63** (500 mg, 2.0 mmol) gave residue **A**. According to *general procedure (3f)*: Boc-protected amine **61** (500 mg, 1.9 mmol) gave residue **B**. According to *general procedure (3e):* Residue **A** and Residue **B** gave the *title compound* **64** (325 mg, 48 %) as a white solid after purification by flash column chromatography (CH_2Cl_2:MeOH, 10:1); $[\alpha]_D^{23.5}$ +6.00 (*c* 0.33, $CHCl_3$); δ_H (400 MHz, $CDCl_3$) 8.86 - 8.98 (m, 1 H, H7), 7.77 - 7.87 (m, 2 H, Ar-H), 7.58 (d, *J* 8.1, 2 H, Ar-H), 7.53 (d, *J* 7.8, 1 H, Ar-H), 7.44 - 7.50 (m, 1 H, H11), 7.22 - 7.39 (m, 5 H, H15, 4 x Ar-H), 7.04 - 7.13 (m, 1 H, Ar-H), 4.75 (sxt, *J* 6.8, 2 H, H9, H13), 1.53 (d, *J* 6.8, 3 H, H10 or H14), 1.45 - 1.50 (m, 3 H, H10 or H14); δ_c (101 MHz, $CDCl_3$) 173.0 (C8), 170.4 (C12), 167.8 (C16), 137.9, 133.2, 131.9, 128.8, 128.5, 127.2, 124.3, 120.1 (8 x Ar-C), 49.9 (C9 or C13), 49.9 (C9 or C13), 18.1 (C10 or C14), 17.9 (C10 or C14); IR ($CHCl_3$) 3735, 3291, 3064, 2982, 2937, 2362, 2342, 2197, 2149, 2038, 1974, 1640; HRMS calculated for $C_{19}H_{21}O_3N_3Na$ $[M+Na]^+$: 362.1475, found 362.1479.

(S)-tert-Butyl 2-((S)-2-(2-iodobenzamido)propanamido)propanoate 65

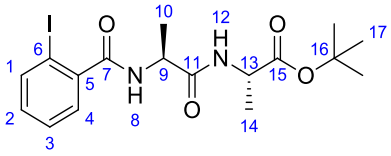

According to *general procedure (3f)*: *tert*-Butyl protected acid **45** (785 mg, 2.21 mmol) gave residue **A**. According to *general procedure (3e):* Residue **A** and alanine *tert*-butyl ester hydrochloride gave the *title compound* **65** (739 mg, 75 %) as a white solid after purification by flash column chromatography (PE:Et_2O, 1:4); $[\alpha]_D^{23.5}$ –18.8 (*c* 1.00, $CHCl_3$); δ_H (400 MHz, $CDCl_3$) 7.71 (d, *J* 7.8, 1 H, H2), 7.37 (d, *J* 7.3, 1 H, H12), 7.21 - 7.27 (m, 2 H, H2, H4), 7.18 (d, *J* 7.8, 1 H, H8), 6.93 - 7.00 (m, 1 H, H3), 4.69 - 4.83 (m, 1 H, H9), 4.21 - 4.31 (m, 1 H, H13), 1.43 (d, *J* 6.8, 3 H, H10), 1.35 (s, 9 H, H17), 1.25 (d, *J* 7.3, 3 H, H14); δ_c (101 MHz, $CDCl_3$) 171.4 (C=O), 171.3 (C=O), 168.6 (C7), 141.2 (C5), 139.4 (C1), 130.8 (C2), 128.0 (C3), 127.7 (C4), 92.3 (C6), 81.3 (C16), 48.9 (C9), 48.5 (C10), 27.6 (C17), 18.4 (C10), 17.7 (C14); IR ($CHCl_3$) 3293, 2980, 2935, 2360, 3242, 2249, 1732, 1643; HRMS calculated for $C_{17}H_{23}O_4N_2INa$ $[M+Na]^+$: 469.05947, found 469.0591.

(S)-tert-Butyl 2-((S)-2-(2-((trimethylsilyl)ethynyl)benzamido)propanamido)propanoate 66

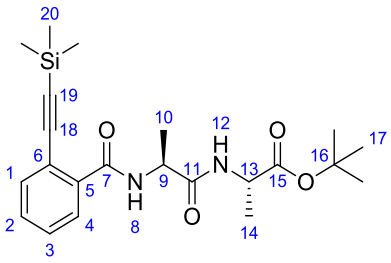

According to *general procedure (3a)*: Aryl iodide **65** (500mg, 1.12 mmol) and ethynyltrimethylsilane (317 µL, 2.24 mmol) gave the *title compound* **66** (243 mg, 52 %) as a pale yellow solid after purification by flash column chromatography (PE:Et_2O, 1:4); $[\alpha]_D^{23.5}$ +4.70 (*c* 1.50, $CHCl_3$); δ_H (400 MHz, $CDCl_3$) 8.09 (d, *J* 7.0, 1 H, H8), 7.89 - 7.93 (m,

1 H, H3), 7.38 - 7.43 (m, 1 H, H1), 7.25 - 7.28 (m, 2 H, H2, H4), 6.93 (d, *J* 7.2, 1 H, H12), 4.66 - 4.73 (m, 1 H, H9), 4.26 - 4.35 (m, 1 H, H13), 1.40 (d, *J* 6.8, 3 H, H10), 1.32 (s, 9 H, H17), 1.23 (d, *J* 7.1, 3 H, H14), 0.15 (s, 9 H, H20); δ_C (101 MHz, $CDCl_3$) 171.8 (C=O), 171.2 (C=O), 165.6 (C7), 134.5 (C5), 134.2 (C1), 130.6 (C2), 130.0(C3), 128.9 (C4), 119.7 (C6), 102.8 (C18), 102.3 (C19), 81.7 (C16), 49.6 (C9), 48.7 (C13), 27.9 (C17), 18.3 (C10), 18.2 (C14), -0.3 (C20); IR ($CHCl_3$) 3319, 3066, 2978, 2246, 2155, 1736, 1685, 1636; HRMS calculated for $C_{22}H_{33}O_4N_2Si$ $[M+H]^+$: 417.2204, found 417.2198.

(S)-tert-Butyl 2-((S)-2-(1-methylene-3-oxoisoindolin-2-yl)propanamido)propanoate 67

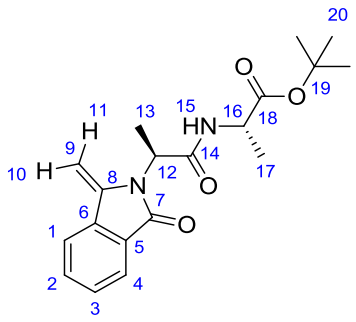

According to *general procedure (3b):* Protected alkyne **66** (486 mg, 1.16 mmol) gave the *title compound* **67** (134 mg, 32 %) as a pale yellow solid after purification by flash column chromatography (CH_2Cl_2:EtOAc, 3:1); $[\alpha]_D^{23.5}$ -22.2 (*c* 1.0, MeOH); δ_H (400 MHz, $CDCl_3$) 7.77 (d, *J* 7.6, 1 H, H4), 7.62 (d, *J* 7.0, 1 H, H1), 7.54 (td, *J* 7.5, 1.0, 1 H, H3), 7.42 - 7.48 (m, 1 H, H2), 6.38 - 6.45 (m, 1 H, H15), 5.22 (d, *J* 2.7, 1 H, H10), 5.15 (q, *J* 7.1, 1 H, H12), 4.88 (d, *J* 2.7, 1 H, H11), 4.39 (quin, *J* 7.1, 1 H, H16), 1.53 (d, *J* 7.3, 3 H, H13), 1.31 - 1.37 (m, 9 H, H20), 1.24 (d, *J* 7.1, 3 H, H17); δ_C (101 MHz, $CDCl_3$) 171.7 (C18), 169.3 (C14), 167.1 (C7), 139.3 (C8), 136.6 (C6), 132.4 (C2), 129.6 (C3), 128.3 (C5), 123.4 (C4), 119.9 (C1), 91.5 (C9), 82.0 (C19), 49.6 (C12), 48.9 (C16), 27.9 (C20), 18.3 (C17), 14.2 (C13); HRMS calculated for $C_{19}H_{24}O_4NaN_2$ $[M+Na]^+$: 367.1628, found 367.1629; IR (MeOH) 3330, 2980, 2938, 1712, 1679, 1381.

(S)-tert-Butyl 2-((S)-2-(2-ethynylbenzamido)propanamido)propanoate 68

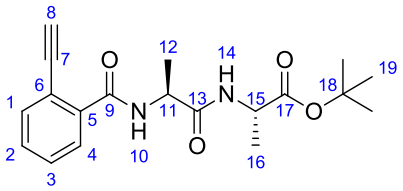

According to *general procedure (3h)*: Silyl protected acetylene **66** (150 mg, 0.36 mmol) gave the *title compound* **68** (115 mg, 93 %) as a yellow oil; $[\alpha]_D^{23.5}$ +4.70 (*c* 1.50, $CHCl_3$); δ_H (400 MHz, $CDCl_3$) 7.92 – 7.96 (m, 1 H, H4), 7.89 (d, *J* 7.0, 1 H, H10), 7.53 - 7.58 (m, 1 H, H1), 7.39 - 7.44 (m, 2 H, H2, H3), 6.93 (d, *J* 7.0, 1 H, H14), 4.74 - 4.84 (m, 1 H, H11), 4.42 – 4.46 (m, 1 H, H15), 3.55 (s, 1 H, H8), 1.51 (d, *J* 7.1, 3 H, H12), 1.45 (s, 9 H, H19), 1.36 (d, *J* 7.1, 3 H, H16); δ_c (101 MHz, $CDCl_3$) 171.7 (C=O), 171.4 (C=O), 165.8 (C9), 135.9 (C5), 134.0 (C1), 130.6 (C2), 129.6 (C4), 129.2 (C3), 118.8 (C6), 84.2 (C8), 81.9 (C7), 81.7 (C18), 49.7 (C11), 48.7 (C15), 27.9 (C19), 18.4 (C16), 18.3 (C12); IR ($CHCl_3$) 3292, 2979, 2934, 2857, 2361, 1767; HRMS calculated for $C_{19}H_{24}O_4NaN_2$ $[M+Na]^+$: 367.1628, found 367.1629.

tert-Butyl 2-((S)-2-(2-((2-((S)-2-((((9H-fluoren-9-yl)methoxy)carbonyl)amino)propanamido)phenyl)ethynyl)benzamido)propanamido)propanoate 69

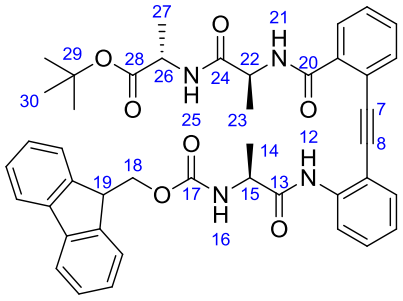

According to *general procedure (3f)*: ^{t}Bu-ester protected acid **48** (500 mg, 0.72 mmol) gave a yellow residue **A**. According to *general procedure (3e)*: Residue **A** and L-alanine tert-butyl ester hydrochloride (273mg, 1.44 mmol) gave the *title compound* **69** (385 mg, 53%) as a

white solid after purification by flash column chromotography (PE:Et_2O, 1:1); $[\alpha]_D^{23.5}$ +42.8 (*c* 1.00, $CHCl_3$); δ_H (400 MHz, $CDCl_3$) 9.51 (s, 1 H, H12), 8.57 (d, *J* 8.3, 1 H, N-H), 7.58 - 7.66 (m, 4 H, Ar-H), 7.47 - 7.56 (m, 3 H, Ar-H), 7.35 - 7.43 (m, 2 H, Ar-H), 7.25 - 7.34 (m, 4 H, Ar-H), 7.15 - 7.22 (m, 3 H, Ar-H), 6.96 (td, *J* 7.5, 0.9, 1 H, Ar-H), 6.15 (d, *J* 8.3, 1 H, H16), 5.31 (t, *J* 7.5, 1 H, H15), 5.12 (t, *J* 7.4, 1 H, H22), 4.37 (dd, *J* 10.3, 7.3, 1 H, H18a), 4.29 (t, *J* 7.3, 1 H, H26), 4.22 (dd, *J* 10.3, 7.6, 1 H, H18b), 4.10 (t, *J* 7.5, 1 H, H19), 1.52 (d, *J* 6.8, 3 H, H14), 1.45 (d, *J* 6.8, 3 H, H23), 1.23 (s, 9 H, H30), 1.08 (d, *J* 7.3, 3 H, H27); δ_C (100 MHz, $CDCl_3$) 172.3 (C13), 171.6 (C24), 171.5 (C28), 166.0 (C20), 155.8 (C17), 143.7, 143.6, 141.1, 140.6, 134.0, 133.9, 132.0, 130.9, 129.8, 128.1, 127.6, 127.2, 126.9, 125.0, 123.2, 122.4, 119.8, 119.3, 112.0 (18 x Ar-C), 95.2, 89.8 (C7, 8), 81.3 (C29), 67.1 (C18), 50.8 (C22), 48.9 (C15), 48.4 (C26), 46.9 (C19), 27.7 (C30), 21.0 (C14), 20.0 (C23), 17.9 (C27); IR ($CHCl_3$) 3280, 1672, 1642; HRMS calculated for $C_{43}H_{44}N_4NaO_7$ $[M+Na]^+$: 751.3102, found 751.3083.

(S)-tert-Butyl 2-((S)-2-(2-((2-((S)-2-((S)-2-((tert-butoxycarbonyl)amino)propanamido)propanamido)phenyl)ethynyl)benzamido)propanamido)propanoate 70

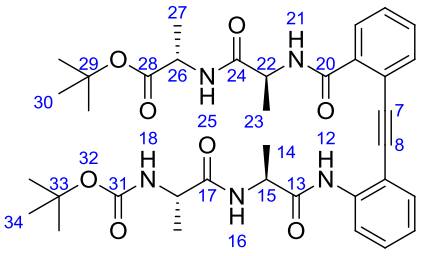

According to *general procedure (3g)*: Fmoc-protected amine **69** (80 mg, 0.15 mmol) gave Residue **A**. According to *general procedure (3e)*: Residue **A** and Boc-Ala-OH (27 mg, 0.19 mmol) gave the *title compound* **70** (28 mg, 24 %) as a white residue after purification by flash column chromatography (PE:Et_2O, 1:1**)**; $[\alpha]_D^{23.5}$ +9.80 (*c* 0.95, $CHCl_3$); δ_H (400 MHz,

$CDCl_3$) 9.49 (s, 1 H, H12), 8.55 (d, *J* 7.8, 1 H, H25), 8.26 - 8.32 (m, 1 H, H18), 7.66 (d, *J* 7.1, 1 H, Ar-H), 7.61 (dd, *J* 7.7, 1.1, 1 H, Ar-H), 7.43 (qd, *J* 7.5, 1.3, 2 H, Ar-H), 7.22 - 7.35 (m, 3 H, Ar-H), 6.98 - 7.04 (m, 2 H, H16, Ar-H), 5.65 - 5.72 (m, 1 H, H21), 5.44 - 5.53 (m, 1 H, H35), 5.27 - 5.35 (m, 1 H, H22), 4.35 - 4.44 (m, 1 H, H15), 4.16 - 4.26 (m, 1 H, H26), 1.54 (d, *J* 6.8, 3 H, H23), 1.48 (d, *J* 6.8, 3 H, H36), 1.43 (s, 9 H, C30), 1.39 (s, 9 H, C34), 1.30 (d, *J* 7.3, 3 H, H14), 1.28 (d, *J* 7.1, 3 H, H27); δ_C (100 MHz, $CDCl_3$) 172.4 (C24), 172.3 (C17), 172.0 (C13), 166.0 (C20), 155.4 (C28), 152.6 (C31), 140.6, 134.2, 134.1, 132.2, 131.1, 129.9, 128.2, 127.2, 123.3, 122.6, 119.4, 112.1 (12 x Ar-C), 95.3, 89.9 (C7, 8), 81.8 (C29), 79.8 (C33), 50.2 (C26), 49.9 (C35), 49.0 (C22), 48.8 (C15), 28.4 (C34), 28.0 (C30), 20.5 (C23), 20.4 (C36), 19.1 (C27), 18.6 (C14); δ_H (DMSO-d_6, 500 MHz) 9.47 (s, 1 H, H12), 8.82 (d, *J* 7.5, 1 H, H14), 8.29 (d, *J* 8.0, 1 H, Ar-H), 8.14 - 8.26 (m, 2 H, H8, H18), 7.77 (dd, *J* 7.8, 0.9, 1 H, Ar-H), 7.70 - 7.73 (m, 1 H, Ar-H), 7.59 (td, *J* 7.5, 1.4, 1 H, Ar-H), 7.53 (td, *J* 7.6, 1.3, 2 H, Ar-H), 7.39 - 7.44 (m, 1 H, Ar-H), 7.14 (td, *J* 7.7, 1.1, 1 H, Ar-H), 6.93 (d, *J* 8.0, 1 H, H4), 5.01 - 5.10 (m, 1 H, H9), 4.63 - 4.71 (m, 1 H, H15), 3.93 - 4.07 (m, 2 H, H5, H19), 1.33 - 1.42 (m, 24 H, H1, H10, H16, H23), 1.18 (d, *J* 7.3 Hz, 6 H, H6, H20); δ_C (DMSO-d_6, 126 MHz) 173.4, 172.5, 172.4 (C11), 172.0, 167.6 (C13), 155.5 (C3), 140.6, 137.3, 133.0, 132.3, 131.1, 130.3, 129.1, 128.8, 124.1, 121.0, 120.5, 112.7 (12 x Ar-C), 94.7, 89.3 (2 x alkynyl-C), 80.7 (C22), 78.5 (C2), 50.0 (C5), 49.1 (C9), 49.1 (C15), 48.8 (C19), 28.7 (C23), 28.0 (C1), 19.5 (C10), 18.5 (C16), 18.4 (C6), 17.1 (C20); IR ($CHCl_3$) 3272, 2979, 2934, 1641, 1581; HRMS calculated for $C_{36}H_{47}N_5NaO_8$ $[M+Na]^+$: 700.3317, found 700.3290.

N,N'-((2S,2'S)-((Ethyne-1,2-diylbis(2,1-phenylene))bis(azanediyl))bis(1-oxopropane-2,1-diyl))bis(2,2-dimethylpropanamide) 71

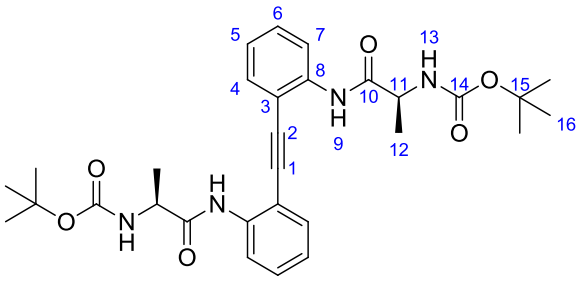

According to *general procedure (3a)*: Iodide **47** (490 mg, 1.26 mmol) and alkyne **51** (405 mg, 1.40 mmol) gave the *title compound* **71** (287 mg, 41 %) as an off-white solid after purification by flash column chromatography (PE:Et_2O, 1:1); $[\alpha]_D^{23.5}$ +4.60 (*c* 1.75, $CHCl_3$); δ_H (400 MHz, $CDCl_3$) 8.83 (br. s., 2 H, H9), 8.30 (d, *J* 7.9, 2 H, H7), 7.52 (d, *J* 7.3, 2 H, H3), 7.24 - 7.35 (m, 2 H, H6), 7.03 (t, *J* 7.5, 2 H, H5), 5.18 - 5.39 (m, 2 H, H13), 4.20 - 4.44 (m, 2 H, H11), 1.38 (d, *J* 7.0, 6 H, H12), 1.21 (s, 18 H, H16); δ_C (101MHz, $CDCl_3$) 171.3 (C10), 155.8 (C14), 138.6 (C8), 132.6 (C4), 130.0 (C6), 123.9 (C5), 120.2 (C7), 112.6 (C3), 91.0 (C1), 80.4 (C15), 65.8, 51.2 (C11), 28.0 (C16), 17.8 (C12); IR ($CHCl_3$) 3319, 2977, 2931, 2855, 2250, 1688; HRMS calculated for $C_{30}H_{38}N_4NaO_6$ $[M+Na]^+$:573.2684, found 573.2683.

N,N'-((2S,2'S)-(((2S,2'S)-((Ethyne-1,2-diylbis(2,1-phenylene))bis(azanediyl))bis(1-oxopropane-2,1-diyl))bis(azanediyl))bis(1-oxopropane-2,1-diyl))bis(2,2-dimethylpropanamide) 72

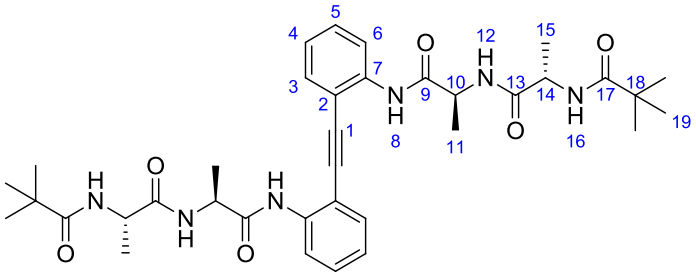

According to *general procedure (3f)*: Boc-protected amine **71** (160 mg, 0.29 mmol) gave yellow residue **A**. According to *general procedure (3e)*: Residue **A** and Boc-Ala-OH (164 mg, 0.87 mmol) gave the *title compound* **72** (60 mg, 30 %) as a colourless gel after purification by flash column chromatography (CH_2Cl_2:MeOH, 19:1); $[\alpha]_D^{23.5}$ +11.5 (*c* 1.00, $CHCl_3$); δ_H (DMSO-d_6, 500MHz) 9.56 (s, 2 H, H8), 8.15 (d, *J* 7.1, 2 H, H12), 7.84 (d, *J* 8.2, 2 H, H6), 7.70 (d, *J* 7.6, 2 H, H3), 7.38 - 7.43 (m, 2 H, H5), 7.20 (td, *J* 7.6, 0.9, 2 H, H4), 6.90 (d, *J* 7.6, 2 H, H16), 4.54 - 4.67 (m, 2 H, H10), 3.95 - 4.02 (m, 2 H, H14), 1.32 - 1.37 (m, 24 H, H11, 19), 1.11 (d, *J* 6.9, 6 H, H15); δ_C (DMSO-d_6, 125 MHz) 172.9 (C9), 171.3 (C13), 155.1 (C17), 138.5 (C7), 132.7 (C3), 129.4 (C5), 124.5 (C4), 122.7 (C6), 115.0 (C2), 91.0 (C1), 78.0 (C18), 49.4 (C14), 48.8 (C10), 28.2 (C19), 17.9 (C15), 17.8 (C11); HRMS calculated for $C_{36}H_{48}N_6NaO_8$ $[M+Na]^+$: 715.3426, found 715.3416.

3.11.4 X-Ray Crystallography

Single crystals of the three-stranded mimic **56** were obtained by vapour diffusion ($CHCl_3$/hexane). Low temperature (100 K) diffraction studies were carried out using Beamline I19 (EH1) at Diamond Light Source. Raw frame data were reduced using CrysAlisPRO[117] and the structure was solved using SuperFlip.[118] Full-matrix least-squares refinement of the structures was carried out using CRYSTALS.[119] Crystallographic data (excluding structure factors) have been deposited with the Cambridge Crystallographic Data Centre (CCDC 1049256).

Single-Crystal X-Ray Diffraction Data for Three-Stranded Meander 56

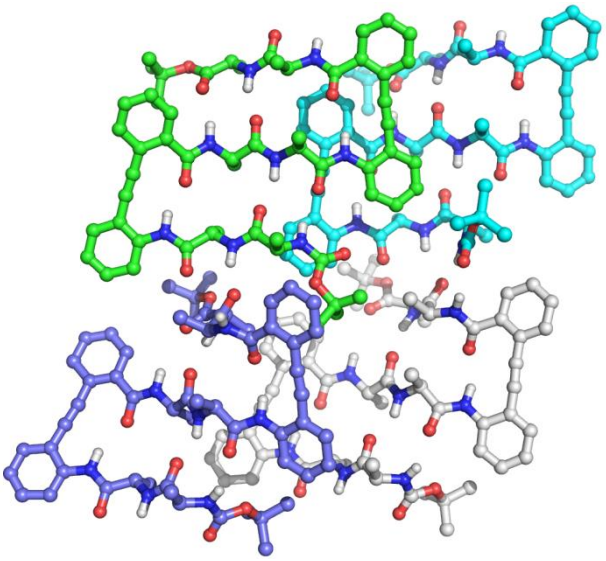

3.11.4.1 Crystal Data

a = 20.4305(7) Å α = 90°

b = 22.9599(10) Å β = 106.160(4)°

c = 27.6036(12) Å γ = 90°

Volume 12436.7(9) Å³ *Crystal* monoclinic

		Class	
Space group	P 1 2_1 1	*Z* =	8
Formula	C_{57} H_{66} N_8 O_{11}	M_r	1039.20
Cell determined from	10757 reflections	*Cell θ range* =	2 - 23°
Temperature	100K		
Shape	plates		
Colour	clear_pale_colourless	*Size*	0.01 × 0.04 × 0.06 mm
D_x	1.11 Mg m^{-3}	*F000*	4416.000
μ	0.078 mm^{-1}		
Absorption correction	multi-scan		
T_{min}	0.60	T_{max}	1.00

3.11.4.2 Data Collection

Diffractometer	multi-scan
Scan type	ω scans
Reflections measured	16032
Independent reflections	16032
Rint	0.1832
θ_{max}	23.7387

h =	-21 → 21
k =	0 → 24
l =	0 → 30

3.11.4.3 Refinement

$\Delta\rho_{min}$ =	-0.57 e Å^{-3}
$\Delta\rho_{max}$ =	0.54 e Å^{-3}
Reflections used	11556
Cutoff: I >	-3.00σ(I)
Parameters refined	2737
S =	1.03
R-factor	0.115
weighted R-factor	0.216
Δ/σ_{max}	0.0056
Refinement on	F^2
w =	$w' \times [1 - (\Delta F_{obs} / 6 \times \Delta F_{est})^2]^2$
w′ =	$[P_0T_0'(x) + P_1T_1'(x) + ...P_{n-1}T_{n-1}'(x)]^{-1}$, where P_i are the coefficients of a Chebychev series in $t_i(x)$, and x = $F_{calc}^2/F_{calc}^2{}_{max}$.
P_0 - P_{n-1} =	0.283E+04 0.437E+04 0.265E+04 0.111E+04 256.

3.12 References

1. Cheng, P.-N., Pham, J. D. & Nowick, J. S. The Supramolecular Chemistry of β-Sheets. *J. Am. Chem. Soc.* **135,** 5477–5492 (2013).
2. Chou, K.-C., Pottle, M., Némethy, G., Ueda, yuzo & Scheraga, H. A. Structure of β-sheets: Origin of the right-handed twist and of the increased stability of antiparallel over parallel sheets. *J. Mol. Biol.* **162,** 89–112 (1982).
3. Datta, S., Shamala, N., Gurunath, R. & Balaram, P. Observation of a mixed antiparallel and parallel beta-sheet motif in the crystal structure of Boc-Ala-Ile-Aib-OMe. *Int. J. Pept. Protein Res.* **48,** 209–214 (1996).
4. Hakimi, O., Knight, D. P., Vollrath, F. & Vadgama, P. Spider and mulberry silkworm silks as compatible biomaterials. *Compos. Part B Eng.* **38,** 324–337 (2007).
5. Wimley, W. C. The versatile β-barrel membrane protein. *Curr. Opin. Struct. Biol.* **13,** 404–411 (2003).
6. Timm, D. E., Baker, L. j., Mueller, H., Zidek, L. & Novotny, M. V. Structural basis of pheromone binding to mouse major urinary protein (MUP-I). *Protein Sci.* **10,** 997–1004 (2001).
7. Papagerogiou, A. C., Shapiro, R. & Acharya, K. R. Molecular recognition of human angiogenein by placental ribonuclease inhibitor - an X-ray crystallographic study at 2.0 Angstrom resolution. *EMBO J.* **16,** 5162–5177 (1997).
8. Sprague, E. R., Redd, M. J., Johnson, A. D. & Wolberger, C. Structure of the C-terminal domain of Tup1, a corepressor of transcription in yeast. *EMBO J.* **19,** 3016–3027 (2000).
9. Forst, D., Welte, W., Wacker, T. & Diederichs, K. Structure of the sucrose-specific porin ScrY from Salmonella typhimurium and its complex with sucrose. *Nat. Struct. Biol.* **5,** 37–46 (1998).
10. Gray, H. B. & Winkler, J. R. Electron transfer in proteins. *Annu. Rev. Biochem.* **65,** 537–561 (1996).
11. Card, P. B., Erbel, P. J. A. & Gardner, K. H. Structural Basis of ARNT PAS-B Dimerization: Use of a Common Beta-sheet Interface for Hetero- and Homodimerization. *J. Mol. Biol.* **353,** 664–677 (2005).
12. Rajagopal, S., Meyer, S. C., Goldman, A., Zhou, M. & Ghosh, I. A minimalist approach toward protein recognition by epitope transfer from functionally evolved beta-sheet surfaces. *J. Am. Chem. Soc.* **128,** 14356–14363 (2006).

13. Lyu, P. C., Liff, M. I., Marky, L. A. & Kallenbach, N. R. Side-chain Contributions to the Stability of Alpha-Helical Structure in Peptides. *Science* **250,** 669–673 (1990).

14. Lyu, P. C., Wemmer, D. E., Zhou, H. X., Pinker, R. J. & Kallenbach, N. R. Capping interactions in isolated .alpha. helixes: position-dependent substitution effects and structure of a serine-capped peptide helix. *Biochemistry (Mosc.)* **32,** 421–425 (1993).

15. Zhou, N. E., Kay, C. M., Sykes, B. D. & Hodges, R. S. A single-stranded amphipathic .alpha.-helix in aqueous solution: Design, structural characterization, and its application for determining .alpha.-helical propensities of amino acids. *Biochemistry (Mosc.)* **32,** 6190–6197 (1993).

16. De Alba, E., Santoro, J., Rico, M. & Jiménez, M. A. De novo design of a monomeric three-stranded antiparallel β-sheet. *PRS* **8,** 854–865 (1999).

17. Blanco, F., Ramírez-Alvarado, M. & Serrano, L. Formation and stability of β-hairpin structures in polypeptides. *Curr. Opin. Struct. Biol.* **8,** 107–111 (1998).

18. Maynard, A. J., Sharman, G. J. & Searle, M. S. Origin of β-Hairpin Stability in Solution: Structural and Thermodynamic Analysis of the Folding of a Model Peptide Supports Hydrophobic Stabilization in Water. *J. Am. Chem. Soc.* **120,** 1996–2007 (1998).

19. Smith, C. K. & Regan, L. Construction and Design of β-Sheets. *Acc. Chem. Res.* **30,** 153–161 (1997).

20. Kim, S., Kim, J. H., Lee, J. S. & Park, C. B. Beta-Sheet-Forming, Self-Assembled Peptide Nanomaterials towards Optical, Energy, and Healthcare Applications. *Small* **11,** 3623–3640 (2015).

21. Nowick, J. S., Smith, E. M. & Pairish, M. Artificial β-sheets. *Chem. Soc. Rev.* **25,** 401–415 (1996).

22. Feigel, M. 2,8-Dimethyl-4-(carboxymethyl)-6-(aminomethyl)phenoxathiin S-dioxide: an organic substitute for the β-turn in peptides? *J. Am. Chem. Soc.* **108,** 181–182 (1986).

23. Wagner, G. & Feigel, M. Parallel β-sheet conformation in macrocycles. *Tetrahedron* **49,** 10831–10842 (1993).

24. Brandmeier, V., Sauer, W. H. B. & Feigel, M. Antiparallel β-Sheet Conformation in Cyclopeptides Containing a Pseudo-amino Acid with a biphenyl moiety. *Helv. Chim. Acta* **77,** 70–85 (1994).

25. Gardner, R. R., Liang, G.-B. & Gellman, S. H. An Achiral Dipeptide Mimetic That Promotes .beta.-Hairpin Formation. *J. Am. Chem. Soc.* **117,** 3280–3281 (1995).

26. Kemp, D. S. & Li, Z. Q. 2-amino-2'-carboxydiphenylacetylenes as β-turn mimetics - Synthesis and Conformational Properties. *Tetrahedron Lett.* **36,** (1995).

27. Gretchikhine, A. B. & Ogawa, M. Y. Photoinduced Electron Transfer Along a β-Sheet Mimic. *J. Am. Chem. Soc.* **118,** 1543–1544 (1996).

28. Jiang, L. J., Moehle, K., Dhanapal, B., Obrecht, D. & Robinson, J. A. Combinatorial biomimetic chemistry: Parallel synthesis of a small library of beta-hairpin mimetics based on loop III from human platelet-derived growth factor B. *Helv. Chim. Acta* **83,** (2000).

29. Favre, M., Moehle, K., Jiang, L. Y., Pfeiffer, B. & Robinson, J. A. Structural mimicry of canonical conformations in antibody hypervariable loops using cyclic peptides containing a heterochiral diproline template. *J. Am. Chem. Soc.* **121,** (1999).

30. Späth, J., Stuart, F., Jiang, L. & Robinson, J. A. Stabilization of a β-Hairpin Conformation in a Cyclic Peptide Using the Templating Effect of a Heterochiral Diproline Unit. *Helv. Chim. Acta* **81,** 1726–1738 (1998).

31. Shankaramma, S. C. *et al.* Macrocyclic Hairpin Mimetics of the Cationic Antimicrobial Peptide Protegrin I: A New Family of Broad-Spectrum Antibiotics. *ChemBioChem* **3,** 1126–1133 (2002).

32. Robinson, J. A. *et al.* Properties and structure-activity studies of cyclic beta-hairpin peptidomimetics based on the cationic antimicrobial peptide protegrin I. *Bioorg. Med. Chem.* **13,** (2005).

33. DeMarco, S. J. *et al.* Discovery of novel, highly potent and selective beta-hairpin mimetic CXCR4 inhibitors with excellent anti-HIV activity and pharmacokinetic profiles. *Bioorg. Med. Chem.* **14,** (2006).

34. Descours, A., Moehle, K., Renard, A. & Robinson, J. A. A New Family of β-Hairpin Mimetics Based on a Trypsin Inhibitor from Sunflower Seeds. *ChemBioChem* **3,** 318–323 (2002).

35. Fasan, R. *et al.* Structure-activity studies in a family of beta-hairpin protein epitope mimetic inhibitors of the p53-HDM2 protein-protein interaction. *Chembiochem* **7,** (2006).

36. Athanassiou, Z. *et al.* Structural Mimicry of Retroviral Tat Proteins by Constrained β-Hairpin Peptidomimetics: Ligands with High Affinity and Selectivity for Viral TAR RNA Regulatory Elements. *J. Am. Chem. Soc.* **126,** 6906–6913 (2004).

37. Fasan, R. *et al.* Using a beta-hairpin to mimic an alpha-helix: Cyclic peptidomimetic inhibitors of the p53-HDM2 protein-protein interaction. *Angew. Chem. Int. Ed.* **43,** (2004).

38. Kemp, D. S., Bowen, B. R. & Muendel, C. C. Synthesis and conformational analysis of epindolidione-derived peptide models for β-sheet formation. *J. Org. Chem.* **55,** 4650–4657 (1990).

39. Kemp, D. S. & Bowen, B. R. Synthesis of peptide-functionalized diacylaminoepindolidiones as templates for β-sheet formation. *Tetrahedron Lett.* **29,** 5077–5080 (1988).

40. Kemp, D. S. & Bowen, B. R. Conformational analysis of peptide-functionalized diacylaminoepindolidiones 1H NMR evidence for β-sheet formation. *Tetrahedron Lett.* **29,** 5081–5082 (1988).

41. Nowick, J. S., Mahrus, S., Smith, E. M. & Ziller, J. W. Triurea Derivatives of Diethylenetriamine as Potential Templates for the Formation of Artificial β-Sheets1. *J. Am. Chem. Soc.* **118,** 1066–1072 (1996).

42. Nowick, J. S. *et al.* An Unnatural Amino Acid that Mimics a Tripeptide β-Strand and Forms β-Sheetlike Hydrogen-Bonded Dimers. *J. Am. Chem. Soc.* **122,** 7654–7661 (2000).

43. Almeida, A. M., Li, R. & Gellman, S. H. Parallel β-Sheet Secondary Structure Is Stabilized and Terminated by Interstrand Disulfide Cross-Linking. *J. Am. Chem. Soc.* **134,** 75–78 (2012).

44. Lingard, H. *et al.* Diphenylacetylene-Linked Peptide Strands Induce Bidirectional β-Sheet Formation. *Angew. Chem. Int. Ed.* **53,** 3650–3653 (2014).

45. Junquera, E. & Nowick, J. S. Folding of an Artificial β-Sheet in Competitive Solvents. *J. Org. Chem.* **64,** 2527–2531 (1999).

46. Tsang, K. Y., Diaz, H., Graciani, N. & Kelly, J. W. Hydrophobic Cluster Formation Is Necessary for Dibenzofuran-Based Amino Acids to Function as .beta.-Sheet Nucleators. *J. Am. Chem. Soc.* **116,** 3988–4005 (1994).

47. Schneider, J. P. & Kelly, J. W. Synthesis and Efficacy of Square Planar Copper Complexes Designed to Nucleate .beta.-Sheet Structure. *J. Am. Chem. Soc.* **117,** 2533–2546 (1995).

48. Nesloney, C. L. & Kelly, J. W. A 2,3‘-Substituted Biphenyl-Based Amino Acid Facilitates the Formation of a Monomeric β-Hairpin-like Structure in Aqueous Solution at Elevated Temperature. *J. Am. Chem. Soc.* **118,** 5836–5845 (1996).

49. Lengyel, G. A. & Horne, W. S. Design Strategies for the Sequence-Based Mimicry of Side-Chain Display in Protein β-Sheets by α/β-Peptides. *J. Am. Chem. Soc.* **134,** 15906–15913 (2012).

50. Boersma, M. D. *et al.* Evaluation of Diverse α/β-Backbone Patterns for Functional α-Helix Mimicry: Analogues of the Bim BH3 Domain. *J. Am. Chem. Soc.* **134,** 315–323 (2012).

51. Horne, W. S., Price, J. L., Keck, J. L. & Gellman, S. H. Helix Bundle Quaternary Structure from α/β-Peptide Foldamers. *J. Am. Chem. Soc.* **129,** 4178–4180 (2007).

52. Freire, F. *et al.* Diacid Linkers That Promote Parallel β-Sheet Secondary Structure in Water. *J. Am. Chem. Soc.* **130,** 7839–7841 (2008).

53. Liu, C. *et al.* Characteristics of Amyloid-Related Oligomers Revealed by Crystal Structures of Macrocyclic β-Sheet Mimics. *J. Am. Chem. Soc.* **133,** 6736–6744 (2011).

54. Davidson, A. *et al.* Simultaneous recognition of HIV-1 TAR RNA bulge and loop sequences by cyclic peptide mimics of Tat protein. *Proc. Natl. Acad. Sci. U. S. A.* **106,** (2009).

55. Srinivas, N. *et al.* Peptidomimetic Antibiotics Target Outer-Membrane Biogenesis in Pseudomonas aeruginosa. *Science* **327,** (2010).

56. Kortemme, T., Ramírez-Alvarado, M. & Serrano, L. Design of a 20-Amino Acid, Three-Stranded β-Sheet Protein. *Science* **281,** 253–256 (1998).

57. Schenck, H. L. & Gellman, S. H. Use of a Designed Triple-Stranded Antiparallel β-Sheet To Probe β-Sheet Cooperativity in Aqueous Solution. *J. Am. Chem. Soc.* **120,** 4869–4870 (1998).

58. Sharman, G. J. & Searle, M. S. Cooperative Interaction between the Three Strands of a Designed Antiparallel β-Sheet. *J. Am. Chem. Soc.* **120,** 5291–5300 (1998).

59. Doig, A. J. A three stranded β-sheet peptide in aqueous solution containing N-methyl amino acids to prevent aggregation. *Chem. Commun.* 2153–2154 (1997).

60. Das, C., Balaram, P. & Raghothama, S. A four stranded β-sheet structure in a designed, synthetic polypeptide. *Chem. Commun.* 967–968 (1999).

61. Venkatraman, J., Naganagowda, G. A., Sudha, R. & Balaram, P. De novo design of a five-stranded β-sheet anchoring a metal-ion binding site. *Chem. Commun.* 2660–2661 (2001).

62. Griffioen, A. W. *et al.* Anginex, a designed peptide that inhibits angiogenesis. *Biochem. J.* **354,** 233–242 (2001).

63. Boehm, T., Folkman, J., Browder, T. & O'Reilly, M. S. Antiangiogenic therapy of experimental cancer does not induce acquired drug resistance. *Nature* **390,** 404–407 (1997).

64. Gupta, S. K. & Singh, J. P. Inhibition of endothelial cell proliferation by platelet factor-4 involves a unique action on S phase progression. *J. Cell Biol.* **127,** 1121–1127 (1994).

65. O'Reilly, M. S. *et al.* Angiostatin: A novel angiogenesis inhibitor that mediates the suppression of metastases by a lewis lung carcinoma. *Cell* **79,** 315–328 (1994).

66. Schaft, D. W. J. van der, Toebes, E. A. H., Haseman, J. R., Mayo, K. H. & Griffioen, A. W. Bactericidal/permeability-increasing protein (BPI) inhibits angiogenesis via induction of apoptosis in vascular endothelial cells. *Blood* **96,** 176–181 (2000).

67. Dings, R. P. M. *et al.* β-sheet is the bioactive conformation of the anti-angiogenic anginex peptide. *Biochem. J.* **373,** 281–288 (2003).

68. Dings, R. P. M. *et al.* Anti-tumor activity of the novel angiogenesis inhibitor anginex. *Cancer Lett.* **194,** 55–66 (2003).

69. Hegedüs, Z. *et al.* Foldameric α/β-Peptide Analogs of the β-Sheet-Forming Antiangiogenic Anginex: Structure and Bioactivity. *J. Am. Chem. Soc.* **135,** 16578–16584 (2013).

70. Haass, C. & Selkoe, D. J. Soluble protein oligomers in neurodegeneration: lessons from the Alzheimer's amyloid β-peptide. *Nat. Rev. Mol. Cell Biol.* **8,** 101–112 (2007).

71. Schenk, D. *et al.* Immunization with amyloid-β attenuates Alzheimer-disease-like pathology in the PDAPP mouse. *Nature* **400,** 173–177 (1999).

72. Kayed, R. *et al.* Common structure of soluble amyloid oligomers implies common mechanism of pathogenesis. *Science* **300,** 486–489 (2003).

73. Fawzi, N. L., Libich, D. S., Ying, J., Tugarinov, V. & Clore, G. M. Characterizing Methyl-Bearing Side-chain Contacts and Dynamics Mediating Amyloid β Protofibril Interactions Using ^{13}C methyl-DEST and Lifetime Line Broadening. *Angew. Chem. Int. Ed.* **53,** 10345-10349 (2014).

74. Vácha, R., Linse, S. & Lund, M. Surface Effects on Aggregation Kinetics of Amyloidogenic Peptides. *J. Am. Chem. Soc.* **136,** 11776-11782 (2014).

75. Pham, J. D., Chim, N., Goulding, C. W. & Nowick, J. S. Structures of Oligomers of a Peptide from β-Amyloid. *J. Am. Chem. Soc.* **135,** 12460–12467 (2013).

76. Benilova, I., Karran, E. & De Strooper, B. The toxic Aβ oligomer and Alzheimer's disease: an emperor in need of clothes. *Nat. Neurosci.* **15,** 349–357 (2012).

77. Kreutzer, A. G., Hamza, I. L., Spencer, R. K. & Nowick, J. S. X-ray Crystallographic Structures of a Trimer, Dodecamer, and Annular Pore Formed by an Aβ17–36 β-Hairpin. *J. Am. Chem. Soc.* (2016). doi:10.1021/jacs.6b01332

78. Salveson, P. J., Spencer, R. K. & Nowick, J. S. X-ray Crystallographic Structure of Oligomers Formed by a Toxic β-Hairpin Derived from α-Synuclein: Trimers and Higher-Order Oligomers. *J. Am. Chem. Soc.* (2016). doi:10.1021/jacs.5b13261

79. Buchanan, L. E. *et al.* Mechanism of IAPP amyloid fibril formation involves an intermediate with a transient β-sheet. *Proc. Natl. Acad. Sci.* **110,** 19285–19290 (2013).

80. Cheng, P.-N., Liu, C., Zhao, M., Eisenberg, D. & Nowick, J. S. Amyloid β-sheet mimics that antagonize protein aggregation and reduce amyloid toxicity. *Nat. Chem.* **4,** 927–933 (2012).

81. Zheng, J., Baghkhanian, A. M. & Nowick, J. S. A Hydrophobic Surface Is Essential To Inhibit the Aggregation of a Tau-Protein-Derived Hexapeptide. *J. Am. Chem. Soc.* **135,** 6846–6852 (2013).

82. Mutter, M., Hersperger, R., Gubernator, K. & Müller, K. The construction of new proteins: V. A template-assembled synthetic protein (TASP) containing both a 4-helix bundle and β-barrel-like structure. *Proteins Struct. Funct. Bioinforma.* **5,** 13–21 (1989).

83. Mutter, M. *et al.* Template-assembled synthetic proteins with four-helix-bundle topology. Total chemical synthesis and conformational studies. *J. Am. Chem. Soc.* **114,** 1463–1470 (1992).

84. Earnest, I. *et al.* Template-Assembled Synthetic Proteins (TASP). Cyclic Templates with Incorporated Turn-Inducing Mimics. *Helv. Chim. Acta* **76,** 1539–1563 (1993).

85. Grove, A., Mutter, M., Rivier, J. E. & Montal, M. Template-assembled synthetic proteins designed to adopt a globular, four-helix bundle conformation form ionic channels in lipid bilayers. *J. Am. Chem. Soc.* **115,** 5919–5924 (1993).

86. Tuchscherer, G., Dömer, B., Sila, U., Kamber, B. & Mutter, M. The TASP concept : Mimetics of peptide ligands, protein surfaces and folding units. *Tetrahedron* **49,** 3559–3575 (1993).

87. Offermann, D. A. *et al.* Synthesis and Incorporation into Cyclic Peptides of Tolan Amino Acids and Their Hydrogenated Congeners: Construction of an Array of A–B-loop Mimetics of the Cε3 Domain of Human IgE. *J. Org. Chem.* **77,** 3197–3214 (2012).

88. Spivey, A. C., McKendrick, J., Srikaran, R. & Helm, B. A. Solid-phase synthesis of an A-B loop mimetic of the C epsilon 3 domain of human IgE: Macrocyclization by Sonogashira coupling. *J. Org. Chem.* **68,** 1843–1851 (2003).

89. Makabe, K. Crystal structure of OspA mutant. *Be Publ.* null–null (2011).

90. *Molecular Operating Environment (MOE)*, 2013.08; Chemical Computing Group Inc., 1010 Sherbrooke St. West, Suite 910, Montreal, QC, Canada, H3A 2R7, **2016**.

91. *The PyMOL Molecular Graphics System*. Version 1.8, Schrodinger, LLC.

92. Mukaiyama, T. New Synthetic Reactions Based on the Onium Salts of Aza-Arenes [New synthetic methods (29)]. *Angew. Chem. Int. Ed. Engl.* **18,** 707–721 (1979).

93. Kundu, N. G. & Khan, M. W. Palladium-Catalysed Heteroannulation with Terminal Alkynes: a Highly Regio- and Stereoselective Synthesis of (Z)-3-Aryl(alkyl)idene Isoindolin-1-ones. *Tetrahedron* **56,** 4777–4792 (2000).

94. Shepard, M. S. & Carreira, E. M. Asymmetric Photocycloadditions with an Optically Active Allenylsilane: Trimethylsilyl as a Removable Stereocontrolling Group for the Enantioselective Synthesis of exo-Methylenecyclobutanes. *J. Am. Chem. Soc.* **119,** 2597–2605 (1997).

95. Claridge, T. D. W. & Pérez-Victoria, I. Enhanced 13C resolution in semi-selective HMBC: a band-selective, constant-time HMBC for complex organic structure elucidation by NMR. *Org. Biomol. Chem.* **1,** 3632–3634 (2003).

96. LaPlante, S. R. *et al.* Compound Aggregation in Drug Discovery: Implementing a Practical NMR Assay for Medicinal Chemists. *J. Med. Chem.* **56,** 5142–5150 (2013).

97. Wishart, D. S., Sykes, B. D. & Richards, F. M. Relationship between nuclear magnetic resonance chemical shift and protein secondary structure. *J. Mol. Biol.* **222,** 311–333 (1991).

98. Wishart, D. S., Sykes, B. D. & Richards, F. M. The chemical shift index: a fast and simple method for the assignment of protein secondary structure through NMR spectroscopy. *Biochemistry (Mosc.)* **31,** 1647–1651 (1992).

99. Haque, T. S., Little, J. C. & Gellman, S. H. Stereochemical Requirements for β-Hairpin Formation: Model Studies with Four-Residue Peptides and Depsipeptides. *J. Am. Chem. Soc.* **118,** 6975–6985 (1996).

100. Fesinmeyer, R. M. *et al.* Chemical shifts provide fold populations and register of beta hairpins and beta sheets. *J. Biomol. NMR* **33,** 213–231 (2005).

101. Marsh, J. A., Singh, V. K., Jia, Z. & Forman-Kay, J. D. Sensitivity of secondary structure propensities to sequence differences between α- and γ-synuclein: Implications for fibrillation. *Protein Sci. Publ. Protein Soc.* **15,** 2795–2804 (2006).

102. Wishart, D. S. & Sykes, B. D. in *Methods in Enzymology* (ed. Thomas L. James, N. J. O.) **239,** 363–392 (Academic Press, 1994).

103. Wang, Y. & Jardetzky, O. Probability-based protein secondary structure identification using combined NMR chemical-shift data. *Protein Sci.* **11,** 852–861 (2002).

104. Hegedüs, Z. *et al.* Foldameric probes for membrane interactions by induced β-sheet folding. *Chem. Commun.* **52,** 1891–1894 (2016).

105. Czerski, L., Vinogradova, O. & Sanders, C. R. NMR-Based amide hydrogen-deuterium exchange measurements for complex membrane proteins: development and critical evaluation. *J. Magn. Reson. San Diego Calif 1997* **142,** 111–119 (2000).

106. Schneider, T. L., Halloran, K. T., Hillner, J. A., Conry, R. R. & Linton, B. R. Application of H/D Exchange to Hydrogen Bonding in Small Molecules. *Chem. Eur. J.* **19,** 15101–15104 (2013).

107. Steffel, L. R., Cashman, T. J., Reutershan, M. H. & Linton, B. R. Deuterium Exchange as an Indicator of Hydrogen Bond Donors and Acceptors. *J. Am. Chem. Soc.* **129,** 12956–12957 (2007).

108. Shan, S. & Herschlag, D. The change in hydrogen bond strength accompanying charge rearrangement: Implications for enzymatic catalysis. *Proc. Natl. Acad. Sci.* **93,** 14474–14479 (1996).

109. Rose, G. D., Glerasch, L. M. & Smith, J. A. in *Advances in Protein Chemistry* (ed. C.B. Anfinsen, J. T. E. and F. M. R.) **37,** 1–109 (Academic Press, 1985).

110. Iqbal, M. & Balaram, P. Membrane channel forming polypeptides. 270-MHz proton magnetic resonance studies of the aggregation of the 11-21 fragment of suzukacillin in organic solvents. *Biochemistry (Mosc.)* **20,** 7278–7284 (1981).

111. Rothemund, S. *et al.* Temperature coefficients of amide proton NMR resonance frequencies in trifluoroethanol: a monitor of intramolecular hydrogen bonds in helical peptides. *J. Biomol. NMR* **8,** 93–97 (1996).

112. Kessler, H. Conformation and Biological Activity of Cyclic Peptides. *Angew. Chem. Int. Ed. Engl.* **21,** 512–523 (1982).

113. Abraham, M. H. *et al.* An NMR Method for the Quantitative Assessment of Intramolecular Hydrogen Bonding; Application to Physicochemical, Environmental, and Biochemical Properties. *J. Org. Chem.* **79,** 11075–11083 (2014).

114. Nakamura, S., Sato, H., Hirata, Y., Watanabe, N. & Hashimoto, S. Total synthesis of zaragozic acid C by an aldol-based strategy. *Tetrahedron* **61,** 11078–11106 (2005).

115. Jones, I. M. & Hamilton, A. D. Designed Molecular Switches: Controlling the Conformation of Benzamido-diphenylacetylenes. *Org. Lett.* **12,** 3651–3653 (2010).

116. Jones, I. M. & Hamilton, A. D. Anion-Dependent Switching: Dynamically Controlling the Conformation of Hydrogen-Bonded Diphenylacetylenes. *Angew. Chem. Int. Ed.* **50,** 4597–4600 (2011).

117. *CrysAlisPRO*. (Oxford Diffraction / Agilent Technologies UK Ltd, Yarnton, England).

118. Palatinus, L. & Chapuis, G. SUPERFLIP - a computer program for the solution of crysal structures by charge flipping in arbitary dimensions. *J. Appl. Crystallogr.* **40,** 786 – 790 (2007).

119. Betteridge, P. W., Carruthers, J. R., Cooper, R. I., Prout, K. & Watkin, D. J. CRYSTALS version 12: software for guided crystal structure analysis. *J. Appl. Crystallogr.* **36,** 1487 (2003).

Chapter 4 – Scope of the Meander Motif

4.1 Introduction

For the meander architecture to achieve the challenges laid down by Gellman, the molecules must be fully adaptable. This means being able to increase the number of strands, the number of residues in each strand, adjust the stereochemistry such that each side-chain can be projected above or below the plane, and allow the incorporation of basic, acidic, and unnatural residues. By creating architecture with this flexibility there is an opportunity to create a library of compounds for biomedical applications. This chapter will explore each of these aims in turn (Figure 4.1)

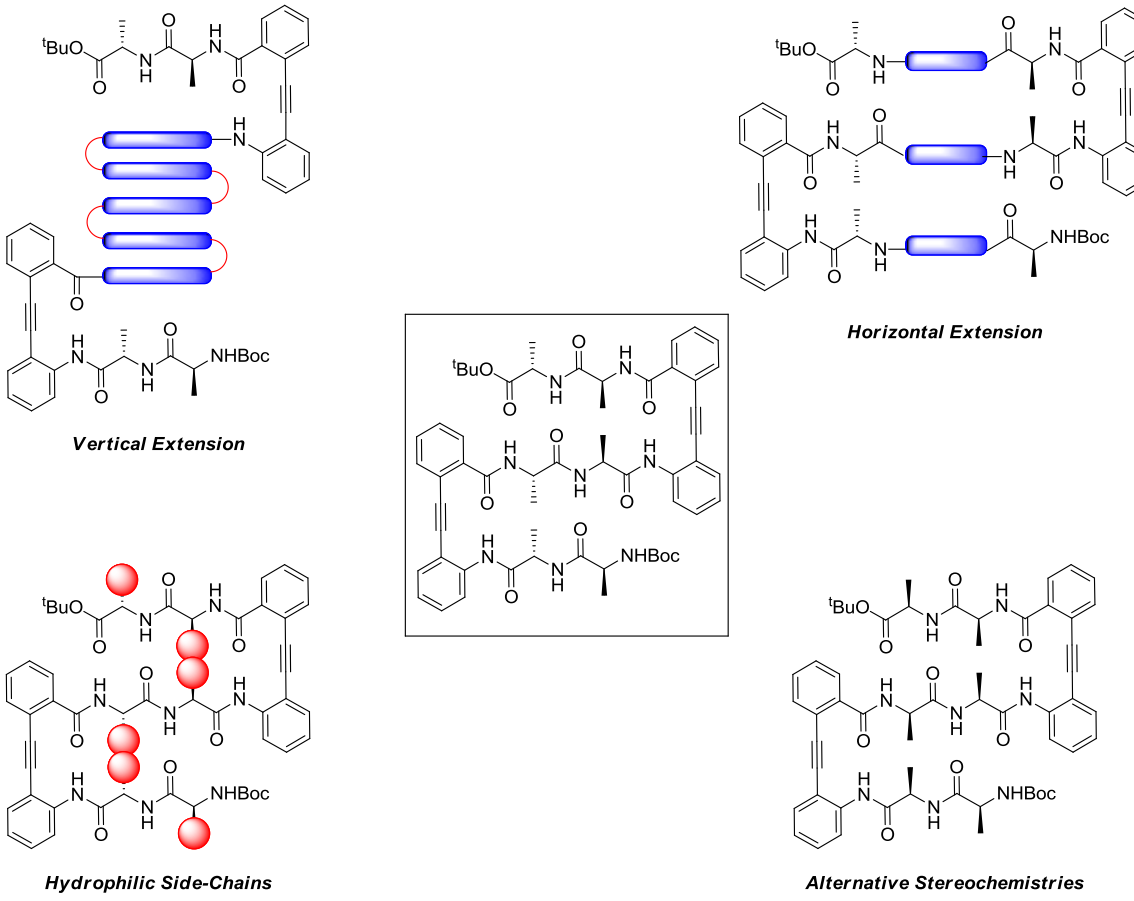

Figure 4.1 Schematic showing the four aims for the chapter.

4.2 Vertical Extension – Increasing the Number of Strands

4.2.1 Synthesis

With an effective modular synthesis in place it should be trivial to indefinitely extend the meander. To test this hypothesis it was decided to combine two four stranded precursors, **57**, to form the seven-stranded **80**. The synthesis, mediated by EDC/HOBt as coupling reagents proceeded as expected to afford the target molecule in 28 % yield (Scheme 4.1).

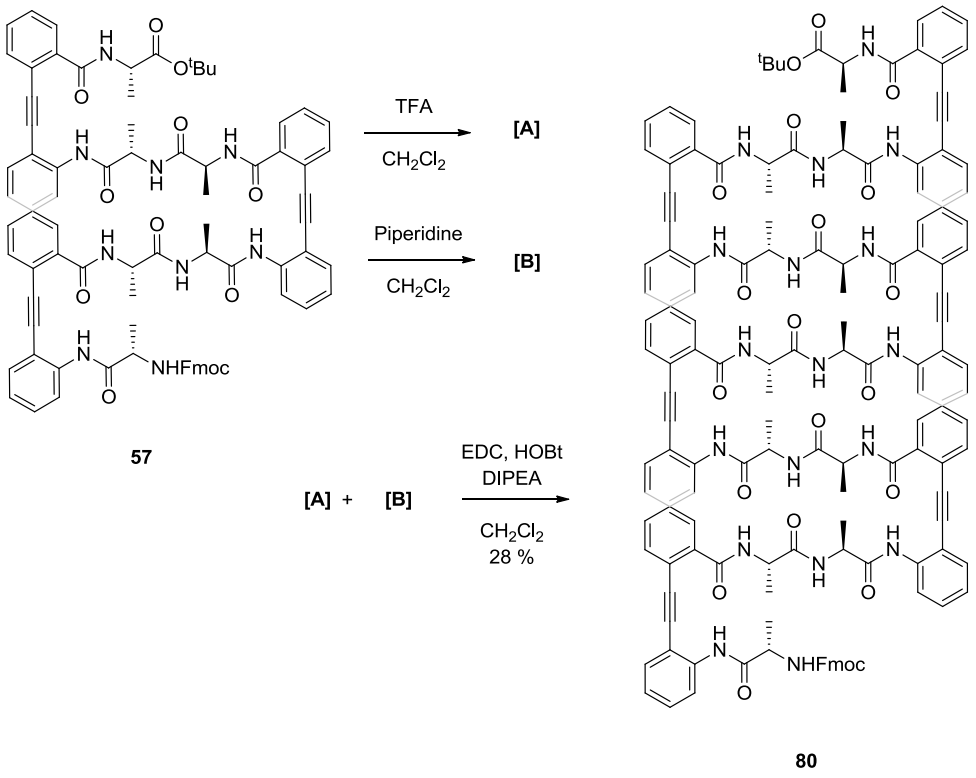

Scheme 4.1 Synthesis of seven-stranded meander **80** projecting six side-chains, and six side-chains below the plane of the molecule.

4.2.2 7-Strand Analysis

Unfortunately, due to the large number of very similar residues complete structural assignment was not possible due to spectral overlay. However the molecule was identified through correct spectral integration and MALDI mass spectrometry and despite the lack of structural assignment some analytical techniques could be applied.

4.2.2.1 NMR Analysis

Using the same assay as previously (Section 3.9.2) seven-stranded meander **80** showed no aggregation behaviour (Figure 4.2).

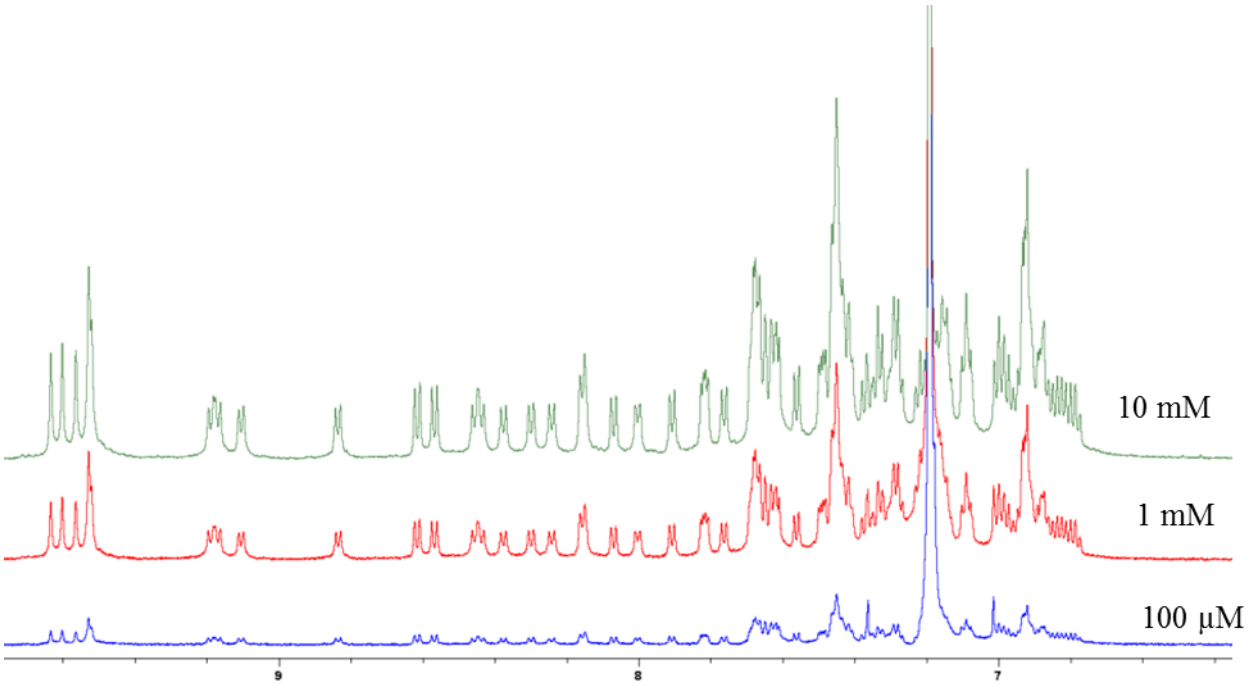

Figure 4.2 ^{1}H NMR spectra overly from aggregation assay for seven-stranded 80. Green = 10 mM, Red = 1 mM, Blue = 100 µM.

Additionally the compound showed high solubility in chloroform and the ^{1}H spectrum showed excellent dispersion in the region downfield of 8 ppm, further indicating a well-folded structure.

Although incomplete structural assignment precluded the ability to conduct any of the previous NMR assays, certain features could be picked out from the ^{1}H spectrum. The amide N-Hs within the Kemp turn are all present between 9.52 and 9.63 ppm as seen for the three and four stranded mimics. As noted in the chemical shift analysis (Section 3.9.4), increasing the number of strands does not result in a further upfield shift of these protons. The α-protons, identified by their COSY relationship to amide N-Hs, fall between 5.15 and 5.90 ppm. Previous analysis has shown that the possible cooperative effect would result in an

increasing downfield shift of the α-protons. The average chemical shift of the non-terminal α-protons for seven stranded **80** is 5.76 pm, as compared to 5.64 ppm and 5.74 ppm for three-stranded **56** and four-stranded **59** respectively. This further confirms the cooperative hypothesis, but shows, perhaps unsurprisingly, that there are diminishing returns from increasing the number of strands.

4.2.2.2 Circular Dichroism

In the original paper on the diphenylacetylene motif, Kemp explored conformation through the use of circular dichroism, showing that the turn displayed a minimum at 225 nm correlating well with β-sheet spectra for natural proteins.[1] The chiral perturbations of the diphenylacetylene chromophore occur at 255 and 320 nm. These therefore do not confound the data below 255 nm which is most indicative of secondary structure. Furthermore a greater ellipticity at 255 nm was also found to be indicative of a stabilized sheet. It was therefore decided to further explore the conformation of the seven-stranded **80** through circular dichroism.

Sheet mimics **56**, **59** and **80**, turn mimic **70**, and control molecule **53** were dissolved in trifluoroethanol and made up to a concentration of 100 μM. Trifluoroethanol was chosen due to its low absorbance in the far UV region (< 200 nm). Chlorinated solvents such as dichloromethane and chloroform are unsuitable for circular dichroism due to their absorbance in this region.[2] Trifluoroethanol is also known to favour the formation of secondary structures.[3] Spectra were recorded every 0.5 nm from 200 to 260 nm and repeated ten times on a ChiraScan^{TM} CD Spectrometer. The data was smoothed according to the Savitsky-Golay algorithm with a polynomial of three and a smoothing window of twenty.[4] The data is presented as both degrees rotation (Figure 4.3) and mean residue ellipticity (Figure 4.4).

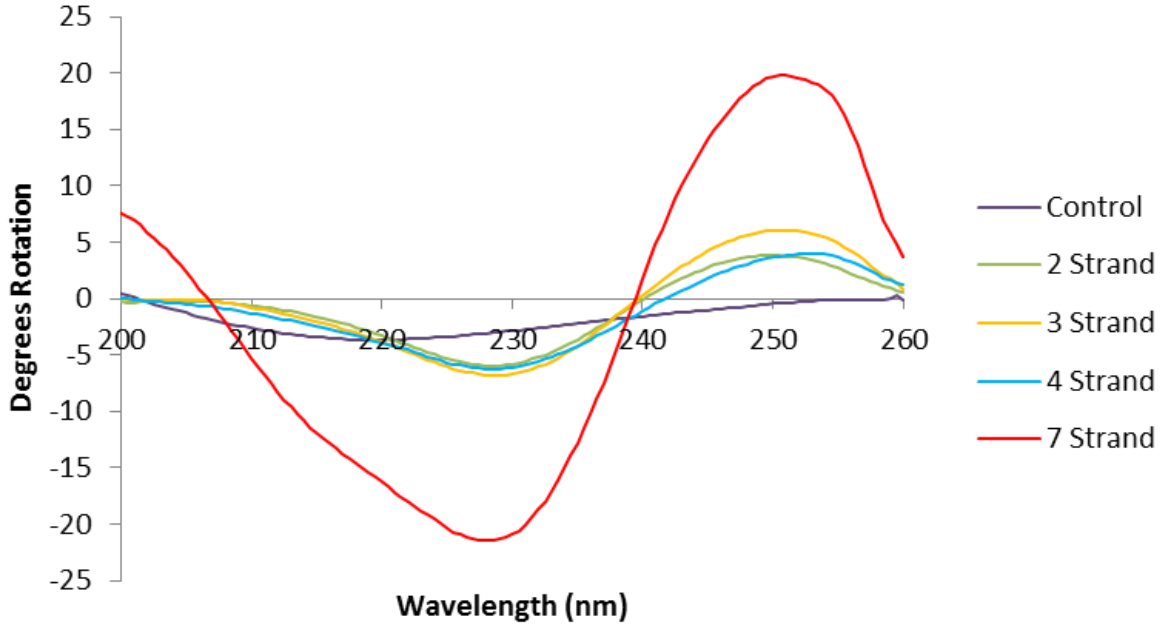

Figure 4.3 Circular Dichroism of meanders at 100 µM in TFE as measured by degrees rotation. All meander and turn mimics have a maximum at 255 nm and a minimum at 230 nm, indicative of a well-folded structure in solution. The control shows shape indicative of random coil.

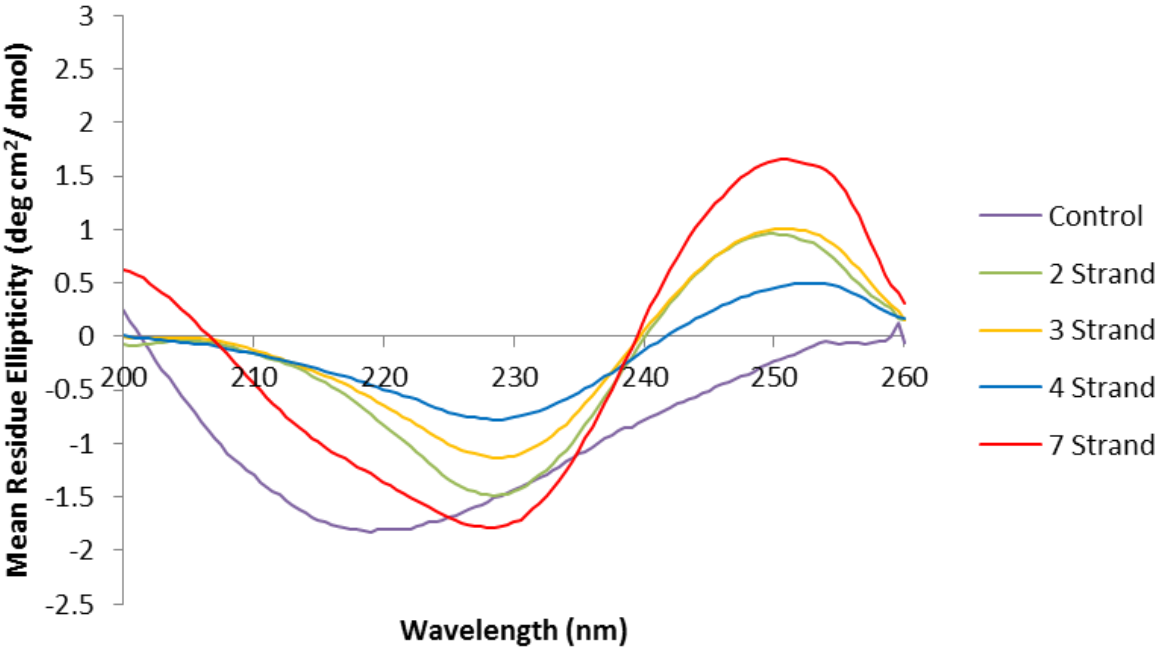

Figure 4.4 Circular Dichroism of meanders at 100 µM in TFE as measured by mean residue ellipticity. This weights the degrees rotation by the number of residues in each molecule.

In contrast to the control the four sheet mimics all show a clear shape, indicative of β-sheet structure and similar to those of the single Kemp turn. The control shows a shape indicative of random coil.

4.2.2.2.1 Melt Experiment

Circular dichroism also allows for the exploration of the effect of temperature on structure. Recall from Section 3.9.7 that the variable temperature NMR studies had provided little evidence for the proposed sheet structure. One possible reason for this was that the structure was unfolded at higher temperatures, and a CD melt experiment allows us to test this hypothesis. As before four-stranded meander **59** was dissolved in 100 µM trifluoroethanol and the CD spectrum recorded between 185 and 260 nm at 10 °C intervals from 25°C to 75°C (Figure 4.5).

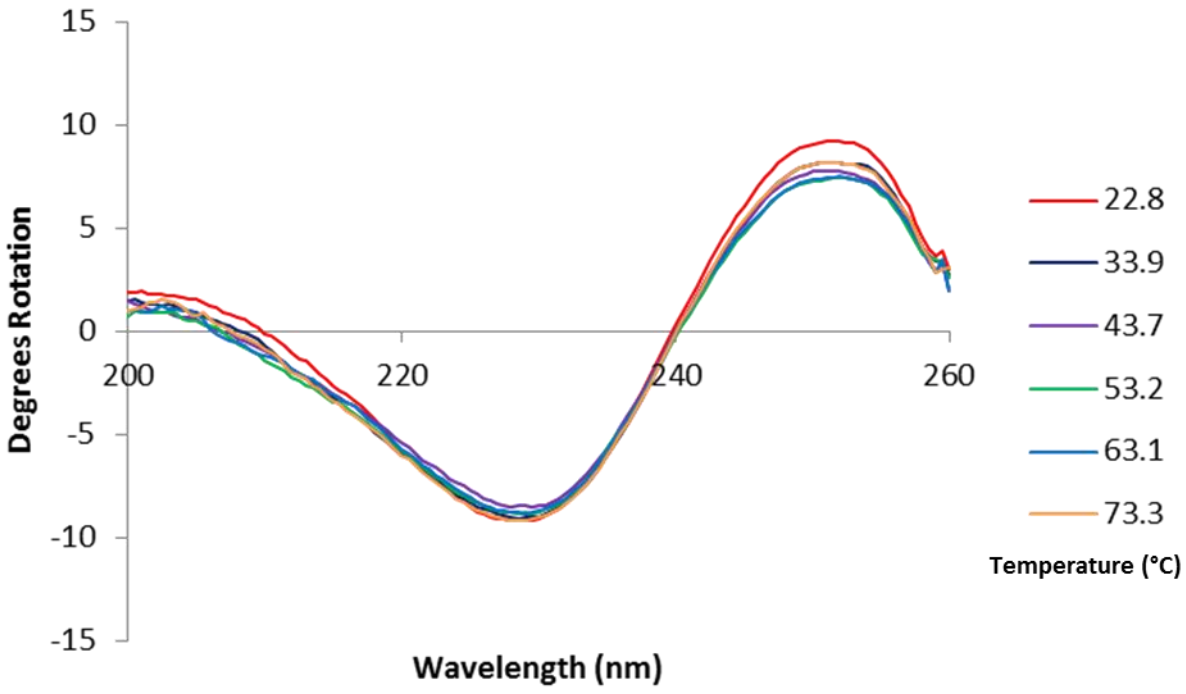

Figure 4.5 CD spectra at a concentration of 100 µM in TFE in degrees rotation of four-stranded mimic **59** at six different temperatures. The lack of change in shape is indicative of a well preserved structure as the temperature increases.

These results indicate that temperature does little to affect the structure of mimic **59**. There is some slightly increased disorder at the low wavelengths at the higher temperatures but the

defining maxima (255 nm) and minima (~ 230 nm) are retained with little change in peak height.

4.2.3 Conclusions

Despite the inability to obtain full structural characterisation on 7-stranded meander **80**, sufficient data has been collected to provide a weight of evidence for the molecule adopting the proposed structure and therefore presenting an extended surface. Rudimentary calculations based on extrapolation from the single crystal X-ray structure of three-stranded **56** suggest that this compound has a surface area across one face of 560 $Å^2$. Combined with a molecular weight of 3 kDa, the meander could represent the surface area of an entire small protein.

4.3 Horizontal Extension – Increasing the number of amino acids per strand

Natural β-sheets are rarely only two amino acids across, more commonly lying between five and seven. For effective mimicry of a target β-sheet it is therefore vital that the motif can accommodate an increased number of amino acids per strand and maintain a well-folded conformation. It should be noted however, that the current synthetic route always requires an even number of amino acids per strand.

4.3.1 Synthesis

To create a meander with four amino acids per strand it was decided to extend the modular building block **48** by one amino acid on each strand. This proceeded well, starting from tri-peptide species **69**, synthesised as a precursor to the two-strand mimic **70** studied in Chapter 3 (Scheme 4.2)

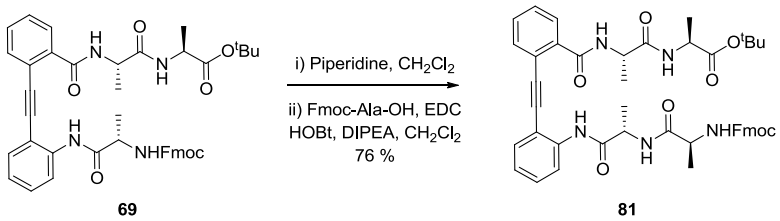

Scheme 4.2 Synthesis of monomer unit for creation of meander with four amino acids per strand.

From here the same strategy of orthogonal deprotection and coupling of the two species was attempted (Scheme 4.3).

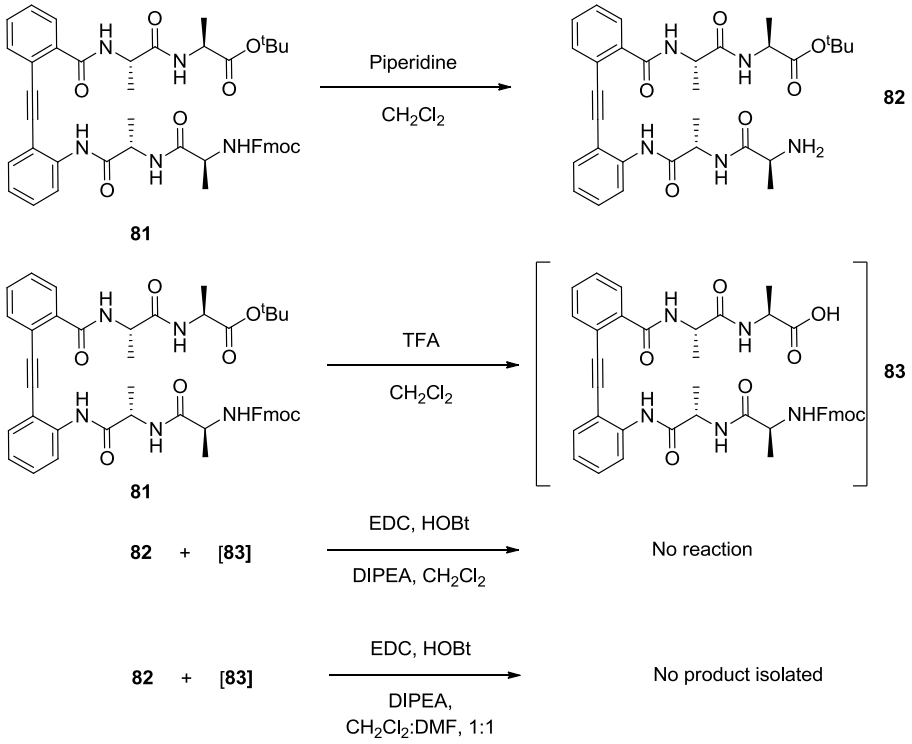

Scheme 4.3 Attempted synthesis of meander with four amino acids per strand.

Deprotection proceeded well with the free acid **83** identified by mass spectrometry and the free amine **82** successfully purified by column chromatography. However in the final coupling step an insoluble gel was formed and no product was identified by mass spectrometry or NMR of the crude mixture. In an attempt to improve solubility, the reaction was run in a 1:1 mixture of dichloromethane and DMF. No gelation occurred and the product could be identified in the crude reaction mixture by mass spectrometry. However following

work-up no product could be isolated. The same result was obtained on running the reaction in neat DMF. To assess whether these difficulties were due to a lack of solubility or reactivity two test reactions were performed (Scheme 4.4).

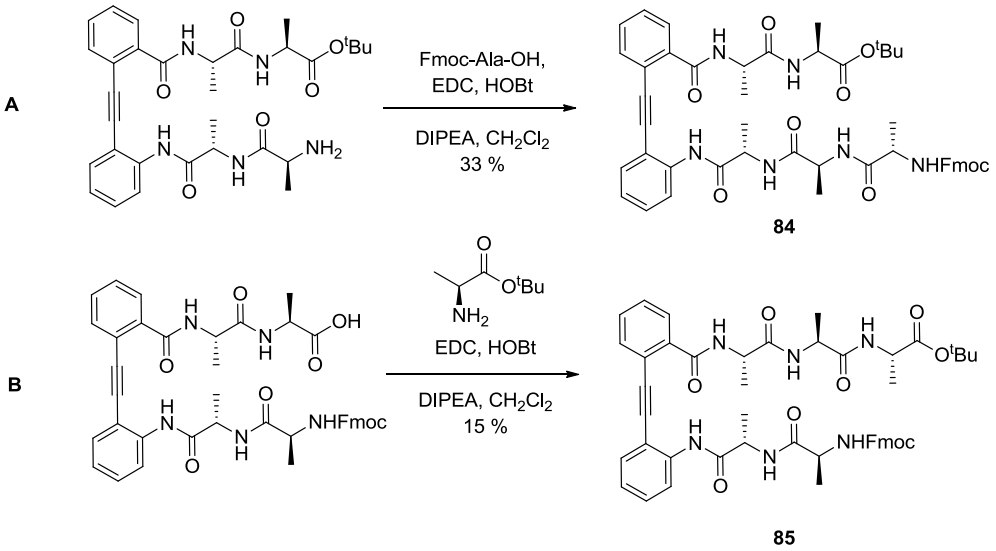

Scheme 4.4 Single amino-acid extensions to test both the reactivity of the free acid and amine and solubility of the resulting products.

These reactions both show that reactions are possible at the terminal amine and acid, albeit with low yields. It was also noted that the solubility of compounds **84** and **85** were far lower than the precursor **81**. The combination of these two factors led to the conclusion that solubility problems were preventing successful purification.

4.3.1.1 Use of Alternative Hydrophobic Side-chains

It was therefore decided to pursue the four-residue meander with alternative hydrophobic side-chains, with the aim of increasing solubility in chlorinated solvents. Initially phenylalanine and valine were chosen as the alternative residue. Phenylalanine was chosen for its hydrophobic bulk, whilst valine was chosen to increase the number of rotatable bonds. Again starting from the monomer unit **48**, both termini were extended to yield precursors **86** - **89** (Scheme 4.5).

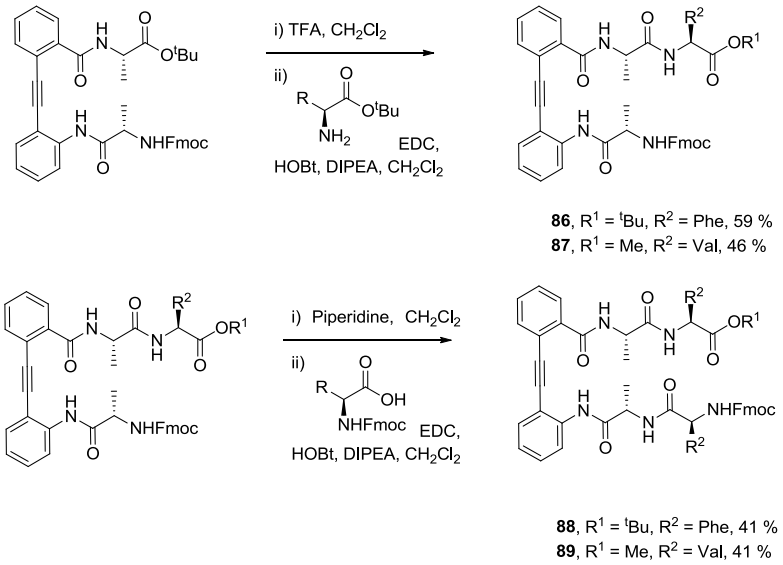

Scheme 4.5 Synthesis of monomer units with alternative side-chains to aid solubility.

Unfortunately the same problem was encountered upon attempting to couple these extended monomer units together, with insoluble and intractable gels resulting.

4.3.2 Conclusions and Future Work

If, as suspected, solubility remains the major barrier to the successful synthesis and purification of these elongated meanders then a number of alternative strategies could be explored in future work.

There are two possible factors contributing to insolubility; the hydrophobic nature of the compounds themselves and a tendency to aggregate. These two factors are most probably related as, for example introducing a charge increases hydrophilicity and prevents aggregation *via* electrostatic interactions.

Such a charge could be introduced through the incorporation of acidic or basic side-chains such as lysine or glutamic acid. Problems may still arise with solubility in the synthesis given the necessity of side-chain protecting groups. The synthesis of meanders incorporating lysine side-chains (although not towards an elongated strand) is fully explored in Section 4.5.

Alternatively the diphenylacetylene linker itself can be modified. The simplest modification is to substitute the phenyl groups with pyridines. As an illustration, substituting both phenyl groups within monomer unit **48** reduces clogP from 7.57 to 6.15. Additional groups, such as carboxylates, could be appended to the phenyl rings. However as substitution of the ring increases the synthesis does become less viable. Finally other group members have started to explore stripping back diphenylacetylene to just the acetylene bolt (Figure 4.6).[5]

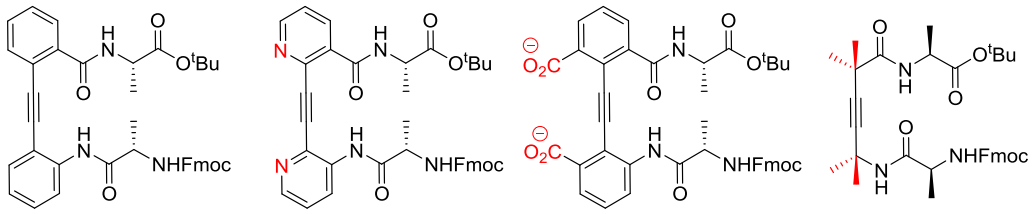

Figure 4.6 Strategies to improve the solubility of the diphenylacetylene linker.

The advantages are both improved solubility (clogP of the equivalent monomer unit 4.99) and, if used in a biological system, less bulk to negatively disrupt any interactions. Consider the overlay of three-stranded meander **56** with a natural protein in Figure 3.59; whilst displaying an excellent RMSD value for a five-vector match the diphenylacetylene linker does project out of the plane, potentially adversely affecting protein affinities due to steric clashing. However this system does require a non-trivial enantioselective synthesis.

If the insolubility is solely down to aggregation then there is extensive precedent in the use of *N*-methylation to prevent this from occurring (Figure 4.7). The work of Doig in this respect was highlighted in Section 3.4, Figure 3.19. The strategy has also been used by Kelly,[6,7] and most recently by Nowick.[8]

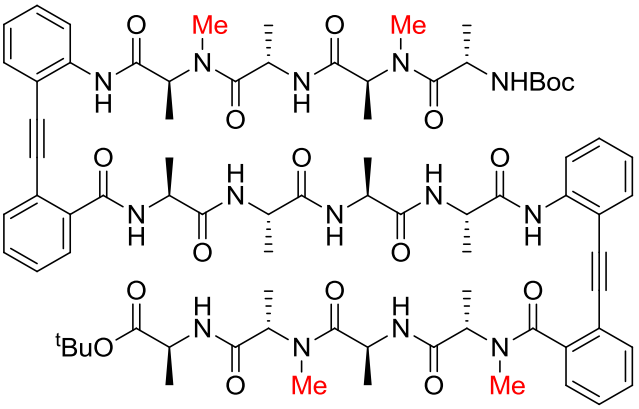

Figure 4.7 *N*-Methylation of the proposed four-residue per strand meander to prevent aggregation.

4.4 Incorporation of D-Amino Acids

Part of the beauty of peptidomimetic systems is the ability to incorporate unnatural residues – both in terms of chemical moiety and stereochemistry.[9] In this case it was decided to use the unnatural D-alanine and to incorporate it in such a way as to project all of the side-chains on the same face of the sheet mimic. The use of such unnatural stereochemistry would also allow for the study of how well the meander accommodates changes in bond angles along the peptide backbone.

As for the all L-amino acid system a molecular mechanics conformational search was used to assess the impact of this increased steric crowding on the conformation of the final molecule (Figure 4.8).

Instead of attempting to place all of the residues on the same face the molecule has been forced to adopt a sandwich-like structure. The network of six hydrogen bonds remains but instead of adopting the pleated structure of meander **56** the molecule now double backs on itself to accommodate the potential for steric clash. This structure is also interesting in its ability to present side-chains on a highly curved surface.

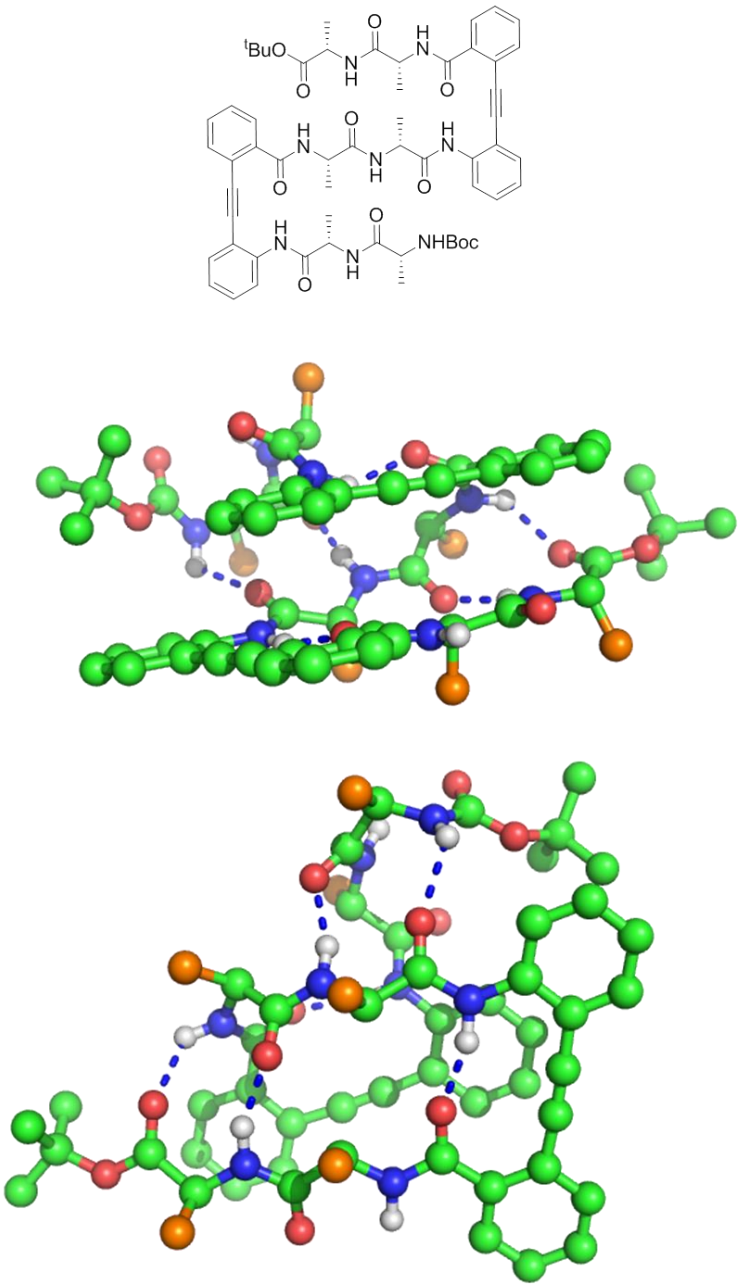

Figure 4.8 Proposed structure and two perspectives of the lowest energy structure from a conformational search for a three-stranded meander incorporating three D-amino acids. Hydrogen bonding network indicated and side-chains shown in orange.

4.4.1 Synthesis

The synthesis followed the same principles as described in Chapter 3. However the only commercially available starting material for the *C*-terminal protected D-alanine was the methyl ester, necessitating a change in protecting group strategy. The construction of fully protected monomer unit **92** proceeded well and it was found that the Fmoc group could be

cleaved by piperidine in dichloromethane whilst leaving the methyl ester untouched. This allowed for coupling to the free acid of the all L-amino acid monomer unit **49** to afford meander precursor **93** with all the side-chains on the same face (Scheme 4.6).

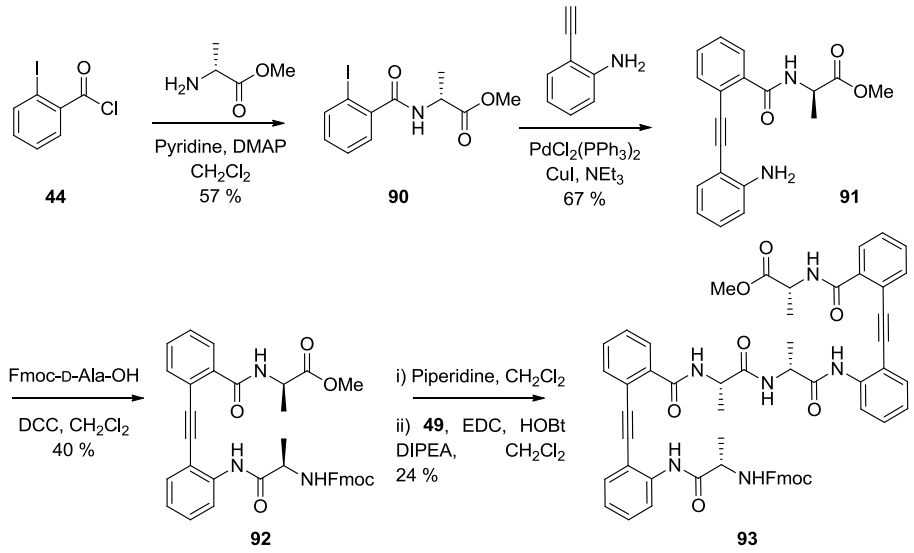

44 **90** **91** **92** **93**

Scheme 4.6 Synthesis of monomer unit **92** containing two D amino acids and subsequent coupling to free acid **49**.

Extension of this precursor according to Scheme 4.7 proceeded in adequate yield. For the final coupling the methyl ester was deprotected with 1 M lithium hydroxide in a 1:1 mixture of water and tetrahydrofuran. The resulting crude residue was reacted with L-alanine *tert*-butyl ester hydrochloride to reveal the final molecule **95** after flash column chromatography.

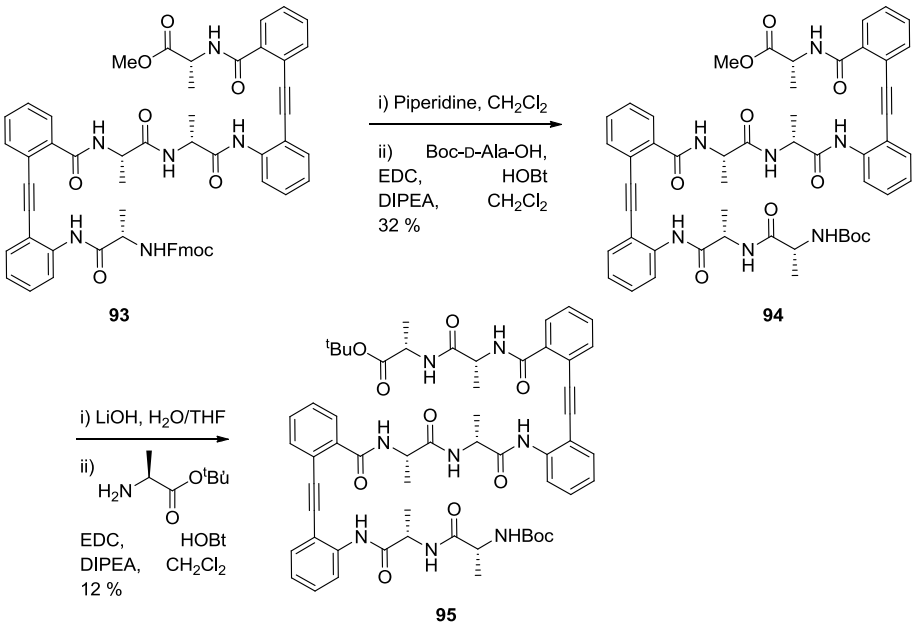

Scheme 4.7 Elongation of initial meander **93** to full three-stranded meander **95**.

As for the original meanders the double-stranded control compound **97** was also synthesised (Scheme 4.8).

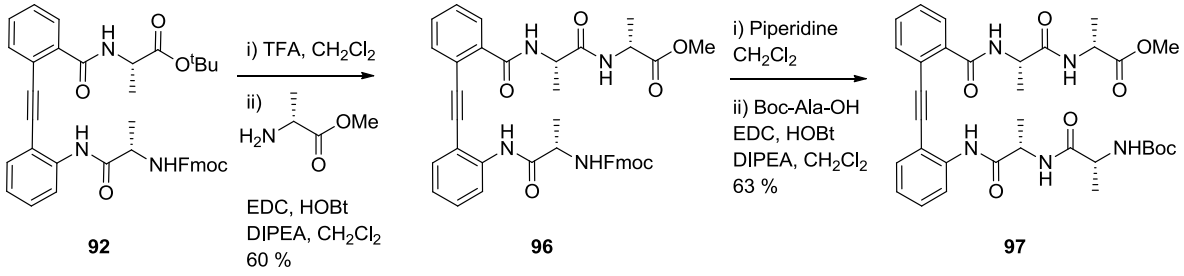

Scheme 4.8 Synthesis of control compound **97**. This represents a good control to isolate the factors in determining the conformation of meander **95**.

4.4.2 Conformational Analysis

The final three-stranded compound **95** displayed excellent solubility in chloroform with non-aggregating behaviour and was therefore amenable to the full suite of solution phase analysis. It was decided to calculate the secondary structure propensity scores, ***A*** values, and perform the hydrogen deuterium exchange experiments on the three-stranded species and the relevant controls. Attempts were made to grow crystals *via* vapour diffusion with a variety of solvents but these were unsuccessful.

4.4.2.1 Secondary Structure Propensity Scores

As for the meanders bearing conventional side-chain geometry the secondary structure propensity scores were computed using the program developed by Forman-Kay *et al.* (Figure 4.9).[10]

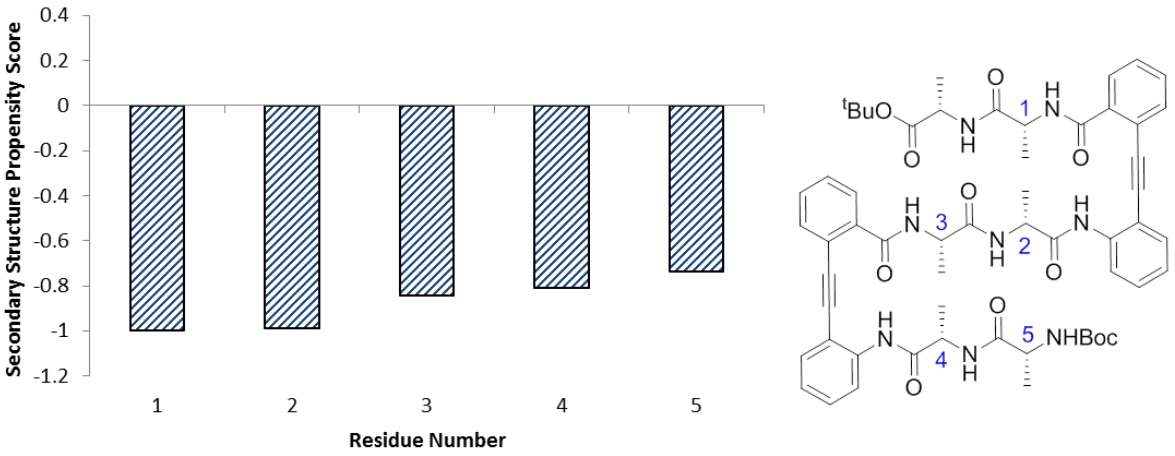

Figure 4.9 Secondary structure propensity scores in chloroform for three-stranded meander **95**.

These show all the residues populating the extended confirmation, strongly indicative of the proposed sheet structure being adopted. The overall β-sheet score is 89.6 %, slightly less than the corresponding three-stranded meander at 94.0 %. Given the potential for steric hindrance to somewhat disrupt the molecule from sitting in a flat, fully extended confirmation (as observed in the computational results) this is in line with expectations.

4.4.2.2 Hydrogen Bond Acidity- A Value

The determination of the ***A*** value for each amide N-H with the unnatural meander was determined as in Section 3.9.9 (Figure 4.10).

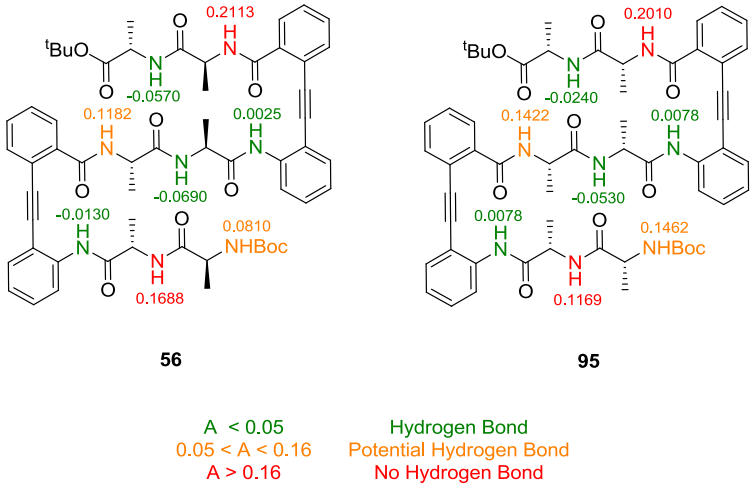

Figure 4.10 *A* values for the amide N-Hs within all L-amino acids three-stranded meander **56** and **95** containing both L and D amino acids.

Comparison of the two three-stranded molecules reveals the same pattern, namely the conservation of the desired hydrogen bonding network. Closer inspection of the terminal residues (coloured in orange) shows higher values much closer to the no hydrogen bonding threshold of 0.15. This is indicative of increased fraying of the termini in this system and is in line with the other analyses with a weaker bias towards the desired, planar confirmation.

4.4.2.3 Hydrogen Deuterium Exchange

As previously (Section 3.9.6), three-stranded mixed stereochemistry meander **95** was dissolved in chloroform at a concentration of 10 mM and subsequently 20 µL of methanol added and the spectra recorded over the following hundred minutes (Figure 4.11).

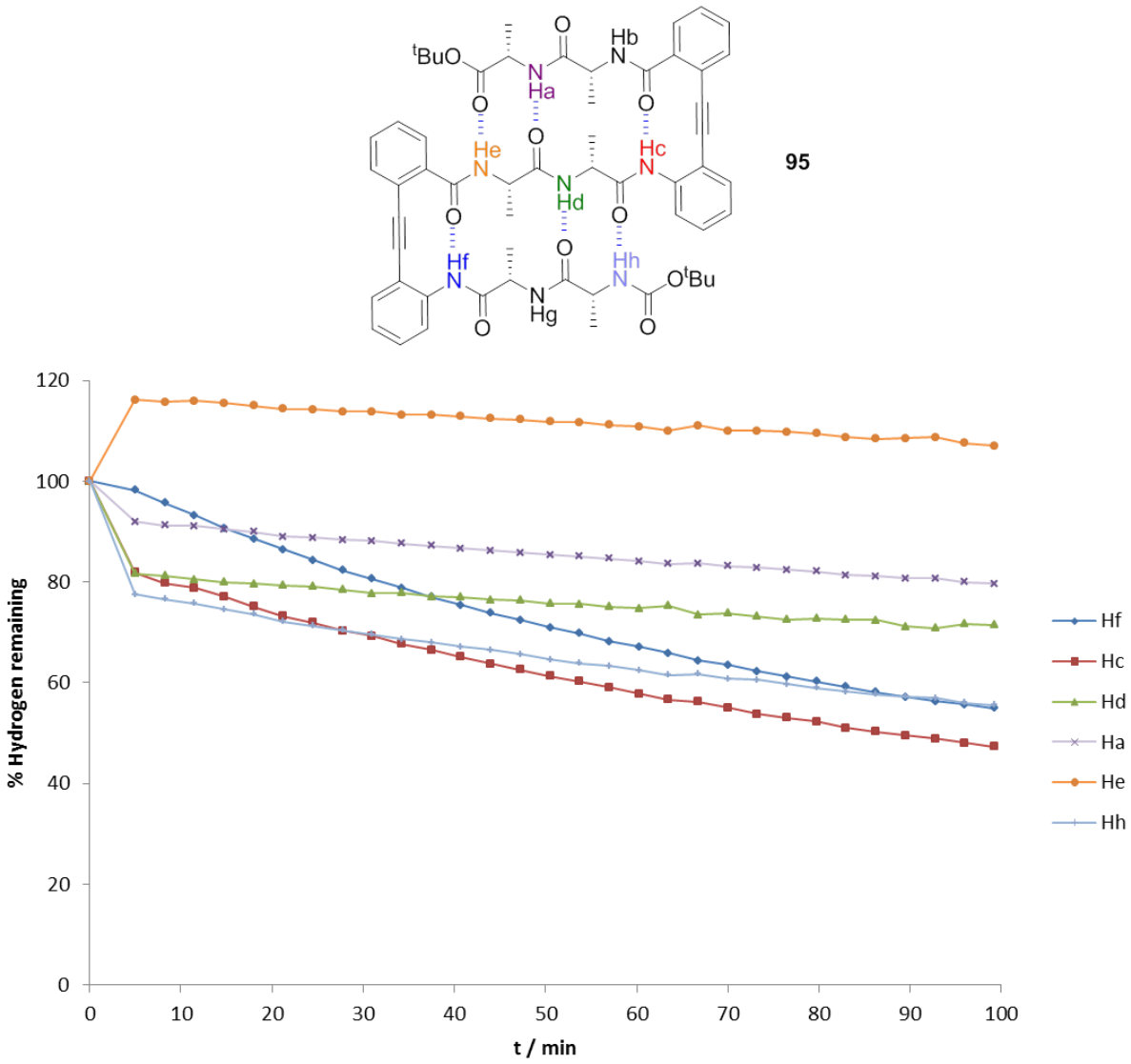

Figure 4.11 Hydrogen/deuterium exchange for three-stranded L/D hybrid meander **95**. Amide N-Hs that underwent complete exchange prior to the first ^{1}H spectrum acquisition at t = 5 min are omitted for clarity (***Hb*** and ***Hg***). The experiment was performed in triplicate with the average values shown.

The trends from this experiment differ sharply from those revealed by the meanders formed of only L-amino acids. There the amide N-Hs within the Kemp turn motif (***Hc*** and ***Hf***) showed the slowest rate of exchange, with intermediate rates of exchange for the majority of the other amide N-Hs and complete exchange within five minutes for the carbamate N-H, ***Hh*** (Table 4.1).

Amide	Meander 56 Rate[a]	Meander 97 Rate[a]
a	1.07	0.16
c	0.16	0.51
d	0.85	0.13
e	1.14	0.10
f	0.11	0.71
h	-[b]	0.32

[a] Rate is the initial rate as for the first twenty minutes of each experiment and is in arbitrary units. [b] Peak decays to 0 within first five minutes of experiment so no rate could be determined.

Table 4.1 Comparison of initial rates of *H*/*D* exchange in the all L-amino acid and mixed D/L meanders

Here however, the slowest rate of exchange is for ***He***, usually one of the weaker bonds owing to the flexibility of the *C*-terminus. The fastest rates of exchange are for the amide N-Hs of the Kemp turns, with around 50 % exchange occurring within the timeframe of the experiment. Finally, the carbamate N-H shows similar exchange to these Kemp turn N-Hs, instead of rapid and complete exchange. To see if this pattern was consistent with an unnatural, two-stranded turn, the experiment was repeated on compound **97** (Figure 4.12).

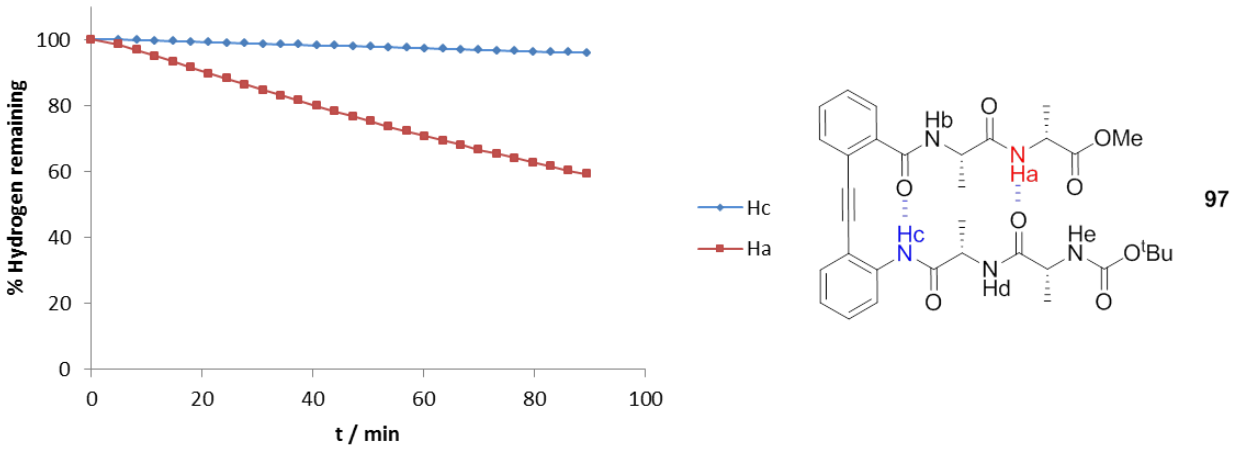

Figure 4.12 Hydrogen/deuterium exchange for two-stranded unnatural turn mimic **97**. Amide N-Hs that underwent complete exchange prior to the first ^{1}H spectrum acquisition at t = 5 min are omitted for clarity. The experiment was performed in triplicate with the average values shown.

This experiment reveals the same trends for the turn with conventional stereochemistry, namely extremely slow exchange for ***Hc***, and intermediate exchange for ***Ha***, and complete exchange in five minutes for the external and carbamate N-Hs.

Combined these two experiments indicate that a hydrogen bond network is present in chloroform, but that in the larger, three-stranded system, it substantially differs from that of conventional stereochemistry meander **59**. These results could point towards the adoption of the sandwich structure seen in the conformational computational studies but given that the proposed hydrogen bonding network is the same for both structures it is difficult to draw any definitive conclusions.

4.4.2.4 Conclusions

These data provide evidence of the ability of this scaffold to accommodate amino acid residues of unnatural stereochemistry and maintain conformational bias. This means that the system allows a chemist to exert complete control over side-chain display and the decoration of each surface. This therefore is an example of the meander system fulfilling the second of Gellman's challenges, the incorporation of unnatural functional groups.

4.5 Incorporation of Hydrophilic Residues

With the principle demonstrated for any size of mimic and stereochemistry of residue, it was now necessary to show the ability to incorporate hydrophilic residues and test the conformation in aqueous solution. Lysine was chosen as the test residue. The inclusion of a reactive side-chain meant that further consideration needed to be given to protecting group strategy. Ideally, the *N*- and *C*-termini, and reactive side-chains should all possess protecting groups labile to orthogonal conditions. Typically this would be acid, base, reductive, and fluoride mediated; however with the diphenylacetylene linker the use of reducing conditions to cleave protecting groups such as benzyl esters would likely also reduce the acetylene. Therefore initially the SEM group, resistant to base and acid but easily removed with fluoride, was chosen as a carboxyl protecting group.

4.5.1 Synthesis

4.5.1.1 SEM Ester

The commercially available Fmoc-Lys(Boc)-OH was *C*-terminally protected with SEM-Cl in quantitative yield.[11] Deprotection of the Fmoc group of **99** proceeded smoothly, although the coupling of the free amine with 2-iodobenzoyl chloride had to be performed immediately to avoid degradation of the amine. This degradation may explain the low yield for this coupling step (Scheme 4.9).

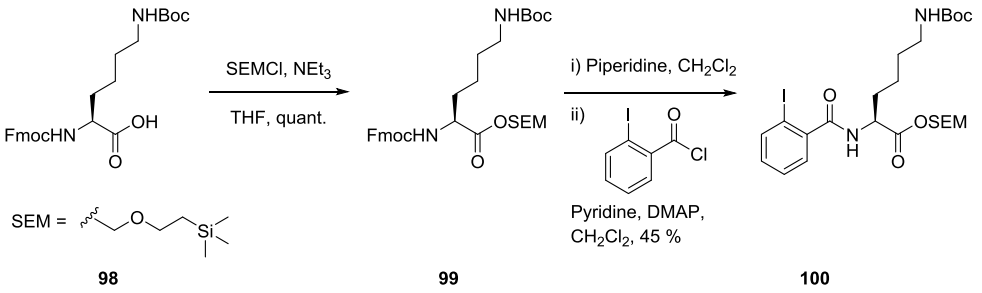

Scheme 4.9 Initial steps towards incorporation of the SEM ester.

The subsequent Sonogashira and DCC-mediated amide coupling proceeded in good yield to afford monomer unit **102** (Scheme 4.10).

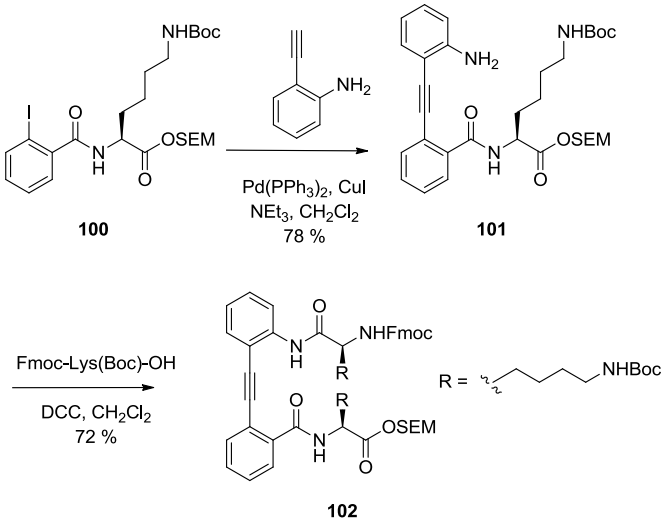

Scheme 4.10 Synthesis of monomer **102** incorporating the SEM ester.

Pleasingly, after Fmoc deprotection of **102** to reveal the free amine, coupling with the free acid of the alanine monomer unit **49**, proceeded well to afford initial meander **103** (Scheme 4.11).

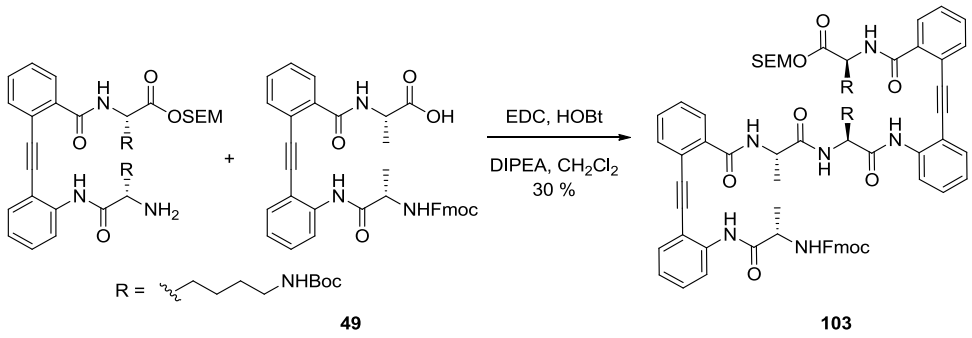

Scheme 4.11 Formation of initial meander **103** incorporating SEM ester and protected lysine side-chains.

The Fmoc group could be successfully deprotected in the presence of the SEM ester allowing for chain elongation to meander precursor **104** (Scheme 4.12).

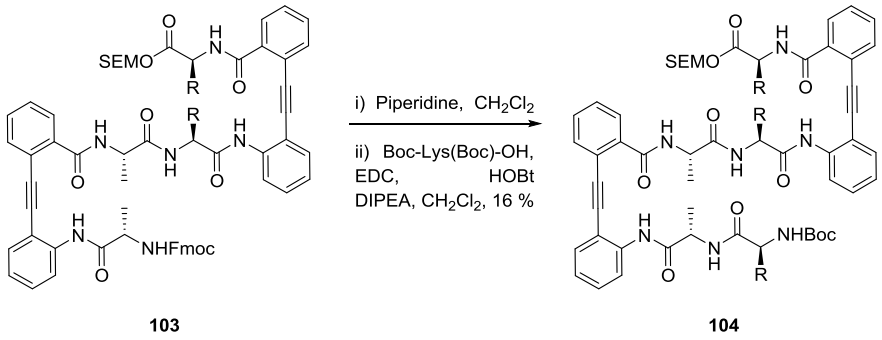

Scheme 4.12 Single amino acid elongation after Fmoc deprotection to meander precursor **102**.

Attempts were then made to deprotect the SEM group. Literature indicated that this should be completed in good yield in the presence of a fluoride ion.[12] However subjecting meander **104** to 1M TBAF in tetrahydrofuran yielded an intractable mixture with no product identifiable by mass spectrometry, and when the crude mixture was subjected to coupling conditions with alanine *tert*-butyl ester hydrochloride as the nucleophile no desired product was isolated (Scheme 4.13).

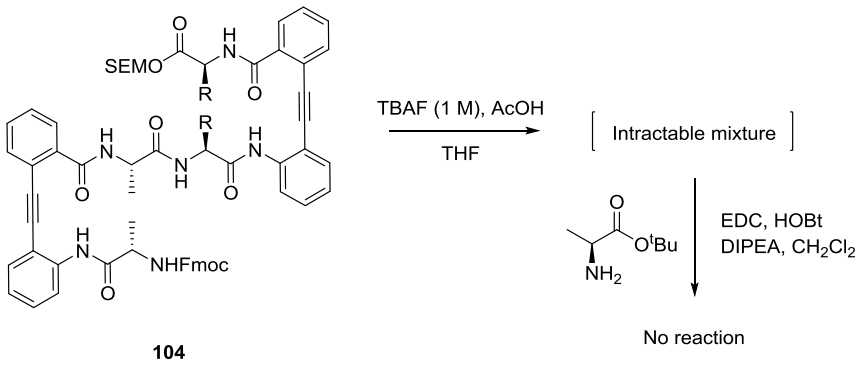

Scheme 4.13 Unsuccessful attempts at deprotection of SEM ester.

Efforts to understand this were also unsuccessful as the attempted deprotection of the simple precursor **100** also yielded an intractable mixture (Scheme 4.14).

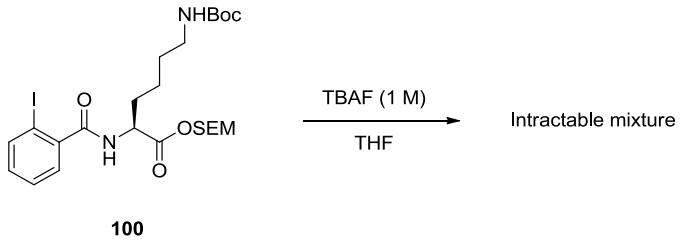

Scheme 4.14 Test reaction for SEM ester deprotectionl.

Given that such conditions have been successfully used to deprotect the alkyne in the synthesis of control molecule **68** it would appear that either the SEM group, or the combination of the SEM and lysine side-chain are responsible for the intractable mixture.

4.5.1.2 Methyl Ester

With the failure of SEM as a carboxyl protecting group it was decided to utilise the methyl ester protecting group used in the unnatural meander synthesis (Section 4.4.1). Again starting from Fmoc-Lys(Boc)-OH, various conditions were explored to successfully form the methyl ester **105** (Table 4.2).

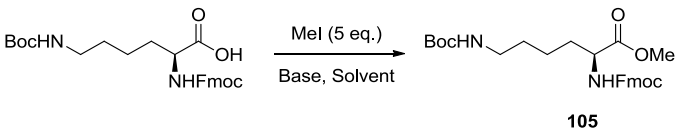

105

Entry	Solvent	Base	Scale (mmol)	Temperature (°C)	Time (h)	Yield (%)
1	THF	DIPEA	0.1	20	2	0
2	CH_2Cl_2	DIPEA	0.1	20	2	43
3	CH_2Cl_2	Pyridine	0.1	20	2	0
4	CH_2Cl_2	DIPEA	0.1	40	16	67
5	CH_2Cl_2	DIPEA	0.5	40	16	95

Table 4.2 Optimisation of methyl ester synthesis.

It was found that this could be achieved with five equivalents of methyl iodide in dichloromethane using DIPEA as a stoichiometric base. Pleasingly the yield was observed to increase on scale up. From this point the synthesis successfully proceeded to monomer unit **108** (Scheme 4.15).

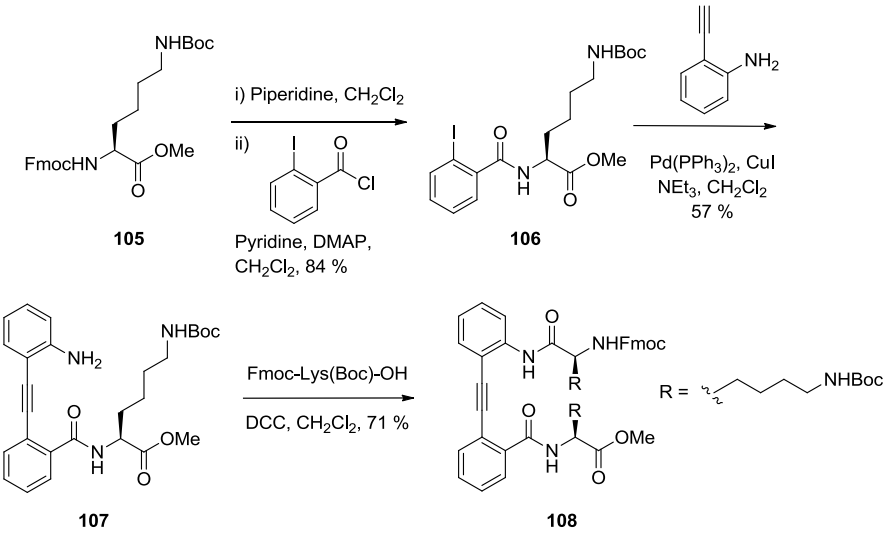

Scheme 4.15 Synthesis of monomer unit **108** incorporating the methyl ester.

Fmoc deprotection of amine **108** proceeded well, and coupling to alanine monomer unit **49** was achieved in moderate yield (Scheme 4.16).

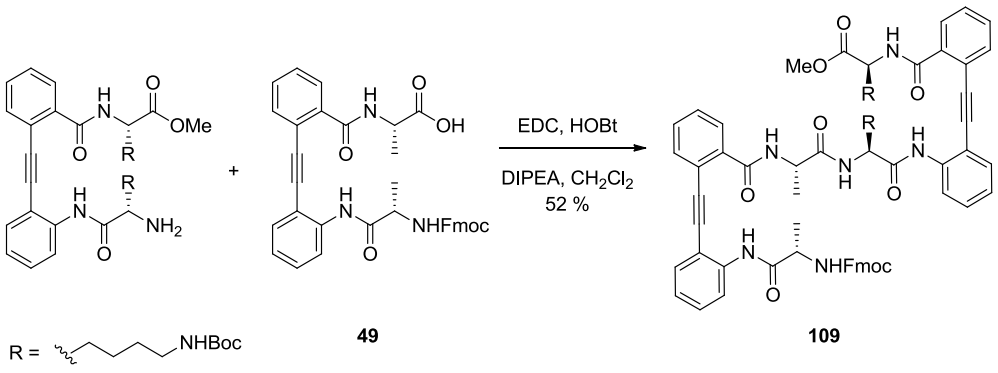

Scheme 4.16 Synthesis of initial meander **107** incorporating lysine side-chains and methyl ester as *C*-terminal protection.

Attempts to perform the first extension, shown as the first step in Scheme 4.17, saw the product identified by mass spectrometry but it could not be isolated in sufficient purity for characterisation. This result is consistent with unpublished work of other group members that methyl esters are less susceptible to successful purification than the equivalent *tert*-butyl ester.[13] However, with reasonable confidence that an appreciable amount of the desired species was present the final deprotection was attempted.

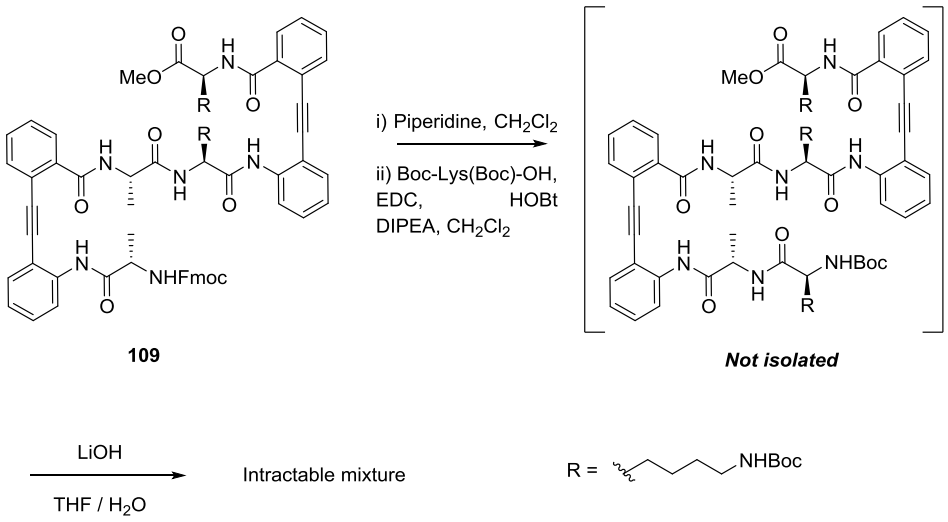

Scheme 4.17 Single amino acid extension to meander precursor and unsuccessful ester hydrolysis.

Frustratingly, this again resulted in an intractable mixture that could not be reacted further and no evidence of the free acid in mass spectrometry or by staining with a TLC plate with bromocresol green. Again to test the reason for this a simpler substrate, **106**, was subjected to the deprotection conditions. Here the reaction proceeded well, with clean conversion by TLC and the product clearly identifiable by mass spectrometry (Scheme 4.18).

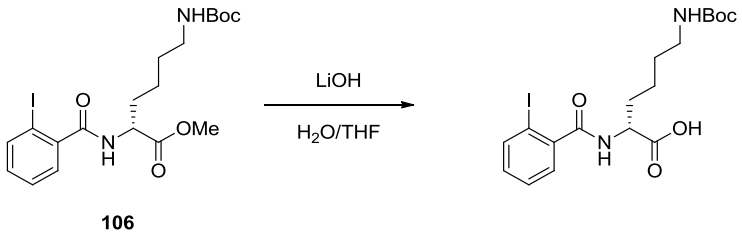

Scheme 4.18 Test reaction for ester hydrolysis.

The success of this deprotection however provided little evidence for why failure occurred at a later stage.

4.5.1.3 Azides

This struggle in effecting a base or fluoride mediated late stage deprotection prompted a change in strategy. The possibility of protecting the side-chain amine was investigated with the literature revealing that free primary amines could be successfully masked as azides.[14]

The azide should successfully be carried through the synthesis and the amine revealed in the last step through the Staudinger reaction. This new strategy has the added advantage of allowing deprotection of the side-chains and main chain termini in separate steps, meaning that conformational analysis of the effect of hydrophilic side-chains can be explored without the complication of additional main chain acid and amine groups.

To test whether the Staudinger conditions resulted in decomposition of the meander motif or the Fmoc and *tert*-butyl protecting groups currently in use, the alanine monomer unit **48** was subjected to the reaction conditions for sixteen hours (Scheme 4.19).[15] Pleasingly, no reaction was observed by TLC and after work up and purification by flash column chromatography the starting material was recovered in quantitative yield.

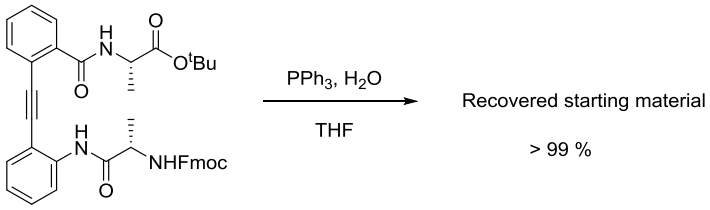

48

Scheme 4.19 Test of conditions for the Staudinger reaction on monomer unit **48**.

In order to convert the amine into the azide, the necessary reagent was synthesised from sulfuryl chloride, sodium azide and imidazole according to a literature procedure (Scheme 4.20).[16]

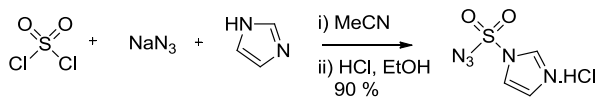

110

Scheme 4.20 Synthesis of azidation reagent **110**.

Fortunately, despite having a nitrogen:carbon ratio of 5:2 this reagent is a stable crystalline solid, and unaffected by heating or impact. This reagent, with stoichiometric base and

catalytic copper sulphate is able to convert Boc-Lys-OH into its corresponding azide in good yield (Scheme 4.21). This reaction proved highly scalable. Due to the presence of K_2CO_3 it was feared that this reaction would not be tolerant of the Fmoc group, hence the use of Boc-Lys-OH as the starting material.

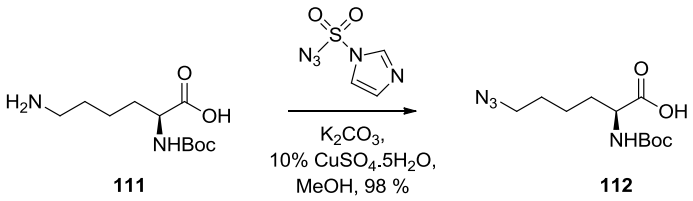

Scheme 4.21 Azidation of Boc-Lys-OH

It was intended that the synthetic route towards the monomer unit remain the same. Therefore attempts were made to protect the acid as a *tert*-butyl ester (Table 4.3).

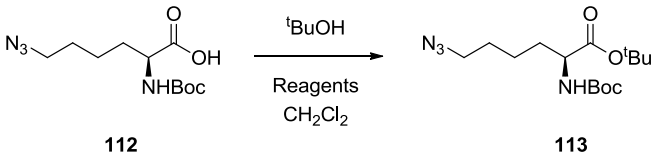

Entry	Reagents	Yield (%)
1	$POCl_3$, DIPEA	-
2	DCC, DMAP, DIPEA	41
3	EDC, HOBt, DIPEA	-
4	HBTU, DMAP, DIPEA	-

Table 4.3 Conditions for formation of *tert*-butyl ester

Disappointingly the previous $POCl_3$ method was unsuccessful with only starting material recovered and DCC/DMAP gave only low yields. However these yields were maintained on scale up.

Pleasingly it was possible to selectively deprotect the carbamate in the presence of the ester by using a lower concentration of TFA in dichloromethane (5:1) and shorter reaction times (5 min). However attempts to couple this amine with 2-iodobenzoyl chloride were unsuccessful. Adopting a methodology that did not require acid protection was also unsuccessful (Scheme 4.22).

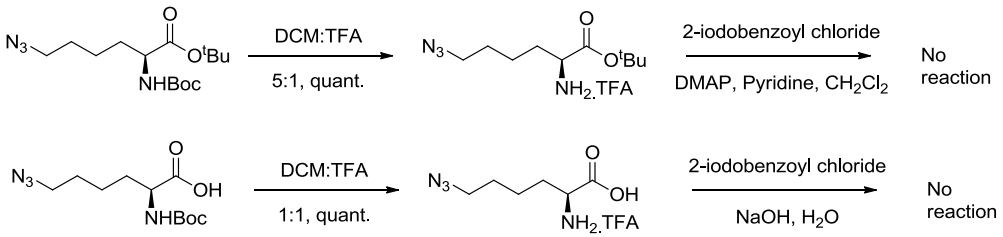

Scheme 4.22 Unsuccessful attempts at Boc deprotection and subsequent coupling with 2-iodobenzoyl chloride.

With this lack of success, it was decided to change step order and perform a late stage diazotransfer reaction. Protection of Fmoc-Lys(Boc)-OH as the *tert*-butyl ester, and subsequent removal of the *N*-terminus Fmoc protecting group proceeded smoothly. Pleasingly, amide bond formation with 2-iodobenzoyl chloride was now successful and the selective removal of the Boc carbamate in the presence of the *tert*-butyl ester allowed for diazotransfer (Scheme 4.23).

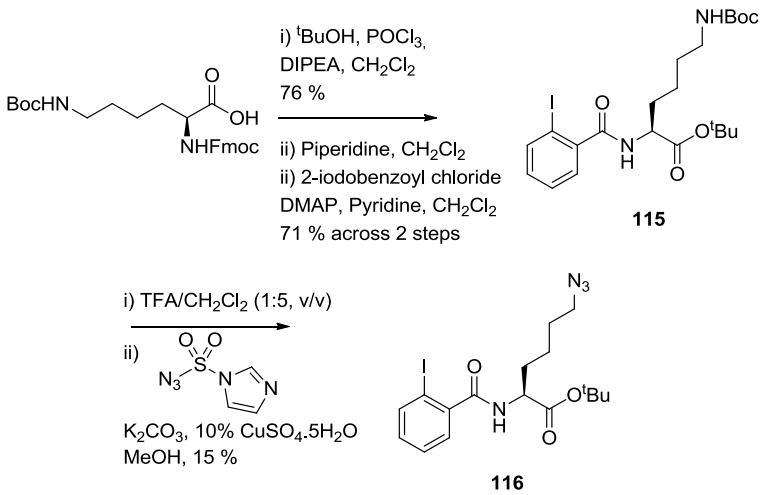

Scheme 4.23 Alternative route to reach iodide **113** with a late stage azidation.

The yield for the formation of the azide was disappointing and attempts to improve it with purification of the deprotected amine by column chromatography was unsuccessful. The completion of the azide monomer unit **112** proceeded with moderate yields (Scheme 4.24).

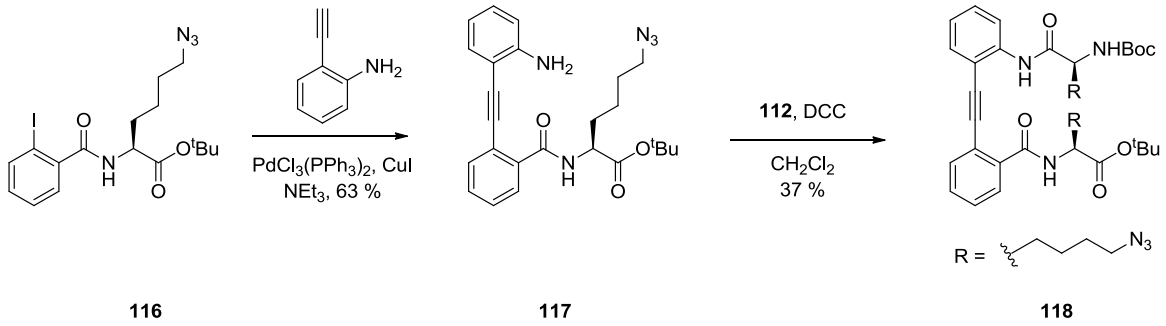

Scheme 4.24 Synthesis of monomer unit 115 incorporating azide side-chains.

Reduced concentration TFA deprotection allowed for selective removal of the Boc group and coupling with the free acid of the alanine monomer unit **49**, was successful, albeit in low yield (Scheme 4.25).

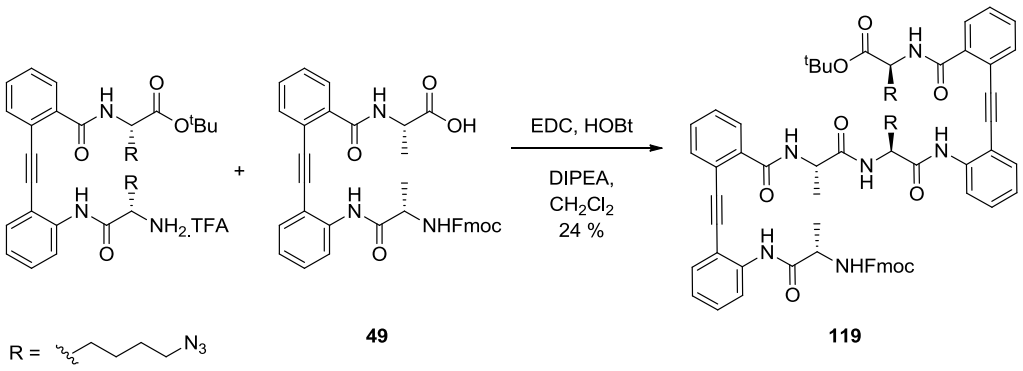

Scheme 4.25 Formation of initial meander 116.

This low yield would appear to correlate with the observed lack of reactivity with the azide side-chain throughout the synthesis and so is not unexpected. Unfortunately attempted extension of this initial meander *via* *tert*-butyl deprotection and alanine *tert*-butyl ester hydrochloride was unsuccessful and the azide incorporation strategy had to be abandoned.

4.5.1.4 Alternative Disconnection Strategy

Due to these frustrations it was decided to avoid the protecting group difficulties by changing the order of the steps. Although this would no longer be a general method that could be used in the construction of larger meanders it would allow for the synthesis of a hydrophilic three-stranded meander and conformational analysis in an aqueous environment.

In order to avoid the problematic final ester hydrolysis and coupling this step was performed first, and the resulting two amino acid species elaborated into the relevant monomer unit (Scheme 4.26).

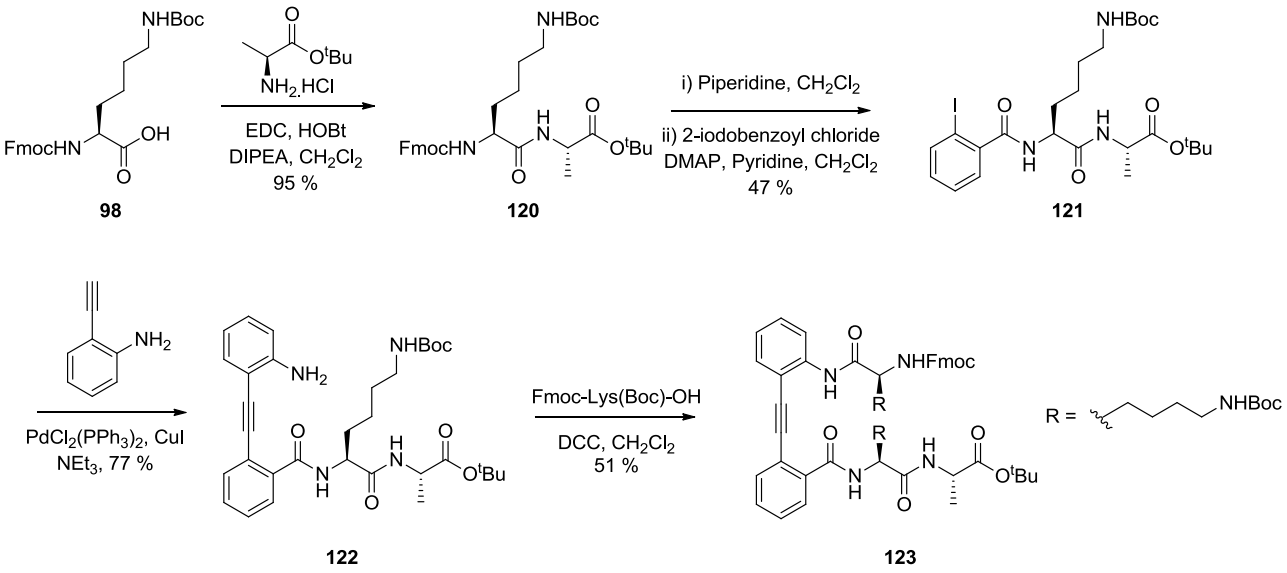

Scheme 4.26 Synthesis of dipeptide 120 and subsequent elaboration into monomer unit **123**.

Fmoc-deprotection of **123** and EDC/HOBt mediated coupling with the free acid **49** proceeded in moderate yield (Scheme 4.27). The single elongation with Fmoc-Lys(Boc)-OH revealed the Boc-protected meander **125**.

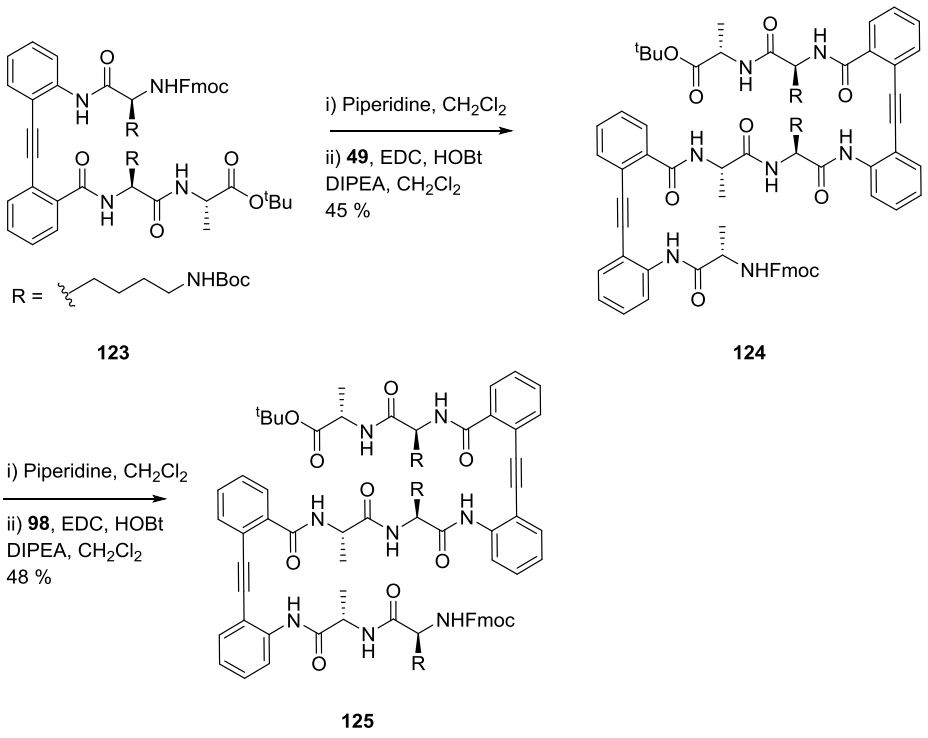

Scheme 4.27 Synthesis of protected meander **125**.

Finally the reduced concentration TFA protocol successfully deprotected the Boc groups whilst leaving the *tert*-butyl ester intact (Scheme 4.28).

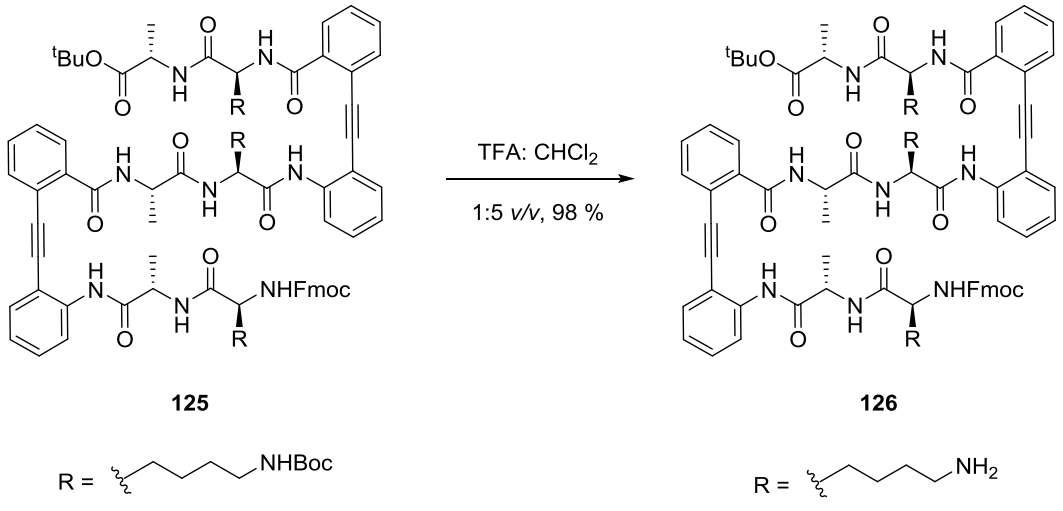

Scheme 4.28 Boc-deprotection to reveal final hydrophilic meander **126**.

4.5.2 Conformational Analysis

4.5.2.1 NMR

An initial NMR of hydrophilic meander **126** was taken in DMSO-d_6. Pleasingly the compound displayed excellent spectral dispersion, indicative of a well-folded structure. Although the meander showed excellent solubility in water the NMR spectra obtained in 9:1 H_2O/D_2O were of insufficient resolution to be interpreted.

4.5.2.1.1 ROESY

A ROESY spectrum of meander **126** was obtained in DMSO-d_6 (Figure 4.13).

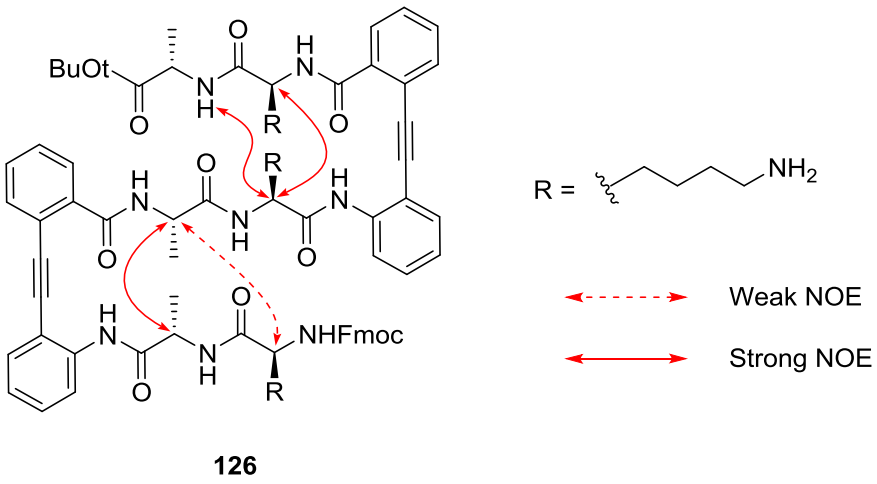

Figure 4.13 Cross-strand NOE interactions from DMSO-d_6 ROESY spectrum of meander **126**.

There are three strong cross-strand interactions that point towards the desired conformation. However the weak NOE, indicated by the dashed line, could be indicative of a poorly folded structure. By measuring the crystal structure of three-stranded **56** the equivalent distance from α*H* to α*H* is 6.5 Å, most likely beyond the NOE detection limit. Therefore for this interaction to be observed there must be an alternative conformation that is populated to an appreciable extent.

4.5.2.1.2 Secondary Structure Propensity Score

As for the systems in Chapter 3 (Section 3.9.5) and the mixed L/D stereochemistry meander above (Section 4.4.2.1), the secondary structure propensity score was calculated for hydrophilic meander **126** in DMSO-d_6 (Figure 4.14).

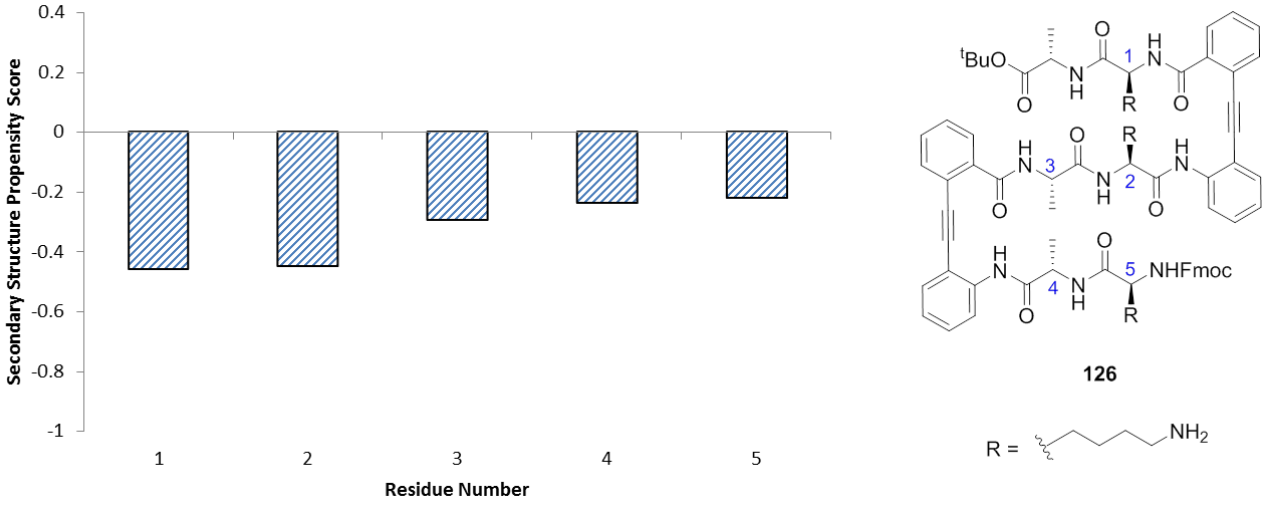

Figure 4.14 Secondary structure propensity scores for hydrophilic meander **126** in DMSO-d_6. These show that β-sheet structure is present but not to the same extent as the comparable all alanine meander **56**.

All the residues showed evidence of sitting in the β-sheet conformation although the values are lower than those of the comparable three-stranded meander **56** in DMSO-d_6 (Figure 3.47). By way of direct comparison for the whole molecule the β-sheet score is 34.2 % compared to 48.8 % for **56**. Therefore these results point towards the desired conformation being present but not to the same extent as for the all alanine equivalents. This ties in well with the NOE data suggesting the population of some conformations away from the fully folded meander.

4.5.2.2 Circular Dichroism

As for the hydrophobic versions, the CD spectrum of meander **126** in trifluoroethanol was obtained. Additionally the spectra in water could also be recorded to see if folding was still observed in a solvent that did not promote such folding. The two spectra are compared in Figure 4.15.

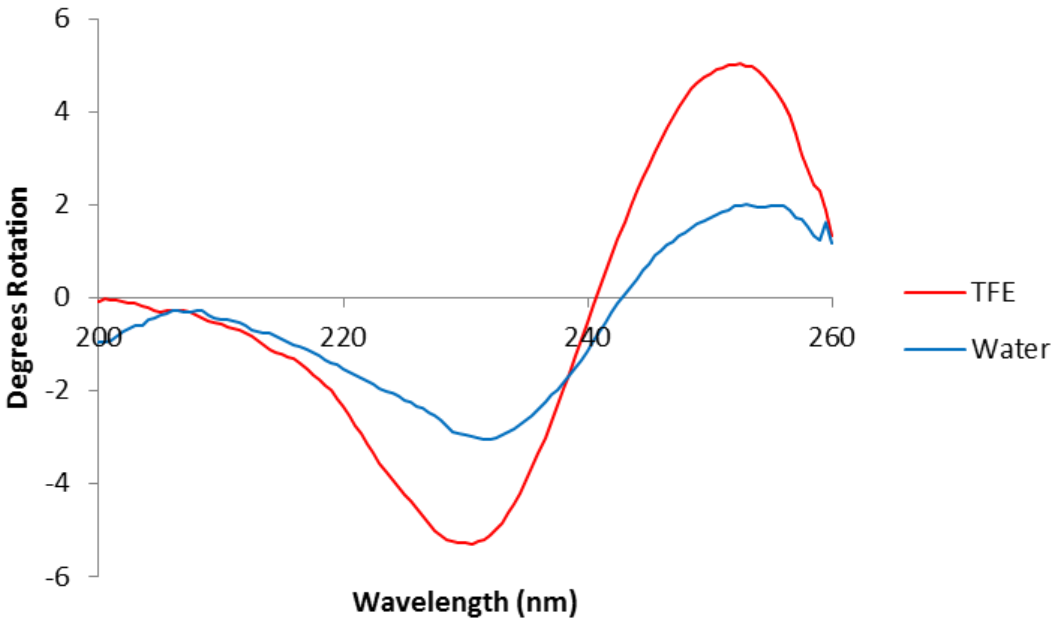

Figure 4.15 CD spectra of hydrophilic meander **126** in TFE and water showing a maximum and minimum indicative of β-sheet structure.

Pleasingly the characteristic maximum and minimum are preserved in both solvents indicating a well folded, sheet like structure. These features are of lower amplitude in water, but this is to be expected as TFE is known to promote folding when compared to water.

Furthermore a melt experiment was performed in water from 25 to 85 °C (Figure 4.16). This showed no dramatic change in structure as a result of an increase in temperature, although there was a general trend of the minimum decreasing in amplitude as the temperature increased. This is indicative of less defined folding as would be expected on increasing temperature.

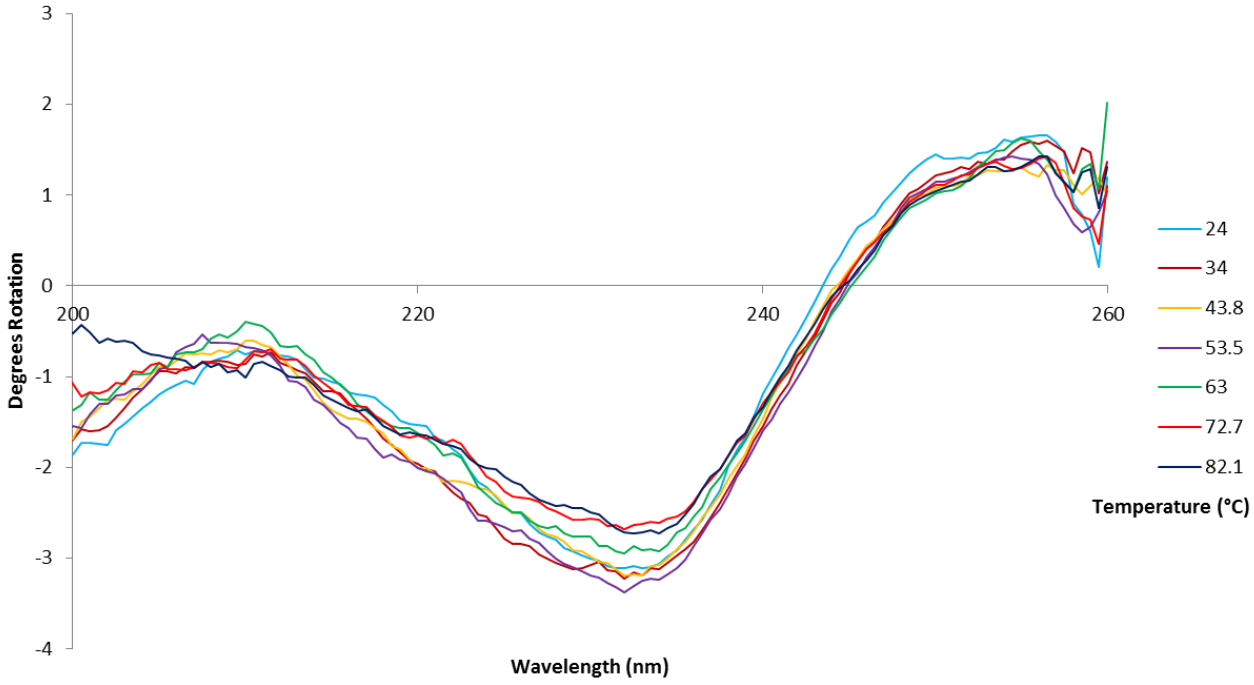

Figure 4.16 CD melt experiment in water on hydrophilic meander **126** showing only small perturbations in the amplitude of the minimum at 230 nm as the temperature increases.

4.5.3 Conclusions

The problems in the synthesis of hydrophilic meander **126** were eventually overcome and the analysis showed the conformation to be maintained to some extent in DMSO-d_6, with excellent spectral dispersion and cross-strand NOE interactions. Furthermore the CD and melt spectra showed that the desired conformation was present in an aqueous environment and preserved at high temperatures. Pleasingly this shows that the meanders can reliably display folding properties in a full range of solvents and with the side-chain display of different functional groups. As such the first two of Gellman's challenges have been met, but the challenge of creating a simple and general synthesis remains.

4.5.4 Future Work

4.5.4.1 Solid-Phase Synthesis

The ability to incorporate the diphenylacetylene turn motif into solid phase peptide synthesis would enable the rapid construction of meanders with the full diversity of side-chains. There are two potential methods of incorporation outlined in Figure 4.17 below.

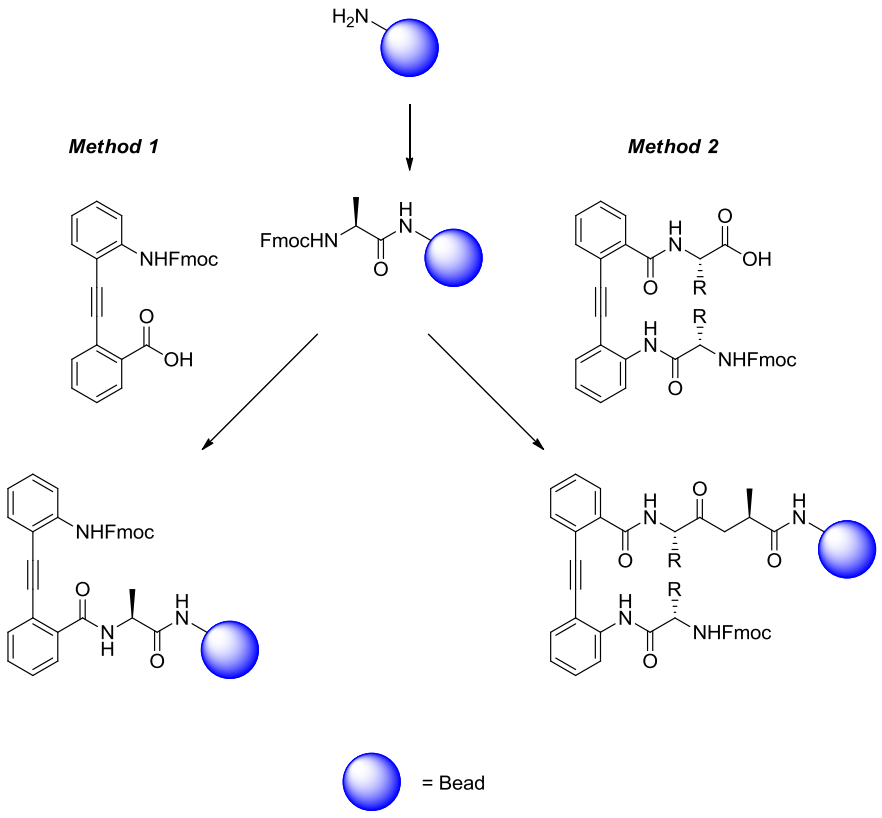

Figure 4.17 General methods for incorporation of the diphenylacetylene turn motif into solid phase synthesis.

Method 1 represents the most general and most favourable method. After incorporation of a single amino acid onto the bead, the deprotected amine could then couple with the benzoic acid terminus of the diphenylacetylene, incorporating the whole motif as an unnatural amino acid. The Fmoc-protected aniline could then be unmasked to continue the synthesis. An additional advantage of this approach is that the side-chain protecting groups normally employed in solid phase synthesis can be used. However initial work in the group has shown this method to be difficult to achieve, with a lack of reactivity for both the benzoic acid and

the aniline.[17] Whether these issues can be overcome by extensive optimisation remains to be seen.

Method 2 is less likely to require optimisation as only conventional peptide bonds (not incorporating anilines or benzoic acids) need to be made in the solid phase. However it does require pre-construction of the entire turn unit and deprotection of the *C*-terminus whilst the *N*-terminus and side-chains remain protected. Whilst the synthesis of such units is robust for the hydrophobic amino acids, there remains a need to find conditions for the selective removal of such a protecting group. Finding the correct conditions for the removal of the SEM-ester whilst leaving the rest of the molecule untouched would satisfy such a need.

It should be noted that Spivey has used solid phase synthesis in the creation of his large macrocyclic peptides incorporating the diphenylacetylene motif.[18] However this is done *via* a late stage, on resin Sonogashira reaction, a strategy that is not viable for the inclusion of more than one such motif.

Performing the synthesis on the solid phase could also overcome the solubility problems highlighted in the attempts to extend each strand of the meander horizontally.

4.5.4.2 Biological Targets

With the ability to incorporate reactive functionalities and control their facial display attention will turn to use of the meanders in a biological setting.

4.5.4.2.1 Anginex

As described in Section 3.5.1, anginex is a fully designed, anti-angiogenic peptide that demonstrated that the inhibition of angiogenesis was a viable therapeutic strategy against cancer. It was shown that anginex is active when in a three-stranded β-sheet form.[19] As discussed in Section 1.6, peptides are poor drugs due to poor cell penetration and metabolic

liabilities. Therefore the specific residues found in the β-sheet region of anginex could be mimicked and these problems overcome. The low RMSD value of the crystal structure of three-stranded meander **56** when compared to a canonical β-sheet implies an excellent goodness-of-fit could be found and the strong conformational preference of the meander could reduce the entropic penalty paid by anginex on binding, given that the natural peptide remains partially unfolded in solution.[20]

4.5.4.2.1.1 Protein Aggregation

As highlighted in Section 3.5.2 there remains a highly important and unmet need in both better understanding and preventing the protein aggregation implicated in diseases such as diabetes, Parkinson's and Alzheimers.

For example building off Nowick's work that showed that a hydrophobic surface is needed to prevent the aggregation of a Tau-Protein derived peptide the meander represents the perfect surface mimic on which to project such hydrophobic residues.

More speculatively, work has shown that the endogenous polyamines, spermine, spermidine, and putrescine can modulate Aβ fibrillation and reduce toxicity.[21, 22]

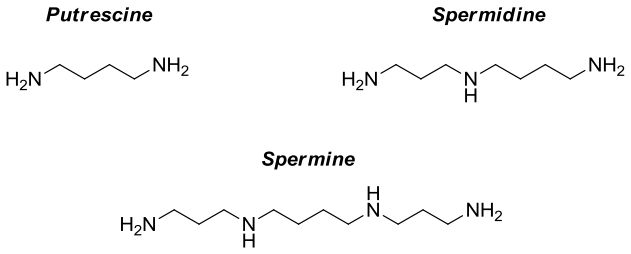

Figure 1 Endogenous polyamines that have been shown to modulate Aβ fibrillation and reduce toxicity.

The Aβ peptide at neutral pH possesses a net negative charge of three and it is therefore proposed that the modulation of aggregation occurs due to a weak electrostatic interaction. There is also some evidence that the polyamines compete with the Aβ peptide for a metal ion,

further affecting the aggregation pathways. However, these amines have little in the way of conformational constraint and so the meander can be used to see if the controlled display of these amines improves activity. This approach could be particularly successful in outcompeting the Aβ peptide for the metal ion where pre-organisation would play a key role.

4.5.4.2.2 Antibacterials

Finally this system, and specifically meander **126**, can display a hydrophilic, cationic face and a hydrophobic face. This makes them ideal as potential anti-bacterial compounds. For example the β-peptide helix developed by Gellman that successfully mimics the magainin class of antibiotics by displaying a cationic and hydrophobic face (Figure 1.5).[23]

4.5.4.3 Combining Turn and Strand Mimics

Ultimately however these sheet mimics remain peptidic in nature. Therefore the ultimate challenge becomes incorporating the strand mimic from Chapter 2 and the diphenylacetylene in the construction of a fully synthetic β-sheet. This could occur in two different ways.

The first is that the artificial strands simply replace the peptide strands (Figure 4.18).

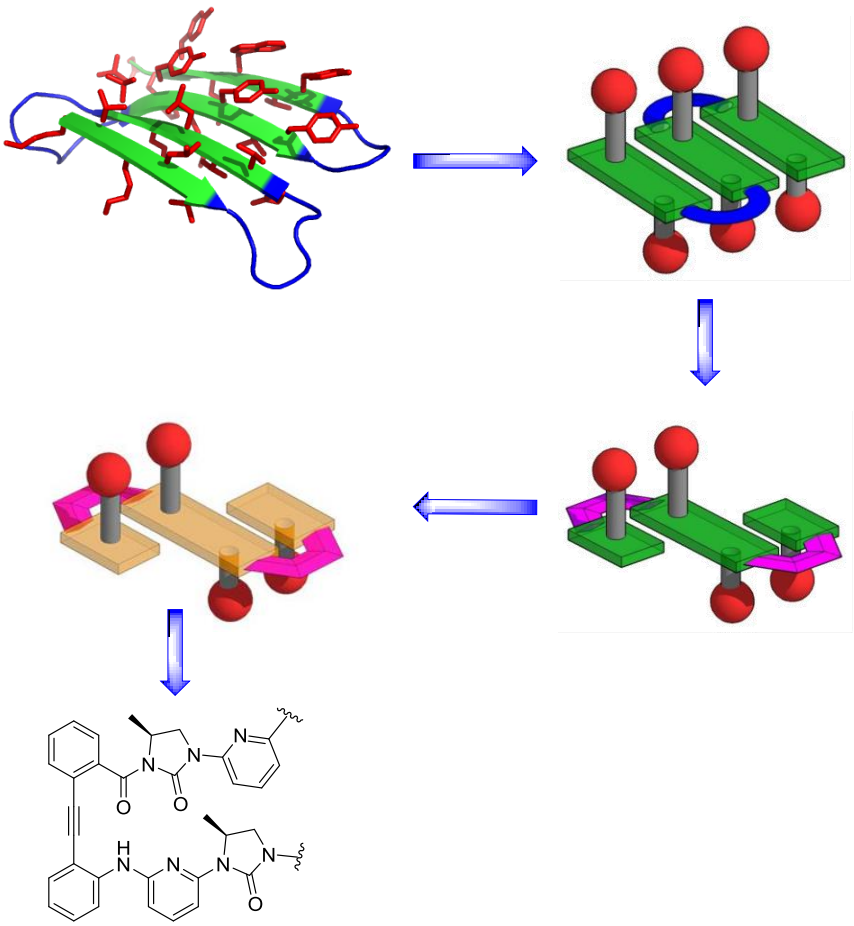

Figure 4.18 Schematic showing the development of a non-peptidic β-sheet mimic. The change in colour from green to orange represents the change from peptidic to non-peptidic strands.

This would represent a fitting culmination of the two projects, creating an artificial mini-protein with conformation controlled by hydrogen bonding and dipolar repulsion. Such a molecule would admirably meet all of Gellman's challenges. An example of this strategy has been demonstrated by the Smith group in using a turn linker and γ-peptides to form a parallel sheet structure (Figure 4.19).[24]

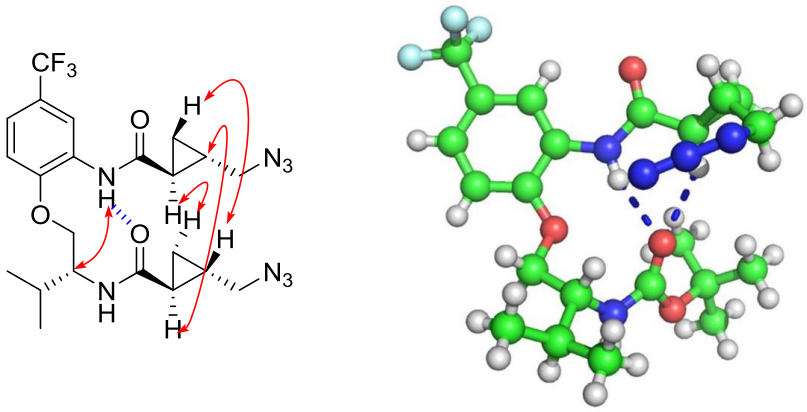

Figure 4.19 Parallel sheet structure of valine derived γ-peptides using an *Orn* derived turn linker. Conformation demonstrated by NOE interactions and X-ray crystal structure (CCDC: 674636).

The second takes inspiration from the TASP concept highlighted in Section 3.6. The meander, as a fully controllable surface that can be modified with a range of reactive side-chains such as amines and azides can act as the template for the projection of multiple different structures (Figure 4.20).

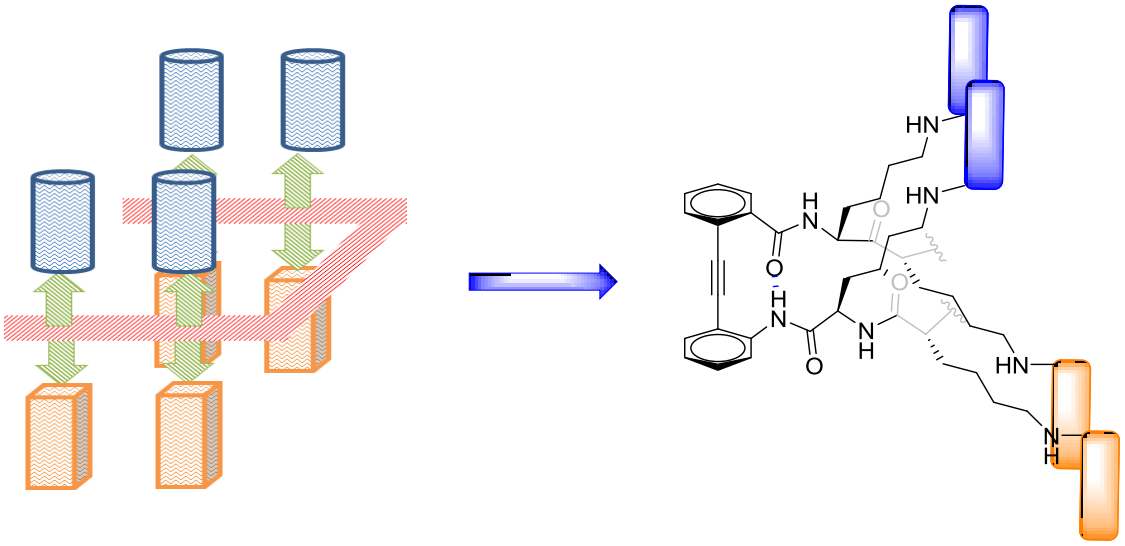

Figure 4.20 TASP concept as applied to the diphenylacetylene motif.

Here the projection of the strands enables the construction of two or three sheet-like structures at perpendicular to each other, thus using the folding properties to build entirely new synthetic topologies.

4.6 Experimental

4.6.1 General Information

For ‘Solvents and Reagents’, ‘Chromatography’, and ‘Spectroscopy’, see Chapter 2, Section 2.14.1

4.6.2 General Experimental Procedures

General procedure (4a): Synthesis of SEM Ester

To a stirring solution of acid (1 eq.) in tetrahydrofuran (0.1 M) was added SEM-Cl (1 eq.) and triethylamine (2 eq.). The reaction mixture was stirred at room temperature for 3 h and subsequently diluted with tetrahydrofuran (10 $mL.mmol^{-1}$). The resulting mixture was partitioned with ammonium chloride solution (10 $mL.mmol^{-1}$), extracted with dichloromethane (3 x 10 $mL.mmol^{-1}$), the combined organic layers dried over magnesium sulfate and concentrated *in vacuo*.

General procedure (4b): Synthesis of Methyl Ester

To a stirring solution of acid (1 eq.) in dichloromethane (0.1 M) was added *N*,*N*-diisopropylethylamine (2 eq.) and methyl iodide (5 eq.). The reaction mixture was stirred at room temperature for 16 h and quenched with methanol (5 $mL.mmol^{-1}$). The resulting mixture was partitioned with water (10 $mL.mmol^{-1}$), extracted with dichloromethane (3 x 10 $mL.mmol^{-1}$), the combined organic layers dried over magnesium sulfate and concentrated *in vacuo*.

General procedure (4c): Deprotection of Methyl Ester

Methyl ester (1 eq.) was stirred in a 1:1 by volume mixture of tetrahydrofuran and 1 M aqueous lithium hydroxide (0.5 M overall concentration). After 1 h the reaction mixture was

diluted with water (5 mL.mmol^{-1}), extracted with dichloromethane (3 x 5 mL.mmol^{-1}), the combined organic layers dried over magnesium sulfate and concentrated *in vacuo*.

General procedure (4d): Synthesis of Diazotransfer Reagent

According to a literature procedure,[16] sulfuryl chloride (1.0 eq.) was added dropwise to a stirring suspension of sodium azide (1.0 eq.) in acetonitrile (1 M) at 0 °C. The reaction mixture was warmed to room temperature and stirred for 16 h before the portion wise addition of imidazole (1.9 eq.) at 0 °C. The reaction was again warmed to room temperature and stirred for a further 3 h. The mixture was filtered and washed with ethyl acetate (2 mL.mmol^{-1}). HCl was generated *in situ* through the dropwise addition of acetyl chloride (1.5 eq.) to ethanol (3 M) at 0 °C. This solution of acetyl chloride in ethanol was added to the filtrate, filtered again and washed with ethyl acetate. The resulting solid was dried *in vacuo*.

General procedure (4e): Synthesis of Azides

According to a literature procedure,[16] to a stirred solution of amine (1.00 eq.) in methanol (0.1 M) was added diazotransfer reagent **110** (1.20 eq.), potassium carbonate (2.25 eq.) and copper(II) sulfate pentahydrate (0.10 eq.). The reaction mixture was stirred at room temperature for 16 h, diluted with dichloromethane (0.05 M) and partitioned with water (10 mL.mmol^{-1}). The mixture was extracted with dichloromethane (3 x 10 mL.mmol^{-1}), the combined organic layers dried over magnesium sulfate and concentrated *in vacuo*.

General procedure (4f): Synthesis of *tert*-Butyl Esters

To a stirred solution of acid (1 eq.) in dichloromethane (0.1 M) was added phosphoryl chloride (5 eq.), *N*,*N*-diisopropylethylamine (10 eq.) and *tert*-butanol (10 eq.). The reaction mixture was stirred at room temperature for 16 h, diluted with dichloromethane (0.05 M) and partitioned with water (10 mL.mmol^{-1}). The mixture was extracted with dichloromethane

(3 x 10 mL.mmol^{-1}), the combined organic layers dried over magnesium sulfate and concentrated *in vacuo*.

General procedure (4g): Deprotection of Boc-carbamate in the presence of a *tert*-butyl ester

To a stirred solution of Boc protected amine (1 eq.) in dichloromethane (0.05 M) was added trifluoroacetic acid (CH_2Cl_2:TFA 5:1 *v/v*) and the reaction mixture stirred for 10 min. The mixture was concentrated *in vacuo* and the residue trifluoroacetic acid removed by repeated co-evaporation with toluene.

4.6.3 Characterisation Data

Seven-Stranded Meander 80

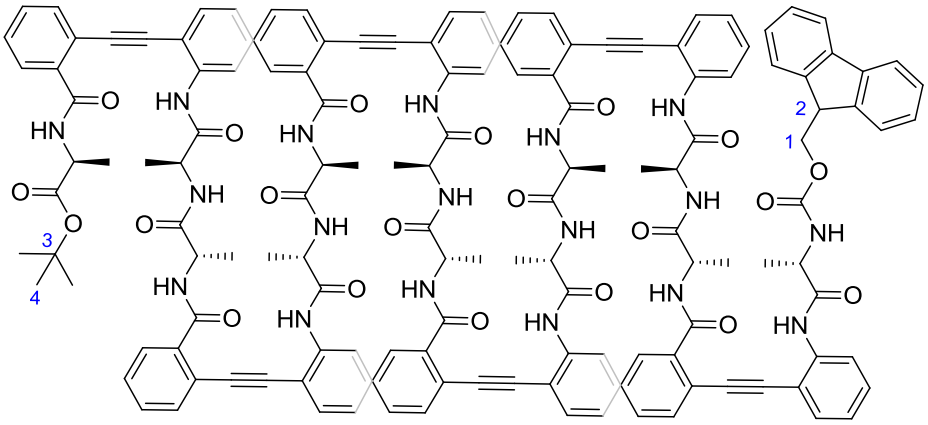

According to *general procedure (3f)*: tBu-ester protected acid **57** (80 mg, 0.05 mmol) gave residue **A** as a yellow paste. According to *general procedure (3g)*: Fmoc-protected amine **57** (80 mg, 0.05 mmol) gave residue **B** as a white solid. According to *general procedure (3e)*: Acid **A** and amine **B** gave the *title compound* **80** (35 mg, 28 %) as a white solid after purification by flash column chromatography (PE:Et_2O, 1:4); $[\alpha]_D^{23.5}$ +11.2 (*c* 1.10, $CHCl_3$); δ_H (600 MHz, $CDCl_3$) 9.63 (s, 1 H, N-H), 9.60 (s, 1 H, N-H), 9.56 (s, 1 H, N-H), 9.51 - 9.54 (m, 3 H, N-H), 9.15 - 9.21 (m, 2 H, N-H), 9.11 (d, *J* 7.7, 1 H, N-H), 8.84 (d, *J* 7.7, 1 H, N-H), 8.61 (dd, *J* 8.2, 1.0, 1 H, Ar-H), 8.57 (dd, *J* 8.3, 1.0, 1 H, Ar-H), 8.45 (t, *J* 9.0, 2 H, N-H), 8.38 (d, *J* 8.0, 1 H, N-H), 8.31 (d, *J* 8.0, 1 H, N-H), 8.25 (d, *J* 8.0, 1 H, N-H), 8.13 - 8.17 (m, 2 H, Ar-H), 8.06 (dd, *J* 8.0, 1.3, 1 H, Ar-H), 7.98 - 8.01 (m, 1 H, Ar-H), 7.91 (dd, *J* 7.7, 1.0, 1 H, Ar-H), 7.82 - 7.83 (m, 1 H, Ar-H), 7.80 - 7.81 (m, 1 H, Ar-H), 7.76 (dd, *J* 8.0, 1.0, 1 H, Ar-H), 7.64 - 7.70 (m, 8 H, Ar-H), 7.59 - 7.64 (m, 4 H, Ar-H), 7.56 (dd, *J* 7.7, 1.0, 1 H, Ar-H), 7.49 - 7.51 (m, 1 H, Ar-H), 7.47 - 7.49 (m, 1 H, Ar-H), 7.41 – 7.46 (m, 10 H, Ar-H), 7.36 - 7.39 (m, 1 H, Ar-H), 7.26 - 7.35 (m, 7 H, N-H, 6 x Ar-H), 7.22 (td, *J* 7.5, 1.0, 1 H, Ar-H), 7.12 - 7.18 (m, 2 H, Ar-H), 7.06 - 7.11 (m, 2 H, Ar-H), 6.97 - 7.02 (m, 2 H, Ar-H), 6.76 - 6.96 (m, 8 H, N-H, 7 x Ar-H), 6.00 (d, *J* 8.0, 1 H, N-H), 5.72 - 5.90 (m, 5 H, 5 x α-H),

5.64 - 5.70 (m, 1 H, α-H), 5.55 - 5.62 (m, 2 H, 2 x α-H), 5.44 - 5.49 (m, 1 H, α-H), 5.36 - 5.41 (m, 1 H, α-H), 5.13 - 5.19 (m, 1 H, α-H), 4.72 - 4.78 (m, 1 H, α-H), 4.60 - 4.69 (m, 2 H, H1, H1'), 4.25 - 4.30 (m, 1 H, H2), 1.52 - 1.63 (m, 21 H, β-H), 1.42 - 1.51 (m, 9 H, β-H), 1.38 (s, 9 H, H4), 1.34 (d, *J* 6.9, 6 H, β-H); δ_C (151 MHz, $CDCl_3$) 173.1, 173.1, 173.0, 172.8, 172.8, 172.7, 172.6, 172.4, 172.4, 172.4, 172.3, 172.2 (12 x C=O), 167.0, 166.6, 166.5, 166.3, 166.2, 165.9 (6 x C=O adjacent to ring), 156.0 (Carbamate C=O), 144.2, 144.1, 141.3, 141.3, 141.1, 140.9, 140.6, 140.6, 140.3, 140.3, 136.1, 134.6, 134.6, 134.3, 134.1, 133.9, 133.9, 133.7, 133.5, 132.1, 132.0, 131.9, 131.5, 131.1, 130.9, 130.7, 130.6, 130.5, 130.5, 129.8, 129.8, 129.7, 129.6, 128.7, 128.6, 128.6, 128.5, 128.5, 128.2, 128.1, 127.9, 127.5, 127.2, 127.0, 125.5, 123.4, 123.2, 123.1, 123.0, 122.8, 122.7, 122.5, 122.4, 122.4, 122.2, 121.9, 120.4, 119.8, 119.5, 119.4, 119.2, 112.5, 112.3, 112.1, 111.9, 111.9 (78 x Ar-C), 96.0, 95.9, 95.7, 95.6, 95.3, 94.4, 90.1, 89.8, 89.7, 89.7, 89.7, 89.5 (12 x alkynyl C), 82.4 (C3), 67.2 (C1), 52.1, 51.4, 50.9, 50.3, 50.1, 50.1, 49.7, 49.6, 49.5, 49.3, 49.0, 48.9 (12 x α-C), 47.3 (C2), 27.9 (C4), 21.3, 21.2, 21.1, 21.1, 20.8, 20.8, 20.7, 20.7, 20.5, 20.2, 18.9, 17.8 (12 x β-C); IR ($CHCl_3$) 3293, 2978, 1729; HRMS (performed by MALDI) calculated for $C_{145}H_{134}N_{18}NaO_{21}$ $[M+Na]^+$: 2485.99, found 2486.15.

(S)-tert-Butyl 2-((S)-2-(2-((2-((S)-2-((S)-2-((((9H-fluoren-9-yl)methoxy)carbonyl)amino)propanamido)propanamido)phenyl)ethynyl)benzamido)propanamido)propanoate 81

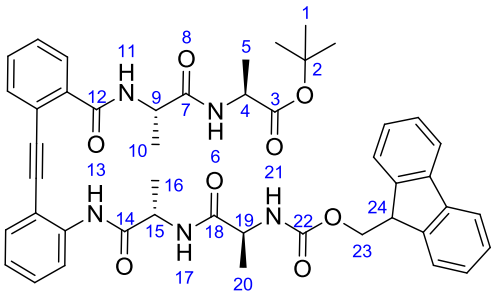

According to *general procedure (3g)*: Fmoc-protected amine **69** (300 mg, 0.41 mmol) gave residue **A**. According to *general procedure (3e)*: Residue **A** and Fmoc- L-Ala-OH (257 mg, 0.82 mmol) gave the *title compound* **81** (250 mg, 76 %) as a white fluffy powder after purification by flash column chromatography (PE:Et_2O, 1:9); $[\alpha]_D^{23.5}$ +13.5 (*c* 1.00, $CHCl_3$); δ_H (400 MHz, $CDCl_3$) 9.47 (s, 1 H, H13), 8.55 (d, *J* 7.5, 1 H, Ar-H), 8.39 (d, *J* 8.0, 1 H, H6), 7.65 (d, *J* 7.1, 3 H, Ar-H), 7.57 (dd, *J* 8.0, 1.0, 1 H, Ar-H), 7.50 - 7.54 (m, 2 H, Ar-H), 7.42 (dd, *J* 7.8, 1.5, 1 H, Ar-H), 7.37 (td, *J* 8.0, 1.0, 1 H, Ar-H), 7.21 - 7.32 (m, 6 H, H11, 5 x Ar-H), 7.15 - 7.20 (m, 2 H, H17, Ar-H), 6.97 (td, *J* 7.5, 1.0, 1 H, Ar-H), 6.46 (d, *J* 8.0, 1 H, H21), 5.50 - 5.62 (m, 1 H, H15), 5.29 - 5.41 (m, 1 H, H9), 4.36 - 4.52 (m, 2 H, H4, H19), 4.22 - 4.32 (m, 2 H, H23, H23'), 4.10 - 4.18 (m, 1 H, H24), 1.52 (d, *J* 6.8, 3 H, H16), 1.45 (d, *J* 6.8, 3 H, H10), 1.33 - 1.40 (m, 12 H, H1, H5), 1.31 (d, *J* 7.1, 3 H, H20); δ_C (101 MHz, $CDCl_3$) 172.4, 172.3, 172.3, 172.1 (4 x C=O), 166.1 (C12), 156.1 (C22), 143.8, 141.1, 140.5, 134.0, 132.1, 130.9, 129.8, 128.1, 127.6, 127.1, 126.9, 126.9, 125.1, 123.2, 122.5, 119.8, 119.3, 112.0 (18 x Ar-C), 95.2, 89.8 (2 x alkynyl-C), 82.0 (C2), 67.1 (C23), 50.5 (C19), 49.8 (C15), 49.0 (C9), 48.8 (C4), 47.0 (C24), 27.8 (C1), 20.4 (C16), 20.3 (C10), 19.3 (C5), 18.8 (C20); IR ($CHCl_3$); 3295, 3279 (broad), 2930, 2150, 1672, 1632, 1522; LRMS calculated for $C_{46}H_{49}N_5NaO_8$ $[M+Na]^+$: 822.3, found 822.2.

(S)-tert-Butyl 2-((S)-2-(2-((2-((5S,8S,11S)-1-(9H-fluoren-9-yl)-5,8,11-trimethyl-3,6,9-trioxo-2-oxa-4,7,10-triazadodecanamido)phenyl)ethynyl)benzamido)propanamido)propanoate 84

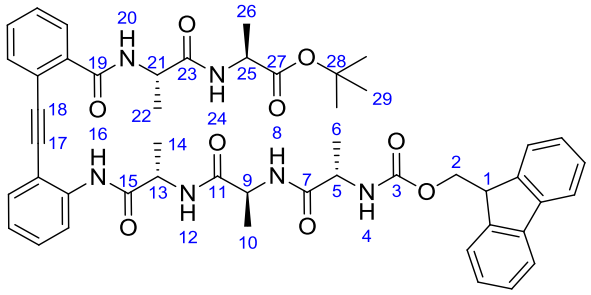

According to *general procedure (3g)*: Fmoc-protected amine **81** (47 mg, 0.08 mmol) gave residue **A**. According to *general procedure (3e)*: Residue **A** and Fmoc- L-Ala-OH (50 mg, 0.16 mmol) gave the *title compound* **84** (36 mg, 33 %) as an off-white solid after purification by flash column chromatography (PE:Et_2O, 1:9); $[\alpha]_D^{23.5}$ +69.8 (*c* 0.10, $CHCl_3$); δ_H (400 MHz, $CDCl_3$) 9.57 (s, 1 H, H16), 8.70 (d, *J* 8.6, 1 H, Ar-H), 8.55 (d, *J* 7.8, 1 H, H24), 7.74 - 7.80 (m, 3 H, Ar-H), 7.71 (dd, *J* 7.7, 1.1, 1 H, Ar-H), 7.63 (d, *J* 7.3, 2 H, Ar-H), 7.48 - 7.57 (m, 4 H, 3 x Ar-H, H8), 7.38 - 7.46 (m, 3 H, Ar-H), 7.28 - 7.34 (m, 4 H, 3 x Ar-H, H20), 7.07 (td, *J* 7.6, 1.0, 1 H, Ar-H), 6.14 (d, *J* 7.6, 1 H, H4), 5.67 – 5.71 (m, 1 H, H13), 5.45 - 5.56 (m, 1 H, H21), 4.82 - 4.92 (m, 1 H, H9), 4.58 - 4.67 (m, 1 H, H25), 4.46 - 4.54 (m, 1 H, H5), 4.37 (d, *J* 7.3, 2 H, H2, H2'), 4.21 - 4.25 (m, 1 H, H1), 1.65 (d, *J* 6.6, 3 H, H14), 1.52 - 1.58 (m, 12 H, H22, H29), 1.49 (d, *J* 7.1, 3 H, H6), 1.41 (dd, *J* 8.4, 7.2, 6 H, H10, H26); δ_C (101 MHz, $CDCl_3$) 173.1, 172.3, 172.3, 172.1, 172.1 (5 x C=O), 166.1 (C19), 155.8 (C3), 144.0, 143.9, 141.3, 140.6, 134.2, 132.3, 131.1, 129.9, 128.3, 127.7, 127.2, 127.0, 125.2, 123.4, 122.6, 120.0, 119.5, 112.1 (18 x C=O), 95.3 (C18), 89.9 (C17), 82.7 (C28), 66.9 (C2), 50.3 (C5), 49.9 (C13), 49.0 (C21), 48.8 (C9), 48.8 (C25), 47.2 (C1), 28.1 (C29), 20.6 (C14), 20.5 (C22), 19.8 (C6), 19.5 (C10), 19.5 (C26); IR ($CHCl_3$); 3278 (broad), 2930, 1672, 1632, 1522; HRMS calculated for $C_{49}H_{54}N_6NaO_9$ $[M+Na]^+$: 893.3845, found 893.3826.

(S)-tert-Butyl 2-((S)-2-((S)-2-(2-((2-((S)-2-((S)-2-((((9H-fluoren-9-yl)methoxy)carbonyl)amino)propanamido)propanamido)phenyl)ethynyl)benzamido)propanamido)propanamido)propanoate 85

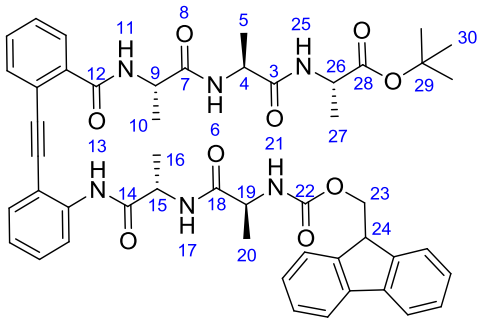

According to *general procedure (3f)*: Boc-protected amine **81** (100 mg, 0.125 mmol) gave residue **A**. According to *general procedure (3e)*: Residue **A** and L-alanine *tert*-butyl ester hydrochloride (50 mg, 0.25 mmol) gave the *title compound* **84** (16 mg, 14 %) as a white residue after purification by flash column chromatography (Et_2O); $[\alpha]_D^{23.5}$ +291 (*c* 0.80, $CHCl_3$); δ_H (400 MHz, $CDCl_3$) 9.49 (s, 1 H, H13), 8.48 - 8.59 (m, 2 H, H6, Ar-H), 7.68 (d, *J* 7.6, 2 H, Ar-H), 7.61 (dd, *J* 7.6, 1.0, 1 H, Ar-H), 7.57 (d, *J* 7.3, 2 H, Ar-H), 7.45 (dd, *J* 7.7, 1.3, 1 H, Ar-H), 7.39 - 7.43 (m, 1 H, Ar-H), 7.18 - 7.36 (m, 6 H, H11, 5 x Ar-H), 6.97 - 7.04 (m, 2 H, H17, Ar-H), 6.73 (d, *J* 8.6, 1 H, H25), 6.57 (d, *J* 6.8 Hz, 1 H, H21), 5.55 (br. s., 1 H, H15), 5.38 (br. s., 1 H, H9), 4.49 - 4.58 (m, 1 H, H4), 4.13 - 4.47 (m, 4 H, H19, H23, H23', H24, H2), 1.54 (d, *J* 6.8, 3 H, H16), 1.45 (d, *J* 6.6, 3 H, H10), 1.35 - 1.40 (m, 6 H, 2 of H5, H20, H27), 1.31 (s, 9 H, H30), 1.18 (d, *J* 8.0, 3 H, H5 or H20 or H27); δ_C (101 MHz, $CDCl_3$) 172.9, 172.1, 171.4, 171.2 (4 x C=O), 166.0 (C12), 156.3 (C22), 144.0, 141.3, 140.6, 134.3, 132.4, 131.9, 131.1, 129.8, 127.7, 127.1, 127.1, 125.3, 123.4, 119.9, 119.4, 118.8, 114.6, 112.2 (18 x Ar-C), 91.0, 90.0 (2 x alkynyl-C), 80.3 (C29), 67.1 (C23), 50.6 (C4 or C19 or C26), 49.9 (C15), 49.0 (C4 or C19 or C26), 48.9 (C9), 48.5 (C4 or C19 or C26), 46.9 (C24), 27.8 (C30), 20.5 (C16), 20.3 (C10), 19.3 (C5 or C20 or C27), 19.0 (C5 or C20 or C27), 18.6

(C5 or C20 or C27); IR ($CHCl_3$) 3287 (broad), 3067, 2979, 2934, 2250, 1722, 1644, 1526, 1450; HRMS calculated for $C_{49}H_{54}N_6NaO_9$ $[M+Na]^+$: 893.3845, found 893.3834.

(S)-tert-Butyl 2-((S)-2-(2-((2-((S)-2-((((9H-fluoren-9-yl)methoxy)carbonyl)amino)propanamido)phenyl)ethynyl)benzamido)propanamido)-3-phenylpropanoate 86

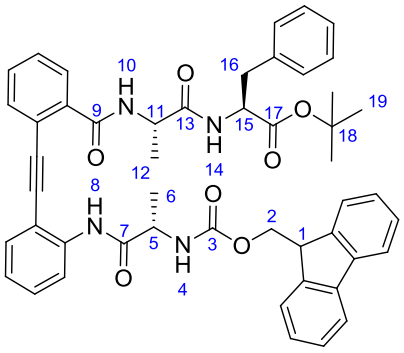

According to *general procedure (3f)*: *tert*-Butyl ester **48** (230 mg, 0.35 mmol) gave residue **A**. According to *general procedure (3e)*: Residue **A** and L-phenylalanine *tert*-butyl ester hydrochloride (100 mg, 0.38 mmol) gave the *title compound* **86** (166 mg, 59 %) as an off white solid after flash column chromatography (PE:Et_2O, 1:4); $[\alpha]_D^{23.5}$ -20.6 (*c* 1.00, $CHCl_3$); δ_H (500 MHz, $CDCl_3$) 9.70 (s, 1 H, H8), 8.78 (d, *J* 8.5, 1 H, Ar-H), 7.84 (d, *J* 8.5, 1 H, H14), 7.81 (dd, *J* 7.6, 4.1, 2 H, Ar-H), 7.77 (d, *J* 7.9, 1 H, Ar-H), 7.74 (d, *J* 7.6, 1 H, Ar-H), 7.70 (d, *J* 7.3, 2 H, Ar-H), 7.60 (dd, *J* 7.7, 1.1, 1 H, Ar-H), 7.53 (t, *J* 7.6, 1 H, Ar-H), 7.42 - 7.48 (m, 4 H, Ar-H), 7.31 - 7.38 (m, 3 H, H10, 2 x Ar-H), 7.13 - 7.18 (m, 1 H, Ar-H), 7.07 - 7.11 (m, 2 H, Ar-H), 7.00 - 7.03 (m, 2 H, Ar-H), 6.17 (d, *J* 8.2, 1 H, H4), 5.41 - 5.50 (m, 1 H, H5), 5.33 (t, *J* 7.1, 1 H, H11), 4.78 (m, 1 H, H15), 4.57 (dd, *J* 10.6, 6.8, 1 H, H2), 4.24 (t, *J* 7.4, 1 H, H1), 4.03 (dd, *J* 10.1, 8.2, 1 H, H2'), 2.94 (d, *J* 6.3, 2 H, H16, H16'), 1.68 (d, *J* 6.9, 3 H, H6), 1.60 (d, *J* 6.9, 3 H, H12), 1.30 (s, 9 H, H19); δ_C (126 MHz, $CDCl_3$) 172.3 (C17), 170.0 (C7, C13), 165.9 (C9), 155.7 (C3), 144.1, 143.6, 141.3, 141.1, 140.7, 136.0, 134.1, 132.1, 131.0, 129.9, 129.2, 128.1, 127.6, 127.2, 127.0, 126.7, 125.4, 125.1, 123.3, 119.8, 119.4, 112.0 (22 x

Ar-C), 95.3, 89.9 (2 x alkynyl-C), 81.6 (C18), 67.1 (C2), 53.7 (C15), 50.8 (C5), 48.9 (C11), 46.9 (C1), 38.4 (C16), 27.7 (C19), 21.1 (C6), 20.2 (C12); IR ($CHCl_3$) 3294, 2978, 1676, 1645, 1527, 1449; HRMS calculated for $C_{49}H_{48}N_4NaO_7$ $[M+Na]^+$: 827.3415, found 827.3399.

Methyl (2-((2-((S)-2-((((9H-fluoren-9-yl)methoxy)carbonyl)amino)propanamido)phenyl)ethynyl)benzoyl)-L-alanyl-L-valinate 87

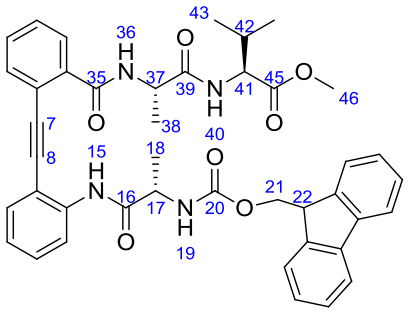

According to *general procedure (3f): tert*-Butyl ester **48** (500 mg, 0.76 mmol) gave a yellow residue **A**. According to *general procedure (3e):* Residue **A** and L-valine methyl ester hydrochloride (250 mg, 1.52 mmol) gave the *title compound* **87** (250 mg, 46 %) as a white solid after purification by flash column chromotography (PE:Et_2O, 1:1); $[\alpha]_D^{23.5}$ +37.3 (c 1.00, $CHCl_3$); δ_H (400 MHz, $CDCl_3$) 9.64 (s, 1 H, H15), 8.70 (d, *J* 8.3, 1 H, Ar-H), 7.76 - 7.81 (m, 2 H, 2 x Ar-H), 7.64 - 7.72 (m, 5 H, 4 x Ar-H, H40), 7.53 (d, *J* 7.6, 1 H, Ar-H), 7.49 (t, *J* 7.6, 1 H, Ar-H), 7.36 - 7.44 (m, 4 H, 4 x Ar-H), 7.30 - 7.35 (m, 2 H, 2 x Ar-H), 7.27 - 7.30 (m, 1 H, H36), 7.09 (t, *J* 7.6, 1 H, Ar-H), 6.06 (d, *J* 8.6, 1 H, H19), 5.44 - 5.52 (m, 1 H, H17), 5.27 - 5.36 (m, 1 H, H37), 4.52 - 4.57 (m, 1 H, H21), 4.46 - 4.51 (m, 1 H, H41), 4.27 - 4.31 (m, 1 H, H21'), 4.22 - 4.26 (m, 1 H, H22), 3.58 (s, 3 H, H46), 1.95 - 2.04 (m, 1 H, H42), 1.63 (d, *J* 6.8, 3 H, H18), 1.54 (d, *J* 6.6 Hz, 3 H, H38), 0.77 (d, *J* 6.6, 3 H, H43), 0.71 (d, *J* 6.8, 3 H, H43'); δ_C (101 MHz, $CDCl_3$) 172.9, 172.4, 171.8, 166.1, 155.9 (5 x C=O), 143.9, 143.7, 141.3, 140.8, 134.2, 134.0, 132.2, 131.1, 129.9, 128.2, 127.7, 127.1, 126.9, 125.3, 123.3, 122.6, 119.9, 112.0 (18 x Ar-C), 95.2, 90.0 (C7, 8), 67.3 (C21), 57.4 (C41), 51.8

(C46), 50.8 (C17), 49.0 (C37), 46.9 (C22), 31.2 (C42), 21.2 (C18), 20.1 (C38), 18.8 (C43), 17.8 (C44); HRMS calculated for $C_{42}H_{42}O_7N_4Na$ $[M+Na]^+$: 737.2946, found 737.2933; IR(CH_2Cl_2) 3280, 2950, 2375, 2300, 1610, 1495.

S)-tert-Butyl 2-((S)-2-(2-((2-((S)-2-((S)-2-((((9H-fluoren-9-yl)methoxy)carbonyl)amino)-3-phenylpropanamido)propanamido)phenyl)ethynyl)benzamido)propanamido)-3-phenylpropanoate 88

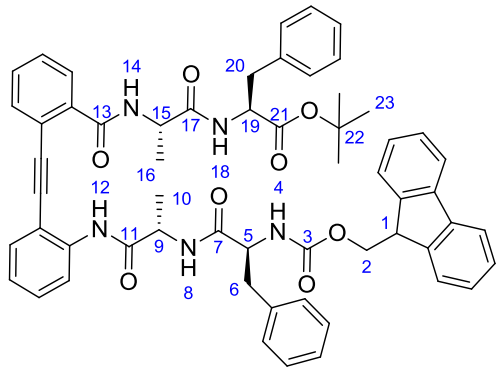

According to *general procedure (3g)*: Fmoc-protected amine **69** (130 mg, 0.17 mmol) gave residue **A**. According to *general procedure (3e)*: Residue **A** and Fmoc- L-Phe-OH (74 mg, 0.19 mmol) gave the *title compound* **88** (66 mg, 41 %) after purification by flash column chromatography (PE: Et_2O, 1:4); $[\alpha]_D^{23.5}$ +46.3 (*c* 0.80, $CHCl_3$); δ_H (500 MHz, $CDCl_3$) 9.48 (s, 1 H, H12), 8.58 (d, *J* 8.3, 2 H, H18, Ar-H), 7.62 - 7.68 (m, 4 H, Ar-H), 7.40 - 7.49 (m, 4 H, Ar-H), 7.28 - 7.36 (m, 4 H, Ar-H), 7.14 - 7.19 (m, 5 H, H14, 4 x Ar-H), 7.06 - 7.12 (m, 7 H, Ar-H), 7.02 (td, *J* 7.5, 1.1, 2 H, Ar-H), 6.85 (d, *J* 7.6, 1 H, H8), 6.45 (d, *J* 9.0, 1 H, H4), 5.55 (t, *J* 7.1, 1 H, H9), 5.47 (t, *J* 7.0, 1 H, H15), 4.78 (m, 1 H, H19), 4.45 (m, 1 H, H5), 4.05 - 4.23 (m, 3 H, H1, H2, H2'), 3.03 (d, *J* 6.4, 2 H, H20, H20'), 2.83 (dd, *J* 13.0, 5.9, 1 H, H6), 2.73 (dd, *J* 13.0, 9.0, 1 H, H6'), 1.48 (d, *J* 6.8, 3 H, H10), 1.42 (d, *J* 6.9, 3 H, H16), 1.28 (s, 9 H, H23); δ_C (151 MHz, $CDCl_3$) 172.6, 171.9, 171.2, 171.0, 166.0 (C13), 156.2 (C3), 143.9, 143.8, 141.1, 140.7, 136.5, 136.2, 134.2, 132.3, 131.1, 129.9, 129.6, 129.3, 128.5, 128.3, 128.2, 127.6, 127.1, 127.0, 126.9, 125.3, 125.2, 123.3, 122.7, 119.9, 119.4, 111.9 (26 x

Ar-C), 95.3, 90.0 (2 x alkynyl-C), 82.6 (C22), 67.2 (C2), 56.3 (C5), 54.4 (C19), 49.8 (C9), 46.9 (C1), 39.0 (C6), 39.0 (C20), 27.9 (C23), 20.5 (C10, C16); IR ($CHCl_3$) 3285 (broad), 2977, 2929, 1708, 1644, 1579, 1391; HRMS calculated for $C_{58}H_{57}N_5NaO_8$ $[M+Na]^+$: 974.4099, found 974.4081.

Methyl (2-((2-((S)-2-((S)-2-((tert-butoxycarbonyl)amino)-3-methylbutanamido)propanamido)phenyl)ethynyl)benzoyl)-L-alanyl-L-valinate 89

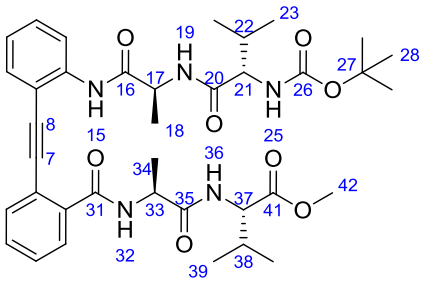

According to *general procedure (3g):* Fmoc-protected amine **69** (250 mg, 0.35 mmol) was deprotected to give residue **A**. According to *general procedure (e):* Residue **A** and *N*-(*tert*-butoxycarbonyl)-L-valine (174 mg, 0.80 mmol) gave the *title compound* **89** (125 mg, 41 %) as a white residue after purification by flash column chromatography (PE:Et_2O, 1:1**)**; $[\alpha]_D^{23.5}$ +60.9 (*c* 1.00, $CHCl_3$); δ_H (400 MHz, $CDCl_3$) 9.62 (br. s, 1 H, H15), 8.65 (d, *J* 7.8, 1 H, Ar-H), 8.28 (d, *J* 8.6, 1 H, H36), 7.68 - 7.74 (m, 2 H, 2 x Ar-H), 7.48 - 7.55 (m, 2 H, 2 x Ar-H), 7.41 (td, *J* 7.6, 1.3, 1 H, Ar-H), 7.34 - 7.39 (m, 1 H, Ar-H), 7.29 (d, *J* 7.3, 1 H, H32), 7.08 (td, *J* 7.5, 1.0, 1 H, Ar-H), 6.95 (d, *J* 8.1, 1 H, H19), 5.59 - 5.71 (m, 2 H, H17, H25), 5.40 - 5.51 (m, 1 H, H33), 4.51 - 4.57 (m, 1 H, H37), 3.98 - 4.07 (m, 1 H, H21), 3.79 (s, 3 H, H42), 2.09 - 2.23 (m, 2 H, H22, H38), 1.62 (d, *J* 6.8, 3 H, H18), 1.53 (d, *J* 6.8, 3 H, H34), 1.47 (s, 9 H, H28), 0.92 - 0.98 (m, 12 H, H23, H24, H39, H40); δ_C (101 MHz, $CDCl_3$) 173.0, 172.2, 172.1, 171.2, 166.0 (5 x C=O), 155.9 (C26), 140.8, 134.2, 134.1, 132.3, 131.1, 129.9, 128.2, 127.1, 123.3, 122.7, 119.4, 112.0 (12 x Ar-C), 95.2, 90.1 (C7, 8), 79.7 (C27), 60.2 (C37), 57.7 (C21), 52.1 (C42), 49.6 (C17), 49.2 (C33), 31.4, 31.3 (C22, 38), 28.3 (C28), 20.8

(C18), 20.3 (C34), 19.3, 18.9, 18.1, 17.8 (C23, 24, 39, 40); IR (CH_2Cl_2) 3300, 2995, 1700, 1650, 1210; HRMS calculated for $C_{37}H_{50}O_8N_5$ $[M+H]^+$: 692.3654, found 692.3655.

(R)-Methyl (1-((2-iodophenyl)amino)-1-oxopropan-2-yl)carbamate 90

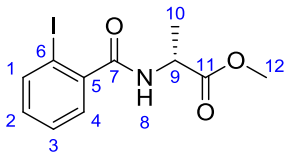

According to *general procedure (3d)*: 2-benzoyl chloride **44** (5.00 g, 22.8 mmol) and D-alanine methyl ester hydrochloride (3.50 g, 37.6 mmol) gave the *title compound* **90** (4.50 g, 57 %) as a white powder after purification by flash column chromatography (PE:Et_2O, 1:1); $[\alpha]_D^{23.5}$ -2.10 (*c* 1.00, $CHCl_3$); δ_H (400 MHz, $CDCl_3$) 7.89 (dd, *J* 8.0, 0.6, 1 H, Ar-H), 7.44 (dd, *J* 7.6, 1.9, 1 H, Ar-H), 7.40 (td, *J* 7.5, 1.0, 1 H, Ar-H), 7.13 (td, *J* 7.7, 1.7, 1 H, Ar-H), 6.44 (d, *J* 5.9, 1 H, H8), 4.83 (quin, *J* 7.3, 1 H, H9), 3.81 (s, 3 H, H12), 1.58 (d, *J* 7.2, 3 H, H10); δ_C (101 MHz, $CDCl_3$) 173.1 (C11), 168.5 (C7), 141.4, 140.0, 131.3, 128.3, 128.1 (5 x Ar-C), 92.3 (C6), 52.6 (C9), 48.6 (C12), 18.4 (C10); IR ($CHCl_3$) 3267, 3061, 2994, 2949, 2360, 1738, 1647, 1539; HRMS calculated for $C_{11}H_{13}N_1O_3I$ $[M+H]^+$: 333.9935, found 333.9935.

(R)*-Methyl 2-(2-((2-aminophenyl)ethynyl)benzamido)propanoate 91*

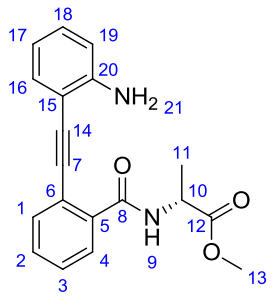

According to *general procedure (3a)*: Iodide **90** (2.0 g, 6.1 mmol) and alkyne **43** (1.0 g, 9.1 mmol) gave the *title compound* **91** (1.3 g, 67 %) as a pale yellow solid after purification

by flash column chromatography (Et_2O); $[\alpha]_D^{23.5}$ -4.60 (*c* 1.00, $CHCl_3$); δ_H (400 MHz, $CDCl_3$) 7.84 (td, *J* 7.7, 1.3, 1 H, H3), 7.63 (dd, *J* 7.7, 1.1, 1 H, H1), 7.47 (td, *J* 7.6, 1.5, 1 H, H2), 7.34 - 7.44 (m, 3 H, H4, H9, H16), 7.16 (ddd, *J* 8.3, 7.2, 1.6, 1 H, H18), 6.67 - 6.74 (m, 2 H, H17, H19), 4.79 (quin, *J* 7.2, 1 H, H10), 4.63 (br. s., 2 H, H21), 3.74 (s, 3 H, H13), 1.52 (d, *J* 7.1, 3 H, H11); δ_C (126 MHz, $CDCl_3$) 173.2 (C12), 166.8 (C8), 149.0 (C20), 135.4 (C5), 133.2 (C1), 131.9 (C16), 130.6 (C2), 130.3 (C18), 128.6 (C3), 128.2 (C4), 121.1 (C6), 117.3 (C17), 114.2 (C19), 106.6 (C15), 92.3, 92.3, 52.4 (C10), 48.8 (C13), 18.3 (C11); IR ($CHCl_3$) 3460, 3347, 2208, 1736, 1642, 1494; HRMS calculated for $C_{19}H_{19}N_2O_3$ $[M+H]^+$: 323.1390, found 323.1391.

(R)-Methyl 2-(2-((2-((R)-2-((((9H-fluoren-9-yl)methoxy)carbonyl)amino)propanamido)phenyl)ethynyl)benzamido)propanoate 92

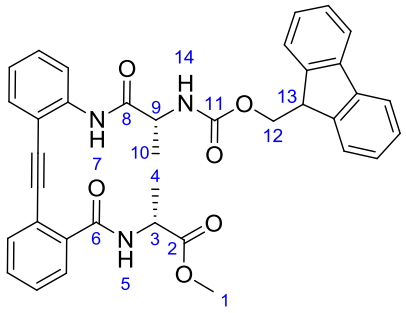

According to *general procedure (3c)*: Aniline **91** (2.91 g, 9.00 mmol) and Fmoc-D-Ala-OH (3.6 g, 11.7 mmol) gave the *title compound* **92** (2.20 g, 40 %) after purification by flash column chromatography (PE:Et_2O, 1:4); $[\alpha]_D^{23.5}$ -2.00 (*c* 1.00, $CHCl_3$); δ_H (500 MHz, $CDCl_3$) 9.34 (br. s., 1 H, H7), 8.55 (d, *J* 8.4, 1 H, Ar-H), 7.76 (d, *J* 7.4, 2 H, Ar-H), 7.63 - 7.69 (m, 2 H, Ar-H), 7.56 (dd, *J* 7.4, 3.3, 2 H, Ar-H), 7.53 (dd, *J* 7.7, 1.4, 1 H, Ar-H), 7.35 - 7.48 (m, 4 H, Ar-H), 7.26 - 7.31 (m, 3 H, Ar-H), 7.11 (t, *J* 7.3, 1 H, Ar-H), 6.91 (d, *J* 6.1, 1 H, H14), 6.36 (d, *J* 7.7, 1 H, H5), 4.97 (t, *J* 7.3, 1 H, H3), 4.90 (t, *J* 7.0, 1 H, H9), 4.25 – 4.28 (m, 1 H, H12), 4.15 - 4.23 (m, 1 H, H12'), 4.10 (d, *J* 7.3, 1 H, H13), 3.68 (s, 3 H, H1), 1.61 (d, *J* 7.7, 3 H, H4), 1.54 (d, *J* 7.8, 3 H, H10); δ_C (126 MHz, $CDCl_3$) 173.4 (C2), 172.3 (C8), 167.1 (C6),

155.7 (C11), 144.0, 143.9, 141.2, 140.1, 135.9, 133.6, 131.8, 130.9, 130.0, 128.5, 127.6, 127.4, 127.0, 125.1, 123.4, 121.6, 119.9, 112.1 (18 x Ar-C), 94.0, 89.7 (2 x alkynyl-C), 66.9 (C12), 52.6 (C1), 51.3 (C3), 48.8 (C9), 47.1 (C13), 19.7 (C4), 18.5 (C10); IR ($CHCl_3$) 3293 (broad), 3017, 2950, 2360, 2340, 1720, 1650, 1527; HRMS calculated for $C_{37}H_{33}N_3O_6Na$ $[M+Na]^+$: 638.2261, found 638.2259.

(R)-Methyl 2-(2-((2-((R)-2-((S)-2-(2-((2-((S)-2-((((9H-fluoren-9-yl)methoxy)carbonyl)amino)propanamido)phenyl)ethynyl)benzamido)propanamido)propanamido)phenyl)ethynyl)benzamido)propanoate 93

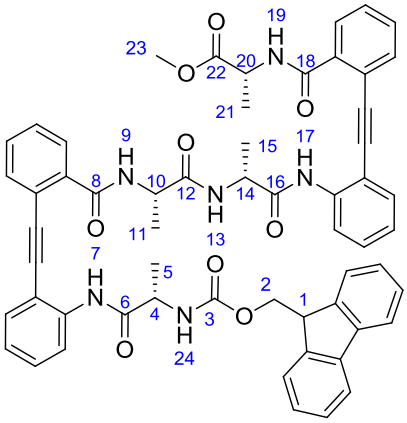

According to *general procedure (3f)*: tBu-ester protected acid **48** (1.70 g, 2.58 mmol) gave residue **A**. According to *general procedure (3g)*: Fmoc-protected amine **92** (2.20 g, 3.57 mmol) gave residue **B** According to *general procedure (3e)*: Residue **A** and **B** gave the *title compound* **93** (600 mg, 24 %) as a white solid after purification by flash column chromatography (PE: Et_2O, 1:4); $[\alpha]_D^{23.5}$ -37.1 (*c* 1.00, $CHCl_3$); δ_H (500 MHz, $CDCl_3$) 9.55 (s, 1 H, H7 or H17), 9.27 (s, 1 H, H7 or H17), 8.66 (d, *J* 8.4, 1 H, Ar-H), 8.43 (d, *J* 8.5, 1 H, Ar-H), 7.92 (d, *J* 7.6, 1 H, H13), 7.77 (dd, *J* 7.6, 3.0, 2 H, Ar-H), 7.62 - 7.71 (m, 6 H, Ar-H), 7.53 (dd, *J* 7.6, 1.3, 1 H, Ar-H), 7.44 - 7.51 (m, 3 H, Ar-H), 7.36 - 7.42 (m, 5 H, Ar-H), 7.30 - 7.33 (m, 1 H, H9), 7.21 - 7.26 (m, 2 H, Ar-H), 7.07 - 7.11 (m, 1 H, Ar-H), 7.02 (t, *J* 7.6, 1 H, Ar-H), 6.94 (d, *J* 6.9, 1 H, H19), 6.14 (d, *J* 7.9, 1 H, H24), 5.28 - 5.34 (m, 1 H, H4), 5.24 (t,

J 7.1, 2 H, H10, H14), 5.19 (t, *J* 7.5, 1 H, H14), 4.87 (t, *J* 7.0, 1 H, H20), 4.57 (dd, *J* 10.4, 6.8, 1 H, H2), 4.45 (dd, *J* 10.5, 8.0, 1 H, H2'), 4.23 - 4.28 (m, 1 H, H1), 3.68 (s, 3 H, H23), 1.63 (d, *J* 6.8, 3 H, H5), 1.55 (d, *J* 6.8, 3 H, H11), 1.50 (d, *J* 7.1, 3 H, H21), 1.47 (d, *J* 6.9, 3 H, H15); δ_C (126 MHz, $CDCl_3$) 173.4, 172.4, 172.2, 171.5 (4 x C=O), 166.8 (C8 or C18), 166.0 (C8 or C18), 156.0 (C3), 144.2, 143.6, 141.3, 141.2, 140.6, 140.3, 135.9, 134.2, 134.1, 133.4, 132.2, 131.7, 131.0, 130.8, 129.9, 129.9, 128.5, 128.1, 127.6, 127.4, 127.2, 127.0, 125.4, 125.2, 123.3, 123.2, 122.6, 121.6, 119.9, 119.5 (30 x Ar-C), 95.0, 93.9, 90.1, 89.9 (4 x alkynyl-C), 67.0 (C2), 52.6 (C23), 51.0 (C4), 49.6 (C14), 49.2 (C10), 48.8 (C20), 47.1 (C1), 21.1 (C5), 20.2 (C11), 19.0 (C15), 18.5 (C21); IR ($CHCl_3$) 3288 (broad), 2361, 2340, 1646, 1579, 1525, 1449; HRMS calculated for $C_{58}H_{52}N_6O_9Na$ $[M+Na]^+$: 999.3688, found 999.3684.

(R)-Methyl 2-(2-((2-((R)-2-((S)-2-(2-((2-((S)-2-((R)-2-((tert-butoxycarbonyl)amino)propanamido)propanamido)phenyl)ethynyl)benzamido)propanamido)propanamido)phenyl)ethynyl)benzamido)propanoate 94

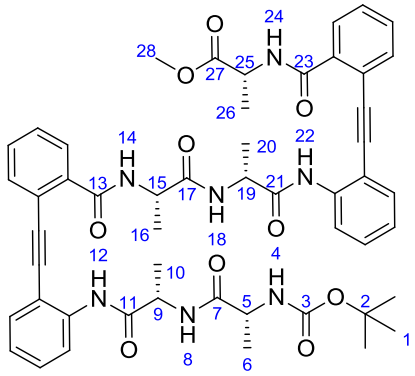

According to *general procedure (3g)*: Fmoc-protected amine **93** (600 mg, 0.61 mmol) gave residue **A**. According to *general procedure (3e)*: Reside **A** and Boc-D-Ala-OH (193 mg, 1.02 mmol) gave the *title compound* **94** (125 mg, 32 %) as an off-white solid after purification by flash column chromatography (Et_2O); $[\alpha]_D^{23.5}$ -39.9 (*c* 0.10, $CHCl_3$); δ_H (400 MHz, $CDCl_3$) 9.42 (s, 1 H, H12 or H22), 9.23 (s, 1 H, H12, or H22), 8.53 (d, *J* 8.1, 1 H, Ar-H), 8.40 (d, *J* 8.3, 1 H, Ar-H), 8.34 (d, *J* 7.1, 1 H, H18), 7.55 - 7.61 (m, 4 H, Ar-H),

7.40 - 7.43 (m, 1 H, Ar-H), 7.33 - 7.39 (m, 2 H, Ar-H), 7.19 - 7.31 (m, 6 H, 4 x Ar-H, H8, H24), 6.88 - 7.00 (m, 4 H, 3 x Ar-H, H14), 5.61 - 5.72 (m, 1 H, H4), 5.41 (t, *J* 7.2, 1 H, H25), 5.31 (br. s., 1 H, H9), 5.17 (t, *J* 7.1, 1 H, H19), 4.81 (t, *J* 7.1, 1 H, H15), 4.20 – 4.32 (br. s, 1 H, H5), 3.58 (s, 3 H, H28), 1.52 (d, *J* 6.6, 3 H, H26), 1.48 (dd, *J* 6.7, 1.3, 6 H, H10, H20), 1.39 - 1.45 (m, 3 H, H16), 1.33 - 1.39 (m, 12 H, H1, H6); δ_C (101 MHz, $CDCl_3$) 173.4, 172.5, 172.5, 171.9, 171.8 (5 x C=O), 166.7 (C13 or C23), 165.9 (C13 or C23), 155.6 (C3), 140.6, 140.3, 135.8, 134.1, 133.4, 132.1, 131.7, 131.0 (2C), 130.8, 129.9, 129.8, 128.4, 128.1, 127.5 (2C), 127.1, 125.5, 123.2, 122.7, 121.5, 120.0, 119.5, 112.1 (24 x Ar-C), 95.1, 93.9, 90.0, 89.9 (4 x alkynyl-C), 79.8 (C2), 52.5 (C28), 50.3 (C5), 49.9 (C25), 49.6 (C19), 49.0 (C9), 48.7 (C15), 28.3 (C1), 20.5 (C26), 20.4 (C16), 20.3 (C20), 19.1 (C10), 18.4 (C6); IR ($CHCl_3$) 3284 (broad), 2979, 2873, 2216, 1744, 1697, 1644, 1606, 1483; HRMS calculated for $C_{51}H_{56}N_7O_{10}$ $[M+H]^+$: 926.4083, found 926.4086.

(S)-tert-Butyl 2-((R)-2-(2-((2-((R)-2-((S)-2-(2-((2-((S)-2-((R)-2-((tert-butoxycarbonyl)amino)propanamido)propanamido)phenyl)ethynyl)benzamido)propanamido)propanamido)phenyl)ethynyl)benzamido)propanamido)propanoate 95

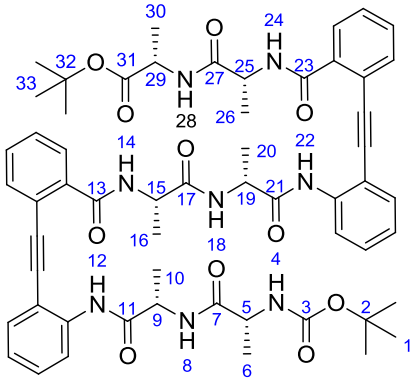

According to *general procedure (4c)*: Methyl ester **94** (150 mg, 0.16 mmol) gave residue **A**. According *general procedure (3e)*: Residue **A** and L-alanine *tert*-butyl ester hydrochloride (42 mg, 0.22 mmol) gave the *title compound* **95** (20 mg, 12 %) as an off-white solid after purification by flash column chromatography (Et_2O); $[\alpha]_D^{23.5}$ -48.9 (*c* 0.35, $CHCl_3$);

δ_H (500 MHz, $CDCl_3$) 9.55 (s, 1 H, H12), 9.48 (s, 1 H, H22), 8.75 - 8.82 (m, 1 H, H18), 8.59 - 8.66 (m, 2 H, Ar-H), 8.36 (d, *J* 7.4, 1 H, H28), 7.80 (d, *J* 7.4, 1 H, Ar-H), 7.71 (d, *J* 7.7, 1 H, H14), 7.68 - 7.70 (m, 1 H, Ar-H), 7.65 (td, *J* 6.5, 0.9, 2 H, Ar-H), 7.46 - 7.51 (m, 2 H, Ar-H), 7.44 (td, *J* 7.6, 1.1, 1 H, Ar-H), 7.39 (td, *J* 7.7, 1.1, 1 H, Ar-H), 7.29 - 7.36 (m, 3 H, 2 x Ar-H, H8), 7.24 - 7.27 (m, 2 H, Ar-H), 7.22 (d, *J* 6.9, 1 H, H24), 7.06 (td, *J* 7.6, 0.9, 1 H, Ar-H), 6.99 - 7.03 (m, 1 H, Ar-H), 5.85 – 5.90 (m, 1H, H4), 5.64 - 5.75 (m, 2 H, H9, H19), 5.46 - 5.60 (m, 2 H, H15, H25), 4.52 (t, *J* 7.2, 1 H, H29), 4.33 - 4.46 (m, 1 H, H5), 1.59 - 1.65 (m, 9 H, H10, H16, H20), 1.53 (d, *J* 6.8, 3 H, H26), 1.49 (d, *J* 6.9, 3 H, H6), 1.42 (br. s., 9 H, H1 or H33), 1.38 (d, *J* 7.1, 3 H, H30), 1.21 (s, 9 H, H1 or H33); δ_C (126 MHz, $CDCl_3$) 172.8, 172.5, 172.5, 172.1, 172.1, 172.0, 166.4 (C13 or C23), 166.3 (C13 or C23), 155.6 (C3), 140.9, 140.8, 134.5, 134.3, 134.1, 133.9, 132.1, 132.0, 131.0, 130.8, 129.9, 129.8, 128.1, 128.0, 127.9, 126.9, 125.5, 123.2, 123.0, 122.9, 122.7, 119.5, 112.1, 111.8 (24 x Ar-C), 95.2, 94.8, 90.1, 90.0 (4 x alkynyl-C), 81.9 (C2 or C32), 79.7 (C2 or C32), 50.2 (C5), 49.8 (C9), 49.6 (C19), 49.2 (C15), 49.0 (C25), 48.6 (C29), 28.3 (C1 or C33), 27.7 (C1 or C33), 20.5 (C10 or C16 or C20), 20.4 (C10 or C16 or C20), 20.3 (C26), 20.1 (C10 or C16 or C20), 19.0 (C30), 18.5 (C6); IR ($CHCl_3$) 3287, 3245, 2981, 2875, 2218, 2205, 1746, 1690, 1641 ; HRMS calculated for $C_{57}H_{66}N_8O_{11}Na$ $[M+Na]^+$: 1061.4743, found 1061.4741.

(R)-Methyl 2-((S)-2-(2-((2-((S)-2-((((9H-fluoren-9-yl)methoxy)carbonyl)amino)propanamido)phenyl)ethynyl)benzamido)propanamido)propanoate 96

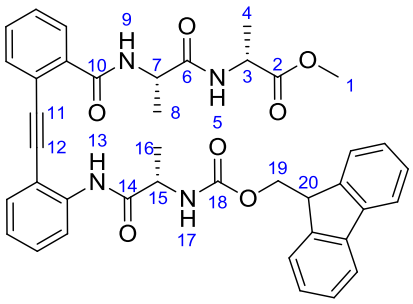

According to *general procedure (3f)*: *tert*-butyl ester **48** (330 mg, 0.50 mmol) gave residue **A**. According *general procedure (3e)*: Residue **A** and D-alanine methyl ester hydrochloride (100 mg, 0.72 mmol) gave the *title compound* **96** (205 mg, 60 %) as an off-white solid after purification by flash column chromatography (Et_2O); $[\alpha]_D^{23.5}$ -20.1 (*c* 0.10, $CHCl_3$); δ_H (500 MHz, $CDCl_3$) 9.61 (s, 1 H, H13), 8.68 (d, *J* 8.3, 1 H, Ar-H), 7.77 - 7.83 (m, 3 H, Ar-H), 7.65 - 7.72 (m, 3 H, H5, 2 x Ar-H), 7.61 (d, *J* 7.6, 1 H, Ar-H), 7.54 (dd, *J* 7.6, 1.5, 1 H, Ar-H), 7.49 (t, *J* 7.5, 1 H, Ar-H), 7.38 - 7.44 (m, 4 H, Ar-H), 7.35 - 7.38 (m, 1 H, Ar-H), 7.29 - 7.34 (m, 2 H, Ar-H), 7.25 - 7.29 (m, 1 H, H9), 7.10 (td, *J* 7.6, 1.0, 1 H, Ar-H), 6.18 (d, *J* 5.6, 1 H, H17), 5.35 - 5.44 (m, 1 H, H15), 5.24 (t, *J* 7.0, 1 H, H7), 4.52 (t, *J* 7.3, 1 H, H3), 4.34 - 4.46 (m, 2 H, H19, H19'), 4.23 - 4.29 (m, 1 H, H20), 3.55 (s, 3 H, H1), 1.65 (d, *J* 6.8, 3 H, H16), 1.53 (d, *J* 6.6, 3 H, H8), 1.30 (d, *J* 7.3, 3 H, H4); δ_C (126 MHz, $CDCl_3$) 172.7, 172.5, 172.2 (3 x C=O), 166.0 (C10), 156.0 (C18), 144.0, 143.6, 141.3, 141.2, 140.6, 134.1, 133.9, 132.2, 129.9, 128.2, 127.7, 127.0, 125.0, 123.3, 122.7, 120.0, 119.4, 112.1 (18 x Ar-C), 95.2 (C11), 90.0 (C12), 67.2 (C19), 52.2 (C1), 51.0 (C15), 49.0 (C7), 47.9 (C3), 46.9 (C20), 21.1 (C16), 20.3 (C8), 17.9 (C4); IR ($CHCl_3$) 3291 (broad), 2980, 2883, 1697, 1648, 1525; HRMS calculated for $C_{40}H_{38}N_4O_7Na$ $[M+Na]^+$: 709.2633, found 709.2630.

(R)-Methyl 2-((S)-2-(2-((2-((S)-2-((R)-2-((tert-butoxycarbonyl)amino)propanamido)propanamido)phenyl)ethynyl)benzamido)propanamido)propanoate 97

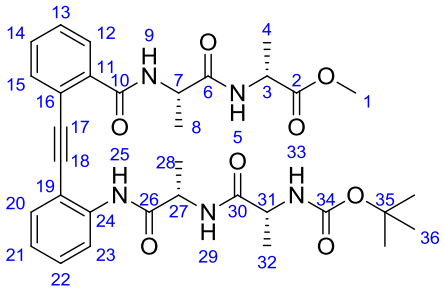

According to *general procedure (3g)*: Fmoc-protected amine **96** (221 mg, 0.33 mmol) gave residue **A**. According *general procedure (3e)*: Residue **A** and Boc-D-Ala-OH (92 mg, 0.49 mmol) gave the *title compound* **97** (132 mg, 63 %) as an off-white solid after purification by flash column chromatography (Et_2O); $[\alpha]_D^{23.5}$ -9.50 (*c* 1.00, $CHCl_3$); δ_H (500 MHz, $CDCl_3$) 9.49 (s, 1 H, H25), 8.53 (dd, *J* 8.6, 0.5, 1 H, H12), 8.27 (d, *J* 7.3, 1 H, H5), 7.64 (d, *J* 7.1, 1 H, H23), 7.58 (td, *J* 7.7, 1.1, 1 H, H22), 7.36 - 7.44 (m, 2 H, H13, H20), 7.23 - 7.32 (m, 4 H, H9, H14, H21, H29), 6.98 (dd, *J* 7.5, 1.1, 1 H, H15), 5.41 - 5.48 (m, 1 H, H27), 5.38 (d, *J* 7.1, 1 H, H33), 5.28 (t, *J* 7.1, 1 H, H7), 4.53 (t, *J* 7.3, 1 H, H3), 4.17 - 4.31 (m, 1 H, H31), 3.61 (s, 3 H, H1), 1.52 (d, *J* 6.8, 3 H, H28), 1.47 (d, *J* 6.8, 3 H, H8), 1.33 - 1.44 (m, 12 H, H4, H36), 1.32 (d, *J* 7.1, 3 H, H32); δ_C (125 MHz, $CDCl_3$) 173.1, 172.7, 172.3, 171.9 (4 x C=O), 165.9 (C10), 155.3 (C34), 140.6 (C24), 134.1 (C22), 133.8 (C11), 132.1 (C13), 131.0 (C20), 129.7 (C14), 128.1 (C21), 127.2 (C23), 123.2 (C15), 122.6 (C16), 119.4 (C12), 112.1 (C19), 95.2 (C17), 89.9 (C18), 79.9 (C35), 52.3 (C1), 50.4 (C27), 49.7 (C7), 48.9 (C3), 47.9 (C31), 28.2 (C36), 20.4 (C28), 20.2 (C8), 18.5 (C32), 18.1 (C4); IR ($CHCl_3$) 3185, 2933, 2895, 1715; HRMS calculated for $C_{33}H_{41}N_5O_8Na$ $[M+Na]^+$: 658.2848, found 658.2839.

(S)-(2-(Trimethylsilyl)ethoxy)methyl 2-((((9H-fluoren-9-yl)methoxy)carbonyl)amino)-6-((tert-butoxycarbonyl)amino)hexanoate 99

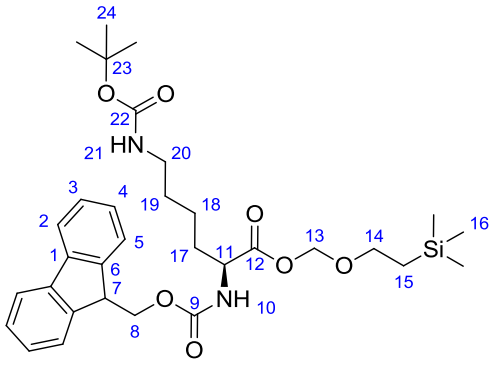

According to *general procedure (4a)*: Fmoc-Lys(Boc)-OH **98** (2.00 g, 4.27 mmol) and SEM-Cl (800 µL, 4.27 mmol) gave the *title compound* **99** (2.15 g, 84 %) as a white foam after purification by flash column chromatography (PE: Et_2O, 1:1); $[\alpha]_D^{23.5}$ -1.00 (*c* 1.00, $CHCl_3$); δ_H (400 MHz, $CDCl_3$) 7.75 (d, *J* 7.6, 2 H, H2), 7.59 (d, *J* 7.1, 2 H, H5), 7.35 - 7.41 (m, 2 H, H3), 7.26 - 7.33 (m, 2 H, H4), 5.41 - 5.50 (m, 1 H, H10), 5.27 - 5.38 (m, 2 H, H13, H13'), 4.51 - 4.65 (m, 1 H, H21), 4.38 (s, 3 H, H11, H14, H14'), 4.17 - 4.25 (m, 1 H, H7), 3.62 - 3.75 (m, 2 H, H8, H8'), 3.10 (d, *J* 5.9, 2 H, H20, H20'), 1.82 - 1.95 (m, 1 H, H17), 1.63 - 1.75 (m, 1 H, H17'), 1.46 - 1.56 (m, 2 H, H19, H19'), 1.33 - 1.45 (m, 11 H, H18, H18', H24), 0.89 - 0.99 (m, 2 H, H15, H15'), 0.00 (s, 9 H, H16); δ_C (101 MHz, $CDCl_3$) 172.1 (C12), 156.0 (C9), 156.0 (C22), 143.8 (C1), 143.7 (C6), 127.7 (C2), 127.0 (C3), 125.1 (C4), 119.9 (C5), 89.8 (C13), 79.1 (C23), 68.1 (C8), 67.0 (C14), 53.8 (C11), 47.1 (C7), 40.0 (C20), 32.0 (C17), 29.6 (C19), 28.4 (C24), 22.3 (C18), 17.9 (C15), -1.5 (C16); IR ($CHCl_3$) 3260 (broad), 2978, 2952, 2929, 2896, 2865, 1755, 1716, 1688; LRMS calculated for $C_{32}H_{40}N_2NaO_7Si$ $[M+Na]^+$: 621.3, found 621.3.

(S)-(2-(Trimethylsilyl)ethoxy)methyl 6-((tert-butoxycarbonyl)amino)-2-(2-iodobenzamido)hexanoate 100

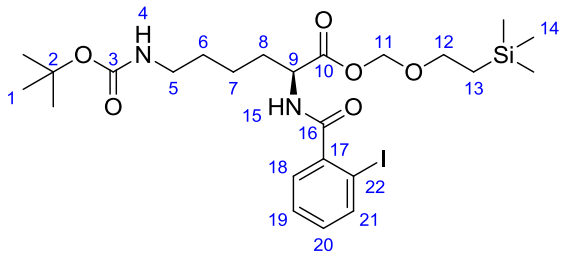

According to *general procedure (3g)*: Fmoc-protected amine **98** (2.15 g, 3.27 mmol) gave residue **99**. According to *general procedure (3d)*: 2-iodobenzoyl chloride (2.1 g, 3.54 mmol) and residue **99** gave the *title compound* **100** (900 mg, 45 %) as an off-white solid after purification by flash column chromatography (Et_2O); $[\alpha]_D^{23.5}$ -3.20 (*c* 1.00, $CHCl_3$); δ_H (400 MHz, $CDCl_3$) 7.85 (dd, *J* 8.1, 0.7, 1 H, H21), 7.40 (dd, *J* 7.0, 2.0, 1 H, H18), 7.35 (dd, *J* 7.3, 1.0, 1 H, H19), 7.08 (td, *J* 8.0, 1.5, 1 H, H20), 6.39 - 6.50 (m, 1 H, H15), 5.37 (d, *J* 5.0, 1 H, H11), 5.33 (d, *J* 5.1, 1 H, H11'), 4.75 - 4.83 (m, 1 H,9), 4.50 - 4.61 (m, 1 H, H4), 3.68 - 3.75 (m, 2 H, H12, H12'), 3.04 - 3.16 (m, 2 H, H5, H5'), 1.97 - 2.07 (m, 1 H, H8), 1.78 - 1.87 (m, 1 H, H8'), 1.47 - 1.58 (m, 4 H, H6, H6', H7, H7'), 1.37 (s, 9 H, H1), 0.91 - 0.98 (m, 2 H, H13, H13'), -0.01 (m, 9 H, H14); δ_C (101 MHz, $CDCl_3$) 171.7 (C10), 168.9 (C16), 156.1 (C3), 141.6 (C17), 140.0 (C21), 131.3 (C20), 128.4 (C19), 128.2 (C18), 92.4 (C11), 90.0 (C22), 79.2 (C2), 68.3 (C12), 52.6 (C9), 40.0 (C5) 32.0 (C8), 29.7 (C7), 28.4 (C1), 22.5 (C6), 18.0 (C13), -1.4 (C14); IR ($CHCl_3$) 3305 (broad), 3054, 2953, 2247, 1741, 1694, 1654, 1586, 1519; HRMS calculated for $C_{24}H_{39}N_2NaO_6ISi$ $[M+Na]^+$: 629.1514, found 629.1504.

(S)-(2-(Trimethylsilyl)ethoxy)methyl 2-(2-((2-aminophenyl)ethynyl)benzamido)-6-((tert-butoxycarbonyl)amino)hexanoate 101

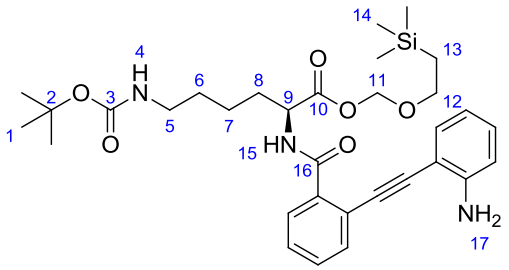

According to *general procedure (3a)*: Iodide **100** (880 mg, 1.45 mmol) and alkyne **43** (339 mg, 2.90 mmol) gave the *title compound* **101** (669 mg, 78 %) as a pale yellow solid after purification by flash column chromatography (PE: Et_2O, 3:7); $[\alpha]_D^{23.5}$ -50.3 (*c* 1.00, $CHCl_3$); δ_H (400 MHz, $CDCl_3$) 7.85 (dd, *J* 7.3, 1.2, 1 H, Ar-H), 7.61 (dd, *J* 7.7, 1.1, 1 H, Ar-H), 7.45 (td, *J* 7.0, 1.5, 1 H, Ar-H), 7.33 - 7.42 (m, 3 H, H15, 2 x Ar-H), 7.11 - 7.17 (m, 1 H, Ar-H), 6.65 - 6.73 (m, 2 H, Ar-H), 5.32 (q, *J* 6.1, 2 H, H11, H11'), 4.76 - 4.83 (m, 1 H, H9), 4.61 - 4.67 (m, 2 H, H17), 4.45 - 4.55 (m, 1 H, H4), 3.70 (dd, *J* 8.8, 7.8 Hz, 2 H, H12, H12'), 2.85 - 3.02 (m, 2 H, H5, H5'), 1.89 - 2.03 (m, 1 H, H8), 1.71 - 1.83 (m, 1 H, H8'), 1.28 - 1.47 (m, 13 H, H1, H6, H6', H7, H7'), 0.90 - 0.98 (m, 2 H, H13, H13'), 0.00 (s, 9 H, H14); δ_C (101 MHz, $CDCl_3$) 171.9 (C10), 165.8 (C16), 156.0 (C3), 149.0, 135.6, 133.3, 132.1, 130.7, 130.4, 128.7, 128.3, 121.1, 117.4, 114.3, 106.6 (12 x Ar-C), 92.4 (C11), 92.3, 89.9 (2 x alkynyl-C), 79.1 (C2), 68.2 (C12), 53.0 (C9), 40.0 (C5), 32.0 (C8), 29.7 (C6), 28.4 (C1), 22.7 (C7), 18.0 (C13), -1.5 (C14); IR ($CHCl_3$) 3347 (broad), 3061, 2952, 2209, 1740, 1693, 1653, 1603, 1476; HRMS calculated for $C_{32}H_{46}N_2NaO_7Si$ $[M+Na]^+$: 596.3151, found 596.3162.

(S)-(2-(Trimethylsilyl)ethoxy)methyl 2-(2-((2-((S)-2-((((9H-fluoren-9-yl)methoxy)carbonyl)amino)-6-((tert-butoxycarbonyl)amino)hexanamido)phenyl)ethynyl)benzamido)-6-((tert-butoxycarbonyl)amino)hexanoate 102

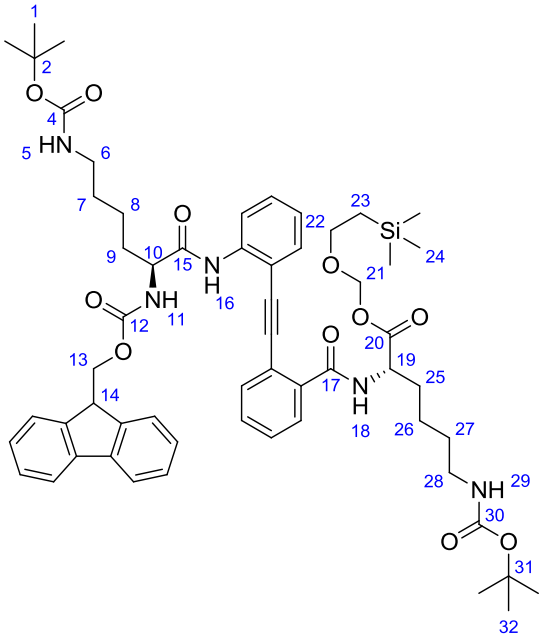

According to *general procedure (3c)*: Aniline **101** (650 mg, 1.09 mmol) and Fmoc-Lys(Boc)-OH **98** (665 mg, 1.42 mmol) gave the *title compound* **102** (812 mg, 71 %) as a pale yellow oil after purification by flash column chromatography (PE:Et_2O, 1:1); $[\alpha]_D^{23.5}$ -20.1 (*c* 0.20, $CHCl_3$); δ_H (400 MHz, $CDCl_3$) 9.33 (br. s., 1 H, H16), 8.49 (d, *J* 8.3 Hz, 1 H, Ar-H), 7.78 (d, *J* 7.6, 2 H, Ar-H), 7.71 (d, *J* 7.8, 1 H, Ar-H), 7.68 (d, *J* 7.6, 1 H, Ar-H), 7.58 (dd, *J* 7.3, 4.2, 2 H, Ar-H), 7.54 (dd, *J* 7.7, 1.3, 1 H, Ar-H), 7.38 - 7.49 (m, 5 H, Ar-H), 7.28 - 7.35 (m, 2 H, Ar-H), 7.08 - 7.17 (m, 2 H, H11, Ar-H), 6.38 - 6.48 (m, 1 H, H18), 5.33 (d, *J* 5.9, 1 H, H21), 5.19 (d, *J* 6.1, 1 H, H21'), 4.93 (br. s., 2 H, H10, 29), 4.83 - 4.89 (m, 1 H, H19), 4.68 - 4.76 (m, 1 H, H5), 4.28 – 4.34 (m, 1 H, H13), 4.07 - 4.22 (m, 2 H, H13', H14), 3.61 - 3.70 (m, 2 H, H22, 22'), 3.07 (m, 4 H, H6, H6', H28, H28'), 1.86 – 2.06 (m, 4 H, H 9, H9' H25, H25'), 1.45 - 1.50 (m, 15 H, H1, H7, H7', H8, H26, H27, H27'), 1.41 (s, 9 H, H32), 1.16 (d, *J* 6.4, 2 H, H8', H26'), 0.85 - 0.94 (m, 2 H, H23, H23'), 0.00 (s, 9 H, H24);

δ_C (101 MHz, $CDCl_3$) 171.9 (C20), 171.3 (C15), 167.5 (C17), 156.1 (C4), 155.9 (C30), 143.9, 143.7, 141.2, 141.1, 139.8, 136.3, 133.3, 131.6, 130.7, 128.6, 127.6, 127.0, 125.2, 123.6, 121.2, 120.2, 119.8, 112.3 (18 x Ar-C), 93.8 (C21), 89.9, 89.6 (2 x alkynyl-C), 78.9 (C2, 31), 68.1 (C22), 66.9 (C13), 55.4 (C10), 52.8 (C19), 47.0 (C14), 40.2 (C6), 39.8 (C28), 33.0 (C9), 31.9 (C25), 29.6 (C7, 27), 28.4 (C1), 28.3 (C32), 22.7 (C26), 22.3 (C8), 17.8 (C23), -1.5 (C24); IR ($CHCl_3$) 3343 (broad), 2932, 2861, 2361, 2340, 1692, 1649, 1522, 1450; HRMS calculated for $C_{58}H_{75}N_5O_{11}SiNa$ $[M+Na]^+$: 1068.5123, found 1068.5094.

(S)-(2-(Trimethylsilyl)ethoxy)methyl 2-(2-((2-((S)-2-((S)-2-(2-((2-((S)-2-((((9H-fluoren-9-yl)methoxy)carbonyl)amino)propanamido)phenyl)ethynyl)benzamido)propanamido)-6-((tert-butoxycarbonyl)amino)hexanamido)phenyl)ethynyl)benzamido)-6-((tert-butoxycarbonyl)amino)hexanoate 103

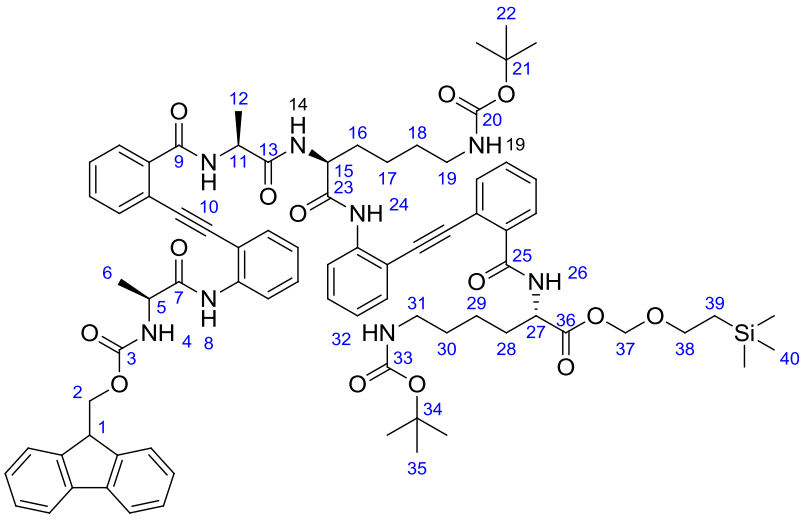

According to *general procedure (3g)*: Fmoc-protected amine **102** (812 mg, 0.78 mmol) gave residue **A**. According to *general procedure (3f)*: *tert*-butyl ester **48** (561 mg, 0.85 mmol) gave residue **B**. According to *general procedure (3e)*: Residue **A** and residue **B** gave the *title compound* **103** (330 mg, 30 %) as a pale yellow oil after purification by flash column chromatography (PE: Et_2O, 2:3); $[\alpha]_D^{23.5}$ +2.20 (*c* 1.00, $CHCl_3$); δ_H (600 MHz, DMSO-d_6) 9.32 (br. s., 1 H, H24), 9.28 (br. s., 1 H, H8), 8.66 (d, *J* 7.3, 1 H, H26), 8.35 (d, *J* 6.8, 1 H,

H4), 8.26 (d, *J* 7.7, 1 H, Ar-H), 8.15 (d, *J* 7.3, 1 H, Ar-H), 7.95 (d, *J* 6.6, 1 H, H14), 7.88 (d, *J* 5.9, 1 H, Ar-H), 7.76 (m, 3 H, Ar-H), 7.70 (m, 3 H, Ar-H), 7.49 - 7.60 (m, 7 H, Ar-H), 7.40 - 7.44 (m, 4 H, 3 x Ar-H, H26), 7.30 (br. s., 2 H, Ar-H), 7.14 - 7.20 (m, 2 H, Ar-H), 6.34 (br. s., 1 H, H19 or H32), 6.16 - 6.28 (m, 1 H, H19 or H32), 5.26 (br. s., 1 H, H37), 5.19 (br. s., 1 H, H37'), 4.81 (br. s., 1 H, H15), 4.72 (br. s., 1 H, H11), 4.65 (s, 2 H, H5, H27), 4.32 (m, 1 H, H2), 4.24 - 4.30 (m, 1 H, H2'), 4.16 - 4.21 (m, 1 H, H1), 3.64 - 3.70 (m, 2 H, H38, H38'), 2.83 - 2.94 (m, 4 H, H19, H19', H31, H31'), 1.70 - 1.93 (m, 4 H, H16, H16', H28, H28'), 1.46 - 1.48 (m, 3 H, H5), 1.41 (br. s., 9 H, H22 or H35), 1.39 (br. s., 9 H, H22 or H35), 1.36 (m, 3 H, H11), 0.87 (br. s., 2 H, H39, H39'), 0.00 (br. s., 9 H, H40); δ_C (151 MHz, DMSO-d_6) 172.8 (C13, C36), 172.3 (C23), 171.8 (C7), 168.6 (C25), 167.6 (C9), 156.8 (C3), 156.5 (C20 or C33), 156.4 (C20 or C33), 144.8, 144.7, 141.7, 140.6, 140.5, 138.5, 138.1, 133.9, 133.6, 132.9, 132.8, 131.2, 131.1, 130.5, 130.4, 129.5, 129.5, 129.1, 129.0, 128.5, 127.9, 126.1, 126.1, 124.7, 124.6, 122.1, 121.6, 121.5, 121.3, 120.9, 114.4, 114.0 (30 x Ar-C), 95.1, 94.9, 90.0, 90.0 (4 x alkynyl-C) 89.9 (C37), 78.4 (C21 or C34), 78.3 (C21 or C34), 67.9 (C38), 67.1 (C2), 54.6 (C15), 53.9 (C27), 52.1 (C5), 50.0 (C11), 47.8 (C1) 33.0 (C16), 31.4 (C28), 30.3 (C17 or C29), 30.2 (C17 or C29), 29.2 (C22, C35), 23.8 (C18 or C30), 23.5 (C18 or C30, 19.2 (C5), 19.0 (C11), 18.5 (C39), -0.5 (C40); N.B C19 and C31 are obscured by the DMSO-d_6 solvent peak. From HSQC they are expected to be at 40.8 and 41.0; IR ($CHCl_3$) 3284 (broad), 3065, 2979, 2214, 1689, 1648, 1523, 1482; HRMS calculated for $C_{79}H_{95}N_8O_{14}Si$ $[M+Na]^+$: 1407.6732, found 1407.6711.

Lysine Meander, Single Extension, Fully Protected 104

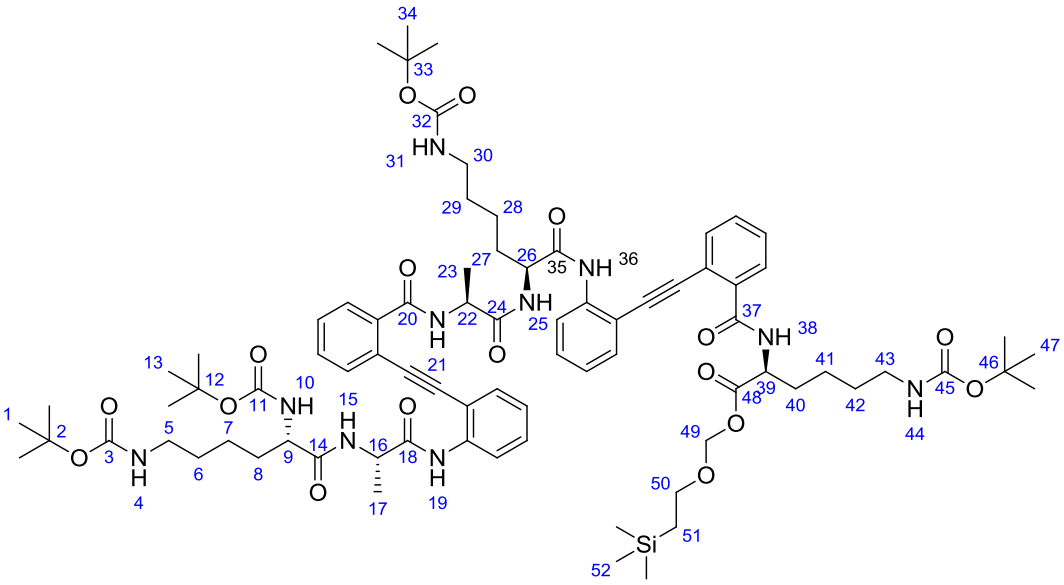

According to *general procedure (3g)*: Fmoc-protected amine **103** (150 mg, 0.12 mmol) gave residue **A**. According to *general procedure (3e)*: Residue **A** and Boc-Lys(Boc)-OH (82 mg, 0.24 mmol) gave the *title compound* **104** (30 mg, 16 %) as an off-white solid after purification by flash column chromatography (PE: Et_2O, 1:3); $[\alpha]_D^{23.5}$ +6.50 (*c* 0.50, $CHCl_3$); δ_H (600 MHz, DMSO-d_6) 9.56 (s, 1 H, H19 or H36), 9.47 (s, 1 H, H19 or H36), 8.99 (d, *J* 7.4 Hz, 1 H, N-H), 8.68 (d, *J* 7.5, 1 H, N-H), 8.29 (d, *J* 7.5, 1 H, Ar-H), 8.23 (d, *J* 8.3, 3 H, Ar-H), 7.78 - 7.86 (m, 3 H, Ar-H), 7.73 (d, *J* 7.5, 1 H, Ar-H), 7.55 - 7.67 (m, 6 H, Ar-H), 7.43 - 7.49 (m, 2 H, Ar-H), 7.22 (t, *J* 7.0, 1 H, Ar-H), 7.19 (t, *J* 7.5, 1 H, Ar-H), 6.87 - 6.92 (m, 1 H, N-H), 6.73 - 6.81 (m, 2 H, N-H), 6.61 - 6.67 (m, 1 H, N-H), 5.29 (d, *J* 6.2, 1 H, H49), 5.17 (d, *J* 6.2, 1 H, H49'), 4.97 - 5.06 (m, 1 H, H16 or H22), 4.78 - 4.90 (m, 2 H, H9 or H16 or H22 or H26 or H39), 4.56 - 4.65 (m, 1 H, H9 or C26 or C39), 3.98 - 4.07 (m, 1 H, H9 or C26 or C39), 3.61 - 3.69 (m, 2 H, H50, H50'), 2.81 - 2.98 (m, 6 H, H5, H5', H30, H30', H43, H43'), 1.76 - 1.91 (m, 3 H, alkyl-H), 1.63 - 1.75 (m, 2 H, alkyl-H), 1.54 - 1.58 (m, 1 H, alkyl-H), 1.37 - 1.45 (m, 54H, H1, H13, H34, H47, 18 x alkyl-H) H 0.83 - 0.88 (m, 2 H, H51, H51'), 0.00 (s, 9 H, H52); δ_C (151 MHz, DMSO-d_6) 172.3 (C14 or C18 or C24 or C35

or C48), 171.8 (C14 or C18 or C24 or C35 or C48), 171.8 (C14 or C18 or C24 or C35 or C48), 171.4 (C14 or C18 or C24 or C35 or C48), 171.1 (C14 or C18 or C24 or C35 or C48), 167.7 (C20 or C37), 166.6 (C20 or C37), 155.5 (C3 or C11 or C32 or C45), 155.5 (C3 or C11 or C32 or C45), 155.4 (C3 or C11 or C32 or C45), 155.3 (C3 or C11 or C32 or C45), 139.8, 139.6, 139.2, 137.4, 136.7, 132.9, 132.6, 131.8, 131.8, 130.5, 130.4, 129.7, 129.6, 128.6, 128.6, 128.3, 128.0, 124.9, 123.8, 123.7, 121.0, 120.6, 120.4, 113.0, 112.7 (24 x Ar-C), 94.2, 93.9, 89.0, 88.8 (4 x alkynyl-C), 88.7 (C49), 78.0 (C2 or C12 or C33 or C46), 77.3 (C2 or C12 or C33 or C46), 77.3 (C2 or C12 or C33 or C46), 77.2 (C2 or C12 or C33 or C46), 66.8 (C50), 54.1 (C9 or C26 or C39), 53.4 (C9 or C26 or C39), 52.8 (C9 or C26 or C39), 48.8 (C16 or C22), 48.7 (C16 or C22), 38.2 (C5 or C30 or C43), 34.4 (C5 or C30 or C43), 32.2 (C5 or C30 or C43), 31.6 (C8 or C27 or C40), 30.4 (C8 or C27 or C40), 30.1 (C8 or C27 or C40), 29.4 (C6 or C29 or C42), 29.2 (C6 or C29 or C42), 29.1 (C6 or C29 or C42), 28.3 (C1 or C13 or C34 or C47), 28.2 (C1 or C13 or C34 or C47), 28.2 (C1 or C13 or C34 or C47), 28.1 (C1 or C13 or C34 or C47), 22.9 (C7 or C28 or C41), 22.8 (C7 or C28 or C41), 22.6 (C7 or C28 or C41), 18.8 (C17 or C23), 18.2 (C17 or C23), 17.3 (C51), -1.5 (C52); IR ($CHCl_3$) 3305 (broad), 3285, 3209, 2930, 2420, 1715, 1698; HRMS calculated for $C_{80}H_{113}N_{10}O_{17}Si$ $[M+H]^+$: 1513.8049, found 1513.8044.

(S)-Methyl 2-((((9H-fluoren-9-yl)methoxy)carbonyl)amino)-6-((tert-butoxycarbonyl)amino)hexanoate 105

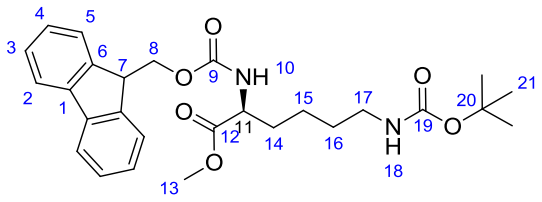

According to *general procedure (4b)*: Fmoc-Lys(Boc)-OH **98** (250 mg, 0.53 mmol) and methyl iodide (180 µL, 2.65 mmol) gave the *title compound* **105** (243 mg, 95 %) as a white

solid after flash column chromatography (PE:Et_2O, 1:1); $[\alpha]_D^{25.0}$ -1.00 (*c* 1.00, $CHCl_3$); δ_H (400 MHz, $CDCl_3$) 7.67 (d, *J* 7.3, 2 H, H5), 7.52 (dd, *J* 7.1, 3.2, 2 H, H4), 7.28 - 7.34 (m, 2 H, H3), 7.20 - 7.26 (m, 2 H, H2), 5.42 (d, *J* 7.6, 1 H, H10), 4.55 (br. s., 1 H, H18), 4.22 - 4.39 (m, 3 H, H8, H8', H11), 4.10 - 4.17 (m, 1 H, H7), 3.66 (s, 3 H, H13), 3.02 (d, *J* 5.9, 2 H, H17, H17'), 1.71 - 1.84 (m, 1 H, H14), 1.61 (s, 1 H, H14'), 1.38 - 1.47 (m, 2 H, H16, H16'), 1.35 (s, 9 H, H21), 1.23 - 1.32 (m, 2 H, H15, H15'); δ_C (101 MHz, $CDCl_3$) 172.9 (C12), 156.0 (C19), 155.9 (C9), 143.7 (C6), 141.2 (C1), 127.6 (C3), 127.0 (C2), 125.0 (C4), 119.9 (C5), 79.1 (C20), 66.9 (C8), 53.7 (C11), 52.3 (C13), 47.1 (C7), 39.9 (C17), 32.0 (C14), 29.5 (C16), 28.3 (C21), 22.3 (C15); IR ($CHCl_3$) 3339, 2950, 2865, 2360, 2341, 2249, 1691; HRMS calculated for $C_{27}H_{34}N_2NaO_6$ $[M+Na]^+$: 505.2309, found 505.2305.

(S)-Methyl 6-((tert-butoxycarbonyl)amino)-2-(2-iodobenzamido)hexanoate 106

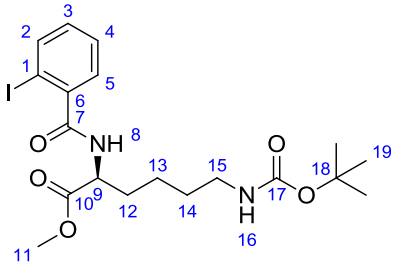

According to *general procedure (3g)*: Fmoc-protected amine **105** (800 mg, 1.66 mmol) gave Residue **A**. According to *general procedure (3d)*: Residue **A** and 2-iodobenzoyl chloride (880 mg, 3.32 mmol) gave the *title compound* **106** (683 mg, 84 %) as a pale yellow oil after flash column chromatography (PE:Et_2O, 1:1); $[\alpha]_D^{23.5}$ -14.5 (*c* 1.00, $CHCl_3$); δ_H (400 MHz, $CDCl_3$) 7.78 (d, *J* 7.2, 1 H, H2), 7.26 - 7.36 (m, 2 H, H4, H5), 7.02 (td, *J* 7.5, 1.8, 1 H, H3), 6.56 (d, *J* 7.3, 1 H, H8), 4.66 - 4.75 (m, 1 H, H9), 4.62 (br. s., 1 H, H16), 3.70 (s, 3 H, H11), 3.04 (d, *J* 5.6, 2 H, H15, H15'), 1.87 - 1.98 (m, 1 H, H12), 1.69 - 1.81 (m, 1 H, H12'), 1.40 - 1.52 (m, 4 H, H13, H13', H14, H14'), 1.31 (s, 9 H, H19); δ_C (101 MHz, $CDCl_3$) 172.4 (C10), 168.9 (C7), 156.0 (C17), 141.5 (C6), 139.8 (C2), 131.1 (C3), 128.3 (C4), 128.0 (C5),

92.3 (C1), 79.0 (C18), 52.4 (2C, C9, C11), 39.9 (C15), 31.8 (C12), 29.5 (C14), 28.3 (H19), 22.5 (C13); IR ($CHCl_3$) 3295, 3058, 2975, 2933, 2865, 2360, 2341, 2246, 1738, 1691. HRMS calculated for $C_{21}H_{26}N_2NaO_5I$ $[M+Na]^+$: 513.0881, found 513.0851.

(S)-Methyl 2-(2-((2-aminophenyl)ethynyl)benzamido)-6-((tert-butoxycarbonyl)amino)hexanoate 107

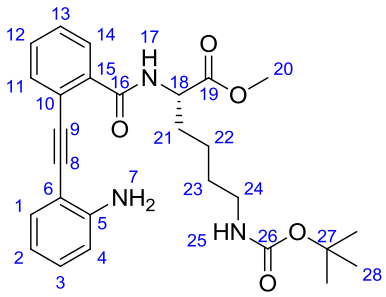

According to *general procedure (3a)*: Iodide **106** (680 mg, 1.39 mmol) and alkyne **43** (250 mg, 2.09 mmol) gave the *title compound* **107** (380 mg, 57 %) as a pale yellow oil after flash column chromatography (PE:Et_2O, 1:1); $[\alpha]_D^{25.0}$ +14.0 (*c* 0.50, $CHCl_3$); δ_H (400 MHz, $CDCl_3$) 7.65 (dd, *J* 7.7, 1.1, 1 H, H13), 7.42 (dd, *J* 7.6, 1.2, 1 H, H11), 7.26 (td, *J* 7.5, 1.7, 1 H, H12), 7.18 - 7.23 (m, 2 H, H14, H17), 7.16 (dd, *J* 7.8, 1.5, 1 H, H1), 6.92 - 6.98 (m, 1 H, H3), 6.46 - 6.54 (m, 2 H, H2, H4), 4.55 - 4.62 (m, 1 H, H25), 4.47 (br. s., 2 H, H7), 4.33 - 4.41 (m, 1 H, H18), 3.52 (s, 3 H, H20), 2.70 – 2.82 (m, 2 H, H24, H24'), 1.66 - 1.79 (m, 1 H, H21), 1.51 - 1.63 (m, 1 H, H21'), 1.22 (s, 9 H, H28), 1.09 - 1.20 (m, 4 H, H22, H22', H23, H23'); δ_C (101 MHz, $CDCl_3$) 172.6 (C19), 167.0 (C16), 156.0 (C26), 149.0 (C5), 135.6 (C15), 133.2 (C11), 132.0 (C1), 130.6 (C12), 130.3 (C14), 128.7 (C13), 128.3 (C3), 121.0 (C10), 117.3 (C2), 114.3 (C4), 106.5 (C6), 92.3 (C9), 92.2 (C8), 79.0 (C27), 52.8 (C18), 52.3 (C20), 40.0 (C24), 32.0 (C21), 29.5 (C23), 28.3 (C28), 22.6 (C22); IR ($CHCl_3$) 3431 (broad), 3348, 2977, 2950, 2210, 1741, 1690, 1655; HRMS calculated for $C_{27}H_{33}N_3NaO_5$ $[M+Na]^+$: 502.2312, found 502.2308.

(S)-Methyl 2-(2-((2-((S)-2-((((9H-fluoren-9-yl)methoxy)carbonyl)amino)-6-((tert-butoxycarbonyl)amino)hexanamido)phenyl)ethynyl)benzamido)-6-((tert-butoxycarbonyl)amino)hexanoate 108

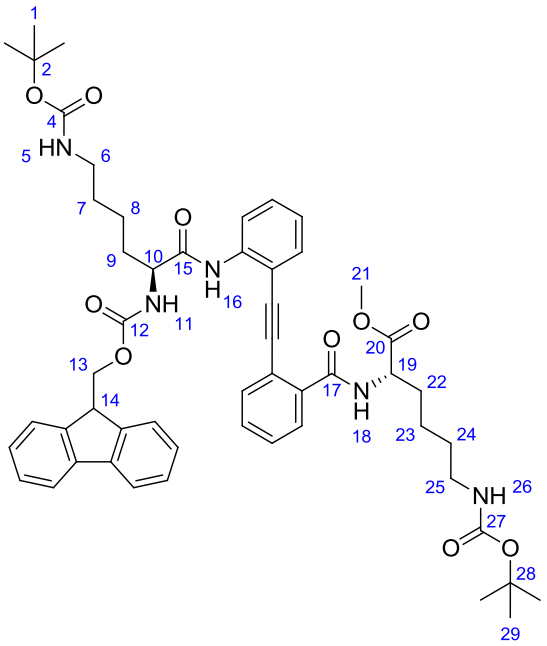

According to *general procedure (3c)*: Aniline **107** (150 mg, 0.31 mmol) and Fmoc-Lys(Boc)-OH **98** (187 mg, 0.40 mmol) gave the *title compound* **108** (200 mg, 71 %) as a pale yellow oil after purification by flash column chromatography (PE:Et_2O, 1:4); $[\alpha]_D^{25.0}$ -14.0 (*c* 1.00, $CHCl_3$); δ_H (400 MHz, $CDCl_3$) 9.11 (s, 1 H, H16), 8.28 (d, *J* 8.6, 1 H, Ar-H), 7.56 (d, *J* 7.6, 2 H, Ar-H), 7.47 (dd, *J* 7.6, 1 H, Ar-H), 7.44 (d, *J* 7.4, 1 H, Ar-H), 7.36 (dd, *J* 7.3, 3.7, 3 H, Ar-H), 7.32 (dd, *J* 7.7, 1.3, 1 H, Ar-H), 7.05 - 7.25 (m, 7 H, Ar-H), 6.98 (d, *J* 7.3, 1 H, H18), 6.88 - 6.94 (m, 1 H, Ar-H), 6.33 (d, *J* 8.1, 1 H, H11), 4.62 - 4.80 (m, 3 H, H10, H19, H5 or H26), 4.56 (br. s., 1 H, H5 or H26), 4.02 - 4.10 (m, 1 H, H13), 3.92 - 4.01 (m, 1 H, H13'), 3.84 - 3.91 (m, 1 H, H14), 3.40 (s, 3 H, H21), 2.86 (br. s., 4 H, H6, H6', H25, H25'), 1.39 - 1.89 (m, 6 H, 6 of H7, H7', H8, H8', H9, H9', H22, H22', H23, H23', H24, H24'), 1.26 - 1.32 (m, 6 H, 6 of H7, H7', H8, H8', H9, H9', H22, H22', H23, H23', H24, H24'), 1.23 (s, 9 H, H1 or H29), 1.19 (s, 9 H, H1 or H29); δ_C (101 MHz, $CDCl_3$) 172.7 (C15), 171.4 (C20), 167.6 (C17), 156.1 (C4, C27), 155.9 (C12), 143.9, 143.7, 141.1, 141.0, 139.8, 136.3, 133.2,

131.5, 130.6, 129.8, 128.5, 127.5, 126.9, 125.1, 125.0, 123.5, 121.1, 119.8 (18 x Ar-C), 93.8, 89.4 (2 x alkynyl-C), 78.8 (C2 or C28), 78.8 (C2 or C28), 66.8 (C13), 55.3 (C21), 52.7 (C10), 52.3 (C19), 46.9 (C14), 40.1 (C6 or C25), 39.7 (C6 or C25), 33.8 (C7 or C24), 33.0 (C7 or C24), 31.7 (C9 or C22), 29.5 (C9 or C22), 28.3 (C1 or C29), 28.2 (C1 or C29), 22.6 (C8 or C23), 22.3 (C8 or C23); IR ($CHCl_3$) 3276 (broad), 3066, 2978, 2930, 2863, 1745, 1712; HRMS calculated for $C_{53}H_{63}N_5NaO_{10}$ $[M+Na]^+$: 952.4467, found 952.4460.

(S)-Methyl 2-(2-((2-((S)-2-((S)-2-(2-((2-((S)-2-((((9H-fluoren-9-yl)methoxy)carbonyl)amino)propanamido)phenyl)ethynyl)benzamido)propanamido)-6-((tert-butoxycarbonyl)amino)hexanamido)phenyl)ethynyl)benzamido)-6-((tert-butoxycarbonyl)amino)hexanoate 109

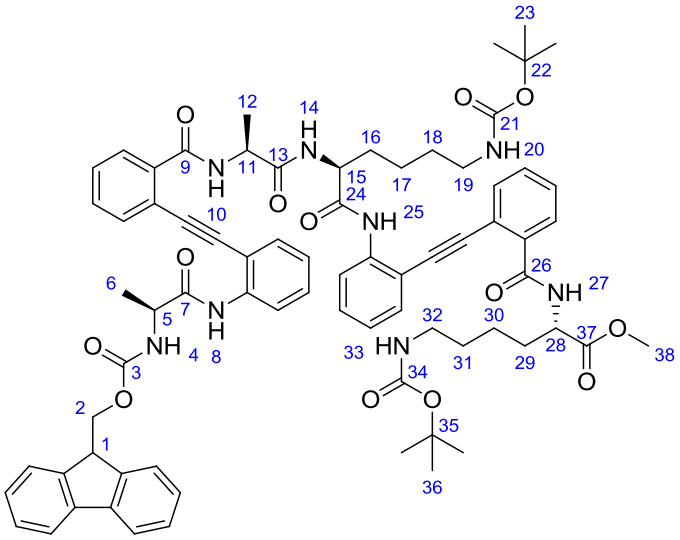

According to *general procedure (3g)*: Fmoc-protected amine **108** (106 mg, 0.15 mmol) gave residue **A**. According to *general procedure (3f)*: *tert*-Butyl ester **48** (300 mg, 0.45 mmol) gave residue **B**. According to *general procedure (3e)*: Residue **A** and residue **B** gave the *title compound* **109** (100 mg, 52 %) as a pale yellow solid after purification by flash column chromatography (PE:Et_2O, 1:4); $[\alpha]_D^{25.0}$ +16.0 (*c* 0.50, $CHCl_3$); δ_H (400 MHz, $CDCl_3$) 9.55 (br. s., 1 H, H8 or H25), 9.23 (br. s., 1 H, H8 or H25), 8.57 (d, *J* 8.3, 1 H, Ar-H), 8.25 - 8.34 (m, 1 H, Ar-H), 7.65 (d, *J* 7.3, 3 H, H27, 2 x Ar-H), 7.58 (t, *J* 8.2, 6 H, H20, H33, 4 x Ar-H),

7.36 - 7.46 (m, 4 H, Ar-H), 7.25 - 7.31 (m, 5 H, Ar-H), 7.07 - 7.22 (m, 5 H, H4, 5 x Ar-H), 6.90 - 7.03 (m, 3 H, H14, 2 x Ar-H), 5.98 - 6.08 (m, 1 H, H10), 5.28 - 5.38 (m, 1 H, H5), 5.17 (br. s., 1 H, H11), 4.98 - 5.07 (m, 1 H, H28), 4.79 - 4.89 (m, 1 H, H15), 4.49 - 4.60 (m, 1 H, H2), 4.13 - 4.29 (m, 2 H, H1, H2'), 3.56 (s, 3 H, H38), 2.46 - 3.09 (m, 4 H, H19, H19, H32, H32'), 1.63 - 1.96 (m, 4 H, H16, H16', H29, H29'), 1.43 - 1.52 (m, 6 H, H6, H12), 1.18 - 1.41 (m, 24 H, H22, H36 and 6 of H17, H17', H18, H18', H30, H30', H31, H31'), 0.89 - 1.01 (m, 2 H, 2 of H17, H17', H18, H18', H30, H30', H31, H31'); δ_C (101 MHz, $CDCl_3$); 172.9, 172.7, 172.4, 170.8 (4 x C=O), 167.4 (C9 or C26), 166.1 (C9 or C26), 156.1 (C3 or C21 or C34), 156.0 (C3 or C21 or C34), 155.7 (C3 or C21 or C34), 144.1, 143.7, 143.5, 141.2, 140.3, 136.5, 134.1, 133.6, 133.2, 132.1, 131.6, 131.1, 130.8, 130.3, 129.9, 128.7, 127.8, 127.6, 127.0, 125.5, 125.4, 125.0, 123.5, 123.4, 121.4, 120.6, 120.0, 119.8, 112.4, 112.1 (30 x Ar-C), 95.2, 93.8, 90.0, 89.8 (4 x alkynyl-C), 79.0 (2C, C22, C35), 67.3 (C2), 53.5 (C28), 52.5 (C15), 52.3 (C38), 50.9 (C5), 49.2 (C11), 47.1 (C1), 40.2 (C19 or C32), 40.0 (C19 or C32), 33.5 (C16 or C29), 32.3 (C16 or C29), 30.3 (C18 or C31), 29.4 (C18 or C31), 28.5 (C23 or C36), 28.4 (C23 or C36), 22.9 (C17 or C30), 22.6 (C17 or C30), 21.1 (C6), 20.0 (C12); IR ($CHCl_3$) 3279 (broad), 3066, 2978, 2932, 2684, 2218, 1745, 1713; HRMS calculated for $C_{74}H_{83}N_8O_{13}$ $[M+H]^+$: 1291.6074, found 1292.6108.

(S)-tert-Butyl 6-azido-2-((tert-butoxycarbonyl)amino)hexanoate 113

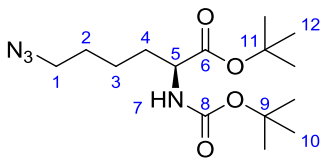

According to *general procedure (4f)*: Carboxylic acid **112** (400 mg, 1.54 mmol) and *tert*-butanol gave the *title compound* **113** (200 mg, 40 %) as a colourless oil after purification by flash column chromatography (PE:Et_2O, 2:1); $[\alpha]_D^{23.5}$ +8.00 (*c* 1.00, $CHCl_3$); δ_H (400 MHz, $CDCl_3$) 4.95 - 5.17 (m, 1 H, H7), 4.08 - 4.27 (m, 1 H, H5), 3.27 (t, *J* 6.8, 2 H, H1, H1'), 1.76

- 1.83 (m, 1 H, H4), 1.57 - 1.68 (m, 4 H, H2, H2', H3, H4'), 1.47 (s, 9 H, H10 or H12), 1.44 (s, 9 H, H10 or H12), 1.41 - 1.43 (m, 1 H, H3'); δ_C (101 MHz, $CDCl_3$) 171.7 (C6), 155.3 (C8), 81.8 (C9 or C11), 79.5 (C9 or C11), 53.6 (C5), 51.1 (C1), 32.4 (C4), 28.4 (C2), 28.2 (C10 or C12), 27.9 (C10 or C12), 22.3 (C3); IR ($CHCl_3$) 2943, 2855, 2595, 2155, 2146, 2077, 1699; LRMS calculated for $C_{15}H_{28}N_4NaO_4$ $[M+Na]^+$: 351.2, found 351.2.

Fmoc-L-Lysine-tert-butyl ester 114

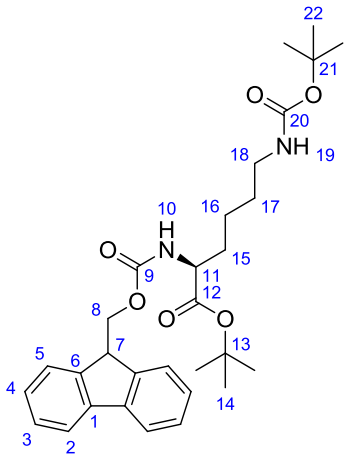

According to *general procedure (4f)*: Fmoc-Lys(Boc)-OH **98** (5.00 g, 10.6 mmol) and *tert*-butanol (10.0 mL, 106 mmol) gave the *title compound* **114** (3.4 g, 61 %) as a white solid after purification by flash column chromatography (PE:Et_2O, 1:1); $[\alpha]_D^{23.5}$ +3.00 (*c* 1.00, $CHCl_3$); δ_H (400 MHz, $CDCl_3$) 7.67 (d, *J* 7.6, 2 H, H2), 7.52 (d, *J* 7.6, 2 H, H5), 7.31 (t, *J* 7.0, 2 H, H3), 7.22 (t, *J* 7.0, 2 H, H4), 5.38 (d, *J* 7.6, 1 H, H10), 4.48 - 4.59 (m, 1 H, H19), 4.25 - 4.34 (m, *J* 7.1, 2.7, 2 H, H8, H8'), 4.10 - 4.21 (m, 2 H, H7, H11), 2.96 - 3.08 (m, 2 H, H18, H18'), 1.68 - 1.80 (m, 1 H, H15), 1.53 - 1.65 (m, 1 H, H15'), 1.41 - 1.47 (m, *J* 6.6, 2 H, H17, H17'), 1.38 (s, 9 H, H14 or H22), 1.35 (s, 9 H, H14 or H22), 1.18 - 1.31 (m, 2 H, H16, H16'); δ_C (101 MHz, $CDCl_3$) 171.5 (C12), 155.9 (C20), 155.9 (C9), 143.9 (C6'), 143.7 (C6), 141.2 (C1), 127.6 (C3), 127.0 (C4), 125.0 (C5), 119.9 (C2), 82.0 (C13), 79.0 (C21), 66.8 (C8), 54.1 (C11), 47.1 (C7), 40.1 (C18), 32.3 (C15), 29.5 (C17), 28.3 (C22), 27.9 (C14), 22.2 (C16); IR

($CHCl_3$) 3338 (broad), 3067, 2977, 2933, 2867, 2250, 1699, 1510; HRMS calculated for $C_{30}H_{40}N_2NaO_6$ $[M+Na]^+$: 547.2779, found 547.2791.

(S)-tert-Butyl 6-((tert-butoxycarbonyl)amino)-2-(2-iodobenzamido)hexanoate 115

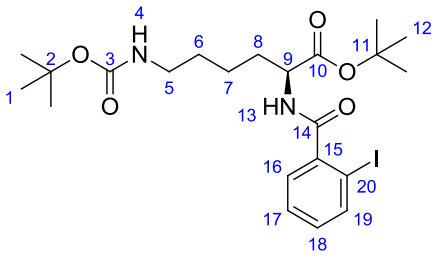

According to *general procedure (3g)*: Fmoc-protected amine **114** (6.0 g, 11.2 mmol) gave Residue **A**. According to *general procedure (3d)*: Residue **A** and 2-iodobenzoyl chloride (4.0 g, 15 mmol) gave the *title compound* **115** (4.8 g, 90 %) as a colourless liquid after purification by flash column chromatography (Et_2O); $[\alpha]_D^{23.5}$ -4.20 (*c* 1.00, $CHCl_3$); δ_H (400 MHz, $CDCl_3$) 7.80 (dd, *J* 7.9, 0.9, 1 H, H19), 7.36 (dd, *J* 8.0, 2.0, 1 H, H16), 7.31 (td, *J* 7.3, 1.0, 1 H, H17), 7.03 (td, *J* 7.5, 2.0 Hz, 1 H, H18), 6.31 - 6.46 (m, 1 H, H13), 4.57 - 4.63 (m, 1 H, H9), 4.46 - 4.56 (m, 1 H, H4), 2.96 - 3.13 (m, 2 H, H5, H5'), 1.86 - 1.97 (m, 1 H, H8), 1.68 - 1.77 (m, 1 H, H8'), 1.44 - 1.54 (m, 3 H, H6, H6', H7), 1.42 (s, 9 H, H1), 1.34 – 1.37 (m, 1H, H7'), 1.33 (s, 9 H, H12); δ_C (101 MHz, $CDCl_3$) 171.2 (C10), 168.7 (C14), 156.0 (C3), 141.7 (C15), 139.9 (C19), 131.2 (C18), 128.3 (C17), 128.1 (C16), 92.4 (C20), 82.4 (C11), 79.1 (C2), 53.0 (C9), 40.1 (C5), 32.2 (C8), 29.6 (C6), 28.4 (C1), 28.0 (C12), 22.4 (C7); IR ($CHCl_3$) 3307 (broad), 3054, 2977, 2935, 2861, 1703, 1657, 1625; HRMS calculated for $C_{22}H_{34}N_2NIO_5$ $[M+H]^+$: 533.1507, found 533.1503.

(S)-tert-Butyl (6-azido-1-((2-iodophenyl)amino)-1-oxohexan-2-yl)carbamate 116

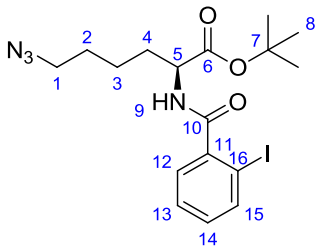

According to *general procedure (4g)*: Boc protected lysine **115** (1.2 g, 2.25 mmol) gave Residue **A**. According to *general procedure (4e)*: Residue **A** gave the *title compound* **116** (110 mg, 10 %) as a colourless oil after purification by flash column chromatography (PE:Et_2O, 3:2); $[\alpha]_D^{23.5}$ +5.00 (*c* 0.60, $CHCl_3$); δ_H (400 MHz, $CDCl_3$) 7.79 (dd, *J* 7.8, 0.7, 1 H, H15), 7.34 (dd, *J* 8.0, 2.0, 1 H, H12), 7.30 (td, *J* 7.1, 1.0, 1 H, H13), 7.00 - 7.06 (m, 1 H, H14), 6.40 (d, *J* 8.0, 1 H, H9), 4.59 - 4.66 (m, 1 H, H5), 3.17 - 3.26 (m, 2 H, H1, H1'), 1.88 - 1.99 (m, 1 H, H4), 1.69 - 1.76 (m, 1 H, H4'), 1.47 - 1.65 (m, 3 H, H2, H3, H3'), 1.43 (s, 10 H, H2', H8); δ_C (101 MHz, $CDCl_3$) 171.1 (C6), 168.7 (C10), 141.7 (C11), 140.0 (C15), 131.3 (C14), 128.3 (C12), 128.2 (C13), 92.4 (C16), 82.6 (C7), 52.9 (C5), 51.1 (C1), 32.1 (C4), 28.5 (C2), 28.0 (C8), 22.4 (C3); IR ($CHCl_3$) 3299 (broad), 3056, 2979, 2933, 2866, 2094, 1730, 1650, 1586, 1526; HRMS calculated for $C_{17}H_{23}N_4NaIO_3$ $[M+Na]^+$: 481.0707, found 481.0708.

(S)-tert-Butyl 2-(2-((2-aminophenyl)ethynyl)benzamido)-6-azidohexanoate 117

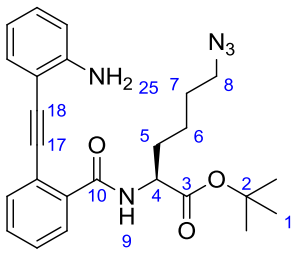

According to *general procedure (3a)*: Iodide **116** (275 mg, 0.60 mmol) and alkyne **43** (140 mg, 1.20 mmol) gave the *title compound* **117** (170 mg, 64 %) after purification by flash column chromatography (PE:Et_2O, 1:1); $[\alpha]_D^{25.0}$ -3.00 (*c* 1.00, $CHCl_3$); δ_H (400 MHz, $CDCl_3$)

7.65 (d, *J* 7.8, 1 H, Ar-H), 7.12 - 7.19 (m, 3 H, Ar-H), 6.86 - 6.94 (m, 2 H, Ar-H), 6.57 (d, *J* 7.8, 1 H, Ar-H), 6.51 (t, *J* 7.5, 1 H, Ar-H), 6.40 (d, *J* 7.8, 1 H, H9), 5.34 (br. s., 2 H, H25), 4.46 - 4.53 (m, 1 H, H4), 4.22 (td, *J* 6.8, 3.9, 2 H, H8, H8'), 1.77 - 1.90 (m, 3 H, H5, H5', H7), 1.57 - 1.68 (m, 1 H, H7'), 1.34 - 1.42 (m, 1 H, H6), 1.29 (s, 9 H, H1), 1.22 - 1.27 (m, 1 H, H6'); δ_C (101 MHz, $CDCl_3$) 170.7 (C3), 168.7 (C10), 148.2, 144.9, 141.3, 139.7, 131.1, 128.7, 128.1, 128.0, 127.6, 117.1, 116.5, 113.4 (12 x Ar-C), 92.2 (2C, C17, C18), 82.4 (C2), 52.6 (C4), 49.8 (C8), 31.7 (C7), 29.4 (C5), 27.8 (C1), 22.1 (C6); IR ($CHCl_3$) 3452, 3345, 3130, 3058, 2930, 2863, 2243, 1727, 1654, 1617; HRMS calculated for $C_{25}H_{29}N_5NaO_3$ $[M+Na]^+$: 470.2163, found 470.2159.

(S)-tert-Butyl 6-azido-2-(2-((2-((S)-6-azido-2-((tert-butoxycarbonyl)amino)hexanamido)phenyl)ethynyl)benzamido)hexanoate 118

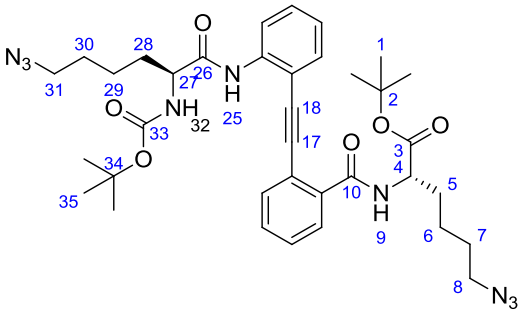

According to *general procedure (3c)*: Aniline **117** (175 mg, 0.39 mmol) and acid **112** (139 mg, 0.51 mmol) gave the *title compound* **118** (100 mg, 37 %) as a colourless oil after purification by flash column chromatography (Et_2O); $[\alpha]_D^{23.5}$ -12.5 (*c* 1.00, $CHCl_3$); δ_H (400 MHz, $CDCl_3$) 11.73 (s, 1 H, H25), 8.62 (d, *J* 8.1, 1 H, Ar-H), 7.79 - 7.85 (m, 1 H, Ar-H), 7.48 (d, *J* 8.0, 1 H, Ar-H), 7.30 - 7.36 (m, 3 H, Ar-H), 7.08 (td, *J* 7.4, 2.3, 2 H, Ar-H), 6.49 (d, *J* 8.0, 1 H, H9), 5.41 (d, *J* 8.0, 1 H, H32), 4.68 - 4.74 (m, 1 H, H4), 4.48 (t, *J* 6.8, 2 H, H8, H8' or H31, H31'), 4.38 - 4.45 (m, 1 H, H27), 3.24 (t, *J* 6.8, 2 H, H8, H8' or H31, H31'), 2.13 - 2.23 (m, 1 H, H7 or H30), 1.99 - 2.11 (m, 3 H, 3 of H7, H7', H30, H30'), 1.75 -

1.88 (m, 2 H, H6, H29), 1.55 - 1.71 (m, 4 H, H5, H5', H28, H28'), 1.44 - 1.49 (m, 18 H, H1, H35), 1.28 - 1.40 (m, 2 H, H6', H29'); δ_C (101 MHz, $CDCl_3$) 170.9 (C3 or C26), 170.9 (C3 or C26), 168.8 (C10), 155.4 (C33), 147.4, 141.3, 139.9, 135.9, 131.3, 128.9, 128.2, 128.1, 127.0, 123.6, 121.3, 117.7 (12 x Ar-C), 92.2 (2C, C17, C18), 82.7 (C2 or C34), 79.7 (C2 or C34), 55.4 (C27), 52.5 (C4), 51.1 (C8 or C31), 50.3 (C8 or C31), 32.0 (C7 or C30), 29.4 (C7 or C30), 28.4 (C5 or C28), 28.2 (C5 or C28), 27.9 (2C, C1, C35), 22.4 (C6 or C29), 22.2 (C6 or C29); IR ($CHCl_3$) 3735, 3566, 2891, 2345, 2322, 1771, 1716; HRMS calculated for $C_{26}H_{48}N_9O_6$ $[M+H]^+$: 702.3722, found 702.3706.

Initial Azide Meander 119

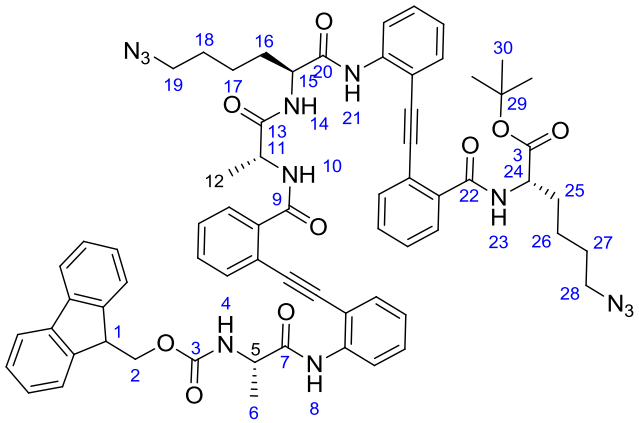

According to *general procedure (4g)*: Boc-protected amine **118** (100 mg, 0.15 mmol) gave Residue **A**. According to *general procedure (3f)*: *tert*-Butyl ester protected acid **48** (187 mg, 0.28 mmol) gave Residue **B**. According to *general procedure (3e)*: Residue **A** and Residue **B** gave the *title compound* **119** (40 mg, 24 %) after purification by flash column chromatography (Et_2O); $[\alpha]_D^{23.5}$ +8.50 (*c* 0.80, $CHCl_3$); δ_H (500 MHz, $CDCl_3$) 11.46 (s, 1 H, H21), 9.55 (s, 1 H, H8), 8.59 (d, *J* 8.4, 1 H, Ar-H), 8.46 (dd, *J* 8.4, 0.8, 1 H, Ar-H), 7.96 (d, *J* 8.2, 1 H, H14), 7.70 (dd, *J* 8.0, 0.6, 1 H, Ar-H), 7.60 - 7.68 (m, 4 H, Ar-H), 7.45 - 7.52 (m, 3 H, Ar-H), 7.41 (td, *J* 7.6, 1.0, 1 H, Ar-H), 7.29 - 7.34 (m, 3 H, Ar-H), 7.24 - 7.28 (m, 4 H,

H10, 3 x Ar-H), 7.22 (dd, *J* 7.3, 0.8, 1 H, Ar-H), 7.18 (dd, *J* 7.0, 1.4, 1 H, Ar-H), 7.12 (td, *J* 7.5, 0.9, 1 H, Ar-H), 7.06 (td, *J* 7.4, 0.9, 1 H, Ar-H), 6.94 - 7.04 (m, 3 H, Ar-H), 6.55 (d, *J* 7.9, 1 H, H23), 5.96 (d, *J* 8.4, 1 H, H4), 5.37 - 5.43 (m, 1 H, H5), 5.21 - 5.27 (m, 1 H, H11), 4.63 - 4.67 (m, 1 H, H24), 4.52 - 4.56 (m, 1 H, H15), 4.24 - 4.38 (m, 3 H, H2, H19 or H28, H19' or H28'), 4.17 (dd, *J* 10.3, 7.8, 1 H, H2'), 4.06 - 4.10 (m, 1 H, H1), 2.81 - 2.88 (m, 2 H, H19 or H28, H19' or H28'), 1.87 - 2.05 (m, 3 H, H25, H18 or H27, H18' or H27'), 1.79 - 1.86 (m, 1 H, H16), 1.73 - 1.77 (m, 1 H, H25'), 1.58 - 1.63 (m, 1 H, H16'), 1.56 (d, *J* 6.8, 3 H, H6), 1.53 (d, *J* 6.8, 3 H, H12), 1.45 - 1.50 (m, 1 H, H17 or H26), 1.39 (s, 10 H, H17' or H26', H30), 1.19 - 1.29 (m, 4 H, 4 of H17, H17', H18, H18', H26, H26', H27, H27'); δ_C (126 MHz, $CDCl_3$) 172.9 (C=O), 172.5 (C=O), 171.0 (C=O), 170.0 (C=O), 168.9 (C9 or C22), 166.1 (C9 or C22), 155.9 (C3), 147.4, 143.9, 143.6, 141.5, 141.2, 141.1, 140.7, 139.9, 135.9, 134.3, 134.1, 132.1, 131.2, 131.1, 130.0, 129.0, 128.2, 128.1, 127.6, 127.3, 127.1, 127.0, 125.3, 125.2, 123.7, 123.3, 122.6, 121.6, 120.7 (30 x Ar-C), 119.8, 95.2 (Alkynyl-C), 92.3 (2C, Alkynyl-C), 89.9 (Alkynyl-C), 82.7 (C29), 67.2 (C2), 54.1 (C15), 52.5 (C24), 50.9 (C5), 50.8 (C19 or C28), 50.2 (C19 or C28), 49.3 (C11), 46.9 (C1), 32.4 (C16), 32.1 (C25), 29.5 (C18 or C27), 28.2 (C18 or C27), 28.0 (C30), 22.5 (C17 or C26), 22.2 (C17 or C26), 21.1 (C6), 19.9 (C12); IR ($CHCl_3$) 5420, 3350, 3282. 2945, 2877, 2355, 1685, 1598; HRMS calculated for $C_{67}H_{68}N_{12}NaO_9$ $[M+Na]^+$: 1207.5124, found 1207.5095.

(S)-tert-Butyl 2-((S)-2-((((9H-fluoren-9-yl)methoxy)carbonyl)amino)-6-((tert-butoxycarbonyl)amino)hexanamido)propanoate 120

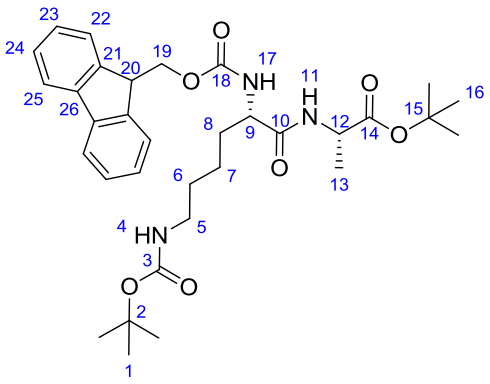

According to *general procedure (3e)*: Fmoc-Lys(Boc)-OH **98** (2.5 g, 5.3 mmol) and L-alanine *tert*-butyl ester hydrochloride (1.0 g, 5.3 mmol) gave the *title compound* **120** (3.0 g, 95 %) as a pale yellow foam after purification by flash column chromatography (PE:Et_2O, 1:4); $[\alpha]_D^{25.0}$ -18.0 (*c* 0.50, $CHCl_3$); δ_H (400 MHz, $CDCl_3$) 7.77 (d, *J* 7.3, 2 H, H25), 7.60 (d, *J* 7.3, 2 H, H22), 7.38 - 7.43 (m, 2 H, H24), 7.32 (tt, *J* 7.2, 1.3, 2 H, H23), 6.57 (d, *J* 5.6, 1 H, H11), 5.55 (d, *J* 6.8, 1 H, H17), 4.70 (br. s., 1 H, H4), 4.35 - 4.48 (m, 3 H, H12, H19, H19'), 4.15 - 4.25 (m, 2 H, H9, H20), 3.03 - 3.19 (m, 2 H, H5, H5'), 1.82 - 1.94 (m, 1 H, H8), 1.63 - 1.74 (m, 1 H, H8'), 1.50 - 1.58 (m, 2 H, H6, H6'), 1.46 (s, 9 H, H1 or H16), 1.44 (s, 9 H, H1 or H16), 1.39 - 1.42 (m, 2 H, H7, H7'), 1.38 (d, *J* 7.1, 3 H, H13); δ_C (101 MHz, $CDCl_3$) 171.8 (C14), 171.0 (C10), 156.2 (C3 or C18), 156.1 (C3 or C18), 143.8 (C21), 141.3 (C26), 127.7 (C24), 127.1 (C23), 125.1 (C22), 119.9 (C25), 82.1 (2C, C2, C15), 67.1 (C19), 54.6 (C9), 48.7 (C12), 47.1 (C20), 39.8 (C5), 32.4 (C8), 29.5 (C1 or C16), 28.4 (C1 or C16), 27.9 (C6), 22.3 (C7), 18.4 (C13); IR ($CHCl_3$) 3309 (broad), 3067, 2978, 2934, 2865, 1736, 1712, 1690; HRMS calculated for $C_{33}H_{45}N_3O_7Na$ $[M+Na]^+$: 618.3150, found 618.3145.

(S)-tert-Butyl 2-((S)-6-((tert-butoxycarbonyl)amino)-2-(2-iodobenzamido)hexanamido)propanoate 121

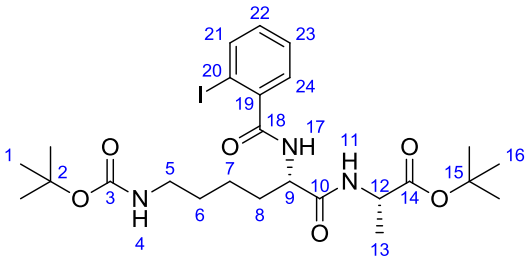

According to *general procedure (3g)*: Fmoc-protected amine **120** (2.0 g, 3.5 mmol) gave Residue **A**. According to *general procedure (3d)*: Residue **A** and 2-iodobenzoyl chloride (1.8 g, 7.0 mmol) gave the *title compound* **121** (1.0 g, 47 %) as an off-white solid after purification by flash column chromatography (Et_2O); $[\alpha]_D^{23.5}$ -12.5 (*c* 1.00, $CHCl_3$); δ_H (400 MHz, $CDCl_3$) 7.85 (d, *J* 7.8, 1 H, H21), 7.33 - 7.41 (m, 2 H, H22, H24), 7.10 (td, *J* 7.5, 2.0, 1 H, H23), 6.88 (d, *J* 8.0, 1 H, H17), 6.73 (d, *J* 8.0, 1 H, H11), 4.74 - 4.83 (m, 1 H, H4), 4.67 - 4.71 (m, 1 H, H9), 4.43 (quin, *J* 7.2, 1 H, H12), 3.04 - 3.22 (m, 2 H, H5, H5'), 1.95 - 2.05 (m, 1 H, H8), 1.77 - 1.86 (m, 1 H, H8'), 1.50 - 1.61 (m, 4 H, H6, H6', H7, H7'), 1.47 (s, 9 H, H1 or H16), 1.41 (s, 9 H, H1 or H16), 1.38 (d, *J* 7.1, 3 H, H13); δ_C (101 MHz, $CDCl_3$) 171.7 (H14), 170.5 (H10), 169.1 (C18), 156.1 (C3), 141.5 (C19), 139.8 (C21), 131.2 (C22), 128.3 (C23), 128.1 (C24), 92.4 (C20), 81.9 (C2 or C15), 79.0 (C2 or C15), 53.2 (C9), 48.8 (C12), 39.9 (C5), 32.2 (C8), 29.5 (C6), 28.4 (C1 or C16), 27.9 (C1 or C16), 22.5 (C7), 18.2 (C13); IR ($CHCl_3$) 3273 (broad), 2066, 2891, 2937, 2864, 2365, 1690, 1641; HRMS calculated for $C_{25}H_{39}N_3O_6I$ $[M+H]^+$: 604.1878, found 604.1885.

(S)-tert-Butyl 2-((S)-2-(2-((2-aminophenyl)ethynyl)benzamido)-6-((tert-butoxycarbonyl)amino)hexanamido)propanoate 122

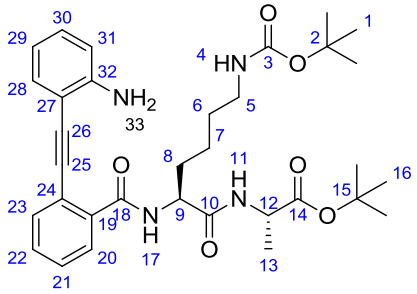

According to *general procedure (3a)*: Iodide **121** (1.00 g, 1.65 mmol) and alkyne **43** (0.40 g, 3.32 mmol) gave the *title compound* **122** (0.75 g, 77 %) after purification by flash column chromatography (Et_2O); $[\alpha]_D^{23.5}$ -5.00 (*c* 1.00, $CHCl_3$); δ_H (400 MHz, $CDCl_3$) 7.78 (dd, *J* 7.7, 1.1, 1 H, Ar-H), 7.60 (dd, *J* 7.6, 1.0, 1 H, Ar-H), 7.44 (td, *J* 7.6, 1.5, 1 H, Ar-H), 7.40 (d, *J* 7.8, 1 H, H17), 7.34 - 7.38 (m, 2 H, Ar-H), 7.13 (td, *J* 7.7, 1.5, 1 H, Ar-H), 6.82 (d, *J* 7.6, 1 H, H11), 6.64 - 6.72 (m, 2 H, Ar-H), 4.73 (br. s., 2 H, H33), 4.63 - 4.70 (m, 2 H, H4, H9), 4.38 (quin, *J* 7.1, 1 H, H12), 2.91 - 3.07 (m, 2 H, H5, H5'), 1.92 - 1.98 (m, 1 H, H8), 1.68 - 1.79 (m, 1 H, H8'), 1.45 (s, 9 H, H1 or H16), 1.41 (s, 13 H, H1 or H16, H6, H6', H7, H7'), 1.28 (d, *J* 7.1, 3 H, H13); δ_C (101 MHz, $CDCl_3$) 171.8 (C14), 170.8 (C10), 167.4 (C18), 156.0 (C3), 149.0, 135.7, 133.2, 132.1, 130.6, 130.3, 128.4, 128.2, 121.2, 117.4, 114.4, 106.7 (12 x Ar-C), 92.3 (C25 or C26), 92.3 (C25 or C26), 81.9 (C2 or C15), 78.9 (C2 or C15), 53.6 (C9), 48.7 (C12), 39.9 (C5), 32.1 (C8), 29.5 (C6), 28.4 (C1 or C16), 27.9 (C1 or C16), 22.6 (C7), 18.1 (C13); IR ($CHCl_3$) 3344 (broad), 3064, 2980, 2935, 2867, 2248, 2210, 1691, 1635, 1593, 1516; HRMS calculated for $C_{33}H_{45}N_4O_6$ $[M+H]^+$: 593.3345, found 593.3330.

(S)-tert-Butyl 2-((S)-2-(2-((2-((S)-2-((((9H-fluoren-9-yl)methoxy)carbonyl)amino)-6-((tert-butoxycarbonyl)amino)hexanamido)phenyl)ethynyl)benzamido)-6-((tert-butoxycarbonyl)amino)hexanamido)propanoate 123

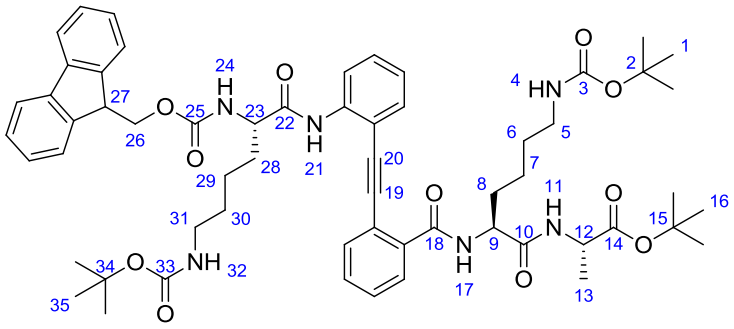

According to *general procedure (3c)*: Aniline **122** (690 mg, 1.16 mmol) and Fmoc-Lys(Boc)-OH **98** (706 mg, 1.51 mmol) gave the *title compound* **123** (800 mg, 51 %) after purification by flash column chromatography (2:1, PE:Et_2O); $[\alpha]_D^{23.5}$ +9.50 (*c* 1.00, $CHCl_3$); δ_H (400 MHz, $CDCl_3$) 9.43 (s, 1 H, H21), 8.62 (d, *J* 8.3, 1 H, Ar-H), 7.76 (dd, *J* 7.5, 2.6, 2 H, Ar-H), 7.60 - 7.69 (m, 5 H, H11, 4 x Ar-H), 7.52 (dd, *J* 7.7, 1.3, 1 H, Ar-H), 7.47 (td, *J* 7.7, 0.7, 1 H, Ar-H), 7.28 - 7.43 (m, 6 H, Ar-H), 7.05 - 7.11 (m, 2 H, H17, 1 x Ar-H), 6.07 (d, *J* 8.2, 1 H, H24), 5.32 - 5.39 (m, 1 H, H9), 5.10 - 5.18 (m, 1 H, H23), 4.87 - 4.97 (m, 1 H, H4 or H32), 4.64 - 4.74 (m, 1 H, H4 or H32), 4.50 (dd, *J* 9.8, 7.0, 1 H, H26), 4.26 - 4.37 (m, 2 H, H12, H26'), 4.18 - 4.24 (m, 1 H, H27), 2.97 - 3.16 (m, 4 H, H5, H5', H31, H31'), 1.82 - 2.05 (m, 4 H, H8, H8', H28, H28'), 1.43 - 1.57 (m, 8 H, H6, H6, H7, H7', H29, H29', H30, H30'), 1.40 (s, 18 H, 2 of H1/H16/H35), 1.34 (s, 9 H, H1 or H16 or H35), 1.14 (d, *J* 7.1, 3 H, H13); δ_C (101 MHz, $CDCl_3$) 171.6 (C10 or C14 or C22), 171.5 (C10 or C14 or C22), 171.2 (C10 or C14 or C22), 166.9 (C18), 156.4 (C3 or C25 or C33), 156.0 (C3 or C25 or C33), 155.9 (C3 or C25 or C33), 143.8, 143.6, 141.2, 140.4, 133.8, 132.1, 131.0, 129.9, 128.3, 127.7, 127.1, 125.2, 125.1, 123.4, 122.2, 119.9, 119.5, 112.0 (18 x Ar-C), 94.8 (C19 or C20), 89.6 (C19 or C20), 81.4 (C2 or C15 or C34), 78.9 (C2 or C15 or C34), 78.8 (C2 or C15 or C34), 67.3

(C26), 54.7 (C9), 52.6 (C23), 48.4 (C12), 47.0 (C27), 40.4 (C5 or C31), 40.1 (C5 or C31), 34.0 (C8 or C28), 33.5 (C8 or C28), 29.9 (C6 or C30), 29.7 (C6 or C30), 28.4 (C1 or C16 or C35), 28.4 (C1 or C16 or C35), 27.9 (C1 or C16 or C35), 22.2 (C7 or C29), 22.1 (C7 or C29), 17.8 (C13); IR ($CHCl_3$) 3294(broad), 3066, 2981, 2940, 2866, 2364, 2245, 1689, 1643, 1527; HRMS calculated for $C_{59}H_{47}N_6O_{11}Na$ $[M+Na]^+$: 1065.5308, found 1065.5256.

(S)-tert-Butyl 2-((S)-2-(2-((2-((S)-2-((S)-2-(2-((2-((S)-2-((((9H-fluoren-9-yl)methoxy)carbonyl)amino)propanamido)phenyl)ethynyl)benzamido)propanamido)-6-((tert-butoxycarbonyl)amino)hexanamido)phenyl)ethynyl)benzamido)-6-((tert-butoxycarbonyl)amino)hexanamido)propanoate 124

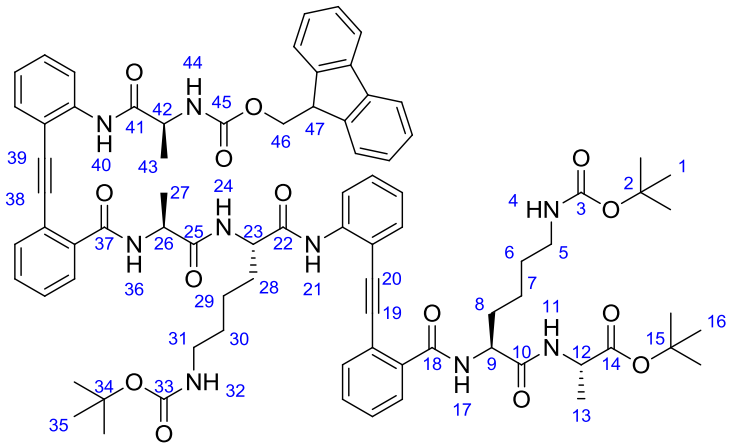

According to *general procedure (3g)*: Fmoc-protected amine **123** (700 mg, 0.67 mmol) gave residue **A**. According to *general procedure (3f)*: *tert*-Butyl ester **48** (873 mg, 1.34 mmol) gave residue **B**. According to *general procedure (3e)*: Residue **A** and residue **B** gave the *title compound* **124** (450 mg, 48 %) as an off-white foam after purification by flash column chromatography (Et_2O); $[\alpha]_D^{23.5}$ +52.9 (*c* 1.00, $CHCl_3$); δ_H (400 MHz, $CDCl_3$) 9.74 (s, 1 H, H21 or H40), 9.26 (s, 1 H, H21 or H40), 8.72 (d, *J* 8.1, 1 H, Ar-H), 8.69 (d, *J* 7.0, 1 H, H11), 8.59 (d, *J* 8.0, 1 H, Ar-H), 8.31 (d, *J* 8.0, 1 H24), 7.98 (d, *J* 7.3, 2 H, H36, 1 x Ar-H), 7.70 - 7.80 (m, 4 H, Ar-H), 7.64 - 7.70 (m, 2 H, Ar-H), 7.56 (dd, *J* 7.7, 1.3, 1 H, Ar-H), 7.51 (td,

J 8.3, 1.2, 2 H, Ar-H), 7.33 - 7.45 (m, 5 H, Ar-H), 7.21 - 7.28 (m, 3 H, Ar-H), 7.11 (td, *J* 7.5, 1.0, 1 H, Ar-H), 7.07 (td, *J* 7.5, 0.9, 1 H, Ar-H), 6.95 (d, *J* 9.0, 1 H, H17), 6.12 (d, *J* 8.8, 1 H, H44), 5.59 - 5.71 (m, 2 H, H23, H42), 5.42 - 5.55 (m, 2 H, H9, H26), 4.84 - 4.96 (m, 1 H, H4 or H32), 4.70 - 4.78 (m, 1 H, H46), 4.51 - 4.63 (m, 2 H, H12, H46'), 4.36 (t, *J* 7.2, 2 H, H4 or H32, H47), 2.65 - 3.13 (m, 4 H, H5, H5', H31, H31'), 1.67 - 2.01 (m, 4 H, H8, H8', H28, H28'), 1.63 (d, *J* 6.6, 3 H, H43), 1.53 (d, *J* 6.8, 3 H, H27), 1.44 - 1.51 (m, 2 H, 2 of H6, H6', H30, H30'), 1.43 (s, 9 H, H1 or H16 or H35), 1.41 (s, 9 H, H1 or H16 or H35), 1.37 - 1.39 (m, 2 H, 2 of H6, H6', H30, H30'), 1.34 (s, 9 H, H1 or H16 or H35), 1.25 - 1.31 (m, 2 H, 2 of H7, H7', H29, H29'), 1.14 - 1.22 (m, 2 H, 2 of H7, H7', H29, H29'); δ_C (101 MHz, $CDCl_3$) 173.2 (C14), 172.7 (C10 or C22 or C25 or C41), 172.5 (C10 or C22 or C25 or C41), 171.4 (C10 or C22 or C25 or C41), 171.3 (C10 or C22 or C25 or C41), 166.2 (C18 or C37), 166.2 (C18 or C37), 156.1 (C3 or C33 or C45), 155.9 (C3 or C33 or C45), 155.7 (C3 or C33 or C45), 144.0, 143.9, 141.2, 140.9, 140.5, 134.2, 133.8, 132.1, 132.0, 131.0, 130.9, 130.0, 129.8, 128.2, 127.7, 127.6, 127.6, 127.2, 127.0, 125.5, 125.4, 123.3, 123.1, 122.8, 122.3, 119.8, 119.3, 119.3, 112.0, 111.7 (30 x Ar-C), 95.6 (C20 or C39), 94.8 (C20 or C39), 89.9 (C19 or C38), 89.6 (C19 or C38), 82.0 (C15), 78.7 (C2 or C34), 78.7 (C2 or C34), 67.4 (C46), 53.4 (C23), 52.3 (C9), 50.8 (C42), 48.8 (C26), 48.5 (C12), 47.1 (C47), 40.3 (C5 or C31), 40.1 (C5 or C31), 34.2 (C8 or C28), 34.1 (C8 or C28), 29.8 (C6 or C30), 29.4 (C6 or C30), 28.4 (C1 or C16 or C35), 28.3 (C1 or C16 or C35), 27.9 (C1 or C16 or C35), 22.7 (C7 or C29), 22.5 (C7 or C29), 19.6 (C43), 19.2 (C27); IR ($CHCl_3$) 3285, 3065, 2980, 2934, 2866, 2248, 1692, 1642, 1579, 1522; HRMS calculated for $C_{80}H_{94}N_9O_{14}$ $[M+H]^+$: 1404.6915, found 1404.6893.

(S)-tert-Butyl 2-((S)-2-(2-((2-((S)-2-((S)-2-(2-((2-((S)-2-((S)-2-((((9H-fluoren-9-yl)methoxy)carbonyl)amino)-6-((tert-butoxycarbonyl)amino)hexanamido)propanamido)phenyl)ethynyl)benzamido)propanamido)-6-((tert-butoxycarbonyl)amino)hexanamido)phenyl)ethynyl)benzamido)-6-((tert-butoxycarbonyl)amino)hexanamido)propanoate 125

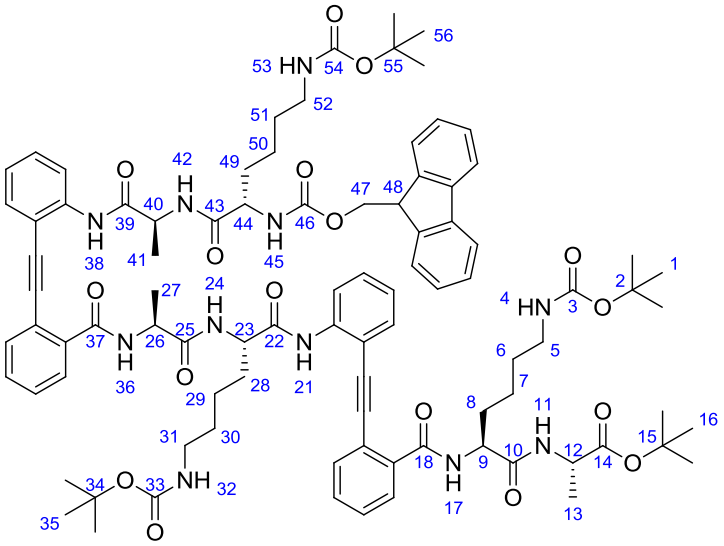

According to *general procedure (3g)*: Fmoc-protected amine **125** (210 mg, 0.15 mmol) gave Residue **A**. According to *general procedure (3e)*: Residue **A** and Fmoc-Lys(Boc)-OH **98** (140 mg, 0.30 mmol) gave the *title compound* **125** (110 mg, 45 %) as a white solid after purification by flash column chromatography (Et_2O); $[\alpha]_D^{23.5}$ +34.5 (*c* 0.50, $CHCl_3$); δ_H (400 MHz, $CDCl_3$) 9.69 (s, 1 H, H21 or H38), 9.42 (s, 1 H, H21 or H38), 9.16 (d, *J* 7.5, 1 H, H24), 8.76 (d, *J* 8.3, 1 H, Ar-H), 8.69 (d, *J* 8.3, 2 H, H11, Ar-H), 8.07 (d, *J* 7.8, 1 H, Ar-H), 7.96 (d, *J* 8.0, 1 H, H36), 7.64 - 7.74 (m, 5 H, Ar-H), 7.60 (dd, *J* 7.3, 2.7, 2 H, Ar-H), 7.55 (dd, *J* 7.7, 1.3, 1 H, Ar-H), 7.51 (td, *J* 6.0, 1.0, 1 H, Ar-H), 7.46 - 7.50 (m, 1 H, Ar-H), 7.36 - 7.45 (m, 5 H, H45, 4 x Ar-H), 7.31 (t, *J* 7.0, 2 H, Ar-H), 7.14 - 7.20 (m, 2 H, Ar-H), 7.06 - 7.12 (m, 3 H, H17, H42), 6.96 - 7.01 (m, 1 H, Ar-H), 6.88 - 6.94 (m, 1 H, Ar-H), 5.81 - 5.91 (m, 1 H, H40), 5.64 - 5.78 (m, 2 H, H23, H26), 5.51 - 5.60 (m, 1 H, H9), 4.98 - 5.11 (m,

1 H, H4 or H32 or H53), 4.86 - 4.93 (m, 1 H, H4 or H32 or H53), 4.77 - 4.85 (m, 1 H, H4 or H32 or H53), 4.60 - 4.67 (m, 1 H, H12), 4.43 - 4.51 (m, 1 H, H44), 4.33 - 4.40 (m, 2 H, H47, H47'), 4.20 - 4.27 (m, 1 H, H48), 3.12 (br. s., 2 H, 2 of H5, H5', H31, H31', H52, H52'), 2.79 - 3.05 (m, 4 H, 4 of H5, H5', H31, H31', H52, H52'), 1.77 - 2.11 (m, 6 H, H8, H8', H28, H28', H49, H49'), 1.62 (d, *J* 6.8, 3 H, H41), 1.36 - 1.47 (m, 45 H, 3 of H1, H16, H35, H56; H6, H6', H7, H7', H13, H27, H29, H29', H30, H30', H50, H50', H51, H51'), 1.33 (s, 9 H, H1 or H16 or H35 or H56); δ_C (101 MHz, $CDCl_3$) 173.1, 172.6, 172.3, 171.9, 171.5, 171.4, 166.5 (C18 or C37), 165.7 (C18 or C37), 156.7 (C46), 156.0 (C3 or C33 or C54), 156.0 (C3 or C33 or C54), 155.8 (C3 or C33 or C54), 143.9, 143.8, 141.1, 141.0, 140.8, 140.2, 134.8, 134.3, 134.1, 132.1, 131.0, 129.9, 129.7, 128.3, 128.2, 127.5, 127.5, 126.9, 125.5, 125.3, 125.3, 123.3, 123.2, 122.8, 122.4, 119.8, 119.7, 119.5, 119.2, 111.9 (30 x Ar-C), 95.8, 95.1, 89.9, 89.7 (4 x alkynyl-C), 82.0 (C15), 78.8 (C2 or C34 or C55), 78.7 (2C, 2 of C2, C34, C55) , 67.1 (C47), 54.9 (C44), 53.8 (C23), 52.3 (C9), 49.7 (40), 48.7 (C26), 48.5 (C12), 47.1 (C48), 40.5 (C5 or C31 or C52), 40.3 (C5 or C31 or C52), 40.2 (C5 or C31 or C52), 34.5 (C8 or C28 or C49), 33.3 (C8 or C28 or C49), 33.3 (C8 or C28 or C49), 30.0 (C6 or C29 or C51), 29.7 (C6 or C29 or C51), 29.6 (C6 or C29 or C51), 28.4 (2C, 2 of C1, C16, C35, C56), 28.3 (C1 or C16 or C35 or C56), 27.9 (C1 or C16 or C35 or C56), 22.8 (C7 or C29 or C50), 22.6 (C7 or C29 or C50), 22.5 (C7 or C29 or C50), 20.5 (C41), 20.0 (C13 or C27), 19.3 (C13 or C27); IR ($CHCl_3$) 3285, 3067, 2980, 2934, 2865, 2248, 1690, 1638, 1580, 1523; HRMS calculated for $C_{91}H_{114}N_{11}O_{17}$ $[M+H]^+$: 1632.8389, found 1632.8379.

(S)-tert-Butyl 2-((S)-2-(2-((2-((S)-2-((S)-2-(2-((2-((S)-2-((S)-2-((((9H-fluoren-9-yl)methoxy)carbonyl)amino)-6-aminohexanamido)propanamido)phenyl)ethynyl)benzamido)propanamido)-6-aminohexanamido)phenyl)ethynyl)benzamido)-6-aminohexanamido)propanoate 126

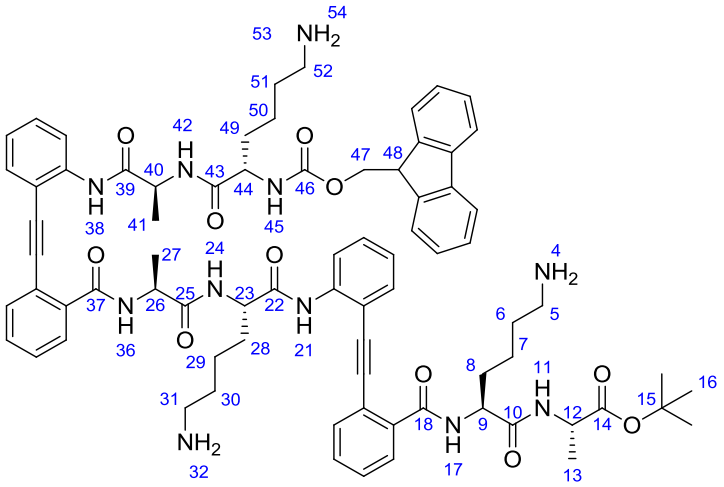

According to *general procedure (4g)*: Boc-protected amine **125** (70 mg, 0.04 mmol) gave the *title compound* **126** (56 mg, 98 %) as a white solid; $[\alpha]_D^{23.5}$ +52.8 (*c* 0.35, $CHCl_3$); δ_H (500 MHz, DMSO-$_{d6}$) 9.54 (s, 1 H, H21), 9.50 (s, 1 H, H38), 8.70 (d, *J* 8.1, 1 H, H17), 8.67 (d, *J* 7.3, 1 H, H36), 8.41 (d, *J* 7.8, 1 H, H24), 8.29 (d, *J* 7.0, 1 H, H42), 8.25 (d, *J* 6.6, 1 H, H11), 8.13 (dd, *J* 8.0, 4.8, 1 H, Ar-H), 7.88 (d, *J* 6.7, 2 H, Ar-H), 7.67 - 7.76 (m, 11 H), 7.57 (d, *J* 7.0, 1 H, Ar-H), 7.49 - 7.54 (m, 4 H, H45, 3 x Ar-H), 7.37 - 7.41 (m, 3 H, Ar-H), 7.28 - 7.33 (m, 2 H, Ar-H), 7.11 - 7.18 (m, 2 H, Ar-H), 4.94 - 5.01 (m, 1 H, H23), 4.81 - 4.88 (m, 1 H, H40), 4.69 (quin, *J* 7.2, 1 H, H26), 4.51 - 4.58 (m, 1 H, H9), 4.24 - 4.30 (m, 2 H, H47, H47'), 4.18 - 4.22 (m, 1 H, H48), 4.01 - 4.07 (m, 1 H, H44), 3.95 - 4.00 (m, 1 H, H12), 2.53 - 2.83 (m, 6 H, 6 H, H5, H5', H31, H31', H52, H52'), 1.60 - 1.84 (m, 5 H, Alkyl-H), 1.47 - 1.57 (m, 5 H, Alkyl-H), 1.43 - 1.47 (m, 2 H, Alkyl-H), 1.40 (d, *J* 7.0, 3 H, H41), 1.35 - 1.38 (m, 4 H, Alkyl-H), 1.33 (s, 9 H, H16), 1.22 - 1.31 (m, 5 H, Alkyl-H), 1.14 (d, *J* 7.3, 3 H, H13); δ_C (126 MHz, DMSO-$_{d6}$) 172.4, 172.0, 171.9, 171.6, 171.3, 171.0 (6 x C=O), 167.5

(C18 or C37), 167.0 (C18 or C37), 156.0 (C46), 143.8, 143.7, 140.7, 139.6, 139.6, 137.5, 137.2, 136.0, 131.9, 131.9, 130.5, 130.4, 129.7, 128.9, 128.7, 128.6, 128.2, 127.6, 127.1, 126.1, 125.3, 125.2, 124.9, 123.9, 123.9, 120.3, 120.3, 120.1, 113.2, 113.1 (30 x Ar-C), 93.9, 93.9, 93.8, 89.0 (4 x alkynyl-C), 80.4 (C15), 65.6 (C47), 54.1 (C44), 53.5 (C23), 53.1 (C9), 49.0 (C40), 48.8 (C26), 48.3 (C12), 46.6 (C48), 38.7 (C5 or C31 or C52), 38.6 ((C5 or C31 or C52), 38.6 (C5 or C31 or C52), 31.9 (C8 or C28 or C49), 31.3 (C8 or C28 or C49), 31.3 (C8 or C28 or C49), 27.5 (C16), 26.8 (C6 or C30 or C51), 26.7 (C6 or C30 or C51), 26.6(C6 or C30 or C51), 22.5 (C7 or C29 or C50), 22.4 (C7 or C29 or C50), 22.2 (C7 or C29 or C50), 18.4 (C41), 18.0 (C27), 16.7 (C13); IR ($CHCl_3$) 3282 (broad), 3066, 2985, 2947, 1675, 1641, 1580, 1527; HRMS calculated for $C_{76}H_{90}N_{11}O_{11}$ $[M+H]^+$: 1332.6816, found 1332.6815.

4.7 References

1. Kemp, D. S. & Li, Z. Q. 2-amino-2'-carboxydiphenylacetylenes as β-turn mimetics - Synthesis and Conformational Properties. *Tetrahedron Lett.* **36,** (1995).
2. Dichloromethane - High Purity Solvents. *Sigma-Aldrich* Available at: https://www.sigmaaldrich.com/chemistry/solvents/dichloromethane-center.html. (Accessed: 1st March 2016)
3. Roccatano, D., Colombo, G., Fioroni, M. & Mark, A. E. Mechanism by which 2,2,2-trifluoroethanol/water mixtures stabilize secondary-structure formation in peptides: A molecular dynamics study. *Proc. Natl. Acad. Sci.* **99,** 12179–12184 (2002).
4. Greenfield, N. J. Using circular dichroism spectra to estimate protein secondary structure. *Nat. Protoc.* **1,** 2876–2890 (2006).
5. Knipe, P. C (Post-Doctoral Research Assistant, Hamilton Group, University of Oxford) Unpublished. (2015).
6. Schneider, J. P. & Kelly, J. W. Synthesis and Efficacy of Square Planar Copper Complexes Designed to Nucleate .beta.-Sheet Structure. *J. Am. Chem. Soc.* **117,** 2533–2546 (1995).
7. Nesloney, C. L. & Kelly, J. W. A 2,3'-Substituted Biphenyl-Based Amino Acid Facilitates the Formation of a Monomeric β-Hairpin-like Structure in Aqueous Solution at Elevated Temperature. *J. Am. Chem. Soc.* **118,** 5836–5845 (1996).
8. Spencer, R. K., Kreutzer, A. G., Salveson, P. J., Li, H. & Nowick, J. S. X-ray Crystallographic Structures of Oligomers of Peptides Derived from β2-Microglobulin. *J. Am. Chem. Soc.* **137,** 6304–6311 (2015).
9. Stevenazzi, A., Marchini, M., Sandrone, G., Vergani, B. & Lattanzio, M. Amino acidic scaffolds bearing unnatural side chains: An old idea generates new and versatile tools for the life sciences. *Bioorg. Med. Chem. Lett.* **24,** 5349–5356 (2014).
10. Marsh, J. A., Singh, V. K., Jia, Z. & Forman-Kay, J. D. Sensitivity of secondary structure propensities to sequence differences between α- and γ-synuclein: Implications for fibrillation. *Protein Sci. Publ. Protein Soc.* **15,** 2795–2804 (2006).
11. Motozaki, T. *et al.* Total Synthesis of (+)-Tubelactomicin A. 1. Stereoselective Synthesis of the Lower-Half Segment by an Intramolecular Diels−Alder Approach. *Org. Lett.* **7,** 2261–2264 (2005).
12. Li, W. R., Ewing, W. R., Harris, B. D. & Joullie, M. M. Total synthesis and structural investigations of didemnins A, B, and C. *J. Am. Chem. Soc.* **112,** 7659–7672 (1990).

13. Dewis, L. (Masters Research Student, Hamilton Group, University of Oxford), Unpublished. (2014).

14. Marinescu, L., Thinggaard, J., Thomsen, I. B. & Bols, M. Radical Azidonation of Aldehydes. *J. Org. Chem.* **68,** 9453–9455 (2003).

15. Staudinger, H. & Meyer, J. Über neue organische Phosphorverbindungen III. Phosphinmethylenderivate und Phosphinimine. *Helv. Chim. Acta* **2,** 635–646 (1919).

16. Goddard-Borger, E. D. & Stick, R. V. An Efficient, Inexpensive, and Shelf-Stable Diazotransfer Reagent: Imidazole-1-sulfonyl Azide Hydrochloride. *Org. Lett.* **9,** 3797–3800 (2007).

17. Gianella-Borradori, M. (Post-Doctoral Research Assistant, Hamilton Group, University of Oxford), Unpublished. (2015).

18. Offermann, D. A. *et al.* Synthesis and Incorporation into Cyclic Peptides of Tolan Amino Acids and Their Hydrogenated Congeners: Construction of an Array of A–B-loop Mimetics of the Cε3 Domain of Human IgE. *J. Org. Chem.* **77,** 3197–3214 (2012).

19. Dings, R. P. M. *et al.* Anti-tumor activity of the novel angiogenesis inhibitor anginex. *Cancer Lett.* **194,** 55–66 (2003).

20. Dings, R. P. M. *et al.* β-sheet is the bioactive conformation of the anti-angiogenic anginex peptide. *Biochem. J.* **373,** 281–288 (2003).

21. Luo, J. *et al.* Cellular Polyamines Promote Amyloid-Beta (Aβ) Peptide Fibrillation and Modulate the Aggregation Pathways. *ACS Chem. Neurosci.* **4,** 454–462 (2013).

22. Luo, J. *et al.* Endogenous Polyamines Reduce the Toxicity of Soluble Aβ Peptide Aggregates Associated with Alzheimer's Disease. *Biomacromolecules* **15,** 1985–1991 (2014).

23. Porter, E. A., Weisblum, B. & Gellman, S. H. Mimicry of Host-Defense Peptides by Unnatural Oligomers: Antimicrobial β-Peptides. *J. Am. Chem. Soc.* **124,** 7324–7330 (2002).

24. Jones, C. R. *et al.* A Nonpeptidic Reverse Turn that Promotes Parallel Sheet Structure Stabilized by C-H···O Hydrogen Bonds in a Cyclopropane γ-Peptide. *Angew. Chem. Int. Ed.* **47,** 7099–7102 (2008).

Chapter 5 – Understanding β-Sheet Folding: Quantification of non-covalent structural determinants in β-turn mimics

5.1 The Folding Problem

How proteins fold into their precisely defined structures to enable their function remains one of biology's biggest questions. To answer it would open up enormous avenues of protein and foldamer design. Fully understanding the huge numbers of interactions that govern quaternary and tertiary structure remain almost completely intractable, but ever since Pauling, Corey and Bransons' discovery of secondary structure chemists and biologists have sought to understand the forces governing the creation of the highly canonical helices and sheets.[1,2]

As highlighted in Chapter 3, there remains an important need to better appreciate how β-sheets form in order to build our understanding of how and why the toxic oligomers of misfolded proteins form.

Owing to the ease of creating short, soluble segments of α-helix, their folding properties are relatively well understood.[3,4] However, the forces governing the stability of the β-sheet are poorly illuminated and the diphenylacetylene system and techniques utilised in Chapters 3 and 4 present an opportunity to investigate them.

5.2 β-Sheet Propensity

5.2.1 Statistical Analysis of β-Sheet Propensity

In 1974 Chou and Fasman, having noted that certain amino acids were found more extensively in certain secondary structures, completed a rigorous statistical analysis of this observation for 2473 residues in fifteen different proteins.[5] For each amino acid they

calculated P_α, P_β, P_C; the chance of it being found in an α-helix, β-sheet or random coil respectively. The sheet propensity score for alanine was arbitrarily set at one. The rank order for P_β showed that, in general the bulkier the amino acid the greater the β-sheet propensity, with methionine, valine and isoleucine having the highest values (Figure 5.1).

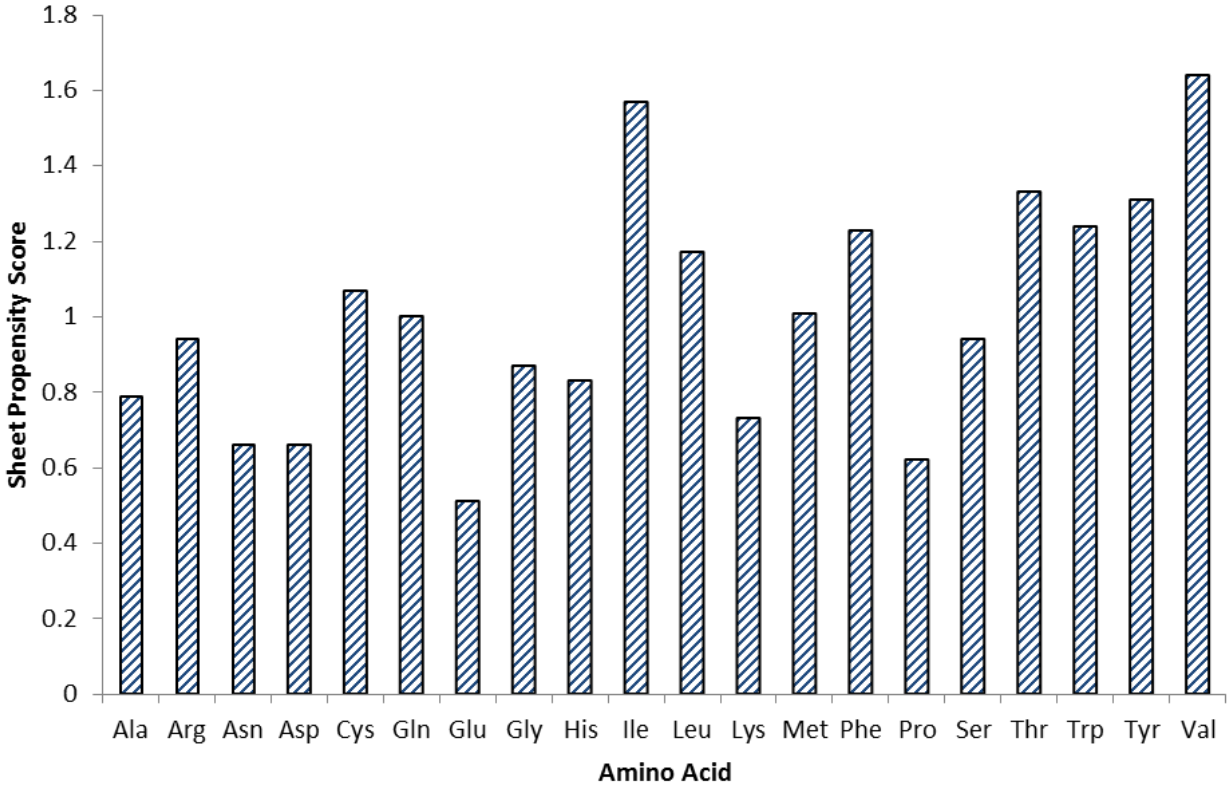

Figure 5.1 Statistically derived β-sheet propensity scores for each amino acid.

These scores were then used in a subsequent paper to predict the initiation and termination of helix and sheet regions.[6] Without the need for complex computational calculations, Chou and Fasman were able to show if any five residue sequence contained three or more β-forming amino acids (methionine, valine, isoleucine), it would nucleate a β-sheet in both directions. This simple model was able to locate 95 % of sheet regions and predict 86 % of the sheet residues across nineteen different proteins. The power of this model demonstrates the importance of short range interactions (single residue information, and neighbouring residue information) in controlling secondary structure.

Similar techniques have been used to analyse turn propensities,[7] and even much more recent studies, incorporating machine learning, have struggled to improve on the simple elegance of their observations.[8]

5.2.2 Thermodynamic Calculation of β-Sheet Propensity

5.2.2.1 Studies on Fully Peptidic Systems

Kim and Berg developed a model system based on a designed zinc-finger peptide to calculate the β-sheet propensity of different amino acids.[9,10] They had previously shown *via* NMR studies that the designed peptide only folded into a β-sheet in the presence of a zinc ion (Figure 5.2).

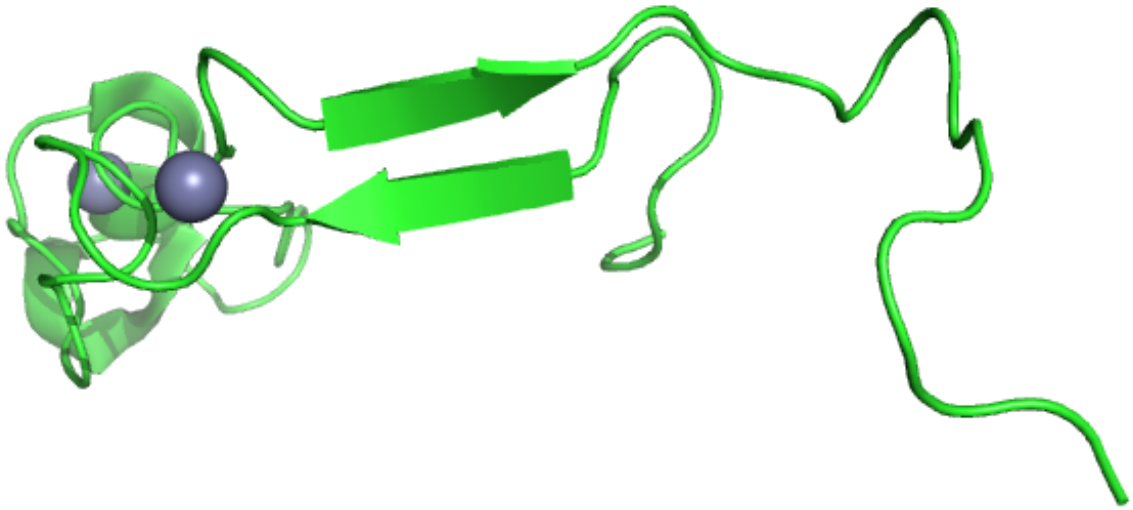

Figure 5.2 Example of a zinc finger protein containing a β-sheet (PDB: 2J2S).[11]

They worked on the assumption that if different amino acids affected the stability of the sheet due to their different propensities, this would be reflected in the affinity for the metal ion. After creating a library of different peptides by performing single-site mutational studies with each amino acid the assay revealed the relative metal-binding free energy of each peptide. From these free energies the stability of the sheet secondary structure could be extrapolated. The researchers then compared their results with an extended study across a larger range of

proteins conducted by Chou and Fasman in 1990.[12] With the exceptions of proline and glycine there was an excellent correlation between the statistical and thermodynamic observations (Figure 5.3).

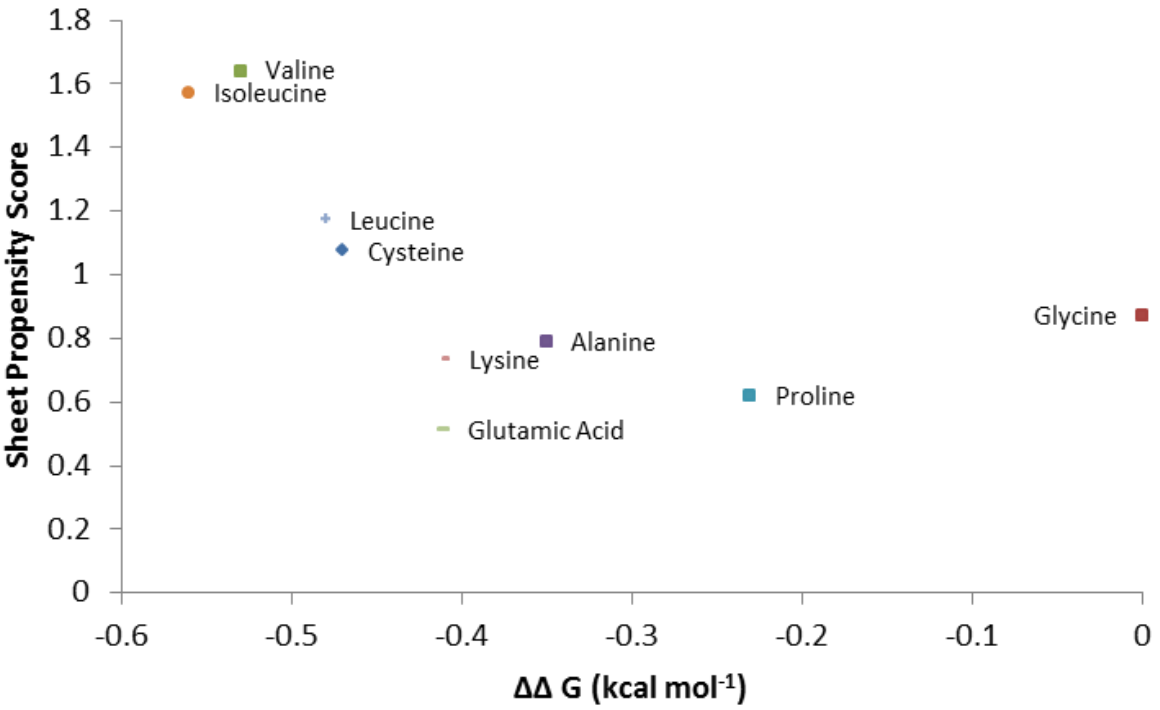

Figure 5.3 Comparison of statistical β-sheet propensities (y-axis) with experimentally derived binding energies (x-axis) for selected amino acids.

Critics could question the link between the metal-binding energies and β-sheet propensity and so a year later Kim repeated the study on an alternative system.[13] The immunoglobin-binding domain B1 from protein G (GB1), a small, globular protein containing a four-stranded β-sheet, undergoes a two-state, reversible, thermal unfolding transition,[14,15] and as such was an ideal model system.

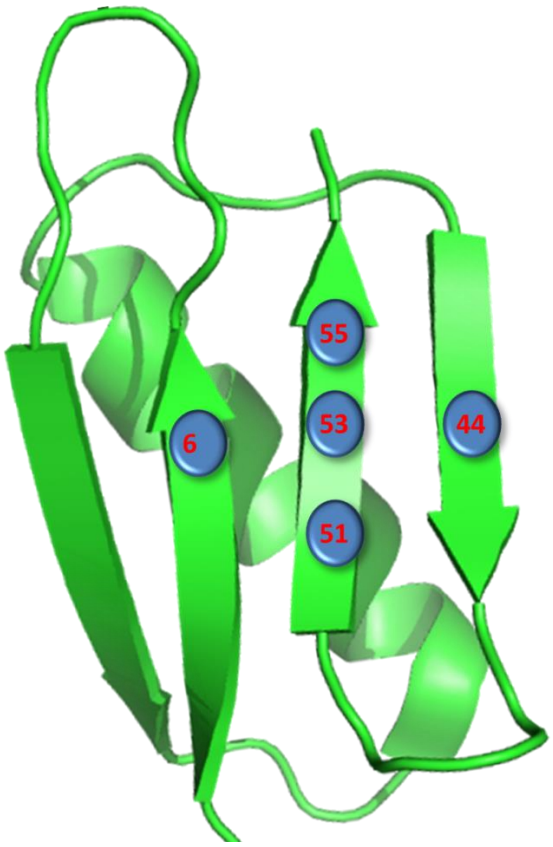

Figure 5.4 X-ray crystal structure showing the location of β-sheet residues in GB1 (PDB: 2GB1). Residue 53 was chosen for single-site mutational studies as it sat in the middle of the sheet, and would therefore be unaffected by interactions due to being on the end or edge of a β-sheet.

Residue 53 was chosen as it was in the middle of the sheet and thus avoided the potential effects of the substitution being made on the edge or the ends of the β-sheet (Figure 5.4). Single-site mutations were made and the conservation of sheet structure confirmed through binding to the Fc domain of IgG and NMR spectroscopy. The sheet stability was assessed through thermal unfolding as measured by circular dichroism and the changes in overall stability attributed entirely to the ability of the mutation to preserve the β-sheet conformation. The results revealed a range of 2 kcal mol^{-1} and correlated well with the previous zinc-finger model system and by extension, the statistical results of Chou and Fasman.

5.2.2.2 Studies of Model Chemical Systems

Studies by Kemp and Nowick have assessed β-sheet propensities using model chemical systems.[16,17] Using the diurea group as a turn inducer (for a more detailed discussion see

Chapter 3) for a parallel β-sheet, Nowick and Insaf explored the propensities of the hydrophobic residues glycine, alanine, valine and leucine in chloroform.[17] By comparing the chemical shift of the amide N-H, ***Hc***, in the turn and corresponding control across a complete suite of mixed compounds the ability of each side-chain to promote sheet formation could be assessed (Figure 5.5).

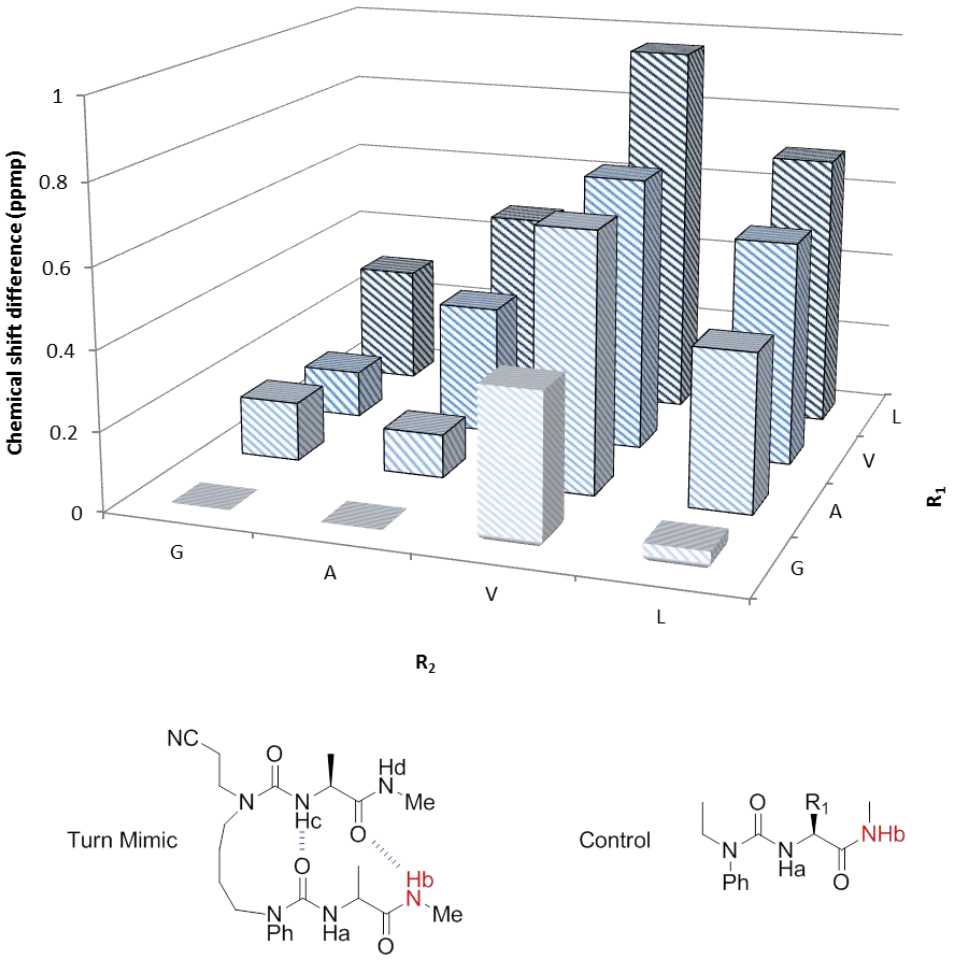

Figure 5.5 ^{1}H NMR chemical shift differences between the H_b the amide N-H of the artificial sheet and the corresponding control. A larger difference indicates an increased downfield shift in the turn mimics and therefore greater hydrogen bonding, considered an indicator of sheet formation.

As established by the whole-protein studies, the bulkier, more hydrophobic side-chains such as valine and leucine stabilised sheet structure. This particular study showed the propensities of valine and leucine to be extremely similar, in contrast to the propensities previously derived. It was reasoned that having an overly large side-chain next to a turn element could

result in destabilising steric hindrance, thus lowering the sheet forming propensity of valine. This conclusion also reinforces observations that location within a sheet is also a relevant factor.

5.3 The Basis for β-Sheet Propensity

Although these trends were now firmly established in an experimental and statistical basis, and it was clear that bulkier, more hydrophobic amino acids tended to form β-sheets the reason for these propensities remained unclear. Both enthalpy and entropy have a role to play as the free energy changes on progression from random and isolated coil in solution, to an extended strand within a sheet. The enthalpic changes occur as the existing hydrogen bonds to solvent are broken, to be replaced by new ones to the surrounding strands, and by the changes in steric clash as the interactions between main chain and side-chains change upon a change in conformation. Similarly, the strand itself sees an entropic loss as it loses degrees of freedom within its new, highly restricted sheet environment, whilst the 'thrown-off' solvent molecules experience an entropic gain. The interplay between these factors and their relative contributions remains to be explored (Figure 5.6).

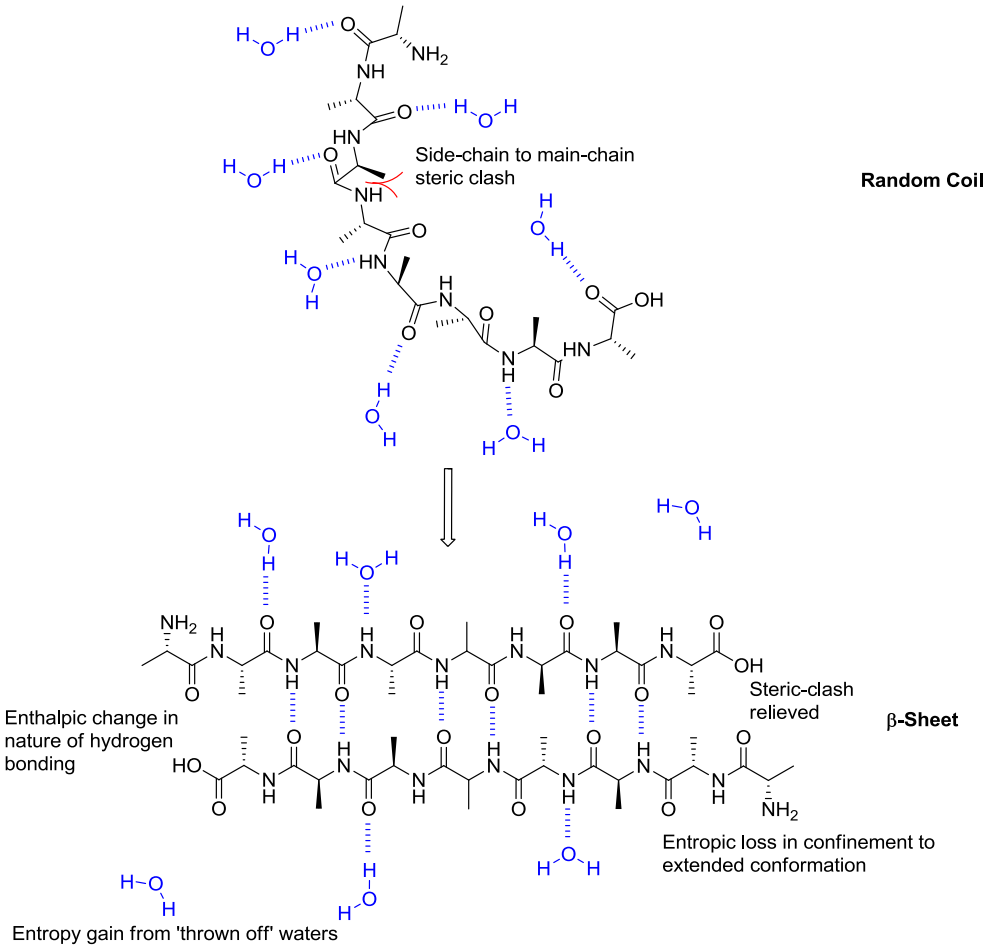

Figure 5.6 Representation of entropic and enthalpic changes on moving from random coil to β-sheet in solution. The interactions shown are representative only and extensive networks with solvent molecules are likely to be present.

5.3.1 Experimental

Englander employed the hydrogen-deuterium exchange experiment to examine the effects of primary structure on N-H exchange.[18] The effect of the side-chain for all twenty amino acids was investigated on dipeptide models and the researchers were able to identify the role of both inductive and side-chain blocking effects. They showed that for all peptides the exchange can be both acid- and base-catalysed and noted that bulkier side-chains lead to slower rates of exchange (Figure 5.7, Left).

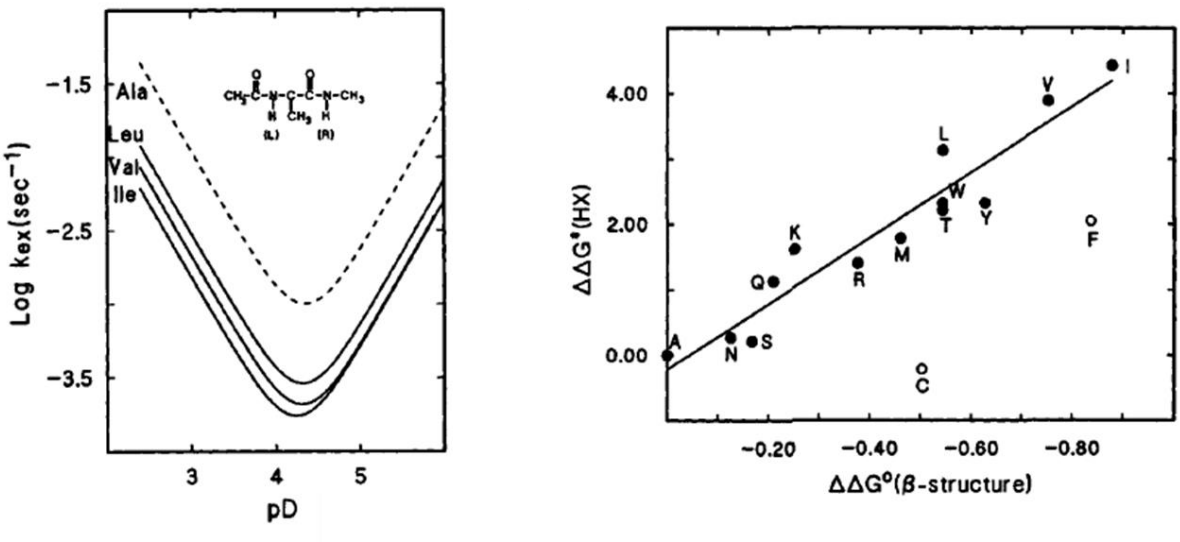

Figure 5.7 Left: Decreasing exchange rates with increasing steric bulk for a model dipeptide. As the exchange reaction can be both acid- and base-catalysed there is a minimum rate where neither is occurring to any appreciable extent, before rapid rate increases upon a slight change of pD in either direction. Right: Correlation between the side-chain blocking effect and the thermodynamic β-sheet stabilisation energies determined by Minor and Kim. Adapted and reprinted by permission from Proteins: Structure, Function, and Genetics. Copyright 1994, John Wiley & Sons.

With these results in hand they proposed that the side-chain blocking effect, whereby the larger side-chain displays a slower rate of exchange indicative of the amide N-H being inaccessible to solvent, could explain β-sheet propensity.[19] If the amide N-Hs were less accessible to solvent they would experience weaker hydrogen bonds as a random coil in solution. The enthalpic gain on progressing to a hydrogen-bonded strand would therefore be greater for bulkier side-chains (Figure 5.8).

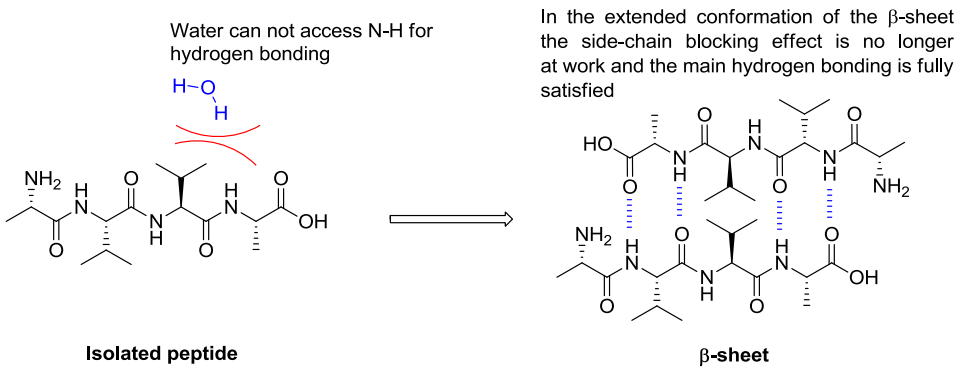

Figure 5.8 The role of the side-chain blocking effect in β-sheet formation.

Comparison of the values obtained by Kim and Berg to the HX activation energy due to side-chain blocking showed an excellent correlation of 0.96 (Figure 5.7, Right), provided that

cysteine and phenylalanine were omitted. The activation energy for these residues is as expected, falling near to alanine and tyrosine respectively and the authors were therefore at a loss to describe the difference in sheet propensity. The blocking effect was estimated to contribute an enthalpic stabilisation of up to 0.9 kJ mol^{-1} relative to alanine.

5.3.2 Computational

Using first principles density functional theory, Rossmeisl calculated the interaction energies between fourteen different amino acids in polypeptides.[20] By summing the enthalpy of the broken and newly formed hydrogen bonds, the free energy change in confining the polypeptide to the sheet region of the Ramachandran plot, and the effect of side-chain interference with solvent as investigated by Englander the researchers computed an interaction energy that correlated directly with the well-established β-sheet propensities. This interaction energy (ΔE) could be broken down into two separate components, E_{conf} and $E_{H\text{-}Bond}$, the energy required to adopt the correct conformation for β-sheet formation and the energy associated with the breaking and making of hydrogen bonds respectively and such that;

$$\Delta E = E_{conf} + E_{H-bond}$$

The computation showed that changes in ΔE were purely due to changes in E_{conf} and that across all the amino acids investigated any changes in $E_{H\text{-}bond}$ were immaterial. The proposed reasoning was that due to main-chain, side-chain steric clashes polypeptides containing bulky amino acids were unable to fully relax and explore all the conformational possibilities as a random coil (Figure 4.X).

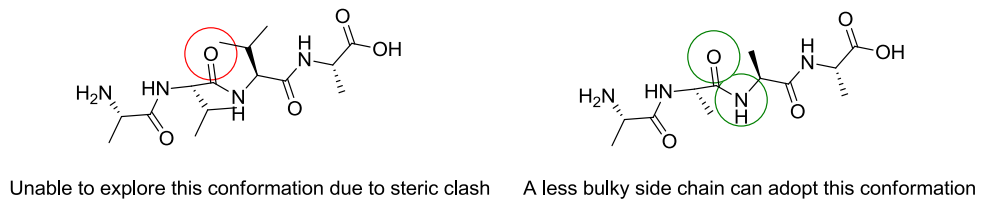

Figure 5.9 The steric clashes that prevent peptides with bulky side-chains fully exploring the conformational space of the random coil.

There is therefore a reduced entropic penalty on being restricted to the sheet configuration and an enthalpic gain due to relief of the chain clashes in the extended strand conformation. By claiming insignificance of hydrogen bond strength this paper differs from the conclusions of Englander, who argues that the side-chain blocking effect has a crucial effect on hydrogen bond strength. Furthermore the paper appears to neglect the role of solvent in both an entropic and enthalpic manner.

However work by Scheiner provided further support for Rossmeisl's conclusions.[21,22] He investigated the effect of changing the dihedral angles about the N-Cα and C_α-C(O) bonds on the hydrogen bond strength between a dipeptide and a proton acceptor molecule. Even if the geometry of the hydrogen bond itself did not change it was found that restricting the dihedral angles to those found in a canonical β-strand drastically reduced the strength of the hydrogen bond by making the amide N-H a poorer proton donor (Figure 5.10). The reason for this observation was proposed to be electrostatics; by placing the carbonyl group in close proximity to the N-H the partial negative charge wards off potential hydrogen bond acceptors.

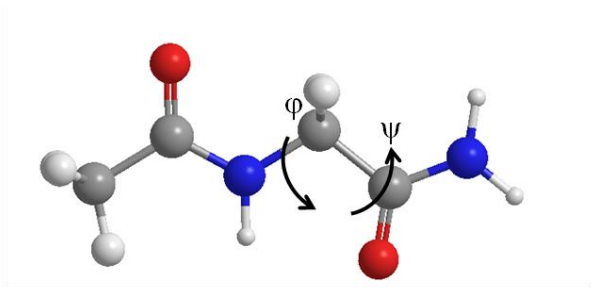

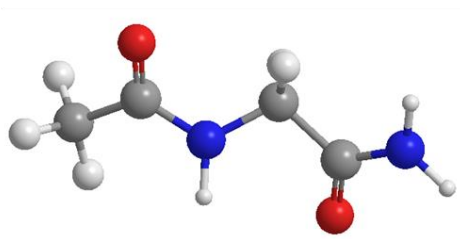

β-sheet: φ = -140°; ψ = 140°
Letter *e* in the Ramachandran Plot

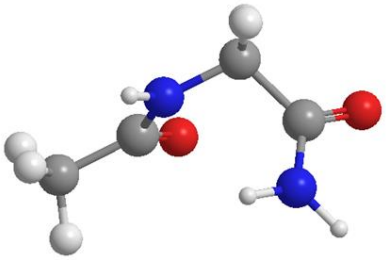

α-helix: φ = -60°; ψ = -40°
Letter *a* in the Ramachandran Plot

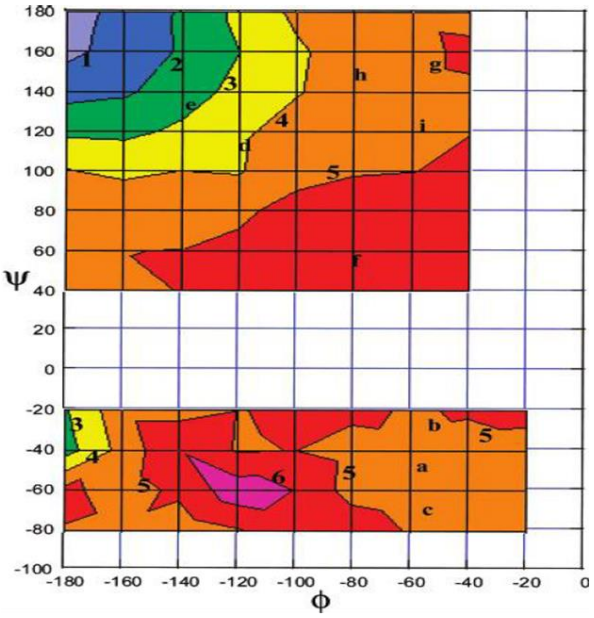

Strength of this hydrogen bond measured as φ and ψ angles are rotated

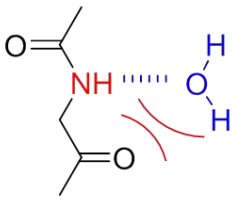

Electrostatic repulsion between carbonyl and hydrogen bond acceptor responsible for weak bonding.

Figure 5.10 Peptide labelled with ψ and φ angles; Angles observed for a canonical α-helix and β-sheet; Energy plot of the hydrogen bond strength (kcal mol^{-1}) between a dipeptide and a water molecule. Region e indicates the typical angles found within an anti-parallel β-sheet. Plot reprinted with permission from Journal of Physical Chemistry B, Copyright 2007 American Chemical Society.

By establishing that hydrogen bond interactions play a much weaker role in sheet formation that compared to other secondary structure, such as α-helices, Scheiner establishes a reason for the instability of β-sheets and the importance of additional enthalpic and entropic factors. However the effect of different side-chains on the hydrogen bond strength was not investigated.

As demonstrated in Chapters 3 and 4, cooperativity (that the addition of each strand to pre-existing sheet further stabilises that sheet) may be a large stabilising feature in formation of extended β-sheets. Sheridan showed that the strength of an individual hydrogen bond could be increased by up to 25 % in a sheet containing four or five strands.[23] Such cooperativity helps explain the stability of the sheet structure relative to random coil.

5.4 The Influence of Side-Chain Identity on Hydrogen Bond Strength

The research detailed above provides an overview of our understanding of the energetics of β-sheet stability and formation. Englander has demonstrated that the side-chain blocking effect displays an excellent correlation with β-sheet propensity and provided a plausible explanation, but there remains a need for model systems that can delineate the entropic and enthalpic components outlined above. For example, if adjusted for the side-chain blocking effect would the hydrogen bond strengths still correlate with sheet propensity? Or would there be, as suggested by Rossmeisl, a negligible difference such that the energy for changing conformation fully explained the propensity? These questions cannot be answered on a whole protein as it is not practical to isolate a single hydrogen bond. Instead, model systems provide a unique opportunity; Nowick writes that such artificial constructs 'demonstrate that even relatively simple model systems can provide information to the folding and interactions of large proteins.'[24]

5.4.1 The Diphenylacetylene Motif as a Model System

The diphenylacetylene motif, as a turn mimic allowing for the construction of model short anti-parallel β-sheets, provides an ideal platform for such a study. Its simple and scalable synthesis allows for a rapid construction of a library of different compounds. The small number of residues forced to lie in an extended conformation makes the library easy to study, with each hydrogen bond identifiable and amenable to investigation.

By extending the monomer unit **48** by one amino acid at each terminus and varying the nature of the side-chain it should be possible to study the central hydrogen bond (Figure 5.11).

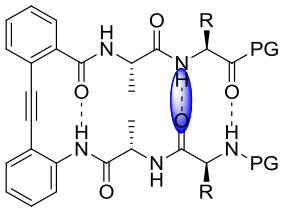

Figure 5.11 Canonical structure of diphenylacetylene-dipeptide motif. The side-chains to be varied are denoted by the R groups. The hydrogen bond to be studied is highlighted in blue.

5.4.2 Experimental Techniques

Each turn mimic would first be examined by circular dichroism to check for the adoption of sheet conformation, before the strength of the hydrogen bond could be examined by two orthogonal, kinetic and thermodynamic, NMR assays.

As shown in Chapter 3, Section 3.9.9, the NMR '*A* value' developed by Abraham can be used as a comparative tool in the quantitative assessment of hydrogen bond strengths.[25] However this method, although trivial to perform and having no need for control molecules, does not provide absolute values for the hydrogen bond strength.

Linton *et al*. were able to extend their methods in hydrogen-deuterium exchange to allow for the calculation of the absolute values.[26] This can be calculated as Bai *et al*. showed that the rate of deuterium exchange is directly correlated to the hydrogen bonding equilibrium according to the following relationship:[27]

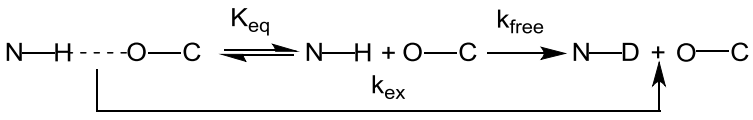

Figure 5.12 Relationship between the rate of hydrogen-deuterium exchange and hydrogen bonding equilibrium.

where K_{eq} is the equilibrium between the bound and unbound states, k_{ex} the rate of exchange from the bound state (the molecule of interst) and k_{free} the rate of exchange from the unbound state (a suitable control). From this relationship it can be shown that:

$$K_{eq} = \frac{k_{op}}{k_{cl}} = \frac{k_{ex}}{k_{free}}$$

Equation 5.1 Calculation of K_{eq} from exchange rates of turn mimic and control compound.

where k_{op} and k_{cl} are the rates of the opening and closing of the hydrogen bond respectively. Therefore, if a suitable control can be made to allow for the measurement of k_{free} the strength of the bond can be derived from the Gibbs free energy equation:

$$\Delta G_{HDX} = -RTlnK_{eq}$$

Equation 5.2 Calculation of free energy of hydrogen bond from K_{eq}

These two methods can then be compared to see if they concur. These initial methods only provide values in chloroform. In the first instance this is valuable as it allows for the removal of additional solvent effects and a simplification of the system. However, ultimately the methods need to be adapted to incorporate biologically relevant aqueous solvents.

5.5 Synthesis

5.5.1 Turn Mimics

For ease of synthesis it was decided to create the library of turn mimics through elongation of monomer unit **48** introduced in Chapter 3. The alanine, valine and phenylalanine mimics, **70**, **89**, and **90**, respectively, had previously been synthesised but are included in Scheme 5.1 for completeness.

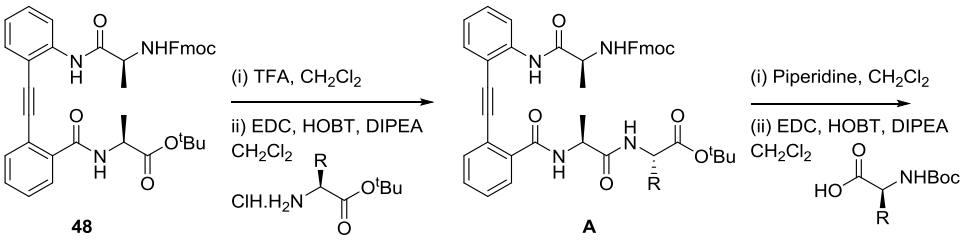

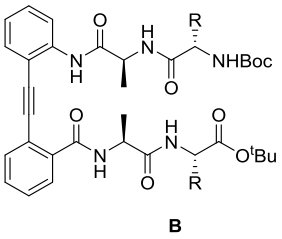

R	A		B	
Me	**69**	53 %	**70**	24 %
H	**130**	46 %	**131**	23 %
	87	46 %	**89**	63 %
	132	45 %	**133**	70 %
	88	50 %	**90**	37 %

Scheme 5.1 Synthesis of a suite of hydrophobic turn mimics.

All of the turn mimics displayed excellent solubility in chloroform and DMSO.

5.5.2 Control Molecules

The single-strand control molecules, **53** and **68**, used in Chapter 3, were deemed unsuitable for a precise study of bonding strength as they did not contain all of the desired residues, nor the same substitution pattern about the diphenylacetylene motif. It was therefore decided to create the *para* substituted system. All five control molecules were successfully synthesised *via* the separate construction of top and bottom strands followed by a late stage Sonogashira reaction (Scheme 5.2).

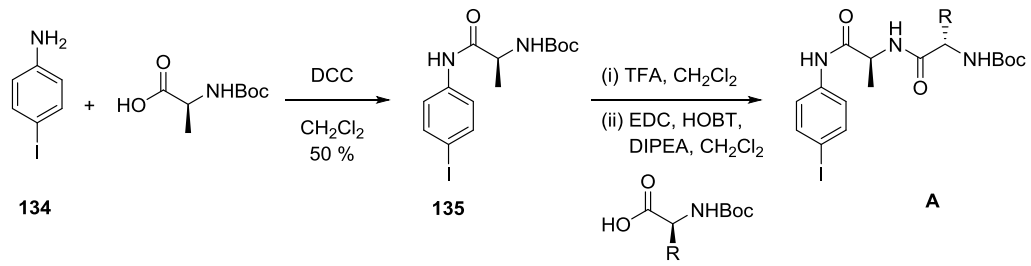

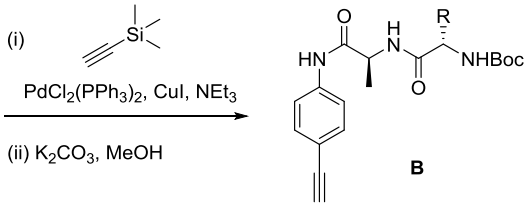

R	A		B	
Me	**136**	63 %	**137**	93 %
H	**138**	62 %	**139**	76 %
	140	56 %	**141**	90 %
	142	77 %	**143**	90 %
	144	72 %	**145**	44 %

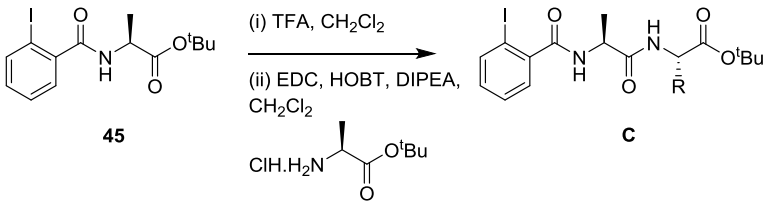

R	C	
Me	**65**	67 %
H	**146**	49 %
	147	44 %
	148	51 %
	149	51 %

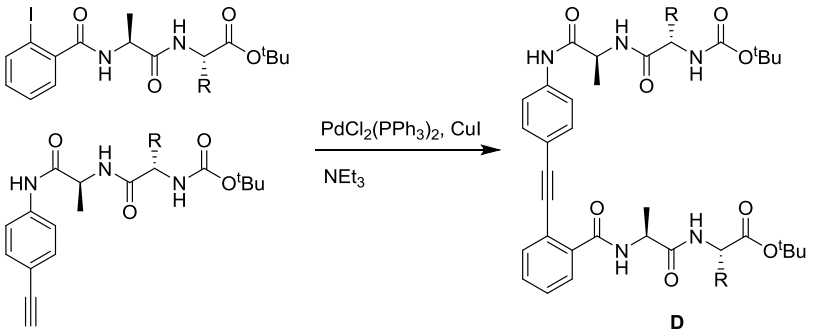

R	D	
Me	**150**	68 %
H	**151**	24 %
	152	47 %
	153	25 %
	154	29 %

Scheme 5.2 Synthesis of control molecules that are unable to form β-sheet structures..

5.6 Analysis

5.6.1 Circular Dichroism

Spectra were obtained for the library of turn mimics at a 100 µM concentration in trifluoroethanol between 185 and 260 nm. Consistent with the spectra obtained of the meanders in Chapter 4, all of the mimics displayed the characteristic minima and maxima of β-sheet structure as templated by the diphenylacetylene motif. The control molecules showed no characteristic shape and so were deemed adequate controls (Figure 5.13).

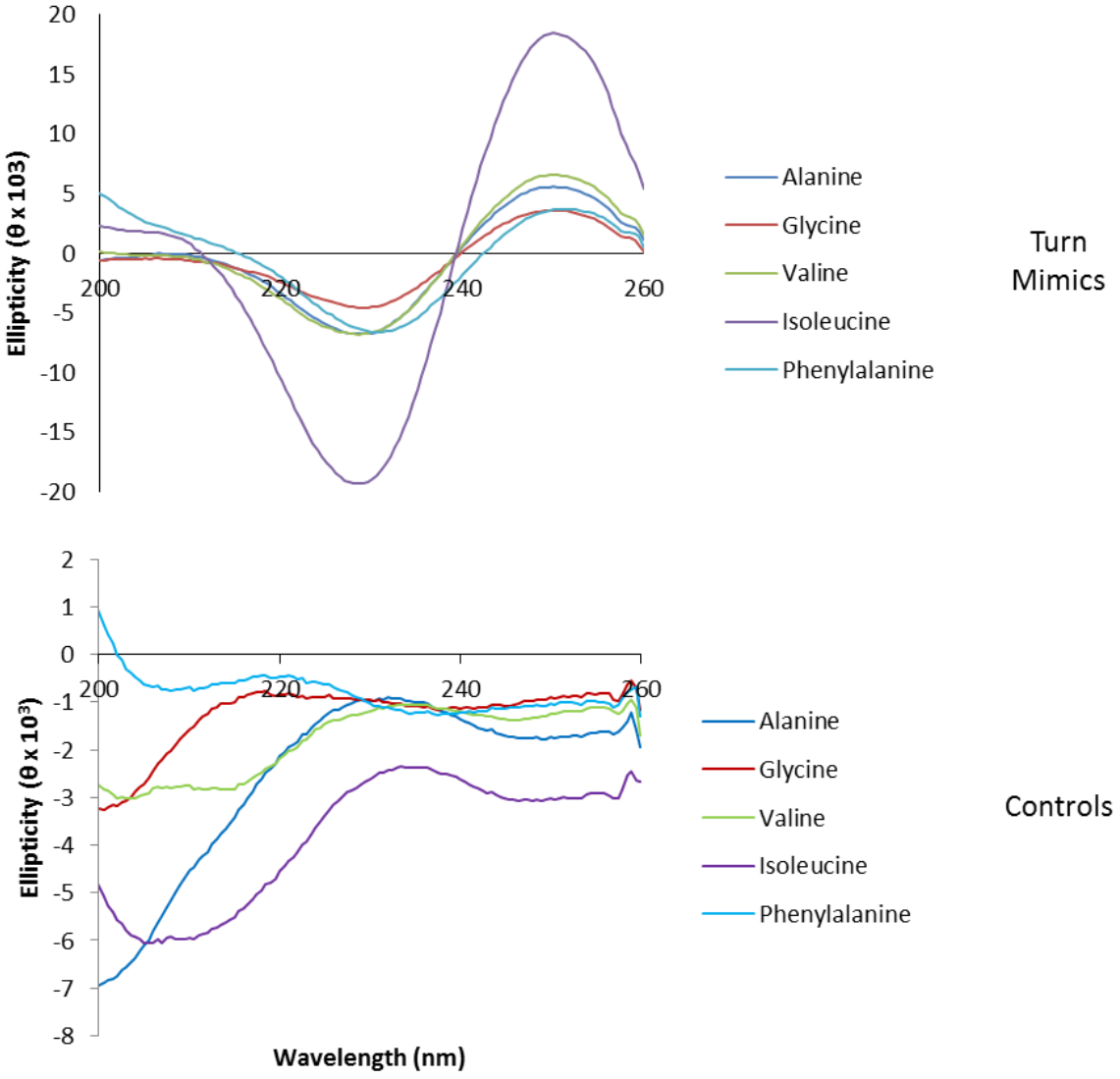

Figure 5.13 Top: CD spectra of turn mimics showing the characteristic maximum and minimum, indicative of well folded β-sheet structure; Bottom: CD spectra of control compounds showing no clear shape, indicative of no defined structure.

5.6.2 NMR

5.6.2.1 A-Values

The ^{1}H NMR spectra of the turn mimics were recorded in deuterated chloroform and DMSO. The spectra were assigned such that the amide N-H within the hydrogen bond of interest (Figure 5.11) could be identified, the chemical shift recorded and the *A* value calculated according to the equation in Section 3.9.9. (Table 5.1, Figure 5.14).

Amino Acid	$\delta_{chloroform}$	δ_{DMSO}	*A* Value
Glycine	8.19	8.15	0.0012
Alanine	8.28	8.20	-0.0041
Valine	8.28	8.16	-0.0095
Isoleucine	8.33	8.21	-0.0095
Phenylalanine	8.62	8.33	-0.0321

Table 5.1 Calculation of *A* values for the turn mimics.

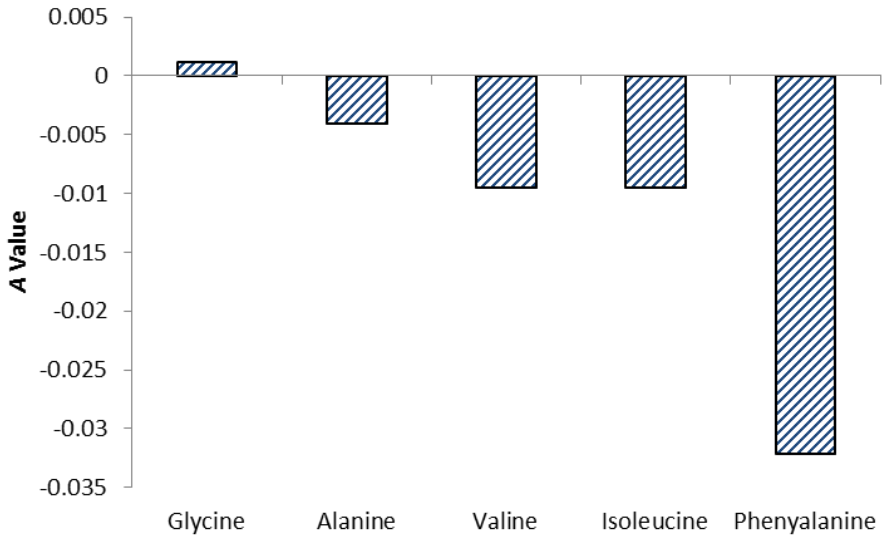

Figure 5.14 Bar chart representation of the *A* values for the turn mimcs.

Recall from Chapter 3 that the smaller the *A* value the stronger the hydrogen bond, with any values less than 0.05 indicating the presence of a hydrogen bond. Thus, hydrogen bonds have been formed in all of these turn mimics, with glycine forming the weakest and phenylalanine the strongest. These results show that increasing bulk results in a stronger hydrogen bond, correlating with the general trend observed in the β-sheet propensity scores. However, valine and isoleucine show a stronger propensity than phenylalanine. In organic solvents the hydrogen bond between the phenylalanine residues may be strengthened by the π-π interaction (Figure 5.15) that brings the donor and acceptor into closer proximity, whilst the hydrophobic effect that aids the formation of clusters including valine and isoleucine is not present.

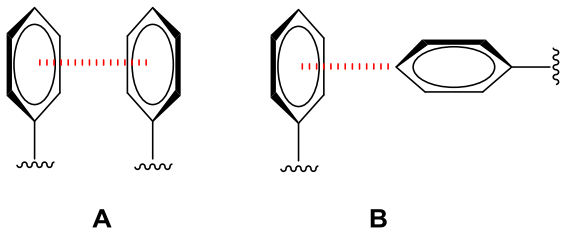

Figure 5.15 Possible modes of π-π interactions. A: Face-to-face most likely in adjacent strands B: Edge-to-face.

However, when compared to the *A* values measured for the various hydrogen bonds in the meanders (Chapter 3) the differences in value are very small. From Figure 3.57 the difference in *A*-value for a similar amide bond to that studied here between the two and three-stranded molecules is 0.065. This compares to a total spread of 0.0333 here, and excluding phenylalanine 0.0107. Furthermore the total range of all hydrogen bound amide N-Hs in the four-stranded meander is 0.1592. This suggests that this data reinforces the conclusions of Rossmeisl, namely that the differences in β-sheet propensity are largely driven by the energy required to change the backbone conformation (E_{conf}) and not the hydrogen bonds within the sheet ($E_{H\text{-}bond}$).

To see if the side-chain blocking effect had any effect on these *A* values the experiment was repeated with the controls (Table 5.2, Figure 5.16).

Amino Acid	**$\delta_{chloroform}$**	**δ_{DMSO}**	***A* Value**
Glycine	7.24	8.42	0.1634
Alanine	6.85	8.34	0.2047
Valine	7.13	8.21	0.1501
Isoleucine	7.13	8.22	0.1515
Phenylalanine	6.46	8.21	0.2393

Table 5.2 Calculation of *A* values for the control molecules.

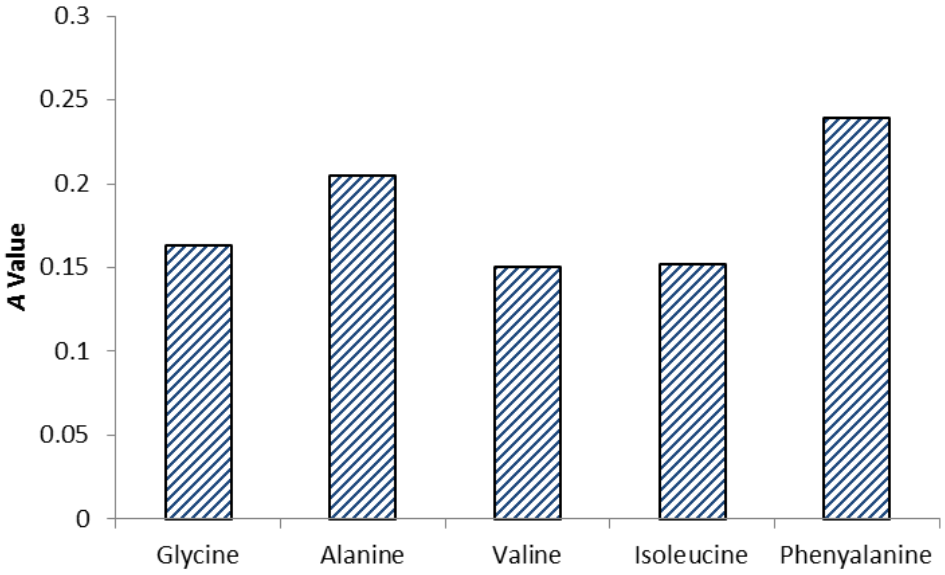

Figure 5.16 Bar chart representation of *A* values for the control compounds.

Pleasingly all of these structures show no hydrogen bonding (*A* values greater than 0.15) and no obvious trends in side-chain dependence. This provides evidence that the observed differences in bonding strength, although small, are not due to the side-chain blocking effect.

5.6.3 Hydrogen-Deuterium Exchange

5.6.3.1 Validation

To confirm the validity and applicability of the method developed by Linton *et al*. it was first tested on data obtained as part of Chapter 3. The hydrogen deuterium exchange for proton ***Hc*** in double strand **70**, and proton ***Ha*** in single stranded control **53** allowed for initial rates to be determined and the bond strength calculated.

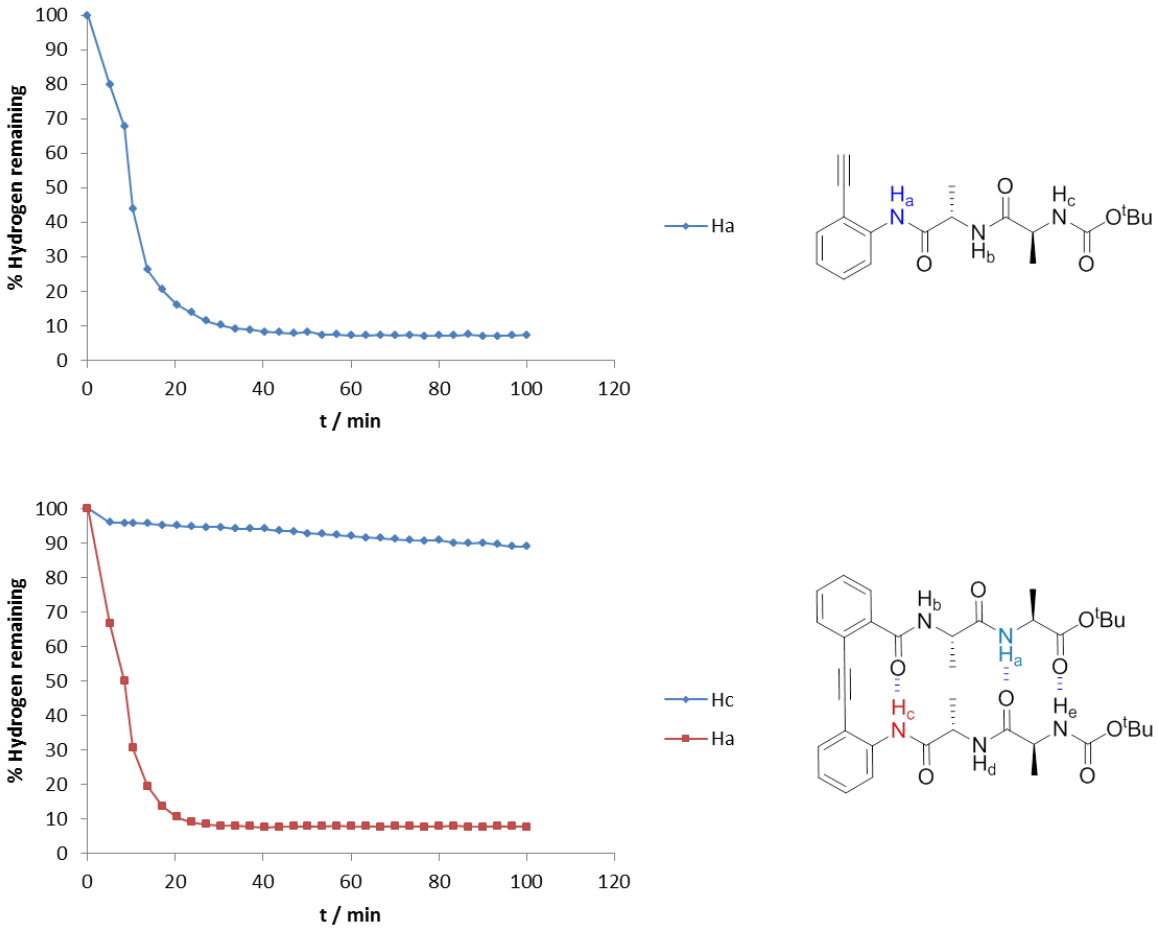

Figure 5.17 Hydrogen-Deuterium exchange data for single strand control **53** and turn mimic **70**. Protons that underwent complete exchange within five minutes are omitted for clarity (Hb and Hc for **53**; Hb, Hd, and He for **70**).

$$k_{ex} = 0.00084\ min^{-1} \quad k_{free} = 0.03086\ min^{-1}$$

$$K_{eq} = \frac{k_{ex}}{k_{free}} = \frac{0.00084}{0.03086} = 0.02722$$

$$\Delta G_{HDX} = -RT \ln 0.02722 = 2.13\ kcal\ mol^{-1}$$

Equation 5.3 Calculation of hydrogen bond strength for bond within Kemp turn.

This falls towards the lower end of expected hydrogen bond strengths, but remains plausible.[28] Possible explanations for this weak bond would be the poor arrangement of the donor and acceptor due to restricted rotation due to the neighbouring sp^2 centres of the aromatic ring. Additionally experimental considerations, such as difficulties in selecting a suitable control and the possibility of aggregation could also be confounding factors.

5.6.3.2 Optimisation

However these reasonable values gave some confidence in the method when applied to these compounds and attempts were therefore made to establish experimental conditions that allowed for calculation of the strength of the bond of interest (Figure 5.11). For this to be determinable the initial rate of exchange of the amide N-H in the control molecule must be measurable. Under the existing experimental conditions the amide N-H of interest underwent complete exchange before the first spectra could be taken. Control molecule **53** was used to establish these conditions. Although it was known to aggregate, by examining the rate of decay of ***N-Hb*** across each run it was hoped that if consistency was observed the aggregation may not have an adverse effect on the rates of exchange. Additionally at this 10 mM concentration the control molecule retained excellent dispersion in the ^{1}H NMR spectra, indicative of negligible self-association, a criteria previously used in propensity studies of other artificial systems.[17]

The rate of exchange was examined across a series of concentrations and volumes when methanol-d_4 was added to a solution of **53** in $CDCl_3$ (Table 4.3).

Entry	Control Concentration (mM)	MeOD added (µL)	Initial Rate
1	10	20	N/A
2	10	10	N/A
3	20	10	N/A
4	40	10	N/A
5	10	2	N/A

Table 4.3 Experimental parameters used in attempts to optimise the hydrogen-deuterium exchange experiment.

Pleasingly the behaviour of ***N-Ha*** across of all these condition was consistent. However across all experimental conditions the proton of interest (***N-Hb***) underwent complete exchange before the first spectra could be obtained. To further confirm that this was not affected by aggregation the triple-stranded meander **56**, known not to aggregate, was subjected to the same conditions as Entry 5, and the external and carbamate N-Hs underwent complete exchange. The new all alanine control, **150**, also known to aggregate in chloroform, showed similar behaviour.

5.6.3.3 Application of Method to Alternative Solvents

Unable to develop suitable assay conditions in chloroform, attention was turned to different solvents. As a hydrogen bond acceptor DMSO is more representative of physiologically relevant solvents. Pleasingly no aggregation was shown by any control molecules in DMSO. Initial studies were therefore performed on turn mimic **70** and control **150** at 10 mM concentration in DMSO-d_6 upon a 20 µL addition of methanol-d_4.

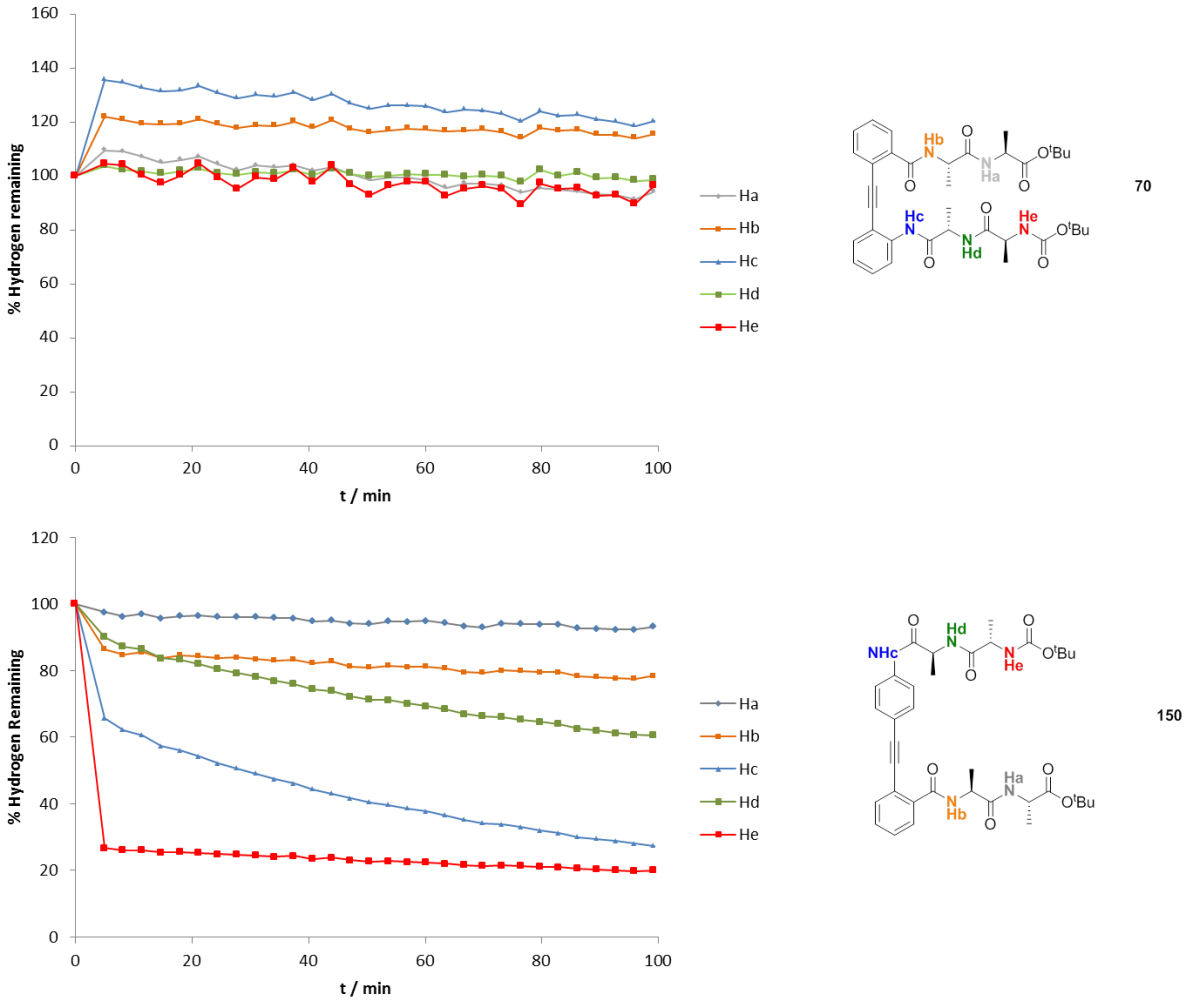

Figure 2 Hydrogen-deuterium exchange experiments performed in DMSO-d_6 for turn mimic 70 and control 150.

The data from these experiments yield some interesting observations. All the amide N-Hs in the turn mimic show no appreciable exchange. It is thought that this is because as a very strong hydrogen bond acceptor, DMSO molecules create a hydrogen bonding network that is harder to disrupt so as to allow for hydrogen-deuterium exchange (Figure 5.18)

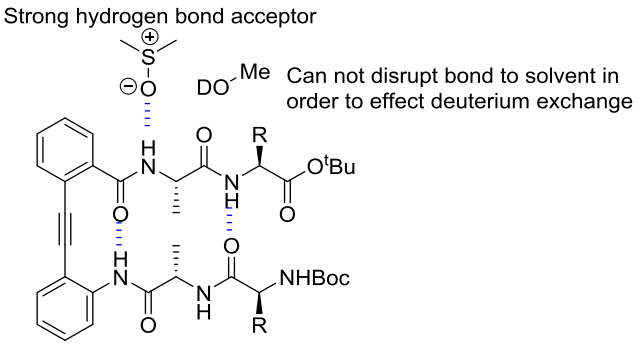

Figure 5.18 Representation of slow exchange in DMSO due to strong hydrogen bonds to solvent.

For the control molecule the analide and carbamate N-Hs, ***Hc*** and ***He***, respectively, show much faster rates of exchange. Pleasingly this points towards the turn conformation being maintained in DMSO. However, for ***Ha***, the amide N-H of interest, the rate of exchange is faster for the turn that the control (although both show only very slow exchange) making calculation of the hydrogen bond strength nonsensical as it would produce a negative value.

To check for consistency in these results and to probe the importance of the deuterium source the experiment was repeated with the addition of 20 µL of D_2O (Figure 5.19).

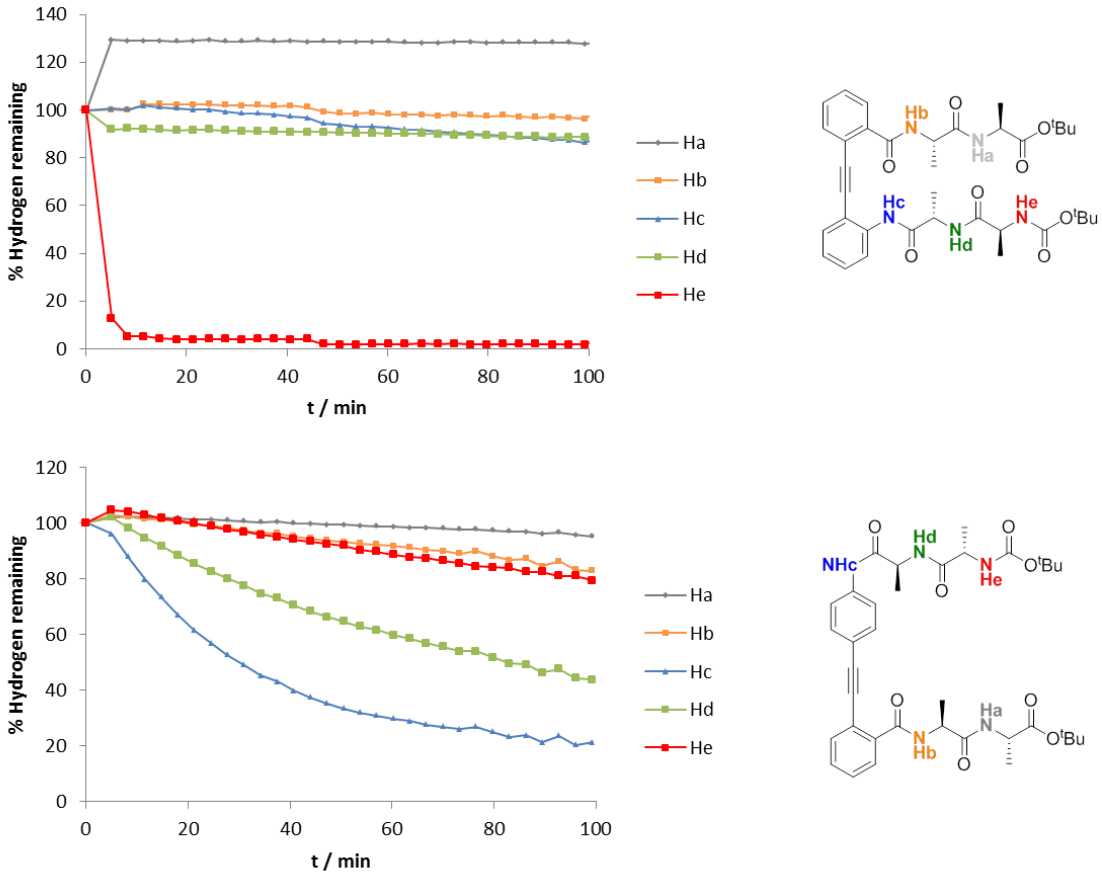

Figure 5.19 Deuterium exchange experiments on the all alanine turn mimic and control.

The amide N-H within the Kemp turn motif here behaves very similarly, with a near zero exchange rate when in the turn motif, and a fast exchange rate in the control. However the carbamate N-H behaves completely differently with near immediate exchange juxtaposed with very slow exchange in the control.

Examining the proton of interest, ***Ha***, the negligible difference in rates would seemingly indicate that no hydrogen bonding is occurring when comparing the turn and control molecules.

5.7 Conclusions and Future Work

A suite of molecules and corresponding controls have been successfully synthesised and their conformations analysed with circular dichroism suggesting adoption of β-sheet structure for

all the turn mimics, and not for the corresponding controls. The suite has then been subjected to two different assays in an attempt to determine the effect of side-chains on hydrogen bond strength in a β-sheet. The hydrogen-deuterium exchange experiment could not be optimised in $CDCl_3$ owing to possible problems with aggregation and overly fast exchange. Data collected in DMSO-d_6 proved difficult to interpret with no firm conclusions drawn.

The use of hydrogen bond acidity, or '***A*** values', proved much more successful with a relative order of hydrogen bond strength deduced and comparison to controls appearing to show that this was independent of the side-chain blocking effect. However the absolute magnitude of the difference between the values indicated that, as suggested by Rossmeisl, it is the energy involved in adopting the extended conformation that dominates sheet propensities.

This work shows that the construction of model chemical systems, and a keen understanding of their folding, provides a tool for probing the properties of Nature's foldamers.

Future work will focus on the development of non-aggregating controls, for example through the incorporation of a suitable *N*-methyl moiety, and a subsequent optimisation of the assay in chloroform.

Ultimately, the diphenylacetylene scaffold will be modified to incorporate water solubilising groups (Chapter 4, Section 4.3.2). The measurement of hydrogen-deuterium exchange by NMR is a very well established technique in aqueous solvents, with exchange, even for solvent exposed N-H groups generally occurring much more slowly than observed for the experiments in this thesis.[18] This should make their study much more tractable. Additionally this allows for the measurement of bond strength in aqueous, physiologically relevant environments, in which entropic and enthalpic differences may lead to markedly different conclusions.

5.8 Experimental

5.8.1 General Information

For ‘Solvents and Reagents’, ‘Chromatography’, and ‘Spectroscopy’, see Chapter 2, Section 2.14.1.

5.8.2 General Experimental Procedures

All procedures used in the synthesis of compounds **130** to **154** are detailed in Chapter 3, Section 3.11.2.

5.8.3 Characterization Data

tert-Butyl (2-((2-((S)-2-((((9H-fluoren-9-yl)methoxy)carbonyl)amino)propanamido)phenyl)ethynyl)benzoyl)-L-alanylglycinate 130

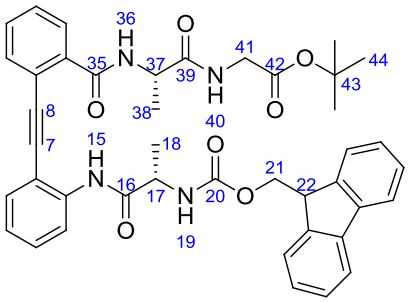

According to *general procedure (3f)*: *tert*-Butyl ester **48** (200 mg, 0.30 mmol) gave a yellow residue **A**. According to *general procedure (3e)*: Residue **A** and L-glycine *tert*-butyl ester hydrochloride (51 mg, 0.30 mmol) gave the *title compound* **130** (100 mg, 46 %) as a white solid after purification by flash column chromotography (PE:Et_2O, 1:1); $[\alpha]_D^{23.5}$ +20.0 (*c* 1.00, $CHCl_3$); δ_H (400 MHz, $CDCl_3$) 9.49 (s, 1 H, H15), 8.58 (d, *J* 7.8, 1 H, Ar-H), 7.66 - 7.70 (m, 2 H, 2 x Ar-H), 7.51 - 7.65 (m, 5 H, H40, 4 x Ar-H), 7.44 (dd, *J* 7.6, 1.5 Hz, 1 H, Ar-H), 7.37 - 7.42 (m, 1 H, Ar-H), 7.26 - 7.35 (m, 4 H, 4 x Ar-H), 7.17 - 7.26 (m, 3 H, H36, 2 x Ar-H), 6.97 - 7.04 (m, 1 H, Ar-H), 6.05 (d, *J* 8.1, 1 H, H19), 5.28 - 5.35 (m, 1 H, H17), 5.19 (s, 1 H, H37), 4.27 - 4.42 (m, 2 H, H21, H21'), 4.14 (m, 1 H, H22), 3.84 (dd, *J* 18.0, 5.4, 1 H, H41), 3.69 (dd, *J* 18.0, 5.1, 1 H, H41'), 1.55 (d, *J* 6.6, 3 H, H18), 1.47 (d, *J* 6.6, 3 H, H38), 1.19 (s, 9 H, H44); δ_C (101 MHz, $CDCl_3$) 173.0, 172.3, 168.4 (3 x C=O), 166.2 (C35), 156.0 (C20), 143.9, 141.3, 140.7, 134.2, 134.1, 132.2, 131.1, 129.9, 128.2, 127.7, 127.2, 127.1, 125.2, 123.4, 122.6, 120.0, 119.5, 112.1 (18 x Ar-C), 95.2, 90.0 (C7, 8), 81.9 (C43), 67.2 (C21), 51.0 (C17), 49.0 (C37), 47.2 (C22), 41.9 (C41), 27.9 (C44), 21.1 (C18), 20.3 (C38); HRMS calculated for $C_{42}H_{42}O_7N_4Na$ $[(M+Na)]^+$: 737.2946, found 737.2941; IR (CH_2Cl_2) 3292, 2974, 2933, 1686, 1649, 1509.

tert-Butyl (2-((2-((S)-2-(2-((tert-butoxycarbonyl)amino)acetamido)propanamido)phenyl)ethynyl)benzoyl)-L-alanylglycinate 131

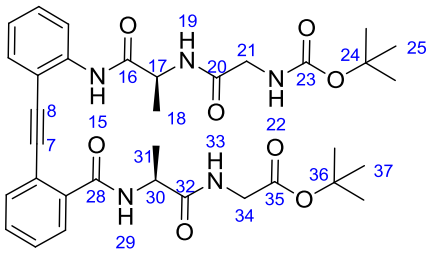

According to *general procedure (3g)*: Fmoc-protected amine **130** (85 mg, 0.12 mmol) was deprotected to give residue **A**. According to *general procedure (3e)*: Residue **A** and *N*-(*tert*-butoxycarbonyl)glycine (22 mg, 0.12 mmol) gave the *title compound* **131** (18.6 mg, 23 %) as a white residue after purification by flash column chromatography (PE:Et_2O, 1:1); $[\alpha]_D^{23.5}$ +45.9 (*c* 1.00, $CHCl_3$); δ_H (400 MHz, $CDCl_3$) 9.52 (br. s, 1 H, H15), 8.60 (d, *J* 8.3, 1 H, Ar-H), 8.14 - 8.23 (m, 1 H, H33), 7.71 - 7.74 (m, 1 H, Ar-H), 7.69 (dd, *J* 7.8, 1.0 Hz, 1 H, Ar-H), 7.51 - 7.53 (m, 1 H, Ar-H), 7.48 - 7.51 (m, 1 H, Ar-H), 7.39 - 7.42 (m, 1 H, Ar-H), 7.34 - 7.37 (m, 1 H, Ar-H), 7.25 (d, *J* 7.3, 1 H, H29), 7.06 - 7.12 (m, 2 H, Ar-H, H19), 5.54 - 5.63 (m, 2 H, H17, H22), 5.37 - 5.45 (m, 1 H, H30), 3.96 - 4.01 (m, 2 H, H34), 3.89 - 3.95 (m, 2 H, H21), 1.62 (d, *J* 6.8, 3 H, H18), 1.57 (d, *J* 6.8, 3 H, H31), 1.48, 1.47 (2 x s, 9 H, H 25, 37); δ_C (101 MHz, $CDCl_3$) 173.1, 172.0, 169.3, 169.0 (4 x C=O), 166.6 (C28), 158.2 (C23), 143.7, 134.3, 134.2, 132.2, 131.1, 129.9, 128.2, 127.2, 123.4, 122.6, 119.5, 114.1 (12 x Ar-C), 95.5, 89.9 (C7, 8), 81.4, 81.0 (C24, 36), 49.9 (C17), 48.9 (C30), 43.9 (C21), 42.2 (C34), 28.4, 28.1 (C25, 37), 20.5 (C18), 20.4 (C31); HRMS calculated for $C_{34}H_{44}O_8N_5[(M+H)]^+$: 650.3184, found 650.3186; IR (CH_2Cl_2) 3306, 2980, 1749, 1514.

Methyl (2-((2-((S)-2-((((9H-fluoren-9-yl)methoxy)carbonyl)amino)propanamido)phenyl)ethynyl)benzoyl)-L-alanyl-L-alloisoleucinate 132

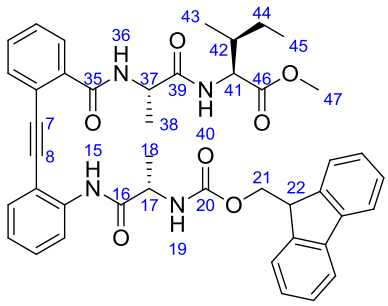

According to *general procedure (3f)*: *tert*-Butyl ester **48** (574 mg, 0.95 mmol) gave yellow residue **A**. According to *general procedure (3e)*: Residue **A** and L-isoleucine methyl ester hydrochloride (182 mg, 0.95 mmol) gave the *title compound* **132** (310 mg, 45 %) as a white solid after purification by flash column chromotography (PE:Et_2O, 1:1); $[\alpha]_D^{23.5}$ +36.6 (*c* 1.00, $CHCl_3$); δ_H (400 MHz, $CDCl_3$) 9.66 (s, 1 H, H15), 8.70 (d, *J* 8.1, 1 H, Ar-H), 7.75 - 7.79 (m, 2 H, 2 x Ar-H), 7.65 - 7.73 (m, 5 H, 4 x Ar-H, H40), 7.53 (dd, *J* 7.6, 1.5, 1 H, Ar-H), 7.47 (td, *J* 7.6, 1.2, 1 H, Ar-H), 7.36 - 7.44 (m, 5 H, 4 x Ar-H, H36), 7.29 - 7.34 (m, 2 H, 2 x Ar-H), 7.09 (td, *J* 7.5, 1.1, 1 H, Ar-H), 6.11 (d, *J* 8.6, 1 H, H19), 5.44 - 5.53 (m, 1 H, H17), 5.26 - 5.34 (m, 1 H, H37), 4.55 - 4.58 (m, 1 H, H41), 4.52 - 4.55 (m, 1 H, H21), 4.27 - 4.31 (m, 1 H, H21'), 4.23 - 4.27 (m, 1 H, H22), 3.58 (s, 3 H, H47), 1.69 - 1.78 (m, 1 H, H42), 1.62 (d, *J* 6.8, 3 H, H18), 1.55 (d, *J* 6.8, 3 H, H38), 0.86 - 0.96 (m, 2 H, H44, H44'), 0.74 (d, *J* 6.8, 3 H, H43), 0.67 (t, *J* 7.3, 3 H, H45); δ_C (101 MHz, $CDCl_3$) 172.8, 172.4, 171.7 (3 x C=O), 166.1 (C35), 155.9 (C20), 143.9, 141.3, 140.8, 134.1, 134.0, 132.1, 131.0, 129.8, 128.1, 127.7, 127.1, 126.9, 125.2, 123.2, 122.6, 119.9, 119.3, 112.0 (18 x Ar-C), 95.2, 89.9 (C7, 8), 67.3 (C21), 56.5 (C41), 51.7 (C47), 50.8 (C17), 49.0 (C37), 46.9 (C22), 37.8 (C42), 25.0 (C44), 21.2 (C18), 20.0 (C38), 15.2 (C43), 11.2 (C45); HRMS calculated for $C_{43}H_{45}O_7N_4$

$[(M+H)]^+$: 729.3283, found 729.3278; IR (CH_2Cl_2) 3300, 2990, 2410, 1680, 1625, 1520, 1490.

Methyl (2-((2-((S)-2-((2S,3R)-2-((tert-butoxycarbonyl)amino)-3-methylpentanamido)propanamido)phenyl)ethynyl)benzoyl)-L-alanyl-L-alloisoleucinate 133

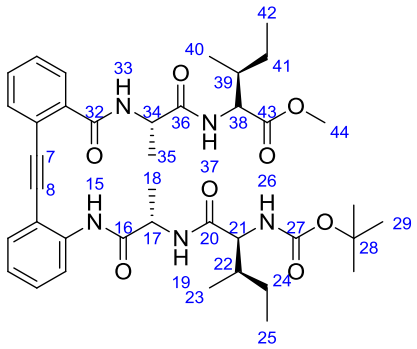

According to *general procedure (3g)*: Fmoc-protected amine **132** (255 mg, 0.35 mmol) was deprotected to give residue **A**. According to *general procedure (3e)*: Residue **A** and *N*-(*tert*-butoxycarbonyl)-L-isoleucine (82 mg, 0.35 mmol) gave the *title compound* **13** (178 mg, 70 %) as a white residue after purification by flash column chromatography (PE:Et_2O, 1:1); $[\alpha]_D^{23.5}$ +61.3 (*c* 1.00, $CHCl_3$); δ_H (400 MHz, $CDCl_3$) 9.63 (br. s, 1 H, H15), 8.67 (d, *J* 7.8, 1 H, Ar-H), 8.33 (d, *J* 8.6, 1 H, H37), 7.74 (d, *J* 7.6, 1 H, Ar-H), 7.71 (dd, *J* 7.8, 1.0, 1 H, Ar-H), 7.53 - 7.56 (m, 1 H, Ar-H), 7.49 - 7.53 (m, 1 H, Ar-H), 7.43 (m, 1 H, Ar-H), 7.36 - 7.40 (m, 1 H, Ar-H), 7.30 - 7.36 (m, 1 H, H33), 7.09 (td, *J* 7.6, 1.0, 1 H, Ar-H), 6.98 (d, *J* 8.1, 1 H, H19), 5.73 (d, *J* 8.8, 1 H, H26), 5.62 - 5.69 (m, 1 H, H17), 5.48 (d, *J* 6.8, 1 H, H34), 4.63 (dd, *J* 8.4, 5.0, 1 H, H38), 4.03 - 4.10 (m, 1 H, H21), 3.80 (s, 3 H, H44), 1.83 - 1.98 (m, 2 H, H22, 39), 1.63 (d, *J* 6.8, 3 H, H18), 1.54 (d, *J* 6.6, 3 H, H35), 1.48 (s, 9 H, H29), 0.87 - 0.98 (m, 16 H, H23, H24, H24', H25, H40, H41, H41', H42); δ_C (101 MHz, $CDCl_3$) 172.9, 172.2, 172.1, 171.3, 166.0 (5 x C=O), 155.9 (C27) 140.8, 134.2, 134.1, 132.3, 131.1, 129.9, 128.2, 127.1, 123.3, 122.7, 119.4, 112.0 (12 x Ar-C), 95.3, 90.1 (C7, 8), 79.5 (C28), 59.6 (C21), 56.8 (C38), 51.3 (C44), 49.6 (C17), 49.2 (C34), 38.1 (C39), 37.7 (C22), 28.4 (C29),

25.3 (C41), 24.8 (C24), 20.8 (C18), 20.4 (C35), 15.4 (C40), 15.3 (C23), 11.6 (C42), 11.5 (C25); HRMS calculated for $C_{39}H_{53}O_8N_5Na$ $[(M+Na)]^+$: 742.3786, found 742.3784; IR (CH_2Cl_2) 3330, 2950, 1700, 1680, 1520, 1480.

tert-Butyl (S)-(1-((4-iodophenyl)amino)-1-oxopropan-2-yl)carbamate 135

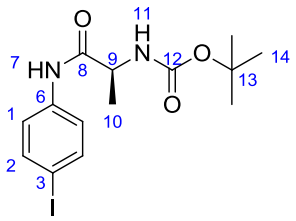

According to *general procedure (3c)*: 4-iodo-aniline **134** (1.00 g, 4.57 mmol) was reacted with *N*-(*tert*-butoxycarbonyl)-L-alanine (1.12 g, 5.94 mmol) to give the *title compound* **135** (900 mg, 50 %) as a white solid after purification by flash column chromotography (CH_2Cl_2:EtOAc, 9:1); The recorded data is in line with reported values;[29] $[\alpha]_D^{23.5}$ -30.4 (*c* 1.00, MeOH); δ_H (400 MHz, $CDCl_3$) 8.91 (br. s, 1 H, H7), 7.55 (d, *J* 8.3, 2 H, H2), 7.26 (d, *J* 8.6, 2 H, H1), 5.24 - 5.29 (m, 1 H, H11), 4.34 - 4.49 (m, 1 H, H9), 1.47 (s, 9 H, H14), 1.44 (d, *J* 7.1, 3 H, H10); δ_C (101 MHz, $CDCl_3$) 171.2 (C8), 156.3 (C12), 137.8 (2C, C2, C6), 121.5 (C1), 87.3 (C3), 80.8 (C13), 50.8 (C9), 28.3 (C14), 17.5 (C10); HRMS calculated for $C_{14}H_{18}O_3N_2{}^{127}I$ $[(M-H)]^-$: 389.0368, found 389.0363; IR (CH_2Cl_2) 3311, 2979, 2931, 1673, 1531, 1487.

tert-Butyl ((S)-1-(((S)-1-((4-iodophenyl)amino)-1-oxopropan-2-yl)amino)-1-oxopropan-2-yl)carbamate 136

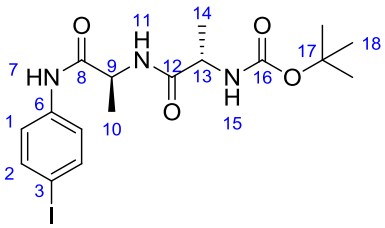

According to *general procedure (3f)*: Boc-protected amine **21** (900 mg, 3.10 mmol) gave yellow residue **A**. According to *general procedure (3e)*: Residue **A** and *N*-(*tert*-butoxycarbonyl)-L-alanine (586 mg, 3.10 mmol) gave the *title compound* **136** (900 mg, 63 %) as a white solid after purification by flash column chromotography (CH_2Cl_2:EtOAc, 3:1); $[\alpha]_D^{23.5}$ -12.7 (*c* 1.00, $CHCl_3$); δ_H (400 MHz, $CDCl_3$) 8.69 (br. s, 1 H, H7), 7.60 (d, *J* 8.5, 2 H, H2), 7.44 (d, *J* 6.9, 2 H, H1), 6.64 (d, *J* 7.3, 1 H, H11), 4.91 (br. s, 1 H, H15), 4.55 - 4.64 (m, 1 H, H9), 4.10 - 4.16 (m, 1 H, H13), 1.48 (d, *J* 7.1, 3 H, H10), 1.44 (s, 9 H, H18), 1.41 (d, *J* 7.1, 3 H, H14); δ_C (101 MHz, $CDCl_3$) 172.8 (C8 or C12), 170.0 (C8 or C12), 156.2 (C16), 137.8 (C6), 137.7(C2), 121.8 (C1), 87.4 (C3), 81.3 (C17), 51.2 (C13), 49.6 (C9), 28.2 (C18), 17.5 (C14), 17.2 (C10); HRMS calculated for $C_{17}H_{24}O_4N_3{}^{127}INa$ $[(M+Na)]^+$: 484.0704, found 484.0706; IR (CH_2Cl_2) 3334, 3283, 2981, 2932, 1649, 1527.

tert-Butyl ((S)-1-(((S)-1-((4-ethynylphenyl)amino)-1-oxopropan-2-yl)amino)-1-oxopropan-2-yl)carbamate 137

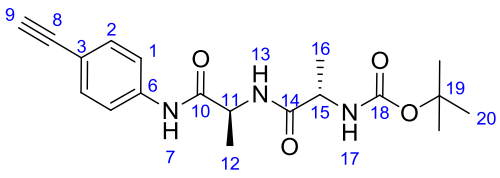

According to *general procedure (3a)*: Iodide **135** (900 mg, 1.95 mmol) and ethynyltrimethylsilane (554 µL, 3.90 mmol) gave a pale brown residue **A**. This was then

deprotected according to *general procedure (3b)* to give the *title compound* **137** (703 mg, 93 %) as a pale yellow solid after purification by flash column chromatography (CH_2Cl_2:EtOAc, 3:1); $[\alpha]_D^{23.5}$ -46.6 (*c* 1.00, $CHCl_3$); δ_H (400 MHz, $CDCl_3$) 8.76 (br. s, 1 H, H7), 7.45 (d, *J* 8.1, 2 H, H1), 7.24 - 7.29 (m, 2 H, H2), 6.71 (d, *J* 7.1, 1 H, H13), 4.89 (d, *J* 5.6, 1 H, H17), 4.45 - 4.53 (m, 1 H, H15), 3.95 - 4.07 (m, 1 H, H11), 2.88 (s, 1 H, H9), 1.31 (d, *J* 7.1, 3 H, H16), 1.27 (s, 9 H, H20), 1.24 (d, *J* 7.1, 3 H, H12); δ_C (101 MHz, $CDCl_3$) 173.0 (C10 or C14), 170.3 (C10 or C14), 156.8 (C18), 138.6 (C6), 132.8 (C2), 119.6 (C1), 117.5 (C3), 86.6 (C8), 83.5 (C9), 81.0 (C19), 49.7 (C15), 49.2 (C11), 28.3 (C20), 17.8 (C12), 17.5 (C16); HRMS calculated for $C_{19}H_{26}O_4N_3$ $[(M+H)]^+$: 360.1918, found 360.1921; IR (CH_2Cl_2) 3291, 2980, 2934, 1656, 1509.

tert-Butyl (S)-(2-((1-((4-iodophenyl)amino)-1-oxopropan-2-yl)amino)-2-oxoethyl)carbamate 138

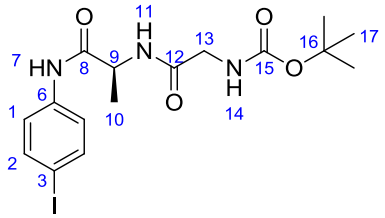

According to *general procedure (3f)*: Boc-protected amine **135** (840 mg, 2.90 mmol) gave yellow residue **A**. According to *general procedure (3e)*: Residue **A** and *N*-(*tert*-butoxycarbonyl)-glycine (175 mg, 2.90 mmol) gave the *title compound* **138** (800 mg, 62 %) as a white solid after purification by flash column chromotography (CH_2Cl_2:EtOAc, 3:1); $[\alpha]_D^{23.5}$ -28.2 (*c* 1.00, $CHCl_3$); δ_H (400 MHz, $CDCl_3$) 9.20 (br. s, 1 H, H7), 7.55 (d, *J* 8.8, 2 H, H2), 7.33 (d, *J* 8.6, 2 H, H1), 7.29 (br. s, 1 H, H11), 5.55 (br. s, 1 H, H14), 4.65 - 4.76 (m, 1 H, H9), 3.79 - 3.89 (m, 2 H, H13, H13'), 1.43 - 1.45 (m, 3 H, H10), 1.42 (s, 9 H, H17); δ_C (101 MHz, $CDCl_3$) 170.7 (C8 or C12), 170.1 (C8 or C12), 153.1 (C15), 137.7 (2C, C2,

C6), 121.8 (C1), 87.5 (C3), 80.5 (C16), 49.7 (C9), 44.3 (C13), 28.2 (C17), 17.9 (C10); HRMS calculated for $C_{16}H_{22}O_4N_3{}^{127}INa$ $[(M+Na)]^+$: 470.0547, found 470.0551; IR (CH_2Cl_2) 3389, 3318, 3261, 2981, 1688, 1652, 1519.

tert-Butyl (S)-(2-((1-((4-ethynylphenyl)amino)-1-oxopropan-2-yl)amino)-2-oxoethyl)carbamate 139

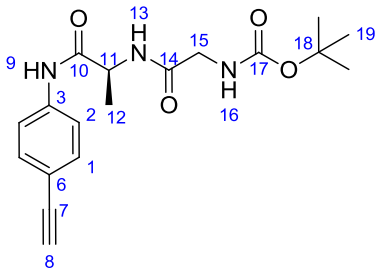

According to *general procedure (3a)*: Iodide **138** (400 mg, 0.89 mmol) and ethynyltrimethylsilane (250 μL, 1.79 mmol) gave a pale brown residue **A**. This was then deprotected according to *general procedure (3b)* to give the *title compound* **139** (232 mg, 76 %) as a pale yellow solid after purification by flash column chromatography (CH_2Cl_2:EtOAc, 3:1); $[\alpha]_D^{23.5}$ -48.0 (*c* 1.00, MeOH); δ_H (400 MHz, $CDCl_3$) 8.91 (br. s, 1 H, H9), 7.55 - 7.60 (m, 2 H, H2), 7.41 - 7.45 (m, 2 H, H1), 6.84 (d, *J* 7.3, 1 H, H13), 5.25 (br. s, 1 H, H16), 4.68 (quin, *J* 7.2, 1 H, H11), 3.83 (d, *J* 5.6, 2 H, H15), 3.04 (s, 1 H, H8), 1.49 (m, 3 H, H12), 1.45 (s, 9 H, H19); δ_C (101 MHz, $CDCl_3$) 172.0 (C10 or C14), 170.6 (C10 or C14), 156.4 (C17), 138.4 (C3), 132.8 (C1), 119.6 (C2), 116.1 (C6), 83.1 (C7), 77.2 (C18), 76.7 (C8), 49.6 (C11), 44.5 (C15), 28.2 (C19), 17.4 (C12); HRMS calculated for $C_{18}H_{23}O_4N_3Na$ $[(M+Na)]^+$: 368.1581, found 368.1581; IR (CH_2Cl_2) 3291, 2979, 2933, 1661, 1601, 1510, 1452.

tert-Butyl ((S)-1-(((S)-1-((4-iodophenyl)amino)-1-oxopropan-2-yl)amino)-3-methyl-1-oxobutan-2-yl)carbamate 140

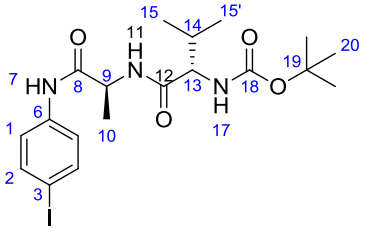

According to *general procedure (3f)*: Boc protected amine **135** (840 mg, 2.90 mmol) gave yellow residue **A**. According to *general procedure (3e)*: Residue **A** and *N*-(*tert*-butoxycarbonyl)-L-valine (629 mg, 2.90 mmol) gave the *title compound* **140** (800 mg, 56 %) as a white solid after purification by flash column chromotography (CH_2Cl_2:EtOAc, 3:1); $[\alpha]_D^{23.5}$ -36.9 (*c* 1.00, $CHCl_3$); δ_H (400 MHz, $CDCl_3$) 9.09 (br. s, 1 H, H7), 7.55 (d, *J* 8.8, 2 H, H2), 7.33 (d, *J* 8.6, 2 H, H1), 7.20 (d, *J* 6.8, 1 H, H11), 5.23 (d, *J* 7.3, 1 H, H17), 4.63 - 4.73 (m, 1 H, H9), 4.00 - 4.08 (m, 1 H, H13), 2.09 - 2.16 (m, 1 H, H14), 1.43 - 1.44 (m, 3 H, H10), 1.42 (s, 9 H, H20), 0.95 (d, *J* 6.8, 3 H, H15), 0.92 (d, *J* 6.8, 3 H, H15'); δ_C (101 MHz, $CDCl_3$) 172.3 (C8 or C12), 170.4 (C8 or C12), 156.1 (C18), 137.7 (C6), 137.7 (C2, 4), 121.8 (C1, 5), 87.4 (C3), 80.4 (C19), 60.1 (C13), 49.7 (C9), 30.7 (C14), 28.3 (C20), 19.2 (C15), 17.8 (C15'), 17.5 (C10); HRMS calculated for $C_{19}H_{29}O_4N_3{}^{127}I$ $[(M+H)]^+$: 490.1197, found 490.1196; IR (CH_2Cl_2) 3324, 3288, 1652, 1265, 733.

tert-Butyl ((S)-1-(((S)-1-((4-ethynylphenyl)amino)-1-oxopropan-2-yl)amino)-3-methyl-1-oxobutan-2-yl)carbamate 141

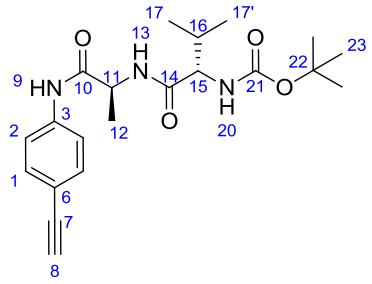

According to *general procedure (3a)*: Iodide **140** (400 mg, 0.82 mmol) and ethynyltrimethylsilane (232 µL, 1.64 mmol) gave pale brown residue **A**. This was then deprotected according to *general procedure (3b)* to give the *title compound* **141** (285 mg, 90 %) as a pale yellow solid after purification by flash column chromatography (CH_2Cl_2:EtOAc, 3:1); $[\alpha]_D^{23.5}$ -50.0 (*c* 1.00, $CHCl_3$); δ_H (400 MHz, $CDCl_3$) 8.84 (br. s., 1 H, H9), 7.57 (d, *J* 8.3, 2 H, H2), 7.40 - 7.46 (m, 2 H, H1), 6.68 (d, *J* 6.6, 1 H, H13), 5.01 (d, *J* 6.1, 1 H, H20), 4.61 - 4.73 (m, 1 H, H11), 3.92 - 4.03 (m, 1 H, H15), 3.04 (s, 1 H, H8), 2.14 - 2.24 (m, 1 H, H16), 1.47 (d, *J* 7.1 Hz, 3 H, H12), 1.44 (s, 9 H, H23), 0.99 (d, *J* 6.8 Hz, 3 H, H17), 0.94 (d, *J* 6.8, 3 H, H17'); δ_C (101 MHz, $CDCl_3$) 172.1 (C10 or C14), 170.1 (C10 or C14), 156.3 (C21), 138.4 (C3), 132.8 (C1), 119.5 (C2), 117.5 (C6), 83.5 (C7), 77.2 (C22), 76.7 (C8), 60.5 (C15), 49.6 (C11), 30.3 (C16), 28.2 (C23), 19.3 (C17), 17.7 (C17'), 17.2 (C12); HRMS calculated for $C_{21}H_{30}O_4N_3$ $[(M+H)]^+$: 388.2231, found 388.2234; IR (CH_2Cl_2) 3292, 2974, 2933, 1686, 1649, 1527, 1509.

tert-Butyl ((2S,3S)-1-(((S)-1-((4-iodophenyl)amino)-1-oxopropan-2-yl)amino)-3-methyl-1-oxopentan-2-yl)carbamate 142

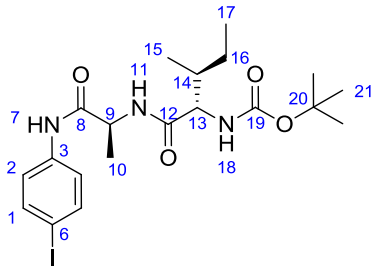

According to *general procedure (3f)*: Boc-protected amine **135** (840 mg, 2.90 mmol) gave yellow residue **A**. According to *general procedure (3e)*: Residue **A** and *N*-(*tert*-butoxycarbonyl)-L-isoleucine (670 mg, 2.90 mmol) gave the *title compound* **142** (900 mg, 77 %) as a white solid after purification by flash column chromotography (CH_2Cl_2:EtOAc, 3:1); $[\alpha]_D^{23.5}$ -27.8 (*c* 1.00, $CHCl_3$); δ_H (400 MHz, $CDCl_3$) 9.15 (br. s, 1 H, H7), 7.51 - 7.55 (m, 2 H, H1), 7.37 (d, *J* 6.6, 1 H, H11), 7.31 (d, *J* 8.8, 2 H, H2), 5.32 (d, *J* 7.1, 1 H, H18), 4.63 - 4.74 (m, 1 H, H9), 4.07 - 4.14 (m, 1 H, H13), 1.79 - 1.85 (m, 1 H, H14), 1.42 - 1.42 (m, 3 H, H10), 1.41 (s, 9 H, H21), 1.04 - 1.19 (m, 2 H, H16, H16'), 0.90 (d, *J* 6.8, 3 H, H15), 0.83 - 0.87 (m, 3 H, H17); δ_C (101 MHz, $CDCl_3$) 172.4 (C8 or C12), 170.5 (C8 or C12), 156.1 (C19), 137.7 (C3), 137.6 (C1), 121.8 (C2), 87.3 (C6), 80.2 (C20), 59.3 (C13), 49.7 (C9), 37.1 (C14), 28.2 (C21), 24.8 (C16), 17.5 (C10), 15.5 (C15), 11.2 (C17); HRMS calculated for $C_{20}H_{31}O_4N_3{}^{127}I$ $[(M+H)]^+$: 504.1354, found 504.1346; IR (CH_2Cl_2) 3466, 2932, 1657, 1387.

tert-Butyl ((2S,3S)-1-(((S)-1-((4-ethynylphenyl)amino)-1-oxopropan-2-yl)amino)-3-methyl-1-oxopentan-2-yl)carbamate 143

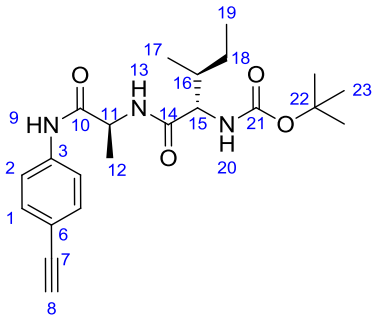

According to *general procedure (3a)*: Iodide **142** (400 mg, 0.82 mmol) and ethynyltrimethylsilane (232 µL, 1.64 mmol) gave pale brown residue **A**. This was then deprotected according to *general procedure (3b)* to give the *title compound* **143** (285 mg, 90 %) as a pale yellow solid after purification by flash column chromatography (CH_2Cl_2:EtOAc, 3:1); $[\alpha]_D^{23.5}$ -44.7 (*c* 1.00, $CHCl_3$); δ_H (400 MHz, $CDCl_3$) 8.87 (br. s, 1 H, H9), 7.58 (d, *J* 8.3, 2 H, H2), 7.40 - 7.45 (m, 2 H, H1), 6.71 (d, *J* 6.8, 1 H, H13), 5.01 (d, *J* 6.8, 1 H, H20), 4.60 - 4.73 (m, 1 H, H11), 3.95 - 4.06 (m, 1 H, H15), 3.04 (s, 1 H, H8), 1.86 - 1.99 (m, 1 H, H16), 1.47 (d, *J* 7.1, 3H, H12), 1.43 (s, 9 H, H23), 1.05 - 1.27 (m, 2 H, H18, H18'), 0.95 (d, *J* 6.8, 3 H, H17), 0.90 (t, *J* 7.3, 3 H, H19); δ_C (101 MHz, $CDCl_3$) 172.0 (C10 or C14), 170.1 (C10 or C14), 156.3 (C21), 138.4 (C3), 132.8 (C1), 119.5 (C2), 117.5 (C6), 83.5 (C7), 80.8 (C22), 76.6 (C8), 59.8 (C15), 49.6 (C11), 36.9 (C16), 28.2 (C23), 24.8 (C18), 17.3 (C12), 15.7 (C17), 11.4 (C19); HRMS calculated for $C_{22}H_{31}O_4N_3Na$ $[(M+Na)]^+$: 424.2207, found 424.2203; IR (CH_2Cl_2) 3427, 3344, 3301, 1708, 1674, 1637.

tert-Butyl ((S)-1-(((S)-1-((4-iodophenyl)amino)-1-oxopropan-2-yl)amino)-1-oxo-3-phenylpropan-2-yl)carbamate 144

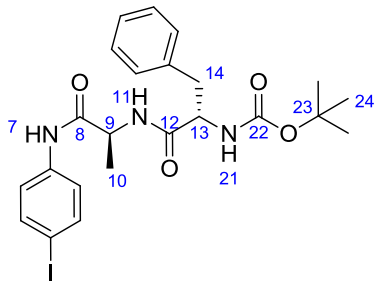

According to *general procedure (3f)*: Boc protected amine **135** (600 mg, 2.07 mmol) gave yellow residue **A**. According to *general procedure (3e)*: Residue **A** and *N*-(*tert*-butoxycarbonyl)-L-phenylalanine (550 mg, 2.07 mmol) gave the *title compound* **144** (800 mg, 72%) as a white solid after purification by flash column chromotography (CH_2Cl_2:EtOAc, 3:1); $[\alpha]_D^{23.5}$ -3.10 (*c* 1.00, $CHCl_3$); δ_H (400 MHz, $CDCl_3$) 8.70 (br. s, 1 H, H7), 7.57 - 7.62 (m, 2 H, 2 x Ar-H), 7.39 (d, *J* 8.6, 2 H, 2 x Ar-H), 7.25 - 7.28 (m, 3 H, 3 x Ar-H), 7.15 - 7.20 (m, 2 H, 2 x Ar-H), 6.44 (d, *J* 7.3, 1 H, H11), 4.97 (d, *J* 4.2, 1 H, H21), 4.54 - 4.65 (m, 1 H, H9), 4.31 - 4.39 (m, 1 H, H13), 3.09 - 3.16 (m, 1 H, H14), 3.04 - 3.08 (m, 1 H, H14'), 1.41 (d, *J* 7.1, 3 H, H10), 1.40 (s, 9 H, H24); δ_C (101 MHz, $CDCl_3$) 171.7 (C8 or C12), 169.8 (C8 or C12), 155.9 (C22), 137.8, 135.7, 129.1, 128.9, 128.6, 127.4, 121.8, 87.4 (8 x Ar-C), 81.2 (C23), 56.2 (C13), 49.6 (C9), 37.7 (C14), 28.2 (C24), 17.1 (C10); HRMS calculated for $C_{23}H_{28}O_4N_3{}^{127}INa$ $[(M+Na)]^+$: 560.1017, found 560.1017; IR (CH_2Cl_2) 3331, 3285, 2931, 1650, 1526, 1513.

tert-Butyl ((S)-1-(((S)-1-((4-ethynylphenyl)amino)-1-oxopropan-2-yl)amino)-1-oxo-3-phenylpropan-2-yl)carbamate 145

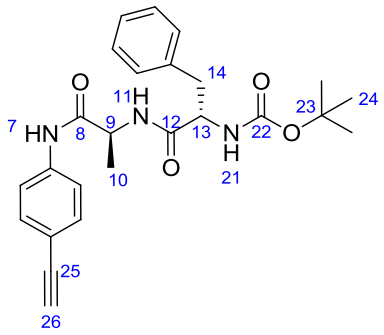

According to *general procedure (3a)*: Iodide **135** (600 mg, 1.12 mmol) and ethynyltrimethylsilane (320 µL, 2.23 mmol) gave pale brown residue **A**. This was then deprotected according to *general procedure (3b)* to give the *title compound* **145** (213 mg, 44 %) as a pale yellow solid after purification by flash column chromatography (CH_2Cl_2:EtOAc, 3:1); $[\alpha]_D^{23.5}$ -8.20 (*c* 1.00, MeOH); δ_H (400 MHz, $CDCl_3$) 8.72 - 8.84 (m, 1 H, H7), 7.58 - 7.62 (m, 1 H, Ar-H), 7.57 (d, *J* 9.0, 1 H, Ar-H), 7.41 - 7.47 (m, 1 H, Ar-H), 7.37 (d, *J* 8.3, 1 H, Ar-H), 7.23 - 7.28 (m, 3 H, 3 x Ar-H), 7.15 - 7.19 (m, 2 H, 2 x Ar-H), 6.57 (d, *J* 6.4, 1 H, H11), 4.98 - 5.04 (m, 1 H, H21), 4.56 - 4.66 (m, 1 H, H9), 4.33 - 4.44 (m, 1 H, H13), 3.06 - 3.19 (m, 2 H, H14), 3.05 (s, 1 H, H26), 1.40 (s, 9 H, H24), 1.37 - 1.39 (m, 3 H, H10); δ_C (101 MHz, $CDCl_3$) 171.7 (C8 or 12), 169.8 (C8 or C12), 155.9 (C22), 138.4, 135.7, 132.8, 129.1, 127.3, 121.8, 119.5, 117.5 (8 x Ar-C), 83.5 (C25), 81.1 (C23), 76.7 (C26), 56.2 (C13), 49.7 (C9), 37.8 (C14), 28.2 (C24), 17.2 (C10); HRMS calculated for $C_{25}H_{29}O_4N_3Na$ $[(M+Na)]^+$: 458.2050, found 458.2044; IR (CH_2Cl_2) 3290, 2979, 1652, 1601, 1528, 1509.

Methyl (2-iodobenzoyl)-L-alanylglycinate 146

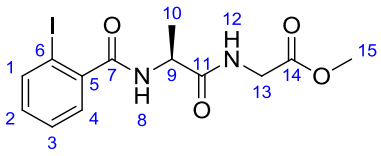

According to *general procedure (3f): tert*-Butyl ester **45** (667 mg, 2.09 mmol) gave yellow residue **A**. According to *general procedure (3e):* Residue **A** and glycine methyl ester hydrochloride (336 mg, 2.09 mmol) gave the *title compound* **146** (400 mg, 49 %) as a white solid after purification by flash column chromotography (CH_2Cl_2:EtOAc, 3:1); $[\alpha]_D^{23.5}$ -1.60 (*c* 1.00, MeOH); δ_H (400 MHz, $CDCl_3$) 7.77 - 7.81 (m, 1 H, Ar-H), 7.28 - 7.37 (m, 2 H, 2 x Ar-H), 7.01 - 7.07 (m, 1 H, Ar-H), 6.90 (br. d, *J* 4.4, 1 H, H8), 6.48 (br. d, *J* 7.3, 1 H, H12), 4.68 - 4.77 (m, 1 H, H9), 4.00 (d, *J* 5.4, 2 H, H13, H13'), 3.68 (s, 3 H, H15), 1.45 - 1.50 (m, 3 H, H10); δ_C (101 MHz, $CDCl_3$) 172.0, 170.0, 169.2 (3 x C=O), 141.2 (C5), 139.9 (C1), 131.4 (C2), 128.4 (C3), 128.2 (C4), 92.4 (C6), 52.4 (C9), 49.2 (C15), 41.3 (C13), 18.1 (C10); HRMS calculated for $C_{13}H_{16}O_4N_2{}^{127}I$ $[(M+H)]^+$: 391.0149, found 391.0160; IR (CH_2Cl_2) 3302, 3068, 2362, 1750, 1646, 1531.

Methyl (2-iodobenzoyl)-L-alanyl-L-valinate 147

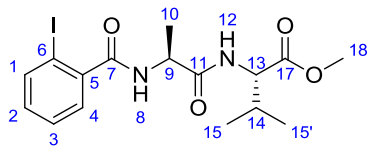

According to *general procedure (3f)*: *tert*-Butyl ester **45** (1.00 g, 3.13 mmol) gave yellow residue **A**. According to *general procedure (3e)*: Residue **A** and L-valine methyl ester hydrochloride (523 mg, 3.13 mmol) gave the *title compound* **147** (600 mg, 44 %) as a white solid after purification by flash column chromotography (PE:Et_2O, 2:3); $[\alpha]_D^{23.5}$ -8.70 (*c* 1.00, $CHCl_3$); δ_H (400 MHz, $CDCl_3$) 7.77 - 7.82 (m, 1 H, Ar-H), 7.28 - 7.38 (m, 2 H, 2 x Ar-H),

7.01 - 7.07 (m, 1 H, Ar-H), 6.62 (d, *J* 8.6, 1 H, H8), 6.42 (d, *J* 7.1, 1 H, H12), 4.64 - 4.74 (m, 1 H, H9), 4.48 (dd, *J* 8.8, 4.9, 1 H, H13), 3.69 (s, 3 H, H18), 2.08 - 2.19 (m, 1 H, H14), 1.45 - 1.48 (m, 3 H, H10), 0.88 - 0.91 (m, 3 H, H15), 0.84 - 0.88 (m, 3 H, H15'); δ_C (101 MHz, $CDCl_3$) 172.1, 171.6, 169.0 (3 x C=O), 141.3 (C5), 139.9 (C1), 131.4 (C2), 128.4 (C3), 128.2 (C4), 92.4 (C6) 57.4 (C13), 52.3 (C18), 49.5 (C9), 31.2 (C14), 19.1 (C15), 18.1 (C10), 17.8 (C15'); HRMS calculated for $C_{16}H_{22}O_4N_2{}^{127}I$ $[(M+H)]^+$: 433.0619, found 433.0622; IR (CH_2Cl_2) 3258, 2966, 1737, 1626, 1532.

Methyl (2-iodobenzoyl)-L-alanyl-L-alloisoleucinate 148

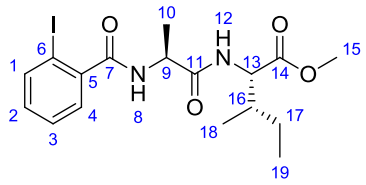

According to *general procedure (3f)*: *tert*-Butyl ester **45** (667 mg, 2.09 mmol) gave yellow residue **A**. According to *general procedure (3e)*: Residue **A** and L-isoleucine methyl ester hydrochloride (380 mg, 2.09 mmol) gave the *title compound* **148** (472 mg, 51 %) as a white solid after purification by flash column chromotography (CH_2Cl_2:EtOAc, 3:1); $[\alpha]_D^{23.5}$ +2.60 (*c* 1.00, $CHCl_3$); δ_H (400 MHz, $CDCl_3$) 7.78 (d, *J* 7.8, 1 H, Ar-H), 7.29 - 7.33 (m, 2 H, 2 x Ar-H), 6.99 - 7.06 (m, 1 H, Ar-H), 6.87 (br. d, *J* 8.3, 1 H, H12), 6.56 (br. d, *J* 7.3, 1 H, H8), 4.72 - 4.80 (m, 1 H, H9), 4.49 (m, 1 H, H13), 3.67 (s, 3 H, H15), 1.81 - 1.91 (m, 1 H, H16), 1.44 - 1.49 (m, 3 H, H10), 1.29 - 1.39 (m, 1 H, H17), 1.06 - 1.19 (m, 1 H, H17'), 0.82 - 0.87 (m, 3 H, H18), 0.77 - 0.82 (m, 3 H, H19); δ_C (101 MHz, $CDCl_3$) 172.1, 171.7 (2C, 3 x C=O), 141.4 (C5), 139.9 (C1), 131.3 (C2), 128.4 (C3), 128.2 (C4), 92.4 (C6), 56.8 (C13), 52.2 (C15), 49.4 (C9), 37.7 (C16), 25.1 (C17), 18.3 (C10), 15.6 (C18), 11.6 (C19); HRMS calculated for $C_{17}H_{24}O_4N_2{}^{127}I$ $[(M+H)]^+$: 447.0775, found 447.0771; IR (CH_2Cl_2) 3262, 2966, 1734, 1682, 1626, 1531.

Methyl (2-iodobenzoyl)-L-alanyl-L-phenylalaninate 149

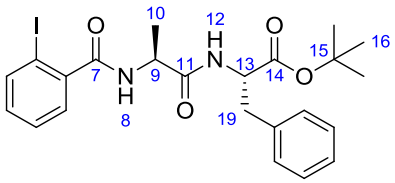

According to *general procedure (3f)*: *tert*-Butyl ester **45** (667 mg, 2.09 mmol) gave yellow residue **A**. According to *general procedure (3e)*: Residue **A** and L-phenylalanine *tert*-butyl ester hydrochloride (539 mg, 2.09 mmol) gave the *title compound* **149** (668 mg, 61 %) as a white solid after purification by flash column chromotography (CH_2Cl_2:EtOAc, 3:1); $[\alpha]_D^{23.5}$ +24.2 (*c* 1.00, $CHCl_3$); δ_H (400 MHz, $CDCl_3$) 7.83 - 7.86 (m, 1 H, Ar-H), 7.33 - 7.36 (m, 2 H, Ar-H), 7.23 - 7.28 (m, 2 H, Ar-H), 7.20 - 7.23 (m, 1 H, Ar-H), 7.16 - 7.19 (m, 2 H, Ar-H), 7.06 - 7.12 (m, 1 H, Ar-H), 6.80 (br. d, *J* 7.8, 1 H, H8), 6.69 (br. d, *J* 7.6, 1 H, H12), 4.74 - 4.77 (m, 1 H, H9), 4.71 - 4.74 (m, 1 H, H13), 3.10 (m, 2 H, H19), 1.50 (d, *J* 7.1, 3 H, H10), 1.41 (s, 9 H, H16); δ_C (101 MHz, $CDCl_3$) 171.3 (C11 or C14), 170.2 (C11 or C14), 168.8 (C7), 141.4, 139.8, 136.1, 131.3, 129.5, 128.5, 128.4, 128.1, 127.0 (9 x Ar-C), 92.5 (C6), 82.4 (C15), 53.9 (C13), 49.4 (C9), 37.9 (C19), 28.0 (C16), 18.6 (C10); HRMS calculated for $C_{23}H_{28}O_4N_2{}^{127}I$ $[(M+H)]^+$: 523.1088, found 523.1086; IR (CH_2Cl_2) 3290, 2978, 1730, 1641, 1525, 1154.

tert-Butyl (2-((4-((S)-2-((S)-2-((tert-butoxycarbonyl)amino)propanamido)propanamido)phenyl)ethynyl)benzoyl)-L-alanyl-L-alaninate 150

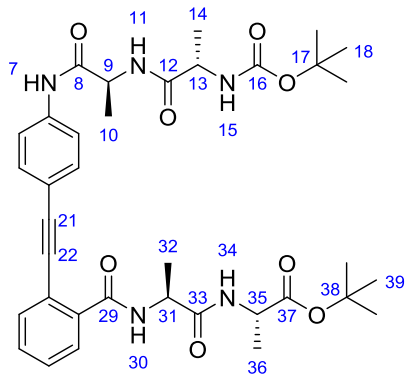

According to *general procedure (3a)*: Alkyne **137** (270 mg, 0.61 mmol) and iodide **65** (217 mg, 0.61 mmol) gave the *title compound* **150** (282 mg, 68 %) as a pale yellow solid after purification by flash column chromatography (CH_2Cl_2:MeOH, 97.5:2.5); $[\alpha]_D^{23.5}$ +6.70 (*c* 1.00, $CHCl_3$); δ_H (400 MHz, DMSO-d_6) 10.17 (br. s, 1 H, H7), 8.46 (d, *J* 7.3, 1 H, H30), 8.34 (d, *J* 6.8, 1 H, H34), 8.08 (d, *J* 7.3, 1 H, H11), 7.66 - 7.70 (m, 2 H, 2 x Ar-H), 7.59 - 7.64 (m, 2 H, Ar-H, H27), 7.51 - 7.54 (m, 2 H, 2 x Ar-H), 7.48 - 7.51 (m, 2 H, 2 x Ar-H), 6.98 - 7.01 (m, 1 H, H15), 4.52 - 4.61 (m, 1 H, H31), 4.38 - 4.46 (m, 1 H, H9), 4.10 - 4.18 (m, 1 H, H35), 3.98 - 4.04 (m, 1 H, H13), 1.37 - 1.41 (m, 18 H, H18, 39), 1.34 (d, *J* 3.2, 3 H, H32), 1.32 (d, *J* 3.2, 3 H, H10), 1.27 (d, *J* 7.3, 3 H, H36), 1.20 (d, *J* 7.3, 3 H, H14); δ_C (101 MHz, DMSO-d_6) 172.6, 171.8, 171.6, 171.5 (4 x C=O), 166.3 (C29), 155.2 (C16), 139.5, 137.9, 132.5, 132.1, 130.0, 128.4, 128.3, 120.0, 118.9, 116.7 (10 x Ar-C), 93.6, 86.9 (C21, 22), 80.3, 78.1 (C17, 38), 49.6 (C13), 49.0 (C9), 48.5 (C31), 48.4 (C35), 28.2 (C18 or C39), 27.6 (C18 or C39), 18.5 (2C, C10, 32), 18.0 (C14), 16.9 (C36); HRMS calculated for $C_{36}H_{47}O_8N_5Na$ $[(M+Na)]^+$: 700.3317, found 700.3309; IR (CH_2Cl_2) 3297, 2979, 1652, 1514, 1155.

Methyl (2-((4-((S)-2-(2-((tert-butoxycarbonyl)amino)acetamido)propanamido)phenyl)ethynyl)benzoyl)-L-alanylglycinate 151

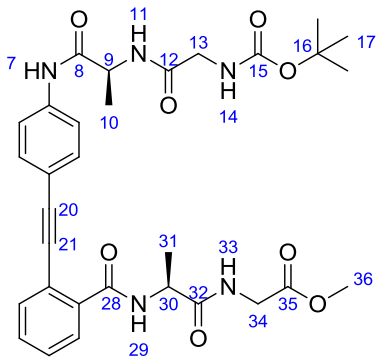

According to *general procedure (3a)*: Alkyne **139** (182 mg, 0.53 mmol) and iodide **146** (257 mg, 0.66 mmol) gave the *title compound* **151** (78 mg, 24 %) as a pale yellow solid after purification by flash column chromatography (CH_2Cl_2:EtOAc, 3:1); $[\alpha]_D^{23.5}$ -12.8 (*c* 1.00, $CHCl_3$); δ_H (400 MHz, $CDCl_3$) 9.13 (br. s, 1 H, H7), 7.94 - 8.01 (m, 1 H, Ar-H), 7.88 (d, *J* 7.1, 1 H, H29), 7.62 (d, *J* 8.6, 2 H, 2 x Ar-H), 7.57 - 7.60 (m, 1 H, Ar-H), 7.45 - 7.49 (m, 3 H, 3 x Ar-H), 7.41 - 7.44 (m, 1 H, Ar-H), 7.22 - 7.26 (m, 1 H, H33), 6.99 (d, *J* 7.8, 1 H, H11), 5.42 (t, *J* 5.7, 1 H, H14), 4.78 - 4.87 (m, 1 H, H30), 4.69 - 4.76 (m, 1 H, H9), 3.97 - 4.03 (m, 2 H, H34), 3.86 (d, *J* 5.1, 2 H, H13), 3.70 (s, 3 H, H36), 1.46 - 1.50 (m, 6 H, H10, H31), 1.45 (s, 9 H, H17); δ_C (101 MHz, $CDCl_3$) 172.3, 170.4, 170.1, 170.1 (4 x C=O), 166.7 (C28), 154.0 (C 15), 138.8, 134.6, 133.6, 133.6, 132.3, 130.9, 129.7, 128.6, 120.2, 119.7 (10 x Ar-C), 95.9, 86.8 (C20, 21), 80.8 (C16), 52.3 (C36), 49.7 (C9), 49.4 (C30), 44.6 (C13), 41.2 (C34), 28.2 (C17), 17.9, 17.6 (C10, 31); HRMS calculated for $C_{31}H_{37}O_8N_5Na$ $[(M+Na)]^+$: 631.2568, found 631.2563; IR (CH_2Cl_2) 3306, 2980, 1659, 1594, 1514.

Methyl (2-((4-((S)-2-((S)-2-((tert-butoxycarbonyl)amino)-3-methylbutanamido)propanamido)phenyl)ethynyl)benzoyl)-L-alanyl-L-valinate 152

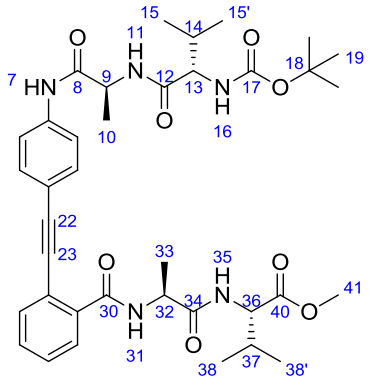

According to *general procedure (3a)*: Alkyne **141** (235 mg, 0.61 mmol) and iodide **147** (327 mg, 0.76 mmol) gave the *title compound* **152** (200 mg, 47 %) as a pale yellow solid after purification by flash column chromatography (CH_2Cl_2:EtOAc, 1:1); $[\alpha]_D^{23.5}$ -48.5 (*c* 1.00, $CHCl_3$); δ_H (400 MHz, $CDCl_3$) 9.06 (br. s, 1 H, H7), 8.00 - 8.03 (m, 1 H, Ar-H), 7.92 (d, *J* 7.1, 1 H, H31), 7.62 - 7.66 (m, 2 H, 2 x Ar-H), 7.59 - 7.62 (m, 1 H, Ar-H), 7.48 - 7.52 (m, 2 H, 2 x Ar-H), 7.44 (td, *J* 6.9, 1.6, 2 H, 2 x Ar-H), 7.13 (d, *J* 8.6, 1 H, H35), 6.78 (d, *J* 7.1, 1 H, H11), 5.14 (d, *J* 6.4, 1 H, H16), 4.80 - 4.90 (m, 1 H, H32), 4.65 - 4.75 (m, 1 H, H9), 4.48 - 4.55 (m, 1 H, H36), 3.94 - 4.03 (m, 1 H, H13), 3.74 (s, 3 H, H41), 2.10 - 2.26 (m, 2 H, H14, 37), 1.46 - 1.50 (m, 6 H, H10, 33), 1.44 (s, 9 H, H19), 0.99 (d, *J* 6.8, 3 H, H15), 0.92 - 0.96 (m, 3 H, H15'), 0.87 (d, *J* 6.8, 6 H, H38, H38'); δ_C (101 MHz, $CDCl_3$) 172.2, 172.0, 171.8, 170.3 (4 x C=O), 166.5 (C30), 156.3 (C17), 138.9, 134.4, 133.7, 132.4, 132.1, 132.0, 130.9, 129.9, 128.6, 119.6 (10 x Ar-C), 96.1, 86.7 (C22, 23), 80.7 (C18), 60.4 (C13), 57.3 (C36), 52.1 (C41), 49.7 (C9), 49.4 (C32), 31.1, 30.5 (C14, 37), 28.2 (C19), 19.3, 18.9, 17.7, 17.6 (C15, 16, 38, 39), 17.6, 17.5 (C10, 33); HRMS calculated for $C_{37}H_{49}O_8N_5Na$ $[(M+Na)]^+$: 714.3473, found 714.3468; IR (CH_2Cl_2) 3324, 3059, 2480, 1651, 1515.

Methyl (2-((4-((S)-2-((2S,3S)-2-((tert-butoxycarbonyl)amino)-3-methylpentanamido)propanamido)phenyl)ethynyl)benzoyl)-L-alanyl-L-alloisoleucinate 153

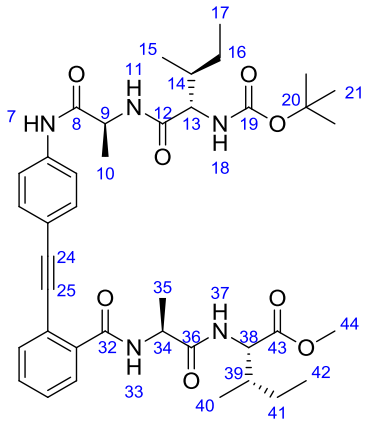

According to *general procedure (3a)*: Alkyne **143** (250 mg, 0.62 mmol) and iodide **148** (348 mg, 0.78 mmol) gave the *title compound* **153** (111 mg, 25 %) as a pale yellow solid after purification by flash column chromatography (CH_2Cl_2:EtOAc, 1:1); $[\alpha]_D^{23.5}$ -54.5 (*c* 1.00, $CHCl_3$); δ_H (400 MHz, $CDCl_3$) 9.08 (br. s, 1 H, H7), 7.99 - 8.03 (m, 1 H, Ar-H), 7.91 (d, *J* 7.3, 1 H, H33), 7.67 - 7.70 (m, 1 H, Ar-H), 7.64 - 7.66 (m, 1 H, Ar-H), 7.59 - 7.61 (m, 1 H, Ar-H), 7.49 - 7.51 (m, 2 H, 2 x Ar-H), 7.43 - 7.46 (m, 2 H, 2 x Ar-H), 7.13 (d, *J* 8.6, 1 H, H37), 6.75 - 6.83 (m, 1 H, H11), 5.11 - 5.20 (m, 1 H, H18), 4.79 - 4.89 (m, 1 H, H34), 4.65 - 4.75 (m, 1 H, H9), 4.52 - 4.59 (m, 1 H, H38), 3.98 - 4.04 (m, 1 H, H13), 3.73 (s, 3 H, H44), 1.82 - 1.88 (m, 2 H, H14, 39), 1.45 - 1.48 (m, 6 H, H10, 35), 1.44 (s, 9 H, H21), 1.34 - 1.40 (m, 2H, 2 of H16, H16', H41, H41'), 1.13 - 1.20 (m, 2 H, 2 of 2 of H16, H16', H41, H41'), 0.90 - 0.96 (m, 6 H, H15, H40), 0.82 - 0.87 (m, 6 H, H17, H42); δ_C (101 MHz, $CDCl_3$) 172.1, 171.7, 171.2, 170.3 (4 x C=O), 166.5 (C32), 156.2 (C19), 138.9, 134.5, 133.6, 132.4, 132.1, 132.0, 130.8, 129.9, 128.6, 119.6 (10 x Ar-C), 96.1, 86.6 (C24, 25), 80.6 (C20), 59.7 (C13), 56.6 (C38), 52.1 (C44), 49.7 (C9), 49.4 (C34), 37.7, 36.9 (C14, 39), 28.2 (C21), 25.0, 24.8 (C16, 41), 17.6, 17.5 (C10, 35), 15.7, 15.4 (C15, 40), 11.5, 11.4 (C17, 42);

HRMS calculated for $C_{39}H_{53}O_8N_5Na$ $[(M+Na)]^+$: 742.3786, found 742.3784; IR (CH_2Cl_2) 3289, 2966, 1645, 1514, 735.

tert-Butyl (2-((4-((S)-2-((S)-2-((tert-butoxycarbonyl)amino)-3-phenylpropanamido)propanamido)phenyl)ethynyl)benzoyl)-L-alanyl-L-phenylalaninate 154

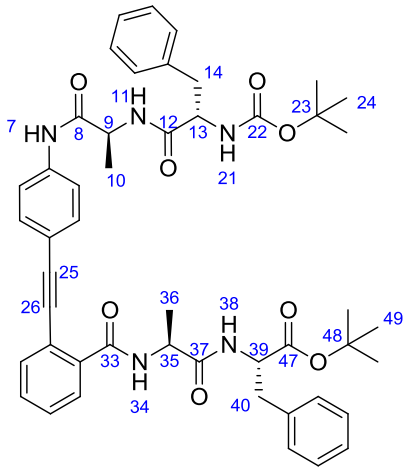

According to *general procedure (3a)*: Alkyne **145** (170 mg, 0.39 mmol) and iodide **149** (256 mg, 0.49 mmol) gave the *title compound* **154** (93 mg, 29 %) as a pale yellow solid after purification by flash column chromatography (CH_2Cl_2:EtOAc, 3:1); $[\alpha]_D^{23.5}$ -8.60 (*c* 0.50, MeOH); δ_H (500 MHz, $CDCl_3$) 8.60 (br. s., 1 H, H7), 7.74 - 7.80 (m, 1 H, Ar-H), 7.59 (d, *J* 8.8, 2 H, 2 x Ar-H), 7.42 - 7.47 (m, 1 H, Ar-H), 7.35 - 7.41 (m, 3 H, 3 x Ar-H), 7.20 - 7.30 (m, 8 H, 8 x Ar-H), 7.14 - 7.19 (m, 3 H, 3 x Ar-H), 6.46 (d, *J* 7.4, 1 H, H38), 6.41 (d, *J* 6.8, 1 H, H11 or H34), 6.27 (d, *J* 7.6, 1 H, H11 or H34), 4.87 - 4.98 (m, 1 H, H21), 4.71 - 4.78 (m, 1 H, H39), 4.62 - 4.70 (m, 1 H, H9 or H35), 4.57 (quin, *J* 7.2, 1 H, H9 or H35), 4.27 - 4.37 (m, 1 H, H13), 3.01 - 3.17 (m, 4 H, H14, 40), 1.36 - 1.44 (m, 24 H, H10, H24, H36, H49); δ_C (126 MHz, $CDCl_3$) 171.6, 171.1, 170.1, 168.8 (4 x C=O), 166.9 (C33), 156.0 (C22), 141.3, 139.9, 137.8, 137.7, 135.9, 135.7, 131.4, 129.5, 129.4, 129.1, 129.0, 128.6, 128.5, 128.4, 128.2, 127.4, 127.1, 121.8 (18 x Ar-C), 92.4, 87.4 (C25, 26), 82.6, 81.3 (C23, 48),

56.3 (C13), 53.7 (C39), 49.6, 49.4 (C9, 35), 38.0, 37.6 (C14, 40), 28.2, 28.0 (C23, 48), 18.5, 16.9 (C10, 36); HRMS calculated for $C_{48}H_{54}O_8N_5$ $[(M-H)]^-$: 828.3978, found 828.3986; IR (MeOH) 3303, 2928, 1649, 1537.

5.9 References

1. Pauling, L. & Corey, R. B. Configurations of Polypeptide Chains with Favored Orientations Around Single Bonds: Two New Pleated Sheets. *Proc. Natl. Acad. Sci. U. S. A.* **37,** 729–740 (1951).

2. Pauling, L. & Corey, R. B. The pleated sheet, a new layer configuration of polypeptide chains. *Proc. Natl. Acad. Sci. U. S. A.* **37,** 251–256 (1951).

3. O'Neil, K. T. & DeGrado, W. F. A Thermodynamic Scale for the Helix-Forming Tendencies of the Commonly Occurring Amino Acids. *Science* **250,** 646–651 (1990).

4. Muñoz, V. & Serrano, L. Elucidating the folding problem of helical peptides using empirical parameters. *Nat. Struct. Mol. Biol.* **1,** 399–409 (1994).

5. Chou, P. Y. & Fasman, G. D. Conformational parameters for amino acids in helical, β-sheet, and random coil regions calculated from proteins. *Biochemistry (Mosc.)* **13,** 211–222 (1974).

6. Chou, P. Y. & Fasman, G. D. Prediction of protein conformation. *Biochemistry (Mosc.)* **13,** 222–245 (1974).

7. Wilmot, C. M. & Thornton, J. M. Analysis and prediction of the different types of Beta-turn in proteins. *J. Mol. Biol.* **203,** 221 – 232 (1988).

8. Singh, H., Singh, S. & Raghava, G. P. S. In silico platform for predicting and initiating β-turns in a protein at desired locations. *Proteins Struct. Funct. Bioinforma.* **83,** 910–921 (2015).

9. Kim, C. A. & Berg, J. M. Thermodynamic β-sheet propensities measured using a zinc-finger host peptide. *Nature* **362,** 267–270 (1993).

10. Krizek, B. A., Amann, B. T., Kilfoil, V. J., Merkle, D. L. & Berg, J. M. A consensus zinc finger peptide: design, high-affinity metal binding, a pH-dependent structure, and a His to Cys sequence variant. *J. Am. Chem. Soc.* **113,** 4518–4523 (1991).

11. Allen, M. D. *et al.* Solution structure of the nonmethyl-CpG-binding CXXC domain of the leukaemia-associated MLL histone methyltransferase. *EMBO J.* **25,** 4503–4512 (2006).

12. Chou, P. Y. *Prediction of Protein Structure and the Principles of Protein Conformation*. (Plenum Press, 1990).

13. Minor, D. L. & Kim, P. S. Measurement of the β-sheet-forming propensities of amino acids. *Nature* **367,** 660–663 (1994).

14. Alexander, P., Fahnestock, S., Lee, T., Orban, J. & Bryan, P. Thermodynamic analysis of the folding of the streptococcal protein G IgG-binding domains B1 and B2: why small

proteins tend to have high denaturation temperatures. *Biochemistry (Mosc.)* **31,** 3597–3603 (1992).

15. Gronenborn, A. M. *et al.* A novel, highly stable fold of the immunoglobulin binding domain of streptococcal protein G. *Science* **253,** 657–661 (1991).

16. Kemp, D. S. Peptidomimetics and the template approach to nucleation of β-sheets and α-helices in peptides. *Trends Biotechnol.* **8,** 249–255 (1990).

17. Nowick, J. S. & Insaf, S. The Propensities of Amino Acids To Form Parallel β-Sheets. *J. Am. Chem. Soc.* **119,** 10903–10908 (1997).

18. Bai, Y., Milne, J. S., Mayne, L. & Englander, S. W. Primary structure effects on peptide group hydrogen exchange. *Proteins Struct. Funct. Bioinforma.* **17,** 75–86 (1993).

19. Bai, Y. & Englander, S. W. Hydrogen bond strength and β-sheet propensities: The role of a side-chain blocking effect. *Proteins Struct. Funct. Bioinforma.* **18,** 262–266 (1994).

20. Rossmeisl, J., Kristensen, I., Gregersen, M., Jacobsen, K. W. & Nørskov, J. K. β-Sheet Preferences from First Principles. *J. Am. Chem. Soc.* **125,** 16383–16386 (2003).

21. Scheiner, S. The Strength with Which a Peptide Group Can Form a Hydrogen Bond Varies with the Internal Conformation of the Polypeptide Chain. *J. Phys. Chem. B* **111,** 11312–11317 (2007).

22. Scheiner, S. & Kar, T. Underlying source of the relation between polypeptide conformation and strength of NH···O hydrogen bonds. *J. Mol. Struct.* **844–845,** 166–172 (2007).

23. Sheridan, R. P., Lee, R. H., Peters, N. & Allen, L. C. Hydrogen-bond cooperativity in protein secondary structure. *Biopolymers* **18,** 2451–2458 (1979).

24. Nowick, J. S. Chemical Models of Protein β-Sheets. *Acc. Chem. Res.* **32,** 287–296 (1999).

25. Abraham, M. H. *et al.* An NMR Method for the Quantitative Assessment of Intramolecular Hydrogen Bonding; Application to Physicochemical, Environmental, and Biochemical Properties. *J. Org. Chem.* **79,** 11075–11083 (2014).

26. Schneider, T. L., Halloran, K. T., Hillner, J. A., Conry, R. R. & Linton, B. R. Application of H/D Exchange to Hydrogen Bonding in Small Molecules. *Chem. Eur. J.* **19,** 15101–15104 (2013).

27. Bai, Y. W., Englander, J. J., Mayne, L., Milne, J. S. & Englander, S. W. Structural-Perturbation Approaches to Thermodynamics of Site-Specific Protein-DNA Interactions. *Energ. Biol. Macromol.* **249,** 344 – 356 (1995).

28. Dixon, D. A., Dobbs, K. D. & Valentini, J. J. Amide-Water and Amide-Amide Hydrogen Bond Strengths. *J. Phys. Chem.* **98,** 13435–13439 (1994).

29. Maeda, K., Kamiya, N. & Yashima, E. Poly(phenylacetylene)s Bearing a Peptide Pendant: Helical Conformational Changes of the Polymer Backbone Stimulated by the Pendant Conformational Change. *Chem. – Eur. J.* **10,** 4000–4010 (2004).

Appendix I: Rights Permissions

The figures for which permission was required for use or adaptation are listed below with the reference from which they were taken. The corresponding permissions follow in order.

Figures 1.1 and ***1.2***

Seebach, D., Hook, D. F. & Glättli, A. Helices and other secondary structures of β- and γ-peptides. *Pept. Sci.* **84,** 23–37 (2006).

Figure 1.17

Nelson, J. C., Saven, J. G., Moore, J. S. & Wolynes, P. G. Solvophobically Driven Folding of Nonbiological Oligomers. *Science* **277,** 1793–1796 (1997).

Figure 1.20

Berl, V., Huc, I., Khoury, R. G., Krische, M. J. & Lehn, J.-M. Interconversion of single and double helices formed from synthetic molecular strands. *Nature* **407,** 720–723 (2000).

Figure 3.7

Nowick, J. S., Smith, E. M. & Pairish, M. Artificial β-sheets. *Chem. Soc. Rev.* **25,** 401–415 (1996).

Figure 3.18

Schenck, H. L. & Gellman, S. H. Use of a Designed Triple-Stranded Antiparallel β-Sheet To Probe β-Sheet Cooperativity in Aqueous Solution. *J. Am. Chem. Soc.* **120,** 4869–4870 (1998).

Figure 3.22

Schenk, D. *et al.* Immunization with amyloid-β attenuates Alzheimer-disease-like pathology in the PDAPP mouse. *Nature* **400,** 173–177 (1999).

Figure 5.7

Bai, Y. & Englander, S. W. Hydrogen bond strength and β-sheet propensities: The role of a side chain blocking effect. *Proteins Struct. Funct. Bioinforma.* **18,** 262–266 (1994).

Figure 5.10

Scheiner, S. The Strength with Which a Peptide Group Can Form a Hydrogen Bond Varies with the Internal Conformation of the Polypeptide Chain. *J. Phys. Chem. B* **111,** 11312–11317 (2007).